frontiers | Research Topics

Immune evasion and defense strategies in parasitic protozoa-host interactions

Edited by
Jian Du, Hong-Juan Peng, Bang Shen and Yongliang Zhang

Published in
Frontiers in Microbiology
Frontiers in Cellular and Infection Microbiology

ISSN 1664-8714
ISBN 978-2-83250-973-9
DOI 10.3389/978-2-83250-973-9

About Frontiers

Frontiers is more than just an open access publisher of scholarly articles: it is a pioneering approach to the world of academia, radically improving the way scholarly research is managed. The grand vision of Frontiers is a world where all people have an equal opportunity to seek, share and generate knowledge. Frontiers provides immediate and permanent online open access to all its publications, but this alone is not enough to realize our grand goals.

Frontiers journal series

The Frontiers journal series is a multi-tier and interdisciplinary set of open-access, online journals, promising a paradigm shift from the current review, selection and dissemination processes in academic publishing. All Frontiers journals are driven by researchers for researchers; therefore, they constitute a service to the scholarly community. At the same time, the *Frontiers journal series* operates on a revolutionary invention, the tiered publishing system, initially addressing specific communities of scholars, and gradually climbing up to broader public understanding, thus serving the interests of the lay society, too.

Dedication to quality

Each Frontiers article is a landmark of the highest quality, thanks to genuinely collaborative interactions between authors and review editors, who include some of the world's best academicians. Research must be certified by peers before entering a stream of knowledge that may eventually reach the public - and shape society; therefore, Frontiers only applies the most rigorous and unbiased reviews. Frontiers revolutionizes research publishing by freely delivering the most outstanding research, evaluated with no bias from both the academic and social point of view. By applying the most advanced information technologies, Frontiers is catapulting scholarly publishing into a new generation.

What are Frontiers Research Topics?

Frontiers Research Topics are very popular trademarks of the *Frontiers journals series*: they are collections of at least ten articles, all centered on a particular subject. With their unique mix of varied contributions from Original Research to Review Articles, Frontiers Research Topics unify the most influential researchers, the latest key findings and historical advances in a hot research area.

Find out more on how to host your own Frontiers Research Topic or contribute to one as an author by contacting the Frontiers editorial office: frontiersin.org/about/contact

Immune evasion and defense strategies in parasitic protozoa-host interactions

Topic editors

Jian Du — Anhui Medical University, China

Hong-Juan Peng — Southern Medical University, China

Bang Shen — Huazhong Agricultural University, China

Yongliang Zhang — National University of Singapore, Singapore

Citation

Du, J., Peng, H.-J., Shen, B., Zhang, Y., eds. (2022). *Immune evasion and defense strategies in parasitic protozoa-host interactions*. Lausanne: Frontiers Media SA.

doi: 10.3389/978-2-83250-973-9

Table of contents

frontiers in Microbiology

REVIEW
published: 22 October 2020
doi: 10.3389/fmicb.2020.589604

The Host Autophagy During *Toxoplasma* Infection

Minmin Wu[1,2,3†], *Obed Cudjoe*[1,2,3†], *Jilong Shen*[1,2,3], *Ying Chen*[1,2,3,4*] and *Jian Du*[1,2,3*]

[1]Department of Biochemistry and Molecular Biology, School of Basic Medical Sciences, Anhui Medical University, Hefei, China, [2]The Key Laboratory of Zoonoses of Anhui, Anhui Medical University, Hefei, China, [3]The Key Laboratory of Pathogen Biology of Anhui Province, Anhui Medical University, Hefei, China, [4]School of Nursing, Anhui Medical University, Hefei, China

Autophagy is an important homeostatic mechanism, in which lysosomes degrade and recycle cytosolic components. As a key defense mechanism against infections, autophagy is involved in the capture and elimination of intracellular parasites. However, intracellular parasites, such as *Toxoplasma gondii*, have developed several evasion mechanisms to manipulate the host cell autophagy for their growth and establish a chronic infection. This review provides an insight into the autophagy mechanism used by the host cells in the control of *T. gondii* and the host exploitation by the parasite. First, we summarize the mechanism of autophagy, xenophagy, and LC3-associated phagocytosis. Then, we illustrate the process of autophagy proteins-mediated *T. gondii* clearance. Furthermore, we discuss how the parasite blocks and exploits this process for its survival.

Keywords: *Toxoplasma gondii*, autophagy, xenophagy, LC3-associated phagocytosis, IFN-γ mediated pathogen elimination

OPEN ACCESS

Edited by:
Lihua Xiao,
South China Agricultural University, China

Reviewed by:
Carlos Subauste,
Case Western Reserve University, United States
Vern B. Carruthers,
University of Michigan, United States

***Correspondence:**
Ying Chen
cy.juice@aliyun.com
Jian Du
dujane@163.com

[†]*These authors have contributed equally to this work*

Specialty section:
This article was submitted to Infectious Diseases, a section of the journal Frontiers in Microbiology

Received: *31 July 2020*
Accepted: *28 September 2020*
Published: *22 October 2020*

Citation:
Wu M, Cudjoe O, Shen J, Chen Y and Du J (2020) The Host Autophagy During Toxoplasma Infection. Front. Microbiol. 11:589604. doi: 10.3389/fmicb.2020.589604

INTRODUCTION

Toxoplasma gondii (*T. gondii*) is an obligate intracellular protozoan parasite, which can infect warm-blooded animals and cause morbidity and mortality in humans and animals worldwide (Halonen and Weiss, 2013). *T. gondii* is unified as a single species in the genus *Toxoplasma*, although recent estimates based on genomic barcoding show a much greater diversity across continents. Most strains of *Toxoplasma* isolated in Europe and North America belong to three main clonal lineages known as Types I, II, and III strains, which have different virulence in mice and may cause different human sequelae (Darde et al., 1992; Howe and Sibley, 1995; Howe et al., 1997; Machacova et al., 2016). *T. gondii* strains in South America are genetically more diverse than those in North America and Europe. However, Chinese 1 strain was reported to be the dominant strain, differing from the three main clones previously reported in East Asia, particularly in China (Zhou et al., 2010; Chen et al., 2011; Wang et al., 2013; Li et al., 2014).

Toxoplasma gondii is transmitted through food-borne, animal-to-human, congenital, blood transfusion, and organ transplantation (Montoya and Liesenfeld, 2004; Chu et al., 2017; Yu et al., 2017). *T. gondii* can cause human congenital and acquired infection. The congenital form may be subclinical or manifest as destructive damage to the internal organs, eyes, and brain (Halonen and Weiss, 2013; Hampton, 2015). Available data suggest about a third of the world's population have developed long lasting serum antibodies in response to previous subclinical infection. Most of the toxoplasmosis is asymptomatic (Halonen and Weiss, 2013;

Parlog et al., 2014). In rare cases, acquired toxoplasmosis could cause serious, disseminated diseases such as meningoencephalitis, pneumonia, or myocarditis. In addition, acquired ocular disease generally occurs either alone as a result of reactivation from chronic infection, or as a complication of acute systemic disease, including newly acquired disease (Montoya and Remington, 1996; Montoya and Liesenfeld, 2004; Hampton, 2015). In the acute phase of infection, tachyzoites rapidly replicate and spread to various organs through the blood or lymphatic system. In the chronic phase, *T. gondii* forms tissue cysts (bradyzoites) in which the parasite can survive for a long time or even lifetime lurking in the brain, tissue, muscle, retina, etc. (Lyons et al., 2002; Halonen and Weiss, 2013; Li et al., 2016).

Autophagy, a well-conserved and tightly regulated process in eukaryotes, which is key for cellular homeostasis, cell survival, and degradation of damaged cytoplasmic components or harmful exogenous substrates (Levine and Kroemer, 2008; Wang et al., 2009). As a key defense mechanism against infections, it also involves catching parasites inside cells and then clearing them out (Besteiro, 2017). Moreover, autophagy is thought to be an integral component of the innate immune response, targeting intracellular parasites, and parasites in damaged vacuoles and phagosomes, limiting their growth (Huang and Brumell, 2014). Recent study has shown that 4-Hydroxybenzaldehyde restricts the intracellular growth of *Toxoplasma* by activating SIRT1-mediated autophagy in macrophages (Lee et al., 2020). However, intracellular pathogens have also evolved diverse mechanisms to avoid autophagy (Steele et al., 2015). In this review, we focus on recent progress on understanding interactions between *T. gondii* and host autophagy pathways.

MECHANISMS OF AUTOPHAGY

Autophagy is a conservative catabolism system in cells, in which double-membraned autophagosome engulfs cytoplasmic components and degrades them after fusion with lysosomes (Choi et al., 2013; Paulus and Xavier, 2015; Galluzzi et al., 2017). Autophagy is mainly dependent on autophagy (ATG) proteins leading to the formation of autophagosome and lysosomal degradation of autophagy substrates. This pathway involves several different steps, such as the formation of a cup-shaped double membrane capable of engulfing specific substances or chunks of cytoplasm; membrane elongation and closure to form autophagosomes; transport and fusion of autophagosomes and lysosomes; and finally, degradation of the enclosed cytoplasmic contents within the autophagosome and nutrient recycling (Nakatogawa et al., 2009; Parzych and Klionsky, 2014; **Figure 1**). Starvation and the mammalian target of rapamycin (mTOR) kinase inhibition induce autophagy to provide nutrients for the basic physiological processes of the cells and to maintain homeostasis. Nutrient deprived conditions induce autophagosome formation *via* the mTORcomplex 1 (mTORC1) inhibition in mammalian cells. The initiation complex of ULK1 activates the phosphatidylinositol 3-kinase (PI3K) complex of Beclin1-Vps34-Vps15-Atg14L (Deretic, 2011; Choi et al., 2014; Paulus and Xavier, 2015). The expansion or elongation of the phagophore need the involvement of two ubiquitin-like (UBL) conjugation systems. The first UBL conjugation system involves the formation of Atg12-Atg5-Atg16 complex. In yeast cells, Atg12 binds covalently to Atg5. This Atg12-Atg5 conjugation is highly dependent on Atg7 (E1 activating enzyme) and Atg10 (E2 activating enzyme). Then, Atg16 non-covalently binds to Atg5 forming the Atg12-Atg5-Atg16 complex, following the Atg12-Atg5 conjugation. The second UBL conjugation system involves the Atg8 or LC3 (in mammals) system. Atg8/LC3 is activated by the EI-like enzyme Atg7 and transferred to the E2-like enzyme Atg3. In the final step, phosphatidylethanolamine (PE) binds to the C-terminal glycine Atg8 to form LC3-phosphatidylethanolamine conjugate (LC3-II) and incorporated into the autophagosomal membrane (Hwang et al., 2012; Huang and Brumell, 2014; Biering et al., 2017; Choi et al., 2017; Wacker et al., 2017). The lysosome subsequently fuses with the outer membrane of the autophagosome to deliver their cytoplasmic cargo for degradation and recycling (Melzer et al., 2008; Paulus and Xavier, 2015; Selleck et al., 2015). Cytoplasmic cargoes are captured in double-membrane structure, called "autophagosomes," which then mature into autolysosomes that degrade or otherwise eliminate captured cargoes. Another strategy employed by host cells to capture and degrade invading intracellular pathogens is xenophagy. It is a key defense mechanism against various infections involving the elimination intracellular pathogens such as protozoans, bacteria, and viruses (Mizushima et al., 2011; Paulus and Xavier, 2015; Galluzzi et al., 2017). Xenophagy is also considered as an innate component of cellular immune response.

Autophagy proteins may be involved in certain cellular pathways leading to the elimination of intracellular pathogens but do not constitute autophagy. These cellular pathways are established under certain cellular conditions; some bypass proteins involved in elongation and closure (Atg7, Atg5, and LC3), while others bypass proteins necessary for initiation (ULK1) and nucleation (Beclin1; Steele et al., 2015; Galluzzi et al., 2017). LC3-associated phagocytosis (LAP) is an example of such a process, involves the recruitment of LC3 to single-membrane phagosomes, which surround intracellular pathogens or dead cells (Paulus and Xavier, 2015). This process is independent of the ULK1 initiation complex, while the PtdIns3K complex is important for LAP initiation (Martinez et al., 2015; Besteiro, 2019). During PAMP receptor activation, PI3PK complex is recruited to the phagosomal membrane (Ma et al., 2012). This complex lacks ATG14 but is composed of Rubicon and UV resistance-associated gene (UVRAG; Martinez et al., 2015). With Rubicon's help, NADPH oxidase 2 (NOX2) then enters the phagosomes. Activation of NOX2 and PI3PK leads to the production reactive oxygen species (ROS) and initiate lipidation of the phagosomal membrane, respectively, and ultimately leading to the formation of LAPosome (LC3-decorated phagosome; Ueyama et al., 2011). Fusing with lysosomes to form a lytic compartment, the LAPosomes then degrades the cargo. Although the effect of LC3 on LAPosome is still unknown, some studies suggested

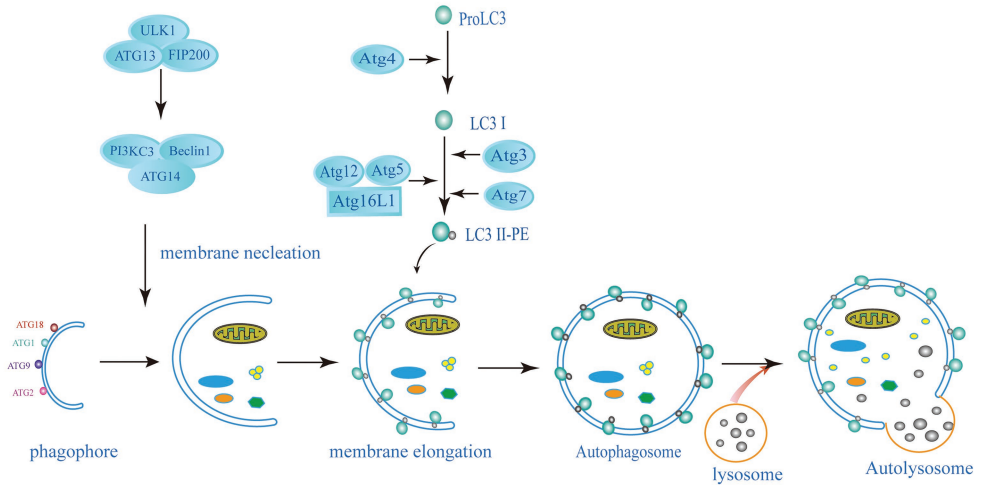

FIGURE 1 | Schematic diagram of the autophagy pathway. The induction of autophagy causes the assembly and elongation of the phagophore and finally forms a structure that can surround the components in cytoplasm. The phagophore expands and develops into a double-membrane structure of autophagosomes. Targets in cytoplasm, like organelles, proteins, and microorganisms, are isolated. Autolysosome has formed by the fussing of autophagosome and lysosome, where hydrolytic enzymes in the autolysosome degrade cytoplasmic cargo. The left side shows the key proteins related to mammalian autophagy (ATG, autophagy-related: ATG3, ATG5, ATG7, ATG4, ATG12, ATG13, ATG14, ATG16L1, FIP200, ULK1, PI3KC3, Beclin1, LC3, and PE).

that LC3 could accelerate its maturation by fusion with lysosomes (Martinez et al., 2015; Besteiro, 2019).

MECHANISMS OF HOST AUTOPHAGY PROTEINS-MEDIATED *T. GONDII* CLEARANCE

Toxoplasma gondii replicate in the host cell by forming a special endocytic vacuole, called parasitophorous vacuole (PV). The membrane of PV allows *T. gondii* to develop while protected from intracellular cytoplasmic defense mechanisms (Orlofsky, 2009; Portillo et al., 2017). Increasing literature indicates that *T. gondii* actively induces autophagic pathways in the infected host cells (Orlofsky, 2009; Wang et al., 2009; Chu et al., 2017; Saeij and Frickel, 2017; Subauste, 2019). Two types of immune response are required in the control of *T. gondii*: clearance of *T. gondii* by CD40-mediated autophagy and IFN-γ-induced the clearance of *T. gondii* through autophagy proteins. Both of them are essential for killing parasites within host cells.

Clearance of *T. gondii* by CD40-Mediated Autophagy

The parasitic vacuole is formed during the active invasion of *T. gondii*. Vacuolar membranes have been extensively modified by removing many proteins from host cells and inserting parasite-derived proteins into parasitic vacuoles. Once the PV is formed, its nonfusion properties will be unchanged (Subauste, 2009). So, whether there is a way to change the nonfusion properties of PV is the key question in the interaction between *T. gondii* and the immune system. Previous studies have demonstrated that this can be achieved *via* stimulation of CD40 (Andrade et al., 2006; Subauste et al., 2007b). In macrophages infected with *T. gondii*, stimulation with CD40 can induce the fusion of the PV with lysosomes in an autophagy-dependent manner.

As a member of the TNF receptor superfamily, CD40 expresses on various nonhematopoietic cells and APCs (Subauste, 2009; Van Grol et al., 2013). Several studies have demonstrated that CD40 triggers signaling pathways, which are upstream of ULK1 and Beclin1-PI3KC3 complexes to activate autophagy. CD40 stimulates autophagy *via* pathways involving CaMKKβ, AMP-activated protein kinase (AMPK), and ULK1, leading to kill *T. gondii* (Liu et al., 2016). The phosphorylation of Ser-555 ULK1 and autophagy mediated by ULK1 are caused by AMPK (Russell et al., 2013). CD40 can induce phosphorylation of Thr-172 AMPK mediated by CaMKKβ. Besides direct effects on the ULK1/2 complex, AMPK also inhibit mTORC1 by phosphorylating Raptor (a mTORC1 binding partner). CD40 also interacts with TRAF6 to stimulate TNF-α production in macrophages. Recruitment of TRAF6 in the cytoplasmic tail of CD40 enhances the expression of TNF-α. It causes phosphorylation of Bcl-2 at Ser-87 in JNK-dependent way, and binding Beclin 1 to PI3KC3 to induce autophagy (Subauste et al., 2007a; Liu et al., 2016). CD40 can also induce the death of *T. gondii* by lowering the level of P21 and upregulating the autophagy molecule Beclin 1 (Portillo et al., 2010; **Figure 2**). CD40 signaling triggers pathogen-lysosome fusion *via* the autophagic mechanism. ULK1/2 complexes and the Beclin1-PI3KC3 complex activation promote the formation and maturation of autophagosome by recruiting Atg proteins to the isolation membrane (Liu et al., 2016). The phagophore is produced by polymerization of Atg8 (LC3) and Atg12-Atg5 UBL conjugation systems (Kihara et al., 2001; Ohsumi, 2001). The isolation membrane envelops organelles and cytosol, which leads to forming the autophagosomes.

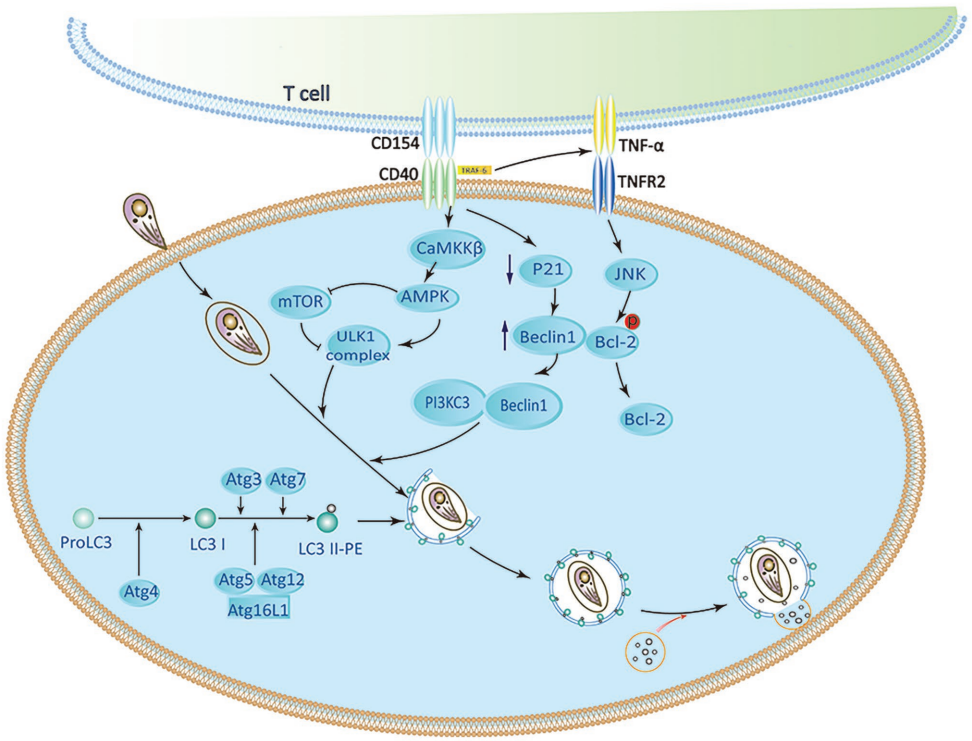

FIGURE 2 | CD40 induces activation of autophagy signaling pathway. CaMKKβ-mediated Threonine-172 AMP-activated protein kinase (AMPK) phosphorylation can be induced by CD40, which leads to Serine-555 ULK1 phosphorylation and ULK1-mediated autophagy. CD40 may upregulate Beclin 1 protein levels by reducing p21. The accumulation of TRAF6 in the cytoplasmic tail of CD40 enhances TNF-α autocrine production, which leads to the phosphorylation of Bcl-2 at Serine 87 in JNK-dependent way and separation of Bcl-2 from Beclin1. ULK1, Beclin 1, PI3KC3, ATG5, ATG7, and lysosomal enzymes play an important role in killing of *Toxoplasma gondii* caused by CD40 (Subauste, 2009; Liu et al., 2016).

Therefore, autophagosomes are recruited around the PV and fused with late endosomal lysosomes to kill *T. gondii* (Zhao et al., 2007; Subauste, 2009; Chu et al., 2017).

IFN-γ Restricts *T. gondii* Through Autophagy-Independent Effects of Autophagy Proteins

To restrict the infection, IFN-γ-stimulated murine cells are armed with effector molecules, such as the immunity-related p47GTPases (IRGs) and guanylate-binding proteins (GBPs; Feng et al., 2008). Studies have revealed that the LC3 conjugation system is necessary to recruit IRGs and GBPs to the parasitophorous vacuole membrane (PVM; Choi et al., 2014; Haldar et al., 2014; Ohshima et al., 2014; Lee et al., 2015). Atg5 is an important autophagic gene and is particularly useful for targeting IRGs and GBPs to PVM containing *T. gondii*. Without ATG5, IRGs and GBPs are usually induced by IFN-γ, and they form aggregates in the cytoplasm instead of targeting vacuoles containing pathogens (Zhao et al., 2008; Choi et al., 2014, 2017; Biering et al., 2017). Once these GTPases are recruited to the LC3-tagged PVM, the PVM surrounding parasites shows extensive vesiculation and blebbing with clusters of small vesicles in the purlieu of the vacuole. At these sites, IRGs localize to small vesicular forms with dense coats from the adjacent PVM, stripping the PV membrane of *T. gondii*. Denuded parasites are enveloped in autophagic vacuoles that eventually fuse with lysosomes and ultimately limit the growth of *T. gondii* growth (Ling et al., 2006; Zhao et al., 2008; Clough et al., 2016; Coppens, 2017). PVMs of type I virulent strains are much less intensely loaded with IRG proteins than those of type II or type III avirulent strains in single infection or co-infections (Khaminets et al., 2010). Although IRGs and GBPs participate in the disruption of parasite PVM, the molecular mechanisms of how these IFN-γ induced GTPases interact with the autophagic machinery are poorly understood (Melzer et al., 2008; Whitmarsh and Hunter, 2008; Choi et al., 2014; Biering et al., 2017; **Figure 3**).

Although some studies have identified p47 IRGs as the primary IFN-γ-induced mechanism of anti-*Toxoplasma* infection in mice during the acute phase, there is a lack of multitude of IRGs in humans (Subauste, 2009; Clough et al., 2016; Krishnamurthy et al., 2017). Immunity-related GTPase family M protein (IRGM) and immunity-related GTPase cinema (IRGC) are the only two human IRGs. But neither of them are induced by IFN-γ. IRGM plays a role in autophagy and host resistance against *Mycobacterium tuberculosis*; but its role in toxoplasmosis has not been determined (Portillo et al., 2010;

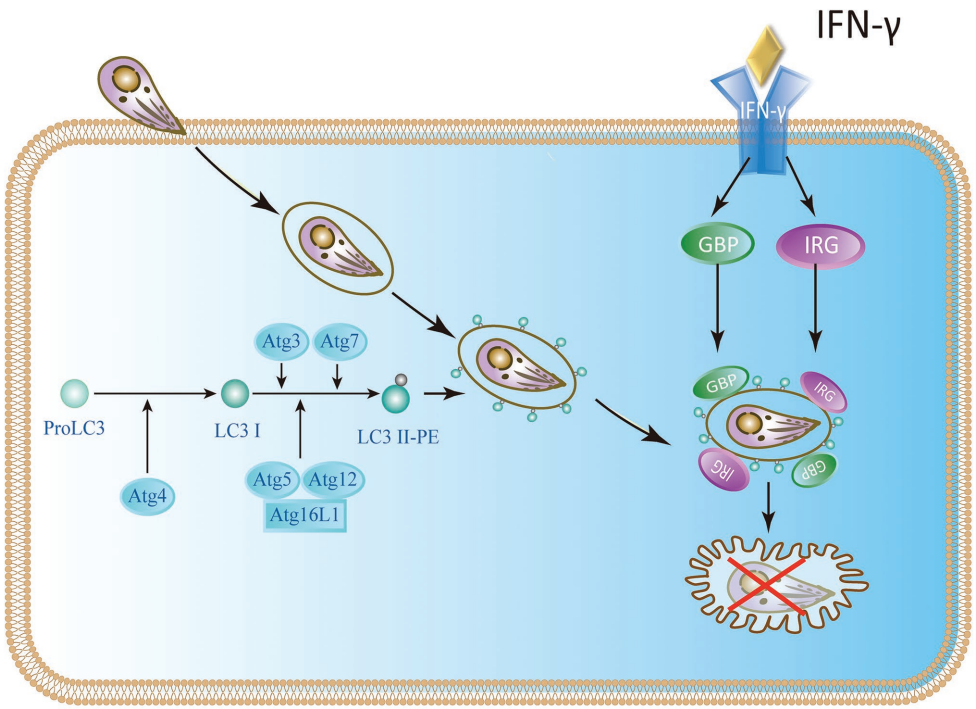

FIGURE 3 | IFN-γ restricts the growth of *T. gondii* in mouse cells. In mice, the Atg proteins Atg7, Atg3, and the Atg12-Atg5-Atg16L1 complex play a key role in the delivery and binding of LC3 to the autophagosome membrane. They are also involved in targeting immunity-related p47GTPases (IRG) and guanylate-binding protein (GBP) to *Toxoplasma* parasitophorous vacuole membrane (PVM).

Deretic, 2011; Niedelman et al., 2013; Krishnamurthy et al., 2017). Furthermore, seven IFN-γ-inducible Guanylate binding proteins (GBPs) expressed in humans are involved in IFN-γ dependent clearance of pathogens such as *Chlamydia* and viruses. There is currently no evidence of GBP-mediated inhibition of *T. gondii* in humans (Ohshima et al., 2014). Selleck et al. identified new roles for ubiquitination and recruitment of autophagic adapters p62 and NDP52, which could control *T. gondii* replication in IFN-γ activated human cells (Choi et al., 2014; Lee et al., 2015; Selleck et al., 2015; Clough et al., 2016). The IFN-γ mediated ubiquitin-driven restriction pathways of *Toxoplasma* type II varies with cell type. Ubiquitin-targeted PVs found in HeLa cells do not acidify but instead restrict *Toxoplasma* type II by stunting growth. However, IFN-γ stimulated human umbilical vein endothelial cells (HUVEC) have been shown to restrict *Toxoplasma* in a manner independent of autophagy, where HUVEC exhibits vacuolar lysosomal acidification and subsequent parasite destruction. Thus, we conclude that the two different human cell types deploy the same initial defense molecules ubiquitin, p62 and NDP52 to similar numbers but diverge in the ultimate strategy (Clough et al., 2016; Saeij and Frickel, 2017). Neither of these mechanisms works in all cell types, suggesting the IFN-γ mediated control of *T. gondii* exists multiple overlapping pathways in human cells (Niedelman et al., 2013; Selleck et al., 2015; Bando et al., 2018). In addition, ATG16L1 and ATG7 are required to encapsulate PV in multiple host membranes. They do not destroy vacuoles or transmit parasite to lysosomes, but they limit nutrient absorption and inhibit parasite growth (Choi et al., 2014; Lee et al., 2015; Selleck et al., 2015). Therefore, IFN-γ mainly relies on ubiquitination and core autophagy to mediate membrane engulfment and cell growth restriction in human cells (**Figure 4**).

HOST CELL SIGNALING IS MANIPULATED BY *TOXOPLASMA GONDII* TO AVOID AUTOPHAGY TARGETING

Autophagy is mainly a process of sustaining life. It could not only coordinate the degradation and circulation of important macromolecules such as lipids and amino acids response to stress but also contribute to catching the intracellular parasites and transporting them for destruction (Bando et al., 2018). Avoiding lysosomal degradation is critical for the survival of *T. gondii*. *Toxoplasma* can interfere with the host autophagy machinery to escape targeting or even promote their intracellular growth by exploiting autophagy components (Wang et al., 2009; Deretic, 2011; Ohshima et al., 2014). Currently, it is still unclear how *Toxoplasma* interferes with autophagy.

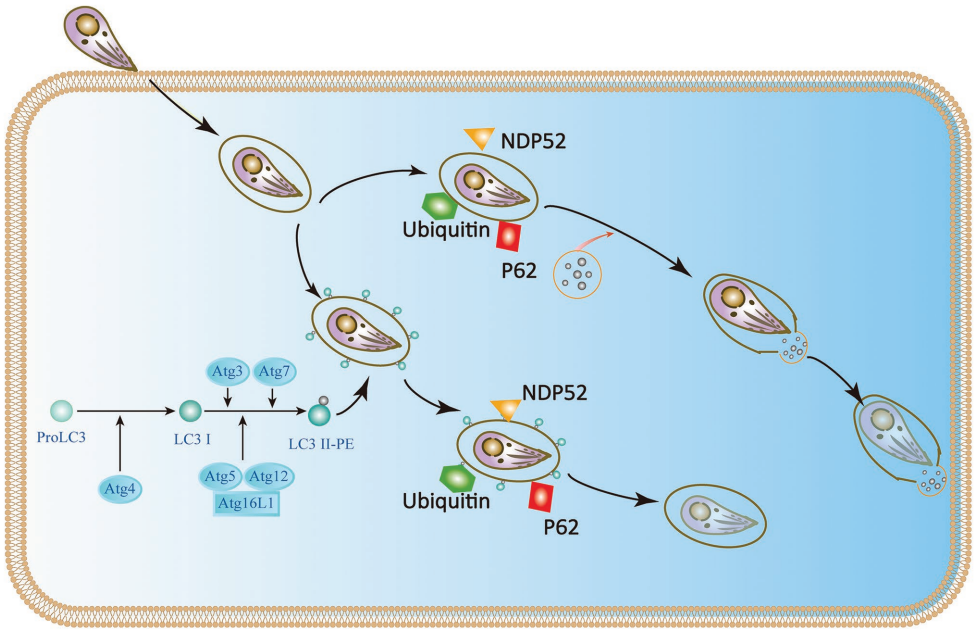

FIGURE 4 | IFN-γ restricts the growth and proliferation of *T. gondii* in human cells. In HeLa cells, the Atg proteins Atg7, Atg3, and the Atg12-Atg5-Atg16L1 complex target ubiquitin to the *Toxoplasma* PVM, which causes the recruitment of p62 and NDP52 and subsequently LC3. The parasite is encapsulated in a double-membrane autophagy structure and cannot grow and replicate further. In human umbilical vein endothelial cells (HUVEC) cells, *T. gondii* encapsulated in parasitophorous vacuole (PV) is recognized by host cell immune effector factors (K63Ub, p62, and NDP52), which leads to lysosomal fusion and subsequent parasite destruction.

Toxoplasma gondii activates host cell signaling cascade of the epidermal growth factor receptor (EGFR) by PI3K to avoid targeting autophagy mechanisms to parasitic vacuoles (Muniz-Feliciano et al., 2013; Coppens, 2017; Portillo et al., 2017). Parasites can induce the phosphorylation of EGFR in host cells by secreting several proteins containing multiple domains homologous to EGFR, such as MIC3 and MIC6. PI3K-mediated Akt phosphorylation can activate the autophagosome negative regulator mTORC1, which leads to reverse regulation of autophagy (Muniz-Feliciano et al., 2013; Coppens, 2017; Lopez Corcino et al., 2019). Thus, the Akt signaling pathway is critical for escaping host autophagy to promote parasite survival (**Figure 5** I). The moving junction is characterized by the expression of RON4. The formation of the moving junction is accompanied by the activation of focal adhesion kinase (FAK) in the mammalian cell during the invasion. The activation of Src depends on FAK, and then causes the transactivation of EGFR. The activation of EGFR recruits STAT3 signaling to block the activation of key stimulators of autophagy, PKR, and eIF2α. They prevent *T. gondii* from becoming a target (Portillo et al., 2017). At the later stage of the intracellular phase of *T. gondii*, EGFR autophosphorylation is maintained through prolonged PKCα/PKCβ-Src signaling, which in turn promote the survival of *Toxoplasma* through Akt (Lopez Corcino et al., 2019; **Figure 5** II).

IFN-γ is a main effector for activating mammalian cell responses to *T. gondii*. Recruitment and loading of effector IRGs on PVM are induced by IFN-γ (Martens et al., 2005; Ling et al., 2006; Khaminets et al., 2010). The deposition of ubiquitin on the PVM is promoted by IRGs and subsequently the accumulation of p62-dependent GBP (Haldar et al., 2015). In mouse macrophages and fibroblasts activated by IFN-γ, LC3 is recruited to PVM and can target IRGs to PVM membrane (Park et al., 2016). Associating with the small GTPase ADP-ribosylation factor 1 (Arf1), Gate-16 mediates IRG recruitment (Sasai et al., 2017). Recruitment of IFN-γ-activated IRGs and GBPs resulted in the vesicle formation and rupture of PVM, resulting in the release of *T. gondii* into the cytoplasm and the death of *T. gondii* in mouse cells (Martens et al., 2005; Zhao et al., 2008, 2009; Choi et al., 2014; Ohshima et al., 2014). Rop18 is a rhoptry protein, also a polymorphic protein kinase. It mainly determines the virulence of parasite in mice (Taylor et al., 2006; Lei et al., 2014). Together with ROP17, ROP18 complexes mediate the protection from the IRG pathway. The phosphorylation ability of ROP18-ROP17 depends on the presence of virulent alleles of pseudokinase ROP5 (Behnke et al., 2011; Reese et al., 2011). GRA7 is a dense granule protein. It is also a part of the complex of ROP18-ROP17-ROP5 (Hermanns et al., 2016). Binding a conserved surface of IRG, ROP5 proteins promote IRG remain in an inactive GDP binding conformation. As a result, GTP-dependent activation of IRG is prevented. Simultaneously, threonines in the nucleotide-binding domain are exposed. Then ROP18 and ROP17 kinases phosphorylate threonines, resulting in permanent inactivation of IRG (Fleckenstein et al., 2012; Reese et al., 2014; **Figure 5** III).

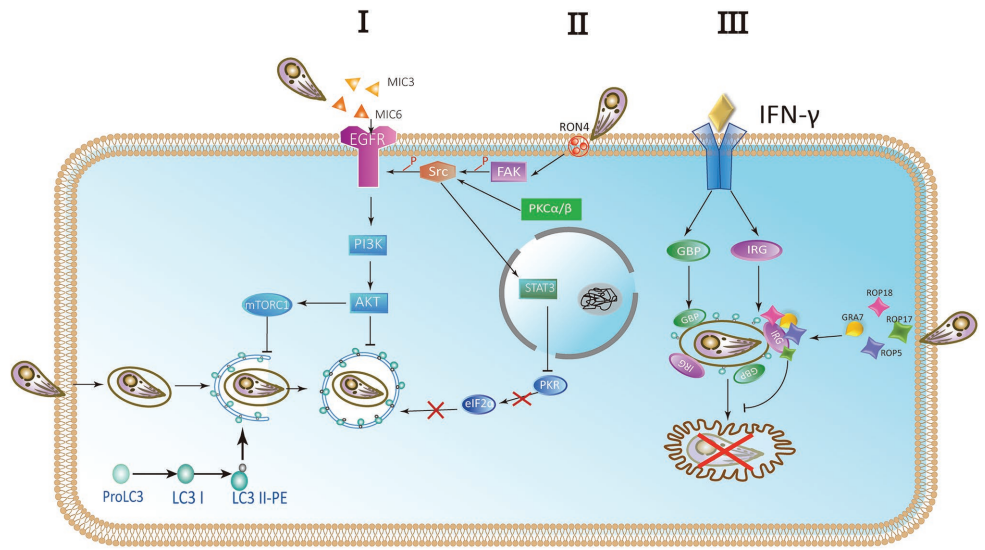

FIGURE 5 | Parasites escape host autophagy destruction. (I) A hypothetical model of *Toxoplasma* controlling host autophagy by the epidermal growth factor receptor (EGFR)-Akt signaling pathway. MIC protein is released from micronemes upon invasion. MIC3 and MIC6 bind to the host EGFR through the EGF-like domain and are activated by phosphorylation. Phosphatidylinositol 3-kinase (PI3K)-induced Akt phosphorylation and Akt-dependent activation of mTORC1 block the autophagy pathway and signify *T. gondii* to survive. (II) During the invasion of host cells, RON4 expression was associated with focal adhesion kinase (FAK) activation. In turn, FAK activates Src leading to the transactivation of EGFR in a Src-dependent way. Furthermore, the STAT3 signaling pathway is facilitated to prevent PKR and eIF2a from activation. Blocking the signaling causes the activation of PKR and eIF2a, resulting in autophagic targeting and the killing of parasite. At later stages of the intracellular stage of *T. gondii*, autophosphorylation of EGFR is maintained through PKCα/PKCβ-Src signaling. (III) The complex of GRA7 and ROP18-ROP17-ROP5 phosphorylates IFN-γ-activated IRGs and GBPs permanently inactivates them to ensure the integrity of PVM and is conducive to the survival of parasite.

CONCLUDING REMARKS

In summary, autophagy is critical in maintaining cellular homeostasis and plays a key role in mechanism against a large number of intracellular pathogens including *T. gondii* as this pathway can degrade intracellular pathogens *via* autophagolysosomes. The interaction between *T. gondii* and host autophagy is a mutual process. However, *T. gondii* has developed complex evolutionary adaptation and evasion mechanisms to avoid host cell phagocytic recognition. Some PVM associated proteins (rhoptries and dense granules) are known to phosphorylate IRGs, inactivating IRGs. In recent years, the mechanism of *T. gondii* recognition and invasion has been extensively investigated. However, the mechanisms by which parasites antagonize these responses in different cell lines are still elusive. For instance, in mouse cells, IRGs contribute to immune control of *T. gondii*, but how it contributes to parasite control in human cells remains enigmatic. Understanding the mechanisms by which these parasites prevent the host's innate immune defenses and escape autophagy may provide the basis to design new therapeutic strategies to treat toxoplasmosis.

AUTHOR CONTRIBUTIONS

JD designed the work. MW and OC wrote the first draft of the manuscript. JS and YC did critical revision of the article. All authors contributed to the article and approved the submitted version.

FUNDING

This work was supported by the National Natural Science Foundation of China (81871674 and 81672046 to JD), the Academic and Technology Leaders reserve candidate Fund of Anhui Province (2016H080 to JD), and the key project of outstanding young talent support program in Anhui province university (gxyqZD2016047 to JD).

ACKNOWLEDGMENTS

The authors would like to thank members of our laboratories for many thoughtful discussions.

REFERENCES

Andrade, R. M., Wessendarp, M., Gubbels, M. J., Striepen, B., and Subauste, C. S. (2006). CD40 induces macrophage anti-*Toxoplasma gondii* activity by triggering autophagy-dependent fusion of pathogen-containing vacuoles and lysosomes. *J. Clin. Invest.* 116, 2366–2377. doi: 10.1172/JCI28796

Bando, H., Sakaguchi, N., Lee, Y., Pradipta, A., Ma, J. S., Tanaka, S., et al. (2018). *Toxoplasma* effector TgIST targets host IDO1 to antagonize the IFN-gamma-induced anti-parasitic response in human cells. *Front. Immunol.* 9:2073. doi: 10.3389/fimmu.2018.02073

Behnke, M. S., Khan, A., Wootton, J. C., Dubey, J. P., Tang, K., and Sibley, L. D. (2011). Virulence differences in *Toxoplasma* mediated by amplification of

a family of polymorphic pseudokinases. *Proc. Natl. Acad. Sci. U. S. A.* 108, 9631–9636. doi: 10.1073/pnas.1015338108

Besteiro, S. (2017). Autophagy in apicomplexan parasites. *Curr. Opin. Microbiol.* 40, 14–20. doi: 10.1016/j.mib.2017.10.008

Besteiro, S. (2019). The role of host autophagy machinery in controlling *Toxoplasma* infection. *Virulence* 10, 438–447. doi: 10.1080/21505594.2018.1518102

Biering, S. B., Choi, J., Halstrom, R. A., Brown, H. M., Beatty, W. L., Lee, S., et al. (2017). Viral replication complexes are targeted by LC3-guided interferon-inducible GTPases. *Cell Host Microbe* 22, 74.e77–85.e77. doi: 10.1016/j.chom.2017.06.005

Chen, Z. W., Gao, J. M., Huo, X. X., Wang, L., Yu, L., Halm-Lai, F., et al. (2011). Genotyping of *Toxoplasma gondii* isolates from cats in different geographic regions of China. *Vet. Parasitol.* 183, 166–170. doi: 10.1016/j.vetpar.2011.06.013

Choi, J., Biering, S. B., and Hwang, S. (2017). Quo vadis? Interferon-inducible GTPases go to their target membranes via the LC3-conjugation system of autophagy. *Small GTPases* 8, 199–207. doi: 10.1080/21541248.2016.1213090

Choi, J., Park, S., Biering, S. B., Selleck, E., Liu, C. Y., Zhang, X., et al. (2014). The parasitophorous vacuole membrane of *Toxoplasma gondii* is targeted for disruption by ubiquitin-like conjugation systems of autophagy. *Immunity* 40, 924–935. doi: 10.1016/j.immuni.2014.05.006

Choi, A. M., Ryter, S. W., and Levine, B. (2013). Autophagy in human health and disease. *N. Engl. J. Med.* 368, 1845–1846. doi: 10.1056/NEJMc1303158

Chu, J. Q., Jing, K. P., Gao, X., Li, P., Huang, R., Niu, Y. R., et al. (2017). *Toxoplasma gondii* induces autophagy and apoptosis in human umbilical cord mesenchymal stem cells via downregulation of Mcl-1. *Cell Cycle* 16, 477–486. doi: 10.1080/15384101.2017.1281484

Clough, B., Wright, J. D., Pereira, P. M., Hirst, E. M., Johnston, A. C., Henriques, R., et al. (2016). K63-linked ubiquitination targets *Toxoplasma gondii* for endo-lysosomal destruction in IFNgamma-stimulated human cells. *PLoS Pathog.* 12:e1006027. doi: 10.1371/journal.ppat.1006027

Coppens, I. (2017). How *Toxoplasma* and malaria parasites defy first, then exploit host autophagic and endocytic pathways for growth. *Curr. Opin. Microbiol.* 40, 32–39. doi: 10.1016/j.mib.2017.10.009

Darde, M. L., Riahi, H., Bouteille, B., and Pestre-Alexandre, M. (1992). Isoenzyme analysis of *Hammondia hammondi* and *Toxoplasma gondii* sporozoites. *J. Parasitol.* 78, 731–734.

Deretic, V. (2011). Autophagy in immunity and cell-autonomous defense against intracellular microbes. *Immunol. Rev.* 240, 92–104. doi: 10.1111/j.1600-065X.2010.00995.x

Feng, C. G., Zheng, L., Jankovic, D., Bafica, A., Cannons, J. L., Watford, W. T., et al. (2008). The immunity-related GTPase Irgm1 promotes the expansion of activated $CD4^+$ T cell populations by preventing interferon-gamma-induced cell death. *Nat. Immunol.* 9, 1279–1287. doi: 10.1038/ni.1653

Fleckenstein, M. C., Reese, M. L., Konen-Waisman, S., Boothroyd, J. C., Howard, J. C., and Steinfeldt, T. (2012). A *Toxoplasma gondii* pseudokinase inhibits host IRG resistance proteins. *PLoS Biol.* 10:e1001358. doi: 10.1371/journal.pbio.1001358

Galluzzi, L., Baehrecke, E. H., Ballabio, A., Boya, P., Bravo-San Pedro, J. M., Cecconi, F., et al. (2017). Molecular definitions of autophagy and related processes. *EMBO J.* 36, 1811–1836. doi: 10.15252/embj.201796697

Haldar, A. K., Foltz, C., Finethy, R., Piro, A. S., Feeley, E. M., Pilla-Moffett, D. M., et al. (2015). Ubiquitin systems mark pathogen-containing vacuoles as targets for host defense by guanylate binding proteins. *Proc. Natl. Acad. Sci. U. S. A.* 112, E5628–E5637. doi: 10.1073/pnas.1515966112

Haldar, A. K., Piro, A. S., Pilla, D. M., Yamamoto, M., and Coers, J. (2014). The E2-like conjugation enzyme Atg3 promotes binding of IRG and Gbp proteins to chlamydia- and *Toxoplasma*-containing vacuoles and host resistance. *PLoS One* 9:e86684. doi: 10.1371/journal.pone.0086684

Halonen, S. K., and Weiss, L. M. (2013). Toxoplasmosis. *Handb. Clin. Neurol.* 114, 125–145. doi: 10.1016/B978-0-444-53490-3.00008-X

Hampton, M. M. (2015). Congenital toxoplasmosis: a review. *Neonatal Netw.* 34, 274–278. doi: 10.1891/0730-0832.34.5.274

Hermanns, T., Muller, U. B., Konen-Waisman, S., Howard, J. C., and Steinfeldt, T. (2016). The *Toxoplasma gondii* rhoptry protein ROP18 is an Irga6-specific kinase and regulated by the dense granule protein GRA7. *Cell. Microbiol.* 18, 244–259. doi: 10.1111/cmi.12499

Howe, D. K., Honore, S., Derouin, F., and Sibley, L. D. (1997). Determination of genotypes of *Toxoplasma gondii* strains isolated from patients with toxoplasmosis. *J. Clin. Microbiol.* 35, 1411–1414. doi: 10.1128/JCM.35.6.1411-1414.1997

Howe, D. K., and Sibley, L. D. (1995). *Toxoplasma gondii* comprises three clonal lineages: correlation of parasite genotype with human disease. *J. Infect. Dis.* 172, 1561–1566. doi: 10.1093/infdis/172.6.1561

Huang, J., and Brumell, J. H. (2014). Bacteria-autophagy interplay: a battle for survival. *Nat. Rev. Microbiol.* 12, 101–114. doi: 10.1038/nrmicro3160

Hwang, S., Maloney, N. S., Bruinsma, M. W., Goel, G., Duan, E., Zhang, L., et al. (2012). Nondegradative role of Atg5-Atg12/Atg16L1 autophagy protein complex in antiviral activity of interferon gamma. *Cell Host Microbe* 11, 397–409. doi: 10.1016/j.chom.2012.03.002

Khaminets, A., Hunn, J. P., Konen-Waisman, S., Zhao, Y. O., Preukschat, D., Coers, J., et al. (2010). Coordinated loading of IRG resistance GTPases on to the *Toxoplasma gondii* parasitophorous vacuole. *Cell. Microbiol.* 12, 939–961. doi: 10.1111/j.1462-5822.2010.01443.x

Kihara, A., Kabeya, Y., Ohsumi, Y., and Yoshimori, T. (2001). Beclin-phosphatidylinositol 3-kinase complex functions at the trans-Golgi network. *EMBO Rep.* 2, 330–335. doi: 10.1093/embo-reports/kve061

Krishnamurthy, S., Konstantinou, E. K., Young, L. H., Gold, D. A., and Saeij, J. P. (2017). The human immune response to *Toxoplasma*: autophagy versus cell death. *PLoS Pathog.* 13:e1006176. doi: 10.1371/journal.ppat.1006176

Lee, J., Choi, J. W., Han, H. Y., Kim, W. S., Song, H. Y., Byun, E. B., et al. (2020). 4-hydroxybenzaldehyde restricts the intracellular growth of *Toxoplasma gondii* by inducing SIRT1-mediated autophagy in macrophages. *Korean J. Parasitol.* 58, 7–14. doi: 10.3347/kjp.2020.58.1.7

Lee, Y., Sasai, M., Ma, J. S., Sakaguchi, N., Ohshima, J., Bando, H., et al. (2015). p62 plays a specific role in interferon-gamma-induced presentation of a *Toxoplasma* vacuolar antigen. *Cell Rep.* 13, 223–233. doi: 10.1016/j.celrep.2015.09.005

Lei, T., Wang, H., Liu, J., Nan, H., and Liu, Q. (2014). ROP18 is a key factor responsible for virulence difference between *Toxoplasma gondii* and *Neospora caninum*. *PLoS One* 9:e99744. doi: 10.1371/journal.pone.0099744

Levine, B., and Kroemer, G. (2008). Autophagy in the pathogenesis of disease. *Cell* 132, 27–42. doi: 10.1016/j.cell.2007.12.018

Li, X., Chen, D., Hua, Q., Wan, Y., Zheng, L., Liu, Y., et al. (2016). Induction of autophagy interferes the tachyzoite to bradyzoite transformation of *Toxoplasma gondii*. *Parasitology* 143, 639–645. doi: 10.1017/S0031182015001985

Li, M., Mo, X. W., Wang, L., Chen, H., Luo, Q. L., Wen, H. Q., et al. (2014). Phylogeny and virulence divergency analyses of *Toxoplasma gondii* isolates from China. *Parasit. Vectors* 7:133. doi: 10.1186/1756-3305-7-133

Ling, Y. M., Shaw, M. H., Ayala, C., Coppens, I., Taylor, G. A., Ferguson, D. J., et al. (2006). Vacuolar and plasma membrane stripping and autophagic elimination of *Toxoplasma gondii* in primed effector macrophages. *J. Exp. Med.* 203, 2063–2071. doi: 10.1084/jem.20061318

Liu, E., Lopez Corcino, Y., Portillo, J. A., Miao, Y., and Subauste, C. S. (2016). Identification of signaling pathways by which CD40 stimulates autophagy and antimicrobial activity against *Toxoplasma gondii* in macrophages. *Infect. Immun.* 84, 2616–2626. doi: 10.1128/IAI.00101-16

Lopez Corcino, Y., Gonzalez Ferrer, S., Mantilla, L. E., Trikeriotis, S., Yu, J. S., Kim, S., et al. (2019). *Toxoplasma gondii* induces prolonged host epidermal growth factor receptor signalling to prevent parasite elimination by autophagy: perspectives for in vivo control of the parasite. *Cell. Microbiol.* 21:e13084. doi: 10.1111/cmi.13084

Lyons, R. E., McLeod, R., and Roberts, C. W. (2002). *Toxoplasma gondii* tachyzoite-bradyzoite interconversion. *Trends Parasitol.* 18, 198–201. doi: 10.1016/s1471-4922(02)02248-1

Ma, J., Becker, C., Lowell, C. A., and Underhill, D. M. (2012). Dectin-1-triggered recruitment of light chain 3 protein to phagosomes facilitates major histocompatibility complex class II presentation of fungal-derived antigens. *J. Biol. Chem.* 287, 34149–34156. doi: 10.1074/jbc.M112.382812

Machacova, T., Ajzenberg, D., Zakovska, A., Sedlak, K., and Bartova, E. (2016). *Toxoplasma gondii* and *Neospora caninum* in wild small mammals:

seroprevalence, DNA detection and genotyping. *Vet. Parasitol.* 223, 88–90. doi: 10.1016/j.vetpar.2016.04.018

Martens, S., Parvanova, I., Zerrahn, J., Griffiths, G., Schell, G., Reichmann, G., et al. (2005). Disruption of *Toxoplasma gondii* parasitophorous vacuoles by the mouse p47-resistance GTPases. *PLoS Pathog.* 1:e24. doi: 10.1371/journal.ppat.0010024

Martinez, J., Malireddi, R. K., Lu, Q., Cunha, L. D., Pelletier, S., Gingras, S., et al. (2015). Molecular characterization of LC3-associated phagocytosis reveals distinct roles for Rubicon, NOX2 and autophagy proteins. *Nat. Cell Biol.* 17, 893–906. doi: 10.1038/ncb3192

Melzer, T., Duffy, A., Weiss, L. M., and Halonen, S. K. (2008). The gamma interferon (IFN-gamma)-inducible GTP-binding protein IGTP is necessary for *Toxoplasma* vacuolar disruption and induces parasite egression in IFN-gamma-stimulated astrocytes. *Infect. Immun.* 76, 4883–4894. doi: 10.1128/IAI.01288-07

Mizushima, N., Yoshimori, T., and Ohsumi, Y. (2011). The role of Atg proteins in autophagosome formation. *Annu. Rev. Cell Dev. Biol.* 27, 107–132. doi: 10.1146/annurev-cellbio-092910-154005

Montoya, J. G., and Liesenfeld, O. (2004). Toxoplasmosis. *Lancet* 363, 1965–1976. doi: 10.1016/s0140-6736(04)16412-x

Montoya, J. G., and Remington, J. S. (1996). Toxoplasmic chorioretinitis in the setting of acute acquired toxoplasmosis. *Clin. Infect. Dis.* 23, 277–282. doi: 10.1093/clinids/23.2.277

Muniz-Feliciano, L., Van Grol, J., Portillo, J. A., Liew, L., Liu, B., Carlin, C. R., et al. (2013). *Toxoplasma gondii*-induced activation of EGFR prevents autophagy protein-mediated killing of the parasite. *PLoS Pathog.* 9:e1003809. doi: 10.1371/journal.ppat.1003809

Nakatogawa, H., Suzuki, K., Kamada, Y., and Ohsumi, Y. (2009). Dynamics and diversity in autophagy mechanisms: lessons from yeast. *Nat. Rev. Mol. Cell Biol.* 10, 458–467. doi: 10.1038/nrm2708

Niedelman, W., Sprokholt, J. K., Clough, B., Frickel, E. M., and Saeij, J. P. (2013). Cell death of gamma interferon-stimulated human fibroblasts upon *Toxoplasma gondii* infection induces early parasite egress and limits parasite replication. *Infect. Immun.* 81, 4341–4349. doi: 10.1128/iai.00416-13

Ohshima, J., Lee, Y., Sasai, M., Saitoh, T., Su Ma, J., Kamiyama, N., et al. (2014). Role of mouse and human autophagy proteins in IFN-gamma-induced cell-autonomous responses against *Toxoplasma gondii*. *J. Immunol.* 192, 3328–3335. doi: 10.4049/jimmunol.1302822

Ohsumi, Y. (2001). Molecular dissection of autophagy: two ubiquitin-like systems. *Nat. Rev. Mol. Cell Biol.* 2, 211–216. doi: 10.1038/35056522

Orlofsky, A. (2009). *Toxoplasma*-induced autophagy: a window into nutritional futile cycles in mammalian cells? *Autophagy* 5, 404–406. doi: 10.4161/auto.5.3.7807

Park, S., Choi, J., Biering, S. B., Dominici, E., Williams, L. E., and Hwang, S. (2016). Targeting by autophaGy proteins (TAG): targeting of IFNG-inducible GTPases to membranes by the LC3 conjugation system of autophagy. *Autophagy* 12, 1153–1167. doi: 10.1080/15548627.2016.1178447

Parlog, A., Harsan, L. A., Zagrebelsky, M., Weller, M., von Elverfeldt, D., Mawrin, C., et al. (2014). Chronic murine toxoplasmosis is defined by subtle changes in neuronal connectivity. *Dis. Model. Mech.* 7, 459–469. doi: 10.1242/dmm.014183

Parzych, K. R., and Klionsky, D. J. (2014). An overview of autophagy: morphology, mechanism, and regulation. *Antioxid. Redox Signal.* 20, 460–473. doi: 10.1089/ars.2013.5371

Paulus, G. L., and Xavier, R. J. (2015). Autophagy and checkpoints for intracellular pathogen defense. *Curr. Opin. Gastroenterol.* 31, 14–23. doi: 10.1097/MOG.0000000000000134

Portillo, J. C., Muniz-Feliciano, L., Lopez Corcino, Y., Lee, S. J., Van Grol, J., Parsons, S. J., et al. (2017). *Toxoplasma gondii* induces FAK-Src-STAT3 signaling during infection of host cells that prevents parasite targeting by autophagy. *PLoS Pathog.* 13:e1006671. doi: 10.1371/journal.ppat.1006671

Portillo, J. A., Okenka, G., Reed, E., Subauste, A., Van Grol, J., Gentil, K., et al. (2010). The CD40-autophagy pathway is needed for host protection despite IFN-gamma-dependent immunity and CD40 induces autophagy via control of P21 levels. *PLoS One* 5:e14472. doi: 10.1371/journal.pone.0014472

Reese, M. L., Shah, N., and Boothroyd, J. C. (2014). The *Toxoplasma* pseudokinase ROP5 is an allosteric inhibitor of the immunity-related GTPases. *J. Biol. Chem.* 289, 27849–27858. doi: 10.1074/jbc.M114.567057

Reese, M. L., Zeiner, G. M., Saeij, J. P., Boothroyd, J. C., and Boyle, J. P. (2011). Polymorphic family of injected pseudokinases is paramount in *Toxoplasma* virulence. *Proc. Natl. Acad. Sci. U. S. A.* 108, 9625–9630. doi: 10.1073/pnas.1015980108

Russell, R. C., Tian, Y., Yuan, H., Park, H. W., Chang, Y. Y., Kim, J., et al. (2013). ULK1 induces autophagy by phosphorylating Beclin-1 and activating VPS34 lipid kinase. *Nat. Cell Biol.* 15, 741–750. doi: 10.1038/ncb2757

Saeij, J. P., and Frickel, E. M. (2017). Exposing *Toxoplasma gondii* hiding inside the vacuole: a role for GBPs, autophagy and host cell death. *Curr. Opin. Microbiol.* 40, 72–80. doi: 10.1016/j.mib.2017.10.021

Sasai, M., Sakaguchi, N., Ma, J. S., Nakamura, S., Kawabata, T., Bando, H., et al. (2017). Essential role for GABARAP autophagy proteins in interferon-inducible GTPase-mediated host defense. *Nat. Immunol.* 18, 899–910. doi: 10.1038/ni.3767

Selleck, E. M., Orchard, R. C., Lassen, K. G., Beatty, W. L., Xavier, R. J., Levine, B., et al. (2015). A noncanonical autophagy pathway restricts *Toxoplasma gondii* growth in a strain-specific manner in IFN-gamma-activated human cells. *MBio* 6, e01157–e01115. doi: 10.1128/mBio.01157-15

Steele, S., Brunton, J., and Kawula, T. (2015). The role of autophagy in intracellular pathogen nutrient acquisition. *Front. Cell. Infect. Microbiol.* 5:51. doi: 10.3389/fcimb.2015.00051

Subauste, C. S. (2009). CD40, autophagy and *Toxoplasma gondii*. *Mem. Inst. Oswaldo Cruz* 104, 267–272. doi: 10.1590/s0074-02762009000200020

Subauste, C. S. (2019). Interplay between *Toxoplasma gondii*, autophagy, and autophagy proteins. *Front. Cell. Infect. Microbiol.* 9:139. doi: 10.3389/fcimb.2019.00139

Subauste, C. S., Andrade, R. M., and Wessendarp, M. (2007a). CD40-TRAF6 and autophagy-dependent anti-microbial activity in macrophages. *Autophagy* 3, 245–248. doi: 10.4161/auto.3717

Subauste, C. S., Subauste, A., and Wessendarp, M. (2007b). Role of CD40-dependent down-regulation of CD154 in impaired induction of CD154 in $CD4^+$ T cells from HIV-1-infected patients. *J. Immunol.* 178, 1645–1653. doi: 10.4049/jimmunol.178.3.1645

Taylor, S., Barragan, A., Su, C., Fux, B., Fentress, S. J., Tang, K., et al. (2006). A secreted serine-threonine kinase determines virulence in the eukaryotic pathogen *Toxoplasma gondii*. *Science* 314, 1776–1780. doi: 10.1126/science.1133643

Ueyama, T., Nakakita, J., Nakamura, T., Kobayashi, T., Kobayashi, T., Son, J., et al. (2011). Cooperation of $p40^{phox}$ with $p47^{phox}$ for Nox2-based NADPH oxidase activation during Fcγ receptor (FcγR)-mediated phagocytosis mechanism for acquisition of $p40^{phox}$ phosphatidylinositol 3-phosphate (PI (3) P) binding. *J. Biol. Chem.* 286, 40693–40705. doi: 10.1074/jbc.M111.237289

Van Grol, J., Muniz-Feliciano, L., Portillo, J. A., Bonilha, V. L., and Subauste, C. S. (2013). CD40 induces anti-*Toxoplasma gondii* activity in nonhematopoietic cells dependent on autophagy proteins. *Infect. Immun.* 81, 2002–2011. doi: 10.1128/IAI.01145-12

Wacker, R., Eickel, N., Schmuckli-Maurer, J., Annoura, T., Niklaus, L., Khan, S. M., et al. (2017). LC3-association with the parasitophorous vacuole membrane of *Plasmodium berghei* liver stages follows a noncanonical autophagy pathway. *Cell. Microbiol.* 19:e12754. doi: 10.1111/cmi.12754

Wang, L., Chen, H., Liu, D., Huo, X., Gao, J., Song, X., et al. (2013). Genotypes and mouse virulence of *Toxoplasma gondii* isolates from animals and humans in China. *PLoS One* 8:e53483. doi: 10.1371/journal.pone.0053483

Wang, Y., Weiss, L. M., and Orlofsky, A. (2009). Host cell autophagy is induced by *Toxoplasma gondii* and contributes to parasite growth. *J. Biol. Chem.* 284, 1694–1701. doi: 10.1074/jbc.M807890200

Whitmarsh, R. J., and Hunter, C. A. (2008). Digest this! A role for autophagy in controlling pathogens. *Cell Host Microbe* 4, 413–414. doi: 10.1016/j.chom.2008.10.008

Yu, Y., Zhao, N., An, J., and Zhang, X. (2017). CCAAT/enhancer-binding protein beta mediates the killing of *Toxoplasma gondii* by inducing autophagy in nonhematopoietic cells. *DNA Cell Biol.* 36, 212–218. doi: 10.1089/dna.2016.3434

Zhao, Y., Ferguson, D. J., Wilson, D. C., Howard, J. C., Sibley, L. D., and Yap, G. S. (2009). Virulent *Toxoplasma gondii* evade immunity-related GTPase-mediated parasite vacuole disruption within primed macrophages. *J. Immunol.* 182, 3775–3781. doi: 10.4049/jimmunol.0804190

Zhao, Z., Fux, B., Goodwin, M., Dunay, I. R., Strong, D., Miller, B. C., et al. (2008). Autophagosome-independent essential function for the autophagy protein Atg5 in cellular immunity to intracellular pathogens. *Cell Host Microbe* 4, 458–469. doi: 10.1016/j.chom.2008.10.003

Zhao, Y., Wilson, D., Matthews, S., and Yap, G. S. (2007). Rapid elimination of *Toxoplasma gondii* by gamma interferon-primed mouse macrophages is independent of CD40 signaling. *Infect. Immun.* 75, 4799–4803. doi: 10.1128/IAI.00738-07

Zhou, P., Nie, H., Zhang, L. X., Wang, H. Y., Yin, C. C., Su, C., et al. (2010). Genetic characterization of *Toxoplasma gondii* isolates from pigs in China. *J. Parasitol.* 96, 1027–1029. doi: 10.1645/GE-2465.1

Conflict of Interest: The authors declare that the research was conducted in the absence of any commercial or financial relationships that could be construed as a potential conflict of interest.

frontiers in Microbiology

ORIGINAL RESEARCH
published: 13 November 2020
doi: 10.3389/fmicb.2020.611190

Interaction Analysis of a *Plasmodium falciparum* PHISTa-like Protein and PfEMP1 Proteins

*Baoling Yang[1,2,3†], Xiaofeng Wang[4†], Ning Jiang[1,3], Xiaoyu Sang[1,3], Ying Feng[1,3], Ran Chen[1,3], Xinyi Wang[1,5] and Qijun Chen[1,3]**

[1]Key Laboratory of Livestock Infectious Diseases in Northeast China, Ministry of Education, Key Laboratory of Zoonosis, Shenyang Agricultural University, Shenyang, China, [2]College of Food Science and Technology, Shenyang Agricultural University, Shenyang, China, [3]The Research Unit for Pathogenic Mechanisms of Zoonotic Parasites, Chinese Academy of Medical Sciences, Shenyang, China, [4]CAS Key Laboratory for Biomedical Effects of Nanomaterials and Nanosafety, Institute of High Energy Physics, Chinese Academy of Sciences (CAS), University of Chinese Academy of Sciences, Beijing, China, [5]College of Basic Sciences, Shenyang Agricultural University, Shenyang, China

Plasmodium falciparum extensively remodels host cells by translocating numerous proteins into the cytoplasm of red blood cells (RBCs) after invasion. Among these exported proteins, members of the *Plasmodium* helical interspersed subtelomeric (PHIST) family are crucial for host cell remodeling and host-parasite interactions, and thereby contribute to malaria pathogenesis. Herein, we explored the function of PF3D7_1372300, a member of the PHIST/PHISTa-like subfamily. PF3D7_1372300 was highly transcribed and expressed during the blood stage of *P. falciparum*, and distributed throughout RBCs, but most abundant at the erythrocyte membrane. Specific interaction of PF3D7_1372300 with the cytoplasmic tail of *P. falciparum* erythrocyte membrane protein 1 (PfEMP1) was revealed by immunofluorescence assay, *in vitro* intermolecular interaction assays. The interaction sites of PF3D7_1372300 with PfEMP1 ATS domain were found involved more than 30 amino acids (aa) at several positions. The findings deepen our understanding of host-parasite interactions and malaria pathogenesis.

Keywords: *Plasmodium falciparum*, PHIST, PfEMP1, proteins interactions, molecular dynamic simulation, malaria

OPEN ACCESS

Edited by:
Jian Du,
Anhui Medical University, China

Reviewed by:
Wenyue Xu,
Army Medical University, China
Qingfeng Zhang,
Tongji University, China
Jun Cao,
Jiangsu Institute of Parasitic Diseases (JIPD), China

****Correspondence:***
Qijun Chen
qijunchen759@syau.edu.cn

†These authors have contributed equally to this work

Specialty section:
This article was submitted to Infectious Diseases, a section of the journal Frontiers in Microbiology

Received: *28 September 2020*
Accepted: *26 October 2020*
Published: *13 November 2020*

Citation:
Yang B, Wang X, Jiang N, Sang X, Feng Y, Chen R, Wang X and Chen Q (2020) Interaction Analysis of a Plasmodium falciparum PHISTa-like Protein and PfEMP1 Proteins. Front. Microbiol. 11:611190. doi: 10.3389/fmicb.2020.611190

INTRODUCTION

Malaria is a globally distributed disease that poses a serious threat to public health (Chiodini, 2018). The World Health Organization (WHO) estimated that in 2018, there were 228 million cases of malaria, resulting in 405,000 deaths (WHO, 2019). Among the malaria parasites that infect humans, *Plasmodium falciparum* is the most virulent species (Milner, 2018). *P. falciparum* has a complex life cycle that involves human hosts and female *Anopheles* spp. mosquitoes as vectors (Bryan et al., 2017). Proliferation and differentiation of *P. falciparum* inside erythrocytes take place within ~48 h of infection (Gruring et al., 2011). During intraerythrocytic development, *P. falciparum* exports a large number of proteins into erythrocytes, some of which form a complex network with host proteins, while others are transferred onto the infected red blood cell (iRBC) surface (Maier et al., 2008; Prajapati and Singh, 2013; Oberli et al., 2014; Warncke et al., 2016). At this stage, *P. falciparum* remodels human erythrocytes, which results in structural and physiological alterations and increased rigidity of the erythrocyte membrane. These changes not only help the parasite to evade host immune

clearance and support intracellular ion homeostasis and nutrient intake but also cause severe pathogenesis (Mok et al., 2007).

Among the exported proteins, members of the *Plasmodium* helical interspersed subtelomeric (PHIST) protein family are crucial for host cell remodeling (Nilsson et al., 2018). The PHIST gene family was originally targeted using a novel algorithm, ExportPred, which proved superior to other algorithms for the prediction of exported proteins in *Plasmodium* parasites (Sargeant et al., 2006). Genes encoding PHIST proteins are mostly located in subtelomeric regions of most of the chromosomes, and the encoded proteins are distributed in various subcellular locations, including submembrane regions (Warncke et al., 2016). Previous studies identified several PHIST proteins in host-parasite protein interaction complexes (Wahlgren et al., 2017). This family includes 72 protein variants, most of which still have no functional annotations. Based on the number and position of tryptophan residues, *P. falciparum* PHIST protein family members cluster into PHISTa, PHISTb, PHISTc, PHISTb-DnaJ, and PHIST/PHISTa-like subgroups (Sargeant et al., 2006; Claessens et al., 2012). The PHISTa subgroup is unique to *P. falciparum*, while homologous PHISTb and PHISTc sequences are present in other *Plasmodium* lineages, including PHISTb type variants in *Plasmodium vivax* and a single copy of the highly variable PHISTc type variant in rodent malarial parasites (Sargeant et al., 2006). Members share similar structural features, including a classical N-terminal signal sequence followed by PEXEL or VTS motifs, *Plasmodium*-specific signal motifs present in exported proteins (Hiller et al., 2004; Marti et al., 2004). In coordination with the translocon machinery, PHIST proteins are positioned at the appropriate locations (de Koning-Ward et al., 2009). The most characteristic feature of PHIST proteins is the carboxyl terminus PHIST domain, which has a conserved helical structure that mediates most of the interactions with other partner proteins (Warncke et al., 2016). Currently, two PHIST variants, PFE1605w (PHISTb type) and PFI1780w (PHISTc type), have been reported to act as anchors *via* specific interactions with the acidic C-terminal segment (ATS) of *P. falciparum* erythrocyte membrane protein 1 (PfEMP1; Mayer et al., 2012; Oberli et al., 2014). Members of this protein family mediate cytoadherence and severe malaria pathogenesis. PfEMP1 proteins are encoded by the *var* gene, and there are ~60 genes in each *P. falciparum* family (Gardner et al., 2002). Each PfEMP1 molecule is composed of a variable duffy binding-like domain (DBL), a cysteine-rich domain region (CIDR), a transmembrane domain, and a C-terminal ATS (Flick and Chen, 2004; Singh et al., 2006). PfEMP1 proteins are associated with severe malaria pathogenesis because they mediate adhesion between iRBCs and host cells. PfEMP1s are synthesized inside the parasite and are transported to the iRBC surface, but the mechanism of intracellular transportation is not clear (Mayer et al., 2012). However, cytoadhesion of PfEMP1 is directly affected by a protein, which is from the PHISTb subfamily, and deletion of PFE1605w severely diminishes iRBC adhesion to the CD36 receptor, although expression of PfEMP1 is not affected (Oberli et al., 2016). This indicates that PFE1605w type PHIST is critical for the structure stability of PfEMP1 on iRBCs. However, the structure and function of PHIST/PHISTa-like subgroups remain poorly understood.

In this study, we systematically characterized a PHIST/PHISTa-like protein (PF3D7_1372300), which was expressed throughout the erythrocytic stage in iRBCs. The protein has a typical four-helix bundle structure, it interacts with PfEMP1 (PF3D7_0800200), and interaction sites were predicted using molecular dynamics (MD) simulation. The findings greatly expand our knowledge of this important protein family in the context of host-parasite interactions.

Abbreviations: ATS, Acidic C-terminal segment; EVs, Extracellular vesicles; IFA, Immunofluorescence assay; iRBCs, Infected red blood cells; MCs, Maurer's clefts; PfEMP1, *Plasmodium falciparum* erythrocyte membrane protein 1; PHIST, *Plasmodium* helical interspersed subtelomeric; PME, Particle-Mesh-Ewald; qPCR, Quantitative real-time PCR; RMSD, Root mean square deviation.

MATERIALS AND METHODS

Ethical Statement

All procedures performed on animals (rats and rabbits) were conducted according to the animal husbandry guidelines of Shenyang Agricultural University. Protocols for experiments were reviewed and approved by the Experimental Animal Committee and the Ethical Committee of Shenyang Agricultural University, Shenyang, China.

Parasite Culture

The *P. falciparum* 3D7 strain was cultured in human O^+ erythrocytes with 5% serum and 0.25% Albumax II, according to the standard methods reported previously (Florens et al., 2004; Hiller et al., 2004). Briefly, parasites were synchronized by three rounds of treatment at 4 h post-invasion with 5% sorbitol and harvested at 8, 16, 24, 32, 40, and 48 h post-infection.

Expression of Recombinant Proteins and Generation of Specific Antibodies

DNA encoding PF3D7_1372300 (residues 27-206) and PF3D7_0800200 (residues 2,466-2,858) were PCR-amplified from *P. falciparum* cDNA using pairwise primers listed in **Supplementary Table S1**. The PF3D7_1372300 and PF3D7_0800200 PCR products were cloned into the pET-28a vector, while the PF3D7_1372300 PCR product was cloned into the pGEX-4T-1 vector. Constructs were expressed in *Escherichia coli* BL21 (DE3) cells as His-tagged and GST-tagged recombinant proteins and were purified according to the manufacturer's instructions (Ramaprasad et al., 2012). SDS-PAGE and Western blotting were used to evaluate the purified recombinant proteins. Two female New Zealand white rabbits and four female Sprague Dawley rats were immunized with His-tagged recombinant proteins emulsified with Freund's adjuvant. Immunizations were performed four times every 2 weeks, and antisera were collected 10 days after the final immunization. IgGs were purified from the immune sera using Protein G Sepharose 4 Fast Flow Resin (GE Healthcare) and Protein A Sepharose 4 Fast Flow resin (GE Healthcare), respectively. The total proteins of iRBCs

and RBCs were used to detect the specificity of the antibodies by Western blotting.

RT-qPCR Transcriptional Analysis of the PF3D7_1372300 Gene

Total RNA from highly synchronized parasites at six post-infection time points was extracted using TRIzol reagent (Invitrogen, United States) according to the manufacturer's instructions. DNase I (TaKaRa, China) was used to remove genomic DNA from RNA samples, and next, oligo (dT) primer and reverse transcriptase were immediately employed. RT-qPCR was carried out using cDNA templates and specific primers (**Supplementary Table S2**) on a QuantStudio 6 Flex Real-Time PCR System (Applied Biosystems, United States) with SYBR Premix Ex Taq (TaKaRa). The seryl-tRNA synthetase gene (PF3D7_1205100; LaCount et al., 2005) served as an internal control for normalization because it is stably expressed during the blood stage of the parasite. Data are expressed as means ± SD of at least three independent experiments.

Expression and Localization Analysis of the Native Protein in Parasites by Western Blotting and Indirect Immunofluorescence Assay

Infected red blood cells at six time-points post-infection were collected and dissolved in SDS-PAGE loading buffer after ultrasonic disruption, and the proteins were separated by 10% SDS-PAGE and were stained by Coomassie Brilliant Blue. Meanwhile, proteins were transferred to a 0.2 μM polyvinylidene fluoride membrane (Bio-Rad, United States). Membranes were blocked with 5% skim milk (BD, United States) for 2 h at 37°C followed by incubation with rabbit anti-PF3D7_1372300 IgG (1:1,000 dilution) for 12 h at 4°C. Rabbit anti-Hsp70 IgG (1:1,000 dilution) was used for normalization. Membranes were further incubated with horseradish peroxidise (HRP)-conjugated goat anti-rabbit IgG (H + L; 1:10,000 dilution; Zsbio, China) for 1 h at 37°C and were visualized with ECL Western blotting (Solarbio, China) using an Azure Biosystems C300 Image Analyzer (Azure, United States).

Thin blood smears of iRBCs at different stages were fixed with cold methanol in −80°C for 15 min and were blocked in 5% skim milk (BD) for 1 h at 37°C. Smears were then incubated with rabbit anti-PF3D7_1372300 antibody (1:100 dilution) at 4°C for 12 h, followed by incubation with Alexa Fluor 488-conjugated goat anti-rabbit IgG at a 1:600 dilution (Invitrogen) at 37°C for 1 h. Parasite nuclei were stained with ProLong Gold Antifade Mountant and DAPI (Invitrogen) at room temperature for 5 min in the dark. High-resolution images were captured with a confocal laser scanning microscope (Leica, SP8, Germany).

Kinetic Analysis of the Interaction Between PF3D7_1372300 and PfEMP1 ATS

An Octet K2 instrument was used to probe the kinetics of PF3D7_1372300-GST and PF3D7_0800200-His. GST and ATS were served as a negative control. ATS-His was loaded onto Ni-NTA biosensors, and PF3D7_1372300-GST at different concentrations were prepared in phosphate-buffered saline (PBS) containing 0.02% Tween-20.

Kinetic studies were performed to determine the binding affinities of PF3D7_1372300-GST and GST (diluted from 1,000 to 62.5 nM) with ATS-His. Association and dissociation were measured for 5 min, and kinetic parameters and affinities were calculated from a non-linear global fit of the data using Octet Data Analysis software version 7.0 (ForteBio, United States).

Dot Blot Assays

Purified ATS bait protein was immobilized on an nitrocellulose (NC) membrane, total protein from iRBCs containing the PF3D7_1372300 target protein (prey) and total protein from RBCs (negative control) were added and incubated for 1 h, respectively. The NC membrane was blocked with 3% BSA in PBS for 1 h, followed by incubation with rat anti-PF3D7_1372300 IgG primary antibodies, and then with HRP-conjugated anti-rat secondary antibodies for 1 h. Meanwhile, purified PF3D7_1372300 bait protein was immobilized on an NC membrane, and total protein from iRBCs containing the ATS target protein (prey) and total protein from RBCs (negative control) were added. The incubation and blocking conditions are as shown above, followed by incubation with rat anti-ATS IgG primary antibodies, and then with HRP-conjugated anti-rat secondary antibodies for 1 h. Dot intensities were measured using ImageJ software for the analysis of binding by plotting on a graph.

Co-localization of PF3D7_1372300 and ATS

The rabbit IgG of PF3D7_1372300 (1:500) and the rat IgG of ATS (1:1,000) were used to detect the co-localization of the two proteins by indirect immunofluorescence. Anti-ATS rat IgG is stored in our laboratory. The specific method was as mentioned above.

Molecular Dynamics Simulation

The 3D structure of PF3D7_1372300 was predicted by Itasser and Modeller softwares. The structure of PfEMP1 was generated by homology modeling. The structure of the protein complex was obtained *via* docking, and the five most promising poses were selected. Finally, MD simulations were carried out for each complex structure.

Verification of Interaction Sites Between PF3D7_1372300 and the ATS Region of PfEMP1 (PF3D7_0800200)

Recombinant proteins PF3D7_1372300-(27-129)-GST and PF3D7_1372300-(130-206)-GST were purified according to the methods described above. SDS-PAGE and Western blotting were used to evaluate the purified recombinant proteins, and kinetic studies were performed to determine the binding affinities between ATS-His and the two GST-tagged recombinant proteins.

RESULTS

Sequence Characteristics of the PF3D7_1372300 Protein

The amino acid sequence of the PF3D7_1372300 protein includes a PHIST domain in the C-terminal region and a 25 amino acid signal peptide domain at the N-terminus, indicating that the protein is secreted from parasites (**Figure 1A**). Sequence alignment with homologs from other species revealed ~93% sequence identity with different *P. falciparum* strains and *Plasmodium* spp. that infects gorillas or chimpanzees, including *Plasmodium adleri*, *Plasmodium billcollinsi*, *Plasmodium blacklocki*, *Plasmodium gaboni*, *Plasmodium praefalciparum*, and *Plasmodium reichenowi* (**Figure 1B**).

Purification of Recombinant Proteins and Detection of Antibodies Specificity

Recombinant proteins of both PF3D7_1372300 and the ATS of PfEMP1 (PF3D7_0800200) were generated (**Figures 2A–C**). Rabbit anti-PF3D7_1372300 IgG and rat anti-ATS IgG specifically detected the native PF3D7_1372300 protein and all PfEMP1 variants from the total proteins of iRBCs, respectively, and both the two antibodies could not detect proteins from the RBCs (negative control; **Figure 2D**).

The PF3D7_1372300 Gene Is Transcribed and Expressed Throughout the Blood Stage of *P. falciparum*

To investigate transcription and expression of the PF3D7_1372300 gene in the *P. falciparum* 3D7 strain during the blood stage, highly synchronized parasites at six time points (8, 16, 24, 32, 40, and 48 h post-invasion) were collected for gene transcription analysis by quantitative real-time PCR (qPCR). The results showed that the PF3D7_1372300 gene was transcribed throughout the blood stage, reached a peak at ~48 h post-invasion, moreover, and transcription remained high during the ring stage (**Figure 3A**).

Expression of the PF3D7_1372300 protein was also confirmed by both immunofluorescence assay (IFA) and Western blotting. The IFA results revealed dotted fluorescence on the membrane of iRBCs but also in the cytoplasm, during the early stage of infection. As parasites developed, expression of the protein became more extensive. The fluorescence was distributed

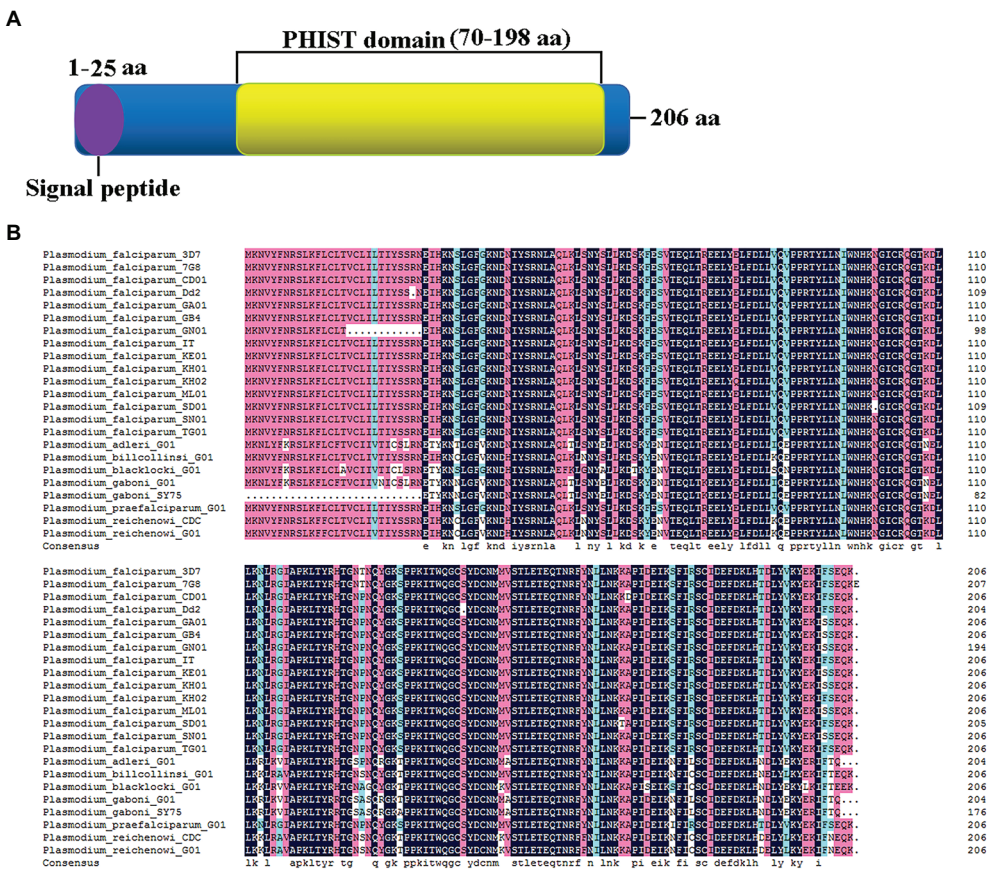

FIGURE 1 | Sequence characteristics of PF3D7_1372300. **(A)** Schematic structure showing the signal peptide (purple) at the N-terminus and a large *Plasmodium* helical interspersed subtelomeric (PHIST) domain (yellow) from the middle to the C-terminus. **(B)** Alignment of PF3D7_1372300 and homologs from different *Plasmodium falciparum* strains and *Plasmodium* spp. that infects gorillas or chimpanzees.

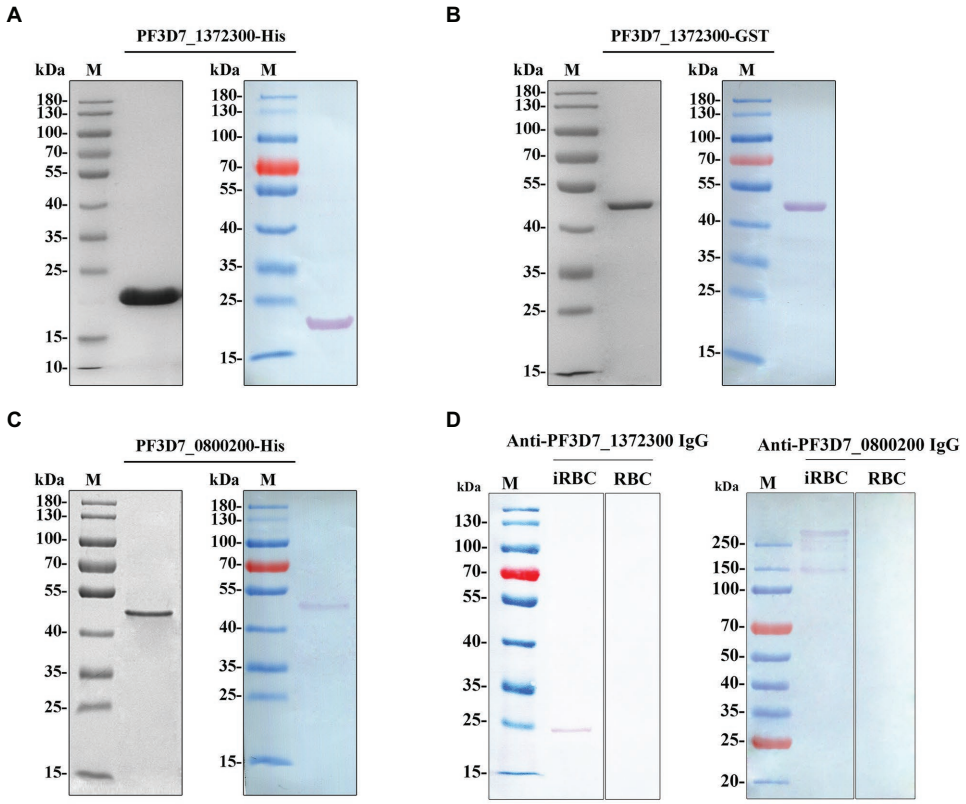

FIGURE 2 | (A–C) Purified PF3D7_1372300 (27-206 aa)-His, PF3D7_1372300 (27-206 aa)-GST, and PF3D7_0800200 [acidic C-terminal segment (ATS) domain, 2,466–2,858 aa]-His proteins analyzed by 10% SDS-PAGE (left) and Western blotting (right). A single protein band was observed with a molecular mass of 21, 46, and 47 kDa. **(D)** Western blotting analysis of the antibody specificity of PF3D7_1372300 and PF3D7_0800200 with total protein of infected red blood cells (iRBCs) and red blood cells (RBCs), respectively.

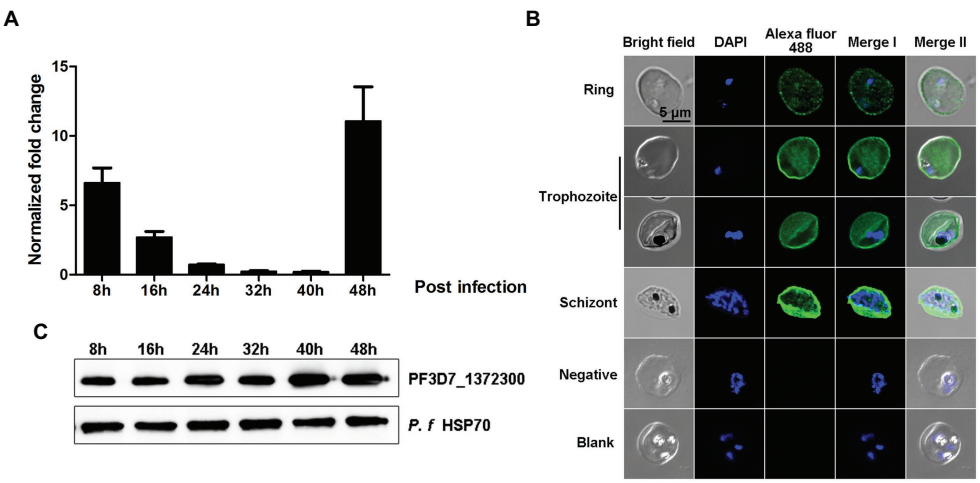

FIGURE 3 | Gene transcription and spatial distribution of the PF3D7_1372300 protein. **(A)** Quantitative real-time PCR was used to measure PF3D7_1372300 gene transcription by the $2^{-\Delta Ct}$ method, and the seryl-tRNA synthetase gene (PF3D7_1205100) served as an internal control for normalization. Results are mean ± SD of three independent experiments. **(B)** Indirect immunofluorescence of PF3D7_1372300. Rabbit anti-PF3D7_1372300 antibody served as the primary antibody, IgG from healthy rabbits was used as a negative control, and buffer without antibody served as a blank control. Parasite nuclei were stained with DAPI. **(C)** Western blotting analysis of the expression of native PF3D7_1372300 during the whole blood stage. Hsp70 protein was used as an internal reference to ensure consistent loading, and rabbit anti-PF3D7_1372300 IgG served as the primary antibody. Scale bar = 5 μm.

throughout the iRBCs, and the fluorescence which was located close to the iRBCs membrane was stronger than that in the cytoplasm of the iRBCs (**Figure 3B**). The results of Western blotting were consistent with the RT-PCR and IFA data (**Figure 3C**).

The co-localization results showed that the two proteins have fluorescence overlap at the erythrocyte membrane during the trophozoite and schizont stages (**Figure 4**).

Binding Between PF3D7_1372300 and the PfEMP1 ATS

Kinetic studies were performed to determine the binding affinities between PF3D7_1372300 and ATS. PF3D7_1372300 fused to glutathione-S-transferase (PF3D7_1372300-GST) and GST alone was diluted from 1,000 to 62.5 nM to capture ATS loaded onto the sensors (**Figures 5A,B**). The Octet K2 system monitored the binding reaction between pairs of proteins in real time, and the binding rates (kon) and dissociation rates (kdis) are listed in **Supplementary Table S3**. To understand the binding affinity value, the equilibrium dissociation constant (KD) was calculated as Kdis/Kon. A KD value between 1.0E-03 and 1.0E-12 M indicates interaction between two molecules. From the results (**Supplementary Table S3**), the KD value for binding of PF3D7_1372300-GST to ATS was 1.19E-07, and the KD value for GST binding to ATS (negative control) was <1.0E-12. This indicates a strong affinity between PF3D7_1372300 and ATS.

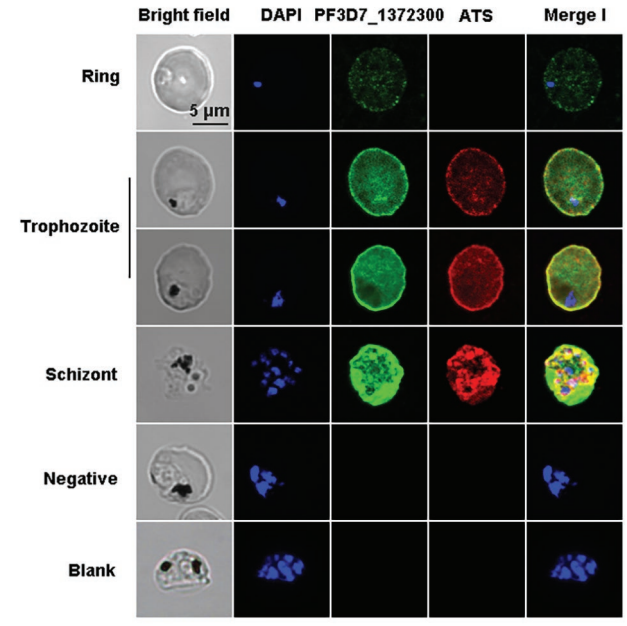

FIGURE 4 | Co-localization of PF3D7_1372300 and ATS using indirect immunofluorescence. Smears of methanol-fixed *Pf*3D7-infected erythrocytes were incubated with anti-PF3D7_1372300 rabbit IgG (1:500) and anti-ATS rat IgG (1:1,000), followed by incubation with Alexa Fluor-conjugated secondary antibody (Alexa Fluor 488, rabbit; Alexa Fluor 594, rat). IgG from healthy rabbits and rats were used as negative controls, and buffer without antibody served as a blank control. Parasite nuclei were stained with DAPI.

Binding of the two proteins was further investigated using dot blot assays. From the results, we can conclude that PF3D7_1372300 in the total protein sample from iRBCs successfully captured PfEMP1 ATS on the blot membrane, while negative control failed to capture PfEMP1 ATS (**Figure 5C**). At the same time, the PfEMP1 ATS in the total protein sample from iRBCs successfully captured PF3D7_1372300 on the blot membrane, while negative control failed to capture PF3D7_1372300 (**Figure 5D**).

Molecular Dynamics Simulation

The sequence from residues 27 to 206 of PF3D7_1372300 was used to predict the 3D structure of PF3D7_1372300, and three structures were obtained by Itasser and Modeller softwares (**Supplementary Figures S1A–C**; Webb and Sali, 2016). PfEMP1 is a large transmembrane protein of 2,858 amino acids (aa) residues, but we only considered the ATS region on the inner part of the membrane. The PfEMP1 sequence from residues 2,486 to 2,759 was used to build the 3D structure using Modeller. Two templates (5MI0 and 2LKL) were identified with sequence identity of 18% and 69%, respectively. The final model of the ATS structure was obtained by further refinement using energy minimization (**Supplementary Figure S1D**). The two proteins were then docked together using the Zdock server (Pierce et al., 2014), and version 3.0.2 was selected, without predefining the interacting and blocking residues. Among the top 100 complex structures, the top nine were initially screened, and representative structures of the five most abundant clusters (Positions 1–5) were selected as the initial structure for MD simulations (**Figure 6**).

All MD simulations were performed using the NAMD 2.10 software package (Phillips et al., 2005) and the CHARMM36m protein force field (Huang et al., 2017). The structures were solvated with water molecules (TIP3P model) and 0.15 mM NaCl, and then subjected to energy minimization. For all simulations, a time step of 2 fs was used, along with periodic boundary conditions and Particle-Mesh-Ewald (PME) for electrostatics. The systems were heated to 300 K with constraining of Cα atoms only for 1 ns. The systems were equilibrated for another 1 ns without constraints before analysis. Finally, each system was run for 25, 35, and 50 ns. Parameters for all simulations were temperature 300 K, switching distance 10 Å, switching cutoff 12 Å, pairlist distance 14 Å, Langevin damping coefficient 1 ps^{-1}, and Langevin pressure control with a target pressure of 1.01325 bar.

The interaction energy of the two proteins in each system was calculated as the sum of electrostatic and Van der Waals energy and was averaged for the whole trajectories. And the root mean square deviation (RMSD) was further calculated, which is an important indicator for measuring the stability of the system. Position 3 yielded the strongest interaction energy (−1,965.03 kJ/mol) and the lowest RMSD (9.4 Å; **Figures 7A,B**; **Supplementary Table S4**). And the preliminary results showed that position 3 forms the most chemical bonds (**Figures 7C,D**; **Supplementary Table S4**). Thus, position 3 was retained for subsequent analyses. We further identified H-bonds, salt-bridges,

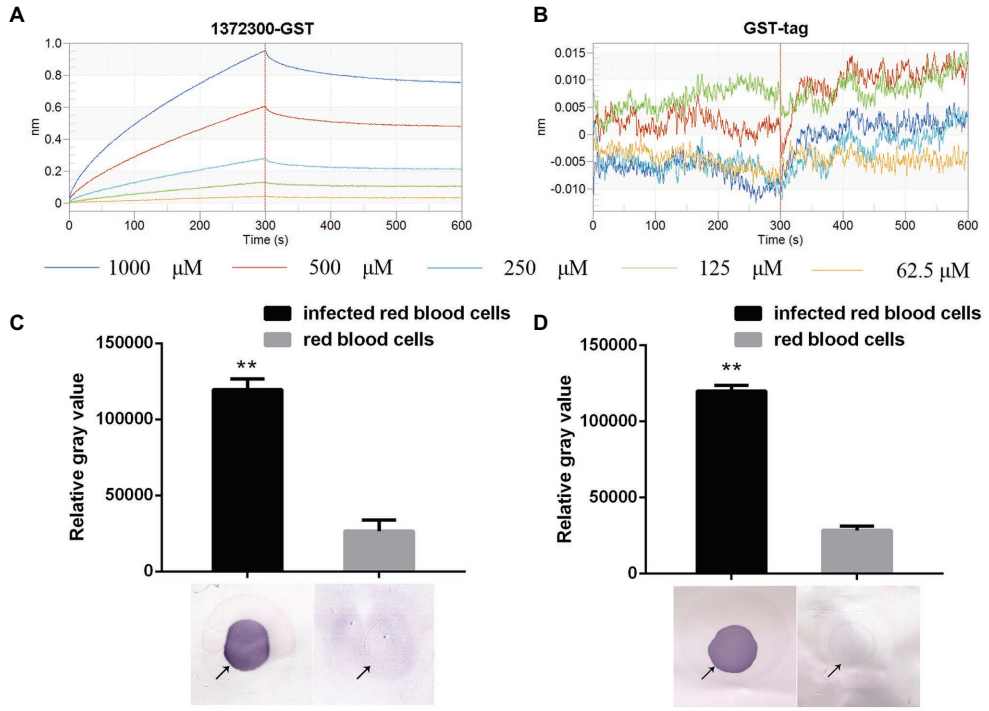

FIGURE 5 | Affinity between PF3D7_1372300 and ATS measured using a ForteBio system. **(A)** PF3D7_1372300-GST. **(B)** GST-tag. Curves correspond to the association and dissociation of PF3D7_1372300-GST/GST-tag at various concentrations and ATS anchored to the sensor chip. The curves can be used to determine KD, Kon, and Kdis. **(C,D)** Affinity between PF3D7_1372300 and ATS measured by dot blot. The arrow shows the position of the droplet. The experiment was repeated in triplicate, and the average relative gray value was calculated by ImageJ software. Statistical analysis was performed using ANOVA. Differences were considered statistically significant at $p \leq 0.05$ (compared with the control red blood cell group, $^{**}p \leq 0.01$).

and hydrophobic contacts between PF3D7_1372300 and ATS in the position 3 analysis. The geometrical criteria of H-bonds were set as distance cutoff 3.5 Å and angle cutoff 30. The threshold of salt bridges was a distance between the carboxyl group (COO^-) and the amino group (NH^{3+}) less than 4.0 Å. Hydrophobic contacts between proteins were defined as a distance between heavy atoms in the side chains of residues Ala, Val, Leu, Ile, Met, Phe, Pro, and Trp less than 4.0 Å, and all the sites involved interactions (**Figure 8A**). Some of the amino acids involved in H-bonds, salt bridges, and hydrophobic interactions are shown in detail in **Figure 8B**.

Verification of Interaction Sites

In order to verify the interaction sites, we divided the PHIST domain of PF3D7_1372300 into two fragments as shown in **Figure 9A**, and expressed and purified the two corresponding recombinant proteins (**Supplementary Figures S2A**,**B**). Kinetic analysis results for the variants are shown in **Figures 9B,C** and **Supplementary Table S5**. The KD value between PfEMP1 ATS and PF3D7_1372300-(27-129)-GST was 1.273E-07 was compared with 2.261E-08 between PfEMP1 ATS and PF3D7_1372300-(130-206)-GST. Thus, both PF3D7_1372300-(27-129)-GST and PF3D7_1372300-(130-206)-GST were interacted with PfEMP1 ATS, but the affinity between ATS and PF3D7_1372300-(27-129)-GST was stronger. This result is consistent with MD simulation data. As shown in **Figure 9A**, PF3D7_1372300-(27-129)-GST contains more sites that interact with PfEMP1 ATS.

DISCUSSION

For the malaria parasite *P. falciparum* to thrive inside human erythrocytes, it must modulate host cells, and this involves networks of protein-protein interactions. A novel exported PHIST protein was recently linked to parasite biology. The functional diversity of PHIST proteins is highlighted by their involvement in PfEMP1 expression, trafficking, and switching, as well as cytoadherence, gametocytogenesis, host cell modification, and generation of extracellular vesicles (EVs; Haldar and Mohandas, 2007; Maier et al., 2009). Several members of the PHIST family are reportedly essential for parasite survival, which highlights their significance in malaria biology (Maier et al., 2008; Zhang et al., 2018).

Different PHIST members are located in distinct subcellular regions. Several are exported to the iRBC surface (Oberli et al., 2014; Tarr et al., 2014; Kumar et al., 2018), while PFE1605w comigrates with PfEMP1 within iRBCs before being located at knobs, where it likely functions as an anchor of PfEMP1 (Oberli et al., 2014). However, PFI1780w was found to

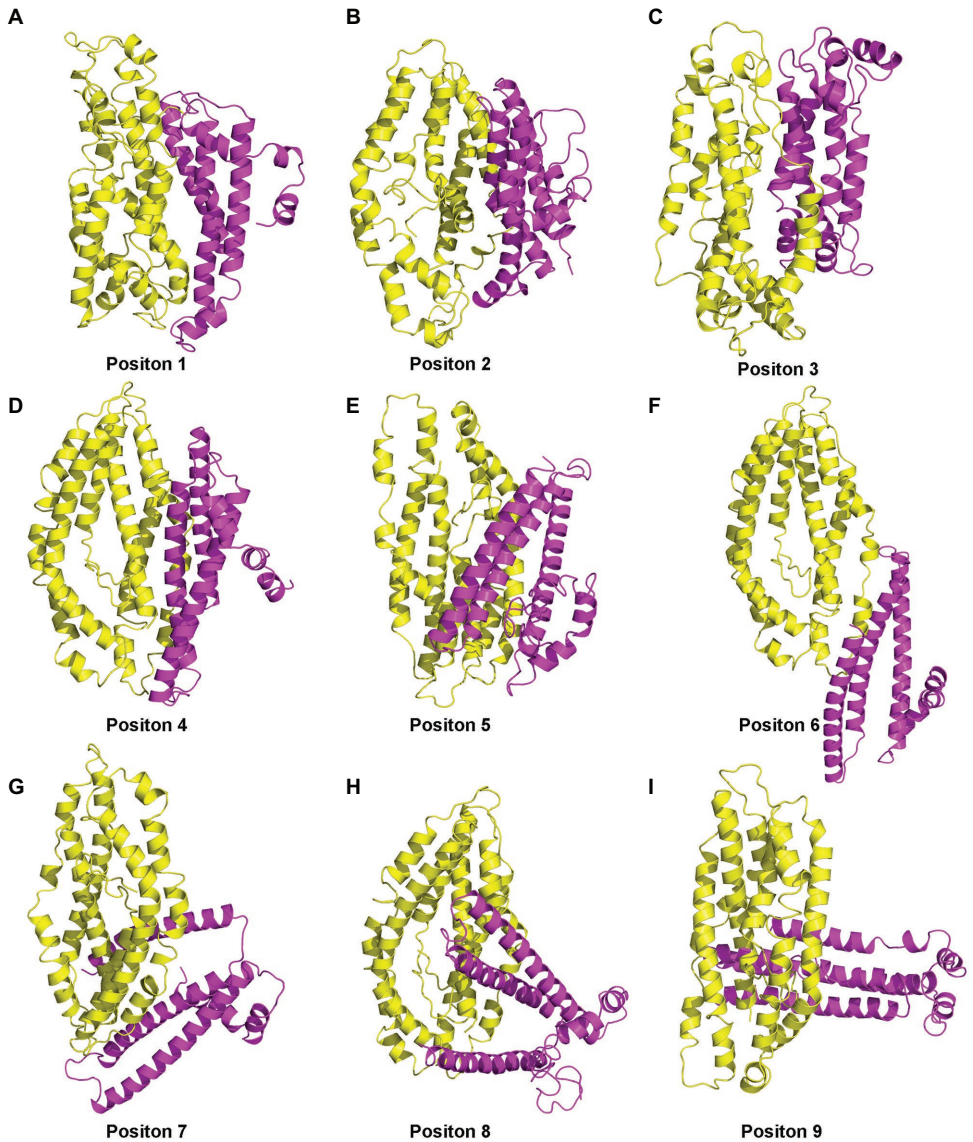

FIGURE 6 | (A–I) Nine complex structures screened out by molecular docking.

be uniformly distributed along the iRBC membrane, and completely absent from knobs (Oberli et al., 2014), while PF3D7_0424000 and PF3D7_0731100 are located to Maurer's clefts (MCs; Maier et al., 2008; Kumar et al., 2018). Although MCs appear to be the final destination of PF3D7_0424000, PF3D7_0731100 was also observed in iRBC-derived EVs (Regev-Rudzki et al., 2013) that carry several other PHIST proteins (Abdi et al., 2017). The presence of PHIST proteins at various locations in host cells indicates that they are potential interaction partners for specific proteins.

In the present study, we studied PF3D7_1372300, a PHIST/PHISTa-like protein with an unknown function. Sequence alignment revealed high similarity not only with homologs in *P. falciparum* strains but also in *Plasmodium* spp. that infects gorillas or chimpanzees. This indicates that the protein emerged after evolving in different *Plasmodium* parasite species, and it is different from PHISTa subgroup, which is unique to *P. falciparum* (**Figure 1**). The PF3D7_1372300 gene was highly transcribed throughout the blood stage of *P. falciparum* (**Figure 3A**), consistent with a previous genome-wide transcription study (Bozdech et al., 2003). Western blotting results showed that the protein was also expressed throughout the blood stage (**Figure 3C**). Comparison of expression at the gene and protein level indicated inconsistencies, which may indicate that expression of PHIST proteins was delayed after transcription (Foth et al., 2011).

Immunofluorescence assay experiments with a PF3D7_1372300 protein-specific antibody revealed dotted fluorescence on the

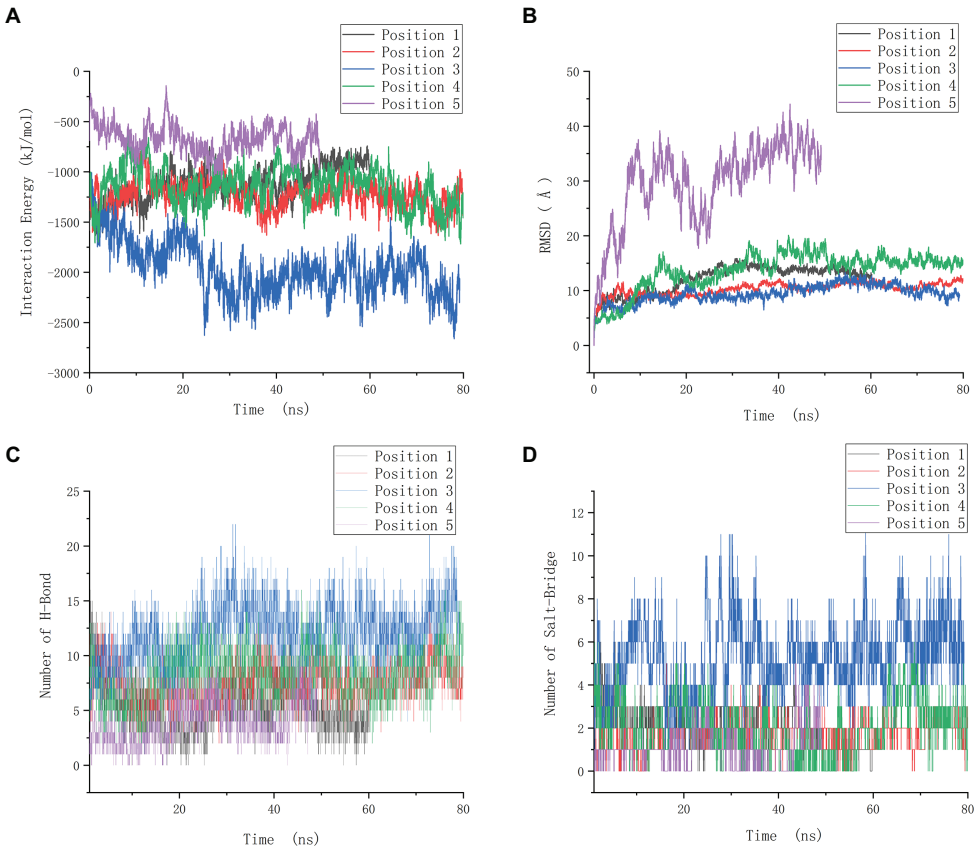

FIGURE 7 | Molecular dynamics data of the positions 1–5. **(A)** Interaction energy of five positions. **(B)** Root mean square deviation (RMSD) of five positions. **(C)** The number of H-bonds of five positions. **(D)** The number of salt-bridges of five positions.

iRBCs during the early stages of infection, and the fluorescence intensity was stronger in the trophozoite and late stages, where fluorescence was mainly located on the erythrocyte membrane (**Figure 3B**). Co-localization of PF3D7_1372300 and ATS revealed that PF3D7_1372300 reached the rim of the iRBC membrane before PfEMP1. In the early stage, the dotted fluorescence signals of PHIST protein were scattered distributed throughout the iRBCs; however, the ATS protein showed no fluorescence signal. During the trophozoite and late stages, significant overlap of fluorescence signals was observed on the erythrocyte membrane (**Figure 4**), unlike previous reports of PFE1605w co-translocated with a PfEMP1 protein (Oberli et al., 2014). We cannot rule out the possibility of variant-specific interactions between different PHISTs and PfEMP1s, especially given the large number of PfEMP1 and PHIST families.

To probe interactions between the two proteins, a ForteBio Octet K2 biomolecular interaction analysis system was applied that uses biofilm interference technology. This approach measures corresponding changes in the interference pattern of the intensity of the interference wave and the wavelength of emitted light to provide binding efficiency or concentration information for biomolecules interacting in real time. The technique can probe intermolecular interactions in a rapid and high-throughput manner. Our protein interaction and dot blot results confirmed that PF3D7_1372300 interacts strongly with the ATS region of PfEMP1 (**Figure 5**).

In the present study, interaction sites on PF3D7_1372300 that bind the ATS of PfEMP1 were explored using MD simulation. A total of 34 PF3D7_1372300 aa residues were predicted to potentially participate in these interactions (**Figure 8**), and these interaction sites were preliminarily verified (**Figure 9**). Furthermore, 36 aa residues of PfEMP1 ATS were predicted to participate in these interactions (**Supplementary Figure S3**). The residues enclosed by a yellow box correspond to conserved interaction sites of ATS predicted in previous studies (Mayer et al., 2012), and five of the residues identified in our MD simulations are located in this predicted conserved interaction region.

In summary, we explored the transcription and expression of a novel PHIST protein (PF3D7_1372300) of *P. falciparum*. We verified the interaction between PF3D7_1372300 and PfEMP1 ATS, and further identified the interaction sites. The findings greatly expand our knowledge of the PHIST protein family in host-parasite interactions, and provide a basis for exploring the functions of this important protein family.

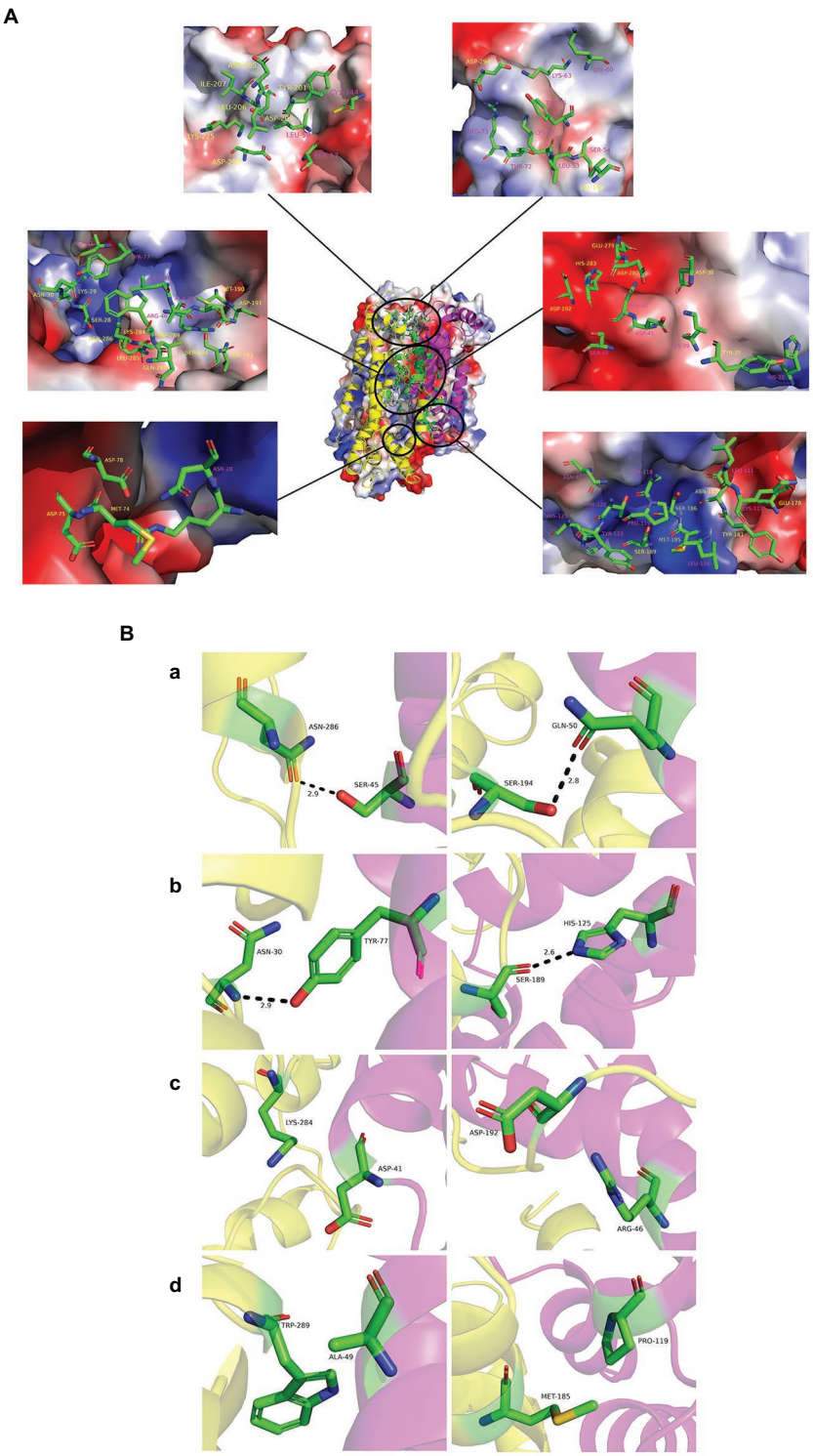

FIGURE 8 | Interaction modes of PF3D7_1372300 and ATS. **(A)** Structure of position 3 and its electrostatic surface were shown in the center. Circles are the sites involved in interactions between the two proteins. The close-up view shows PF3D7_1372300 (purple) and ATS (yellow) residues involved in interactions in electrostatic surface representation. All amino acids are labeled in the figure and shown in stick representation. Carbon atoms are colored green, nitrogen atoms are blue, and oxygen atoms are red. **(B)** PF3D7_1372300 (purple) and ATS (yellow) residues involved in interactions. Rows **(a,b)** show the amino acids involved in the formation of hydrogen bonds (shown as black dotted lines). Row **(c)** shows the amino acids involved in salt bridge formation. Row **(d)** shows the amino acids involved in hydrophobic interactions.

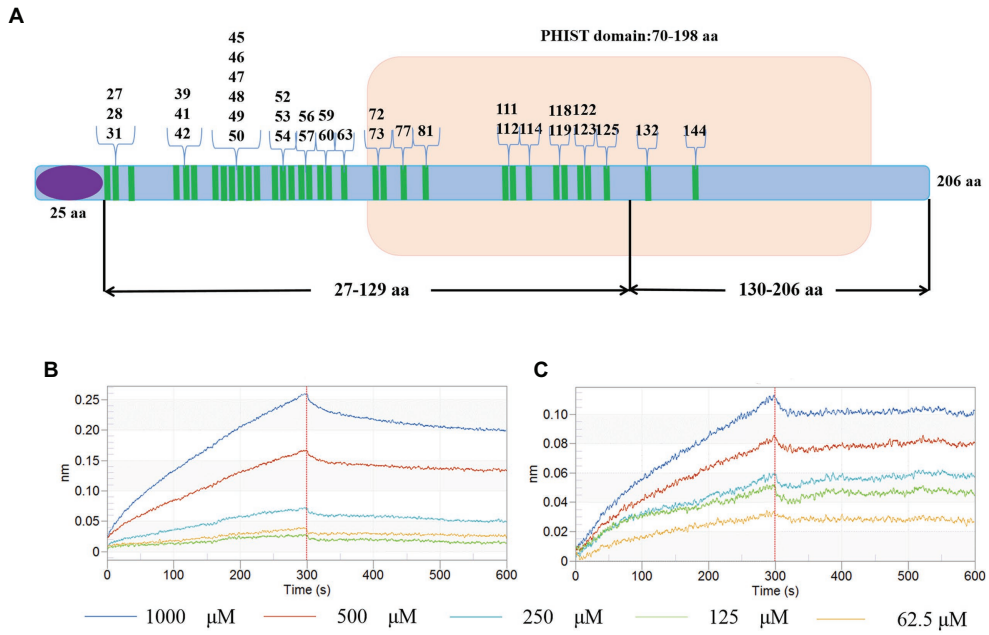

FIGURE 9 | Schematic diagram of interaction sites and interaction verification. **(A)** The blue bar represents PF3D7_1372300, the purple ellipse represents the signal peptide, the part with the light brown background is the PHIST domain, and the green bar represents the amino acids involved in interactions. **(B,C)** Binding affinity for PF3D7_1372300-(27-129)-GST with ATS **(B)** and PF3D7_1372300-(130-206)-GST with ATS **(C)** measured using a ForteBio system.

DATA AVAILABILITY STATEMENT

The original contributions presented in the study are included in the article/**Supplementary Material**, further inquiries can be directed to the corresponding author.

ETHICS STATEMENT

The animal study was reviewed and approved by the Experimental Animal Committee and the Ethical Committee of Shenyang Agricultural University, Shenyang, China.

AUTHOR CONTRIBUTIONS

BY performed most of the experiments, analyzed the data, and wrote the first draft of the manuscript. XiaW and XinW performed the modeling of protein-protein interaction. NJ mentored the study. XS, YF, and RC performed the IFA analysis. QC conceived the study, analyzed that data, and finalized the manuscript. All authors contributed to the article and approved the submitted version.

FUNDING

This study was supported by grants of the National Natural Science Foundation of China (81420108023, 81772219, and 82030060) and CAMS Innovation Fund for Medical Sciences (CIFMS; 2019-I2M-5-042).

SUPPLEMENTARY MATERIAL

The Supplementary Material for this article can be found online at: https://www.frontiersin.org/articles/10.3389/fmicb.2020.611190/full#supplementary-material

REFERENCES

Abdi, A., Yu, L., Goulding, D., Rono, M. K., Bejon, P., Choudhary, J., et al. (2017). Proteomic analysis of extracellular vesicles from a *Plasmodium falciparum* Kenyan clinical isolate defines a core parasite secretome. *Wellcome Open Res.* 2:50. doi: 10.12688/wellcomeopenres.11910.2

Bozdech, Z., Llinás, M., Pulliam, B. L., Wong, E. D., and Derisi, J. L. (2003). The transcriptome of the intraerythrocytic developmental cycle of *Plasmodium falciparum*. *PLoS Biol.* 1:e5. doi: 10.1371/journal.pbio.0000005

Bryan, D., Silva, N., Rigsby, P., Dougall, T., Corran, P., Bowyer, P. W., et al. (2017). The establishment of a WHO reference reagent for anti-malaria (*Plasmodium falciparum*) human serum. *Malar. J.* 16:314. doi: 10.1186/s12936-017-1958-x

Chiodini, J. (2018). Apps from the World Health Organization—The World Malaria Report and more. *Travel Med. Infect. Dis.* 22, 82–84. doi: 10.1016/j.tmaid.2018.03.007

Claessens, A., Adams, Y., Ghumra, A., Lindergard, G., Buchan, C. C., Andisi, C., et al. (2012). A subset of group A-like *var* genes encodes the malaria

parasite ligands for binding to human brain endothelial cells. *Proc. Natl. Acad. Sci. U. S. A.* 109, E1772–E1781. doi: 10.1073/pnas.1120461109

de Koning-Ward, T. F., Gilson, P. R., Boddey, J. A., Rug, M., Smith, B. J., Papenfuss, A. T., et al. (2009). A newly discovered protein export machine in malaria parasites. *Nature* 459, 945–949. doi: 10.1038/nature08104

Flick, K., and Chen, Q. (2004). *var* genes, PfEMP1 and the human host. *Mol. Biochem. Parasitol.* 134, 3–9. doi: 10.1016/j.molbiopara.2003.09.010

Florens, L., Liu, X., Wang, Y., Yang, S., Schwartz, O., Peglar, M., et al. (2004). Proteomics approach reveals novel proteins on the surface of malaria-infected erythrocytes. *Mol. Biochem. Parasitol.* 135, 1–11. doi: 10.1016/j.molbiopara.2003.12.007

Foth, B. J., Zhang, N., Chaal, B. K., Sze, S. K., Preiser, P. R., Bozdech, Z., et al. (2011). Quantitative time-course profiling of parasite and host cell proteins in the human malaria parasite *Plasmodium falciparum*. *Mol. Cell. Proteomics* 10:M110.006411. doi: 10.1074/mcp.M110.006411

Gardner, M. J., Hall, N., Fung, E., White, O., Berriman, M., Hyman, R. W., et al. (2002). Genome sequence of the human malaria parasite *Plasmodium falciparum*. *Nature* 419, 498–511. doi: 10.1038/nature01097

Gruring, C., Heiber, A., Kruse, F., Ungefehr, J., Gilberger, T. W., and Spielmann, T. (2011). Development and host cell modifications of *Plasmodium falciparum* blood stages in four dimensions. *Nat. Commun.* 2:165. doi: 10.1038/ncomms1169

Haldar, K., and Mohandas, N. (2007). Erythrocyte remodeling by malaria parasites. *Curr. Opin. Hematol.* 14, 203–209. doi: 10.1097/MOH.0b013e3280f31b2d

Hiller, N. L., Bhattacharjee, S., van Ooij, C., Liolios, K., Harrison, T., Lopez-Estrano, C., et al. (2004). A host-targeting signal in virulence proteins reveals a secretome in malarial infection. *Science* 306, 1934–1937. doi: 10.1126/science.1102737

Huang, J., Rauscher, S., Nawrocki, G., Ran, T., Feig, M., de Groot, B. L., et al. (2017). CHARMM36m: an improved force field for folded and intrinsically disordered proteins. *Nat. Methods* 14, 71–73. doi: 10.1038/nmeth.4067

Kumar, V., Kaur, J., Singh, A. P., Singh, V., Bisht, A., Panda, J. J., et al. (2018). PHISTc protein family members localize to different subcellular organelles and bind *Plasmodium falciparum* major virulence factor PfEMP-1. *FEBS J.* 285, 294–312. doi: 10.1111/febs.14340

LaCount, D. J., Vignali, M., Chettier, R., Phansalkar, A., Bell, R., Hesselberth, J. R., et al. (2005). A protein interaction network of the malaria parasite *Plasmodium falciparum*. *Nature* 438, 103–107. doi: 10.1038/nature04104

Maier, A. G., Cooke, B. M., Cowman, A. F., and Tilley, L. (2009). Malaria parasite proteins that remodel the host erythrocyte. *Nat. Rev. Microbiol.* 7, 341–354. doi: 10.1038/nrmicro2110

Maier, A. G., Rug, M., O'Neill, M. T., Brown, M., Chakravorty, S., Szestak, T., et al. (2008). Exported proteins required for virulence and rigidity of *Plasmodium falciparum*-infected human erythrocytes. *Cell* 134, 48–61. doi: 10.1016/j.cell.2008.04.051

Marti, M., Good, R. T., Rug, M., Knuepfer, E., and Cowman, A. F. (2004). Targeting malaria virulence and remodeling proteins to the host erythrocyte. *Science* 306, 1930–1933. doi: 10.1126/science.1102452

Mayer, C., Slater, L., Erat, M. C., Konrat, R., and Vakonakis, I. (2012). Structural analysis of the *Plasmodium falciparum* erythrocyte membrane protein 1 (PfEMP1) intracellular domain reveals a conserved interaction epitope. *J. Biol. Chem.* 287, 7182–7189. doi: 10.1074/jbc.M111.330779

Milner, D. A. J. (2018). Malaria pathogenesis. *Cold Spring Harb. Perspect. Med.* 8:a025569. doi: 10.1101/cshperspect.a025569

Mok, B. W., Ribacke, U., Winter, G., Yip, B. H., Tan, C. S., Fernandez, V., et al. (2007). Comparative transcriptomal analysis of isogenic *Plasmodium falciparum* clones of distinct antigenic and adhesive phenotypes. *Mol. Biochem. Parasitol.* 151, 184–192. doi: 10.1016/j.molbiopara.2006.11.006

Nilsson, B. S. K., Ahmad, R., Dantzler, K., Lukens, A. K., De Niz, M., Szucs, M. J., et al. (2018). Quantitative proteomic profiling reveals novel *Plasmodium falciparum* surface antigens and possible vaccine candidates. *Mol. Cell. Proteomics* 17, 43–60. doi: 10.1074/mcp.RA117.000076

Oberli, A., Slater, L. M., Cutts, E., Brand, F., Mundwiler-Pachlatko, E., Rusch, S., et al. (2014). A *Plasmodium falciparum* PHIST protein binds the virulence factor PfEMP1 and comigrates to knobs on the host cell surface. *FEBS J.* 28, 4420–4433. doi: 10.1096/fj.14-256057

Oberli, A., Zurbrügg, L., Rusch, S., Brand, F., Butler, M. E., Day, J. L., et al. (2016). *Plasmodium falciparum Plasmodium* helical interspersed subtelomeric proteins contribute to cytoadherence and anchor *P. falciparum* erythrocyte membrane protein 1 to the host cell cytoskeleton. *Cell. Microbiol.* 18, 1415–1428. doi: 10.1111/cmi.12583

Phillips, J. C., Braun, R., Wang, W., Gumbart, J., Tajkhorshid, E., Villa, E., et al. (2005). Scalable molecular dynamics with NAMD. *J. Comput. Chem.* 26, 1781–1802. doi: 10.1002/jcc.20289

Pierce, B. G., Wiehe, K., Hwang, H., Kim, B. H., Vreven, T., and Weng, Z. (2014). ZDOCK server: interactive docking prediction of protein-protein complexes and symmetric multimers. *Bioinformatics* 30, 1771–1773. doi: 10.1093/bioinformatics/btu097

Prajapati, S. K., and Singh, O. P. (2013). Remodeling of human red cells infected with *Plasmodium falciparum* and the impact of PHIST proteins. *Blood Cells Mol. Dis.* 51, 195–202. doi: 10.1016/j.bcmd.2013.06.003

Ramaprasad, A., Pain, A., and Ravasi, T. (2012). Defining the protein interaction network of human malaria parasite *Plasmodium falciparum*. *Genomics* 99, 69–75. doi: 10.1016/j.ygeno.2011.11.006

Regev-Rudzki, N., Wilson, D. W., Carvalho, T. G., Sisquella, X., Coleman, B. M., Rug, M., et al. (2013). Cell-cell communication between malaria-infected red blood cells via exosome-like vesicles. *Cell* 153, 1120–1133. doi: 10.1016/j.cell.2013.04.029

Sargeant, T. J., Marti, M., Caler, E., Carlton, J. M., Simpson, K., Speed, T. P., et al. (2006). Lineage-specific expansion of proteins exported to erythrocytes in malaria parasites. *Genome Biol.* 7:R12. doi: 10.1186/gb-2006-7-2-r12

Singh, S. K., Hora, R., Belrhali, H., Chitnis, C. E., and Sharma, A. (2006). Structural basis for Duffy recognition by the malaria parasite duffy-binding-like domain. *Nature* 439, 741–744. doi: 10.1038/nature04443

Tarr, S. J., Moon, R. W., Hardege, I., and Osborne, A. R. (2014). A conserved domain targets exported PHISTb family proteins to the periphery of *Plasmodium* infected erythrocytes. *Mol. Biochem. Parasitol.* 196, 29–40. doi: 10.1016/j.molbiopara.2014.07.011

Wahlgren, M., Goel, S., and Akhouri, R. R. (2017). Variant surface antigens of *Plasmodium falciparum* and their roles in severe malaria. *Nat. Rev. Microbiol.* 15, 479–491. doi: 10.1038/nrmicro.2017.47

Warncke, J. D., Vakonakis, I., and Beck, H. P. (2016). *Plasmodium* helical interspersed subtelomeric (PHIST) proteins, at the center of host cell remodeling. *Microbiol. Mol. Biol. Rev.* 80, 905–927. doi: 10.1128/MMBR.00014-16

Webb, B., and Sali, A. (2016). Comparative protein structure modeling using MODELLER. *Curr. Protoc. Protein Sci.* 86, 2.9.1–2.9.37. doi: 10.1002/cpps.20

WHO (2019). *World malaria report 2019*. Geneva: World Health Organization.

Zhang, M., Wang, C., Otto, T. D., Oberstaller, J., Liao, X., Adapa, S. R., et al. (2018). Uncovering the essential genes of the human malaria parasite *Plasmodium falciparum* by saturation mutagenesis. *Science* 360:eaap7847. doi: 10.1126/science.aap7847

Conflict of Interest: The authors declare that the research was conducted in the absence of any commercial or financial relationships that could be construed as a potential conflict of interest.

frontiers in Microbiology

REVIEW
published: 11 January 2021
doi: 10.3389/fmicb.2020.626183

From Metabolite to Metabolome: Metabolomics Applications in *Plasmodium* Research

Xinyu Yu[1,2], Gaoqian Feng[3,4], Qingfeng Zhang[5] and Jun Cao[1,6]**

[1] National Health Commission Key Laboratory of Parasitic Disease Control and Prevention, Jiangsu Provincial Key Laboratory on Parasite and Vector Control Technology, Jiangsu Institute of Parasitic Diseases, Wuxi, China, [2] Medical College of Soochow University, Suzhou, China, [3] Burnet Institute, Melbourne, VIC, Australia, [4] Department of Medicine, The University of Melbourne, Melbourne, VIC, Australia, [5] Key Laboratory of Arrhythmias of the Ministry of Education of China, Research Center for Translational Medicine, East Hospital, Tongji University School of Medicine, Shanghai, China, [6] Center for Global Health, School of Public Health, Nanjing Medical University, Nanjing, China

Advances in research over the past few decades have greatly improved metabolomics-based approaches in studying parasite biology and disease etiology. This improves the investigation of varied metabolic requirements during life stages or when following transmission to their hosts, and fulfills the demand for improved diagnostics and precise therapeutics. Therefore, this review highlights the progress of metabolomics in malaria research, including metabolic mapping of *Plasmodium* vertebrate life cycle stages to investigate antimalarials mode of actions and underlying complex host-parasite interactions. Also, we discuss current limitations as well as make several practical suggestions for methodological improvements which could drive metabolomics progress for malaria from a comprehensive perspective.

Keywords: metabolomics, plasmodium, life stage, antimalarial, mode of action

OPEN ACCESS

Edited by:
Hong-Juan Peng, Southern Medical University, China

Reviewed by:
Xing-Quan Zhu, Chinese Academy of Agricultural Sciences, China
Liang Shaohui, Wenzhou Medical University, China

****Correspondence:***
Qingfeng Zhang
qfzhangsh@aliyun.com
Jun Cao
caojuncn@hotmail.com

Specialty section:
This article was submitted to Infectious Diseases, a section of the journal Frontiers in Microbiology

Received: *05 November 2020*
Accepted: *07 December 2020*
Published: *11 January 2021*

Citation:
Yu X, Feng G, Zhang Q and Cao J (2021) From Metabolite to Metabolome: Metabolomics Applications in Plasmodium Research. Front. Microbiol. 11:626183. doi: 10.3389/fmicb.2020.626183

HIGHLIGHTS

- The number and quality of metabolomics-based approaches for malarial research have significantly improved due to either the growing interest on parasite infection or substantial improvements in instrumentation, enabling the comprehensive profiling of *Plasmodium* metabolome from an overall perspective.
- Recent metabolomics-related advances, including studying the basic biology of *Plasmodium* in their vertebrate host, investigating the mode of action and resistance mechanisms of antimalarials, and exploring the link between host and parasite metabolic plasticity, has fueled its application in *Plasmodium*.
- As a functional hypotheses-generating strategy, an updated framework for malarial metabolomics research is necessary, including the assessment of obtained achievements and suggestions for further investigation.

Abbreviations: F6-P, fructose-6-phosphate; F1,6-BP,fructose-1,6-bisphosphate; DHAP, dihydroxy-acetonephosphate; GlycP, glycerol-3-phosphate; Ac-CoA, acetyl-CoA; Pyr, pyruvate; GADP, glyceraldehyde-3-phosphate; 1,3BPG, 1,3-bisphosphoglycerate; 3-PGA, 3-phosphoglycerate; 2-PGA, 2-phosphoglycerate; PEP, phosphoenolpyruvate; Ala, Alanine; GABA, γ-aminobutyric acid; SSA, succinic semi-aldehyde; Gln, glutamine; Glu, glutamate; αα-KG, α-ketoglutarate; Cit, citrate; OAA, oxaloacetate; Mal, malate; Arg, argine; GlcN6-P, glucosamine-6-phosphate; GlcNAc-6P, N-acetyl-glucosamine-6-phosphate.

OUTSTANDING QUESTIONS

- Given that for *in vitro* culture, the malaria parasites mainly reside inside of host erythrocytes, how can the quality of metabolomics data be improved to reduce unnecessary background noise owing to extremely high sensitivity for metabolomics platforms?
- Can *in vitro* metabolomics analysis for *Plasmodium* provide useful information for *in vivo* studies; if not, are human studies necessary for further investigation and what should be taken into consideration when performing clinical trials?
- What new information can we obtain to understand MoAs for antimalarials through untargeted metabolomics study, and are there any limitations when facing new antimalarials?
- Can obtained results be applied from pre-clinical to clinical scenarios? For example, numerous potential infection-related biomarkers have been revealed by different research, how should a proper interpretation or efficient comparisons be made so that more attention can be paid to those compounds with enough practical value?

DEFINITIONS AND METHODOLOGY: HOW DOES METABOLOMICS FIT IN WITH SYSTEM BIOLOGY

Malaria has been recognized as a significant global health burden, resulting in approximately 228 million new cases and 405 thousand deaths in 2018 worldwide (Sills et al., 2018; World Health Organization, 2019). Malaria is a vector-borne disease caused by the eukaryotic protozoan parasite of genus *Plasmodium* which has a complicate life cycle, transmitting from *Anopheles* mosquitoes to human hosts (Cowman et al., 2016; Haldar et al., 2018; **Figure 1**). With the urgent demands for better understanding of the molecular biology of the malaria parasite (Miller et al., 2013), **system biology** has been proven to be a versatile and robust strategy to explore the complex *Plasmodium* biological process (Hasin et al., 2017; Karczewski and Snyder, 2018; **Box 1**). Advances in these **omics**-based approaches have shed light on parasite biology and further revolutionized the research for parasitic diseases (**Figure 2**; Florens et al., 2002; Gardner et al., 2002; Zhu et al., 2018).

It has been well characterized that the epigenetic mechanism or the physiological effect of post-translational modifications can be regulated by **metabolites**. Therefore, changes in the *Plasmodium* development stages can be captured by omics approaches from a genome to **metabolome** level (Skretas and Wood, 2005; Saito and Matsuda, 2010; Sperber et al., 2015). Metabolomics is defined as an approach that aims at simultaneously detecting small molecules (<1,500 Da) to understand the systemic changes in a different state and allows global **metabolic profiling** in various bio-samples. Metabolomics allows the investigation of metabolic phenotypes associated with gene functions and protein expressions by amplifying changes in transcriptomes and proteomes (Saito and Matsuda, 2010; Horgan and Kenny, 2011; Klassen et al., 2017; Giera et al., 2018). Therefore, metabolome can be visually described as metabolic gears intertwined with genomes and proteomes, which acts as an integral component in the overall system without hypothesizing the effect of any single element. Opposed to conventional "down-top" strategies, metabolomics works well in system biology because it is capable of providing one "top-down" view of biochemical profiles in complex organisms. A surge in metabolomics studies were seen over the past decades with the incredible development of high-resolution platforms (Dunn and Ellis, 2005; Markley et al., 2017; Misra et al., 2017; **Box 2**).

BOX 1 | Systems biology: a comprehensive approach for malarial research. Since 2002, the genome draft of laboratory-adapted and field-isolated strains of *P. falciparum* have been sequenced which enables the investigation of epidemiological and transmission dynamics in malaria endemic areas. This excellent work has opened a window for promoting and accelerating drug and vaccine development. However, the large evolutionary distance from model organisms has hindered the genome annotation and the exact functions of specific genes are hypothetical, putative, or even unknown, making it extremely challenging in identifying functional genes in cellular processes. With the growing demands to overcome this challenge, downstream functional omics strategies including transcriptomics, proteomics, and metabolomics have been and continue to be put forward to characterize the gene functions and to obtain better understanding of the molecular biology of malaria parasites (Hall et al., 2005; Salinas et al., 2014; Lindner et al., 2019). Since the first attempt of genome annotation, proteomics research has also been performed to identify stage-specific proteomes or to reveal the critical cellar regulatory mechanisms, suggesting its potential in identification of drug targets or developing transmission block strategies. Meanwhile, the successful construction of various databases, such as VarDB, PlasmoDB, and MalVac, also makes it possible for researchers to share findings, providing broader applications of acquired genomic data to accelerate the development of malaria biology (Chaudhuri et al., 2008; Cristina et al., 2009; Lakshmanan et al., 2011).

METABOLIC-BASED STRATEGY IN MALARIAL RESEARCH: WHERE ARE WE NOW?

The metabolome is the end-product of intracellular biochemical activities; it is susceptible to changes in the environment, including infection-related stress. Metabolomics studies have been shown to have a critical place in understanding infectious parasite diseases pathology (Kafsack and Llinas, 2010). The complexity of host-parasite interactions resulted from various life cycles, which are often involved in intracellular and/or extracellular stages from insects to vertebrate hosts; considerable efforts have been made to investigate molecular mechanisms to reveal the host immune responses during the invasion and evasion process (Cowman et al., 2016; Gowda and Wu, 2018). However, much less is known about the metabolic interaction and nutrient exchange between parasite and host; therefore, global metabolomics strategy has been put forward for presenting extensive data on *Plasmodium*-infected erythrocytes. Analysis of metabolic profiles for both intracellular and extracellular metabolomes from different life stages is capable of reflecting the perturbations of specific pathways during culture. As

BOX 2 | Overview of metabolomics.

Analytical Platforms

Application of various analytical platforms is of extreme importance in which the fast development will greatly aid in our capabilities to understand the biology from an overall perspective. Technological advances will hugely contribute to the detection of thousands of compounds when facing complex biofluids. Historically, nuclear magnetic resonance (NMR) spectroscopy and mass spectrometry (MS) have been the two most widely applied platforms with highly complementary attributes in various metabolomics researches. Although limited by the sensitivity, NMR still provides a window in the qualitative and quantitative analysis for compounds with high abundance present in almost all biofluids, tissues, or cell extractions. Excellent reproducibility alone with non-destructive property for NMR allows all kinds of sample analysis in a short period, making it an ideal candidate in large-scale metabolomics screening. With the growing demand for capturing low-abundance metabolites to meet the requirement of obtaining metabolic patterns as detailed as possible, the MS platform coupled with chromatography could be another powerful and complementary platform for simultaneous analysis of hundreds of compounds in complex biosamples with sufficient resolution, sensitivity, and reproducibility. Until now, the development trend of analytical platforms still mainly focuses on acquiring more metabolic information in a minimized sample, developing high throughput approaches with improved qualitative and quantitative accuracy.

Analytical Scope

- Untargeted metabolomics
  As a hypothesis generating strategy, it mainly focuses on the global assessment of a broad range of both known and unknown compounds to offer either comprehensive or unbiased approaches to investigate unanticipated perturbations. Using this unbiased strategy, changes of metabolic profiles subjected to different conditions can be revealed, leading to the identification of novel metabolites or metabolic pathways. Then subsequent analysis can be performed to structural or functional characterization of these candidates.
- Targeted metabolomics
  As a hypothesis driven strategy, it mainly emphasizes the detection of clearly defined compounds which holds the advantages in obtaining a comprehensive understanding of the kinetic profile in specific pathways.
- Functional metabolomics
  Functional metabolomics, as one kind of emerging concept, spans from the discovery of differential metabolites to investigate the actual function of specific compounds. Based on untargeted and/or targeted approaches, it further characterizes the functional role of selected metabolites as well as the enzymes in related pathways through both *in vitro* and *in vivo* assays including cell biology and clinical platform. It is able to increase the reliability for metabolomics study and contributes novel knowledge about previous findings.

clarified, after infection, the parasite will massively convert host metabolome into essential molecules to maintain survival during the **erythrocytic asexual stage**, leading to the excretion of products of erythrocyte lysis and parasite metabolism. Actually, this could have a significant effect on the host response, including events at the cellular or molecular level occurring in both host and parasites (Miller et al., 2013; Cowman et al., 2016). However, complicated interactions between *Plasmodium* spp. and their hosts remains a barrier to complete understanding because of poorly understood downstream consequences, which will be discussed below. In addition to applications on *Plasmodium* biology, continuous work has also been done in the development or screening of effective preventive and therapeutic pharmaceuticals. With the advances in whole-cell screening, thousands of compounds with antimalarial capacity and selectivity have been brought to public attention, providing a promising future in the selection of potent drugs to facilitate the therapeutics pipeline (Gamo et al., 2010). However, one critical bottleneck for this strategy is the lack of mechanistic information about their mode of actions (MoAs). Efforts have been made by genomics, transcriptomics, and proteomics for identifying possible mechanisms from different perspectives, while the emerging metabolomics-based method has been shown to be an attractive strategy due to the metabolic pathway specificity for antimicrobials (Vincent and Barrett, 2015; Dos et al., 2016). Identification of MoA in an untargeted manner can significantly enhance the understanding and detects previously unnoticed pharmacological effects that are ignored by conventional biochemical methods. The unbiased nature, as well as the excellent sensitivity of metabolomics, makes it an ideal approach to map drug-specific metabolic profiles in a time-dependent manner and then to facilitate the understanding of MoA for either commercial-available drugs or novel compounds with antimalarial activities. Therefore, in this review, we mainly aim to outline metabolic achievements in the studies of *Plasmodium* spp. (**Table 1**), highlighting the promising applications and providing several suggestions for metabolomics research.

LAYING GROUNDWORK: PROFILING FROM METABOLITE TO METABOLOME

Pioneering efforts were made for the *in vitro* investigation of parasite metabolism early in the 1980s (Zhu, 2004; Macrae et al., 2012; Ng et al., 2014). These studies have reported strikingly distinct metabolic patterns of energy metabolism and has raised the question, how does the parasite adapt to the complex environment by evolving a unique metabolism? Metabolic mapping of *P. falciparum*-infected erythrocytes to track the carbon metabolism has revealed the voraciously consumed level of host glucose, which is almost 100-folds higher than uninfected cells due to the consumption of metabolically-active parasites (Mehta et al., 2006). Surprisingly, glycerol, derived from glucose via glycerol-3-phosphate shuttle, has been proven to serve as an energy source during development, although its origin remains controversial due to the absence of necessary quenching (Lian et al., 2009). Nevertheless, these findings have suggested unique metabolic profiles in parasites which should be further investigated and interpreted with an open mind.

Based on the single metabolite discoveries, successful metabolomics approaches have been performed to map the profile of both parasite-infected host cells and isolated intracellular parasites during life cycles (**Figure 3A**). Owing to the fact that the blood asexual stage is mainly responsible for clinical symptoms caused by the adhesion of infected erythrocyte, it is of great interest to investigate their metabolomic profile during the intraerythrocytic developmental cycle (IDC). Periodically changed metabolites related to the mature stage parasite (trophozoite and schizont stage) during IDC have been identified, suggesting a close relationship between essential parasite growth and metabolome exchange (Olszewski et al., 2009; Sana et al., 2013; Cobbold et al., 2016b). Most of them

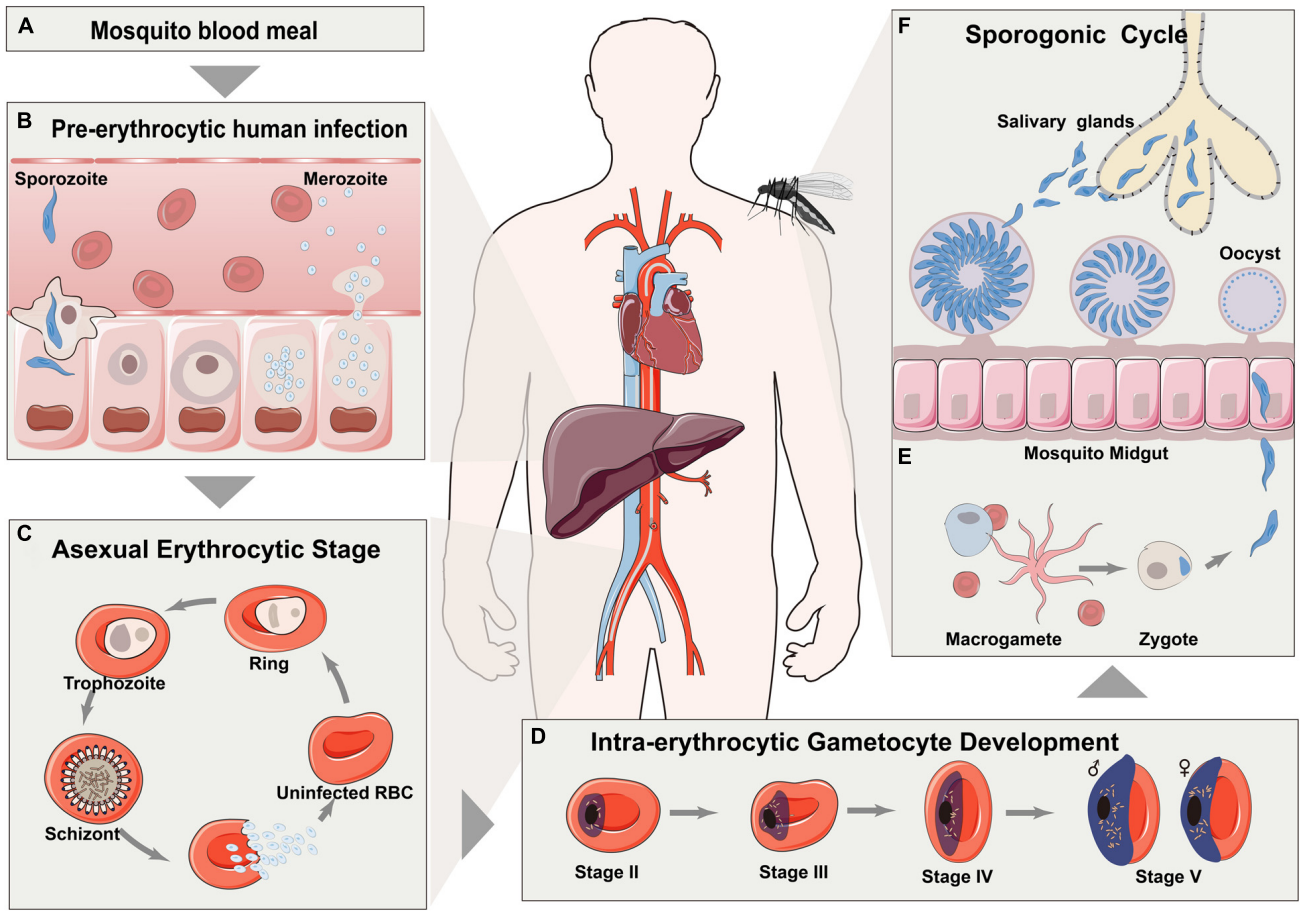

FIGURE 1 | Life cycle of representative plasmodium (*P. falciparum*). **(A)** Malaria is initiated through the bite of *Anopheles* mosquitoes. **(B)** Injected sporozoites are transported to liver through vasculature and then matured in hepatocytes. **(C)** After schizogony by producing hundreds of daughter merozoites, released merozoites then invade into erythrocytes for asexual life cycles. **(D)** A portion of asexually reproducing merozoites undergo reprogramming sexual differentiation to form gametocytes. **(E)** Matured gametocytes are then released into peripheral circulation for ingestion by a mosquito. **(F)** Formed zygotes transform into ookinete in the midgut of mosquito.

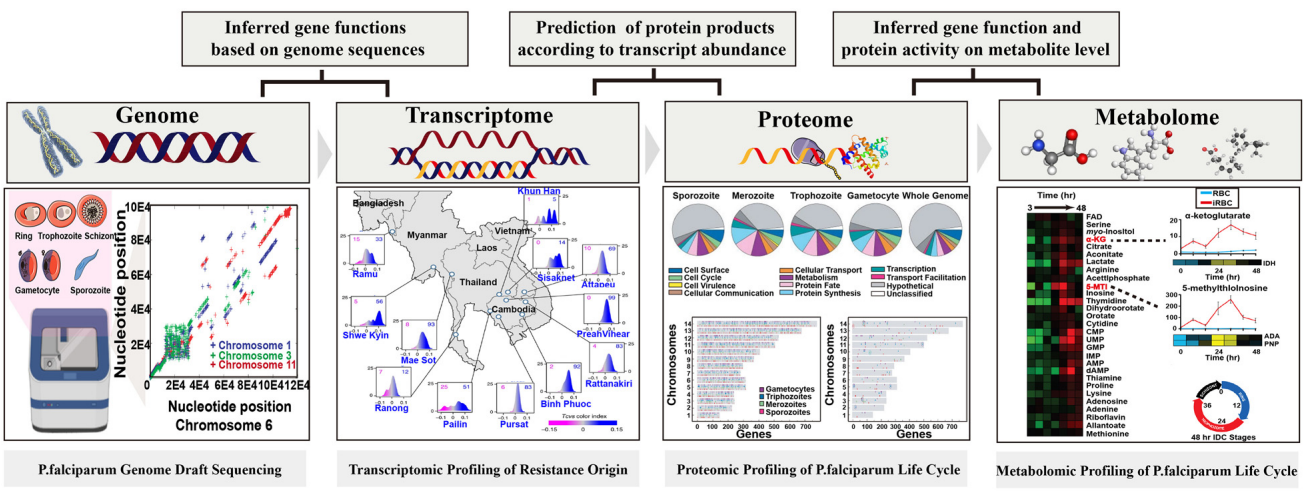

FIGURE 2 | Overview of the relationship between each omics approach and ground-breaking applications in *Plasmodium* spp. Figures of significant achievements are adapted from Gardner et al. (2002), Florens et al. (2002), Olszewski et al. (2009), Zhu et al. (2018) and the copyright of each figure has been achieved.

TABLE 1 | Overall view of representative metabolomics studies in *Plasmodium* spp.

Research scope	Analytical platform	Major findings	References
In vitro life cycle and host specificity	MS	• Highlight key function of glycerol and glycolysis metabolism in adaption to the variable environments	Mehta et al., 2006; Lian et al., 2009
	MS	• Reveal periodic metabolome and clinically important biochemical pathways during IDC in detail	Olszewski et al., 2009
	MS	• Capture stage-specific metabolic profile and elucidate the metabolomic response to physiologically relevant perturbations	Olszewski et al., 2009
	MS	• Profile detailed arginine depletion and metabolism during the *Plasmodium* invasion	Cobbold et al., 2016b
	MS	• Intergrade unbiased discovery-driven and targeted data-mining strategy to facilitate metabolomic profile	Sana et al., 2013
	MS	• Identify parasite-specific waste products in culture supernatant and confirm disturbed amino acids metabolism	Park et al., 2015; Surowiec et al., 2015
	MS	• Compare metabolic profiles of erythrocyte infected with different strains of P. falciparum	Siddiqui et al., 2017
	MS	• Develop one rapid and easily operated purification method for the enrichment of viable ring stage parasites	Brown et al., 2020
	MS	• Characterize substantial remodeling of mitochondrial metabolism to meet the requirement of gametocyte development	Macrae et al., 2013; Lamour et al., 2014
Mode of action for	MS	• Acquire metabolic fingerprints for commercially available antimalarials and candidates in malaria box	Allman et al., 2016
Antimalarials and	MS	• Provide extensive information regarding the impact of antimalarials on parasite metabolism	Cobbold et al., 2016a
Potential compounds	MS	• Develop medium-throughput and phenotypic screening approach for further mechanistic studies	Creek et al., 2016
	MS	• Report detailed antimalarial susceptibility profiling and reveal stage-specific and metabolic profiles to differentiate MoAs	Murithi et al., 2020
	NMR	• Sheds light on the biochemical changes brought about by genome mutations and its association with drug resistance	Teng et al., 2014
Host-parasite	NMR	• Gain global metabolic pattern for *P. berghei* infected mice and laid foundation for exploring metabolic cross-link in rodents	Li et al., 2008
Interaction and	MS	• Assess the importance of central carbon metabolism and address critical glutamine function in adaptive energy metabolism	Srivastava et al., 2016
Malaria severity	NMR	• Characterize glucose and fatty acids metabolism during the energy exchange with host	Vaughan et al., 2010; Ghosh et al., 2011, 2012, 2016
	MS	• First case-control study to identify candidate molecules associated with pathological process	Abdelrazig et al., 2017
	MS	• Develop metabolomics approach to phenotype patients with varied drug susceptibility and disease severity	Gardinassi et al., 2017; Uppal et al., 2017
	NMR/MS	• Evaluate specific metabolic features associated with CM susceptibility and concomitant metabolic acidosis	Sengupta et al., 2016; Leopold et al., 2019
	MS	• Intergrade metabolomics and transcriptomics approach for discrimination of naïve and semi-immune subjects	Gardinassi et al., 2018

are associated with energy metabolism and macromolecular biosynthesis because of excessive metabolic activity for genome replication (Olszewski et al., 2009). Similarly, most prominently alerted glycolysis metabolism has also been revealed by facilitated untargeted profiling and targeted data mining strategies (Sana et al., 2013). In contrast to uninfected erythrocytes with over 90% glucose-to-lactate conversion, disturbed levels of lactic acid resulted from incomplete oxidation suggests both an increased flux of glucose carbon into biomass and the absence of functional tricarboxylic acid (TCA) cycle in energy generation, which correlates well with the minimal oxygen consumption for *P. falciparum in vitro* culture (Brown and Guler, 2020). With the most dramatic change for either accumulated level of non-proteogenic amino acids ornithine and citrulline or sharply depleted arginine in medium (Olszewski et al., 2009), it raises the question for the origin and metabolism of arginine which is not critical for parasite growth. Simultaneous detection of ornithine, citrulline, and arginine by targeted metabolomics has revealed an approximately 1.6-fold up-regulated arginine pool during the asexual stage (especially for trophozoite-stage) resulted from the disruption of nitric oxide metabolism after invasion, proposing one possible mechanism for its metabolism and depletion (Cobbold et al., 2016b). Sufficient information of arginine metabolism, as well as disturbed nitric oxide metabolism, cannot only explain the observed depletion in previous study, but also provide a better understanding for biological events including decreased erythrocyte deformability during parasite invasion. This successful attempt has opened new avenues for capturing

a stage-specific metabolic profile in *Plasmodium* and then in turn act as one problem-oriented strategy for malaria research. Additionally, the invasion process has also been profiled by untargeted detection of excretive metabolites in medium supernatants in a time-dependent manner (Park et al., 2015; Surowiec et al., 2015). The positive metabolome-wide association between those shared metabolites with sufficient specificity in ring, trophozoite, and schizont stages has demonstrated the metabolic heterogeneity during development. As noticed, there is an increasing demand for spatially and temporally regulated lipid metabolism resulting from fast production of merozoites with high metabolic activity during growth and differentiation (Gulati et al., 2015). The lipid-associated metabolic pathway has been considered as one attractive drug target, suggesting the importance for comprehensive profiling of lipid metabolism during *Plasmodium* life cycles. Therefore, analysis of either extracellular metabolite levels in medium or intracellular metabolome from different life cycle stages during *in vitro* culture can be applied to infer novel or unanticipated metabolic pathways to functionally characterize the biological process.

As investigation of parasite differentiation is also of practical importance owing to the fact that mature gametocytes are the prerequisite for spread, the metabolomics attempt is then extended to the linear **sexual gametocyte stage** (Macrae et al., 2013; Lamour et al., 2014). Unlike the asexual stage, precise metabolic profiling for gametocytogenesis by tracking the uptake and metabolism of ^{13}C-glucose has unexpectedly revealed significantly higher glucose utilization resulted from a substantial remodeling of mitochondrial metabolism (Macrae et al., 2013). This proof-of-principle study has allowed one revision for the energy metabolism of sexual stage parasites which switches into an enhanced TCA-cycle metabolism to meet the requirements of gametocyte development in hypoglycemia. Followed by this explorative attempt, detailed metabolic exchange has been investigated to characterize the gametocyte-specific cell biology by profiling the culture medium (Lamour et al., 2014). Consistent with previous results, most distinct patterns still lie in the glucose utilization as a result of host adaption from the asexual stage to the gametocyte stage. Likewise, the observed sharp depletion of medium-derived lipids associated with gametocyte maturation is also worth further investigation to generate better understanding of gametocyte development, which will facilitate yielding new insights for malaria transmission blocking.

Notably, although capture and detection for metabolome is becoming less of a limiting factor owing to instruments with higher resolution and sensitivity, *Plasmodium* metabolomics studies remain facing the technological challenges to acquire parasites with sufficient homogeneity. Almost all the published results focused on the late-stage parasites which can be efficiently separated from the host cells through density gradient centrifugation or by applying magnetic beads to reduce the background contamination, and these enrichment approaches have greatly fueled recent explosive developments for omics-based approaches in late-stage *Plasmodium* biology (Olszewski et al., 2009; Sana et al., 2013; Cobbold et al., 2016b). Unfortunately, non-specific noise has dramatically hindered our methods to investigate the early-stage parasite, especially in these sensitive down-stream approaches. Although challenging, the enrichment of early-stage parasites with sufficient quantity and purity is of practical value. More recently, one rapid and easily to handle purification method for viable ring stage parasites using a combination of selective lysis property of Streptolysin-O and permeability of Percoll has been proposed. This provides a promising tool for asexual parasite research with good quality (over 80%, 22-fold higher than initial parasitemia) (Brown et al., 2020). Nevertheless, metabolic profiling turns out to be one quality verification experiment for the proposed method. On the other hand, it can serve as one quality control strategy by targeted profiling parasite-specific metabolites that are proportional to the enrichment level to facilitate accurate metabolic investigation of early-stage parasite.

Generally, metabolomics analysis from *in vitro* studies have attempted to build the foundation to capture a stage-specific metabolic profile in *Plasmodium* for a comprehensive understanding of *Plasmodium* biology at a cellular level. Considering that metabolite state varies among different stages of the life-cycle due to parasite evolution (Olszewski et al., 2009; Park et al., 2015), researchers should pay more attention to sample treatment and take both periodic and non-periodic stage-dependent metabolic profiles into account. Dynamic profiling through overall metabolome rather than single target metabolites will aid in understanding how the parasite mediates this exchange progress with host cells. For example, although eukaryotic parasites are capable of *de novo* biosynthesis of some necessary nutrients for growth, it turns out to be more advantageous to utilize host-derived compounds (Müller and Kappes, 2007; Brancucci et al., 2017; Mancio-Silva et al., 2017). One practical challenge during research is the rare homogeneity so that synchronization is critical for isolating specific parasite stage. Nevertheless, it remains a mystery since the nature of intracellular parasitism is nutrient and waste exchange between parasite and host or/and the environment, in which host cells are highly compartmentalized, leaving an inherent difficulty for compartmental analysis of metabolites.

FINDING NETWORKS: INFERRING FROM ANTIMALARIAL MoAs TO DRUG RESISTANCE

With the wide application of effective antimalarials worldwide, malarial control has achieved encouraging success. However, it has been facing extreme challenges with the emergence and spread of drug-resistant strains for most of the commercially available antimalarial drugs, creating a heavy burden for public health and economic development (Menard and Dondorp, 2017). It holds the advantage that understanding of MoA will enhance drug development by monitoring their activities and resistance to facilitate further clinical use, including the optimization of dose and pharmacokinetics, guiding the selection of partner drugs, and strategy development for combating the emergence of resistances (Carolino and Winzeler, 2020). Capturing influenced metabolome may also inform us about the biology of specific strains with varied drug resistance, providing a catalog of

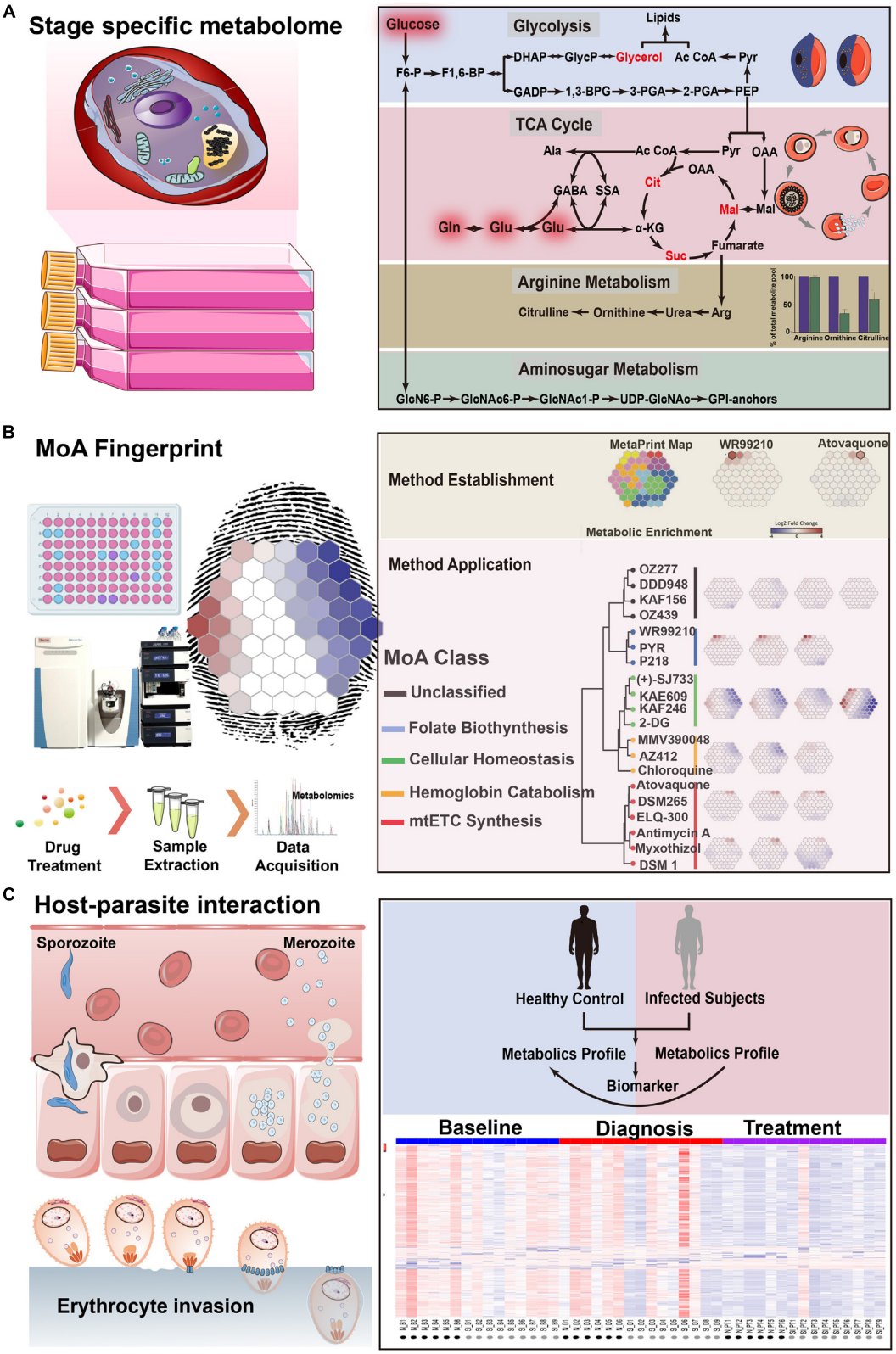

FIGURE 3 | Metabolomics highlights in applications for *Plasmodium* spp. biology**. (A)** An integrated map of an affected metabolic network of *Plasmodium* during different life cycle stages. **(B)** Investigation of antimalarials metabolic fingerprints and mode of action of validated compounds with antimalarial activity. **(C)** Exploration of the link between host response and parasite metabolic plasticity during infection. The copyright of adapted figure has been achieved.

candidate targets or pathways to advance critical malarial-control explorations (**Figure 3B**).

To date, multiple mechanisms of antimalarials have been reported, whereas that of newly available compounds remains yet to be expounded (Olliaro, 2001). The vast majority of them mainly target the essential parasite metabolism to selectively induce lethal outcomes. Thus, metabolomics screening turns out to be an ideal approach to profile these induced perturbations. Until now, applications of metabolomics in the investment of antimalarial MoAs remains largely unexploited. Unlike traditional endpoint assays or phenotype-based methods, which can only provide limited information, metabolomics-based strategies can capture whole-cell metabolic response when facing the treatment of commercially available antimalarials and then be applied for the investigation of related pathways (Allman et al., 2016; Cobbold et al., 2016a; Creek et al., 2016). **Metabolic fingerprint** has been revealed by capturing significantly changed metabolic signatures as well as influenced pathways and, as expected, commercially available drugs (including atovaquone, proguanil, and dihydroartemisinin) displayed distinct metabolic patterns, confirming the feasibility for acquiring unique metabolic perturbation rather than non-specific variance. For example, as a cytochrome bc1 complex inhibitor, disrupted *de novo* pyrimidine synthesis resulted from mitochondrial membrane potential loss has been confirmed by targeting the detection of carbamoyl-L-aspartate and dihydroorotate, the precursor and substrate of affected dihydroorotate dehydrogenase (Cobbold et al., 2016a). In regard to proguanil, a potent prodrug with a poorly understood MoA, significant accumulation of arginine has been observed in which it served as an arginase inhibitor due to structural similarity, suggesting the capability to undercover conventional unknown MoAs with wider perturbations. Although the key mechanism of artemisinin has been characterized, non-specifically released free radicals during the activation process can thus result in multiple effects to the parasite in which more MoAs could be involved in Tilley et al. (2016). Considering the uptake and activation mostly happens in digestive vacuole which results in protein alkylation and the affect hemoglobin catabolism, significantly perturbed hemoglobin-derived metabolism has been observed within 1 h. Unexpectedly, the metabolic profile of dihydroartemisinin also demonstrated the disruption of pyrimidine biosynthesis according to the abundance of isotope-labeled intermediates, even though the specific mechanism differs from atovaquone, indicating dihydroartemisinin could also have an effect on the activity of enzymes such as aspartate carbamoyltransferaseor carbamoyl-phosphate synthase and partly explained the resulted stage susceptibility (Murithi et al., 2020). The proposed method has been extended to screen MoAs for candidates in malaria box, among which 40 of them displayed a drug-like metabolic profile even though they are structurally unrelated. Unlike traditional *in vitro* EC_{50} assay, the proposed method has demonstrated a fast-action manner, suggesting its promising potential in the discovery of fast-acting antimalarial candidates. More recently, another high-throughput metabolomics assay has been put forward for the assessment of stage susceptibility as well as pathway perturbations (Murithi et al., 2020). Likewise, both commercial drugs and antimalarial candidates have been metabolically classified and hierarchically clustered into seven groups to provide a recommended rationale according to their MoAs and drug dynamics. The compounds targeted the same or associated pathways that displayed both similar stage specificity and metabolic profiles; the proposed assay is also capable of differentiating compounds with similar structures. For example, the metabolic profiles of chloroquine and piperaquine, which share the same active structure and displayed similar stage specificity against early ring stages, turn out to be strikingly different, especially for hemoglobin catabolism. From a practical point of view, this research is in favor of the selection of desirable drugs in combination therapies in which combining targets of different life-cycle stages can be applied for optimal therapeutic effect or delaying the emergence of drug resistance.

Likewise, tracking drug-induced perturbation can in turn serve as a powerful tool to profile adapted metabolisms of response phenotypes. Even though genetic or proteomic markers have been regarded as good candidates for monitoring and evaluating resistance, it is still a time and laborintensive task for point-of-care analysis, which is not always suitable for accessing the treatment outcome (Martin et al., 2010; Ariey et al., 2013). However, the exact function of these markers remains unclear from the metabolic level because of the lack of target specificity, suggesting mutations might have a broader impact than expected (Koncarevic et al., 2010; Summers et al., 2012). Thus, global metabolic differences have been characterized between parasites with different susceptibilities for understanding the resistance-related phenotypic diversity (Teng et al., 2014; Siddiqui et al., 2017). Distinct metabolic states for parasites with varied sensitivity have been acquired, especially in amino acid metabolism, phospholipid precursors, and energy metabolism intermediates. The levels of precursors of membrane lipid components or TCA cycle intermediates varied from 5 to 30-fold in resistant strains, suggesting both the membrane lipid and energy metabolism can severe as clues to understanding drug resistance. Another multi-omics integrated attempt has been attempted to enhance the efficiency of metabolomics by associating the decreased level of *PfKelch13* protein with increased levels of glutathione and its precursor, suggesting the perturbation during detoxification enzymes synthesis and regulation (Siddiqui et al., 2017). Hence, metabolomics is able to provide a snapshot of the biochemical status of intercellular activity, telling us how the addressed metabolome changes in response to various factors like drug treatment or adaption to environmental alterations. Moreover, once the responsive metabolome has been identified, the resulted susceptibility or resistance can also be validated by exogenous supplement of targeted molecules.

Currently, the major advantage for metabolomics approaches in the investigation of MoA is the capacity to identify novel drug-related responses at the global level without the need for prior knowledge. Metabolomics has enabled the classification of candidate compounds according to the metabolome-based MoAs, unexpectedly highlighting the effected pathways or enzymes responsible for the antimalarial activity. However, it also brings some limitations; for example, some compounds

can induce either a non-specific metabolic response or an indirect effect on the disruption of metabolic pathways. In general, antimalarial candidates in which selected compounds should or at least cover most common MoA of commercial antimalarials to increase the possibility of positive matching. Meanwhile, dynamic time-course or dose-response relationships should also be investigated before screening because it is highly recommended to apply sub-lethal doses which enables the detection of primary effects rather than an undesirable drug-induced death metabolic signature. Based on the above-mentioned criteria, we do suggest that enough replications analyzed in identical conditions are required to ensure the predictability and variation while more quantitative targeted analysis is also required in some circumstances to provide a more detailed pattern of induced metabolome change. At the same time, multi-omics-based approaches also appear to be an attractive and complementary field to profile both primary and secondary responses.

EXTENDING APPLICATIONS: CHALLENGING FROM PRE-CLINICAL TO CLINICAL

Although *in vitro* parasite culture has been widely explored because of its convenience and maneuverability, it still faces challenges in the absence of a specific immune response and complex nutritional environment. Identifying metabolic perturbations in host **biofluids** is in favor of the understanding of sophisticated host response as well as the development of infection-specific biomarkers. The host-parasite interactions have been extensively reviewed (Kloehn et al., 2016; Ghosh et al., 2018), while the existing challenges are yet to be discussed.

So far, successful attempts have already been made in rodent models (Li et al., 2008; Vaughan et al., 2010; Ghosh et al., 2011, 2012, 2016; Srivastava et al., 2016) and human subjects with symptoms varying from clinically asymptomatic ones to life-threatening ones (metabolic acidosis or cerebral malaria) (Sengupta et al., 2016; Abdelrazig et al., 2017; Gardinassi et al., 2017; Uppal et al., 2017; Gardinassi et al., 2018; Leopold et al., 2019; **Figure 3C**). Remarkable glycolytic up-regulation and energy demand have been observed due to the parasite metabolism shift from glycolysis (asexual stages) to the enhanced TCA cycle (both gametocyte stage and ookinetes), suggesting an adaptive manner of energy metabolism during the host switch from rodent to mosquito (Srivastava et al., 2016). While in human hosts, metabolomics approaches also showed potential in the differentiation of uninfected controls from infected cases with varying severity by using either relative level changes of specific metabolites or unique metabolomes in infected ones. Likewise, lipids metabolism and amino acids metabolic perturbation (especially for aspartate and asparagine) has been shown to have satisfactory sensitivity in patients. Also, distinct metabolic and transcriptomics patterns for semi-immune subjects has indicated a systemic immune response after secondary infections which further resulted in improved symptoms (minor or no symptoms) (Gardinassi et al., 2018). In addition to this situation, closely related lipid composition and glycoprotein for CM-specific susceptibility also suggests a candidate mode for early diagnosis. Particularly, the temporal metabolic profile of specific organic acids (including hydroxyphenyllactic acid, phenylacetic acid, and dimethylglycine) in patients with metabolic acidosis also proposed one possible mechanism to combine the severity of malaria with the dysfunction of the gut microbiota.

Although remarkable metabolomics-based efforts for the investigation of parasite infections have been able to differentiate infected subjects from healthy controls, these approaches are still inadequate for clinical diagnostic application because sometimes these biomarkers are general indicators of infection rather than disease-specific predictors. There remain some open questions that must be answered in the future. For example, do the host responses exactly reflect the severity? Do the parasites have a unique metabolome in the host with varied symptoms or severities? Does the infected host metabolome actually result from the host-parasite interaction? Therefore, one major challenge for investigating host-parasite interactions mainly relies on the biomarker validation in which the valuable biological meaning is required for detailed mechanisms. In most cases, to ensure so-called "novelty," there is an absence of functional information for acquired compounds altogether while the biggest hurdle is how to correlate the candidate metabolites with the phenotypes and further move beyond biomarker identification to mechanism investigation. Theoretically, follow-up validation studies should be performed in other cohorts to ensure objectivity. However, this will result in another problem: how to overcome the individual differences that arise from both genetic and environmental factors to point out the biological meaning of the selected metabolome. Therefore, developing proper normalization strategies as well as a useful database is of great help to obtain a metabolic profile detailed to metabolite concentrations ranging from various influential factors.

On the other hand, metabolome serves as down-stream products like substrates or intermediates for various biochemical reactions, suggesting particular sensitivity to their corresponding enzyme activity and abundance. Although quantitative protein analysis, like enzyme-linked immunosorbent assay or immunoblotting, is of lower throughput, they are more straightforward and readily available to profile metabolite-protein relationships which is in favor of providing useful information associated with metabolomics findings. Additionally, high-throughput omics approaches can also be integrated to transform single metabolomics data into an enhanced understanding of the complex biological process. One guilt-by-association strategy has been put forward in which either known or unknown co-expressed genes in one specific metabolic pathway have been investigated with an associated metabolic profile to predict and validate the pathophysiology (Gerth et al., 2016). This attempt sets both a comprehensive and straightforward overview and framework to explore the infected-related metabolic profiling with corresponding immune function, not only in malaria but also in other parasite diseases.

Generally, acquired potential biomarkers from human subjects or animal models can serve as a starting point for mechanistic research to determine exact biological

functions for more reliable data. In the near future, more blind studies with larger cohort sizes are required to validate the efficiency of discovered potential biomarkers, yielding reliable diagnostic markers, predictors of treatment outcome, and related clinical polymorphisms.

CONCLUSION REMARKS

The advances in metabolomics during the past few decades have opened the door for a deeper biological understanding of the critical metabolic profile in *Plasmodium* spp. With some pioneering studies, solid groundwork has been laid to establish links in metabolic networks from specific metabolites to global metabolome. Promising applications have been achieved as reviewed, including investigating varied metabolic requirements during life stages or through following transmission to their hosts; from these efforts, MoAs or targets of various compounds have been identified and the predictive markers of infection defined. Generally, both the obtained stage-specific metabolic profile and the candidate biomarkers from *in vitro* or *in vivo* studies have strengthened the comprehensive understanding at cellular level, potentially severing as a starting point for future investigations to explore the exact biological functions of acquired metabolome. Meanwhile, globally captured drug-related response has turned out to be helpful in the understanding of novel or unexpected MoAs, further facilitating their clinical use, including the optimization of dose and pharmacokinetics, guiding the selection of partner drugs for combating the emergence of resistances.

However, several questions still remain (as shown in Outstanding Questions). For example, neither rare homogeneity during *in vitro* culture nor the difficulty in interpretation and validation for potential candidates from human subjects has greatly hindered the clinical applications of metabolomics-based research. In our opinion, even though the above-mentioned limitations mainly result from intrinsic characteristics of metabolomics, they can be technologically improved through methodological advances and sophisticated study design. Specifically, a shorter synchronization window or efficient enrichment of a particular stage should be performed to obtain parasites with good quality for accurate metabolome acquisition. Meanwhile, sustained effort is highly recommended for the construction of parasite-specific databases or sharing clinical metabolomic samples in both longitudinal and independent cohorts. In addition to target validating, meta-analysis has shown to be another powerful strategy in which multiple studies for one disease or symptom are compared to exclude those unrelated features for the shared phenotype. Considering the unbiased property of metabolomics, in the investigation of MoAs for antimalarials, we do suggest the selected antimalarial candidates to cover the most common MoAs with available compounds to increase positive hits rather than be classified into an unknown group. Further, dynamic time-course or dose-response experiments should be performed before screening to obtain the primary effects.

One current trend toward standardization of varied metabolomics workflows is a practical way to make the technology and the data more accessible. We believe the future of metabolomics in *Plasmodium* research is to be integrated with traditional system biology strategies routinely used in parasitological studies. More system biology approaches will be generate growing interest from genomics, transcriptomics, proteomics, and metabolomics. These combinatorial strategies will allow for better understanding of the biological events from a more global perspective, yielding a detailed view of its intricate networks. Such approaches can undoubtedly inform many aspects of malaria research including, but not limited to, building basic parasite biological models, development of therapeutics, identification of diagnostic biomarkers, and establishment of human pathophysiology models.

AUTHOR CONTRIBUTIONS

QZ and JC were responsible for providing the idea and framework of the whole work. XY wrote the first draft of the manuscript. GF did critical revision of the article. All authors contributed to the article and approved the submitted version.

FUNDING

This work was supported by the National Key R&D Program of China (No. 2020YFC1200105), National Natural Science Foundation of China (Nos. 81971967, 31671353, and 81971959), and Jiangsu Provincial Project of Invigorating Health Care through Science, Technology and Education, the China Postdoctoral Science Foundation (2020M671397).

REFERENCES

Abdelrazig, S., Ortori, C. A., Davey, G., Deressa, W., Mulleta, D., Barrett, D. A., et al. (2017). A metabolomic analytical approach permits identification of urinary biomarkers for Plasmodium falciparum infection: a case–control study. *Malaria J.* 16, 229. doi: 10.1186/s12936-017-1875-z

Allman, E., Painter, H. J., Samra, J., Carrasquilla, M., and Llinas, M. (2016). Metabolomic profiling of the malaria box reveals antimalarial target pathways. *Antimicrob. Agents Chemother.* 60, 6635–6649. doi: 10.1128/AAC.01224-16

Ariey, F., Witkowski, B., Amaratunga, C., Beghain, J., Langlois, A. C., Khim, N., et al. (2013). A molecular marker of artemisinin-resistant Plasmodium falciparum malaria. *Nature* 505, 50–55. doi: 10.1038/nature12876

Brancucci, N. M. B., Gerdt, J. P., Wang, C., De Niz, M., Philip, N., Adapa, S. R., et al. (2017). Lysophosphatidylcholine regulates sexual stage differentiation in the human malaria parasite *Plasmodium falciparum*. *Cell* 171, 1532–1544. doi: 10.1016/j.cell.2017.10.020

Brown, A. C., and Guler, J. L. (2020). From circulation to cultivation: plasmodium in vivo versus in vitro. *Trends Parasitol.* 36, 914–926. doi: 10.1016/j.pt.2020.08.008

Brown, A. C., Moore, C. C., and Guler, J. L. (2020). Cholesterol-dependent enrichment of understudied erythrocytic stages of human *Plasmodium parasites*. *Sci. Rep.* 10, 4591. doi: 10.1038/s41598-020-61392-6

Carolino, K., and Winzeler, E. A. (2020). The antimalarial resistome-finding new drug targets and their modes of action. *Curr. Opin. Microbiol.* 57, 49–55. doi: 10.1016/j.mib.2020.06.004

Chaudhuri, R., Ahmed, S., Ansari, F. A., Singh, H. V., and Ramachandran, S. (2008). MalVac: database of malarial vaccine candidates. *Malaria J.* 7, 184. doi: 10.1186/1475-2875-7-184

Cobbold, S. A., Chua, H. H., Nijagal, B., Creek, D. J., Ralph, S. A., and Mcconville, M. J. (2016a). Metabolic dysregulation induced in *Plasmodium falciparum* by dihydroartemisinin and other front-line antimalarial drugs. *J. Infect. Dis.* 213, 276–286. doi: 10.1093/infdis/jiv372

Cobbold, S. A., Llinás, M., and Kirk, K. (2016b). Sequestration and metabolism of host cell arginine by the intraerythrocytic malaria parasite *Plasmodium falciparum*. *Cell. Microbiol.* 18, 820–830. doi: 10.1111/cmi.12552

Cowman, A. F., Healer, J., Marapana, D., and Marsh, K. (2016). Malaria: biology and disease. *Cell* 167, 610–624. doi: 10.1016/j.cell.2016.07.055

Creek, D. J., Chua, H. H., Cobbold, S. A., Nijagal, B., Macrae, J. I., Dickerman, B. K., et al. (2016). Metabolomics-based screening of the Malaria Box reveals both novel and established mechanisms of action. *Antimicrob. Agents Chemother.* 60, 6650–6663. doi: 10.1128/AAC.01226-16

Cristina, A., John, B., Brunk, B. P., Jennifer, D., Steve, F., Bindu, G., et al. (2009). PlasmoDB: a functional genomic database for malaria parasites. *Nuclc Acids Res.* 37, 539–543. doi: 10.1093/nar/gkn814

Dos, S. B. S., Da, S. L. C. N., Da, S. T. D., Rodrigues, J. O. F. S., Grisotto, M. A. G., Santos, C. M. T. D., et al. (2016). Application of Omics technologies for evaluation of antibacterial mechanisms of action of plant-derived products. *Front. Microbiol.* 7:1466. doi: 10.3389/fmicb.2016.01466

Dunn, W. B., and Ellis, D. I. (2005). Metabolomics: current analytical platforms and methodologies. *Trends Anal. Chem.* 24, 285–294. doi: 10.1016/j.trac.2004.11.021

Florens, L., Washburn, M. P., Raine, J. D., Anthony, R. M., Grainger, M., Haynes, J. D., et al. (2002). A proteomic view of the *Plasmodium falciparum* life cycle. *Nature* 419, 520–526. doi: 10.1038/nature01107

Gamo, F.-J., Sanz, L. M., Vidal, J., De Cozar, C., Alvarez, E., Lavandera, J.-L., et al. (2010). Thousands of chemical starting points for antimalarial lead identification. *Nature* 465, 305–310. doi: 10.1038/nature09107

Gardinassi, L. G., Arevaloherrera, M., Herrera, S., Cordy, R. J., Tran, V., Smith, M. R., et al. (2018). Integrative metabolomics and transcriptomics signatures of clinical tolerance to *Plasmodium vivax* reveal activation of innate cell immunity and T cell signaling. *Redox Biol.* 17, 158–170. doi: 10.1016/j.redox.2018.04.011

Gardinassi, L. G., Cordy, R. J., Lacerda, M. V. G., Salinas, J. L., Monteiro, W. M., De Melo, G. C., et al. (2017). Metabolome-wide association study of peripheral parasitemia in *Plasmodium vivax* malaria. *Int. J. Med. Microbiol.* 307, 533–541. doi: 10.1016/j.ijmm.2017.09.002

Gardner, M. J., Hall, N., Fung, E., White, O., Berriman, M., Hyman, R. W., et al. (2002). Genome sequence of the human malaria parasite *Plasmodium falciparum*. *Nature* 419, 498–511. doi: 10.1038/nature01097

Gerth, K., Lin, F., Menzel, W., Krishnamoorthy, P., Stenzel, I., Heilmann, M., et al. (2016). Guilt by association: a phenotype-based view of the plant phosphoinositide network. *Annu. Rev. Plant Biol.* 68, 349–374. doi: 10.1146/annurev-arplant-042916-041022

Ghosh, S., Pathak, S., Sonawat, H. M., Sharma, S., and Sengupta, A. (2018). Metabolomic changes in vertebrate host during malaria disease progression. *Cytokine* 112, 32–43. doi: 10.1016/j.cyto.2018.07.022

Ghosh, S., Sengupta, A., Sharma, S., and Sonawat, H. M. (2011). Multivariate modelling with 1H NMR of pleural effusion in murine cerebral malaria. *Malaria J.* 10, 330. doi: 10.1186/1475-2875-10-330

Ghosh, S., Sengupta, A., Sharma, S., and Sonawat, H. M. (2012). Metabolic fingerprints of serum, brain, and liver are distinct for mice with cerebral and noncerebral Malaria: a 1H NMR spectroscopy-based metabonomic study. *J. Proteome Res.* 11, 4992–5004. doi: 10.1021/pr300562m

Ghosh, S., Sengupta, A., Sharma, S., and Sonawat, H. M. (2016). Early prediction of cerebral malaria by 1H NMR based metabolomics. *Malaria J.* 15, 198. doi: 10.1186/s12936-016-1256-z

Giera, M., Filipe, B. D. S., and Siuzdak, G. (2018). Metabolite-induced protein expression guided by metabolomics and systems biology. *Cell Metab.* 27, 270–272. doi: 10.1016/j.cmet.2018.01.002

Gowda, D. C., and Wu, X. (2018). Parasite recognition and signaling mechanisms in innate immune responses to Malaria. *Front. Immunol.* 9:3006. doi: 10.3389/fimmu.2018.03006

Gulati, S., Ekland, E. H., Ruggles, K. V., Chan, R. B., Jayabalasingham, B., Zhou, B., et al. (2015). Profiling the essential nature of lipid metabolism in asexual blood and gametocyte stages of *Plasmodium falciparum*. *Cell Host Microbe* 18, 371–381. doi: 10.1016/j.chom.2015.08.003

Haldar, K., Bhattacharjee, S., and Safeukui, I. (2018). Drug resistance in *Plasmodium*. *Nat. Rev. Microbiol.* 16, 156–170. doi: 10.1038/nrmicro.2017.161

Hall, N., Karras, M., Raine, J. D., Carlton, J. M., Kooij, T. W. A., Berriman, M., et al. (2005). A comprehensive survey of the *Plasmodium* life cycle by genomic, transcriptomic, and proteomic analyses. *Science* 307, 82–86. doi: 10.1126/science.1103717

Hasin, Y., Seldin, M., and Lusis, A. (2017). Multi-omics approaches to disease. *Genome Biol.* 18, 1–15. doi: 10.1186/s13059-017-1215-1

Horgan, R. P., and Kenny, L. C. (2011). 'Omic' technologies: genomics, transcriptomics, proteomics and metabolomics. *Obstetr. Gynaecol.* 13, 189–195. doi: 10.1576/toag.13.3.189.27672

Kafsack, B. F. C., and Llinas, M. (2010). Eating at the table of another: metabolomics of host-parasite interactions. *Cell Host Microbe* 7, 90–99. doi: 10.1016/j.chom.2010.01.008

Karczewski, K. J., and Snyder, M. P. (2018). Integrative omics for health and disease. *Nat. Rev. Genet.* 19, 299–310. doi: 10.1038/nrg.2018.4

Klassen, A., Faccio, A. T., Canuto, G. A. B., Cruz, P. L. R. D., Ribeiro, H. C., Tavares, M. F. M., et al. (2017). Metabolomics: definitions and significance in systems biology. *Adv. Exp. Med. Biol.* 965, 3–17. doi: 10.1007/978-3-319-47656-8_1

Kloehn, J., Blume, M., Cobbold, S., Saunders, E., Dagley, M., and Mcconville, M. (2016). Using metabolomics to dissect host-parasite interactions. *Curr. Opin. Microbiol.* 32, 59–65. doi: 10.1016/j.mib.2016.04.019

Koncarevic, S., Bogumil, R., and Becker, K. (2010). SELDI-TOF-MS analysis of chloroquine resistant and sensitive *Plasmodium falciparum* strains. *Proteomics* 7, 711–721. doi: 10.1002/pmic.200600552

Lakshmanan, V., Rhee, K. Y., and Daily, J. P. (2011). Metabolomics and malaria biology. *Mol. Biochem. Parasitol.* 175, 104–111. doi: 10.1016/j.molbiopara.2010.09.008

Lamour, S. D., Straschil, U., Saric, J., and Delves, M. J. (2014). Changes in metabolic phenotypes of *Plasmodium falciparum* in vitro cultures during gametocyte development. *Malaria J.* 13, 468. doi: 10.1186/1475-2875-13-468

Leopold, S. J., Ghose, A., Allman, E., Kingston, H. W. F., Hossain, A., Dutta, A. K., et al. (2019). Identifying the components of acidosis in patients with severe *Plasmodium falciparum* Malaria using metabolomics. *J. Infect. Dis.* 219, 1766–1776. doi: 10.1093/infdis/jiy727

Li, J. V., Wang, Y., Saric, J., Nicholson, J. K., Dirnhofer, S., Singer, B. H., et al. (2008). Global metabolic responses of NMRI mice to an experimental *Plasmodium berghei* infection. *J. Proteome Res.* 7, 3948–3956. doi: 10.1021/pr800209d

Lian, L., Alhelal, M., Roslaini, A. M., Fisher, N., Bray, P. G., Ward, S. A., et al. (2009). Glycerol: an unexpected major metabolite of energy metabolism by the human malaria parasite. *Malaria J.* 8, 38. doi: 10.1186/1475-2875-8-38

Lindner, S. E., Swearingen, K. E., Shears, M. J., Walker, M. P., and Kappe, S. H. I. (2019). Transcriptomics and proteomics reveal two waves of translational repression during the maturation of malaria parasite sporozoites. *Nat. Commun.* 10, 4964. doi: 10.1038/s41467-019-12936-6

Macrae, J. I., Dixon, M. W. A., Dearnley, M. K., Chua, H. H., Chambers, J. M., Kenny, S., et al. (2013). Mitochondrial metabolism of sexual and asexual blood stages of the malaria parasite *Plasmodium falciparum*. *BMC Biol.* 11:67. doi: 10.1186/1741-7007-11-67

Macrae, J. I., Sheiner, L., Nahid, A., Tonkin, C. J., Striepen, B., and Mcconville, M. J. (2012). Mitochondrial metabolism of glucose and glutamine is required for intracellular growth of *Toxoplasma gondii*. *Cell Host Microbe* 12, 682–692. doi: 10.1016/j.chom.2012.09.013

Mancio-Silva, L., Slavic, K., Ruivo, M. T. G., Grosso, A. R., Modrzynska, K. K., Vera, I. M., et al. (2017). Nutrient sensing modulates malaria parasite virulence. *Nature* 547, 213–216. doi: 10.1038/nature23009

Markley, J. L., Bruschweiler, R., Edison, A. S., Eghbalnia, H. R., Powers, R., Raftery, D., et al. (2017). The future of NMR-based metabolomics. *Curr. Opin. Biotechnol.* 43, 34–40. doi: 10.1016/j.copbio.2016.08.001

Martin, R. E., Marchetti, R. V., Cowan, A. I., Howitt, S. M., Broeer, S., and Kirk, K. (2010). Chloroquine transport via the malaria parasite's chloroquine resistance transporter. *Ence* 325, 1680–1682. doi: 10.1126/science.1175667

Mehta, M., Sonawat, H. M., and Sharma, S. (2006). Glycolysis in *Plasmodium falciparum* results in modulation of host enzyme activities. *J. Vect. Borne Dis.* 43, 95–103. doi: 10.1016/j.ijid.2010.02.2247

Menard, D., and Dondorp, A. (2017). Antimalarial drug resistance: a threat to Malaria elimination. *Cold Spring Harb. Perspect. Med.* 7, a025619. doi: 10.1101/cshperspect.a025619

Miller, L. H., Ackerman, H. C., Su, X. Z., and Wellems, T. E. (2013). Malaria biology and disease pathogenesis: insights for new treatments. *Nat. Med.* 19, 156–167. doi: 10.1038/nm.3073

Misra, B. B., Fahrmann, J. F., and Grapov, D. (2017). Review of emerging metabolomic tools and resources: 2015–2016. *Electrophoresis* 38, 2257–2274. doi: 10.1002/elps.201700110

Müller, S., and Kappes, B. (2007). Vitamin and cofactor biosynthesis pathways in *Plasmodium* and other apicomplexan parasites. *Trends Parasitol.* 23, 112–121. doi: 10.1016/j.pt.2007.01.009

Murithi, J. M., Owen, E., Istvan, E. S., Lee, M. C. S., Ottilie, S., Chibale, K., et al. (2020). Combining stage specificity and metabolomic profiling to advance antimalarial drug discovery. *Chem. Biol.* 27, 158–171. doi: 10.1016/j.chembiol.2019.11.009

Ng, W. W., Kloehn, J., Ng, M., Saunders, E. C., Mcconville, M. J., and Chambers, J. M. (2014). Induction of a stringent metabolic response in intracellular stages of *Leishmania mexicana* leads to increased dependence on mitochondrial metabolism. *PLoS Pathog.* 10:e1003888. doi: 10.1371/journal.ppat.1003888

Olliaro, P. (2001). Mode of action and mechanisms of resistance for antimalarial drugs. *Pharmacol. Therap.* 89, 207–219. doi: 10.1016/S0163-7258(00)00115-7

Olszewski, K. L., Morrisey, J. M., Wilinski, D., Burns, J. M., Vaidya, A. B., Rabinowitz, J. D., et al. (2009). Host-parasite interactions revealed by *Plasmodium falciparum* metabolomics. *Cell Host Microbe* 5, 191–199. doi: 10.1016/j.chom.2009.01.004

Park, Y., Shi, Y. P., Liang, B., Medriano, C. A., Jeon, Y. H., Torres, E., et al. (2015). High-resolution metabolomics to discover potential parasite-specific biomarkers in a *Plasmodium falciparum* erythrocytic stage culture system. *Malaria J.* 14, 122. doi: 10.1186/s12936-015-0651-1

Saito, K., and Matsuda, F. (2010). Metabolomics for functional genomics, systems biology, and biotechnology. *Annu. Rev. Plant Biol.* 61, 463–489. doi: 10.1146/annurev.arplant.043008.092035

Salinas, J. L., Kissinger, J. C., Jones, D. P., and Galinski, M. R. (2014). Metabolomics in the fight against malaria. *Mem. Inst. Oswaldo Cruz* 109, 589–597. doi: 10.1590/0074-0276140043

Sana, T. R., Gordon, D. B., Fischer, S. M., Tichy, S. E., Kitagawa, N., Lai, C., et al. (2013). Global mass spectrometry based metabolomics profiling of erythrocytes infected with *Plasmodium falciparum*. *PLoS One* 8:e60840. doi: 10.1371/journal.pone.0060840

Sengupta, A., Ghosh, S., Das, B. K., Panda, A., Tripathy, R., Pied, S., et al. (2016). Host metabolic responses to *Plasmodium falciparum* infections evaluated by 1H NMR metabolomics. *Mol. BioSyst.* 12, 3324–3332. doi: 10.1039/c6mb00362a

Siddiqui, G., Srivastava, A., Russell, A., and Creek, D. J. (2017). Multi-omics based identification of specific biochemical changes associated with PfKelch13-mutant artemisinin resistant *Plasmodium falciparum*. *J. Infect. Dis.* 215, 1435–1444. doi: 10.1093/infdis/jix156

Sills, J., Koenraadt, C. J. M., and Takken, W. (2018). Integrated approach to malaria control. *Ence* 359, 528–529. doi: 10.1126/science.aar7554

Skretas, G., and Wood, D. W. (2005). Regulation of protein activity with small-molecule-controlled inteins. *Protein Sci.* 14, 523–532. doi: 10.1110/ps.04996905

Sperber, H., Mathieu, J., Wang, Y., Ferreccio, A., Hesson, J., Xu, Z., et al. (2015). The metabolome regulates the epigenetic landscape during naive-to-primed human embryonic stem celltransition. *Nat. Cell Biol.* 17, 1523–1535. doi: 10.1038/ncb3264

Srivastava, A., Philip, N., Hughes, K. R., Georgiou, K., Macrae, J. I., Barrett, M. P., et al. (2016). Stage-specific changes in Plasmodium metabolism required for differentiation and adaptation to different host and vector environments. *PLoS Pathog.* 12:e1006094. doi: 10.1371/journal.ppat.1006094

Summers, R. L., Nash, M. N., and Martin, R. E. (2012). Know your enemy: understanding the role of PfCRT in drug resistance could lead to new antimalarial tactics. *Cell. Mol. Life Sci.* 69, 1967–1995. doi: 10.1007/s00018-011-0906-0

Surowiec, I., Orikiiriza, J., Karlsson, E., Nelson, M., Bonde, M., Kyamanwa, P., et al. (2015). Metabolic signature profiling as a diagnostic and prognostic tool in pediatric *Plasmodium falciparum* Malaria. *Open Forum Infect. Dis.* 2, ofv062. doi: 10.1093/ofid/ofv062

Teng, R., Lehane, A. M., Winterberg, M., Shafik, S. H., Summers, R. L., Martin, R. E., et al. (2014). 1H-NMR metabolite profiles of different strains of *Plasmodium falciparum*. *Biosci. Rep.* 34, e00150. doi: 10.1042/BSR20140134

Tilley, L., Straimer, J., Gnädig, N. F., Ralph, S. A., and Fidock, D. A. (2016). Artemisinin action and resistance in *Plasmodium falciparum*. *Trends Parasitol.* 32, 682–696. doi: 10.1016/j.pt.2016.05.010

Uppal, K., Salinas, J. L., Monteiro, W. M., Val, F., Cordy, R. J., Liu, K., et al. (2017). Plasma metabolomics reveals membrane lipids, aspartate/asparagine and nucleotide metabolism pathway differences associated with chloroquine resistance in Plasmodium vivax malaria. *PLoS One* 12:e0182819. doi: 10.1371/journal.pone.0182819

Vaughan, A. M., O"Neill, M. T., Tarun, A. S., Camargo, N., Phuong, T. M., Aly, A. S. I, et al. (2010). Type II fatty acid synthesis is essential only for malaria parasite late liver stage development. *Cell. Microbiol.* 11, 506–520. doi: 10.1111/j.1462-5822.2008.01270.x

Vincent, I. M., and Barrett, M. P. (2015). Metabolomic-based strategies for anti-parasite drug discovery. *J. Biomol. Screen.* 20, 44–55. doi: 10.1177/1087057114551519

World Health Organization (2019). *World Malaria Report 2018*. Geneva: WHO.

Zhu, G. (2004). Current progress in the fatty acid metabolism in *Cryptosporidium parvum*. *J. Euk. Microbiol.* 51, 381–388. doi: 10.1111/j.1550-7408.2004.tb00384.x

Zhu, L., Tripathi, J., Rocamora, F. M., Miotto, O., Rob, V. D. P., Voss, T. S., et al. (2018). The origins of malaria artemisinin resistance defined by a genetic and transcriptomic background. *Nat. Commun.* 9, 5158. doi: 10.1038/s41467-018-07588-x

Conflict of Interest: The authors declare that the research was conducted in the absence of any commercial or financial relationships that could be construed as a potential conflict of interest.

GLOSSARY

Asexual blood stage: one life cycle refers to the *Plasmodium* infection and development in host erythrocytes. Parasite morphologically transition from ring to trophozoite and further to schizont which is capable to release infectious merozoites for invasion.

Biofluids: any organism derived bio-organic fluids including blood, urine, saliva, cerebrospinal fluid, etc.

Erythrocyte: a set of vertebrate red blood cell.

Metabolic fingerprint: high-throughput classification of candidates according to global patterns of captured metabolite signals without exact identification.

Metabolic profiling: quantification analysis of whole metabolome (known and unknown) as precise possible to obtain the overall metabolic spectrum with respect to their chemical nature or metabolic pathways in biosamples.

Metabolites: small molecules that are biosynthesized, processed, and degraded resulted from cellular metabolic reactions.

Metabolome: chemical entities including both primary and secondary metabolites, metabolic intermediates, and signal compounds in biosamples.

Omics: an extensive term for strategies aim at exhaustively analyzing whole class of biomolecules including genome, transcriptome, proteome and metabolome.

Sexual gametocyte stage: life stage during which a portion of asexually reproducing merozoites undergo reprogrammed sexual differentiation to form gametocytes.

Systems biology: comprehensive analysis from overall perspective without only focusing on specific part.

frontiers in Microbiology

ORIGINAL RESEARCH
published: 12 January 2021
doi: 10.3389/fmicb.2020.595080

Ac-HSP20 Is Associated With the Infectivity and Encystation of *Acanthamoeba castellanii*

Ningning Wang[1†], Hongyu Sun[1†], Di Liu[1], Xiaoming Jiang[1], Meiyu Zheng[1], Wenhe Zhu[1], Quan Liu[3], Wenyu Zheng[2] and Xianmin Feng[1]**

[1]Department of Pathogenic Biology, Jilin Medical University, Jilin City, China, [2]Department of Microsurgery, Jilin City Central Hospital, Jilin City, China, [3]School of Life Sciences and Engineering, Foshan University, Foshan, China

Acanthamoeba castellanii is a pathogenic and opportunistic free-living amoeba that causes *Acanthamoeba* keratitis (AK) and granulomatous amebic encephalitis (GAE) in immunocompromised individuals. The biological and pathogenic characterizations behind this opportunistic protozoan is not fully understood. This study aimed to determine the biological functions of heat shock protein (HSP)-20 of *A. castellanii* (*Ac*-HSP20) involved in the maintenance of life cycle and the infectivity of *A. castellanii*. Immunoscreening *A. castellanii* cDNA library with *A. castellanii* infected rabbit sera identified three positive clones, one of them was a putative heat shock protein (*Ac*-HSP20). The recombinant 23 kDa *Ac*-HSP20 protein (r*Ac*-HSP20) was successfully expressed in *Escherichia coli* BL21 (DE3) and purified using metal affinity chromatography. The rabbits immunized with r*Ac*-HSP20 produced high titer antibody (1:25,600). Immunolocalization with the antibody identified the expression of native *Ac*-HSP20 on the surface of both *A. castellanii* trophozoites and cysts. Further, Western blot with antibody identified that the expression of native Ac-HSP20 was 7.5 times higher in cysts than in trophozoites. Blocking *Ac*-HSP20 on the membrane of trophozoites with specific antibody or silencing *Ac-hsp20* gene transcription by siRNA inhibited their transformation into cysts at the early stage but returned to normal at the late stage by stimulating the transcription of *Ac-hsp20*. Incubation of trophozoites with anti-*Ac*-HSP20 IgG increased macrophage-involved phagocytosis to the protozoa and inhibited trophozoite infectivity on the cornea of rabbits compared with that without antibody. Our study provides that *Ac*-HSP20 is a surface antigen involved in the encystation and infectivity of *A. castellanii* and thus an important target for vaccine and drug development.

Keywords: *Acanthamoeba*, heat shock protein-20, encystation, infectivity, *Acanthamoeba* keratitis

OPEN ACCESS

Edited by:
Bang Shen,
Huazhong Agricultural University, China

Reviewed by:
Shinuo Cao,
Chinese Academy of Agricultural Sciences, China
Hamed Mirjalali,
Shahid Beheshti University of Medical Sciences, Iran

****Correspondence:***
Xianmin Feng
fengxianmin28@163.com
Wenyu Zheng
zwy2002468@sina.com

†These authors have contributed equally to this work

Specialty section:
This article was submitted to Infectious Diseases, a section of the journal Frontiers in Microbiology

Received: *15 August 2020*
Accepted: *01 December 2020*
Published: *12 January 2021*

Citation:
Wang N, Sun H, Liu D, Jiang X, Zheng M, Zhu W, Liu Q, Zheng W and Feng X (2021) Ac-HSP20 Is Associated With the Infectivity and Encystation of Acanthamoeba castellanii. Front. Microbiol. 11:595080. doi: 10.3389/fmicb.2020.595080

INTRODUCTION

Acanthamoeba castellanii is a free-living protozoan that can cause *Acanthamoeba* keratitis (AK) and granulomatous amebic encephalitis (GAE) in immunocompromised individuals. AK is a rare and severe disease in which AK trophozoite adheres and infects the cornea epithelial cell layer and the paracentral corneal stroma, thereby causing permanent visual impairment (Clarke and Niederkorn, 2006; Khan, 2006; Siddiqui and Khan, 2012). The clinical signs of AK include photophobia, annular matrix infiltration, epithelial defect, and orbital edema. GAE is a life-threatening infection in central nervous system (CNS). It usually occurs in immunocompromised

individuals with solid organ transplantations or patients with AIDS (Marciano-Cabral and Cabral, 2003). People become infected through direct contact with contaminated water. The amoebae invade skin, sinuses, or lungs and then reach the CNS through hematogenous route to cause GAE and even death (Parija et al., 2015).

Acanthamoeba castellanii have two stages in its life cycle, including vegetative trophozoite and dormant cyst. Trophozoites usually live in soil and water in the environment fed on bacteria. When external environmental conditions are not suitable for amoeba growth, such as extreme changes in temperatures, pH, osmolarity, and desiccation, the trophozoite transforms into cyst, which is a self-protective form. When stress conditions are removed, the cyst can reverse back to its trophozoite form. Studies have shown that trophozoites are more susceptible to antimicrobial agents than cysts (Lorenzo-Morales et al., 2013; Mahboob et al., 2020), but cysts are resistant to chemicals and could survive in the environment and maintain their pathogenicity for several years. Trophozoites are related to the adhesion and invasion causing diseases, while cysts are related to chronicity, drug resistance, recurrence, and transmission of the infection (Turner et al., 2000, 2004). Meanwhile, cysts could survive several years as a source of recurrent transmission. Therefore, preventing trophozoites from being converted to cysts is important to the treatment of *A.castellanii* infections and blocking its transmission.

Given the difficulty in diagnosing *Acanthamoeba*-caused AK and GAE and the serious consequences of the infection (Visvesvara, 2010), it is needed to develop a vaccine especially for those with immunocompromising conditions. In an effort to identify antigens that are immunogenic and protective as vaccine candidates, a serum from rabbit infected with *A. castellanii* in its corneal stroma was used in the present study to immunoscreen a cDNA library of *A. castellanii* trophozoites. One of the positive clones encoded the heat shock protein (HSP)-20 of *A. castellanii* (*Ac*-HSP20). HSPs are a group of highly conserved proteins found in all organisms that primarily function as molecular chaperones (Lindquist and Craig, 1988). In accordance with their molecular weight, the proteins in HSP superfamily are classified into eight major sub-families: HSP110, HSP100, HSP90, HSP70, HSP60, HSP40, HSP10, and small HSP (sHSP; Feder and Hofmann, 1999). HSP20 is one of the sHSPs with the characteristics of the sHSP family. When cells are under stress, sHSPs could bind to denatured proteins and maintain a competitive folding state to prevent their irreversible aggregation (Sun and MacRae, 2005; Nakamoto and Vígh, 2007). sHSPs play important roles in maintaining life cycle and the pathogenicity of parasites. Knockout of HSP20 in *Plasmodium berghei* affected the substrate-dependent cell movement of sporozoites and reduced sporozoite-matrix adhesion and the spread of natural malaria (Montagna et al., 2012). In *Leishmania* protozoa, the deletion of HSP23 reduces their viability in harsh environment with chemical stressors, such as ethanol and semimetal ions, and loses the ability to infect macrophages (Hombach et al., 2014).

In the present study, we reported the cloning of *Ac*-HSP20 at the first time and its functions in encystation and infectivity of *A. castellanii*. The results showed that this protein is one of the immunodominant antigens and plays a vital role in the maintenance of *Acanthamoeba*'s life cycle.

MATERIALS AND METHODS

A. castellanii Cultivation

Acanthamoeba castellanii cysts were obtained from ATCC (ATCC 30011) and cultured in peptone-yeast extract-glucose medium containing 50 μg/ml of gentamicin, pH 6.5, in a cell culture flask at 25°C to transform into trophozoite form. The cultured trophozoites were fed with heat-killed *Escherichia coli* (ATCC 29552) and harvested at their logarithmic growth phase 3–5 days after cultivation. The cysts were harvested after cultivation for 10–14 days.

Animals

New Zealand white rabbits (8–10 months old weighing 2.5–4 kg) were purchased from the Animal Facility of Jilin University (China). The experimental protocols were approved by the Animal Care and Use Committee of the Jilin Medical College (approval number: 190001). The animal care and treatment in this study followed the statement of the Association for Research in Vision and Ophthalmology.

Rabbit Peritoneal Macrophages

One rabbit was injected with 200 ml of LB broth into the peritoneal cavity, and the cavity liquid was retrieved 3 days after the injection. The macrophages were isolated from the retrieved cavity liquid by adhering on culture flasks. The obtained rabbit macrophages were maintained in RPMI 1640 medium supplemented with 10% fetal bovine serum and 50 μg/ml of streptomycin, 100 U/ml of penicillin, and 50 μg/ml of gentamicin in a cell culture flask at 5% CO_2, 37°C.

Cloning of *Ac*-HSP20

One rabbit was infected with 1×10^4 *A. castellanii* trophozoites through micro-injection into the eye stroma to induce AK. The serum was obtained to immunoscreen the cDNA library *A.castellanii* trophozoite as described before (Wang et al., 2014; Feng et al., 2015). The DNA was extracted from the positive clones for double-stranded DNA sequencing. The obtained DNA sequences were aligned with sequences deposited in GenBank through Basic Local Alignment Search Tool (BLAST) search to conclude their homologs. One of the three positive clones shared 59% amino acid sequence identity with a Hsp20/alpha crystallin superfamily protein of *A. castellanii* (GenBank accession: XP_004336746.1; Zhang et al., 2018), thus named as *Ac*-HSP20 at the first time.

Expression and Purification of Recombinant *Ac*-HSP20 and Preparation of Polyclonal Antibodies

The DNA encoding for *Ac*-HSP20, synthesized in Beijing Genomics Institute, was subcloned into pET-22b expression vector

(New England Biolabs, Beijing, China) by using BamHI and HindIII sites. The sequencing-confirmed recombinant pET-22b-*Ac*-HSP20 plasmid was transformed into *E. coli* BL21 (DE3) competent cell (Beyotime, Beijing, China). The recombinant *Ac*-HSP20 protein (r*Ac*-HSP20) was expressed under the induction of 1 mM of IPTG. The expressed r*Ac*-HSP20 with His-tag at C-terminus was purified *via* nickel affinity and DEAE ion-exchange chromatography. The anti-*Ac*-HSP20 serum was produced by immunizing a rabbit with 400 μg of r*Ac*-HSP20 emulsified with complete Freund's adjuvant and boosted twice with 200 μg of r*Ac*-HSP20 emulsified with incomplete Freund's with 2-week interval. The anti-*Ac*-HSP20 IgG was purified from the antiserum through a HiTrap Protein A HP column (GE Healthcare, United States). The antibody titer of the purified polyclonal antibody was measured using ELISA.

Immunofluorescence Assay

The fresh trophozoites of *A. castellanii* were washed with the pH 7.4 phosphate buffered saline (PBS), overlaid on a coverslip pretreated with 1 mg/ml of poly-L-lysine, and then fixed with 3% paraformaldehyde, followed by permeabilization with 0.25% Triton X-100. The protozoa were incubated with rabbit anti-*Ac*-HSP20 IgG (20 μg/ml) or normal rabbit serum (1:50) and then with Alexa Fluor 488-conjugated anti-rabbit IgG secondary antibody (1 μg/ml, Abcam, United States). The trophozoites were counterstained for the nucleus with 1 μg/ml of 4',6-diamino-2-phenylindole and stained for the cytomembrane with 10 umol 1,1'-dioctadecyl-3,3,3',3'-tetramethylindocarbocyanine perchlorate (DiI). Images were captured with a laser scanning confocal microscope (Olympus, Tokyo, Japan).

Macrophage Phagocytosis of *A. castellanii* Trophozoites

Freshly collected 1×10^5 *A. castellanii* trophozoites were incubated with the same number of macrophages collected from the rabbit peritoneal cavity in the presence of different amounts of rabbit anti-*Ac*-HSP20 IgG (40, 20, 10, 5, 2.5, and 1.25 μg/ml). Normal rabbit serum was used as the control (1:50 dilution). The cells were incubated in a CO_2 incubator at 37°C for 2 h. The change in macrophage phagocytosis of the trophozoites was observed under the microscope. The macrophage phagocytosis rate was calculated by courting the number of macrophages with engulfed trophozoites.

Rabbit Corneal Infection With *A. castellanii*

Eight New Zealand rabbits were randomly divided into two groups with four rabbits each. The eyes of all rabbits were immunosuppressed with 0.5% hydrocortisone ophthalmic solution drops four times daily for 3 consecutive days before exposure to *A. castellanii* trophozoites. In the experimental group, the right eyes of four rabbits were inoculated with 200 μl of 2×10^5 *A. castellanii* trophozoites preincubated with rabbit anti-*Ac*-HSP20 IgG (40 μg/ml) at 37°C for 30 min. In the control group, the right eyes of four rabbits were infected with the same number of trophozoites without incubation with antibody. The left eyes of all rabbits were dropped with 200 μl of sterile saline as the normal control. Corneal scraping was performed on days 3, 7, 14, and 28 after the infection, the living trophozoite number was counted under three randomly-picked fields, and the average was calculated to determine the intensity of corneal infection.

The Expression of *Ac*-HSP20 in *A. castellanii* Trophozoites and Cysts

Freshly collected *A. castellanii* trophozoites were incubated with rabbit anti-*Ac*-HSP20 IgG (40 μg/ml) for 30 min before being placed on ice for 0, 6, 12, and 24 h. In control group, the same numbers of trophozoites were directly put on ice without incubating with antibody. The transformation rate from trophozoite to cyst at different time points was measured and counted under the microscope.

The transcriptional expression levels of *Ac-hsp20* at different cooling time points were measured with real-time quantitative PCR (qPCR). The total RNAs of *A. castellanii* trophozoites or cysts at different time points were extracted using an RNA extraction kit (Beyotime, Beijing, China). The concentration of RNA was measured at A260 and the purity was checked at A260/280. The quality and integrity of RNA were assessed on 1% formaldehyde-agarose gel. The total RNA was treated with DNase I and then reverse transcribed into cDNA by using Oligo dT primers. The transcriptional level of *Ac-hsp20* was quantitatively measured using qPCR (NovoStart SYBR qPCR SuperMix Plus, Novoprotein, Shanghai, China) with specific primers 5'-AAGGCGAGAACTGGGTGA-3' (forward) and 5'-CGGGCTTGGGTACTACAAT-3' (reverse). The beta-actin (β-actin) housekeeping gene was measured as the control by using primers 5'-GTATGCTCCTCCTCAAG-3' (forward) and 5'-TAGAAGGTGTCCATCCA-3' (reverse). All qPCR assays were conducted in an ABI 7500 fast real-time PCR system (ABI7500 Fast, United States).

To determine the protein expression levels of native *Ac*-HSP20 at the different stages of *A. castellanii*, total proteins were extracted from 1×10^8 trophozoites or cysts by suspending in cell lysis buffer containing 10 mM of PMSF for 30 min and sonicating for several times on ice. The lysates were centrifuged at 12,000 rpm for 10 min, and the supernatants were collected as *A. castellanii* trophozoite or cyst extracts for Western blot with anti-*Ac*-HSP20 IgG.

For Western blot, the same amount of trophozoite or cyst extracts (40 μg) was run on SDS-PAGE and then transferred on polyvinylidene fluoride (PVDF) membrane. The membrane was recognized using rabbit anti-*Ac*-HSP20 IgG (2 μg/ml). Meanwhile, the same amount of extracts was recognized using rabbit anti-β-actin serum (1 μg/ml, Bioss, Beijing, China) as the comparative control. Normal rabbit serum was used as negative control. HRP-conjugated goat anti-rabbit IgG were used as secondary antibody (Bioss, Beijing, China). The blots were visualized using ECL chemiluminescence reagents (Beyotime, Beijing, China) and imaged on a luminescence imaging system (Tanon, Beijing, China).

Silence of *Ac-hsp20* expression with siRNA to silence the *Ac-hsp20* gene expression, the siRNA targeting *Ac-hsp20* was designed and performed by GenePharma (Shanghai, China).

The siRNA duplex with sense (5'GACUGGUCAGCUAGCGAG AUTT-3') and anti-sense (5′UGAUCUCGCUAGCUGACCAGCT T-3') sequences were synthesized and conjugated with FITC. The siRNA was added into 1×10^6 *A. castellanii* trophozoites to 200 nM in total volume of 2.5 ml PYG media. The siRNA duplex with sense 5'-UUCUCCGAAC GUGUCACGUTT-3') and anti-sense (5'-ACGUACACGUUCGGAGAATT-3') was used for negative control (NC). After being incubated for 6 h, the trophozoites were washed with PYG medium and the intake of siRNA in the trophozoites was observed and imaged under a fluorescence microscope. Twelve hours after the incubation, qPCR was performed to measure the *Ac-hsp20* mRNA transcription level, and *Ac*-HSP20 protein expression level was performed by Western blot as described above 48 h after the siRNA transfection. To investigate the role of *Ac*-HSP20 in the encystation of *A. castellanii* trophozoite, siRNA transfection was performed in trophozoites. Twelve hours after siRNA transfection, the trophozoites were incubated on ice and the encystation rate was counted under microscope 0, 6, 12, and 24 h after being incubated on ice.

Statistical Analysis

GraphPad Prism8 software was used to analyze the experimental data. The results were expressed as mean ± standard deviation; statistical analysis was performed using one-way or two-way ANOVA to determine the significance of the difference between two groups. $p < 0.05$ indicated statistically significant difference ($^{*}p < 0.05$, $^{**}p < 0.01$, and $^{***}p < 0.001$).

RESULTS

Cloning of *Ac*-HSP20

Three positive clones were obtained after screening 2×10^5 colonies of *A. castellanii* trophozoite cDNA expression library with serum of rabbit infected with *A. castellanii* in its corneal. One of the positive clones shared 59% amino acid sequence identity with HSP20/alpha crystallin superfamily protein of *A. castellanii* (GenBank accession: XP_004336746.1), thus a new putative HSP20 family protein, named as *Ac*-HSP20. The sequence of *Ac*-HSP20 was submitted to GenBank, with accession number MT323119.

Expression of Recombinant *Ac*-HSP20

The 583 bp DNA coding for full-length *Ac*-HSP20 was successfully subcloned into pET22b (**Figure 1A**). The recombinant plasmid DNA was transformed into *E. coli* BL (DE3), and *Ac*-HSP20 was expressed as 26 kDa soluble recombinant protein (r*Ac*-HSP20) in the bacteria under the induction of 1 mM IPTG. The r*Ac*-HSP20 with His-tag was purified using nickel affinity chromatography (**Figure 1B**).

Ac-HSP20 Localization on the Membrane of *A. castellanii* Trophozoite and Cyst

To determine the subcellular localization of *Ac*-HSP20 in *A. castellanii* protozoa, the rabbit anti-*Ac*-HSP20 serum was raised in rabbit and the purified anti-*Ac*-HSP20 IgG was used to recognize native *Ac*-HSP20 expressed on *A. castellanii* trophozoite using IFA. IFA results showed that *Ac*-HSP20 was mainly localized on the cell membrane of *A. castellanii* trophozoite (**Figure 2**).

Anti-*Ac*-HSP20 Antibody Increased Macrophage Phagocytosis on *A. castellanii* Trophozoites

The macrophages were collected from rabbit peritoneal cavity and incubated with the same number of *A. castellanii* trophozoites in the presence of different amounts of rabbit anti-*Ac*-HSP20

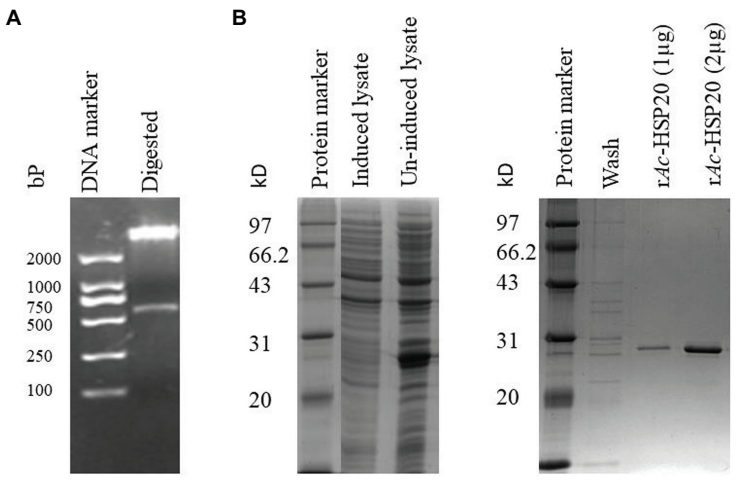

FIGURE 1 | Cloning and expression of recombinant heat shock protein (HSP)-20 of *Acanthamoeba castellanii* (*Ac*-HSP20) in *Escherichia coli* BL21 (DE3). Agarose gel electrophoresis showing a 583 bp insert digested with *Bam*HI and *Hind*III from *Ac-hsp20*/pET22b plasmid DNA **(A)**; SDS-PAGE of r*Ac*-HSP20 expressed in *E. coli* BL21 and the purified r*Ac*-HSP20 (2 μg; **B**).

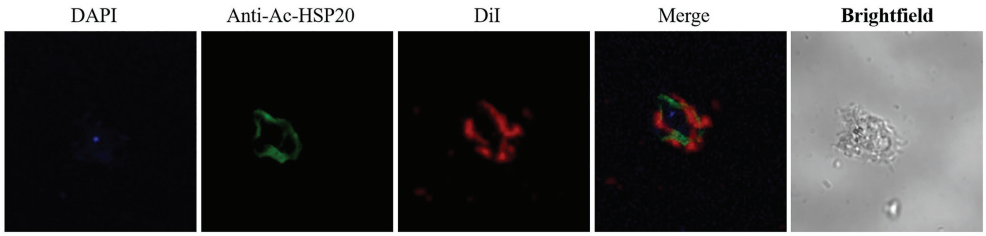

FIGURE 2 | Immunolocalization of *Ac*-HSP20 in *A. castellanii* trophozoite and cyst detected by IFA with anti-*Ac*-HSP20 IgG (20 μg/ml) and visualized by Alexa-Fluor488 labled anti-rabbit IgG secondary antibody (1 μg/ml). Normal rabbit serum (1:50) was used as control. Nuclei were stained with DAPI, membrane was stained with DiI. Scale bars: 10 μm.

IgG (40, 20, 10, 5, 2.5, and 1.25 μg/ml) to determine whether anti-*Ac*-HSP20 antibody induced antibody-dependent macrophage phagocytosis on *A. castellanii*. The rate of macrophage phagocytosis (containing *A. castellanii* trophozoite intracellularly) was 73.1% when the antibody concentration was 40 μg/ml. The phagocytosis dropped to 37.2% when the antibody concentration was decreased to 1.25 μg/ml, which was similar to the culture with addition of or normal rabbit serum (1:50), with statistical significance among the difference antibody amount ($^{***}p < 0.001$ and $^{**}p < 0.01$, **Figure 3**). These results demonstrated that anti-*Ac*-HSP20 IgG induced macrophage phagocytosis on *A. castellanii* trophozites.

Role of *Ac*-HSP20 in the Infectivity of *A. castellanii* Trophozoite to Rabbit Cornea

The right eyes of four rabbits were infected with 2×10^5 *A. castellanii* trophozoites, while another group of four rabbits was infected with the same number of trophozoites preincubated with rabbit anti-*Ac*-HSP20 IgG (40 μg/ml) on their right eyes. Corneal scraping was performed on days 3, 7, 14, and 28 after the infection, and the living trophozoites were counted on the corneal scrapes. The protozoan counting results showed no difference in the living protozoan number between the two groups on days 3 and 7. However, the living protozoan number was significantly reduced on the cornea of rabbits infected with *A. castellanii* trophozoites incubated with anti-*Ac*-HSP20 antibody at late stages (days 14 and 28) compared to the group of rabbits infected with protozoan without antibody ($p < 0.05$, **Figure 4**). No protozoan was observed on the left eyes of rabbits that received sterile saline in each group.

Predominant Expression of *Ac*-HSP20 Protein in *A. castellanii* Cysts

The same amount of trophozoite and cyst extracts was transferred on PVDF membrane and recognized using the rabbit anti-*Ac*-HSP20 IgG to further determine the expression of native HSP20 protein in different forms of *A. castellanii*. Western blot results showed that the expression of native *Ac*-HSP20 was 7.5 times higher in cysts than in trophozoites ($p < 0.05$), while the control β-actin was the same in both forms of *A. castellanii* (**Figures 5A,B**). Both trophozoite and cyst extracts were not recognized by normal rabbit serum. These results indicated that *Ac*-HSP20 was predominantly expressed in cyst and possibly essential for the encystation of *A. castellanii*.

Role of *Ac*-HSP20 in the Encystation of *A. castellanii* Trophozoite

Trophozoites typically begin to transform to cysts after being cooled down on ice, most of them transformed into cysts within 24 h. However, after being incubated with 40 μg/ml of rabbit anti-*Ac*-HSP20 IgG, the cyst transformation was significantly reduced at the early time points (6 and 12 h) compared with group without antibody (PBS). However, no significant difference in cyst transformation was noted between the antibody and PBS groups at 24 h time point, with most trophozoites transformed into cysts at both groups (**Figures 6A,B**). However, gene transcription results showed that incubation with anti-*Ac*-HSP20 IgG significantly increased the *Ac-hsp20* gene transcription level upon temperature cooling down compared with protozoa without antibody incubation ($^{*}p < 0.05$ and $^{**}p < 0.001$, **Figure 6C**).

The transcription of *Ac-hsp20* in *A. castellanii* trophozoites was efficiently silenced by gene-specific siRNA transfection (**Figure 7**). The expression of *Ac*-HSP20 was significantly inhibited at gene transcriptional level (**Figure 7B**) or at protein expression level (**Figures 7C,D**) compared to negative control (xx gene?). The encystation of *A. cantellanii* trophozoites was also significantly inhibited after the *Ac-hsp20* gene transcription was silenced by siRNA transfection (**Figure 8**) at the early cooling down time points (6 and 12 h), but recovered to the similar level to the control group at 24 h time point, consistent to the results of antibody inhibition. The results further suggest that *Ac*-HSP20 is essential for the encystation of *A. castellanii* trophozoites.

DISCUSSION

Acanthamoeba castellanii is a free-living protozoan, and its life cycle includes trophozoite and cyst forms. When the amoeba encounters an unfavorable living environment, the trophozoite form could quickly transform into cyst form as a self-protection mechanism. This encystation process involves massive turnover of cellular components and remodeling of organelle structure

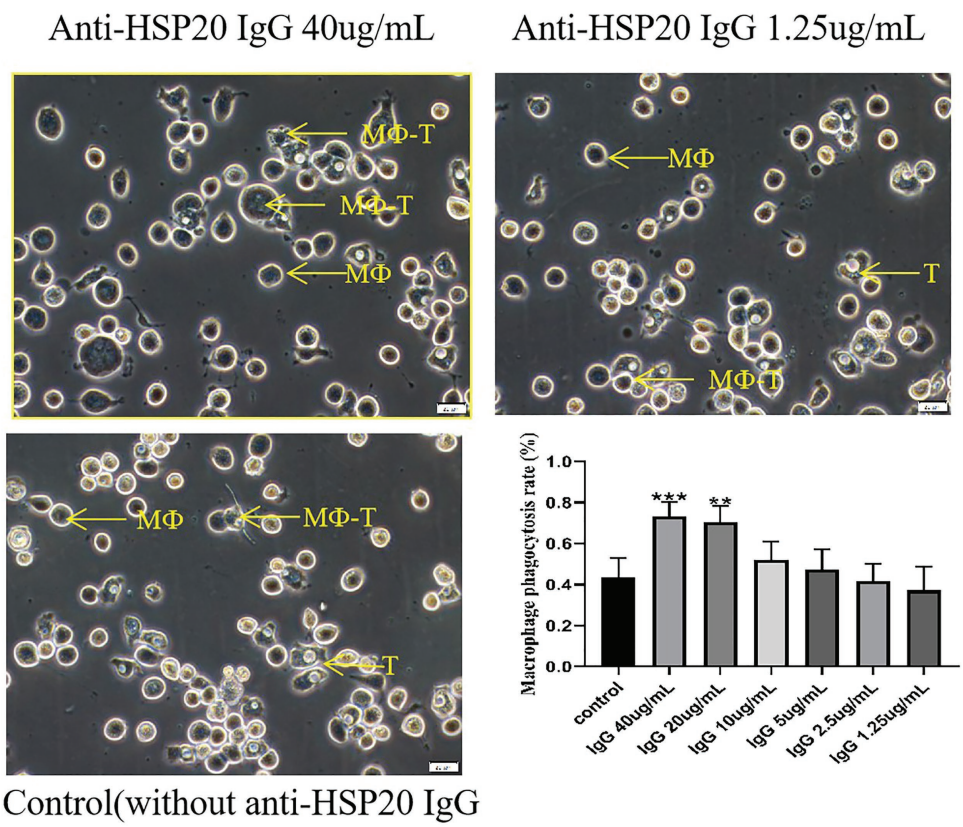

FIGURE 3 | *Ac*-HSP20 antibody induced macrophage phagocytosis on *A. castellanii* trophozoites at a IgG amount-dependent pattern. The phagocytosis of macrophages on *A. castellanii* trophozoites after co-incubation with anti-Ac-HSP20 IgG at 40 μg/ml and 1.25 μg/ml, or normal rabbit serum (1:50) as control, was observed under microscope. The macrophage phagocytosis rate at different amount of anti-*Ac*-HSP20 IgG was shown at downright penal. ***$p < 0.001$, **$p < 0.01$, compared with normal control. МФ, macrophage; T, trophozoites; МФ-T, macrophages with trophozoite phagocytized. Scale bars:20 μm.

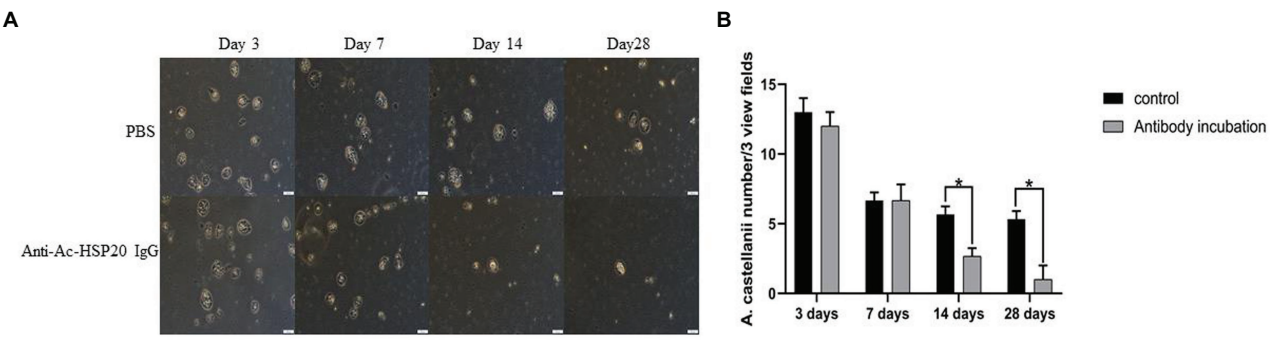

FIGURE 4 | Observation of *A. castellanii* trophozoite on corneal scraping of rabbits after being infected with 2×10^5 *A. castellanii* trophozoites incubated with PBS or with rabbit anti-*Ac*-HSP20 IgG (40 μg/ml) on day 3, 7, 14, and 28 after infection under microscope **(A)**. The average counted number of trophozoites per three view fields at different day points (**B**; *$p < 0.05$). Scale bar: 20 μm.

and function to produce a cryptobiotic cell with resistance to desiccation, heat, freezing, and chemical stresses (Magistrado-Coxen et al., 2019; Baig et al., 2020). However, the detail mechanism involved in the encystation of *A. castellanii* trophozoite is unknown. Identification of molecules involved in the cyst transformation is crucial for understanding the encysting process and self-protection mechanism. Blocking the process by targeting the molecules involved in the encystation

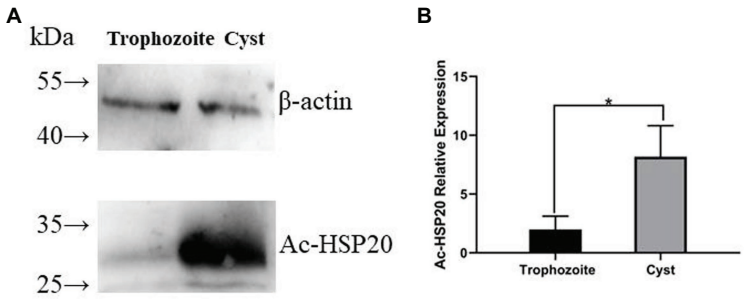

FIGURE 5 | The predominant expression of *Ac*-HSP20 in cysts of *A. castellanii* determined by Western blot with anti-*Ac*-HSP20 IgG. Total 40 μg of *A. castellanii* trophozoite and cyst extracts was transferred on polyvinylidene fluoride (PVDF) membrane, recognized by rabbit anti-*Ac*-HSP20 IgG (2 μg/ml). The same amount of protozoan extracts was equally recognized by anti-β-actin as control **(A)**. Statistical analysis of the predominant expression of *Ac*-HSP20 in cysts of *A. castellanii* (*$p < 0.05$; **B**).

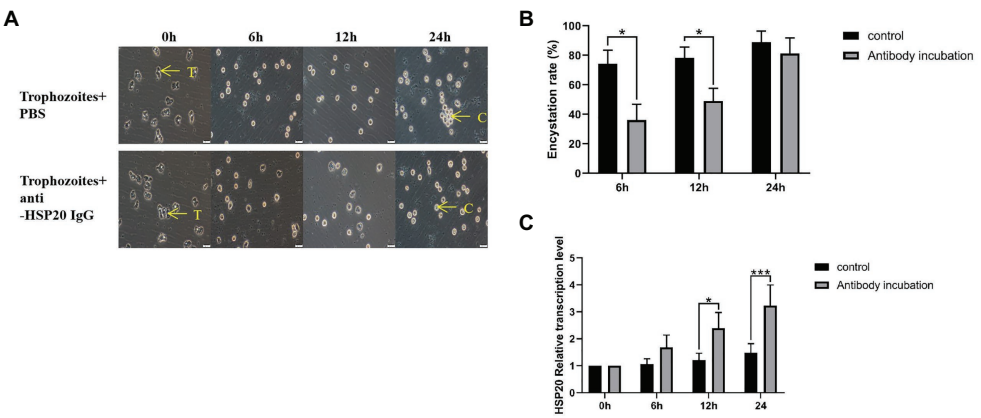

FIGURE 6 | Effect of *Ac*-HSP20 on the encystation of *A. castellanii* trophozoites. The trophozoites were incubated with 40 μg/ml rabbit-anti-*Ac*-HSP20 IgG or PBS control and then cooled down on ice for 0, 6, 12, and 24 h. The transformation from trophozoites to cysts was observed under microscope **(A)**. The encystation rate of *A. castellanii* trophozoites at different ice incubation time points was calculated **(B)**. The *Ac-hsp20* gene transcription level in protozoa at different cooling time points was measured by quantitative PCR (qPCR) compared to trophozoites without antibody incubation (*$p < 0.05$, ***$p < 0.001$; **C**). T, trophozoites; C, cysts. Scale bars: 20 μm.

could be a good approach to interrupt its life cycle because trophozoites are susceptible to chemotherapy and cysts are resistant and contribute to the recurrence and transmission of infection. In this study, a putative *Ac*-HSP20 protein was identified to be an immunodominant protein recognized by the serum from rabbit infected with *A. castellanii*, indicating that this protein was exposed to host immune system during infection. Immunolocalization assay with specific antibody revealed that the native *Ac*-HSP20 was mostly expressed on the surface of trophozoites. Further systematic study with qPCR identified that the expression of *Ac-hsp20* was gradually increased when the trophozoites were cooled down on ice and transformed to cysts (**Figure 6**). The expression of native *Ac*-HSP20 protein was 7.5 times higher in cysts than in trophozoites, as determined using Western blot with anti-*Ac*-HSP20 antibody (**Figure 5**). The predominant expression of *Ac*-HSP20 in cysts indicated its important role in the encystation of *A. castellanii*. Indeed, when *Ac*-HSP20 was neutralized by the specific anti-*Ac*-HSP0 IgG, the transformation of trophozoites to cysts was reduced at the early stage of cooling down on ice (within 12 h) compared with those without antibody incubation ($p < 0.05$, **Figure 6**). However, at the late stage of encystation when the protozoa were placed on ice for 24 h, most trophozoites were transformed into cysts regardless of antibody. Meanwhile, the transcriptional level of *Ac-hsp20* was significantly induced under the pressure of antibody and reached the highest level at 24 h incubation on ice (twice higher than those without antibody, **Figure 6C**). This finding may explain why the antibody neutralization of *Ac*-HSP20 could not offset the complete encystation of *A. castellanii* at the late stage. The antibody pressure could induce the expression of indigenous *Ac*-HSP20. When the expression of *Ac*-HSP20 overtook the antibody pressure, the encystation continued without interruption. These results may provide new clues for the parasite to escape the immune stress from its host. The inhibition of encystation of trophozoites by anti-*Ac*-HSP20 antibody was also confirmed by the silence of

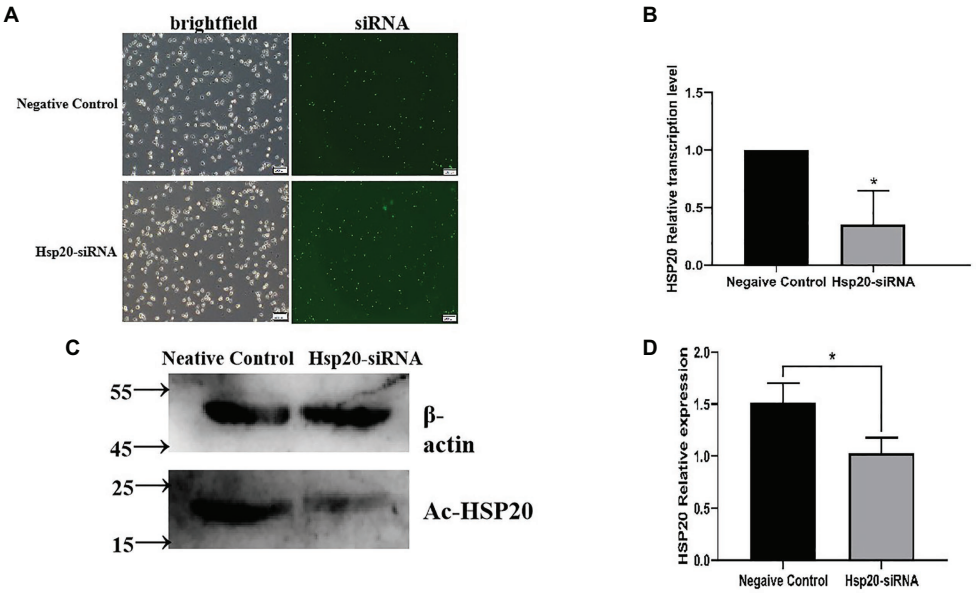

FIGURE 7 | The *Ac-hsp20* gene silence in *A. castellanii* trophozoites by siRNA transfection. The successful transfection of *Ac-hsp20* siRNA into trophozoites was confirmed by the fluorescent staining under microscope after transfection 6 h **(A)**. The *Ac-hsp20* mRNA transcription was significantly inhibited in siRNA group compared to negative control group **(B)**. The inhibited *Ac*-HSP20 protein expression was confirmed in siRNA transfected trophozoites by Western blot with anti-*Ac*-HSP20 IgG **(C)**. Densitometric values were normalized by β-actin and expressed as mean ± *SD*, $n = 3$ **(D)**. $^*p < 0.05$.

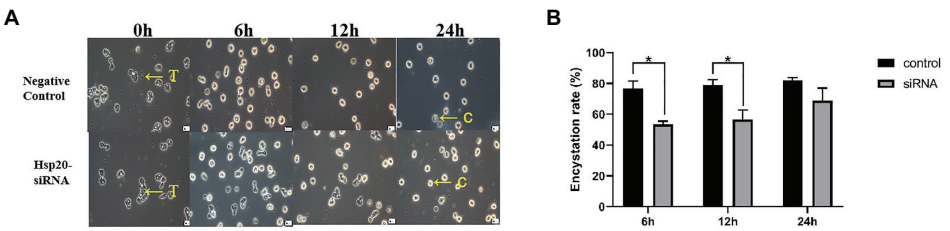

FIGURE 8 | Inhibition of *A. castellanii* encystation through silencing Ac-hsp20 gene transcription in trophozoites. The trophozoites were transfected *Ac*-hsp20-siRNA and then cooled down on ice for 0, 6, 12, and 24 h. The transformation from trophozoites to cysts was observed under microscope **(A)**. The encystation rate of *A. castellanii* trophozoites at different ice incubation time points was calculated (**B**; $^*p < 0.05$). T, trophozoites; C, cysts.

Ac-hsp20 gene in trophozoites by siRNA transfection (**Figure 8**). All results clearly suggested that *Ac*-HSP20 is not only a housekeeping cytoplasmic protein but also a membrane protein involved in the encystation of *A. castellanii*.

Ac-HSP20 belongs to the HSP superfamily, and it is highly conserved during evolution (Ingolia and Craig, 1982; Verbon et al., 1992; Groenen et al., 1994). The present study demonstrated that in addition to being a chaperon protein to protect protozoa from heat shock or other environmental stress, the membrane form of *Ac*-HSP20 played a crucial biological function in the differentiation of *A. castellanii* upon harsh environmental changes as a protective mechanism. The membrane-associated sHSP family has been identified in different species of organism, including protozoa (Caspers et al., 1995; Spinner et al., 2012). It is characterized by the presence of a conserved homologous α-crystallin domain (Spinner et al., 2012). Given their surface exposure, these membrane-associated HSPs are usually immunodominant during infection. Similar to *Ac*-HSP20, the HSP20 protein of *Leishmania* is strongly recognized by sera of dogs with visceral leishmaniasis (Montagna et al., 2012). Rats infected with parasitic nematode *Strongyloides ratti* produce strong immune reactions to two sHSPs (Hombach et al., 2014). Together with the *Ac*-HSP20 reported here, all data demonstrated that sHSP family proteins were induced under stress conditions as stable chaperons and membrane functional proteins.

Considering its presence on the membrane and its critical role in the encystation of *A. castellanii*, *Ac*-HSP20 could be a good target for vaccine or drug development. Indeed, anti-*Ac*-HSP20 antibody induced macrophage-involved ADCC observed in this study, indicating that *Ac*-HSP20-induced

antibody could be involved in the clearance of *A. castellanii* by macrophage phagocytosis during infection. *In-vitro* incubation of *A. castellanii* trophozoites with rabbit anti-*Ac*-HSP20 IgG significantly reduced their adhesion to or infectivity on rabbit cornea at days 14 and 28 after the infection compared with those without antibody incubation. This finding indicated that neutralizing *Ac*-HSP20 on the surface of trophozoites may reduce their infectivity to cornea. The protective immunity induced by the immunization of recombinant *Ac*-HSP20 protein against *A. castellanii* infection in the cornea of rabbit is under investigation.

DATA AVAILABILITY STATEMENT

The datasets presented in this study can be found in online repositories. The names of the repository/repositories and accession number(s) can be found in the article/supplementary material.

ETHICS STATEMENT

The animal study was reviewed and approved by The Animal Care and Use Committee of the Jilin Medical College (approval number: 190001).

AUTHOR CONTRIBUTIONS

XF and WZ: conceptualization. DL, MZ, and HS: data curation. NW, DL, MZ, HS, WZ, and XF: formal analysis. XF: investigation and supervision. NW, DL, MZ, HS, and WZ: validation. NW and HS: writing – original draft. XF and WZ: writing – review and editing. All authors contributed to the article and approved the submitted version.

FUNDING

This work was supported by National Nature Science Foundation of China (project no.31772462), the Medical Specialty from Jilin Provincial Department of Science and Technology (project no.20200708084YY), and the Science and technology planning projects from Department of Education of Jilin Province (JJKH20200452KJ).

ACKNOWLEDGMENTS

We thank Dr. Zheng Wenyu for helping us to construct a rabbit model infected by *Acanthamoeba cantellanii* trophozoites using micromanipulation technique.

REFERENCES

Baig, A. M., Khan, N. A., Katyara, P., Lalani, S., Baig, R., Nadeem, M., et al. (2020). "Targeting the feast of a sleeping beast": nutrient and mineral dependencies of an encysted *Acanthamoeba castellanii*. *Chem. Biol. Drug Des.* doi: 10.1111/cbdd.13755 [Epub ahead of print]

Caspers, G. J., Leunissen, J. A., and de Jong, W. W. (1995). The expanding small heat-shock protein family, and structure predictions of the conserved "alpha-crystallin domain." *J. Mol. Evol.* 40, 238–248. doi: 10.1007/BF00163229

Clarke, D. W., and Niederkorn, J. Y. (2006). The pathophysiology of *Acanthamoeba* keratitis. *Trends Parasitol.* 22, 175–180. doi: 10.1016/j.pt.2006.02.004

Feder, M. E., and Hofmann, G. E. (1999). Heat-shock proteins, molecular chaperones, and the stress response: evolutionary and ecological physiology. *Annu. Rev. Physiol.* 61, 243–282. doi: 10.1146/annurev.physiol.61.1.243

Feng, X., Zheng, W., Wang, Y., Zhao, D., Jiang, X., and Lv, S. (2015). A rabbit model of *Acanthamoeba* keratitis that better reflects the natural human infection. *Anat. Rec.* 298, 1509–1517. doi: 10.1002/ar.23154

Groenen, P. J., Merck, K. B., de Jong, W. W., and Bloemendal, H. (1994). Structure and modifications of the junior chaperone alpha-crystallin. From lens transparency to molecular pathology. *Eur. J. Biochem.* 225, 1–19. doi: 10.1111/j.1432-1033.1994.00001.x

Hombach, A., Ommen, G., MacDonald, A., and Clos, J. (2014). A small heat shock protein is essential for thermotolerance and intracellular survival of *Leishmania donovani*. *J. Cell Sci.* 127, 4762–4773. doi: 10.1242/jcs.157297

Ingolia, T. D., and Craig, E. A. (1982). Four small *Drosophila* heat shock proteins are related to each other and to mammalian alpha-crystallin. *Proc. Natl. Acad. Sci. U. S. A.* 79, 2360–2364. doi: 10.1073/pnas.79.7.2360

Khan, N. A. (2006). *Acanthamoeba*: biology and increasing importance in human health. *FEMS Microbiol. Rev.* 30, 564–595. doi: 10.1111/j.1574-6976.2006.00023.x

Lindquist, S., and Craig, E. A. (1988). The heat-shock proteins. *Annu. Rev. Genet.* 22, 631–677. doi: 10.1146/annurev.ge.22.120188.003215

Lorenzo-Morales, J., Martín-Navarro, C. M., López-Arencibia, A., Arnalich-Montiel, F., Piñero, J. E., and Valladares, B. (2013). *Acanthamoeba* keratitis: an emerging disease gathering importance worldwide? *Trends Parasitol.* 29, 181–187. doi: 10.1016/j.pt.2013.01.006

Magistrado-Coxen, P., Aqeel, Y., Lopez, A., Haserick, J. R., and Samuelson, J. (2019). The most abundant cyst wall proteins of *Acanthamoeba castellanii* are lectins that bind cellulose and localize to distinct structures in developing and mature cyst walls. *PLoS Negl. Trop. Dis.* 13:e0007352. doi: 10.1371/journal.pntd.0007352

Mahboob, T., Nawaz, M., de Lourdes Pereira, M., Tian-Chye, T., Samudi, C., Sekaran, S. D., et al. (2020). PLGA nanoparticles loaded with Gallic acid-a constituent of *Leea indica* against *Acanthamoeba triangularis*. *Sci. Rep.* 10:8954. doi: 10.1038/s41598-020-65728-0

Marciano-Cabral, F., and Cabral, G. (2003). *Acanthamoeba* spp. as agents of disease in humans. *Clin. Microbiol. Rev.* 16, 273–307. doi: 10.1128/cmr.16.2.273-307.2003

Montagna, G. N., Buscaglia, C. A., Münter, S., Goosmann, C., Frischknecht, F., Brinkmann, V., et al. (2012). Critical role for heat shock protein 20 (HSP20) in migration of malarial sporozoites. *J. Biol. Chem.* 287, 2410–2422. doi: 10.1074/jbc.M111.302109

Nakamoto, H., and Vígh, L. (2007). The small heat shock proteins and their clients. *Cell. Mol. Life Sci.* 64, 294–306. doi: 10.1007/s00018-006-6321-2

Parija, S. C., Dinoop, K., and Venugopal, H. (2015). Management of granulomatous amebic encephalitis: laboratory diagnosis and treatment. *Trop. Parasitol.* 5, 23–28. doi: 10.4103/2229-5070.149889

Siddiqui, R., and Khan, N. A. (2012). Biology and pathogenesis of *Acanthamoeba*. *Parasit. Vectors* 5:6. doi: 10.1186/1756-3305-5-6

Spinner, W. G., Thompson, F. J., Emery, D. C., and Viney, M. E. (2012). Characterization of genes with a putative key role in the parasitic lifestyle of the nematode *Strongyloides ratti*. *Parasitology* 139, 1317–1328. doi: 10.1017/S0031182012000637

Sun, Y., and MacRae, T. H. (2005). Small heat shock proteins: molecular structure and chaperone function. *Cell. Mol. Life Sci.* 62, 2460–2476. doi: 10.1007/s00018-005-5190-4

Turner, N. A., Russell, A. D., Furr, J. R., and Lloyd, D. (2000). Emergence of resistance to biocides during differentiation of *Acanthamoeba castellanii*. *J. Antimicrob. Chemother.* 46, 27–34. doi: 10.1093/jac/46.1.27

Turner, N. A., Russell, A. D., Furr, J. R., and Lloyd, D. (2004). Resistance, biguanide sorption and biguanide-induced pentose leakage during encystment of *Acanthamoeba castellanii*. *J. Appl. Microbiol.* 96, 1287–1295. doi: 10.1111/j.1365-2672.2004.02260.x

Verbon, A., Hartskeerl, R. A., Schuitema, A., Kolk, A. H., Young, D. B., and Lathigra, R. (1992). The 14,000-molecular-weight antigen of *Mycobacterium tuberculosis* is related to the alpha-crystallin family of low-molecular-weight heat shock proteins. *J. Bacteriol.* 174, 1352–1359. doi: 10.1128/jb.174.4.1352-1359.1992

Visvesvara, G. S. (2010). Amebic meningoencephalitides and keratitis: challenges in diagnosis and treatment. *Curr. Opin. Infect. Dis.* 23, 590–594. doi: 10.1097/QCO.0b013e32833ed78b

Wang, Y., Feng, X., Li, Y., Ju, X., and Sun, Y. (2014). The construction of full-length cDNA library of *Acanthamoeba* protozoa. *Chin. J. Pathog. Biol.* 9, 452–454.

Zhang, H., Zheng, W., Liu, D., and Feng, X. (2018). Immunological screening of cDNA expression library from *Acanthaoeba*. *Chin. J. Vet. Med.* 54, 17–20.

Conflict of Interest: The authors declare that the research was conducted in the absence of any commercial or financial relationships that could be construed as a potential conflict of interest.

frontiers in Microbiology

ORIGINAL RESEARCH
published: 14 January 2021
doi: 10.3389/fmicb.2020.616688

A Carbamoyl Phosphate Synthetase II (CPSII) Deletion Mutant of *Toxoplasma gondii* Induces Partial Protective Immunity in Mice

Xunhui Zhuo[1†], Kaige Du[1,2†], Haojie Ding[1†], Di Lou[1], Bin Zheng[1] and Shaohong Lu[1]*

[1] Department of Immunity and Biochemistry, Institute of Parasitic Disease, Hangzhou Medical College, Hangzhou, China, [2] Department of Immunity and Biochemistry, Institute of Parasitic Disease, Zhejiang Academy of Medical Sciences, Hangzhou, China

Toxoplasma gondii is an obligate intracellular protozoan parasite. *T. gondii* primarily infection in pregnant women may result in fetal abortion, and infection in immunosuppressed population may result in toxoplasmosis. Carbamoyl phosphate synthetase II (CPSII) is a key enzyme in the *de novo* pyrimidine-biosynthesis pathway, and has a crucial role in parasite replication. We generated a mutant with complete deletion of CPSII via clustered regularly interspaced short palindromic repeats (CRISPR)/cas9 in type-1 RH strain of *T. gondii*. We tested the intracellular proliferation of this mutant and found that it showed significantly reduced replication *in vitro*, though CPSII deletion did not completely stop the parasite growth. The immune responses induced by the infection of RHΔCPSII tachyzoites in mice were evaluated. During infection in mice, the RHΔCPSII mutant displayed notable defects in replication and virulence, and significantly enhanced the survival of mice compared with survival of RH-infected mice. We tracked parasite propagation from ascitic fluid in mice infected with the RHΔCPSII mutant, and few tachyzoites were observed at early infection. We also observed that the RHΔCPSII mutant induced greater accumulation of neutrophils. The mutant induced a higher level of T-helper type-1 cytokines [interferon (IFN)-γ, interleukin (IL)-12]. The mRNA levels of signal transducer and activator of transcription cellular transcription factor 1 and IFN regulatory factor 8 were significantly higher in the RHΔCPSII mutant-infected group. Together, these data suggest that CPSII is crucial for parasite growth, and that strains lack the *de novo* pyrimidine biosynthesis pathway and salvage pathway may become a promising live attenuated vaccine to prevent infection with *T. gondii*.

Keywords: ***Toxoplasma gondii*, carbamoyl phosphate synthetase II, vaccine, immunization, CRISPR/Cas9**

OPEN ACCESS

Edited by:
Hong-Juan Peng,
Southern Medical University, China

Reviewed by:
Chuan Su,
Nanjing Medical University, China
Qijun Chen,
Shenyang Agricultural University, China
Jilong Shen,
Anhui Medical University, China

****Correspondence:***
Shaohong Lu
lsh@zjams.com.cn

† These authors have contributed equally to this work

Specialty section:
This article was submitted to Infectious Diseases, a section of the journal Frontiers in Microbiology

Received: *13 October 2020*
Accepted: *21 December 2020*
Published: *14 January 2021*

Citation:
Zhuo X, Du K, Ding H, Lou D, Zheng B and Lu S (2021) A Carbamoyl Phosphate Synthetase II (CPSII) Deletion Mutant of Toxoplasma gondii Induces Partial Protective Immunity in Mice. Front. Microbiol. 11:616688. doi: 10.3389/fmicb.2020.616688

INTRODUCTION

Toxoplasma gondii is an intracellular parasitic protozoon that can infect a wide range of homeothermic animals including human beings (Dubey et al., 2020). Humans acquire *T. gondii* infection usually through oral intake of oocysts in vegetables or water, or ingestion of tissue cysts in raw or undercooked meat (Blume and Seeber, 2018). Toxoplasmosis is usually asymptomatic in

most immunocompetent adults, but immunodeficient individuals (e.g., organ-transplant recipients and human immunodeficiency virus-infected patients) are at risk (Wang et al., 2017; Odeniran et al., 2020). Infection by *T. gondii* can cause severe consequences in pregnant women, such as miscarriage (Garnaud et al., 2020). In addition, toxoplasmosis in agricultural animals (e.g., pigs) can lead to great economic losses and cause public-health issues around the world; recent prevalence surveys indicated that infection with *T. gondii* remains relatively high in pigs (De Berardinis et al., 2017; Suijkerbuijk et al., 2019).

Prevention or cure of toxoplasmosis is difficult because the parasite lifecycle is very complex. Transmitted oocysts shed by cats are key sources for infection in humans and animals. Tissue cysts, in general, last lifelong in hosts and are important routes of transmission (Elmore et al., 2010; Hill and Dubey, 2016). Currently, toxoplasmosis is treated by pharmacologic agents such as pyrimethamine and sulfadiazine (Deng et al., 2019). However, most marketed drugs do not work in chronic infections of *T. gondii* and cause severe side effects. In addition, drug-resistant parasites have been reported recently, along with increased concerns about treatment failure and increased clinical severity in immunocompromised patients (Montazeri et al., 2018). Therefore, the "ideal" drugs and efficacious therapies for *T. gondii* infection should be discovered and developed.

Vaccination is considered to be another effective method for preventing and controlling toxoplasmosis by providing specific antibodies and inducing cytokines directly against pathogens. Scientists have worked on developing vaccines against *T. gondii* using different strategies, such as recombinant protein- and DNA-based vaccines and dead parasites (Foroutan et al., 2019; Hajissa et al., 2019; Wang et al., 2019). Mice immunized with *T. gondii* extracts or dead parasites may fail to develop robust immune response to reinfection with *T. gondii* (Butcher and Denkers, 2002; Fox and Bzik, 2015). However, Rahman et al. (2019) found that *T. gondii* lysate antigens trigger significant immune responses leading to parasite reduction in pigs upon challenge infection, even though the mechanism of parasite clearance from tissues by early immune response needs further investigation (Rahman et al., 2020). Several studies have demonstrated that subunit vaccines and DNA vaccines induce robust humoral and cellular immunity in mice and provide partial protection against infection by *T. gondii* (Gatkowska et al., 2018; Zheng et al., 2019). For example, Wu et al. (2019) found that immunization of mice with recombinant plant-like calcium-dependent protein kinase 3 could produce humoral and cellular immune responses to acute toxoplasmosis with a prolonged survival time and significantly reduced number of cysts in brain tissues. However, these vaccines do not provide sufficient anti-toxoplasmosis protection because of the parasite's complex mechanism for escaping immune detection in hosts.

"Attenuated parasites" with genetic alterations may offer an efficient means for vaccine development. The only commercial attenuated vaccine against toxoplasmosis (ToxoVax® ; Intervet, Boxmeer, Netherlands) is available for ewes, even though the high cost and side effects limit the use of this vaccine (Verma and Khanna, 2013). Recently, several studies have documented the potential protection proffered by attenuated vaccines against toxoplasmosis in mice. Wang et al. (2020) developed a mutant with a *tkl1* deletion in a *T. gondii* RH strain that elicited strong humoral and cellular immunity in mice whose brain-cyst burden was reduced significantly after infection with oocysts. Thus, the use of attenuated vaccines could be efficacious.

Toxoplasma gondii is an obligate intracellular protozoan that derives most of its nutrients from host cells, including pyrimidine, which is necessary for parasite replication (Hortua Triana et al., 2016; Beraki et al., 2019). *T. gondii* has a pyrimidine-salvaging pathway and *de novo* pyrimidine-biosynthesis pathway that starts with aspartate and glutamine (Fox and Bzik, 2002). Carbamoyl phosphate synthetase II (CPSII) is a predominant enzyme of the *de novo* pyrimidine-biosynthesis pathway. CPSII possesses a unique enzyme architecture that is absent in bacteria and mammals (Fox et al., 2009). CPSII has a bifunctional N-terminal glutamine amidotransferase domain fused with C-terminal carbamoyl-phosphate synthase domains, and accepts glutamine as a donor of amine groups (Fox and Bzik, 2003; Fox et al., 2009). CPSII deletion induces severe uracil auxotrophy with loss of replication and an inability to establish acute infection in mice. Therefore, a strain with knockout of CPSII expression is severely attenuated (Fox and Bzik, 2002). Mutant, with disrupted function of CPSII enzyme, can be used as a live-attenuated vaccine and is able to elicit long-term immunity to lethal acute or chronic *T. gondii* infection in mice (Gigley et al., 2009a,b, but the protection is not always 100%, especially when challenged with type II strain (Gigley et al., 2009b). Thus, we wonder if completely deleting the CPSII gene would produce a more effective attenuated vaccine. To exclude the influence of any residue of the CPSII enzyme, we generated a mutant with complete CPSII deletion in the RH strain via a clustered regularly interspaced short palindromic repeats (CRISPR)/cas9 system, and evaluated the immune protective effect of this strain in a mouse model.

MATERIALS AND METHODS

Ethical Approval of the Study Protocol

Animals were maintained according to the Animal Ethics Procedures and administration of Affairs Concerning Experimental Animals of the People's Republic of China. Animal experiments were approved by the Animal Care and Use Committee of Zhejiang Academy of Medical Sciences (Zhejiang, China).

Plasmid Construction

All primers used in this study are listed in **Supplementary Table 1**. The CRISPR plasmid was generated by replacing the UPRT targeting guide RNA (sgRNA) in pSAG1-CAS9-sgUPRT (kindly provided by Professor Shen Bang) with the corresponding gRNAs using site-directed mutagenesis (New England Biolabs, Ipswich, MA, United States) as described by Shen et al. (2017). Briefly, two sgRNA-targeted CPSII (5′ and 3′) were inserted into the pSAG1-CAS9-sgUPRT plasmid by replacing the UPRT sgRNA. Polymerase chain

reaction (PCR) amplified the U6-sgRNA region from 5′ CPSII sgRNA plasmid using the primers gRNA2-Fw-*Kpn*I and gRNA2-Rv-*Xho*I as listed in **Supplementary Table 1**. The PCR products were digested with *Kpn*I (New England Biolabs) and *Xho*I (New England Biolabs) and the fragment (678 bp) was purified. In parallel, the 3′ CPSII sgRNA plasmid was digested with *Kpn*I and *Xho*I, and the fragment (9663 bp) was purified. the purified PCR products were ligated into the prepared 3′ CPSII sgRNA plasmid backbone to yield the dual sgRNA plasmid. The selection marker DHFR were amplified with primers containing 40 bp of homology to CPSII gene.

Parasite Culture, Transfection, and PCR Diagnosis

Tachyzoites of the RH strain were maintained in human foreskin fibroblasts in complete medium (CM) composed of Dulbecco modified Eagle medium (Gibco; Thermo Fisher Scientific, Inc., Waltham, MA, United States) supplemented with 5% fetal calf serum (Gibco), penicillin (100 U/mL; Life Technologies, Gaithersburg, MD, United States), and streptomycin (100 μg/mL; Life Technologies), purchased from American Tissue Type Collection (Manassas, VA, United States). Parasites were electroporated in a 4 mm gap cuvette by the manufacturer Gene Pulser Xcell (BioRad, Hercules, CA, United States) following the protocol (1700 V, 176 μs of pulse length, two pulses with100 ms interval) as described by Shen et al. (2017). CPSII-deleted parasites were selected with pyrimethamine (Selleck Chemicals, Houston, TX, United States) and cloned by limiting the dilution.

Single positive clones were identified by diagnostic PCRs and primers are listed in **Supplementary Table 1**. The PCRs were carried out by the conditions with an initial melting step at 98°C for 5 min, followed by 30 cycles with each cycle at 98°C for 15 s, 61°C for 30 s, and 72°C for 45 s, followed by a final extension at 72°C for 5 min.

Virulence Testing in Mice

Twenty adult (6–8 weeks) BALB/c mice or 20 ICR mice were obtained from the Experimental Animal Center of Zhejiang Academy of Medical Sciences. Tachyzoites of the RH strain and CPSII-deleted parasites were washed in phosphate-buffered saline (PBS). Three groups of mice were injected (i.p.) with 0.1 mL of PBS containing 1×10^4 tachyzoites of the RH strain or CPSII-deleted parasites. Mice survival was monitored daily, and the survival test was carried out thrice.

Measurement of Parasite Burden

A total of 95 adult ICR mice were randomly divided into three groups: PBS group (25 mice), WT-RH group (35 mice), and ΔCPSII group (35 mice). Three groups of mice were injected (i.p.) with 0.1 mL of PBS or PBS containing 1×10^4 tachyzoites of the RH strain or CPSII-deleted parasites. Mice from each group were euthanized at days 4 and 10 post-infection (dpi) via CO_2 overdose according to the Animal Ethics Procedures. Liver tissues were collected from each mouse and DNA extracted by using the DNeasy Blood & Tissue Kit (QIAGEN, Shanghai, China) according to the manufacturer's protocol. Amplification of parasite DNA was carried out by using primers targeted *T. gondii* repetitive 529 bp gene as listed in **Supplementary Table 1**. Each reaction mixture contained 12.5 μL of 2 × Real time PCR Master Mix (Toyobo, Shanghai, China), 0.5 μL of each primer (10 μM), 1 μL DNA template, and 5.5 μL of sterile distilled water and was performed on a CFX96 Touch™ Real-Time PCR Detection System (BioRad). Parasite equivalents were determined through a standard curve.

In parallel, the ascitic fluid of mice was collected at 4 and 10 dpi with 5 mL of PBS. Parasites were obtained by centrifugation at 300 *g* for 5 min at room temperature. The number of tachyzoites from each mouse was calculated using a cell counter.

Cytokine Measurement

After mice had been injected (i.p.) with 0.1 mL of PBS containing 1×10^4 tachyzoites of RH or CPSII-deleted parasites, serum samples were collected from mice at 2, 4, 8, and 10 dpi for measurement of cytokine levels. Levels of interferon (IFN)-γ and interleukin (IL)-12 were detected using an enzyme-linked immunosorbent assay (ELISA) according to manufacturer (Bio-Swamp, Wuhan, China) instructions. The optical density of each well was measured at 450 nm by a microtiter plate reader (ELX 800; Bio-Tek Instruments, Waltham, MA, United States).

White Blood Cell (WBC) Counts

Blood samples were collected from different mouse groups at 1, 4, and 10 dpi. Each 20 μL of sample was added directly to a dilution solution, and white blood cells (WBCs) were counted by an automated machine (Celltac E; Nihdon Kohden, Tokyo, Japan).

Immunofluorescence Assay

Vero cells, maintained in DMEN (Gibco) supplemented with 2% fetal calf serum (Gibco), penicillin (100 U/mL; Life Technologies), and streptomycin (100 μg/mL; Life Technologies), were added with or absent with uracil after infection with tachyzoites of the ΔCPSII strain. Then, cells were fixed in 4% paraformaldehyde overnight at 4°C, followed by permeabilization with 0.1% Triton X-100 in PBS and blockade with 1% bovine serum albumin in PBS for 1 h at 37°C. After washing thrice with PBS, anti-Dense Granule Protein 7 (GRA7) antibodies were diluted in the same blocking buffer and incubated for 60 min at 37°C. Alexa 594-conjugated anti-rabbit secondary antibodies were added and incubated for 60 min at 37°C. Cell nuclei were stained with 4′,6-diamidino-2-phenylindole. Then, samples were examined under a confocal laser scanning microscope (IX81-FV1000; Olympus, Tokyo, Japan).

Statistical Analyses

The Kaplan–Meier product limit test was used to measure significant differences between survival curves (GraphPad Prism software 8.0). The parasite burdens and the mRNA expression levels of different groups were subjected to Student's *t*-test,

and the percentage and the absolute number of neutrophils and lymphocytes and the production of IFN-γ and IL-12 from different groups were all analyzed with two-way ANOVA via Tukey's multiple comparison test. In all analyses, $p < 0.05$ was considered statistically significant.

RESULTS

Generation of the CPSII Knockout Strain Using the CRISPR/Cas9 System

The strategy for deleting the entire CPSII gene by CRISPR/CAS9-mediated homologous recombination is illustrated in **Figure 1A**. To avoid the effect of CPSII residues, we replaced the entire sequence of CPSII with DHFR-TS* by two sgRNAs. Plasmid templates and homology templates were transfected into the Δ*ku80* RH strain, and selected with pyrimethamine. Single clones were obtained by limiting the dilution and assessed by PCR1/2/3/4/5 to check correct replacement of the target gene by the selection marker DHFR-TS* (**Figure 1A**). We used three pairs of primers targeting areas in genomic CPSII far away from each other to confirm successful knockout of the entire gene. Diagnostic PCRs for one clone of RHΔCPSII are shown in **Figure 1B**. The PCR product of CPSII5′UTR-DHFR-CPSII3′UTR, which is performed by using CPSII-DHFR primers, was sent for sequencing for further confirmation. The results are shown in **Supplementary Figure 1**, and the sequences corresponded to the DHFR-TS* gene. Taken together, these results demonstrated complete deletion of the CPSII gene.

Impact of CPSII on Tachyzoite Growth *in vitro*

Cells infected with the ΔCPSII strain underwent uracil supplementation, and tachyzoites egressed at 72 h. In cells without uracil supplementation, tachyzoites did not egress from cells at any time (**Supplementary Figure 2**). Interestingly, without uracil supplementation to cells, the

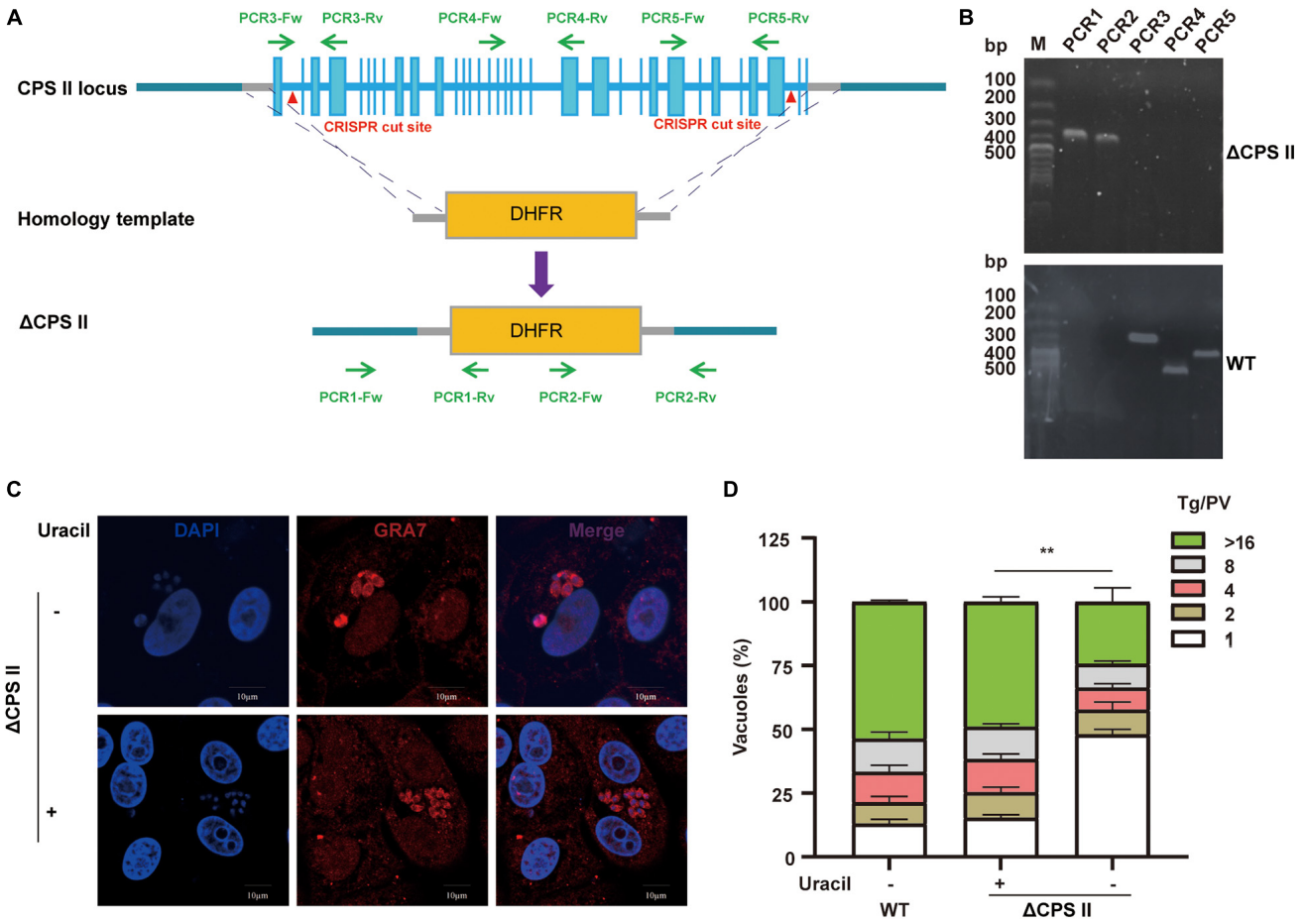

FIGURE 1 | Generation and characterization of a CPSII deletion mutant. **(A)** Schematic illustration of knocking out CPSII by CRISPR/Cas9-mediated homologous gene replacement in the RH Δ*ku80* strain. **(B)** Diagnostic PCRs on a ΔCPSII clone. **(C)** Observation of intracellular replication of ΔCPSII RH strain with or without the addition of 200 μM uracil at 24 hpi by IFA using anti-GRA7 rabbit polyclonal antibody. **(D)** Intracellular replication assay of ΔCPSII RH strain with or without the addition of 200 μM uracil. The number of parasites in each parasitophorous vacuole (PV) was determined at 48 hpi. Values are shown as means ± SEM from three independent experiments. $^{**}P < 0.01$ by two-way ANOVA.

ΔCPSII strain had a slow growth tendency because two to four tachyzoites were observed in single parasitophorous vacuole membrane (**Figure 1C**). Next, we undertook an intracellular replication assay to evaluate parasite proliferation *in vitro*. We found that, without the addition of uracil, growth was notably reduced (**Figure 1D**). These results suggested that CPSII knockout impaired the intracellular proliferation of *T. gondii*.

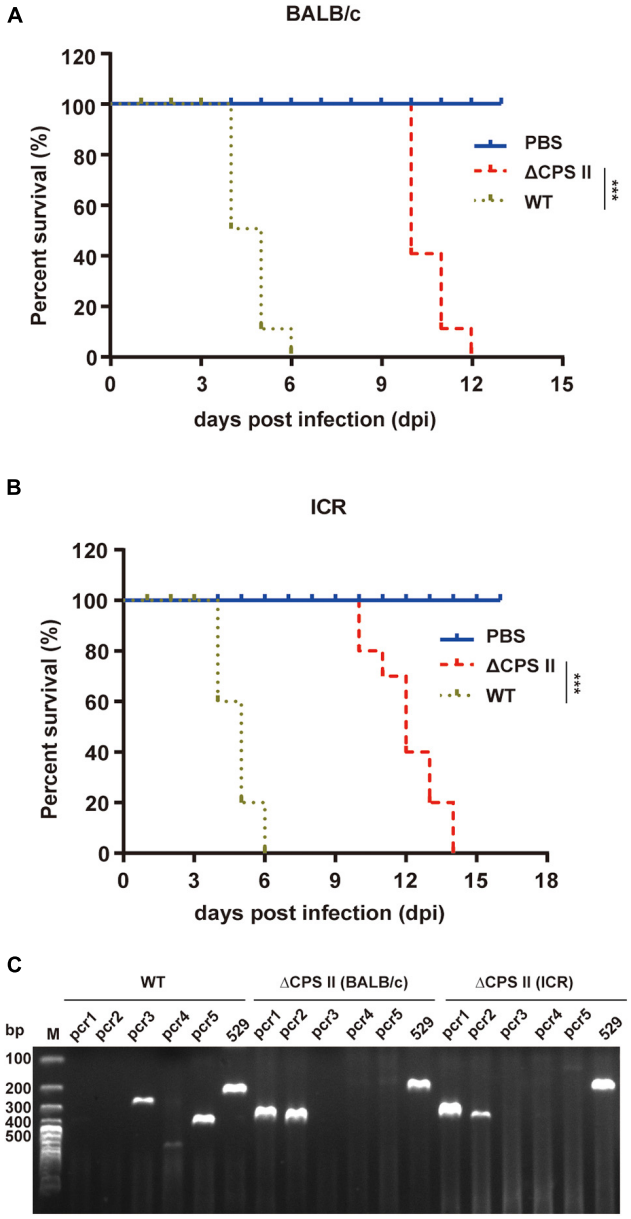

FIGURE 2 | Virulence test of ΔCPSII RH strain in mice. BALB/c **(A)** or ICR **(B)** mice were infected through intraperitoneal injection with 10^4 tachyzoites of RH strain or ΔCPSII RH strain, each group comprised 10 mice. ***$p < 0.001$, Kaplan–Meier product limit test. **(C)** Diagnostic PCRs of ascitic fluid samples collected from toxoplasma-infected mice.

Deletion of CPSII in *T. gondii* Leads to Reduced Virulence in Mice

Mice infected with the ΔCPSII strain lived longer (average, 12 days) compared with those infected with the WT RH strain (average, 5 days) (**Figures 2A,B**). The virulence test was carried out three times and the results were similar.

To exclude the possibility that the ΔCPSII strain was mixed with the WT RH strain, we performed PCR of tachyzoites collected from infected mice. PCR3/4/5 was negative in ΔCPSII-infected mice (**Figure 2C**), which suggested that RH tachyzoites were not mixed into ΔCPSII isolates. These results suggested that the virulence of the ΔCPSII strain was weakened significantly, but that the replication ability was not completely stopped.

Parasite Burden in Mice

Ascitic fluid samples were collected from different mouse groups at 4 and 10 dpi, and the number of tachyzoites was calculated using a hemocytometer. The average number of parasites in WT RH strain-infected mice was $2.7 \pm 0.5 \times 10^6$, whereas parasites were not observed in ΔCPSII strain-infected mice at 4 dpi (**Figure 3A**). The average number of parasites from ΔCPSII strain-infected mice reached a similar level at 10 dpi ($2.7 \pm 0.5 \times 10^6$) compared with that from WT RH strain-infected mice at 4 dpi. Parasite loads in spleen tissues were calculated by real-time PCR based on repetitive 529 bp gene, and we found a similar pattern to that in fluid samples (**Figure 3B**). Parasite loads in WT RH-infected mice were increased notably at 4 dpi whereas a similar level in ΔCPSII strain-infected mice was not observed until 10 dpi. Taken together, these results suggested that deletion of CPSII significantly reduced proliferation efficiency of *T. gondii* in mice.

Increased Number of Neutrophils Upon Infection of the ΔCPSII Strain

The percentage and the absolute numbers of WBCs from blood samples were calculated with an auto-analyzer. We found a significant increase in the percentage and the absolute number of neutrophils at 10 dpi in ΔCPSII strain-infected mice, whereas the percentage and the absolute number of lymphocytes were decreased notably (**Figure 4**). Neutrophil accumulation induced by infection due to the ΔCPSII strain indicated partial activation of adaptive immunity, which may provide protection against toxoplasmosis.

Increased Production of IFN-γ and IL-12 in ΔCPSII Strain-Infected Mice

Production of IFN-γ and IL-12 was evaluated using ELISA kits. Production of IFN-γ and IL-12 was significantly higher in infected mice compared with that in the control group (**Figure 5**). Then, we measured mRNA expression of signal transducer and activator of transcription cellular transcription factor (*stat*)1 and IFN regulatory factor (*irf*)8 using real-time PCR. We found a remarkable increase in expression of *stat1* mRNA and *irf8* mRNA compared with that in

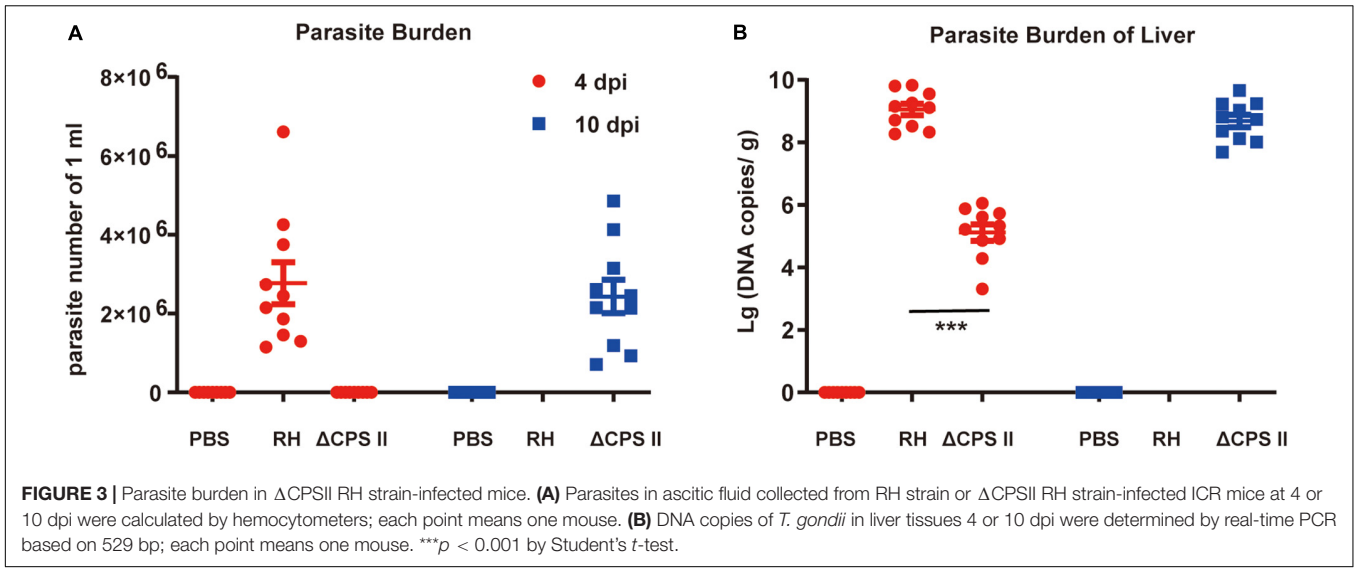

FIGURE 3 | Parasite burden in ΔCPSII RH strain-infected mice. **(A)** Parasites in ascitic fluid collected from RH strain or ΔCPSII RH strain-infected ICR mice at 4 or 10 dpi were calculated by hemocytometers; each point means one mouse. **(B)** DNA copies of *T. gondii* in liver tissues 4 or 10 dpi were determined by real-time PCR based on 529 bp; each point means one mouse. ***$p < 0.001$ by Student's *t*-test.

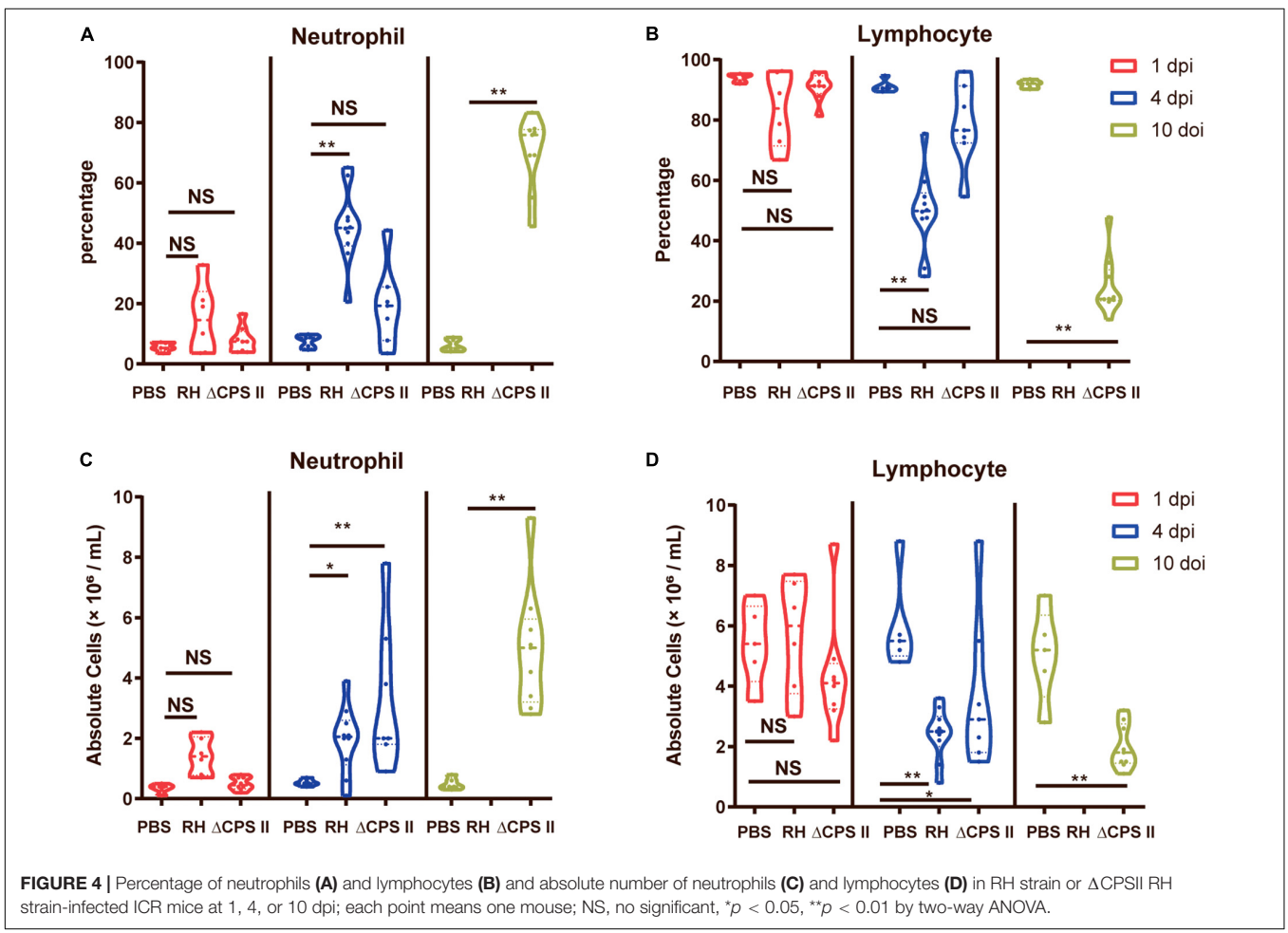

FIGURE 4 | Percentage of neutrophils **(A)** and lymphocytes **(B)** and absolute number of neutrophils **(C)** and lymphocytes **(D)** in RH strain or ΔCPSII RH strain-infected ICR mice at 1, 4, or 10 dpi; each point means one mouse; NS, no significant, *$p < 0.05$, **$p < 0.01$ by two-way ANOVA.

the control group (**Figure 6**). These results suggested that *stat1* and *irf8* induced by the infection by the ΔCPSII strain were likely involved in the increased production of IFN-γ and IL-12.

DISCUSSION

For the last decade, numerous types of vaccines against toxoplasmosis have been evaluated in mice models. Most DNA

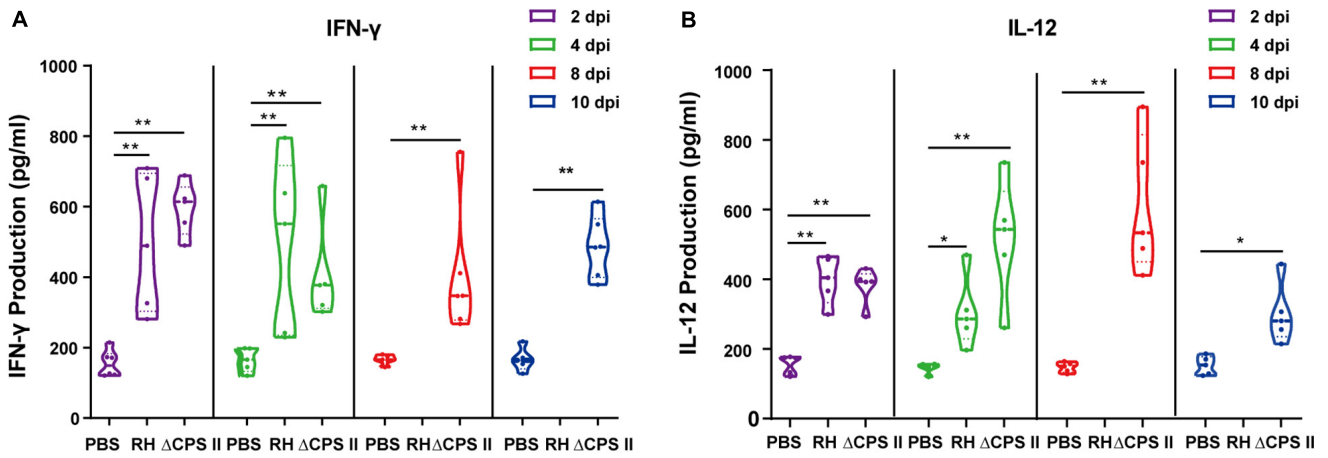

FIGURE 5 | IFN-γ **(A)** and IL-12 **(B)** production in RH strain or ΔCPSII RH strain-infected ICR mice at 2, 4, 8, or 10 dpi; each point means one mouse; $^{*}p < 0.05$, $^{**}p < 0.01$ by two-way ANOVA.

vaccines and recombinant-subunit vaccines have offered partial protection against *T. gondii* infection (Verma and Khanna, 2013). Conversely, several attenuated vaccines, such as RHΔ*tkl1*, RHΔ*ompdc*, and ME49Δ*ldh*, have elicited a potent immune response (Fox and Bzik, 2010; Xia et al., 2018; Wang et al., 2020). These mutants cause a loss of virulence in mice because of uracil auxotrophy; in the absence of uracil *in vivo*, tachyzoites cannot propagate. With defective activity of the *de novo* pyrimidine-biosynthesis pathway, parasites fail to synthesize uridine 5′-monophosphate (UMP) for intracellular replication. These findings are extremely important for developing "ideal" vaccines against toxoplasmosis.

The genomic length of *CPSII* is 24,042 bp and it has 37 extrons, and the mRNA sequence is 5100 bp (Fox et al., 2009). The enzyme CPSII has functional domains at N- and C-terminals. The N-terminal glutamine amidotransferase domain fuses with the C-terminal carbamoyl-phosphate synthase domains, and accepts glutamine as an amine-group donor. It is an important enzyme in the *de novo* pyrimidine-biosynthesis pathway. Reports have shown that tachyzoites with CPSII disrupted, failed to replicate once intracellular without uracil supplementation (Fox and Bzik, 2002; Hortua Triana et al., 2016). The protection of *csp1-1* mutants is not always 100% and the reasons are ambiguous (Fox and Bzik, 2002, 2010, 2015). We assume that the residues of CPSII were the culprits because only part of CPSII is knocked out through homologous recombination according to early reports (Fox and Bzik, 2002; Fox et al., 2009). To achieve better understanding of the immune response induced by RHΔCPSII in mice, we generated a mutant with complete deletion of CSPII. We found that the RHΔCPSII strain reduced intracellular proliferation of tachyzoites in the absence of uracil, but the replication was not dynamic. Two to four tachyzoites in a vacuole were observed by microscopy at 48 or 72 h post-infection, which indicated the slow replication of the mutant.

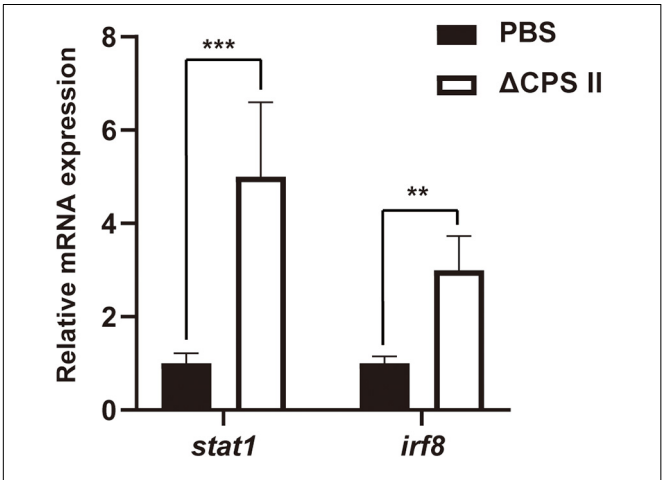

FIGURE 6 | The mRNA level of *stat1* and *irf8* in PBS or ΔCPSII RH strain-infected ICR mice at 10 dpi was evaluated by real-time PCR; $n = 5$, $^{**}p < 0.01$, $^{***}p < 0.001$ by Student's *t*-test.

To further investigate the growth patterns *in vivo*, we carried out experimental infection with RHΔCPSII strain in mice. We found that ICR mice and BALB/c mice infected with the RHΔCPSII strain lived for 10–15 days; our data are not in agreement with the report stating that the cps1-1 mutant is avirulent in mice (Fox and Bzik, 2002). We undertook PCR tests and Sanger sequencing to exclude the possibility that the RHΔCPSII strain was mixed with the wild-type strain. We assumed that *T. gondii* had evolved a compensatory pathway instead of CPSII, or the parasite had acquired a sufficient amount of uracil through the salvage pathway. In our study, no tachyzoites were found in ascitic fluid from ΔCPSII-infected mice at 5 dpi, but many parasites were found at 10 dpi, which is in accordance with our *in vitro* results. Importantly, *T. gondii* can escape the "CPSII deletion" trap, and the mechanism remains obscure. We assume that the salvage pathway takes part in the escape or the parasite evolves a bypass pathway instead of using the CPSII enzyme. The main reason why the S48 strain, as a live attenuated vaccine, is not used widely is that

it may revert to gain the ability to form cysts or oocysts. A live parasite that causes no parasite burden, removes the risk of parasite transmission in the host, and elicits efficacious and long-term immune protection against further infection can be considered to be a "perfect" vaccine. Taken together, we suggest that the RHΔCPSII strain as a live vaccine needs improvement to totally eliminate the dissemination risk even though reports have declared it to be avirulent in mice (Fox and Bzik, 2002; Fox et al., 2009). An advanced strategy would be to combine multiple knockout genes from the *de novo* pyrimidine-biosynthesis pathway and salvage pathway in a single strain to completely delete uracil in designing of a live attenuated vaccine.

Despite the disadvantage mentioned above, we assessed the potential mechanism of the immune response induced by the RHΔCPSII strain for further insight. Upon infection, the percentage and the absolute number of neutrophils were increased significantly. At the early stage of infection, the parasite burden remained low in ΔCPSII group compared with WT group as shown in **Figure 3**, and we can infer that the immune system of mice from the ΔCPSII group was activated in order to eliminate the foreign pathogens. We also found a significant increase in the levels of IFN-γ and IL-12 in infected mice. The latter are key cytokines in immune system because they control *T. gondii* replication via cell-mediated mechanisms (Gazzinelli et al., 1994; Ivanova et al., 2019). A high level of IFN-γ can induce production of the effector proteins, immunity-related GTPases, and guanylate-binding proteins, which further damage parasitophorous vacuoles by fusion with lysosomes (Pifer and Yarovinsky, 2011). IL-12 could be produced by neutrophils and is important for IFN-γ production because it activates natural killer (NK) cells (Gazzinelli et al., 1994; Pifer and Yarovinsky, 2011). In infected mice, especially ΔCPSII-infected mice, which lived much longer, immune responses are induced by parasites and cytokines are then produced to clear the pathogens. Except for NK cells and T cells, neutrophils have been newly identified as another crucial source for the IFN-γ required for T-cell receptor-independent protection against intracellular pathogens (Sturge et al., 2013). Here, we also found notable accumulation of neutrophils after infection by the RHΔCPSII strain, which indicated that a strong immune response had been activated by this strain. The increase in neutrophils is not due to the decrease of lymphocytes by migration from blood to infected tissues, since the absolute number of neutrophils was also significantly increased in ΔCPSII-infected mice. It is not surprising that populations of cluster of differentiation $(CD)4^+$ and $CD8^+$ cells are significantly induced by the cps1-1 RH strain as early as 8 dpi in view of the necessity to establish immunity for controlling infection by *T. gondii* (Dupont et al., 2014). We also observed the mRNA expression of STAT1 and IRF8 to be high at 8 dpi upon infection by the RHΔCPSII strain, indicating the probability of activation of STAT1 and IRF8. STAT1 plays a part in inducing IFN-γ production, whereas IRF8 induces IL-12 expression (Majoros et al., 2017; Jefferies, 2019). Our results suggest that the RHΔCPSII strain elicits an effective cellular immune response.

CONCLUSION

Our findings that a deficiency of CPSII in the RH strain leads to reduced virulence in mice suggest that vaccines targeting the *de novo* pyrimidine-biosynthesis pathway might be efficacious, and these findings could provide research basis for vaccine development. In addition, for the concern of safety and to prevent the possibility of virulence restore, we raised an advanced strategy: *T. gondii* tachyzoites that lack the *de novo* pyrimidine-biosynthesis pathway and salvage pathway, whose resources of uracil are completely shut-off, could be a much safer and promising live attenuated vaccine to prevent infection with *T. gondii*.

DATA AVAILABILITY STATEMENT

The original contributions presented in the study are included in the article/**Supplementary Material**. Further inquiries can be directed to the corresponding author/s.

ETHICS STATEMENT

The animal study was reviewed and approved by the Animal Care and Use Committee of Zhejiang Academy of Medical Sciences (Zhejiang, China).

AUTHOR CONTRIBUTIONS

XZ, SL, HD, DL, and BZ developed the study protocol. XZ, HD, KD, and DL did the experiments. XZ analyzed the data and wrote the manuscript. SL revised the report. All authors read and approved the final manuscript.

FUNDING

This research was supported by the National Natural Science Foundation of China (Grant Nos. 81871684 and 81802037) and Natural Science Foundation of Zhejiang Province of China (LGN18C180004).

SUPPLEMENTARY MATERIAL

The Supplementary Material for this article can be found online at: https://www.frontiersin.org/articles/10.3389/fmicb.2020.616688/full#supplementary-material

Supplementary Figure 1 | Confirmation test of PCR products by sequencing. **(A)** PCR detection of CPSII5′UTR-DHFR-TS*-CPSII3′UTR. **(B)** Sequences of PCR product from ΔCPSII RH strain were aligned with original sequences. Red or blue square means the sequences of 5′ or 3′ UTR of CPSII gene and the rest squares mean the sequences of DHFR gene, as shown in **Figure 1A**.

Supplementary Figure 2 | Parasite growth *in vitro* with or without the addition of uracil. Vero cells were infected with ΔCPSII RH strain with or without the addition of 2 mM uracil. Microscope observation was carried at 24, 48, 72, and 96 hpi.

REFERENCES

Beraki, T., Hu, X., Broncel, M., Young, J. C., O'Shaughnessy, W. J., Borek, D., et al. (2019). Divergent kinase regulates membrane ultrastructure of the Toxoplasma parasitophorous vacuole. *Proc. Natl. Acad. Sci. U S A* 116, 6361–6370.

Blume, M., and Seeber, F. (2018). Metabolic interactions between Toxoplasma gondii and its host. *F1000Research* 7:F1000.

Butcher, B. A., and Denkers, E. Y. (2002). Mechanism of entry determines the ability of Toxoplasma gondii to inhibit macrophage proinflammatory cytokine production. *Infect. Immun.* 70, 5216–5224. doi: 10.1128/iai.70.9.5216-5224.2002

De Berardinis, A., Paludi, D., Pennisi, L., and Vergara, A. (2017). Toxoplasma gondii, a Foodborne Pathogen in the Swine Production Chain from a European Perspective. *Foodborne Pathogens Dis.* 14, 637–648. doi: 10.1089/fpd.2017.2305

Deng, Y., Wu, T., Zhai, S. Q., and Li, C. H. (2019). Recent progress on anti-Toxoplasma drugs discovery: Design, synthesis and screening. *Eur. J. Med. Chem.* 183:111711. doi: 10.1016/j.ejmech.2019.111711

Dubey, J. P., Cerqueira-Cezar, C. K., Murata, F. H. A., Verma, S. K., Kwok, O. C. H., Pedersen, K., et al. (2020). Genotyping of viable Toxoplasma gondii from the first national survey of feral swine revealed evidence for sylvatic transmission cycle, and presence of highly virulent parasite genotypes. *Parasitology* 147, 295–302. doi: 10.1017/s0031182019001586

Dupont, C. D., Christian, D. A., Selleck, E. M., Pepper, M., Leney-Greene, M., Harms Pritchard, G., et al. (2014). Parasite fate and involvement of infected cells in the induction of CD4 + and CD8 + T cell responses to Toxoplasma gondii. *PLoS pathogens* 10:e1004047. doi: 10.1371/journal.ppat.1004047

Elmore, S. A., Jones, J. L., Conrad, P. A., Patton, S., Lindsay, D. S., and Dubey, J. P. (2010). Toxoplasma gondii: epidemiology, feline clinical aspects, and prevention. *Trends Parasitol.* 26, 190–196. doi: 10.1016/j.pt.2010.01.009

Foroutan, M., Ghaffarifar, F., Sharifi, Z., Dalimi, A., and Jorjani, O. (2019). Rhoptry antigens as Toxoplasma gondii vaccine target. *Clin. Exp. Vacc. Res.* 8, 4–26. doi: 10.7774/cevr.2019.8.1.4

Fox, B. A., and Bzik, D. J. (2002). *De novo* pyrimidine biosynthesis is required for virulence of Toxoplasma gondii. *Nature* 415, 926–929. doi: 10.1038/415926a

Fox, B. A., and Bzik, D. J. (2003). Organisation and sequence determination of glutamine-dependent carbamoyl phosphate synthetase II in Toxoplasma gondii. *Int. J. Parasitol.* 33, 89–96. doi: 10.1016/s0020-7519(02)00214-x

Fox, B. A., and Bzik, D. J. (2010). Avirulent uracil auxotrophs based on disruption of orotidine-5′-monophosphate decarboxylase elicit protective immunity to Toxoplasma gondii. *Infect. Immun.* 78, 3744–3752. doi: 10.1128/iai.00287-10

Fox, B. A., and Bzik, D. J. (2015). Non-replicating, cyst-defective type II Toxoplasma gondii vaccine strains stimulate protective immunity against acute and chronic infection. *Infect. Immun.* 83, 2148–2155. doi: 10.1128/iai.02756-14

Fox, B. A., Ristuccia, J. G., and Bzik, D. J. (2009). Genetic identification of essential indels and domains in carbamoyl phosphate synthetase II of Toxoplasma gondii. *Int. J. Parasitol.* 39, 533–539. doi: 10.1016/j.ijpara.2008.09.011

Garnaud, C., Fricker-Hidalgo, H., Evengard, B., Alvarez-Martinez, M. J., Petersen, E., Kortbeek, L. M., et al. (2020). Toxoplasma gondii-specific IgG avidity testing in pregnant women. *Clin. Microbiol. Infect.* 1155–1160. doi: 10.1016/j.cmi.2020.04.014

Gatkowska, J., Wieczorek, M., Dziadek, B., Dzitko, K., Dziadek, J., and Dlugonska, H. (2018). Assessment of the antigenic and neuroprotective activity of the subunit anti-Toxoplasma vaccine in T. gondii experimentally infected mice. *Vet. Parasitol.* 254, 82–94. doi: 10.1016/j.vetpar.2018.02.043

Gazzinelli, R. T., Wysocka, M., Hayashi, S., Denkers, E. Y., Hieny, S., Caspar, P., et al. (1994). Parasite-induced IL-12 stimulates early IFN-gamma synthesis and resistance during acute infection with Toxoplasma gondii. *J. Immunol.* 153, 2533–2543.

Gigley, J. P., Fox, B. A., and Bzik, D. J. (2009a). Cell-mediated immunity to Toxoplasma gondii develops primarily by local Th1 host immune responses in the absence of parasite replication. *J. Immunol.* 182, 1069–1078. doi: 10.4049/jimmunol.182.2.1069

Gigley, J. P., Fox, B. A., and Bzik, D. J. (2009b). Long-term immunity to lethal acute or chronic type II Toxoplasma gondii infection is effectively induced in genetically susceptible C57BL/6 mice by immunization with an attenuated type I vaccine strain. *Infect. Immun.* 77, 5380–5388. doi: 10.1128/iai.00649-09

Hajissa, K., Zakaria, R., Suppian, R., and Mohamed, Z. (2019). Epitope-based vaccine as a universal vaccination strategy against Toxoplasma gondii infection: A mini-review. *J. Adv. Vet. Anim. Res.* 6, 174–182.doi: doi: 10.5455/javar.2019.f329

Hill, D. E., and Dubey, J. P. (2016). Toxoplasma gondii as a Parasite in Food: Analysis and Control. *Microbiol. Spect.* 4, 1–17.

Hortua Triana, M. A., Cajiao Herrera, D., Zimmermann, B. H., Fox, B. A., and Bzik, D. J. (2016). Pyrimidine Pathway-Dependent and -Independent Functions of the Toxoplasma gondii Mitochondrial Dihydroorotate Dehydrogenase. *Infect. Immun.* 84, 2974–2981. doi: 10.1128/iai.00187-16

Ivanova, D. L., Denton, S. L., Fettel, K. D., Sondgeroth, K. S., Gutierrez, J. M., Bangoura, B., et al. (2019). Innate Lymphoid Cells in Protection, Pathology, and Adaptive Immunity During Apicomplexan Infection. *Front. Immunol.* 10:196.doi: 10.3389/fimmu.2019.00196

Jefferies, C. A. (2019). Regulating IRFs in IFN Driven Disease. *Front. Immunol.* 10:325. doi: 10.3389/fimmu.2019.00325

Majoros, A., Platanitis, E., Kernbauer-Holzl, E., Rosebrock, F., Muller, M., and Decker, T. (2017). Canonical and Non-Canonical Aspects of JAK-STAT Signaling: Lessons from Interferons for Cytokine Responses. *Front. Immunol.* 8:29. doi: 10.3389/fimmu.2017.00029

Montazeri, M., Mehrzadi, S., Sharif, M., Sarvi, S., Tanzifi, A., Aghayan, S. A., et al. (2018). Drug Resistance in Toxoplasma gondii. *Front. Microbiol.* 9:2587. doi: 10.3389/fmicb.2018.02587

Odeniran, P. O., Omolabi, K. F., and Ademola, I. O. (2020). Risk factors associated with seropositivity for Toxoplasma gondii in population-based studies among immunocompromised patients (pregnant women, HIV patients and children) in West African countries, Cameroon and Gabon: a meta-analysis. *Acta Tropica* 209:105544. doi: 10.1016/j.actatropica.2020.105544

Pifer, R., and Yarovinsky, F. (2011). Innate responses to Toxoplasma gondii in mice and humans. *Trends Parasitol.* 27, 388–393. doi: 10.1016/j.pt.2011.03.009

Rahman, M., Devriendt, B., Algaba, I. G., Verhaegen, B., Dorny, P., Dierick, K., et al. (2019). QuilA-Adjuvanted T. gondii Lysate Antigens Trigger Robust Antibody and IFNgamma(+) T Cell Responses in Pigs Leading to Reduction in Parasite DNA in Tissues Upon Challenge Infection. *Front. Immunol.* 10:2223.doi: 10.3389/fimmu.2019.02223

Rahman, M., Devriendt, B., Jennes, M., Algaba, I. G., Dorny, P., Dierick, K., et al. (2020). Early Kinetics of Intestinal Infection and Immune Responses to Two Toxoplasma gondii Strains in Pigs. *Front. Cell. Infect. Microbiol.* 10:161.doi: 10.3389/fcimb.2020.00161

Shen, B., Brown, K., Long, S., and Sibley, L. D. (2017). Development of CRISPR/Cas9 for Efficient Genome Editing in Toxoplasma gondii. *Methods Mole. Biol.* 1498, 79–103. doi: 10.1007/978-1-4939-6472-7_6

Sturge, C. R., Benson, A., Raetz, M., Wilhelm, C. L., Mirpuri, J., Vitetta, E. S., et al. (2013). TLR-independent neutrophil-derived IFN-gamma is important for host resistance to intracellular pathogens. *Proc. Natl. Acad. Sci. U S A* 110, 10711–10716. doi: 10.1073/pnas.1307868110

Suijkerbuijk, A. W. M., Over, E. A. B., Opsteegh, M., Deng, H., Gils, P. F. V., Marinovic, A.A. Bonacic, et al. (2019). A social cost-benefit analysis of two One Health interventions to prevent toxoplasmosis. *PLoS One* 14:e0216615. doi: 10.1371/journal.pone.0216615

Verma, R., and Khanna, P. (2013). Development of Toxoplasma gondii vaccine: A global challenge. *Hum. Vac. Immunother.* 9, 291–293. doi: 10.1016/0264-410x(90)90071-s

Wang, J. L., Liang, Q. L., Li, T. T., He, J. J., Bai, M. J., Cao, X. Z., et al. (2020). Toxoplasma gondii tkl1 Deletion Mutant Is a Promising Vaccine against Acute, Chronic, and Congenital Toxoplasmosis in Mice. *J. Immunol.* 204, 1562–1570. doi: 10.4049/jimmunol.1900410

Wang, J. L., Zhang, N. Z., Li, T. T., He, J. J., Elsheikha, H. M., and Zhu, X. Q. (2019). Advances in the Development of Anti-Toxoplasma gondii Vaccines: Challenges, Opportunities, and Perspectives. *Trends Parasitol.* 35, 239–253. doi: 10.1016/j.pt.2019.01.005

Wang, Z. D., Wang, S. C., Liu, H. H., Ma, H. Y., Li, Z. Y., Wei, F., et al. (2017). Prevalence and burden of Toxoplasma gondii infection in HIV-infected people: a systematic review and meta-analysis. *Lancet. HIV* 4, e177–e188.

Wu, M., An, R., Chen, Y., Chen, T., Wen, H., Yan, Q., et al. (2019). Vaccination with recombinant Toxoplasma gondii CDPK3 induces protective immunity

against experimental toxoplasmosis. *Acta Tropica* 199:105148. doi: 10.1016/j.actatropica.2019.105148

Xia, N., Zhou, T., Liang, X., Ye, S., Zhao, P., Yang, J., et al. (2018). Mutant of Toxoplasma Stimulates Protective Immunity Against Acute and Chronic Toxoplasmosis. *Front. Immunol.* 9:1814.doi: 10.3389/fimmu.2018.01814

Zheng, B., Lou, D., Ding, J., Zhuo, X., Ding, H., Kong, Q., et al. (2019). GRA24-Based DNA Vaccine Prolongs Survival in Mice Challenged With a Virulent Toxoplasma gondii Strain. *Front. Immunol.* 10:418.doi: 10.3389/fimmu.2019.00418

Conflict of Interest: The authors declare that the research was conducted in the absence of any commercial or financial relationships that could be construed as a potential conflict of interest.

frontiers in Microbiology

ORIGINAL RESEARCH
published: 18 January 2021
doi: 10.3389/fmicb.2020.612252

Study on Circulating Antigens in Serum of Mice With Experimental Acute Toxoplasmosis

*Qi Liu, Wei Jiang, Yun Chen, Manyu Zhang, Xiaoling Geng and Quan Wang**

Shanghai Veterinary Research Institute, Chinese Academy of Agricultural Sciences, Shanghai, China

Toxoplasma gondii is a ubiquitous apicomplexan protozoan parasite that can infect all warm-blooded animals, causing toxoplasmosis. Thus, efficient diagnosis methods for acute *T. gondii* infection are essential for its management. Circulating antigens (CAgs) are reliable diagnostic indicators of acute infection. In this study, we established a mouse model of acute *T. gondii* infection and explored new potential diagnostic factors. CAgs levels peaked 60 h after *T. gondii* inoculation and 31 CAgs were identified by immunoprecipitation-liquid chromatography-tandem mass spectrometry, among which RuvB-like helicase (TgRuvBL1), ribonuclease (TgRNaseH1), and ribosomal protein RPS2 (TgRPS2) were selected for prokaryotic expression. Polyclonal antibodies against these three proteins were prepared. Results from indirect enzyme-linked immunosorbent assay indicated that anti-rTgRuvBL1, anti-rTgRNase H1, and anti-rTgRPS2 mouse sera were recognized by natural excretory-secretory antigens from *T. gondii* tachyzoites. Moreover, immunofluorescence assays revealed that TgRuvBL1 was localized in the nucleus, while TgRNase H1 and TgRPS2 were in the apical end. Western blotting data confirmed the presence of the three proteins in the sera of the infected mice. Moreover, mice immunized with rTgRuvBL1 (10.0 ± 0.30 days), TgRNaseH1 (9.67 ± 0.14 days), or rTgRPS2 (11.5 ± 0.34 days) had slightly longer lifespan when challenged with a virulent *T. gondii* RH strain. Altogether, these findings indicate that these three proteins can potentially be diagnostic candidates for acute toxoplasmosis. However, they hold poor protective potential against highly virulent *T. gondii* infection.

Keywords: *Toxoplasma gondii*, acute infection, circulating antigens, proteomics, diagnostic candidates

OPEN ACCESS

Edited by:
Hong-Juan Peng,
Southern Medical University, China

Reviewed by:
Shuai Wang,
Xinxiang Medical University, China
Si-Yang Huang,
Yangzhou University, China

***Correspondence:**
Quan Wang
wangquan@shvri.ac.cn

Specialty section:
This article was submitted to Infectious Diseases, a section of the journal Frontiers in Microbiology

Received: *30 September 2020*
Accepted: *23 December 2020*
Published: *18 January 2021*

Citation:
Liu Q, Jiang W, Chen Y, Zhang M, Geng X and Wang Q (2021) Study on Circulating Antigens in Serum of Mice With Experimental Acute Toxoplasmosis. Front. Microbiol. 11:612252. doi: 10.3389/fmicb.2020.612252

INTRODUCTION

Toxoplasma gondii is an obligatory intracellular protozoan parasite that infects virtually any warm-blooded animal, including a third of the human population (Montoya and Liesenfeld, 2004). Infection is mainly acquired by ingestion of undercooked meats containing *T. gondii* cysts (Hide et al., 2009). After ingestion, the parasite causes lifelong infections by converting from rapidly dividing tachyzoites into encysted slow-growing bradyzoites, mainly localizing to the brain, and muscle tissues (Hunter and Sibley, 2012; Wohlfert et al., 2017). Moreover, a latent infection may be reactivated via immune suppression (Dupont et al., 2020). In general, toxoplasmosis is usually asymptomatic in immunocompetent persons, but it can cause life-threatening infections in immunocompromised individuals and developing fetuses

(Nissapatorn, 2009; Csep and Drăghici, 2013; Lima and Lodoen, 2019). Thus, timely and effective diagnosis of acute *T. gondii* infection is imperative.

Convenient serological tests have been widely applied to diagnose toxoplasmosis, which are mainly based on the detection of specific antibodies (IgM and IgG; Robert-Gangneux and Dardé, 2012). IgG can only be detected 13 days after infection, whereas IgM can persist in some patients with toxoplasmosis for over a year (Elsheikha et al., 2020). Thus, the presence of IgG and IgM antibodies does not necessarily indicate an acute infection. The lack of effective serological diagnostic methods for acute toxoplasmosis can lead to delayed treatment and even therapy failure, since available strategies can control acute infections, but not treat chronic toxoplasmosis.

Toxoplasma gondii excretory-secretory antigens (ESA) represent the majority of circulating antigens (CAgs) in the sera of hosts with acute toxoplasmosis (Daryani et al., 2003; Abdollahi et al., 2009). Previous studies have shown that *T. gondii* CAgs can be used as accurate markers for acute toxoplasmosis diagnosis (Hafid et al., 1995; Meira et al., 2008; Abdollahi et al., 2009; Darcy et al., 2010; Xue et al., 2016). Therefore, analysis of CAg profiles and screening of candidate diagnostic molecules should improve the specificity and sensitivity of detection methods for acute infection. Moreover, CAgs modulate the host immune response (Hafid et al., 2005; Abdollahi et al., 2013; Daryani et al., 2014; Carlos et al., 2019; Xue et al., 2019) and the identification of CAg components may be conducive to the discovery of potential candidate antigens for vaccines against toxoplasmosis. To date, CAgs have not been investigated in detail, and only a few CAgs components have been identified. The present study aimed to determine the spectrum of *T. gondii* CAgs in sera of acute infected mice using immunoprecipitation-liquid chromatography (LC)-tandem mass spectrometry (MS/MS). We also aimed to verify three novel CAgs in the sera of infected model mice and to evaluate their protective ability.

MATERIALS AND METHODS

Parasite Strains and Culture

The *T. gondii* strain RH and African green monkey kidney (VERO) cells were stored at our facility. *T. gondii* tachyzoites were grown in VERO cells maintained in Dulbecco's Modified Eagle's Medium (DMEM; Gibco Laboratories, Gaithersburg, MD, United States) supplemented with 2% fetal bovine serum, 100 kU/L streptomycin, and 400 kU/L penicillin at 37°C under a 5% CO_2 atmosphere.

Animals

Eight-week old Kunming mice and New Zealand white female rabbits weighing ∼25 *g* and ∼2 kg, respectively (Shanghai Laboratory Animal Centre, Chinese Academy of Sciences, Shanghai, China) were raised in a sterilized room and fed with sterilized food and water at the Animal Laboratory Centre at the Shanghai Veterinary Research Institute. The Animal Care and Use Committee of the Shanghai Veterinary Research Institute approved the study and the protocols complied with approved guidelines.

ESA and Antisera Preparation

Excretory-secretory antigens were obtained as previously described (Zhou et al., 2005). Briefly, purified tachyzoites (5×10^8/mL) suspended in phosphate-buffered saline (PBS) were incubated at 37°C for 2 h. After centrifugation for 15 min at 1,000 × *g* at 4°C, the supernatant was collected, and the protein density was determined using DC protein assay kits (Bio-Rad Laboratories Inc., Hercules, CA, United States). Thereafter, 1 mg of protein per tube (1.5 mL) was lyophilized. At 0, 2, 4, and 6 weeks, the mice and rabbits were immunized with 100 μg per mouse and 500 μg/kg proteins, respectively, or PBS (the control). The 206 adjuvant was applied as described by the manufacturer (Seppic, Paris, France). Blood was sampled from the tails of mice at the end of each interval for immunoblotting and enzyme-linked immunosorbent assay (ELISA).

Establishment of Double-PcAb Sandwich ELISA

A double-PcAb sandwich ELISA was established to detect CAgs using anti-ESA rabbit and mouse sera as coating and detection antibodies, respectively. Nonspecific protein binding was blocked with PBS containing 0.05% Tween-20 (PBST) and 5% non-fat powdered milk. Briefly, Costar microtiter plates (Corning Inc., Corning, NY, United States) were coated with anti-ESA rabbit serum in 50 mM carbonate buffer overnight at 4°C, then washed with PBST. Nonspecific binding was blocked for 2 h at 37°C. The plates were washed, then 500 ng/mL ESA or samples were added and the plates were incubated for 1 h at 37°C, and washed. Sample dilution buffer was the negative control. Anti-ESA mouse sera were added to the plates and incubated for 1 h at 37°C, followed by three washes with PBST. Secondary HRP-conjugated goat anti-mouse IgG antibody (Cat. No. SE131; Solarbio, Beijing, China) was added, and the plates were incubated for 1 h at 37°C. After five washes with PBST, immune complexes were visualized by incubation with tetramethylbenzidine (TMB) for 20 min. The reaction was stopped by adding 2 M H_2SO_4, and absorbance was measured at 450 nm using an automated MULTISKAN GO microplate reader (Thermo Fisher Scientific Inc., Waltham, MA, United States). All samples were analyzed in triplicate. The optimal coating and detection concentrations were determined using checkerboard titration. The sensitivity of the method was assessed using positive canine sera at 3 days post-challenge with *T. gondii* (Xue et al., 2016).

Development of Acute Infection Models

Control and experimental (n = 3 each) mice were injected with 500 μL of PBS without and with 1×10^7 purified tachyzoites, respectively. Blood (100 μL) samples were collected at 0, 3, 9, 12, 24, 36, 48, and 60 h. Portions of these samples (20 μL) were mixed with sodium citrate anticoagulant for genomic DNA extraction and *T. gondii* detection, and serum

CAgs was detected and purified by immunoprecipitation in 80 μ L of samples.

Evaluation of Infection Models Using ELISA and Nested PCR

We analyzed CAgs in mouse sera using the double-PcAb sandwich ELISA. To detect *T. gondii*, DNA was obtained from anticoagulated blood using a genomic DNA extraction kit (Cat. No. DP308; Tiangen, Beijing, China). Nested PCR was conducted as we previously described (Wang et al., 2012).

Immunoprecipitation

Proteins of interest were immunoprecipitated as described (Xue et al., 2016), mixed with sera at 60 h after challenge (20 μL per mouse), and diluted (1:10) in PBS. Protein G agarose beads (200 μL, 25%; Cat. No. P2009; Beyotime, Nantong, China) were added, and stirred at 4°C for 3 h to remove serum antibodies. The supernatant was collected after centrifugation (260 × *g*, 4°C, 5 min), then 10 μL of anti-ESA mouse serum was added, and stirred slowly overnight at 4°C. Protein G agarose beads (200 μL) were added, and the mixture was stirred at 4°C for 3 h. The beads were collected by centrifugation (260 × *g*, 4°C, 5 min), washed three times with PBS, and boiled in 5× sample buffer (60 μL) for 5 min. The supernatant collected after centrifugation (260 × *g*, 4°C, 5 min) was resolved by 10% sodium dodecyl sulfate-polyacrylamide gel electrophoresis (SDS-PAGE), then analyzed by LC-tandem mass spectrometry (LC-MS/MS; Shanghai Applied Protein Technology Co., Ltd., Shanghai, China).

LC-Electrospray Lonization MS/MS Analysis

Samples were analyzed using a Q Exactive mass spectrometer coupled with an Easy-nLC (Thermo Fisher Scientific Inc.) liquid chromatograph. Briefly, samples were reduced, alkylated, and trypsinized (mass ratio 1:50) at 37°C for 20 h. The enzymolysis product was desalted, lyophilized, dissolved in 0.1% formic acid, and stored at -20°C. For MS analysis, solution A comprised 0.1% formic acid in high performance liquid chromatography (HPLC)-grade water, and solution B comprised 0.1% formic acid in 84% acetonitrile. After the chromatographic column was equilibrated with 95% solution A, samples were loaded from the autosampler to the trap column (0.5 H gradient). To collect mass spectra, the mass-to-charge ratios of peptides and peptide fragments were determined by collecting 20 fragment maps (MS2 scan) after each full scan. The original raw files from the MS test were used to search the UniProt database for proteins using Mascot 2.2 software. The search parameters were as follows: enzyme, trypsin; fixed modification, carbamidomethyl (C); variable modification, oxidation (M); missed cleavage, 2; peptide mass tolerance, 20 ppm; MS/MS tolerance, 0.1 Da; and filter by score ≥ 20.

Expression of TgRuvBL1, TgRNase H1, and TgRPS2 *in vitro* and Antibody Production

To further verify the CAgs components in serum, RuvB-like helicase (TgRuvBL1), ribonuclease (TgRNase H1), and ribosomal protein RPS2 (TgRPS2) were expressed in an *Escherichia coli* (BL 21) system with the pET-28a-c(+) vector. **Table 1** shows the expressed regions, and primers, etc. The sequence of the recombinant plasmid was confirmed by dideoxy chain termination sequencing (Invitrogen, Carlsbad, CA, United States). The recombinant plasmid was transformed into *E. coli* (BL21) competent cells, and cultured in LB medium containing kanamycin (70 μg/mL) at 37°C. Expression was induced with 1 mM isopropyl β-D-thiogalactopyranoside (IPTG) for 6 h at 37°C. Cells were sonicated, then recombinant proteins isolated from inclusion bodies were refolded using TB234 kits (Cat. No: 70123-3; Novagen, San Diego, CA, United States), and purified using His-tag protein purification kits (Cat. No. P2226; Beyotime, Nantong, China). Recombinant proteins were concentrated using 3-kDa centrifugal filters (Merck KGaA, Darmstadt, Germany), and quantified using DC protein assay kits (Bio-Rad Laboratories Inc.). At 0, 2, and 4 weeks, the mice were injected with each protein (100 μg per mouse) or PBS (control). Blood samples were collected from the tail vein of mice at the end of each interval for indirect ELISA and immunofluorescence assay analysis. For indirect ELISA, plates were coated with recombinant proteins (500 ng/mL) or ESA

TABLE 1 | Information of expressed protein.

Protein name	Expressed region	Primers[a]	Restriction enzyme	Form of expression	Recombinant protein weight (Da)	Antiserum dilution
TgRuvBL1	Overall length	F:5′-ACCGGATCCATGGAGCAGSCCGCTCGTGGAG-3′	Bamh I	Inclusion body	41.98 kDa	1:32000
		R: 5′-ACCCTCGAGCTCATCCATGAAAAGGACCCC-3′	Xho I			
TgRNase H1	Overall length	F:5′-ACCGGATCC CGGGAGAGAAGCGAGGCGCCA-3′	Bamh I	Inclusion body	37.52 kDa	1:32000
		R: 5′-ACC GCGGCCGC TTAAACGCCCAGSGTTGGAGAG-3′	Not I			
TgRPS2	Overall length	F:5′-ACCGGATCCATGGCAGSAACGCGGCAGSCTTT-3′	Bamh I	Inclusion body	35.34 kDa	1:32000
		R: 5′-ACCCTCGAGCTAGGCGAGCGGTCGCGACAC-3′	Xho I			

[a] *Enzyme cleavage sites were underlined.*

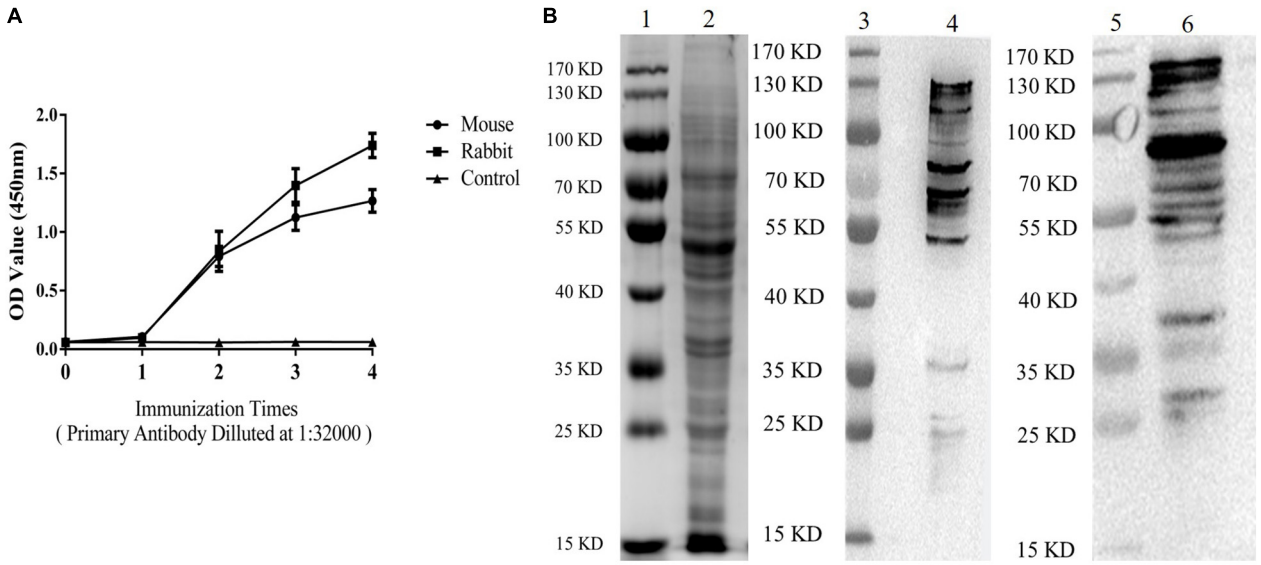

FIGURE 1 | ESA antibodies were tested by ELISA and immunoblotting analyses. **(A)** Levels of ESA antibodies after each immunization (Mouse and Rabbit). Blood sera were sampled from the tails of mice and the ear vein of rabbit 10 days after immunization. **(B)** Western blotting analysis of ESA. Lane 1: marker on gel; Lane 2: ESA on gel; Lane 3: marker on NC membrane; and Lane 4: ESA on NC membrane (anti-ESA mice serum). Lane 5: marker on NC membrane; Lane 6: ESA on NC membrane (anti-ESA rabbit serum).

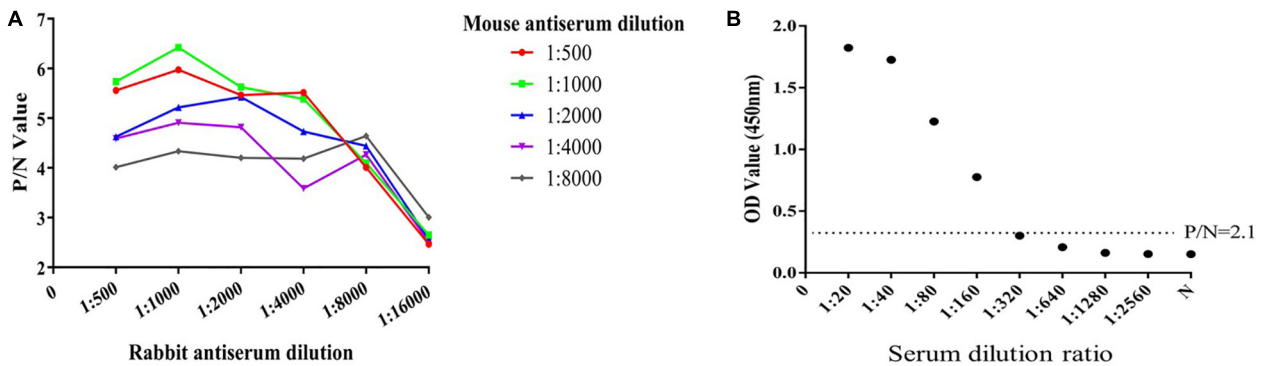

FIGURE 2 | Determination of the optimum working concentration of mouse and rabbit antiserum and the maximum dilution of positive serum. **(A)** The optimal working coating concentration (anti-ESA rabbit serum) and detection concentration (anti-ESA mice serum) were determined using the checkerboard titration method. The P/N value was the criterion standard. **(B)** Sensitivity test using double-PcAb sandwich ELISA. The average optical density (OD) value for negative samples was multiplied by 2.1 to obtain the cut-off value. The horizontal lines represent cut-off values.

(1 μg/mL). Horseradish peroxidase-conjugated goat anti-mouse IgG were diluted 1:5,000.

Immunofluorescence Assays

For Immunofluorescence assays (IFA), infected confluent VERO monolayers were fixed with 4% paraformaldehyde in PBS, permeabilized with 0.5% Triton X-100, and blocked with 1% bovine serum albumin in PBS (BSA-PBS). The primary antibodies used were mouse anti-TgRuvBL1 (1:500), mouse anti-TgRNase H1 (1:500), mouse anti-TgRPS2 (1:500), and rabbit anti-SAG1 (1:4,000). The secondary antibodies used were Alexa Fluor 488-conjugated goat anti-mouse IgG (1:2,000; Thermo Fisher Scientific Inc.) and Alexa Fluor 594-conjugated goat anti-rabbit IgG (1:2,000; Jackson ImmunoResearch, West Grove, PA, United States). Images were acquired with a LSM880 confocal laser scanning microscope (Zeiss, Germany) after the samples were stained with DAPI.

Verification of TgRuvBL1, TgRNase H1, and TgRPS2 in Sera of Acute Infection Model

To verify the presence of TgRuvBL1, TgRNase H1, and TgRPS2 in the sera of infected model. Protein G agarose beads were used to eliminate serum antibodies, then the pooled sera (60 h) from the test and control (negative) group were analyzed by immunoblotting. The positive

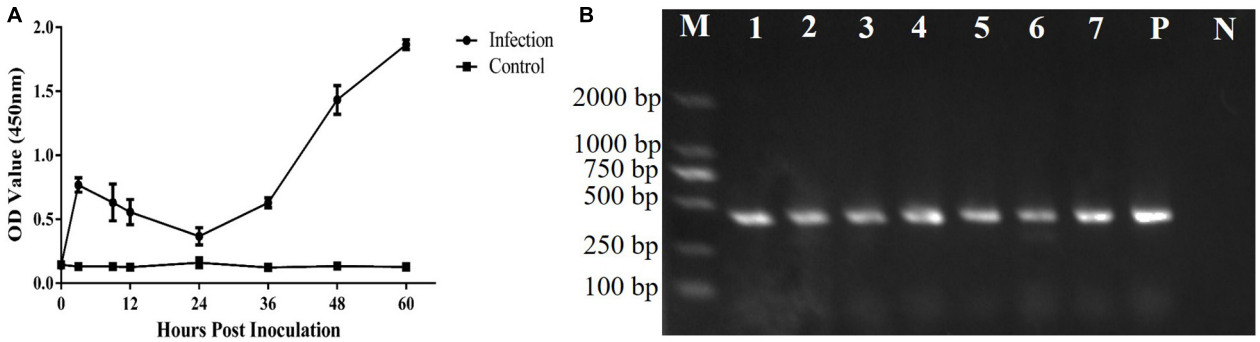

FIGURE 3 | Analyses of CAgs and nested-PCR. **(A)** Sera of 0, 3, 9, 12, 24, 36, 48, and 60 h were tested for CAgs levels. **(B)** Nested-PCR results. Lane M: marker; Lane P: positive control; Lane N: negative control; and Lanes 1–7: Nested-PCR results of 3, 9, 12, 24, 36, 48, and 60 h, The nested-PCR results from one mouse in the test group are shown.

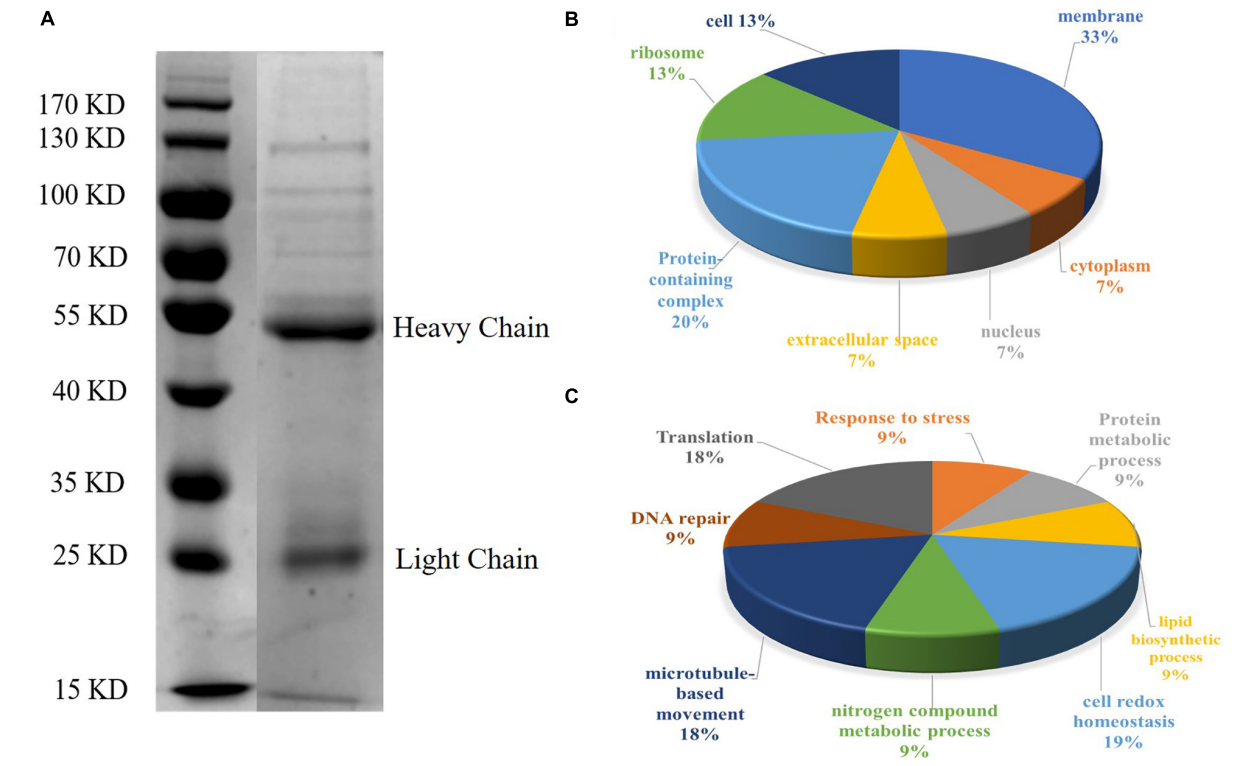

FIGURE 4 | SDS-PAGE analysis and GO annotation of CAgs enriched and purified by immunoprecipitation. **(A)** Circulating antigens enriched and purified by immunoprecipitation were analyzed by SDS-PAGE (10%). Lane 1: marker; Lane 2: immunoprecipitation supernatant (In the original image, there is a crack in a lane near the marker, so it is cut off in the manuscript. Please refer to the original images in the **Supplementary Figure 1**). **(B)** Pie charts showing the GO distributions for the identified circulating antigens based on the cell component. **(C)** Pie charts showing the GO distributions for the identified circulating antigens based on the major biological process categories.

control was ESA. Primary TgRuvBL1, TgRNase H1, and TgRPS2 antisera were diluted 1:1000, and HRP-conjugated goat anti-mouse IgG secondary antibody was diluted 1:5 000.

Mouse Vaccination and Challenge

To further explore the protective ability of TgRuvBL1, TgRNase H1, and TgRPS2, 48 mice were randomly divided into four groups and were subcutaneously injected at weeks 0, 2, and 4 with 100 μg of rTgRuvBL1, rTgRNase H1, rTgRPS2, or PBS (control group), all with 206 adjuvant. Blood was sampled from all mice on week 6. Anti-ESA IgG was determined by ELISA in mice from each group. Afterward, 12 mice from each group were intraperitoneally challenged with 1×10^3 tachyzoites of the *T. gondii* RH strain.

TABLE 2 | CAgs proteins identified by LC-MS/MS after IP enrichment and purification with ESA mouse antibodies.

Resource ID	Protein ID	Protein name	Peptide count	Unique peptide count	Cover percent	Theoretical Mr (Da)/PI	References of analysis in *T. gondii*	GO_Term
1	S7UUF6	PLP1	21	18	17.74%	125493.06/6.01	Kafsack et al., 2009	Apical part of cell
2	A0A086JV38	MIC2-associated protein M2AP	2	2	2.12%	34551.68/4.28	Huynh et al., 2003	Membrane
3	B6D286	SAG1	2	2	12.72%	17922.19/6.46	Grimwood and Smith, 1992	Membrane
4	A0A2G8YCT9	Rhoptry protein ROP28	2	2	0.72%	78578.42/9.5	Jones et al., 2017	Binding
5	A0A2T6ITL9	Protease inhibitor PI1	2	2	1.37%	47808.7/5.06	Morris et al., 2002	Extracellular space
6	S7VNC9	Actin	8	7	23.00%	32058.23/5.66	Dobrowolski and Sibley, 1996	Binding
7	A0A086PH15	Histone H2A	2	2	10.32%	15919.54/10.63	Bogado et al., 2014	Binding
8	Q9NG25	Toxofilin	2	2	6.94%	27131.46/9.57	Poupel et al., 2000	Binding
9	A0A139XN72	Putative myosin regulatory light chain	2	2	5.83%	23123.97/6.86	Herm-Götz et al., 2002	Binding
10	B6KN45	Elongation factor 1-alpha	2	2	4.46%	49005.24/9.02	Wang et al., 2017	Binding
11	A0A086L4P6	Heat shock protein HSP70	2	2	4.35%	72291.98/5.07	Aosai et al., 2002	Response to stress
12	A0A086JS03	Putative transmembrane protein	2	2	2.13%	24896.27/6.85	Xue et al., 2016	Membrane
13	A0A2G8XVZ0	Carbamoylphosphate synthetase	2	2	1.82%	92154.94/8	Fox et al., 2009	Nitrogen compound metabolic process
14	A0A3R7YIU5	Phosphatidylinositol 3-and 4-kinase	2	2	1.44%	53688.12/8.86	Wengelnik et al., 2018	Kinase activity
15	A0A086LU85	Myosin H	2	2	1.42%	78984.17/8.82	Graindorge et al., 2016	Binding
16	A0A3R7YS28	CDPK9	2	2	1.31%	60638.79/7	Long et al., 2016	Binding
17	Q9BLM8	Protein disulfide-isomerase	2	2	1.27%	52801.38/5.14	Wang et al., 2013	Cell redox homeostasis
18	A0A086QXN6	Amine-terminal region of chorein	3	3	0.22%	1101135.3/8.74	Xue et al., 2016	Membrane
19	A0A086PFP4	HECT-domain (Ubiquitin-transferase) domain-containing protein	2	2	0.21%	998277.75/8.37	Xue et al., 2016	Protein metabolic process
20	A0A086KQL2	Putative type I fatty acid synthase	2	2	0.10%	530295.61/5.92	Zhu et al., 2000	Lipid biosynthetic process -
Novel CAgs proteins								
21	A0A086KTM5	RuvB-like helicase	2	2	8.57%	11770.33/5.64	Na	DNA repair
22	A0A086JWF3	Ribonuclease	2	2	4.16%	40446.13/9.59	Na	RNA-DNA hybrid ribonuclease activity
23	A0A086JV11	Uncharacterized protein	2	2	0.27%	433546.48/6.8	Na	Unknown
24	A0A139Y154	Ribosomal protein RPS2	2	2	2.23%	29335.57/10.21	Na	Translation

(Continued)

TABLE 2 | Continued

Resource ID	Protein ID	Protein name	Peptide count	Unique peptide count	Cover percent	Theoretical Mr (Da)/PI	References of analysis in *T. gondii*	GO_Term
25	A0A3R8AB74	Ribosomal protein RPL7	2	2	1.94%	30121.23/10.37	Na	Translation
26	A0A425I0Y7	SAG-related sequence SRS55M	2	2	1.77%	41728.31/4.83	Na	Membrane
27	A0A2T6IQA3	Cation channel family transporter	2	2	1.04%	127269.78/8.94	Na	Binding
28	A0A086L241	Putative Chromosome-associated kinesin KLP1	2	2	0.79%	113375.72/4.99	Na	Microtubule-based movement
29	A0A151HDW0	Putative oxidoreductase	2	2	0.46%	146590.81/6.34	Na	Cell redox homeostasis
30	V4ZW70	SAG-related sequence SRS33	2	2	0.45%	607653.31/7.01	Na	Membrane
31	S8F1G6	Dynein heavy chain family protein	2	2	0.18%	446523/5.3	Na	Microtubule-based movement

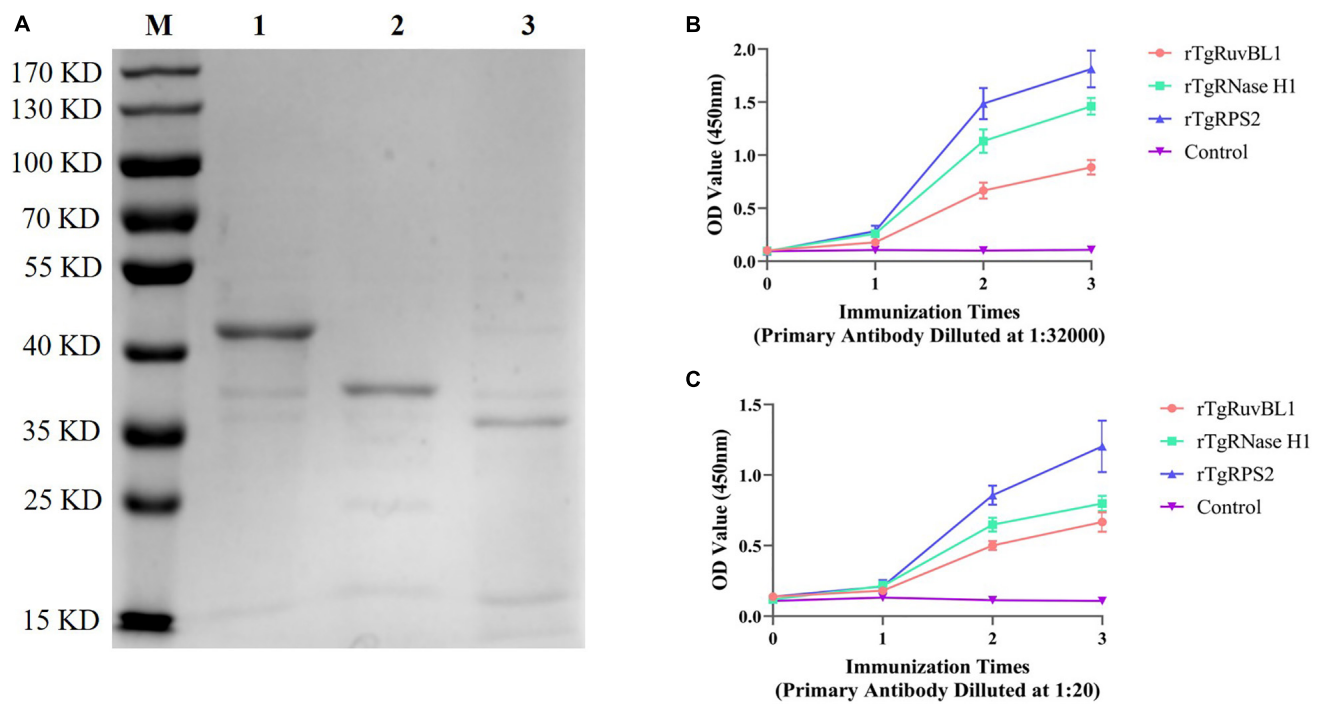

FIGURE 5 | Expression of recombinant proteins and the dynamics of specific antibody amounts in Kunming mice induced by recombinant proteins. **(A)** SDS-PAGE analysis of purified recombinant proteins. M, Marker; 1, rTgRuvBL1; 2, rTgRNase H1; and 3, rTgRPS2. **(B,C)** Plates were coated with recombinant proteins (500 ng/mL) or ESA (1 μg/mL) to detect the dynamics of specific IgG antibody amounts.

Statistical Analysis

All data were statistically analyzed using IBM SPSS 20.0 Data Editor. Differences in data among all groups were compared using one-way ANOVA. Survival of the mice was compared using Kaplan–Meier curves. Differences between groups were considered significant at $P < 0.05$.

RESULTS

Establishment of Double-PcAb Sandwich ELISA

The results of indirect ELISA and immunoblotting assays indicated that anti-ESA mouse and rabbit sera could identify numerous ESA components with good immunogenicity

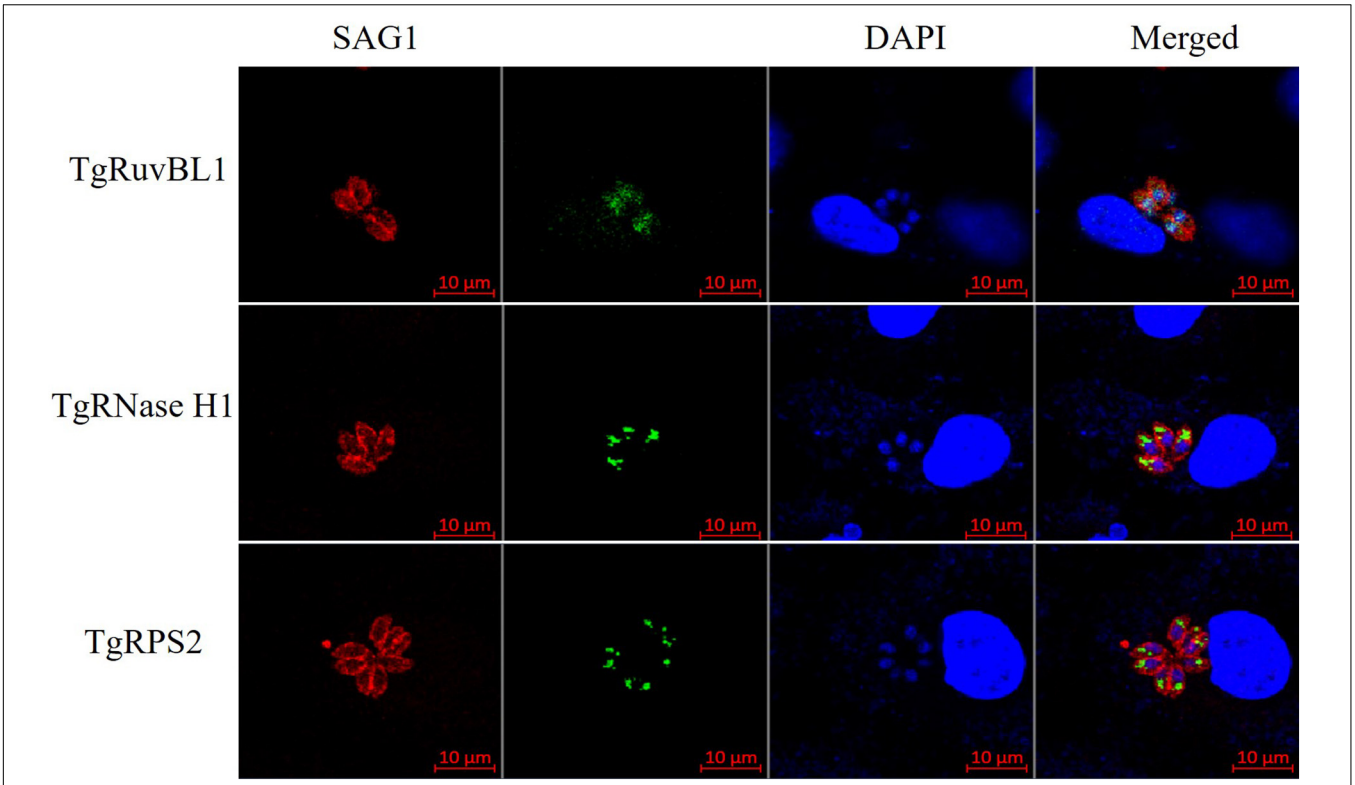

FIGURE 6 | TgRuvBL1, TgRNase H1, and TgRPS2 localize to two subcellular regions. Immunofluorescence analysis showing the localization of the three CAgs, performed in *T. gondii* stained with anti-TgRuvBL1, anti-TgRNase H1, or anti-TgRPS2 antibodies. Surface antigen 1 (SAG1) was used as a marker of the surface.

(**Figures 1A,B**). According to the checkerboard titration results (**Figure 2A**), the P/N value was highest (6.42) at dilutions of 1:1 000 for both anti-ESA rabbit serum coating and mouse serum detection antibodies. The dilution gradient of positive canine sera was detected using the double antibody sandwich ELISA with a P/N cutoff of 2.1. **Figure 2B** shows that the maximum dilution of positive serum was 1:160. These results showed that the double-PcAb sandwich ELISA was sufficiently sensitive.

Establishment of Murine *T. gondii* Infection Model Using Inoculation With Tachyzoites

The *T. gondii* strain RH is lethal in mice. In this study, the mice survived for 65 ± 2 h after inoculation with 1×10^7 tachyzoites. Both *T. gondii* and CAgs were detected in the blood at 3 h (**Figures 3A,B**). The CAgs values initially first increased from 0 to 3 h, decreased from 3 to 24 h, increased from (24 to 60 h), then peaked at 60 h. The decrease in CAgs from 3 to 24 h might have been due to *T. gondii* in the bloodstream invading various organs. These data showed that the *T. gondii* infection model was effective.

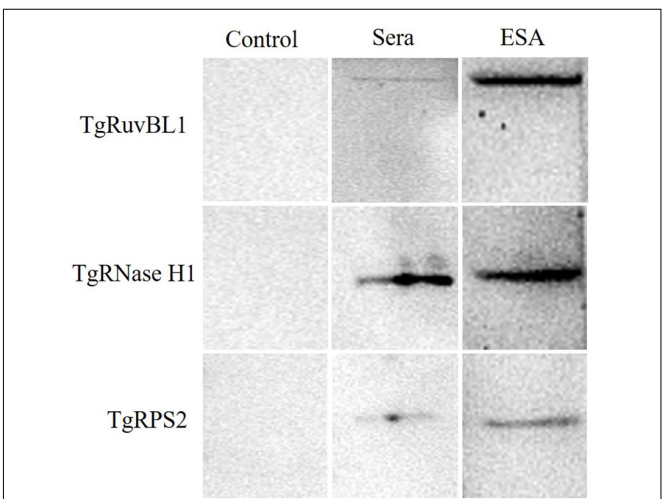

FIGURE 7 | Western blotting of the recombinant proteins. Pooled serum samples from the control group were used as negative control. Pooled serum samples from the test group at 60 h were analyzed by western blotting at a dilution of 1:10. ESA was used as positive control.

Identification of Circulating Antigens in the Sera of Acute *T. gondii* Infected Mice

Sodium dodecyl sulfate-polyacrylamide gel electrophoresis analysis showed that CAgs weighted more than 15 kD (**Figure 4A**). Among 250 protein groups identified by LC-MS/MS (**Supplementary File 1**), the unique peptide counts for 31 proteins were ≥2. **Table 2** shows that the proteins identified by immunoprecipitation-shotgun analysis

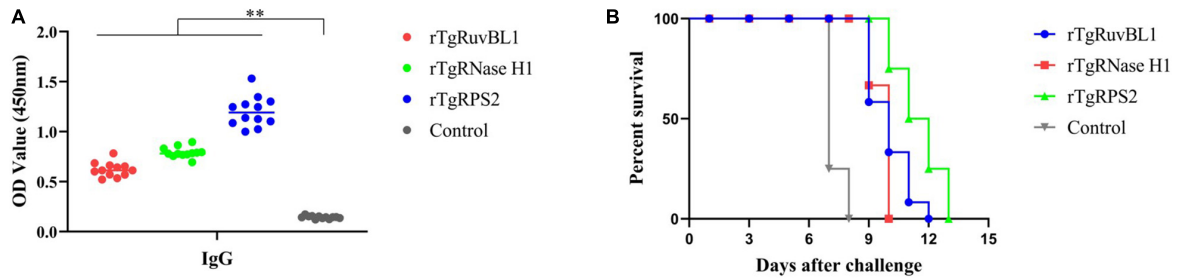

FIGURE 8 | Survival curve of mice after challenge infection with *T. gondii* RH strain. **(A)** Levels of IgG in the sera of mice at week 2 after the final booster immunization. **(B)** Mice were challenged with 10^3 tachyozoites of the RH strain injected intraperitoneally at week 2 after the third immunization. $^*p < 0.05$ and $^{**}p < 0.01$, compared with the control groups.

comprised micronemal proteins (PLP1 and M2AP), surface antigens (SAG1), rhoptry protein (ROP28), dense granule proteins (PI-1), and novel CAgs proteins (RuvB-like helicase, ribonuclease, and ribosomal protein RPS2) and others (**Table 2**).

Gene Ontology Analysis

To further understand the functions of the CAgs herein identified, their gene ontology (GO) was evaluated. **Figures 4B,C** shows the GO annotations of the 31 high-confidence proteins, among which 15 were annotated in cell composition and were related to membrane components (33%), protein-containing complexes (20%), ribosomes (13%), cells (13%), extracellular regions (7%), the nucleus (7%), and the cytoplasm (7%). Only 11 proteins were annotated within biological process, being related to cell redox homeostasis (19%), translation (18%), microtubule-based movement (18%), response to stress (9%), protein metabolic processes (9%), lipid biosynthetic processes (9%), nitrogen compound metabolic processes (9%), and DNA repair (9%).

Expression, Purification, and Antibody Production of Recombinant TgRuvBL1, TgRNase H1, and TgRPS2

The genes encoding TgRuvBL1, TgRNase H1, and TgRPS2 were amplified from the *T. gondii* RH strain. The recombinant proteins were expressed in *E. coli* as inclusion body His-tagged fusion proteins when bacterial growth occurred at 37°C. The inclusion body recombinant proteins were refolded, purified, and concentrated. SDS-PAGE analysis indicated that the recombinant proteins (rTgRuvBL1, rTgRNase H1, and rTgRPS2) were successfully expressed and purified (**Figure 5A**). **Figure 5B** shows that the titer of the antibodies in mice serum reached more than 1:32,000 after three immunizations.

Reactivity of Polyclonal Antibodies Toward *T. gondii*-Derived ESA and Tachyzoites

To characterize the reactivity of anti-recombinant proteins mouse sera with the ESA and *T. gondii* tachyzoites, antisera against rTgRuvBL1, rTgRNase H1, and rTgRPS2 were used as the primary antibody for indirect ELISA and IFA. The ELISA results showed that TgRuvBL1, TgRNase H1, and TgRPS2 antisera were recognized by *T. gondii* tachyzoites-derived natural ESA (**Figure 5C**), indicating that these proteins were present in *T. gondii* ESA. Moreover, IFA using anti-TgRuvBL1, anti-TgRNase H1, or anti-TgRPS2 antibodies revealed that the three proteins were localized in different subcellular compartments in *T. gondii* tachyzoites, including the nucleus (TgRuvBL1) and the apical end (TgRNase H1 and TgRPS2; **Figure 6**).

Detection of Three CAgs in the Sera of Infection Murine Models

Among the newly identified CAgs, the presence of TgRuvBL1, TgRNase H1, and TgRPS2 was verified in mouse sera. Pooled sera from the test and control groups were analyzed by immunoblotting, with ESA being used as positive control. The three CAgs were detected in the sera of mice with acute *T. gondii* infections (**Figure 7**).

Protective Ability of Recombinant Proteins in Kunming Mice

Significantly more IgG antibodies were detected in the sera of mice immunized with rTgRuvBL1, rTgRNase H1, or rTgRPS2 compared with control mice (**Figure 8A**). **Figure 8B** shows survival curves for the four groups of mice. Mice immunized with rTgRuvBL1, rTgRNase H1, or rTgRPS2 survived longer than control mice, all of which died within 8 days of challenge (10.0 ± 0.30, 9.67 ± 0.14, and 11.50 ± 0.34 vs. 7.25 ± 1.31 days; $P < 0.05$).

DISCUSSION

Detection of *T. gondii*-specific IgM and IgG antibodies is the main serological diagnostic method for acute toxoplasmosis. However, detection of IgG antibodies is not reliable for the diagnosis of acute infections, as they induce the production of low levels of IgG antibodies in acute infection and IgG positivity may be indicative of a previous infection.

Moreover, IgM antibodies remain detectable for over a year. Therefore, even the presence of IgM antibodies does not necessarily indicate an acute infection (Elsheikha et al., 2020; Mcleod et al., 2020). ESA are the majority of the CAgs in sera from hosts with acute toxoplasmosis and they were proven to be a serologic marker for the diagnosis of acute toxoplasmosis and the infection route not affecting the detection of CAgs (Hafid et al., 1995; Abdollahi et al., 2009; Darcy et al., 2010; Xue et al., 2016). Particularly, they were shown to be diagnostic markers for cerebral toxoplasmosis in immunocompromised individuals (Meira et al., 2008; Meira et al., 2011). Thus, the identification of CAg components and screening of candidate diagnostic molecules can help improve the specificity and sensitivity of acute infection detection. However, only few studies have focused on the identification of CAgs.

In the current study, a murine model of acute *T. gondii* infection was established, which further demonstrated that CAgs could serve as markers of acute infection in mice in agreement with previous studies (Asai et al., 1987; Hassl et al., 1988; Chen et al., 2008; Azami et al., 2011; Wang et al., 2012; Xue et al., 2016). Moreover, CAgs were detected 3 h post-inoculation, which was consistent with the results of nested PCR. The levels of CAgs decreased during the following 3 to 24 h, and increased in the subsequent 24 to 60 h. The initial reduction might have been due to the host immune response and *T. gondii* in the bloodstream invading various organs.

Herein, 31 CAgs were identified in this study, among which, the diagnostic applications of SAG1, and ubiquitin-transferase domain-containing protein have been investigated (Felgner et al., 2015; Jiang et al., 2015). Moreover, some of the proteins identified, such as PLP1 (Kafsack et al., 2009), M2AP (Huynh et al., 2003), PI1 (Morris et al., 2002), Toxofilin (Poupel et al., 2000), Carbamoylphosphate synthetase (Fox et al., 2009), Myosin H (Graindorge et al., 2016), and CDPK9 (Long et al., 2016), have been shown to impair parasite progression through the lytic cycle, resulting in a loss of or weaker virulence when knocked-down. In addition, although most of the proteins have low reliability, some of them play important roles, such as ROP13 (Turetzky et al., 2010; Kang et al., 2019). Therefore, it is reasonable to believe that the CAgs identified in this study may contribute to the discovery of new virulence factors.

Furthermore, three CAgs – TgRuvBL1, TgRNaseH1, and TgRPS2 – were selected for prokaryotic expression to prepare murine polyclonal antibodies. Polyclonal anti-rTgRuvBL1, anti-rTgRNase H1, and anti-rTgRPS2 antibodies were recognized by natural ESA from *T. gondii* tachyzoites. Moreover, IFA data showed that they localize to two subcellular compartments, including the nucleus (TgRuvBL1) and the apical end (TgRNase H1 and TgRPS2). Of note, as both TgRNase H1 and TgRPS2 localize to the apical end, they may be involved in the invasion or egress of *T. gondii* tachyzoites. However, further research is warranted to explore this hypothesis. Moreover, these three proteins were found in the sera from mice with acute infection, which suggests that they may hold diagnostic potential for acute *T. gondii* infection and that their antibodies may be used in serological detection of CAgs. However, a large number of clinical trials are needed to verify whether they can be used in the diagnosis of acute infections. The present results also provide a theoretical basis for the continued development of rapid, highly specific, and accurate immunological diagnostic strategies.

Most CAgs are ESA that play important roles in inducing appropriate humoral and cellular immune responses against *T. gondii* (Hafid et al., 2005; Jongert et al., 2009; Costa-Silva et al., 2012; Chen et al., 2013; Daryani et al., 2014). Moreover, some proteins identified herein such as PLP1 (Yan et al., 2011), M2AP (Dautu et al., 2007), SAG1 (Mohamed et al., 2003), protease inhibitor PI1 (Cuppari et al., 2008), Histone H2A (Yu et al., 2020), Elongation factor 1-alpha (EF-1α; Wang et al., 2017), CDPK9 (Wang H. L. et al., 2016; Wang J. L. et al., 2016), HSP70 (Mohamed et al., 2003), protein disulfide-isomerase (Wang et al., 2013), and toxofilin (Song et al., 2017) elicit powerful specific immune responses, providing partial protection against acute or chronic *T. gondii* infection. Thus, we evaluated the protective ability of TgRuvBL1, TgRNase H1, and TgRPS2.

We showed that survival was prolonged in mice immunized with rTgRuvBL1, rTgRNase H1, or rTgRPS2, and then lethally challenged with *T. gondii* RH. However, all mice in our study died after challenge with *T. gondii* RH. The protective efficacy of these three recombinant proteins was weaker than that of other proteins, such as rTgEF-1 (14.53 ± 1.72 days; Wang et al., 2017), suggesting that they only weakly protected against infection by a highly virulent *T. gondii* strain. Although the demonstrated protection is not good enough for a vaccine, perhaps other proteins among the newly identified CAgs have better protective efficacy, similar to some other proteins identified in this study [e.g., PLP1 (Yan et al., 2011), EF-1α (Wang et al., 2017), among others].

CONCLUSION

In summary, we identified 31 CAgs in the sera of mice infected with *T. gondii*. Among these CAg molecules, three novel proteins (TgRuvBL1, TgRNase H1, and TgRPS2) were successfully confirmed to be present in the sera of the infection mouse models. Although these proteins only showed a weak protection potential against a highly virulent *T. gondii* strain, they may represent potential diagnostic candidates for acute *T. gondii* infection.

DATA AVAILABILITY STATEMENT

The datasets presented in this study can be found in online repositories. The names of the repository/repositories and accession number(s) can be found below: ProteomeXchange

Consortium via the PRIDE partner repository with the dataset identifier PXD021938 (https://www.ebi.ac.uk/pride/archive/projects/PXD021938).

ETHICS STATEMENT

The animal study was reviewed and approved by The Animal Care and Use Committee of the Shanghai Veterinary Research Institute approved the study and the protocols complied with approved guidelines.

AUTHOR CONTRIBUTIONS

QL and QW participated in the experiment design and wrote the manuscript. QL and WJ analyzed the data. QL, QW, YC, MZ, and XG carried out the experiments. QL carried out bioinformatics analysis. All authors read and approved the final version of the manuscript.

FUNDING

This work was supported by the Shanghai Science and Technology Promotion Agriculture Innovation Program (2019No.3-3) and the National Key Research and Development Programs of China (No. 2016YFD0 501101).

SUPPLEMENTARY MATERIAL

The Supplementary Material for this article can be found online at: https://www.frontiersin.org/articles/10.3389/fmicb.2020.612252/full#supplementary-material

Supplementary Figure 1 | SDS-PAGE analysis of CAg enriched and purified by immunoprecipitation. Circulating antigens enriched and purified by immunoprecipitation were analysed by SDS-PAGE (10 %). Lanes 1, 2, 3, and 4: immunoprecipitation supernatant. Due to the cracks in Lane 1 and Lane 2 is intercepted in the manuscript.

Supplementary File 1 | List of CAgs proteins identified by LC-MS/MS after IP enrichment and purification with ESA antibodies.

REFERENCES

Abdollahi, S. H., Ayoobi, F., Khorramdelazad, H., Hassanshahi, G., Ahmadabadi, B. N., Rezayati, M., et al. (2013). Interleukin-10 serum levels after vaccination with in vivo prepared *Toxoplasma gondii* excreted/secreted antigens. *Oman. Med. J.* 28, 112–115. doi: 10.5001/omj.2013.29

Abdollahi, S. O., Arababadi, M. K., and Hassanshahi, G. (2009). Evaluation of excreted/secreted antigens derived from peritoneal of toxoplasma infected small mice to detect IgG against toxoplasma. *Pak. J. Biol. Sci.* 12, 530–533. doi: 10.3923/pjbs.2009.530.533

Aosai, F., Chen, M., Kang, H. K., Mun, H. S., and Yano, A. (2002). *Toxoplasma gondii*-derived heat shock protein HSP70 functions as a B cell mitogen. *Cell Stress Chaperones* 7, 357–364. doi: 10.1379/146612682002007<0357:tgdhsp>2.0.co;2

Asai, T., Kim, T. J., Kobayashi, M., and Kojima, S. (1987). Detection of nucleoside triphosphate hydrolase as a circulating antigen in sera of mice infected with *Toxoplasma gondii*. *Infect. Immun.* 55, 1332–1335. doi: 10.1128/IAI.55.5.1332-1335

Azami, S. J. P., Keshavarz, H., Rezaian, M., Mohebali, M., and Shojaee, S. (2011). Rapid detection of *Toxoplasma gondii* antigen in experimentally infected mice by Dot- ELISA. *Iran. J. Parasitol.* 6, 28–33.

Bogado, S. S., Dalmasso, C., Ganuza, A., Kim, K., Sullivan, W. J., Angel, S. O., et al. (2014). Canonical histone H2Ba and H2A.X *dimerize in an opposite genomic localization to H2*A.Z/H2B.Z dimers in *Toxoplasma gondii*. *Mol. Biochem. Parasitol.* 197, 36–42. doi: 10.1016/j.molbiopara.2014.09.009

Carlos, J. R. F., Rosalba, C. M., Mónica, E. M. C., Sirenia, G. P., Emmanuel, R. C., and Ricardo, M. F. (2019). Proteomic and structural characterization of self-assembled vesicles from excretion/secretion products of *Toxoplasma gondii*. *Proteomics* 208:103490. doi: 10.1016/j.jprot.2019.103490

Chen, J. L., Yi-yue, G., Jie, Z., Xiao-yan, Q., Jing-fan, Q., Jiang-ping, W., et al. (2013). The dysfunction of CD4+CD25+ regulatory T cells contributes to the abortion of mice Caused by *Toxoplasma gondii* Excreted-secreted antigens in early pregnancy. *PLoS One* 8:e69012. doi: 10.1371/journal.pone.0069012

Chen, R., Lu, S., Lou, D., Lin, A., and Fu, C. (2008). Evaluation of a rapid ELISA technique for detection of circulating antigens of *Toxoplasma gondii*. *Microbiol. Immunol.* 52, 180–187. doi: 10.1111/j.1348-0421.2008.00020.x

Costa-Silva, T. A., Borges, M. M., Galhardo, C. S., and Pereira-Chioccola, V. L. (2012). Immunization with excreted/secreted proteins in AS/n mice activating cellular and humoral response against *Toxoplasma gondii* infection. *Acta Trop.* 124, 203–209. doi: 10.1016/j.actatropica.2012.08.013

Csep, A., and Drăghici, S. (2013). *Toxoplasma gondii* infection in immunocompromised individuals. *BMC Infect. Dis.* 13(Suppl. 1):P4. doi: 10.1186/1471-2334-13-S1-P4

Cuppari, A. F., Sanchez, V., Ledesma, B., Frank, F. M., Goldman, A., Angel, S. O., et al. (2008). *Toxoplasma gondii* protease inhibitor-1 (TgPI-1) is a novel vaccine candidate against toxoplasmosis. *Vaccine.* 26, 5040–5045. doi: 10.1016/j.vaccine.2008.07.031

Darcy, F., Deslee, D., Santoro, F., Charif, H., Auriault, C., Decoster, A., et al. (2010). Induction of a protective antibody-dependent response against toxoplasmosis by in vitro excreted/secreted antigens from tachyzoites of *Toxoplasma gondii*. *Parasite Immunol.* 10, 553–567. doi: 10.1111/j.1365-3024.1988.tb00242.x

Daryani, A., Hosseini, A. Z., and Dalimi, A. (2003). Immune responses against excreted/secreted antigens of *Toxoplasma gondii* tachyzoites in the murine model. *Vet. Parasitol.* 113, 123–134. doi: 10.1016/s0304-4017(03)00044-x

Daryani, A., Sharif, M., Kalani, H., Rafiei, A., and Ahmadpour, E. (2014). Electrophoretic patterns of *Toxoplasma gondii* excreted/secreted antigens and their role in induction of the humoral immune response. *Jundishapur J. Microbiol.* 7:e9525. doi: 10.5812/jjm.9525

Dautu, G., Munyaka, B., Carmen, G., Zhang, G., Omata, Y., Xuenan, X., et al. (2007). *Toxoplasma gondii*: DNA vaccination with genes encoding antigens MIC2, M2AP, AMA1 and BAG1 and evaluation of their immunogenic potential. *Exp. Parasitol.* 116, 273–282. doi: 10.1016/j.exppara.2007.01.017

Dobrowolski, J. M., and Sibley, L. D. (1996). Toxoplasma invasion of mammalian cells is powered by the actin cytoskeleton of the parasite. *Cell* 84, 933–939. doi: 10.1016/S0092-8674(00)81071-5

Dupont, D., Fricker-Hidalgo, H., Brenier-Pinchart, M. P., Garnaud, C., Wallon, M., Pelloux, H., et al. (2020). Serology for toxoplasma in immunocompromised patients: still useful? *Trends Parasitol.* S1471-4922, 30248–30248. doi: 10.1016/j.pt.2020.09.006

Elsheikha, H. M., Marra, C. M., and Zhu, X. Q. (2020). Epidemiology, pathophysiology, diagnosis, and management of cerebral toxoplasmosis. *Clin. Microbiol. Rev.* 34, e115–e119. doi: 10.1128/CMR.00115-19

Felgner, J., Juarez, S., Hung, C., Liang, L. I., Jain, A., Döşkaya, M., et al. (2015). Identification of *Toxoplasma gondii* antigens associated with different types of infection by serum antibody profiling. *Parasitology* 142, 827–838. doi: 10.1017/S0031182014001978

Fox, B. A., Ristuccia, J. G., and Bzik, D. J. (2009). Genetic identification of essential indels and domains in carbamoyl phosphate synthetase II of *Toxoplasma gondii*. *Int. J. Parasitol.* 39, 533–539. doi: 10.1016/j.ijpara.2008.09.011

Graindorge, A., Frénal, K., Jacot, D., Salamun, J., Marq, J. B., and Soldati-Favre, D. (2016). The conoid associated motor myoh is indispensable for *Toxoplasma gondii* entry and exit from host cells. *PLoS Pathog.* 12:e1005388. doi: 10.1371/journal.ppat.1005388

Grimwood, J., and Smith, J. E. (1992). *Toxoplasma gondii*: the role of a 30-kDa surface protein in host cell invasion. *Exp. Parasitol.* 74, 106–111. doi: 10.1016/0014-4894(92)90144-y

Hafid, J., Tran Manh Sung, R., Raberin, H., Akono, Z. Y., Pozzetto, B., and Jana, M. (1995). Detection of circulating antigens of *Toxoplasma gondii* in human infection. *Am. J. Trop. Med. Hyg.* 52, 336–339. doi: 10.4269/ajtmh.1995.52.336

Hafid, J., Vincent, N., Flori, P., Bellete, B., Raberin, H., and Sung, R. T. (2005). Production of antibodies in murine mucosal immunization with *Toxoplasma gondii* excreted/secreted antigens. *Vet. Parasitol.* 128, 23–28. doi: 10.1016/j.vetpar.2004.11.002

Hassl, A., Aspöck, H., and Flamm, H. (1988). Circulating antigen of *Toxoplasma gondii* in patients with AIDS: significance of detection and structural properties. *Zentralbl Bakteriol Mikrobiol Hyg A* 270, 302–309. doi: 10.1016/s0176-6724(88)80167-6

Herm-Götz, A., Weiss, S., Stratmann, R., Fujita-Becker, S., Ruff, C., Meyhöfer, E., et al. (2002). *Toxoplasma gondii* myosin A and its light chain: a fast, single-headed, plus-end-directed motor. *EMBO J.* 21, 2149–2158. doi: 10.1093/emboj/21.9.2149

Hide, G., Morley, E. K., Hughes, J. M., Gerwash, O., Elmahaishi, M. S., Elmahaishi, K. H., et al. (2009). Evidence for high levels of vertical transmission in *Toxoplasma gondii*. *Parasitology* 136, 1877–1885. doi: 10.1017/S0031182009990941

Hunter, C. A., and Sibley, L. D. (2012). Modulation of innate immunity by *Toxoplasma gondii* virulence effectors. *Nat. Rev. Microbiol.* 10, 766–778. doi: 10.1038/nrmicro2858

Huynh, M. H., Rabenau, K. E., Harper, J. M., Beatty, W. L., Sibley, L. D., and Carruthers, V. B. (2003). Rapid invasion of host cells by Toxoplasma requires secretion of the MIC2-M2AP adhesive protein complex. *EMBO J.* 22, 2082–2090. doi: 10.1093/emboj/cdg217

Jiang, W., Liu, Y., Chen, Y., Yang, Q., and Chun, P. (2015). A novel dynamic flow immunochromatographic test (DFICT) using gold nanoparticles for the serological detection of Toxoplasma gondii infection in dogs and cats. *Biosens. Bioelectron.* 72, 133–139. doi: 10.1016/j.bios.2015.04.035

Jones, N. G., Wang, Q., and Sibley, L. D. (2017). Secreted protein kinases regulate cyst burden during chronic toxoplasmosis. *Cell Microbiol.* 19:10.1111/cmi.12651. doi: 10.1111/cmi.12651

Jongert, E., Roberts, C. W., Gargano, N., Förster-Waldl, E., and Petersen, E. (2009). Vaccines against *Toxoplasma gondii*: challenges and opportunities. *Mem. Inst. Oswaldo. Cruz.* 104, 252–266. doi: 10.1590/s0074-02762009000200019

Kafsack, B. F. C., Pena, J. D. O., Coppens, I., Ravindran, S., Boothroyd, J. C., and Carruthers, V. B. (2009). Rapid membrane disruption by a perforin-like protein facilitates parasite exit from host cells. *Science* 323, 530–533. doi: 10.1126/science.1165740

Kang, H. J., Lee, S. H., Kim, M. J., Chu, K. B., Lee, D. H., Chopra, M., et al. (2019). Influenza virus-like particles presenting both *Toxoplasma gondii* ROP4 and ROP13 Enhance Protection against *T. gondii* infection. *Pharmaceutics* 11:342. doi: 10.3390/pharmaceutics11070342

Lima, T. S., and Lodoen, M. B. (2019). Mechanisms of human innate immune evasion by *Toxoplasma gondii*. *Front. Cell Infect. Microbiol.* 9:103. doi: 10.3389/fcimb.2019.00103

Long, S., Wang, Q., and Sibley, L. D. (2016). Analysis of noncanonical calcium-dependent protein kinases in *Toxoplasma gondii* by targeted gene deletion using CRISPR/Cas9. *Infect. Immun.* 84, 1262–1273. doi: 10.1128/IAI.01173-15

Mcleod, R., Cohen, W., Dovgin, S., Finkelstein, L., and Boyer, K. M. (2020). "Human Toxoplasma infection," in *Toxoplasma gondii*, eds L. M. Weiss and K. Kim (Cambridge, MA: Academic), 143–148.

Meira, C. S., Costa-Silva, T. A., Vidal, J. E., Ferreira, I. M. R., and Hiramoto, R. M. (2008). Use of the serum reactivity against *Toxoplasma gondii* excreted-secreted antigens in cerebral toxoplasmosis diagnosis in human immunodeficiency virus-infected patients. *J. Med. Microbiol.* 57(Pt 7), 845–850. doi: 10.1099/jmm.0.47687-0

Meira, C. S., Vidal, J. E., Costa-Silva, T. A., Frazatti-Gallina, N., and Pereira-Chioccola, V. L. (2011). Immunodiagnosis in cerebrospinal fluid of cerebral toxoplasmosis and HIV-infected patients using *Toxoplasma gondii* excreted/secreted antigens. *Diagn. Microbiol. Infect. Dis.* 71, 279–285. doi: 10.1016/j.diagmicrobio.2011.07.008

Mohamed, R. M., Aosai, F., Mei, C., Mun, H. S., Norose, K., Belal, U. S., et al. (2003). Induction of protective immunity by DNA vaccination with *Toxoplasma gondii* HSP70, HSP30 and SAG1 genes. *Vaccine* 21, 2852–2861. doi: 10.1016/s0264-410x(03)00157-9

Montoya, J. G., and Liesenfeld, O. (2004). Toxoplasmosis. *Lancet* 363, 1965–1976. doi: 10.1016/S0140-6736(04)16412-X

Morris, M. T., Coppin, A., Tomavo, S., and Carruthers, V. B. (2002). Functional analysis of *Toxoplasma gondii* protease inhibitor 1. *J. Biol. Chem.* 277, 45259–45266. doi: 10.1074/jbc.M205517200

Nissapatorn, V. (2009).). Toxoplasmosis in HIV/AIDS: a living legacy. *Southeast Asian. J. Trop. Med. Public Health* 40, 1158–1178.

Poupel, O., Boleti, H., Axisa, S., Couture-Tosi, E., and Tardieux, I. (2000). Toxofilin, a novel actin-binding protein from *Toxoplasma gondii*, sequesters actin monomers and caps actin filaments. *Mol. Biol. Cell* 11, 355–368. doi: 10.1091/mbc.11.1.355

Robert-Gangneux, F., and Dardé, M. L. (2012). Epidemiology of and diagnostic strategies for toxoplasmosis. *Clin. Microbiol. Rev.* 25, 264–296. doi: 10.1128/CMR.05013-11

Song, P., He, S., Zhou, A., Lv, G., Guo, J., Zhou, J., et al. (2017). Vaccination with toxofilin DNA in combination with an alum-monophosphoryl lipid A mixed adjuvant induces significant protective immunity against *Toxoplasma gondii*. *BMC Infect. Dis.* 17:19. doi: 10.1186/s12879-016-2147-1

Turetzky, J. M., Chu, D. K., Hajagos, B. E., and Bradley, P. J. (2010). Processing and secretion of ROP13: a unique Toxoplasma effector protein. *Int. J. Parasitol.* 40, 1037–1044. doi: 10.1016/j.ijpara.2010.02.014

Wang, H. L., Wang, Y. J., Pei, Y. J., Bai, J. Z., Yin, L. T., Guo, R., et al. (2016). DNA vaccination with a gene encoding *Toxoplasma gondii* Rhoptry Protein 17 induces partial protective immunity against lethal challenge in mice. *Parasite* 23:4. doi: 10.1051/parasite/2016004

Wang, J. L., Huang, S. Y., Li, T. T., Chen, K., Ning, H. R., and Zhu, X. Q. (2016). Evaluation of the basic functions of six calcium-dependent protein kinases in *Toxoplasma gondii* using CRISPR-Cas9 system. *Parasitol. Res.* 115, 697–702. doi: 10.1007/s00436-015-4791-6

Wang, H. L., Ya-Qing, L., Li-Tian, Y., Xiao-Li, M., Min, G., Jian-Hong, Z., et al. (2013). *Toxoplasma gondii* protein disulfide isomerase (TgPDI) is a novel vaccine candidate against toxoplasmosis. *PLoS One* 8:e70884. doi: 10.1371/journal.pone.0070884

Wang, Q., Jiang, W., Chen, Y. J., Liu, C. Y., Shi, J. L., and Li, X. T. (2012). Prevalence of *Toxoplasma gondii* antibodies, circulating antigens and DNA in stray cats in Shanghai, China. *Parasit Vectors* 5:190. doi: 10.1186/1756-3305-5-190

Wang, S., Zhang, Z., Wang, Y., Gadahi, J. A., Xu, L., Yan, R., et al. (2017). *Toxoplasma gondii* elongation Factor 1-Alpha (TgEF-1α) is a novel vaccine candidate antigen against toxoplasmosis. *Front. Microbiol.* 8:168. doi: 10.3389/fmicb.2017.00168

Wengelnik, K., Daher, W., and Lebrun, M. (2018). Phosphoinositides and their functions in apicomplexan parasites. *Int. J. Parasitol.* 48, 493–504. doi: 10.1016/j.ijpara.2018.01.009

Wohlfert, E. A., Blader, I. J., and Wilson, E. H. (2017). Brains and brawn: toxoplasma infections of the central nervous system and skeletal muscle. *Trends Parasitol.* 33, 519–531. doi: 10.1016/j.pt.2017.04.001

Xue, J., Jiang, W., Chen, Y., Liu, Y., Zhang, H., Xiao, Y., et al. (2016). Twenty-six circulating antigens and two novel diagnostic candidate molecules identified in the serum of canines with experimental acute toxoplasmosis. *Parasites Vectors* 9:374. doi: 10.1186/s13071-016-1643-x

Xue, J., Jiang, W., Li, J., Xiong, W., Tian, Z., Zhang, Q., et al. (2019). *Toxoplasma gondii* RPL40 is a circulating antigen with immune protection effect. *Folia Parasitol.* 66:2019.013. doi: 10.14411/fp.2019.013

Yan, H. K., Yuan, Z.-G., Petersen, E., Zhang, X.-X., Zhou, D.-H., Liu, Q., et al. (2011). *Toxoplasma gondii*: protective immunity against experimental toxoplasmosis induced by a DNA vaccine encoding the perforin-like protein 1. *Exp Parasitol.* 128, 38–43. doi: 10.1016/j.exppara.2011.02.005

Yu, Z., Zhou, T., Luo, Y., Dong, L., Li, C., Chen, M., et al. (2020). Modulation effects of *Toxoplasma gondii* histone H2A1 on murine macrophages and

encapsulation with polymer as a vaccine candidate. *Vaccines* 8:E731. doi: 10.3390/vaccines8040731

Zhou, X. W., Kafsack, B. F. C., Cole, R. N., Beckett, P., Shen, R. F., and Carruthers, V. B. (2005). The opportunistic pathogen *Toxoplasma gondii* deploys a diverse legion of invasion and survival proteins. *J. Biol. Chem.* 280, 34233–34244. doi: 10.1074/jbc.M504160200

Zhu, G., Marchewka, M. J., Woods, K. M., Upton, S. J., and Keithly, J. S. (2000). Molecular analysis of a Type I fatty acid synthase in *Cryptosporidium parvum*. *Mol. Biochem. Parasitol.* 105, 253–260. doi: 10.1016/s0166-6851(99)00183-8

Conflict of Interest: The authors declare that the research was conducted in the absence of any commercial or financial relationships that could be construed as a potential conflict of interest.

frontiers in Microbiology

ORIGINAL RESEARCH
published: 18 January 2021
doi: 10.3389/fmicb.2020.631444

PfAP2-G2 Is Associated to Production and Maturation of Gametocytes in *Plasmodium falciparum via* Regulating the Expression of *PfMDV-1*

Yaozheng Xu[1†], Dan Qiao[2†], Yuhao Wen[3], Yifei Bi[4], Yuxi Chen[1], Zhenghui Huang[3], Liwang Cui[5], Jian Guo[6] and Yaming Cao[1*]*

[1] Department of Immunology, College of Basic Medical Sciences, China Medical University, Shenyang, China, [2] Department of Laboratory Medicine, Ruijin Hospital, Shanghai Jiao Tong University School of Medicine, Shanghai, China, [3] Institut Pasteur of Shanghai, Chinese Academy of Sciences, Shanghai, China, [4] Philosophy, Politics and Economics Department, University College London, London, United Kingdom, [5] Department of Internal Medicine, Morsani College of Medicine, University of South Florida, Tampa, FL, United States, [6] Department of Laboratory Medicine, Shanghai East Hospital, Tongji University School of Medicine, Shanghai, China

OPEN ACCESS

Edited by:
Hong-Juan Peng,
Southern Medical University, China

Reviewed by:
Jianbing Mu,
National Institutes of Health (NIH), United States
Jun Cao,
Jiangsu Institute of Parasitic Diseases (JIPD), China

***Correspondence:**
Jian Guo
guojian1110@126.com
Yaming Cao
ymcao@cmu.edu.cn

[†]These authors have contributed equally to this work

Specialty section:
This article was submitted to Infectious Diseases, a section of the journal Frontiers in Microbiology

Received: 20 November 2020
Accepted: 21 December 2020
Published: 18 January 2021

Citation:
Xu Y, Qiao D, Wen Y, Bi Y, Chen Y, Huang Z, Cui L, Guo J and Cao Y (2021) PfAP2-G2 Is Associated to Production and Maturation of Gametocytes in Plasmodium falciparum via Regulating the Expression of PfMDV-1. Front. Microbiol. 11:631444. doi: 10.3389/fmicb.2020.631444

Gametocyte is the sole form of the *Plasmodium falciparum* which is transmissible to the mosquito vector. Here, we report that an Apicomplexan Apetala2 (ApiAP2) family transcription factor, PfAP2-G2 (Pf3D7_1408200), plays a role in the development of gametocytes in *P. falciparum* by regulating the expression of *PfMDV-1 (Pf3D7_1216500)*. Reverse transcriptase-quantitative PCR (RT-qPCR) analysis showed that *PfAP2-G2* was highly expressed in the ring stage. Indirect immunofluorescence assay showed nuclear localization of PfAP2-G2 in asexual stages. The knockout of *PfAP2-G2* led to a ∼95% decrease in the number of mature gametocytes with a more substantial influence on the production and maturation of the male gametocytes, resulting in a higher female/male gametocyte ratio. To test the mechanism of this phenotype, RNA-seq and RT-qPCR showed that disruption of *PfAP2-G2* led to the down-regulation of male development gene-1 (*PfMDV-1*) in asexual stages. We further found that PfAP2-G2 was enriched at the transcriptional start site (TSS) of *PfMDV-1* by chromatin immunoprecipitation and qPCR assay in both ring stage and schizont stage, which demonstrated that *PfMDV-1* is one of the targets of PfAP2-G2. In addition, RT-qPCR also showed that PfAP2-G (Pf3D7_1222600), the master regulator for sexual commitment, was also down-regulated in the PfAP2-G2 knockout parasites in the schizont stage, but no change in the ring stage. This phenomenon suggested that PfAP2-G2 played a role at the asexual stage for the development of parasite gametocytes and warrants further investigations in regulatory pathways of PfAP2-G2.

Keywords: malaria, *Plasmodium falciparum*, gametocytes, sexual development, transcriptional factor

INTRODUCTION

Malaria is a vector-borne disease caused by protozoan parasites of the genus *Plasmodium*. Nearly half of the world's population is at risk of malaria and hundreds of millions of people suffer from the disease each year. Of the five species that infect humans, *Plasmodium falciparum* is the most lethal. The complete lifecycle of *P. falciparum* includes developmental stages that occur in a mosquito vector, the human liver, and human blood (Ciuffreda et al., 2020). Though the symptoms of the disease are associated with the asexual growth of the parasites in the human blood, the parasites must undergo sexual differentiation to form female and male gametocytes, so that the mature gametocytes in the human peripheral blood can be taken up by the mosquito and transmitted. Therefore, gametocyte is an attractive target for eliminating malaria (Henry et al., 2019; Amoah et al., 2020; Guiguemde et al., 2020).

The Apicomplexan Apetala2 (ApiAP2) family is the sole family of sequence-specific transcriptional factors that have been identified in *Plasmodium* species, with each protein containing one to three copies of the AP2 integrase DNA binding domains (Balaji et al., 2005; De Silva et al., 2008). The DNA-binding specificities of orthologous pairs of AP2 domains are fundamentally conserved, and the timing of orthologous ApiAP2 protein expression is very similar, although the putative target genes of orthologous ApiAP2s are sometimes highly divergent (Oberstaller et al., 2014; Martins et al., 2017). So far, five ApiAP2 proteins have been identified as key stage-specific regulators in the rodent malaria parasite *Plasmodium berghei* (Yuda et al., 2009, 2010; Iwanaga et al., 2012; Kafsack et al., 2014; Josling et al., 2018). Though seven AP2s have been functionally characterized at the cellular level in *P. falciparum*, only PfAP2-G is associated with stage specificity and has been identified as a master regulator of sexual commitment (Flueck et al., 2010; Han et al., 2014; Kafsack et al., 2014; Henriques et al., 2015; Martins et al., 2017; Santos et al., 2017; Sierra-Miranda et al., 2017). Campbell et al. (2010) characterized the DNA binding motifs for 27 distinct AP2 members which were predicted bioinformatically in *P. falciparum*. In addition to regulating target genes, AP2 members may also regulate their own expression (Bischoff and Vaquero, 2010; Campbell et al., 2010). Previous studies of AP2-G2 in *P. berghei* demonstrated that PbAP2-G2 disruptants almost completely lacked mature gametocytes, suggesting that this transcriptional factor played a critical role in the maturation of gametocytes (Sinha et al., 2014; Yuda et al., 2015; Modrzynska et al., 2017). In addition, PbAP2-G2 targeted about 1,500 genes mostly required for asexual replication, repressing them before the commitment to sexual differentiation, which was thought to induce genome-wide gene repression in both asexual blood stages and gametocytes (Sinha et al., 2014; Martins et al., 2017). Recently, Singh et al. (2020) reported that PfAP2-G2 played a critical role in the maturation of gametocytes and bound to the promoters and gene body of a wide array of genes, acting as a repressor.

In this study, we report that PfAP2-G2 plays a role in the production and maturation of gametocytes. First, we detected that *PfAP2-G2* was highly expressed in the ring stage and localized in the nucleus of the parasites. Subsequently, we found that disruption of *PfAP2-G2* almost completely arrested gametocyte development, especially the male gametocytes. We further investigated the expression profile of this transcriptional factor in the asexual stage, and we showed that the expression levels of many genes were decreased significantly in the PfAP2-G2 disruptants, especially the male development gene 1 (*MDV-1*), which is an essential regulator in the development of male gametocytes. Chromatin immunoprecipitation and quantitative PCR (CHIP-qPCR) assay showed that PfAP2-G2 was enriched at the transcriptional start site (TSS) of *PfMDV-1* in the asexual stage. This study implies an important role for PfAP2-G2 in the development of gametocytes in *P. falciparum*, possibly through regulating *PfMDV-1* and other gametocyte-specific genes in the asexual stage.

METHODS

Parasites Culture and Transfection

P. falciparum NF54 parasites were cultured and synchronized following the standard protocols (Trager and Jensen, 2005). Red blood cells were transfected with 100 μg of each of the plasmids PL6CS-hDHFR-AP2-G2 and PL6CS-hDHFR-AP2-G2(-) with pUF1-BSD-Cas9 by electroporation. Schizont-stage parasites were synchronized with Percoll. Transfected parasites were subjected to selection with the WR99210 (Jacobus Pharmaceuticals) and blasticidin (BSD) (Thermo) drugs, which respectively targeted human dihydrofolate reductase and blasticidin S deaminase, to select parasites carrying both pUF1-BSD-Cas9 and PL6CS-hDHFR-AP2-G2(-) or both pUF1-BSD-Cas9 and PL6CS-hDHFR-AP2-G2. After resistant parasites emerged, genomic DNA was extracted for PCR validation, and parasites were cloned by limiting dilution. The knockout and tagging of *PfAP2-G2* were carried out separately, using the CRISPR/Cas9 system, and was confirmed by PCR. For tagging, the coding sequences of 3Ty1-3Flag was fused to the C terminus of *PfAP2-G2*. The selected tagged parasite was confirmed by PCR with genomic DNA and primer pairs P1/P2, by sequencing of PCR products, and by Western blotting. For gene knockout, the entire 397 bp functional domain (4,645 bp away from ATG to 5042 bp) was replaced by the 5′-UTR-hdhfr-3′-UTR drug cassette. PCR was performed with genomic DNA as templates, and primer pairs P3/P4. The selected knockout parasite was confirmed by sequencing of the PCR products. All primers used are listed in **Supplementary Table 1**.

Gametocytes Induction

To compare gametocyte development between the NF54 and the *PfAP2-G2(-)* parasites, tightly synchronized schizont stage cultures were set to a parasitemia of 0.3 with 6% hematocrit and cultivated in 15 ml of the complete medium at 37°C. We regard this day as the first day post-gametocyte induction. The medium was exchanged daily and increased to 25 ml until the parasitemia up to 5%. Cultures were maintained in culture medium for 12 days. The asexual parasites were eliminated by N-acetyl-D-glucosamine (Sangon Biotech) from day 6 post-gametocyte induction when both the NF54 and the *PfAP2-G2(-)*

parasites were at the ring stage and the parasitemia reached about 13%. The cultures of NF54 and the *PfAP2-G2(-)* parasites were treated with N-acetyl-D-glucosamine for 7 days until day 12 post-gametocyte induction. Samples were taken every 24 h starting from day 2 post-gametocyte induction for Giemsa smear preparation.

Indirect Immunofluorescence Assay (IFA)

IFAs were performed as previously described (Zhang et al., 2014). The early differences in gametocyte formation and sex ratio between the *PfAP2-G2(-)* parasites and the NF54 parasites were detected by IFA. Briefly, on day 6 post-gametocytes induction, parasites were collected and adsorbed on slides treated by poly-L-lysine for 10 min. The slides were washed twice with phosphate-buffered saline (PBS, pH 7.0). Then, the parasites were fixed with 4% paraformaldehyde and 0.0075% glutaraldehyde in PBS for 30 min. Following another PBS wash, parasites were permeabilized with 0.25% Triton X-100 in PBS for 15 min and then treated with 50 mM NH_4Cl in PBS for 10 min. After washing the slides with PBS, the parasites were blocked with 3% BSA-PBS for 2 h. Following a PBS wash, rabbit anti-Pfs16 antibody (diluted to 1:250 in 3% BSA-PBS, BEI Resources) and mouse anti-α-tubulin antibody (diluted to 1:1,000 in 3% BSA-PBS, Sigma) were added respectively and the mixtures were incubated at 4°C overnight. After washing the slides with PBS, fluorescein isothiocyanate (FITC)-conjugated goat anti-rabbit immunoglobulin antibody and FITC-conjugated goat anti-mouse immunoglobulin antibody (Thermo) diluted to 1:2,000 in 3% BSA-PBS were added respectively and the mixture was incubated for 1 h. Parasite nuclei were counterstained with DAPI-Aqueous (Abcam). IFA slides were observed under an Olympus FV1200 microscope. The location of PfAP2-G2 by mouse anti-Flag antibody (diluted to 1:1,000 in 3% BSA-PBS, Sigma) was identified by IFA as mixed asexual parasites using the same procedure as described above.

Western Blot Analysis

Parasites pellets were released from infected red blood cells with 0.15% saponin and then lysed in PBS containing 1% SDS and protease inhibitor. After centrifugation, the supernatant was mixed with SDS-PAGE loading buffer, separated in SDS-PAGE, and transferred to a PVDF membrane. The membrane was blocked with 5% non-fat milk in Tris-buffered saline with 0.1% Tween 20 (TBS-T) at room temperature for 2 h and probed with mouse anti-Flag (diluted to 1:1,000 in 5% non-fat milk, Sigma) and rabbit anti-H3 (diluted to 1:2,000 in 5% non-fat milk, Abcam), respectively. After three washes with TBS-T, the membranes were incubated with the secondary antibodies conjugated to HRP (Jackson Immuno Research Laboratories). Chemiluminescent HRP substrate Immobilon Western kit (Millipore) was used to develop the blots.

RNA-seq and RT-qPCR

Total RNA was extracted from tightly synchronized *PfAP2-G2(-)* parasites and NF54 parasites at both ring stage and schizont stage using Trizol (Life Technologies) according to the manufacturer's instructions. Total RNA was dissolved in RNase-free water for downstream uses. The mRNA-seq library was constructed by KAPA Stranded mRNA-seq Kit (KAPA Biosystems, KK8420) according to the manufacturer's instructions. Barcoded libraries were pooled and sequenced with the read lengths of 150 nt from both ends on the HiSeq Ten machine (Illumina, CA). For RT-qPCR, cDNA was synthesized using the FastQuant RT kit (Tiangen). qPCR was performed on the ABI 7900 system with an initial denaturing at 95°C for 5 min, followed by 40 cycles of 10 s at 95°C, 20 s at 50°C and 30 s at 60°C. The housekeeping gene serine-tRNA ligase (Pf3D7_0717700) was used as internal control. RT-qPCR for detecting the expression level of PfAP2-G2 used the same procedure as described above. RT-qPCR was repeated three times and RNA-seq was repeated twice. Primers for RT-qPCR are shown in **Supplementary Table 1**.

Chromatin Immunoprecipitation (ChIP)

The ChIP assay was performed as previously described (Chookajorn et al., 2007) using synchronized ring stage and schizont stage PfAP2-G2-3Ty1-3Flag parasites. Briefly, iRBCs were fixed with 1% formaldehyde solution (Thermo) at room temperature for 20 min and stopped by the addition of 125mM glycine at room temperature for another 5 min. Parasites were released by using 0.15% saponin. Chromatin was sheared to a size range between 200 and 300 bp by Bioruptor UCD-200 (Diagenode). Antibodies against Flag (Sigma) was used in this assay. DNA was extracted by phenol-chloroform. The ChIP-qPCR assay used the same aliquot of immunoprecipitated DNA and was detected on the ABI 7900 system. Primers for CHIP-qPCR are shown in **Supplementary Table 1**.

RNA-seq Data Analysis

The raw data were filtered by trim-galore (version 0.4.4) to remove adapters, short reads and the other low quantity reads with cutoffs (reads quantity $\leq$ 15 and read length $\leq$ 15 nt). The paired and unpaired (reads length$\geq$18) reads were aligned to the *P. falciparum* v36 genome using HISAT2 (version 2.1.0) with default parameters (Kim et al., 2015). Alignment files were converted to "BAM" format and merged using SAMtools. The PCR deduplicates were removed using Picard (version 2.18.6) with default parameters and calculated Transcripts Per Million (TPM) using Stringtie (version 1.3.4, parameters "-e –rf -j 1") (Pertea et al., 2015). Two biological replicates for each sample were counted and mapped reads for all the genes using Stringtie and conducted differential expression analysis using DESeq2 (version 1.16.1) (Feng et al., 2012) in R platform. Finally, each gene in the treatment group against the control group was presented as the volcano plot using the ggplot2 package (version 3.1.1) (Ginestet, 2011) in R. Genes whose TPM was <10 in any replicate of a group were considered as low expression level and genes that were low expression level in both treatment and control group were considered as unchanged in mRNA level. Up-regulated and down-regulated genes were defined using the following cutoff: $|\log_2 \text{fold change}| > 1$.

RESULTS

PfAP2-G2 Is Highly Expressed in the Ring Stage and Localized in the Nuclei of the Parasites

To explore the expression and localization of PfAP2-G2, we established parasites line with *PfAP2-G2* tagged at its C terminus with the 3Ty1-3Flag in the NF54 parasites using the CRISPR/Cas9 system (**Figure 1A**). The selected parasite clone (named D5) was confirmed by PCR and DNA sequencing of the PCR product (**Figure 1B**), as well as by Western blot to detect the tagged protein (**Figure 1C**). We found that tagging of *PfAP2-G2* had no effect on asexual and sexual development of the parasites (**Supplementary Figure 1**). We found that *PfAP2-G2* was expressed throughout the intraerythrocytic development cycle and gametocyte stage IV∼V via RT-qPCR with the expression level reaching the highest in the ring stage and lowest in the schizont stage (**Figure 1D**). IFA of fixed asexual parasites detected that at the ring stage *PfAP2-G2* was shown as a single punctum at the nuclear periphery demarcated by DAPI staining, while in the trophozoite stage, it diffused and overlapped more extensively with the nucleus. However, the anti-Flag staining became much fainter at the schizont stage and the more prominent foci did not overlap with the DAPI staining (**Figure 1E**).

PfAP2-G2 Is Important for Gametocyte Development, Especially for Male Gametocytes

To determine the role of PfAP2-G2 during *P. falciparum* development, we replaced a coding region of *PfAP2-G2* with the hdhfr cassette using the CRISPR/Cas9 system (**Figure 2A**). The knockout strain [named *PfAP2-G2(-)*] was obtained after transfection and cloning and was confirmed by PCR and DNA sequencing of the PCR product (**Figure 2B**). Phenotypic analysis of *PfAP2-G2(-)* parasites was compared with the NF54 strain. Although the *PfAP2-G2(-)* parasites and the NF54 control showed no significant difference in daily asexual parasitemia (data not shown), there was a ∼95% reduction in gametocytemia in the *PfAP2-G2(-)* parasites at day 9 after post-gametocyte induction (**Figure 2C**). However, gametocytes produced by *PfAP2-G2(-)* parasites retained normal morphology observed under a light microscope on day 9 post-gametocyte induction (**Figure 2D**). However, on day 12 post-gametocyte induction when mature gametocytes were visible in the NF54 parasites, gametocytes could not be observed in the *PfAP2-G2(-)* parasites (**Figure 2D**). On day 6 post-gametocyte induction, when the gametocytes were at stage I, we found that deletion of *PfAP2-G2* affected sexual commitment as determined by staining with anti-Pfs16, with the *PfAP2-G2(-)* parasites having lower sexual commitment (4.7%) than the NF54 parasites (11.5%) (**Figure 2E**). Simultaneously, we also found that deletion of *PfAP2-G2* had a substantial impact on the sex ratio as determined by staining with anti-α-tubulin-II antibodies, with the *PfAP2-G2(-)* parasites having significantly higher female/male gametocyte ratio (∼9.1:1) than the NF54 parasites (∼3.7:1) (**Figure 2F**). It is worth mentioning that α-tubulin II expressed normally in the *PfAP2-G2(-)* parasites (**Supplementary Tables 2, 3**) and anti-α-tubulin II reacted with both sexes, but the different intensities allowed differentiation of the male gametocytes (Schwank et al., 2010) (**Supplementary Figure 2**). Altogether, these phenotypic analyses showed more severe developmental defects in male gametocytogenesis in the *PfAP2-G2(-)* parasites.

Downregulation of *PfMDV-1* in AP2-G2(-) Parasites

To determine the effect of PfAP2-G2 deletion on gene expression, we performed RNA-seq analysis and compared the transcriptomes of the NF54 with *PfAP2-G2(-)* parasites at the ring stage and schizont stage. Compared with the NF54 parasites, *PfAP2-G2* deletion resulted in significantly more genes up-regulated (113 genes) than down-regulated (12 genes) in the ring stage (**Figure 3A**, **Supplementary Table 2**). In the schizont stage, however, 41 and 102 genes were up-regulated and down-regulated, respectively in *PfAP2-G2(-)* parasites (**Figure 3B**, **Supplementary Table 3**). GO term analysis did not identify specific clusters of genes with altered expression. However, we found that the expression level of *PfMDV-1*, which is essential to the development of male gametocytes, was significantly decreased in both the ring and schizont stages. The expression level of *PfAP2-G*, the master regulator of sexual commitment, was also decreased in the schizont stage, but not in the ring stage. We selected *PfMDV-1*, *PfAP2-G,* and five other genes related to gametocyte development for RT-qPCR verification, and the results were consistent with those from RNA-seq analysis (**Figures 3C,D**). These results suggested that PfAP2-G2 played a role in the development of gametocytes by regulating the expression of *PfMDV-1* as well as *PfAP2-G* in the asexual stage.

PfMDV-1 Is a Target of PfAP2-G2

Since *PfMDV-1* was decreased both in the ring and schizont stages after *PfAP2-G2* deletion, we suspected that *PfMDV-1* may be one of the targets of PfAP2-G2. To test this hypothesis, we evaluated whether PfAP2-G2 is targeted to the *PfMDV-1* gene. Both D5 and NF54 parasites were subjected to ChIP by using the mouse anti-Flag antibody at the ring and schizont stages. qPCR analysis using primer pairs targeting to different upstream regions of the *PfMDV-1* gene showed significant enrichment of the PfAP2-G2 protein at around 500 bp upstream of the start codon, which corresponds approximately to the transcriptional start site (TSS) of *PfMDV-1* at both ring and schizont stages (**Figures 4A,B**). This result suggests that *PfMDV-1* is one of the targets of PfAP2-G2 in the asexual stage.

DISCUSSION

In this study, we showed that PfAP2-G2, whose *P. berghei* ortholog is downstream in a transcriptional cascade initiated by PbAP2-G (Sinha et al., 2014), played a critical role in the production and maturation of gametocytes. *PfAP2-G2* was highly expressed in the ring stage and localized in the nuclei of early-stage parasites. Deletion of *PfAP2-G2*

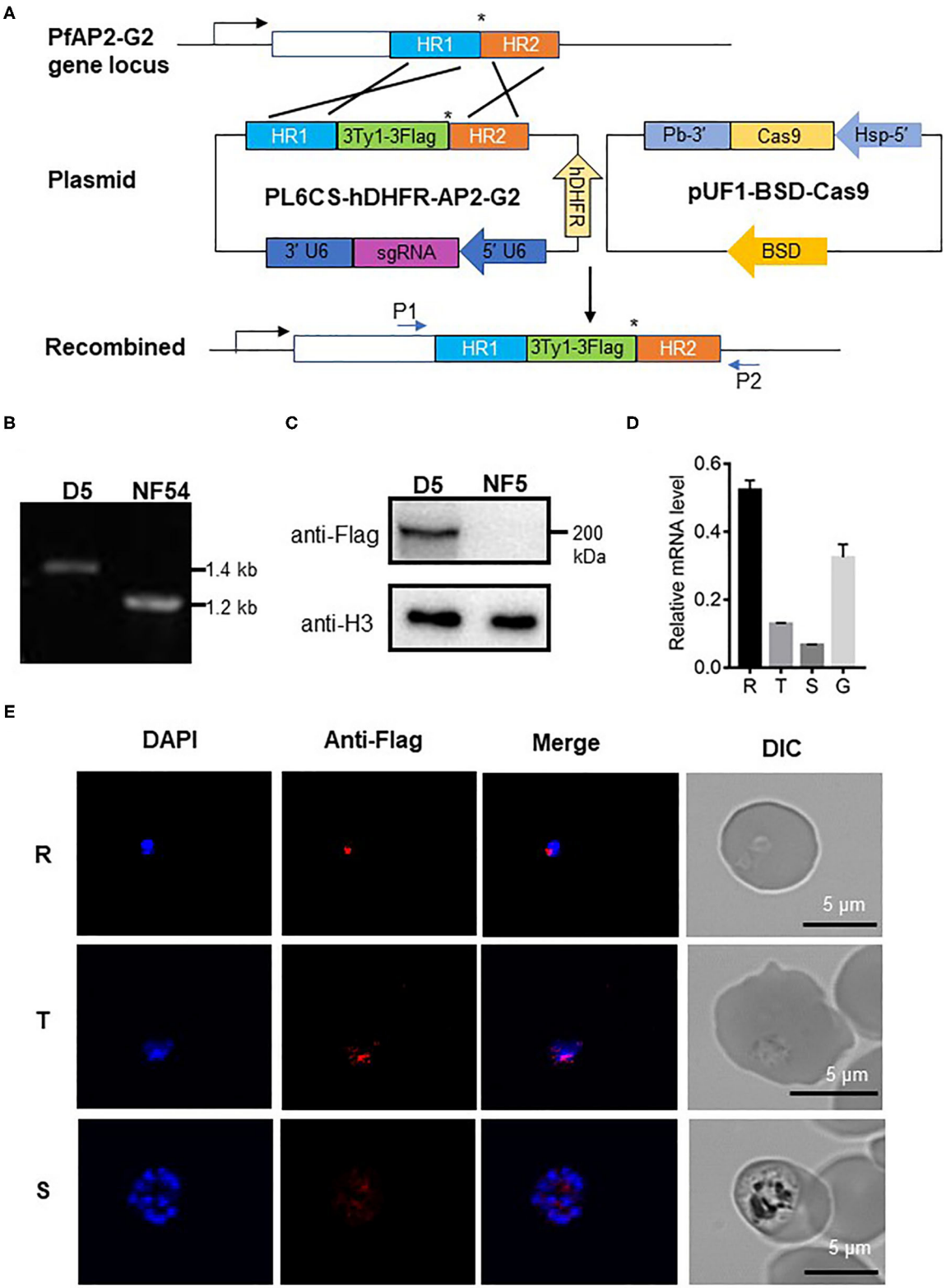

FIGURE 1 | Expression of *PfAP2-G2* in *P. falciparum* development. **(A)** Schematic representation of the generation of transgenic PfAP2-G2-3Ty1-3Flag line. Co-transfection of the plasmid pUF1-BSD-Cas9 with PL6CS-hDHFR-AP2-G2 leads to the integration of the PfAP2-G2-3Ty1-3Flag containing cassette into the

(Continued)

FIGURE 1 | endogenous *PfAP2-G2* locus. HR1 and HR2 are the two homologous arms used for recombination. The asterisk (*)indicates the stop codon. P1 and P2 are primers used to verify plasmid integration. **(B)** PCR analysis of genomic DNA from the NF54 parasites and the PfAP2-G2-3Ty1-3Flag clone D5. Predicted DNA fragment sizes with P1 and P2 are 1,423 bp from D5 parasites and 1,217 bp from the NF54 parasites. **(C)** Western blot analysis of D5 parasites. Proteins were separated by 6% SDS-PAGE and probed with the mouse anti-Flag antibody and against *P. falciparum* H3 as a protein loading control. **(D)** RT-qPCR analysis of *PfAP2-G2* expression in the ring (14∼16 h) (R), trophozoite (34∼36h) (T), schizont (44∼46 h) (S) stages and gametocyte stage IV∼V(G). Primers for RT-qPCR are shown in **Supplementary Table 1**. The experiment was repeated three times. Error bars indicate standard deviation (SD). **(E)** IFA analysis of PfAP2-G2 during asexual parasite development. PfAP2-G2 localization was identified by using the anti-Flag antibody (red), while nuclei were counterstained with DAPI. Scale bars, 5 μm.

reduced gametocyte production and resulted in the nearly complete (>95%) loss of mature gametocytes, especially male gametocytes. In addition, we found that *PfAP2-G2* deletion resulted in down-regulation of *PfMDV-1* in both ring stage and schizont stage. We provided further evidence to show that the *PfMDV-1* was a target of PfAP2-G2 in the asexual stage.

Consistent with the previous findings in *P. berghei* (Sinha et al., 2014; Yuda et al., 2015), deletion of *PfAP2-G2* could significantly reduce the number of mature gametocytes, which may be the consequence of PfAP2-G2 regulating the expression of *PfMDV-1*. PfMDV-1 plays an important role in maintaining membrane structures which are essential for gametocyte maturation in erythrocytes. Disruption of *PfMDV-1* results in a dramatic reduction of mature gametocytes, especially functional male gametocytes, with the majority of sexually committed parasites developmentally arrested at stage I (Guinet et al., 1996; Furuya et al., 2005). We also found that the deletion of *PfAP2-G2* resulted in the reduction of stage I gametocytes, especially male gametocytes. However, given that *PfMDV-1* is only one of the genes whose expressed is decreased after *PfAP2-G2* deletion, the defect in sexual development may also involve other gametocyte-specific genes. Due to a ∼95% reduction in gametocytemia was happened in the *PfAP2-G2(-)* parasites, it is hardly for us to collect the gametocyte samples for RNA-seq, so, we decided to study the mechanisms of PfAP2-G2 in the asexual stage and found that PfAP2-G2 regulated the formation of gametocyte by directly regulate the expression of *PfMDV-1* in ring stage and schizont stage. Simultaneously, the RT-qPCR result of *PfAP2-G2* found that it also highly expressed in gametocyte stage, means PfAP2-G2 may also functionating at gametocyte stage. Recently, Singh et al. (2020) demonstrated that PfAP2-G2 can bound the promoters of genes expressed at several different stages of the parasite life cycle, as well as gene body of genes which correlates with the location of H3K36me3 and several other histone modifications. All these results demonstrated that PfAP2-G2 may have different function in the asexual stage and gametocyte stage, and the function of it in gametocyte stage would be worth to study in the future.

AP2-G2 has been identified as a transcriptional repressor that induces genome-wide transcriptional repression in early gametocytes and contributes to dramatic alterations of cell fate at this stage in *P. berghe*i (Yuda et al., 2015). Similarly, Singh et al. (2020) collected the samples in stage and gametocyte stage III for CHIP-seq, suggesting that PfAP2-G2 acted as a repressor and affected the transcription by interacting with other proteins. However, we found that *PfMDV-1* was down-regulated in *PfAP2-G2(-)* parasites. Here, we propose two hypotheses to explain this phenomenon. First, AP2-G2 may induce genome-wide transcriptional repression in *P. falciparum* throughout the life cycle of parasites. *PfMDV-1* may be up-regulated in gametocytes after the point at which PfAP2-G2 is required for continued development. In that case, *PfAP2-G2* knockout cultures would lack the background levels of gametocytes expressing these genes that are present in wild-type cultures. Second, we found that compared with the NF54 parasites, the deletion of *PfAP2-G2* resulted in significantly more genes up-regulated (113 genes) in the ring stage. Contrasting, in schizont stage, more genes were down-regulated (102 genes). As a result, we speculate that PfAP2-G2 may function as a transcriptional repressor for some of the genes at ring stage, but not all stages. The function of PfAP2-G2 is complicated and so, worth further examination.

In *P. berghei*, ChIP-seq analysis has revealed that targets of PbAP2-G2 mainly included genes that were required for asexual proliferation, whereas gametocyte-specific genes were not considered (Yuda et al., 2015). Targets of AP2-G2 appear to be highly divergent in *P. falciparum* and *P. berghei,* although the phenotypes are similar (Campbell et al., 2010). In this study, RNA-seq analysis showed that a limited number of genes with defined biological functions were up or down regulated in *PfAP2-G2(-)* parasites. Among genes identified as regulons of gametocytes in *P. falciparum* (Josling and Llinas, 2015), we only found reduced expression of *PfMDV-1* in *PfAP2-G2(-)* parasites. Thus, we speculated that *PfMDV-1* might be regulated by PfAP2-G2 directly, as ChIP-qPCR analysis identified binding of PfAP2-G2 to the putative promoter of *PfMDV-1*. We also detected other genes which might be gametocyte-specific genes and were down-regulated at ring stage simultaneously. However, we found that CHIP-qPCR analysis using primer pairs targeting to different upstream regions of these genes showed no significant enrichment of the PfAP2-G2 protein. This may be because of the fact that these genes are important to gametocytes development, loss of *PfAP2-G2* would cause the decrease of gametocytes so that the expression of these genes descends (**Supplementary Figure 3**). Interestingly, the expression of *PfAP2-G* was also down-regulated in *PfAP2-G2(-)* parasites at the schizont stage, which partially explains the reduced gametocytogenesis phenotype. The mechanism of ApiAP2 regulators may be different in Plasmodium species. We speculate that PfAP2-G2 may mainly execute its role at the upstream to regulate *PfAP2-G*, whose expression is the initial of sexual commitment through the next cycle conversion pathway

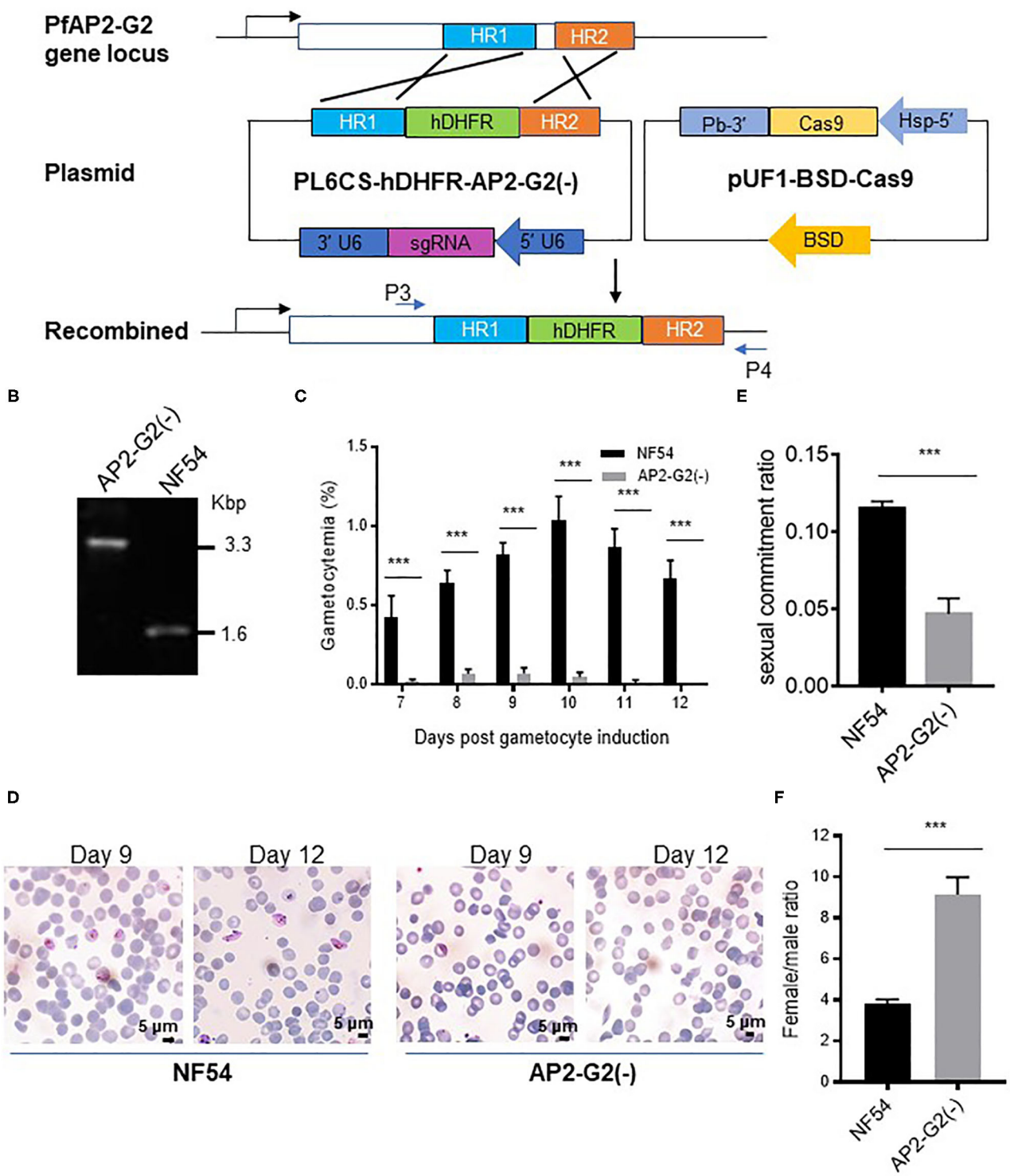

FIGURE 2 | Phenotypic analysis of the *PfAP2-G2(-)* parasites. **(A)** Schematic representation of the generation of transgenic *PfAP2-G2* knockout line. Co-transfection of the plasmid pUF1-BSD-Cas9 with PL6CS-hDHFR-AP2-G2(-) leads to knockout of PfAP2-G2 structural domain in the endogenous locus. HR1 and HR2 are the two homologous arms used for recombination. P3 and P4 are primers used to verify the deletion in *PfAP2-G2*. **(B)** PCR analysis of genomic DNA from the NF54 parasites and the *PfAP2-G2(-)* clone. Predicted DNA fragment sizes with P3 and P4 are 3,330 bp from the *PfAP2-G2(-)* parasites and 1,590 bp from the NF54 parasites.

(Continued)

FIGURE 2 | (C) Daily gametocytemia after day 6 post-gametocyte induction. Results are the mean of three biological replicates (10,000 RBCs counted per sample). **(D)** Giemsa-stained blood smears of NF54 (left) and the *PfAP2-G2(-)* parasites (right) on days 9 and 12 to illustrate the gross morphology of the gametocytes and their disappearance in day 12 culture in the *PfAP2-G2(-)* parasites. Scale bars, 5 μm. **(E)** Sexual commitment ratio on day 6 post-induction. Results are the mean of three biological replicates (1000 infected RBCs counted per sample). **(F)** Female/male gametocyte ratio on day 6 post-induction. Results are the mean of three biological replicates (1000 infected RBCs counted per sample). Sex was differentiated based on the staining of all gametocytes by the anti-Pfs16 antibodies and strong fluorescence of male gametocytes by the anti-α-tubulin II IFA. The experiment was repeated three times. All error bars indicate SD. ***$P < 0.001$.

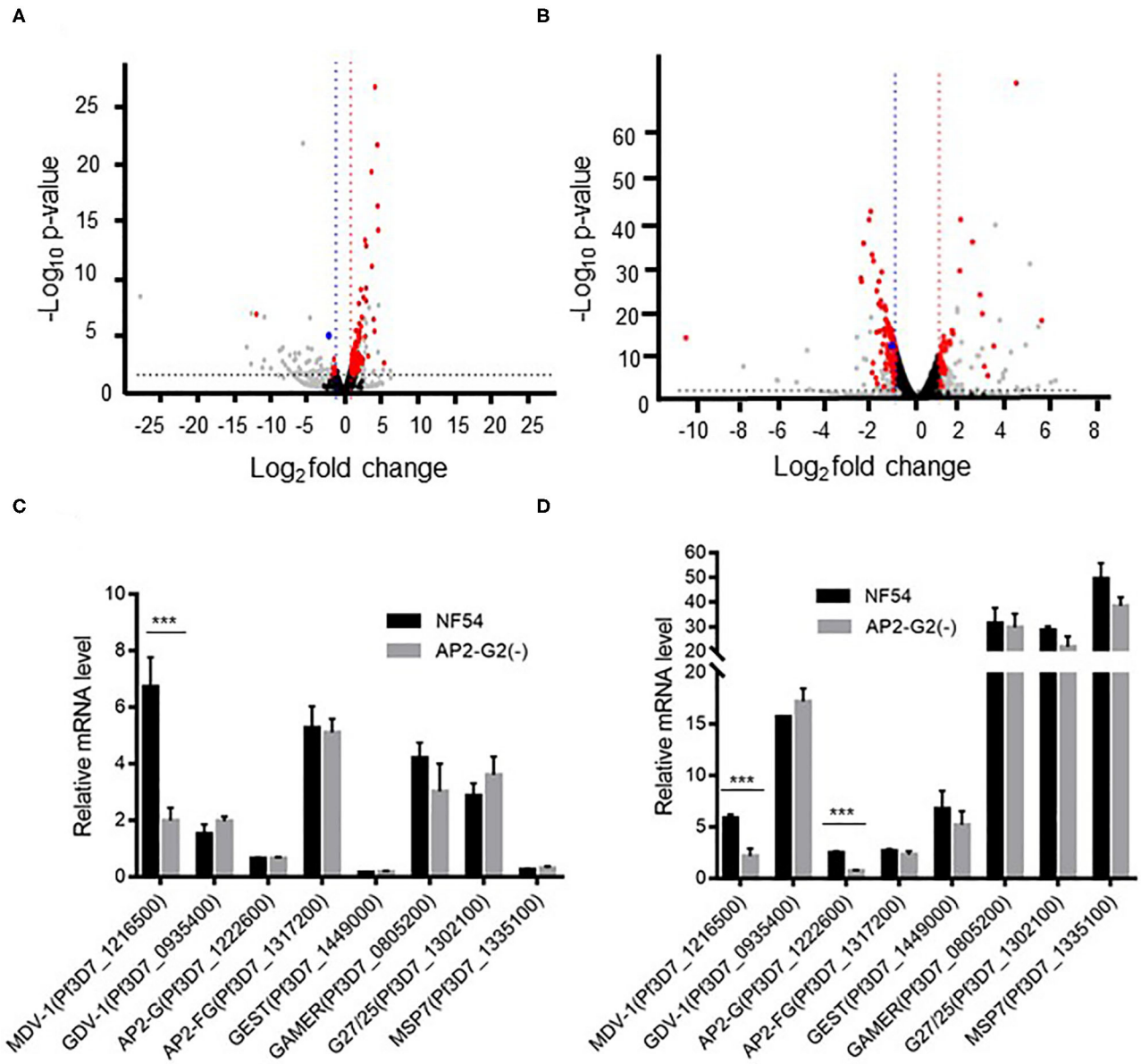

FIGURE 3 | Transcriptomic analysis of NF54 and the *PfAP2-G2(-)* parasites by RNA-seq. **(A,B)** Volcano plot of $\log_2$ fold change (x axis) in gene expression of *PfAP2-G2(-)* parasites vs. NF54 parasites in ring stage **(A)** and schizont stage **(B)** against the significance of change shown as the $-\log_{10}$ *p*-value (y axis). Red dots indicate genes with significant changes in expression level. Blue dots indicate the *PfMDV-1* gene. Gray dots indicate genes whose TPM was <10. Black dots indicate genes whose p-value was more than 0.05 or | $\log_2$ fold change | was <1 **(C,D)** RT-qPCR validation of the RNA-seq data using selected genes essential for gametocyte development at the ring **(C)** and schizont **(D)** stages. A gene (*MSP7*), which is unrelated to gametocyte development, was used as a negative control. Primers for RT-qPCR are shown in **Supplementary Table 1**. The experiment was repeated three times. All error bars indicate SD. ***$P < 0.001$.

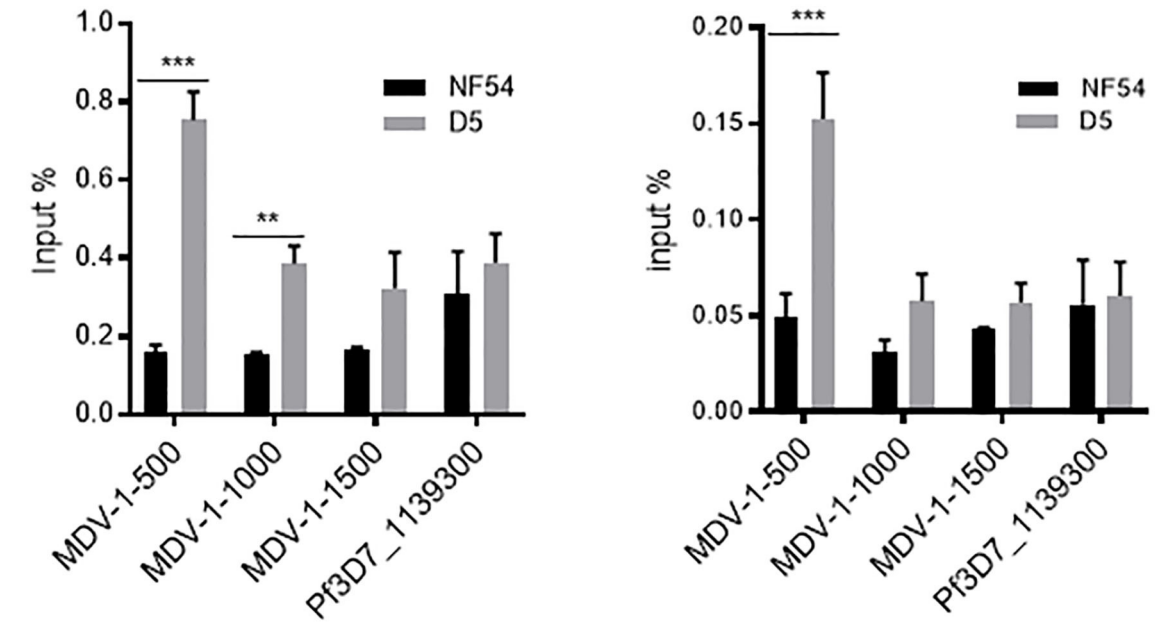

FIGURE 4 | ChIP-qPCR analysis of PfAP2-G2 binding to the promoter region of *PfMDV-1* at ring stage **(A)** and schizont stage **(B)**. MDV1-500, MDV1-1000, and MDV1-1500 indicate primers that are located at about 500 bp, 1,000 bp, 1,500 bp before the start codon of *PfMDV-1*, respectively. TSS of *PfMDV-1* is mapped to about 500 bp upstream of the start codon. *Pf3D7_1139300* was used as a negative control. Primers for ChIP-qPCR are shown in **Supplementary Table 1**. The experiment was repeated three times. All error bars indicate SD. $^{**}P < 0.01$; $^{***}P < 0.001$.

(NCC pathway) (Bancells et al., 2019). In addition, it is possible that PfAP2-G2 is at downstream. It is also possible that there is a feedback regulation and synergy affection between PfAP2-G2 and PfAP2-G. However, we do not know whether PfAP2-G2 affects the expression of *PfAP2-G* directly or indirectly given that PfAP2-G also regulate invasion-related genes expressed in schizont. It is worth mentioning that the expression of *PfAP2-G2* was up-regulated with the primers located close to the start codon, which is in accord with RNA-seq analysis (**Supplementary Figure 4A**). However, we found that there was nearly no expression of *PfAP2-G2* when the primers located in the knockout domain (**Supplementary Figure 4B**). In our opinion, this is because we don't knock out the whole of *PfAP2-G2*, but part of it containing the domain, which is shown on PlasmoDB and previous report (Campbell et al., 2010). Therefore, up-regulation of *PfAP2-G2* in *PfAP2-G2(-)* ring stages might be due to the transcriptional compensatory mechanism. Importantly, we confirm that *PfAP2-G2* can't be translated into protein successfully.

In conclusion, we have shown that PfAP2-G2 is highly expressed in the ring stage and localized in the nuclei of all stages of asexual parasites. More importantly, it plays an important role in the production and maturation of gametocytes, especially the male gametocytes. RNA-seq and ChIP-qPCR analyses suggest that PfAP2-G2 targets the *PfMDV-1* gene and regulates its expression in the asexual stage.

DATA AVAILABILITY STATEMENT

The data presented in the study are deposited in the NCBI repository, accession number PRJNA686696.

AUTHOR CONTRIBUTIONS

YX, JG, YMC, and ZH conceived and designed experiments. YX performed the majority of the experiments. DQ, YW, YB, and YXC collected the samples and conducted the bioinformatics analysis. YX, DQ, YW, YB, JG, YXC, ZH, LC, and YMC wrote the manuscript. All authors discussed and edited the manuscript.

FUNDING

This research was supported by a grant (R01AI150533) from the NIAID, NIH, USA to YMC.

SUPPLEMENTARY MATERIAL

The Supplementary Material for this article can be found online at: https://www.frontiersin.org/articles/10.3389/fmicb.2020.631444/full#supplementary-material

REFERENCES

Amoah, L. E., Acquah, F. K., Nyarko, P. B., Cudjoe, E., Donu, D., Ayanful-Torgby, R., et al. (2020). Comparative analysis of asexual and sexual stage Plasmodium falciparum development in different red blood cell types. *Malar. J.* 19:200. doi: 10.1186/s12936-020-03275-9

Balaji, S., Babu, M. M., Iyer, L. M., and Aravind, L. (2005). Discovery of the principal specific transcription factors of Apicomplexa and their implication for the evolution of the AP2-integrase DNA binding domains. *Nucleic Acids Res.* 33, 3994–4006. doi: 10.1093/nar/gki709

Bancells, C., Llorà-Batlle, O., Poran, A., Nötzel, C., Rovira-Graells, N., Elemento, O., et al. (2019). Revisiting the initial steps of sexual development in the malaria parasite Plasmodium falciparum. *Nat. Microbiol.* 4, 144–154. doi: 10.1038/s41564-018-0291-7

Bischoff, E., and Vaquero, C. (2010). *In silico* and biological survey of transcription-associated proteins implicated in the transcriptional machinery during the erythrocytic development of *Plasmodium falciparum*. *BMC Genomics* 11:34. doi: 10.1186/1471-2164-11-34

Campbell, T. L., De Silva, E. K., Olszewski, K. L., Elemento, O., and Llinas, M. (2010). Identification and genome-wide prediction of DNA binding specificities for the ApiAP2 family of regulators from the malaria parasite. *PLoS Pathog.* 6:e1001165. doi: 10.1371/journal.ppat.1001165

Chookajorn, T., Dzikowski, R., Frank, M., Li, F., Jiwani, A. Z., Hartl, D. L., et al. (2007). Epigenetic memory at malaria virulence genes. *Proc. Natl. Acad. Sci. U.S.A.* 104, 899–902. doi: 10.1073/pnas.0609084103

Ciuffreda, L., Zoiku, F. K., Quashie, N. B., and Ranford-Cartwright, L. C. (2020). Estimation of parasite age and synchrony status in Plasmodium falciparum infections. *Sci. Rep.* 10:10925. doi: 10.1038/s41598-020-67817-6

De Silva, E. K., Gehrke, A. R., Olszewski, K., León, I., Chahal, J. S., Bulyk, M. L., et al. (2008). Specific DNA-binding by apicomplexan AP2 transcription factors. *Proc. Natl. Acad. Sci. U.S.A.* 105, 8393–8398. doi: 10.1073/pnas.0801993105

Feng, J., Meyer, C. A., Wang, Q., Liu, J. S., Shirley Liu, X., and Zhang, Y. (2012). GFOLD: a generalized fold change for ranking differentially expressed genes from RNA-seq data. *Bioinformatics* 28, 2782–2788. doi: 10.1093/bioinformatics/bts515

Flueck, C., Bartfai, R., Niederwieser, I., Witmer, K., Alako, B. T., Moes, S., et al. (2010). A major role for the *Plasmodium falciparum* ApiAP2 protein PfSIP2 in chromosome end biology. *PLoS Pathog.* 6:e1000784. doi: 10.1371/journal.ppat.1000784

Furuya, T., Mu, J., Hayton, K., Liu, A., Duan, J., Nkrumah, L., et al. (2005). Disruption of a *Plasmodium falciparum* gene linked to male sexual development causes early arrest in gametocytogenesis. *Proc. Natl. Acad. Sci. U.S.A.* 102, 16813–16818. doi: 10.1073/pnas.0501858102

Ginestet, C. (2011). ggplot2: elegant graphics for data analysis. *J. R. Stat. Soc. A* 174, 245–246. doi: 10.1111/j.1467-985X.2010.00676_9.x

Guiguemde, K. T., Dieye, Y., Lô, A. C., Ndiaye, M., Lam, A., Manga, I. A., et al. (2020). Molecular detection and quantification of *Plasmodium falciparum* gametocytes carriage in used RDTs in malaria elimination settings in northern Senegal. *Malar. J.* 19:123. doi: 10.1186/s12936-020-03204-w

Guinet, F., Dvorak, J. A., Fujioka, H., Keister, D. B., Muratova, O., Kaslow, D. C., et al. (1996). A developmental defect in *Plasmodium falciparum* male gametogenesis. *J. Cell Biol.* 135, 269–278. doi: 10.1083/jcb.135.1.269

Han, S. T., Zhang, Q. F., and Pan, W. Q. (2014). *In vivo* identification of the interaction between var intron and an ApiAP2 transcription factor in Plasmodium falciparum. *Zhongguo Ji Sheng Chong Xue Yu Ji Sheng Chong Bing Za Zhi* 32, 1–5.

Henriques, G., van Schalkwyk, D. A., Burrow, R., Warhurst, D. C., Thompson, E., Baker, D. A., et al. (2015). The Mu subunit of *Plasmodium falciparum* clathrin-associated adaptor protein 2 modulates *in vitro* parasite response to artemisinin and quinine. *Antimicrob. Agents Chemother.* 59, 2540–2547. doi: 10.1128/AAC.04067-14

Henry, N. B., Sermé, S. S., Siciliano, G., Sombié, S., Diarra, A., Sagnon, N., et al. (2019). Biology of *Plasmodium falciparum* gametocyte sex ratio and implications in malaria parasite transmission. *Malar. J.* 18:70. doi: 10.1186/s12936-019-2707-0

Iwanaga, S., Kaneko, I., Kato, T., and Yuda, M. (2012). Identification of an AP2-family protein that is critical for malaria liver stage development. *PLoS ONE* 7:e47557. doi: 10.1371/journal.pone.0047557

Josling, G. A., and Llinas, M. (2015). Sexual development in Plasmodium parasites: knowing when it's time to commit. *Nat. Rev. Microbiol.* 13, 573–587. doi: 10.1038/nrmicro3519

Josling, G. A., Williamson, K. C., and Llinás, M. (2018). Regulation of Sexual Commitment and gametocytogenesis in malaria parasites. *Annu. Rev. Microbiol.* 72, 501–519. doi: 10.1146/annurev-micro-090817-062712

Kafsack, B. F., Rovira-Graells, N., Clark, T. G., Bancells, C., Crowley, V. M., Campino, S. G., et al. (2014). A transcriptional switch underlies commitment to sexual development in malaria parasites. *Nature* 507, 248–252. doi: 10.1038/nature12920

Kim, D., Langmead, B., and Salzberg, S. L. (2015). HISAT: a fast spliced aligner with low memory requirements. *Nat. Methods* 12, 357–360. doi: 10.1038/nmeth.3317

Martins, R. M., Macpherson, C. R., Claes, A., Scheidig-Benatar, C., Sakamoto, H., Yam, X. Y., et al. (2017). An ApiAP2 member regulates expression of clonally variant genes of the human malaria parasite *Plasmodium falciparum*. *Sci. Rep.* 7:14042. doi: 10.1038/s41598-017-12578-y

Modrzynska, K., Pfander, C., Chappell, L., Yu, L., Suarez, C., Dundas, K., et al. (2017). A knockout screen of ApiAP2 genes reveals networks of interacting transcriptional regulators controlling the *Plasmodium* life cycle. *Cell Host Microbe* 21, 11–22. doi: 10.1016/j.chom.2016.12.003

Oberstaller, J., Pumpalova, Y., Schieler, A., Llinás, M., and Kissinger, J. C. (2014). The Cryptosporidium parvum ApiAP2 gene family: insights into the evolution of apicomplexan AP2 regulatory systems. *Nucleic Acids Res.* 42, 8271–8284. doi: 10.1093/nar/gku500

Pertea, M., Pertea, G. M., Antonescu, C. M., Chang, T. C., Mendell, J. T., and Salzberg, S. L. (2015). StringTie enables improved reconstruction of a transcriptome from RNA-seq reads. *Nat. Biotechnol.* 33, 290–295. doi: 10.1038/nbt.3122

Santos, J. M., Josling, G., Ross, P., Joshi, P., Orchard, L., Campbell, T., et al. (2017). Red Blood Cell Invasion by the Malaria Parasite Is Coordinated by the PfAP2-I Transcription Factor. *Cell Host Microbe* 21, 731–741.e710. doi: 10.1016/j.chom.2017.05.006

Schwank, S., Sutherland, C. J., and Drakeley, C. J. (2010). Promiscuous expression of α-tubulin II in maturing male and female Plasmodium falciparum gametocytes. *PLoS ONE* 5:e14470. doi: 10.1371/journal.pone.0014470

Sierra-Miranda, M., Vembar, S. S., Delgadillo, D. M., Ávila-López, P. A., Herrera-Solorio, A. M., Lozano Amado, D., et al. (2017). PfAP2Tel, harbouring a non-canonical DNA-binding AP2 domain, binds to *Plasmodium falciparum* telomeres. *Cell. Microbiol.* 19. doi: 10.1111/cmi.12742

Singh, S., Santos, J. M., Orchard, L. M., Yamada, N., van Biljon, R., Painter, H. J., et al. (2020). The PfAP2-G2 transcription factor is a critical regulator of gametocyte maturation. *bioRxiv [preprint]*. doi: 10.1101/2020.10.27.355685

Sinha, A., Hughes, K. R., Modrzynska, K. K., Otto, T. D., Pfander, C., Dickens, N. J., et al. (2014). A cascade of DNA-binding proteins for sexual commitment and development in *Plasmodium*. *Nature* 507, 253–257. doi: 10.1038/nature12970

Trager, W., and Jensen, J. B. (2005). Human malaria parasites in continuous culture. 1976. *J. Parasitol.* 91, 484–486. doi: 10.1645/0022-3395(2005)091[0484:HMPICC]2.0.CO;2

Yuda, M., Iwanaga, S., Kaneko, I., and Kato, T. (2015). Global transcriptional repression: an initial and essential step for Plasmodium sexual development. *Proc. Natl. Acad. Sci. U.S.A.* 112, 12824–12829. doi: 10.1073/pnas.1504389112

Yuda, M., Iwanaga, S., Shigenobu, S., Kato, T., and Kaneko, I. (2010). Transcription factor AP2-Sp and its target genes in malarial sporozoites. *Mol. Microbiol.* 75, 854–863. doi: 10.1111/j.1365-2958.2009.07005.x

Yuda, M., Iwanaga, S., Shigenobu, S., Mair, G. R., Janse, C. J., Waters, A. P., et al. (2009). Identification of a transcription factor in the mosquito-invasive stage of malaria parasites. *Mol. Microbiol.* 71, 1402–1414. doi: 10.1111/j.1365-2958.2009.06609.x

Zhang, Q., Siegel, T. N., Martins, R. M., Wang, F., Cao, J., Gao, Q., et al. (2014). Exonuclease-mediated degradation of nascent RNA silences genes linked to severe malaria. *Nature* 513, 431–435. doi: 10.1038/nature13468

Conflict of Interest: The authors declare that the research was conducted in the absence of any commercial or financial relationships that could be construed as a potential conflict of interest.

frontiers in Cellular and Infection Microbiology

ORIGINAL RESEARCH
published: 26 February 2021
doi: 10.3389/fcimb.2021.644983

Theileria annulata Subtelomere-Encoded Variable Secreted Protein-TA05575 Binds to Bovine RBMX2

Zhi Li[1], *Junlong Liu*[1]*, *Shuaiyang Zhao*[1], *Quanying Ma*[1], *Aihong Liu*[1], *Youquan Li*[1], *Guiquan Guan*[1], *Jianxun Luo*[1] *and Hong Yin*[1,2]*

[1] State Key Laboratory of Veterinary Etiological Biology, Key Laboratory of Veterinary Parasitology of Gansu Province, Lanzhou Veterinary Research Institute, Chinese Academy of Agricultural Science, Lanzhou, China, [2] Jiangsu Co-Innovation Center for the Prevention and Control of Important Animal Infectious Disease and Zoonose, Yangzhou University, Yangzhou, China

OPEN ACCESS

Edited by:
Bang Shen,
Huazhong Agricultural University, China

Reviewed by:
Junlong Zhao,
Huazhong Agricultural University, China
Gordon Langsley,
INSERM U1016 Institut Cochin, France

***Correspondence:**
Junlong Liu
liujunlong@caas.cn
Hong Yin
yinhong@caas.cn

Specialty section:
This article was submitted to Parasite and Host, a section of the journal Frontiers in Cellular and Infection Microbiology

Received: 22 December 2020
Accepted: 18 January 2021
Published: 26 February 2021

Citation:
Li Z, Liu J, Zhao S, Ma Q, Liu A, Li Y, Guan G, Luo J and Yin H (2021) Theileria annulata Subtelomere-Encoded Variable Secreted Protein-TA05575 Binds to Bovine RBMX2. Front. Cell. Infect. Microbiol. 11:644983. doi: 10.3389/fcimb.2021.644983

Tropical theileriosis is the disease caused by tick-transmitted apicomplexan parasite *Theileria annulata*, which has ability to transform bovine leukocytes, including B cells, macrophage cells, and dendritic cells. The *T. annulata* transformed cells are characterized as uncontrolled proliferation and shared some cancer-like phenotypes. The mechanism of the transformation by *T. annulata* is still not understood well. In previous reports, the subtelomere-encoded variable secreted proteins (SVSP) of *T. parva* were considered to contribute to phenotypic changes of the host cell, but the role of SVSP of *T. annulata* in host-pathogen relationship remains unknown. In the present study, a member of SVSP family, TA05575 of *T. annulata* was selected as the target molecule to analyze its expression profiles in different life cycle stages of *T. annulata* by qPCR and investigate its subcellular distribution of different passages of *T. annulata* transformed cells using confocal experiments. From the results, the transcription level of TA05575 at schizont stage was significantly higher than the other two life stages of *T. annulata*, and the protein of TA05575 was mainly distributed in nucleus of *T. annulata* infected cells. In addition, the potential proteins of host cells interacting with TA05575 were screened by Yeast-two hybrid system. The results of Co-IP experiment confirmed that TA05575 interacted with RBMX2-like protein that participated in transcription regulation of cells. In addition, a novel BiFC assay and flow cytometry were carried out, and the results further revealed that TA05575-RBMX2-like pair was directly interacted in cell context. Moreover, this interacting pair was found to distribute in intracellular compartments of HEK293T cells by using confocal microscopy. The results of the present study suggest that TA05575 may contribute for cells transformation due its distribution. According to the function of RBMX2, the interaction of TA05575 and RMMX2-like will provide a new information to further understand the mechanisms of cells transformation by *T. annulata*.

Keywords: *Theileria annulata*, TA05575, Yeast-two hybrid, Co-IP, BiFC, RBMX2-like

HIGHLIGHTS

1. We firstly discovered TA05575 is mainly expressed in schizont stage of *T. annulata*.
2. We firstly observed TA05575 protein is mainly distributed in nucleus of *T. annulata*-transformed cells.
3. BiFC and Co-IP assays showed that TA05575 interacted directly with RBMX2-like protein in cell context, and subcellular colocalization of this pair is in the intracellular compartments.

INTRODUCTION

Theileria annulata is a bovine-specific pathogen that causes tropical theileriosis in tropical and subtropical countries, including Asia (India, China), Africa (Egypt, Sudan), Middle East, Europe (Portugal) (Al-Deeb et al., 2015; Anupama et al., 2015; Liu et al., 2015; Gomes et al., 2016; El-Dakhly et al., 2018; Mohammed-Ahmed et al., 2018). The tick-borne diseases for cattle constraints livestock industry, which leads to the economic loss of USD 384.3 million per annum because of the high cost of anti-tick control and treatment, bovine mortality, and decreased animal production (Rajendran and Ray, 2014; Medjkane and Weitzman, 2020). *T. annulata* can infect bovine macrophages, B cells, and dendritic cells whereas *T. parva* invades T cells and B lymphocytes of cattle, which are referred as "schizont-transforming species." *T. annulata* schizont-infected cells was confirmed has some cancer hallmarks, including uncontrolled proliferation, metastasis, genomic instability (Hayashida et al., 2013; Cheeseman and Weitzman, 2015; Tretina et al., 2015). Many studies were focused on host cell signaling pathways affected by the molecules of *T. annulata*, including end-binding protein 1 (EB1) (Woods et al., 2013), *T. annulata* Peptidyl-Prolyl Isomerase1 (TaPin1) (Villoutreix et al., 2015; Marsolier et al., 2019), and *T. annulata* surface protein (TaSP) (Seitzer et al., 2010), yet the key proteins of *T. annulata* directly responsible for host cell transformation remain unknown.

T. annulata contains two large multigene families, which are SVSP (subtelomere-encoded variable secreted protein) and TashAT (*Theileria annulata* schizont AT-hook protein). Although some previous studies have proposed that SVSP family, the largest multigene family in *T. annulata*, maybe associated with host cell transformation, invasion, and immune evasion (Barry et al., 2003; Schmuckli et al., 2009; Weir et al., 2010; Tretina et al., 2015), the detailed roles of SVSP multigene family in host-parasite interactions are unclear. The atypical codon usage, diversity of length, and extensive nucleotide variability are unique characteristics in SVSP multigene family due to its subtelomere localization (Weir et al., 2010), which indicates that the members of this multigene family maybe play an important role in manipulating host cell signaling by binding to various host cell proteins.

Therefore, exploring to the host cell molecules interacting with SVSPs is absolutely necessary at present that will yield a new sight into molecular mechanism of *Theileria*-induced cancer features. In our study, we revealed that the direct interactions between one member of SVSP multigene family-TA05575 and host cell proteins.

Abbreviations: SD/-Trp (SDO), synthetically defined medium without tryptophan; SD/-Trp/X-α-Gal (SDO/X), synthetically defined medium without tryptophan supplemented with X-α-Gal; SD/-Trp/X-α-Gal/AbA, synthetically defined medium without tryptophan supplemented with X-α-Gal; SDO/X/A, synthetically defined medium without tryptophan and leucine supplemented with X-α-Gal and aureobasidin A; DDO, synthetically defined medium without tryptophan and leucine; DDO/X/A, synthetically defined medium without tryptophan and leucine supplemented with X-α-Gal and aureobasidin A; QDO/X/A, synthetically defined medium without tryptophan, leucine, adenine, histidine supplemented with X-α-Gal and aureobasidin A.

MATERIAL AND METHODS

Cell Culture

Theileria annulata schizont-infected cells were preserved at the Vector and Vector borne Disease (VVBD) team, Lanzhou Veterinary Research Institute (LVRI), China. And the cells were cultured using RPMI 1640 medium (Biological Industries, Kibbutz Beit Haemek, Israel) containing 10% fetal bovine serum (Biological Industries, Kibbutz Beit Haemek, Israel) and 100 mg/ml penicillin/streptomycin (Gibco, CA, USA) in an incubator with 5% CO_2 at 37°C. HEK 293T cells were purchased from the China Center for Type Culture Collection, Shanghai, China. The cells were maintained in DMEM (Gibco, NY, USA) plus 10% fetal bovine serum (Gibco, NY, USA).

Quantitative Real-Time Polymerase Chain Reaction (qRT-PCR)

Total RNA of different life cycle stages of *T. annulata* was extracted by using RNeasy Mini kit (QIAGEN, Dusseldorf, Germany) based on the manufacturer's instruction. After measurement of the concentration and quality, 1 microgram of RNA was used for cDNA synthesization by using PrimeScript™ RT reagent kit with gDNA Eraser (Perfect Real Time) (Takara, Dalian, China). The specific primers of this gene were designed based on the sequences deposit online (Piroplasma DB No: TA05575), the sequence of primers as following: TA05575-F (5′-ACCACCAAGCTCCACTCCAT-3′) and TA05575-R (5′-ACTCCTTTGCCACCAGGATCT-3′). qRT-PCR was performed with the SYBR Premix ExTaq reagents (TaKaRa, Dalian, China) and used the Agilent Technologies Stratagene MX3005P (CA, USA). The transcription level of β-actin of *T. annulata* was used for normalization. The specific primers for β-actin of *T. annulata* were β-actin-F (5′-GAGACCACCTACAACAGCATCATG-3′) and β-actin-R (5′- CACCTTGATCTTCATGGTGCTGGG-3′). Relative amounts of transcripts for TA05575 in different life cycle stages and passages of *T. annulata*-infected cells were determined by using the comparative cycle threshold ($2^{-\Delta\Delta CT}$) method.

Immunoblotting Analysis

Cells were lysed in lysis buffer (Beyotime, Shanghai, China, #P0013B) contained with protease inhibitor (Roche, Basel,

Switzerland, #4693132001) and phosphatase inhibitor cocktail (Roche, Basel, Switzerland, #4906845001) for 30 min on ice. The cell lysates were then centrifuged at 14,000 × g at 4 °C for 10 min. Following the centrifuge, the supernatants were collected, and the protein concentration was measured by using Pierce™ BCA Protein Assay Kit (Thermo Fisher Scientific, MA, USA, #23225). Equal amounts of each protein samples were electrophoresed in SDS-PAGE based on the standard protocol, and then transferred onto a PVDF membrane (Millipore, MA, USA). The PVDF membrane was subsequently blocked with 5% bovine serum albumin (BSA) (Amresco, WA, USA) in TBST (50 mM Tris-HCl, 150 mM NaCl, 0.05% Tween-20) buffer for 2 h at room temperature. Following three times washes with TBST buffer, the membrane was incubated with the appropriate primary antibodies at 4°C for overnight. After washing four times with TBST buffer, the membrane was incubated with HRP-coupled secondary antibodies for 1 h at room temperature. Finally, the membrane was washed four times with TBST buffer, and visualized using SuperSignal™ West Pico PLUS Chemiluminescent Substrate (Thermo Fisher Scientific, MA, USA, #34577). GAPDH loading control Monoclonal Antibody (GA1R) (Thermo Fisher Scientific, MA, USA, #MA5-15738) was used to normalize protein levels of HEK 293T cells.

Subcellular Distribution of TA05575 in *T. annulata* Infected Cell Lines

The CELLO v.2.5, a subCELlular LOcation predictor (http://cello.life.nctu.edu.tw/), was used to evaluate the subcellular location of TA05575 in *T. annulata*-infected cells. The cells of different passages (F10, F20, F55, F110, and F165) were cultured onto the glass slides (NEST) in a 12-well cell culture plate at a density of 2.0–3.0 × 10^5 cells/ml for each well for 24 h. For confocal experiment, cells were washed with PBS three times, and fixed with 4% paraformaldehyde for 30 min at room temperature. Following three times wash with PBS, the PBS with 0.5% Triton X-100 was added for permeabilizing the cells at room temperature for 15 min. After washing with PBS, the cells were incubated for blocking in PBS containing 3% BSA for 1 h at 37°C. Primary antibody against TA05575 derived from rabbit was prepared by DETABIO Inc (Nanjing, China). Five hundred μl primary antibody, which diluted was with PBS containing 1% BSA at the ratio 1:100, was added into the wells and incubated at 4°C for overnight. Following five times washing with PBS, the cells were probed with 500 μl goat anti-rabbit Alexa Fluor 488 antibody (Life Technologies, MA, USA) at a 1:1,000 dilution in PBS plus with 1% BSA at 37°C for 1 h. DNA and actin of the cells were stained with Hoechst 3342 (Life Technologies, MA, USA) and Alexa Fluro™ 594 Phalloidin (Life Technologies, MA, USA), respectively. The cells were observed by a confocal microscope (Leica TCS) with a 63× oil objective after an additional five times washes with PBS. No less than100 cells of different passages of *T. annulata*-infected cells were randomly examined per slide, and the most representative images of each glass slide were shown in the present study.

Construction and Identification of Bait Plasmid

The target sequence of TA05575 was obtained from the cDNA of *T. annulata*-infected cells using the PCR with its specific primers. The specific primer TA05575 was designed based on the TA05575 reference sequence and the sequences are as following: TA05575-F (5′-CCGGAATTCCGGATGAATAAATGTGTAACATAT-3′) and TA05575-R (5′-TGCACTGCAGTGCATTTGTCATCTTTTCCAGAACT-3′), and the enzyme restriction sites are underlined. The obtained PCR product for TA05575 was purified by using the Cycle-Pure kit (OMEGA Bio-Tek, Doraville, USA). Then both the purified PCR products of TA05575 and pGBKT7 plasmid were digested with Thermo Scientific™ FastDigest restriction enzymes *EcoR I* (Thermo Fisher Scientific, MA, USA, #FD0274) and *Pst I* (Thermo Fisher Scientific, MA, USA, #FD0614), respectively, which was followed by ligation step. Finally, the bait plasmid (TA05575-pGBKT7) was further identified by sequencing (Sangon Biotech, Shanghai, China) and bioinformatic analysis.

Determination of Autoactivation and Toxicity of the Recombinant Bait Plasmid

To investigate whether the TA05575-pGBKT7 bait plasmid has the abilities of autoactivation and toxicity, the pGBKT7 plasmid (empty vector control) and the bait plasmid were respectively transformed into Y2H Gold component cells using Quick & Easy Yeast Transformation Mix (Clontech, CA, USA) according to the manufacturer's instructions. Then, the transformants were maintained on the agar plates contained different components, including SD/-Trp (SDO), SD/-Trp/X-α-Gal (SDO/X), and SD/-Trp/X-α-Gal/AbA (SDO/X/A) for 3–5 days at 30°C. Only the color of colonies shown white on SDO plates and pale on SDO/X plates, while no colonies on SD/X/A plates, the bait plasmid could be considered not to be autoactivated. If the size of bait plasmid colonies cultured on SDO and SDO/X plates is remarkably smaller than colonies of the empty vector that indicate the bait plasmid is toxic. Only in the case of the bait plasmid are neither toxicity nor autoactivation, it is possible to perform the Y2H screening for TA05575 gene.

Screen the Interaction Proteins With SVSP449 Using Y2H System

To screen the host cell proteins that might be interact with TA05575 of *T. annulata*, the Y2H system was performed. Firstly, the bait plasmid (TA05575-pGBKT7) and prey plasmid (the cDNA library derived from bovine B cells) (Zhao et al., 2017) were co-transformed into Y2H Gold component cells at the library scale using Yeastmaker™ Yeast Transformation System 2 (Clontech, CA, USA). Then, the transformants were cultured on DDO/X/A agar plates at 30°C for 5 days. Finally, the blue colonies were selected and plated on QDO/X/A agar plates for continued culture at 30°C for 3–5 days. Moreover, the plasmids of pGADT7-T and pGBKT7-Lam were used as negative control, pGADT7-T and pGBKT7-53 plasmids served as positive controls, both negative and positive controls were co-transformed into Y2H Gold cells at the small scale according

to the standard protocol, respectively. Co-transformants were plated onto the DDO and DDO/X/A agar plates at 30°C for 3–5 days, respectively. Following the Y2H screening, identification of blue colonies cultured on the QDO/X/A agar plates with PCR was carried out using Matchmaker™ Insert Check PCR Mix (Clontech, CA, USA) according to the protocol provided by the manufacture.

Rescue and Analysis of the Putative Prey Plasmids

Based on the results of colony PCR, the potential prey plasmids were extracted from the blue colonies picked from QDO/X/A agar plates using Easy Yeast Plasmid Isolation kit (Clontech, CA, USA) according to user manual. Three μl of extracted prey plasmids were subsequently transformed into *E. coli* DH5α competent cells (TaKaRa, Dalian, China). The possible positive prey plasmid DNA was extracted from transformants using PureLink™ HiPure Plasmid Midiprep kit (Thermo Fisher Scientific, MA, USA, #K210005) and sequenced.

The sequence of putative prey plasmids was analyzed by using the BLAST function of NCBI for confirming the potential interacting genes of host cell. Meanwhile, the structure and biological function of identified prey genes of bovine were analyzed by the SMART (http://smart.embl-heidelberg.de/) and UniProt database (http://www.uniprot.org/).

Expression and Subcellular Localization of SVSP449 and Its Potential Binding Proteins

The recombinant plasmids (p3×Flag-CMV-prey genes) were constructed by cloning prey genes into the *Hind III* (Thermo Fisher Scientific, MA, USA, #FD0504) and *BamH I* (Thermo Fisher Scientific, MA, USA, #FD0054) digested p3×Flag-CMV vector. In addition, the pcDNA3.1- TA05575-Myc recombinant plasmid was constructed by cloning the TA05575 contained a C-terminal Myc tag into the pcDNA3.1 vector that digested with *BamH I* and *Xho I* (Thermo Fisher Scientific, MA, USA, #FD0694). To observe the expression and subcellular distribution of TA05575 and its potential interacting proteins, the confocal experiment was performed. Firstly, the HEK293T cells were seeded on glass slides in six-well cell culture plate. Then, the recombinant TA05575 and its corresponding prey plasmid were transfected or co-transfected into the cells using Lipofectamine 3000 (Thermo Fisher Scientific, MA, USA, #L3000015) when the confluent rate of the cells was 70–90%. For the immunofluorescence assay, the cells were washed, fixed, permeabilized, and blocked according to the above mentioned protocol after 24 h of transfection. The cells were incubated with mouse anti-Myc tag monoclonal antibody (CST, #2276S) or rabbit anti-Flag tag polyclonal antibody (Sigma, #F7425) at 4°C overnight, respectively. Following washed with PBS, the cells were stained with goat anti-mouse Alexa Fluor 594- or donkey anti-rabbit 488-conjugated secondary antibodies- (Life Technologies, MA, USA) according to the user manual. The nuclear of cells was stained with Hoechst33342 (Life Technologies, MA, USA). The cells were examined with confocal microscope (Leica TCS) using a 63× oil objective. For each slide, more than 100 cells were randomly visualized, and the presented images we selected were the most representative in our experiment.

Co-IP Assay

Co-IP assay was used to identify the interactions of TA05575 and the prey proteins in HEK293T cells. The cells were cultured in 10-cm cell culture dishes (Thermo Fisher Scientific, MA, USA) at an initial density of 2×10^6 cells per dish. Fourteen hours later, 10 μg of TA05575 plasmid and 10 μg of the prey plasmids were co-transfected into the cells. After 48 h of transfection, the cells were washed two times with cold PBS and lysed with 600 μl of IP/lysis buffer (Thermo Fisher Scientific, MA, USA) containing the protease inhibitor (Roche, Basel, Switzerland, #4693132001) and phosphatase inhibitor cocktail (Roche, Basel, Switzerland, #4906845001) on ice. Then, the supernatants of cell lysate were obtained by centrifuging at 16,000 × g at 4°C for 10 min. The immunoprecipitation experiment was carried out with an anti-Flag tag monoclonal antibody derived from mouse (Sigma, #F1804) using a Pierce™ Co-Immunoprecipitation kit (Thermo Fisher Scientific, MA, USA, #26149). In addition, p3×Flag-CMV and pcDNA3.1 plasmid served as negative controls, were also co-transfected into HEK293T cells. The elution from the Co-IP experiment was analyzed with western blotting. Anti-Flag tag monoclonal antibody (Sigma, #F1804) and anti-Myc tag monoclonal antibody derived from rabbit (CST, #2278S) were used to identify its target protein, respectively.

BiFC Assay

To further confirm the interactions of TA05575 with its prey proteins, the BiFC assay was used to identify their intracellular interactions. The BiFC assay depends on the link of two nonfluorescent complementary fragments of Venus, a variant of green fluorescent protein (GFP). Two Venus fragments of the BiFC vectors are fused with the bait and prey proteins, respectively. Once the expressed SVSP449 and its partner interact to each other, they are brought in proximity to each other, leading to structural complementation and stimulate a bright fluorescent signal (Kerppola, 2008). Moreover, the assay can also visualize the subcellular localization of the interacted proteins (Kerppola, 2008).

The vectors of pBiFC-VN173 (Addgene, #22010) and pBiFC-VC155(Addgene, #22011) were purchased from Addgene (Shyu et al., 2006). The TA05575 and its prey plasmids were cloned into the pBiFC-VN173 vector after double enzymes digestion with *Hind III* and *Sal I* (Thermo Fisher Scientific, MA, USA, #FD0644). The recombinant plasmids of pBiFC-VC155-TA05575 or its prey genes were created by cloning the target gene into the pBiFC-VC155 vector, which was digested with *Sal I* and *Kpn I* (Thermo Fisher Scientific, MA, USA, #FD0524) enzymes. The pBiFC-VN173-TA05575/prey recombinant plasmids, and pBiFC-VC155-TA05575/prey plasmids were transfected individually into HEK293T cells. Moreover, the pairwise of pBiFC-VN173-TA05575/pBiFC-VC155-prey and pBiFC-VN155-TA05575/pBiFC-VC173-prey plasmids were co-transfected into HEK293T cells using Lipofectamine 3000. In addition, the pBiFC-VN173 and pBiFC-VC155 empty plasmids were also transfected into HEK293T cells, which were served as the blank controls. The confocal

microscopy experiments were performed to observe the fluorescent signal and subcellular localization in cell context. For confocal experiment, the cells were incubated with mouse anti-Flag tag monoclonal antibody at a dilution ratio of 1:200 or anti-HA tag monoclonal antibody produced in rabbits (CST, #3724S) at a dilution ratio of 1:800 after fixing, permeabilizing, and blocking of HEK293T cells at 4°C overnight. Followed washing the cells with PBS, donkey anti-rabbit 594- or goat anti-mouse Alexa Fluor 594-conjugated secondary antibodies (Life Technologies, MA, USA) was incubated with the cells at dilution ratio 1:1,000 for 1 h at room temperature, respectively. The cells were visualized with confocal microscope (Leica TCS) after staining cells nuclear with Hoechst 33342 (Life Technologies, MA, USA).

Flow Cytometry Analysis

HEK293T cells were seeded at initial density of 0.5×10^6 cells/ml in six-well cell culture plates (Corning, USA). The pBiFC-VN173-TA05575 and its potential plasmids, the pBiFC-VC155-TA05575 and its corresponding plasmids were transfected individually into HEK293T cells. At the same time, pBiFC-VN173-TA05575/pBiFC-VC155-prey pair and pBiFC-VN155-TA05575/pBiFC-VC173-prey pair were also co-transfected into HEK293T cells when the confluent rate of cells was 70–90%. The fluorescence signal of transfected cells was determined by fluorescence microscopy after 48 h of transfection. The cells were harvested and washed with PBS, and then applied on BD Accuri™ C6 Plus Flow Cytometer (USA) for analysis of the mean fluorescence intensity (MFI) of the cells.

Data and Statistical Analysis

Statistical analysis was performed using GraphPad Prism 7 software. The significance of differences between samples was evaluated using unpaired two-tailed Student's *t*-test. The variance was assessed by calculating the standard error of the mean (SEM) in each group. All experiments were carried out independently at least three times. *$p < 0.05$; **$p < 0.01$; ***$p < 0.001$; ****$p < 0.0001$ and NS, not significant ($p < 0.05$).

RESULTS

Analysis of TA05575 at mRNA Levels in Different Life Cycle Stages of *T. annulata*

The relative mRNA levels of TA05575 in schizont stage of *T. annulata* was significantly higher than that of sporozoite and merozoite stages based on the results of qPCR (**Figure 1**), so it was mainly expressed in *T. annulata* schizont stage, which was consistent with the reports of previous studies (Pain et al., 2005; Shiels et al., 2006; Schmuckli et al., 2009).

Subcellular Colocalization of TA05575 in *T. annulata*-Infected Cell Lines

As shown in **Figure 2**, the subcellular distribution of TA05575 was mainly in nucleus (57.76%) and cytoplasm (28.77%) of the *T. annulata*-infected cells based on the results of CELLO v.2.5. Moreover, the findings of confocal microscopy showed that the subcellular distribution of TA05575 was mainly in nucleus and cytoplasm in different passages (F10, F20, F60, F110, and F165) of *T. annulata*-infected cells (**Figure 3**), which was in consistent with the results of CELLO v.2.5.

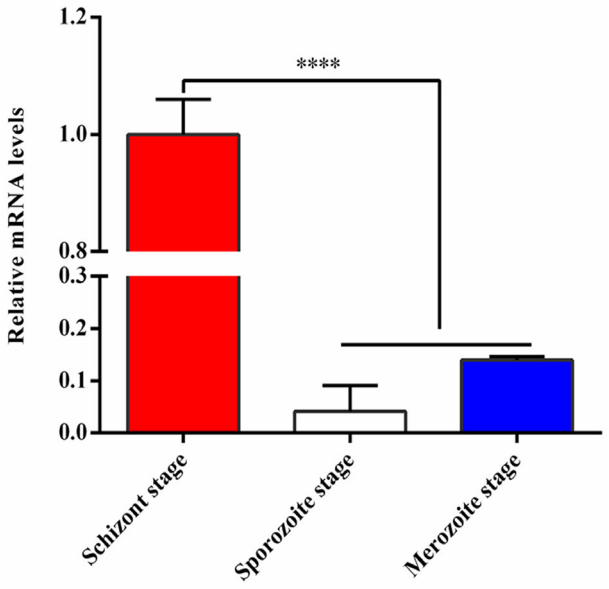

FIGURE 1 | Expression analysis of TA05575 at mRNA level in different life cycle stages of *T. annulata*. ****$p < 0.0001$.

Identification and Bioinformatic Analysis of TA05575

A fragment of TA05575 was successfully amplified from the cDNA of *T. annulata*. In the present study, the length of the TA05575 ORF was 1,350 bp that encoding 450 amino acids, with the predicted size of the TA05575 was about 52 kDa. The TA05575 was predicted to contain a signal peptide from 1 to 21 amino acids and a nuclear localization signal sequence (NLSs) from 217 to 234 amino acids but no GPI-anchors, based on the SignalP-5.0 (http://www.cbs.dtu.dk/services/SignalP-5.0/), NLStradamus (http://www.moseslab.csb.utoronto.ca/NLStradamus/), and PredGPI server (http://gpcr.biocomp.unibo.it/predgpi/pred.htm) analysis, respectively, which indicated that TA05575 was secreted into the host cell cytosol and nucleus. In addition, the target protein did not have putative transmembrane domains after using TMHMM server (http://www.cbs.dtu.dk/services/TMHMM/) analysis. While TA05575 did not have FAINT domain based on the SMART and Pfam identification, which was the typical regions found in SVSP multigene family of *T. annulata*. However, the ORF of reference gene TA05575 was 1,401 bp, encoding 316 aa. The similarity of nucleotide and amino acid sequences of TA05575 obtained in this study and reference gene fragment was 96.1 and 92.4%, respectively.

Analysis for Autoactivation and Toxicity of Bait Plasmid

The recombinant TA05575-pGBKT7 bait plasmid was successfully obtained after sequencing identification. Then, the

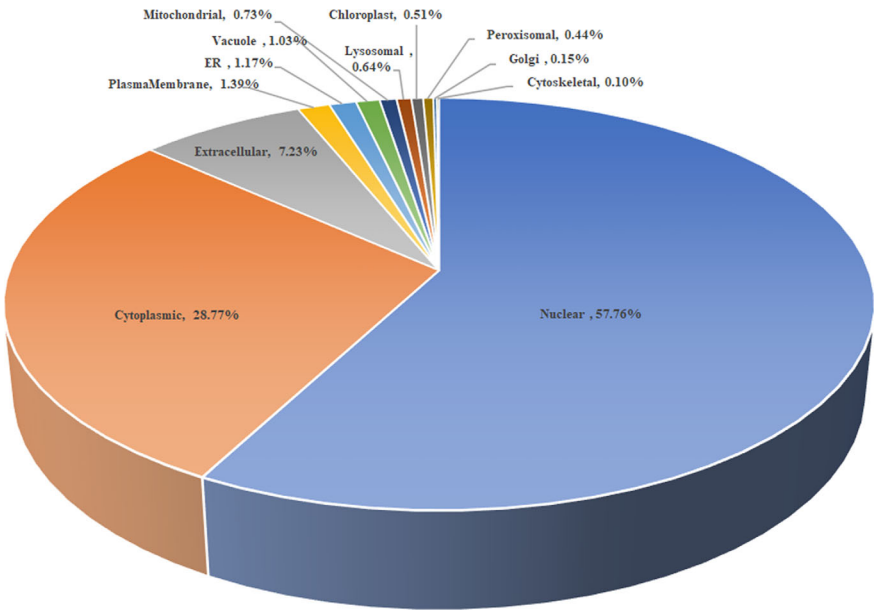

FIGURE 2 | The scheme of subcellular distribution of TA05575 in *T. annulata*-infected cell using CELLO v.2.5. ER represents the endoplasmic reticulum.

characteristics of autoactivation and toxicity of TA05575-pGBKT7 bait plasmid was identified before Y2H screening experiment. As shown in **Figure 4A**, the size of colonies of the bait plasmid cultured on the SDO and SDO/X plates was almost same as the colonies with the control plasmid-pGBKT7 on the same plates. The results demonstrated that TA05575 bait was not toxic in present study. In addition, for bait plasmid, the color of colonies grown on the SDO and SDO/X plates was white and pale blue (**Figure 4A**), which indicated that autoactivation feature of the bait plasmid was not exist in Y2H system. And the results of the colony PCR showed that the transformation efficiency of TA05575 bait plasmid was 71.5% (**Figure 4B**).

Y2H Screening and Identification for Potential Prey Proteins

The potential proteins interact with TA05575 was screened using Y2H system. In this study, the blue colonies for the co-transformants of TA05575 and prey plasmid grown on DDO/X/A plates were picked and cultured on QDO/X/A plates to identify the putative interacting proteins with bait protein (**Figure 4C**). The screened prey plasmids were further confirmed by colony PCR and prey plasmids rescue. The nucleotide sequences of potential plasmids were determined using the BLAST Tool in NCBI. With the BLAST results, the screened prey plasmid had 99.68% similarity with Bos taurus RNA binding motif protein, X-linked 2-like (LOC534630) (RBMX2-like, Accession No: NM_001206548.1). The fragments we screened contained the CDS region from 412 to 1,041 nucleotides of RBMX2-like mRNA, encoding 210 amino acids. And RBMX2-like protein contained a RNA recognition motif (RRM) at the residues at 36 to 114 aa, the biological process of this protein was involved in mRNA splicing *via* spliceosome based on bioinformatic analysis of UniProt and SMART servers. The results of STRING (https://version11.string-db.org/cgi/input.pl?sessionId=1zlnqDY4pkmx&input_page_show_search=on) server indicated that predicted functional partners with RBMX2-like protein included Bos taurus BUD13 homolog, Bos taurus Smad nuclear interacting protein 1 (SNIP1), Splicing factor 3b, subunit 1 and subunit 2 even subunit 3 and Bos taurus PHD finger protein 5A, and so on.

Expression and Subcellular Distribution of TA05575 and Its Putative Interact Protein

The recombinant plasmids of Myc-tagged TA05575 and its potential interacting protein (Flag-tagged RBMX2-like) were successfully constructed. The findings of immunofluorescence assay showed that Myc-tagged TA05575 and Flag-tagged RBMX2-like were both successfully expressed when they were individually or pairwise transfected in HEK293T cells, and the subcellular distribution of these proteins was mainly visualized in the cytoplasm of cells based on the confocal microscopy experiment (**Figures 5A, B**). More importantly, we found that Myc-tagged TA05575 and Flag-tagged RBMX2-like protein were colocalized in the cytoplasm of HEK293T cells, which suggested that TA05575 could interplay with RBMX2-like protein (**Figure 5B**).

Identification of the Interaction of TA05575 With RBMX2-Like by Co-IP

After determination of expression and subcellular distribution of TA05575 and its potential interacting partner, we confirmed the

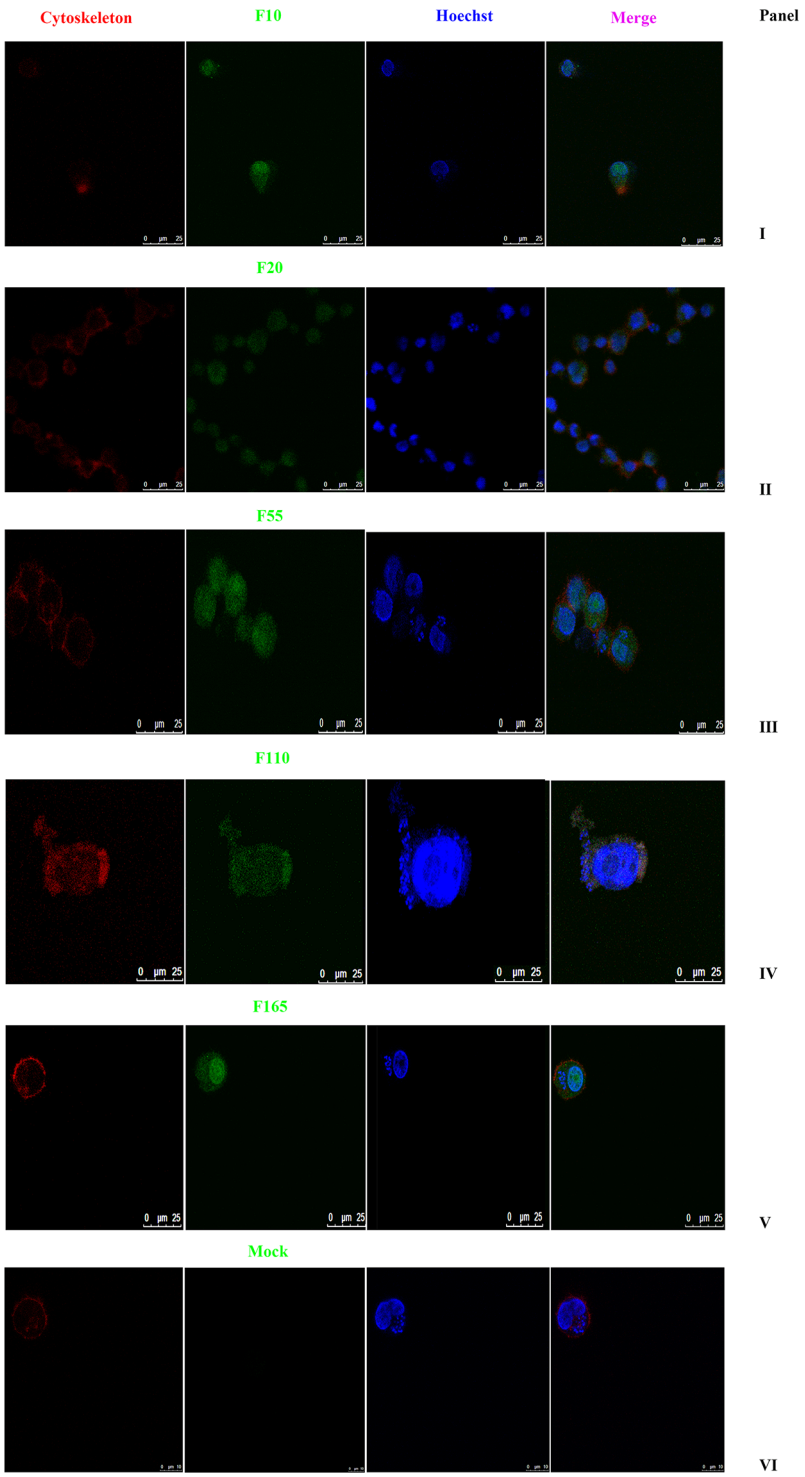

FIGURE 3 | Subcellular localization of TA05575 in *T. annulata*-infected cells. Panels I to V displayed the subcellular localization of TA05575 in different culture passages (F10, F20, F55, F110, and F165) of *T. annulata*-infected cells. Panel VI was the negative control. The TA05575 (Panel I to V) were incubated with rabbit polyclonal antibody against TA05575 and then stained with an Alexa Fluor 488-conjugated goat anti-rabbit antibody. Hoechst 33342 was used to label cell nuclei, Alexa Fluor™ 594 phalloidin was used to label the cytoskeleton. Subcellular localization of TA05575 was visualized by confocal microscopy. Scale bar = 25 μm.

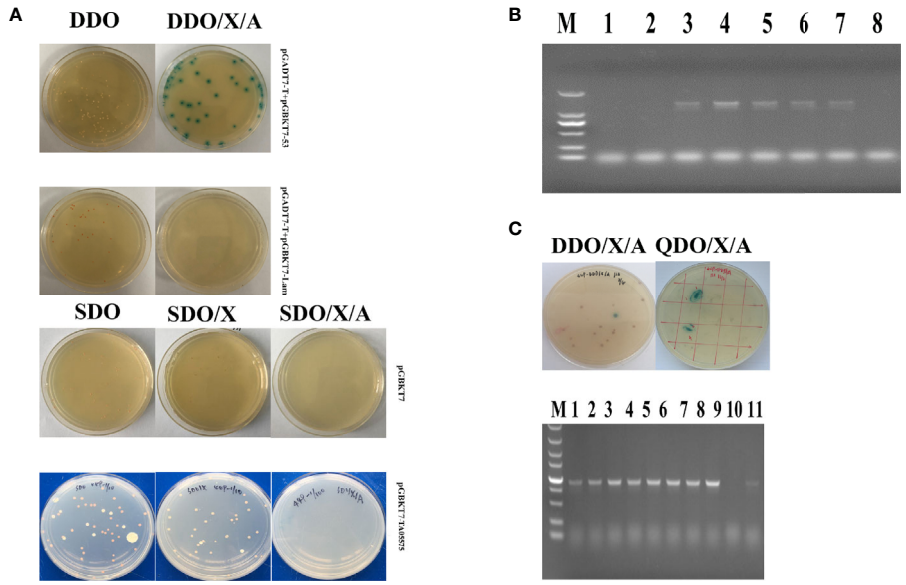

FIGURE 4 | Screen of prey proteins interact with TA05575 by Y2H system. **(A)** Identification for autoactivation and toxicity of pGBKT7-TA05575 in Y2H Gold cells. **(B)** Confirmation for the transformation efficiency of pGBKT7-TA05575 recombinant bait plasmid. The colonies grown on SDO plates were randomly selected and performed to colony PCR using specific primers for TA05575. M: DL 2000 DNA marker; 1-8: the colonies picked from the SDO plate. **(C)** Screening and identification of the possible interacting proteins with TA05575. The co-transformants of pGBKT7-TA05575 and cDNA library of bovine B cells were cultured on DDO/X/A and then grown onto QDO/X/A plates. The co-transformants of pGADT7-T and pGBKT7-Lam plasmids, and pGADT7-T and pGBKT7-53 plasmids grown on DDO an DDO/X/A plates were served as negative and positive controls, respectively.

interactions between TA05575 and RBMX2-like in the HEK293T cells using the Co-IP assay (**Figure 6**). The results of our study demonstrated that TA05575 interacted with RBMX2-like protein, which further supported the findings of confocal microscopy (**Figure 5B**).

TA05575 Binds Directly to RBMX2-Like Protein in Cell Context

To further determine the interaction of TA05575 with RBMX2-like protein in cellular context, BiFC assay was carried out. In the present study, the results showed that no fluorescent signals were detected by flow cytometry method when the plasmids of TA05575-VN, TA05575-VC, RBMX2-like-VN, RBMX2-like-VC were individually transfected in HEK293T cells (**Figures 7A, B**). However, strong fluorescent signals were observed when TA05575-VN and its complementary RBMX2-like-VC or TA05575-VC and RBMX2-like-VN pairs were co-transfected into HEK293T cells (**Figures 7A, B**).

The specificity and subcellular colocation of TA05575-RBMX2-like pair was further determined by visualizing the green BiFC fluorescent signals with confocal microscopy. The strong BiFC green fluorescent signals were observed from co-transfected TA05575-VN/RBMX2-like-VC or TA05575-VC/RBMX2-like-VN pairs in cells (**Figure 7C**), which was consistent with the findings of flow cytometry. Moreover, the green signals of TA05575-RBMX2-like interacting pair colocalized with the red fluorescent signals of RBMX2-like demonstrated their perinuclear subcellular localization in HEK293T cells (**Figure 7C**). These above findings demonstrated that TA05575 of *T. annulata* interplayed with bovine RBMX2-like protein in the intracellular compartments of cell contexts.

DISCUSSION

n the present study, a member of SVSP family, TA05575 was used as a target molecule to investigate its role in host-parasite interactions. Previous findings have analyzed the expression profiles of some SVSP molecules in *T. parva* (Schmuckli et al., 2009) and some results using bioinformatics in *T. annulata* (Weir et al., 2010), however, the expression characteristics of this multigene family in various life cycle stages of *T. annulata* and *T. annulata*-infected cells was not investigated. The findings of our research firstly determined that TA05575 was mainly expressed in the schizont stage in *T. annulata*, which implied it was closely associated with *T. annulata* pathogenecity and in consistent with the previous speculations. Meanwhile, the subcellular localization of TA05575 was observed in different cell culture passages (F10, F20, F55, F110, and F165) in *T. annualta*-infected cells, the results were similar with the CELLO v.2.5 prediction that TA05575 was mainly distributed in the nucleus and cytoplasm compartments in *T. annulata*-transformed cells, and the regions of subcellular distribution was basically not changed when the cell culture passages varied. The above findings indicated that TA05575 was likely to execute its function by manipulating the host cell molecules.

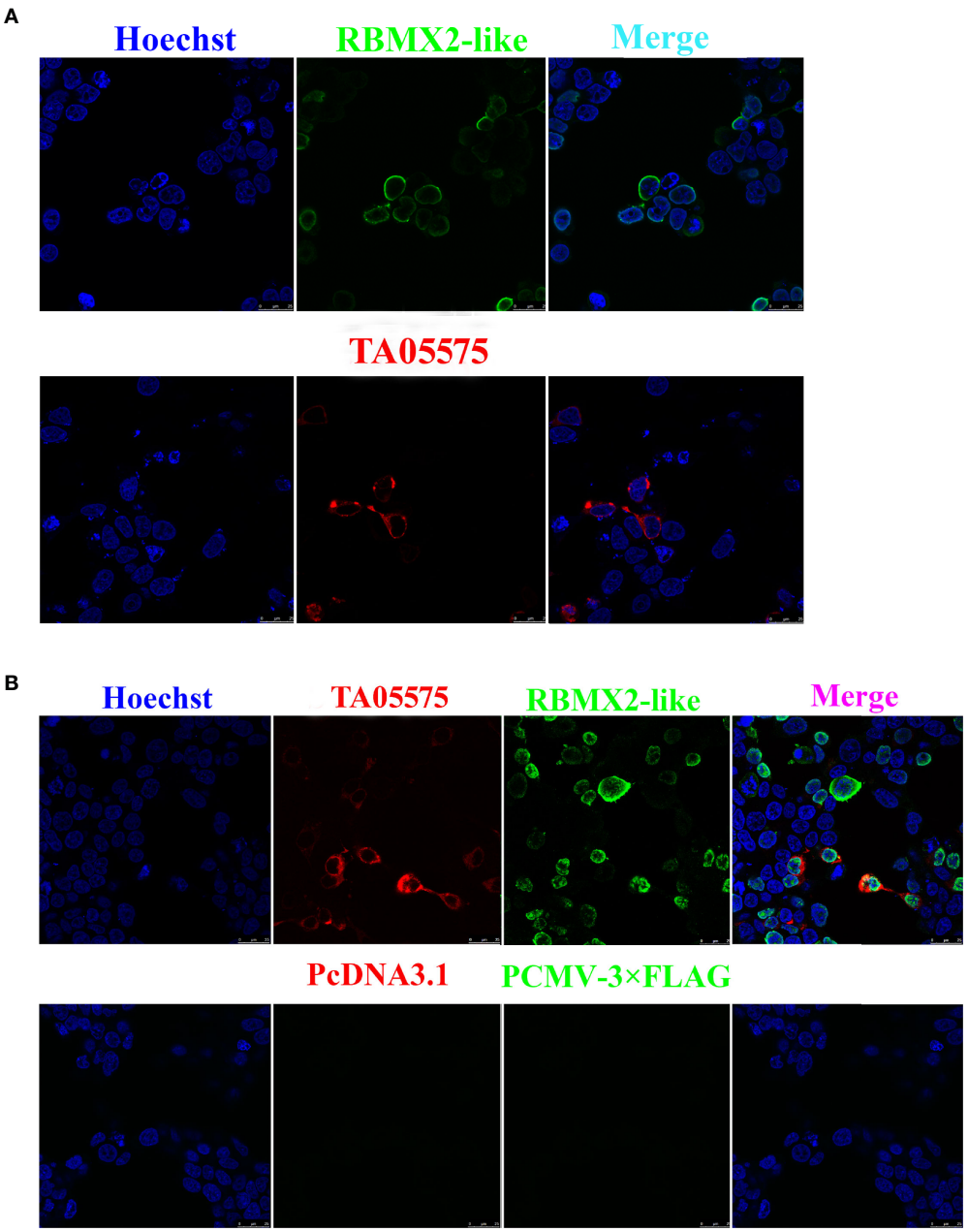

FIGURE 5 | Expression and subcellular distribution analysis of TA05575and its potential interacting protein in HEK293T cells. Confocal microscopy analysis of HEK293T cells expressing TA05575 (4 μg) and its possible prey protein-RBMX2-like (4 μg) **(A)**, and (TA05575 (2 μg)-RBMX2-like (2 μg) **(B)**, respectively. Scale bar = 25 μm.

Herein, to find the possible interacting proteins of host cells with TA05575, Y2H screening system was used in the present study. Finally, The RBMX2-like protein of bovine was identified after sequencing and bioinformatic analysis. To confirm whether the RBMX2-like protein interacts with TA05575, we used Co-IP assay to investigate the interplay between bait and prey proteins in HEK293T cells, and the findings demonstrated that the host cell protein-RBMX-2 like interacted with TA05575, which was further verified the observations of confocal microscopy. To further investigate the interactions of TA05575 and its prey protein, BiFC assay was performed in our study. Both results of confocal microscopy and flow cytometry demonstrated that TA05575-RBMX-2 like pair directly interacted and the subcellular colocalization region is in the cytoplasm of HEK293T cells.

RBMX2-like encodes the protein containing a RRM domain protein of bovine at residues from 56 to 134 aa. The biological process of RBMX2-like maybe involved in mRNA splicing *via* spliceosome. At present, the specific function of RBMX2-like is

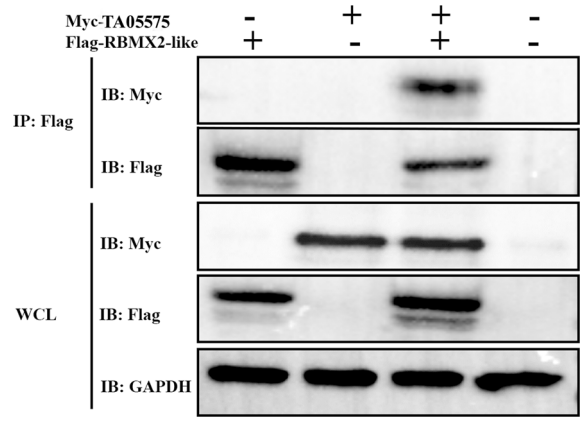

FIGURE 6 | TA05575 interacts with RBMX2-like in HEK293T cells. Co-IP and immunoblotting (IB) detection of the cells expressing TA05575 (10 μg) and its potential pair RBMX2-lik**e** (10 μg). Whole HEK293T cells (WCL) represents IB analysis of the cell lysates for transfection without IP.

not clear, however, serval reports have indicated that it could be used as a molecular marker to assess spermatozoa in MA patients (Ahmadi et al., 2015). Someone found RBMX2 was downregulated in chromosome X in TCs, which might play a role in cell immunology (Zhu et al., 2015), and retention and splicing (RES) complex in RBMX2 was associated with splicing in vertebrate development (Fernandez et al., 2018). Therefore, RBMX2 has a potential role as a molecular marker for *T. annulata* infection due to its unique feature. More importantly, we speculate that the potential alternative splicing of TA05575 is by stabilizing RBMX2-like protein of bovine, and this biological process maybe further affect the parasite transformation in host cells.

In summary, we discovered the TA05575 was mainly expressed in schizont stage of *T. annulata*. Moreover, the subcellular distribution of TA05575 was determined in different cell passages of *T. annualta*-infected cells. The above findings will pave path to elucidate the role of TA05575 during *T. annulata* infection in the future study. More importantly, we firstly identified RBMX2-like interacted with TA05575 using

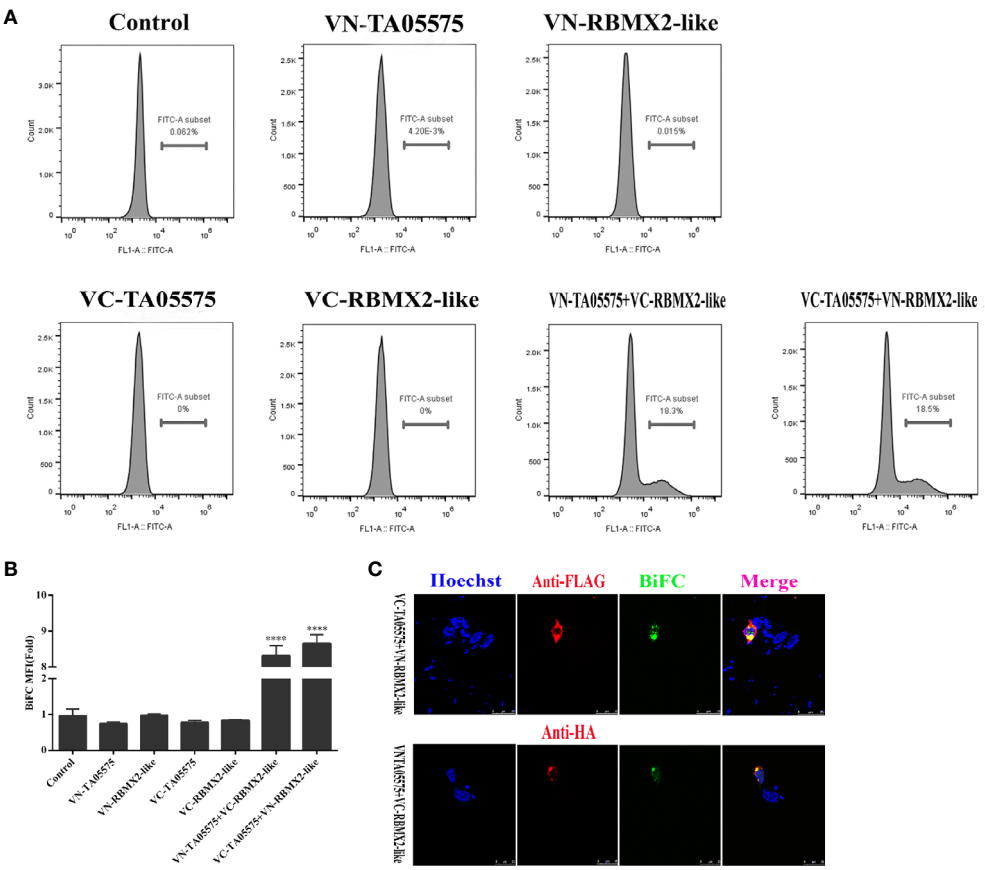

FIGURE 7 | TA05575 directly binds to RBMX2-like in a cell context. TA05575-VN (4 μg), SVSP449-VC (4 μg), RBMX2-like-VN (4 μg), RBMX2-like-VC (4 μg), TA05575-VN (2 μg)-RBMX2-like-VC (2 μg), and TA05575-VC (2 μg)-RBMX2-like-VN (2 μg) were expressed individually or pairwise in HEK293T cells. The MFI of the green-fluorescent signals for BiFC assay was determined using flow cytometry, and the value of MFI is relative to fluorescent signal of un-transfected HEK293T cells, which were served as the control **(A, B)**. HEK293T cells were co-transfected with TA05575-VN (2 μg)-RBMX2-like-VC (2 μg), TA05575-VC (2 μg)-RBMX2-like-VN (2 μg) pairs. The subcellular colocalization of the red of interacting pairs and green-fluorescent signals for BiFC were visualized by confocal microscopy **(C)**. Scale bar =25 μ m. ****$p < 0.0001$.

Y2H system, Co-IP, and BiFC assays. In brief, the investigations into the interactions of *T. annulata* and host cells could provide key insights into the basic biology underlying cancer-like phenotypes.

DATA AVAILABILITY STATEMENT

The raw data supporting the conclusions of this article will be made available by the authors, without undue reservation.

ETHICS STATEMENT

The animal study was reviewed and approved by the Animal Ethics Committee of the Lanzhou Veterinary Research Institute, Chinese Academy of Agricultural Sciences.

AUTHOR CONTRIBUTIONS

ZL, JLL, and HY conceived and designed the experiments. ZL, QM, and SZ performed the experiments. ZL, JLL, AL, YL, GG, and JXL analyzed the data. ZL drafted the manuscript. All authors contributed to the article and approved the submitted version.

FUNDING

This study was supported by the National Key R&D Program of China (2017YFD0500403), National Natural Science Foundation of China (31402189, 31972706), ASTIP, NCBIS (CARS-37), and Central Public-interest Scientific Institution Basal Research Fund (1610312016009), and Jiangsu Co-innovation Center for Prevention and Control of Important Animal Infectious Diseases and Zoonoses, State Key Laboratory of Veterinary Etiological Biology Project.

REFERENCES

Ahmadi, R. D., Sharifi, T. M., Alikhani, M., Parsamatin, P., Sahraneshin, S. F., Sabbaghian, M., et al. (2015). Isoform-Level Gene Expression Profiles of Human Y Chromosome Azoospermia Factor Genes and Their X Chromosome Paralogs in the Testicular Tissue of Non-Obstructive Azoospermia Patients. *J. Proteome Res.* 14 (9), 3595–3605. doi: 10.1021/acs.jproteome.5b00520

Al-Deeb, M. A., Muza_ar, S. B., Abu-Zeid, Y. A., Enan, M. R., and Karim, S. (2015). First Record of a Spotted Fever Group Rickettsia sp. and *Theileria annulata* in *Hyalomma dromedarii* (Acari: Ixodidae) Ticks in the United Arab Emirates. *Fla Entomol.* 98, 135–139. doi: 10.1653/024.098.0123

Anupama, R., Srinivasan, S. R., and Parthiban, M. (2015). Molecular studies on theileriosis and identification of *Theileria orientalis* in India using PCR. *Indian Vet. J.* 92, 9–11.

Barry, J. D., Ginger, M. L., Burton, P., and McCulloch, R. (2003). Why are parasite contingency genes often associated with telomeres? *Int. J. Parasitol.* 33 (1), 29–45. doi: 10.1016/s0020-7519(02)00247-3

Cheeseman, K., and Weitzman, J. B. (2015). Host-parasite interactions: an intimate epigenetic relationship. *Cell. Microbiol.* 17, 1121–1132. doi: 10.1111/cmi.12471

El-Dakhly, K. M., Arafa, W., Ghanem, S. S., Abdel-Fatah, O. R., and Wahba, A. A. (2018). Microscopic and Molecular Detection of *Theileria annulata* Infection of Cattle in Egypt. *J. Adv. Parasitol.* 5, 29–34. doi: 10.17582/journal.jap/2018/5.2.29.34

Fernandez, J. P., Moreno-Mateos, M. A., Gohr, A., Miao, L., Chan, S. H., Irimia, M., et al. (2018). RES complex is associated with intron definition and required for zebrafish early embryogenesis. *PloS Genet.* 14 (7), e1007473. doi: 10.1371/journal.pgen.1007473

Gomes, J., Salgueiro, P., Inácio, J., Amaro, A., Pinto, J., Tait, A., et al. (2016). Population diversity of *Theileria annulata* in Portugal. *Infect. Genet. Evol.* 42, 14–19. doi: 10.1016/j.meegid.2016.04.023

Hayashida, K., Kajino, K., Hattori, M., Wallace, M., Morrison, I., Greene, M. I., et al. (2013). MDM2 regulates a novel form of incomplete neoplastic transformation of *Theileria parva* infected lymphocytes. *Exp. Mol. Pathol.* 94, 228–238. doi: 10.1016/j.yexmp.2012.08.008

Kerppola, T. K. (2008). Bimolecular fluorescence complementation (BiFC) analysis as a probe of protein interactions in living cells. *Annu. Rev. Biophys.* 37, 465–487. doi: 10.1146/annurev.biophys.37.032807.125842

Liu, J., Li, Y., Liu, A., Guan, G., Xie, J., Yin, H., et al. (2015). Development of a multiplex PCR assay for detection and discrimination of *Theileria annulata* and *Theileria sergenti* in cattle. *Parasitol. Res.* 114, 2715–2721. doi: 10.1007/s00436-015-4478-z

Marsolier, J., Perichon, M., Weitzman, J. B., and Medjkane, S. (2019). Secreted parasite pin1 isomerase stabilizes host PKM2 to reprogram host cell metabolism. *Commun. Biol.* 2, 152. doi: 10.1038/s42003-019-0386-6

Medjkane, S., and Weitzman, J. B. (2020). Intracellular *Theileria* parasites PIN down host metabolism. *Front. Cell Dev. Biol.* 8:134. doi: 10.3389/fcell.2020.00134

Mohammed-Ahmed, G. M., Hassan, S. M., El Hussein, A. M., and Salih, D. A. (2018). Molecular, serological and parasitological survey of *Theileria annulata in* North Kordofan State, Sudan. *Vet. Parasitol. Reg Stud. Rep.* 13, 24–29. doi: 10.1016/j.vprsr.2018.03.006

Pain, A., Renauld, H., Berriman, M., Murphy, L., Yeats, C. A., Weir, W., et al. (2005). Genome of the host-cell transforming parasite *Theileria annulata* compared with *T. parva Sci* 309 (5731), 131–133. doi: 10.1126/science.1110418

Rajendran, C., and Ray, D. D. (2014). Diagnosis of tropical bovine theileriosis by ELISA with recombinant merozoite surface protein of *Theileria annulata* (Tams1). *J. Parasitol. Dis.* 38, 41–45. doi: 10.1007/s12639-012-0183-3

Schmuckli, M. J., Casanova, C., Stéfanie, S., Affentranger, S., Parvanova, I., Kang'a, S., et al. (2009). Expression analysis of the *Theileria parva* subtelomere-encoded variable secreted protein gene family. *PLOS One* 4 (3), e4839. doi: 10.1371/journal.pone.0004839

Seitzer, U., Gerber, S., Beyer, D., Dobschanski, J., Kullmann, B., Haller, D., et al. (2010). Schizonts of *Theileria annulata* interact with the microtubule network of their host cell via the membrane protein TaSP. *Parasitol. Res.* 106 (5), 1085–1102. doi: 10.1007/s00436-010-1747-8

Shiels, B., Langsley, G., Weir, W., Pain, A., McKellar, S., and Dobbelaere, D. A. E. (2006). Alteration of host cell phenotype by *Theileria annulata* and *Theileria parva*: mining for manipulators in the parasite genomes. *Int. J. Parasitol.* 36 (1), 9–21. doi: 10.1016/j.ijpara.2005.09.002

Shyu, Y. J., Liu, H., Deng, X., and Hu, C. D. (2006). Identification of new fluorescent protein fragments for bimolecular fluorescence complementation analysis under physiological conditions. *Biotechniques* 40 (1), 61–66. doi: 10.2144/000112036

Tretina, K., Gotia, H. T., Mann, D. J., and Silva, J. C. (2015). *Theileria*-transformed bovine leukocytes have cancer hallmarks. *Trends Parasitol.* 31, 306–314. doi: 10.1016/j.pt.2015.04.001

Villoutreix, B. O., Chluba, J., Lopez, T., Garrido, C., Zhou, X. Z., Lu, K. P., et al. (2015). *Theileria* parasites secrete a prolyl isomerase to maintain host leukocyte transformation. *Nature* 520 (7547), 378–382. doi: 10.1038/nature14044

Weir, W., Karagenç, T., Baird, M., Tait, A., and Shiels, B. R. (2010). Evolution and diversity of secretome genes in the apicomplexan parasite *Theileria annulata*. *BMC Genomics* 11:42. doi: 10.1186/1471-2164-11-42

Woods, K. L., Theiler, R., Mühlemann, M., Segiser, A., Huber, S., Ansari, H. R., et al. (2013). Recruitment of EB1, a master regulator of microtubule dynamics, to the surface of the *Theileria annulata* schizont. *PLOS Pathog.* 9 (5), 1–12. doi: 10.1371/journal.ppat.1003346

Zhao, S. Y., Guan, G. Q., Liu, J. L., Liu, A. H., Li, Y. Q., Yin, H., et al. (2017). Screening and identification of host proteins interacting with *Theileria annulata* cysteine proteinase (TaCP) by yeast-two-hybrid system. *Parasites Vectors* 10 (1), 536. doi: 10.1186/s13071-017-2421-0

Zhu, Y. C., Zheng, M. H., Song, D. L., Ye, L., and Wang, X. D. (2015). Global comparison of chromosome X genes of pulmonary telocytes with mesenchymal stem cells, fibroblasts, alveolar type II cells, airway epithelial cells, and lymphocytes. *J. Transl. Med.* 13, 318. doi: 10.1186/s12967-015-0669-8

Conflict of Interest: The authors declare that the research was conducted in the absence of any commercial or financial relationships that could be construed as a potential conflict of interest.

frontiers in Cellular and Infection Microbiology

ORIGINAL RESEARCH
published: 10 March 2021
doi: 10.3389/fcimb.2021.628667

Comprehensive Analyses of circRNA Expression Profiles and Function Prediction in Chicken Cecums After *Eimeria tenella* Infection

Hailiang Yu[1], Changhao Mi[1], Qi Wang[1], Wenbin Zou[1], Guojun Dai[1], Tao Zhang[1], Genxi Zhang[1], Kaizhou Xie[1], Jinyu Wang[1] and Huiqiang Shi[2]*

[1] College of Animal Science and Technology, Yangzhou University, Yangzhou, China, [2] Technical Research Department, Jiangsu Jinghai Poultry Group Co. Ltd., Haimen, China

OPEN ACCESS

Edited by:
Yongliang Zhang, National University of Singapore, Singapore

Reviewed by:
Shannon Moonah, University of Virginia, United States
Serena Cavallero, Sapienza University of Rome, Italy

***Correspondence:**
Guojun Dai
daigj@yzu.edu.cn

Specialty section:
This article was submitted to Parasite and Host, a section of the journal Frontiers in Cellular and Infection Microbiology

Received: *12 November 2020*
Accepted: *01 February 2021*
Published: *10 March 2021*

Citation:
Yu H, Mi C, Wang Q, Zou W, Dai G, Zhang T, Zhang G, Xie K, Wang J and Shi H (2021) Comprehensive Analyses of circRNA Expression Profiles and Function Prediction in Chicken Cecums After Eimeria tenella Infection. Front. Cell. Infect. Microbiol. 11:628667. doi: 10.3389/fcimb.2021.628667

Coccidiosis is an important intestinal parasitic disease that causes great economic losses to the global poultry production industry. Circular RNAs (circRNAs) are long non-coding RNAs that play important roles in various infectious diseases and inflammatory responses. However, the expression profiles and functions of circRNAs during *Eimeria tenella* (*E. tenella*) infection remain unclear. In this study, high-throughput sequencing was carried out to detect circRNAs in chicken cecal tissues from the control (JC), resistant (JR), and susceptible (JS) groups on day 4.5 postinfection (pi), respectively. A total of 104 circRNAs were differentially expressed, including 47 circRNAs between the JS and JC groups, 38 between the JR and JS groups, and 19 between the JR and JC groups. Functional analyses indicated that these differentially expressed circRNAs were involved in pathways related to *E. tenella* infection; the adaptive immune response was enriched in the JS *vs* JC group, the NF-kappa B signaling and natural killer cell-mediated cytotoxicity pathways were enriched in the JS *vs* JC and JR *vs* JC groups, while the B cell receptor signaling pathway was enriched in only the JR *vs* JC group. Moreover, the coexpression network of differentially expressed circRNAs and mRNAs suggested that circRNA2202 and circRNA0759 associated with *DTX1* in the JS *vs* JC group, circRNA4338 associated with *VPREB3* and *CXCL13L3* in the JR *vs* JC group, and circRNA2612 associated with *IL8L1* and *F2RL2* in the JR *vs* JS group were involved in the immune response upon *E. tenella* infection. In conclusion, our results provide valuable information on the circRNAs involved in the progression of chicken *E. tenella* infection and advance our understanding of the circRNA regulatory mechanisms of host resistance and susceptibility to *E. tenella* infection in chickens.

Keywords: chicken, circRNAs, *E. tenella*, cecum, expression profiles

INTRODUCTION

Avian coccidiosis is an intestinal parasitic disease caused by *Eimeria* protozoa and hinders the development of the global poultry industry (Shirley and Lillehoj, 2012). The global poultry industry has annual economic losses of up to $3 billion due to coccidiosis. Seriously, the subclinical economic losses caused by infected chickens are even more severe, including the impact on weight gain and egg production (Sharman et al., 2010; Blake and Tomley, 2014). To date, there are seven species of *Eimeria* that have been recognized worldwide, and each genus of coccidia is parasitic in a specific region. *E. tenella* parasitizes the chicken cecum, mainly causing bleeding of the cecum epithelium and bloody stools (Yu et al., 2019). In addition, due to the high tolerance and survival rate of coccidia oocysts in the environment, *E. tenella* is common in the poultry industry. At present, the prevention strategies for coccidiosis are mainly divided into three types: anticoccidial drugs, vaccines, and strict feeding hygiene management (Swaggerty et al., 2015). Drug resistance issues and violations of antibiotic bans have attracted much attention (Xie et al., 2020). In this regard, selecting breeds and lines with natural resistance to coccidiosis based on the genetic variability of chickens and genes related to resistance is an effective, long-term prevention strategy (Kim et al., 2009). Genetically distinct lines of broilers have shown differences in resistance or susceptibility to *Salmonella enteritidis* (Swaggerty et al., 2005), *Campylobacter jejuni* (Li et al., 2008), and *E. tenella* (Swaggerty et al., 2011) infections. Broiler breeders with an efficient innate immune response are more resistant to *E. tenella* (Swaggerty et al., 2011), and a novel selected mean based on a higher phenotype of some pro-inflammatory mediators was formed to produce broilers that are naturally more resistant to *E. tenella* (Swaggerty et al., 2015).

Circular RNAs (circRNAs) are a special type of endogenous non-coding RNA that are widespread in animals and plants (Li et al., 2019). Compared to linear RNA, circRNA is formed through the back-splicing of covalently bound 3′-and 5′-ends. Therefore, they are more highly conserved and stable (Jeck et al., 2013). Previous studies have shown that circRNAs can play a regulatory role as miRNA sponges and can also act as posttranscriptional regulators and templates for translating proteins to perform biological functions (Hansen et al., 2013; Jeck et al., 2013; Memczak et al., 2013). Increasing evidence has shown that circRNAs play an important regulatory role in pathological processes such as *Alzheimer's* disease, cancer, and viral infections (Li et al., 2015; Li et al., 2017; Cervera-Carles et al., 2020). However, the expression and regulatory mechanisms of circRNAs during *E. tenella infection* are unclear. In this study, we first investigated the expression profile and function of circRNAs in cecal tissues of broilers infected with *E. tenella* in different groups (the control, resistant, and susceptible groups) to understand the complex mechanisms of resistance and susceptibility to *E. tenella* mediated by circRNAs.

MATERIALS AND METHODS

Samples and Challenge

A total of 20 full-sib family broilers were selected from 200 Jinghai Yellow Chickens at Jinghai Yellow Chicken Resource Farm in Jiangsu Province, China. One male and four female parents in each family were artificially fertilized to produce the F1 generation (the number of F1 generations of each family was not less than 10). The offspring of each family were raised separately in oocyst-free cages and fed antibiotic-free feed and water. At 18 days old, F1 individuals from each family were randomly divided into two groups: the treatment group and the control group. Each chicken in the treatment group was orally infected with the same dose of sporulated *E. tenella* oocysts (3.5×10^4 oocysts/bird). In this study, the clinical symptoms (emaciation, drooping wings, and dying death), fecal scores (Morehouse and Baron, 1970), and cecal lesion scores (Johnson and Reid, 1970) were used together to discriminate susceptible (JS, severe clinical symptoms, fecal scores >3, and cecal lesion scores >3) from resistant (JR, slight clinical symptoms, fecal scores = 0, and cecal lesion scores ≤1) birds. Thus, the most resistant and most susceptible families were selected for subsequent sequencing (**Figure 1**). Each chicken in the control group of the resistant family received the same amount of normal saline (JC).

Parasite oocysts were collected from the Department of Parasitology, College of Veterinary Medicine, Yangzhou

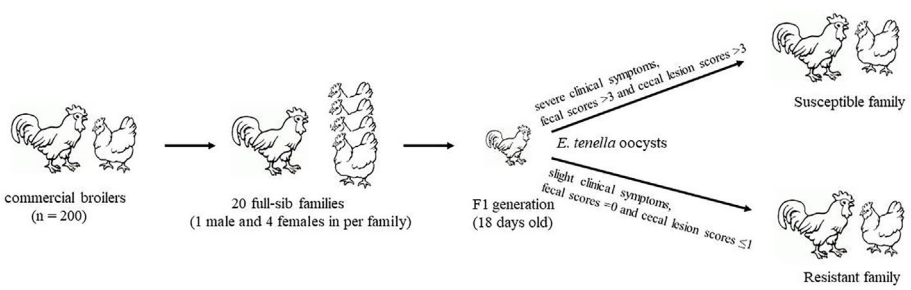

FIGURE 1 | Workflow of sample selection.

University (Jiao et al., 2018). On the 4.5th day postinfection [the point time to identify the resistance and susceptibility chickens according to whether cecum bleeding or not (Rose and Hesketh, 1976)], the cecal tissues of the three broilers in the JS, JR, and JC groups were collected, snap-frozen, and preserved at −80°C for later use. All animal protocols were approved by the Animal Welfare Committee of Yangzhou University, and all efforts were made to minimize the suffering of the chickens.

Library Construction and High-Throughput Sequencing Analysis

Total RNA from cecal samples in each group was extracted using TRIzol reagent (Invitrogen, Carlsbad, CA, USA) according to the manufacturer's instructions. The purity of RNAs was checked using a NanoPhotometer® spectrophotometer (IMPLEN, CA, USA). The concentration and integrity of RNAs were determined using the Qubit® RNA Assay Kit in Qubit® 2.0 Flurometer (Life Technologies, CA, USA) and Bioanalyzer 2100 system (Agilent Technologies, CA, USA), respectively. The quality of the RNA samples met the experimental requirements (RIN> = 7 28S/18S> = 0.7) and were used for RNA sequencing.

Ribosomal RNA was removed using the Ribo-Zero Gold rRNA Removal Kit (Illumina), and the remaining RNA was fragmented by a fragmentation reagent. Then, the libraries were constructed using TruSeq Stranded Total RNA with Ribo-Zero Gold (Illumina, Cat. no. RS-122-2301) according to the manufacturer's instructions. Whole transcriptome sequencing, including circRNA sequencing and mRNA sequencing, was carried out on an Illumina HiSeq 2500 (OE Biotech, Shanghai, China), and the reading length was 2 × 150 BP (pe150).

Differentially Expressed circRNA and mRNA Analysis

The clean reads were aligned to a reference genome using HISAT2 (Kim et al., 2015). Then, CIRI (v2.0.3) was employed to detect and identify the circRNAs (Gao et al., 2015). The expression of circRNAs was calculated using spliced reads per million mapped reads (RPM). For mRNAs, Cufflinks (Trapnell et al., 2010) was used to calculate the fragments per kilobase of transcript per million mapped reads (FPKM) value (Roberts et al., 2011) of expression of each gene, and the read counts of each gene were obtained by HTSeq-count (Anders et al., 2015). The DESeq (2012) R package was also used to perform differential expression analysis. Finally, the differentially expressed circRNAs and mRNAs were screened based on fold change (FC) > 2, and the *P-value* was <0.05.

CircRNA Functional Analysis

Gene Ontology (GO) analysis was performed to determine the basic functions of the host genes of differentially expressed circRNAs, including three classes: biological process (BP), cellular component (CC), and molecular function (MF). The Kyoto Encyclopedia of Genes and Genomes (KEGG) was used to analyze the functional pathways of the host genes of the circRNAs. GO terms and KEGG pathways were considered to be significantly enriched based on a *P-value* <0.05.

Construction of the circRNA-mRNA Coexpression Network

We used the Pearson correlation coefficient (*PCC*) to calculate the correlation between differentially expressed circRNAs and differentially expressed mRNAs and constructed a coexpression network. CircRNA-mRNA interaction pairs were extracted with the value of *PCC* ≥0.8 and *P-value* <0.05, and the top 100 coexpression of circRNA-mRNA network map was then constructed using the R network package.

Real-Time PCR

Total RNA was extracted from original cecal tissues and used to synthesize cDNA using an RT-PCR Kit (TaKaRa Biotech, Dalian). Seven circRNAs were selected to verify the reliability of RNA-Seq, including six circRNAs, and β-actin was used as an internal reference gene. Primer sequences (**Table 1**) were synthesized by Sangon Biotech Co., Ltd. (Shanghai, China). Then, qRT-PCR was performed using SYBR Green (TaKaRa Biotech, Dalian). The reactions were carried out as follows: initial denaturation at 94°C for 30 s, followed by 40 cycles of denaturation for 5 s at 95°C and annealing for 34 s at 60°C. Data at multiple points were collected for dissolution curve analysis, and the procedure was as follows: 95°C for 15 s, 60°C for 1 min, 95°C for 15 s, and 60°C for 15 s. Each sample was analyzed in triplicate. The qRT-PCR results were analyzed using the $2^{-\Delta\Delta Ct}$ method (Livak and Schmittgen, 2001).

RESULTS

Identification of circRNAs in Cecal Tissues by RNA-Seq

We obtained 1000.44 M raw reads from nine libraries by Illumina sequencing. After removing adapter reads and low-quality reads, a total of 967.44 M clean reads were used for the identification of circRNAs. The accuracy of base recognition (Q30) in each sample was greater than 95% (**Table 2**). A total of

TABLE 1 | Primer sequences for differentially expressed circRNAs.

circRNAs	Primer sequences (5'-3')	Length/bp
β-actin	F: CCTGAACCTCTCATTGCCA	152
	R: GAGAAATTGTGCGTGACATCA	
circRNA_4375|	F: CTTAGAAACAACGAGGGACGA	183
Chr31:5251588_5267684_-	R: TCAGGACTCACAGTGATGGGA	
circRNA_6530|	F: AGTCACACCTCCCGATCAAGG	121
ChrZ:38536561_38537174_+	R: GGTGCGGAGTGAGAGGTACA	
circRNA_6300|	F: TGCAGACCAGATACGGGGTA	136
ChrW:4831150_4838596_+	R: CCCAAGCACTGGAAGGGCTA	
circRNA_0759|	F: GGACATTGCTATGTTTGCAGG	162
Chr1:130466378_130493459_-	R: ACATCACCACCTCTCGAGTTC	
circRNA_4340|	F: CCATAAAAGCACCGGCTCTC	250
Chr31:2362269_2405166_-	R: CATATTCCAACCCCTTGCCG	
circRNA_1909|	F: GGGTATAAAAGGGCATCGAG	227
Chr15:8218348_8230982_-	R: AGCCATAACCATAGCCACTG	

bp, base pair; circRNA, circular RNA; F, forward; R, reverse.

TABLE 2 | Sequencing data and quality parameters.

Sample	Raw reads	Clean reads	Multiple mapped (%)	Uniquely mapped (%)	Q30 (%)	GC (%)
JC1	107.54 M	104.92 M	6299668 (6.00)	93010583 (88.65)	96.13	47.73
JC2	109.24 M	105.23 M	13308196 (12.65)	84687626 (80.48)	95.89	53.21
JC3	111.36 M	107.18 M	8417074 (7.85)	93783447 (87.50)	95.86	48.32
JR1	110.64 M	107.46 M	7548912 (7.02)	94792432 (88.21)	95.81	48.05
JR1	102.58 M	100.09 M	6540337 (6.53)	88766317 (88.69)	96.21	47.62
JR1	117.57 M	114.35 M	9002737 (7.87)	99731881 (87.22)	96.01	47.96
JS1	115.24 M	110.56 M	8323574 (7.53)	97330051 (88.03)	95.55	47.73
JS2	110.87 M	106.66 M	7483362 (7.02)	93909225 (88.04)	95.77	47.61
JS3	115.40 M	110.99 M	9413810 (8.48)	96283860 (86.75)	95.77	48.21

M, the size of the data volume; Q30, the percentage of bases with a Qphred value greater than 30 in Raw base to the total base; GC, the percentage of the total number of G and C in CleanBase to the total number of bases.

6,725 circRNAs were identified in all nine cecal samples of broilers (JR *vs* JC, 5,439; JR *vs* JS, 5,752; JS *vs* JC, 5,352). The majority of them were sense-overlapping circRNAs (88.80%), while a small proportion (1.20%) of circRNAs contained intronic sequences (**Figure 2A**). In addition, the lengths of these circRNAs were mostly concentrated at 200–2,000 nt (**Figure 2B**), which was consistent with the reported length distribution of circRNAs. Most of the circRNAs were distributed on chromosome 1, followed by distribution on chromosomes 2 and 3 (**Figure 2C**).

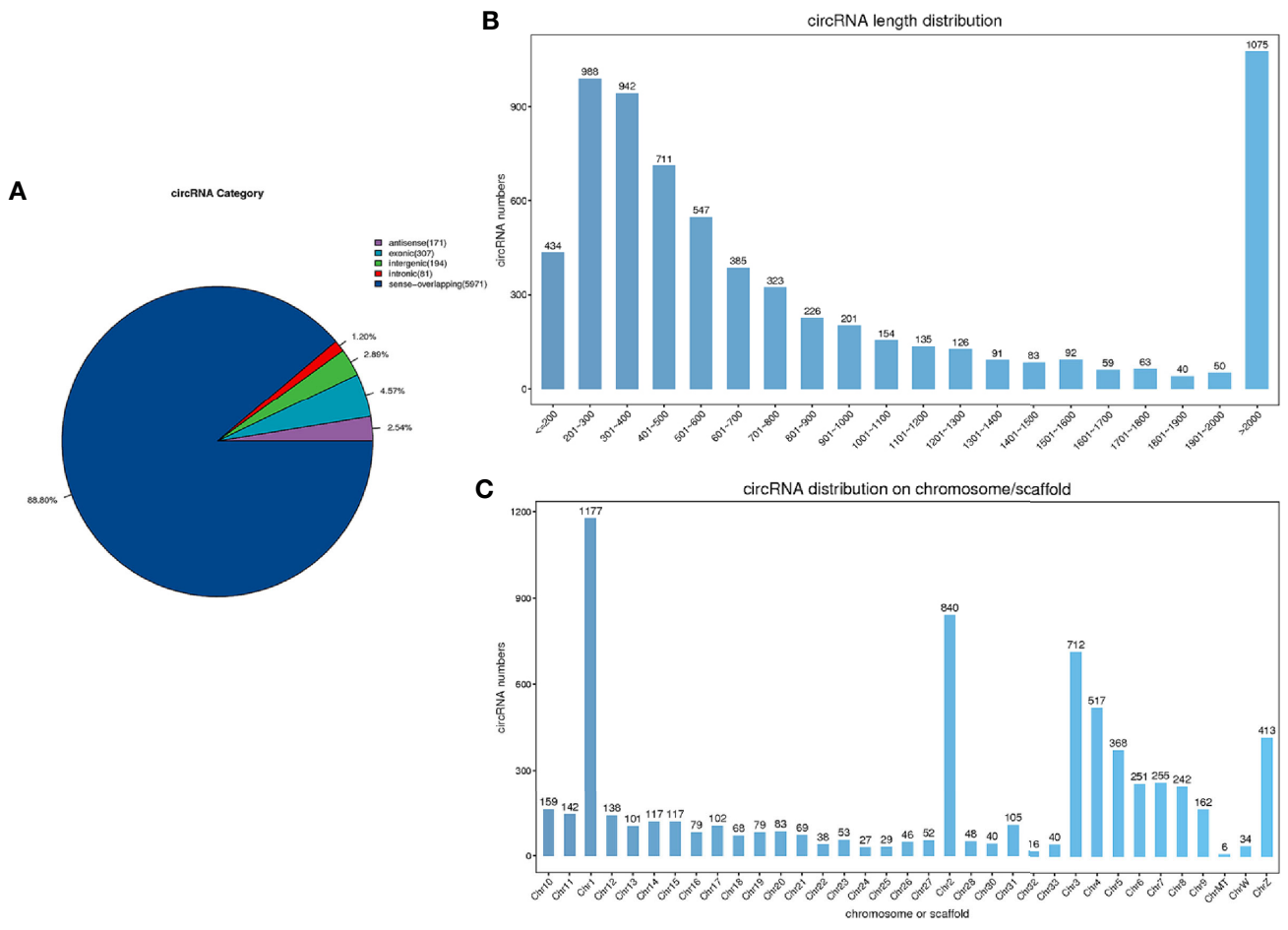

FIGURE 2 | Characteristics of circRNAs in chicken cecal tissues during *E. tenella* infection. **(A)** circRNA category. **(B)** The length distribution of circRNAs. **(C)** Chromosomal distribution of circRNAs.

Differentially Expressed circRNAs in Chicken Cecal Tissues During *E. tenella* Infection

To further investigate the regulatory role of these circRNAs in cecal tissues challenged with *E. tenella*, we analyzed the differential expression of circRNAs from circRNA expression profiling based on a fold change (FC) > 2 and a *P-value* <0.05. *A* total of 47 (17 upregulated and 30 downregulated), 38 (19 upregulated and 19 downregulated), and 19 (9 upregulated and 10 downregulated) differentially expressed circRNAs were identified in the JS *vs* JC, JR *vs* JS, and JR *vs* JC groups, respectively (**Figures 3B–D**, **Supplementary Table 1**). Three circRNAs showed differential expression in the JR *vs* JS and JR *vs* JC groups, seven circRNAs showed differential expression in the JS *vs* JC and JR *vs* JC groups, and 18 circRNAs showed differential expression in the JR *vs* JS and JS *vs* JC groups (**Figure 3A**). Hierarchical clustering analysis showed that the expression patterns of significantly differentially expressed circRNAs were different between the control group and the treatment group (**Figures 3E–G**).

GO Enrichment and KEGG Pathway Analyses of Differentially Expressed circRNAs

Because most circRNAs are derived from middle exons of protein-coding genes, the processing of circRNAs can affect splicing of their precursor transcripts, resulting in changes in the expression of linear host genes (Li et al., 2018). To explore the functions of differentially expressed circRNAs, host genes of these circRNAs were used for GO and KEGG enrichment analyses. The list of host genes is shown in **Supplementary Table 1**. The top 30 significantly enriched GO terms are shown in **Figure 3** (**Figures 4A–C**, **Supplementary Table 2**). Biological processes, adaptive immune response, immune response, and regulation of immune response were enriched in the JS *vs* JC group. Positive regulation of B cell activation and the B cell receptor signaling pathway were enriched in the JR *vs* JC group. The adaptive immune response and apoptotic process were enriched in the JR *vs* JS group. For the cellular component, the immunoglobulin complex, circulating and blood microparticle were enriched in the JR *vs* JC group. Regarding molecular function, antigen binding was enriched in the JS *vs* JC group, antigen binding and immunoglobulin receptor binding were enriched in the JR *vs* JC group, and antigen binding was enriched in the JR *vs* JS group.

Some signaling pathways that are potentially involved in the regulation of *E. tenella* infection and host resistance were significantly ($P < 0.05$) enriched in the top 10 KEGG pathways in different groups, such as the NF-kappa B signaling pathway and natural killer cell-mediated cytotoxicity in the JS *vs* JC and JR *vs* JC groups, the B cell receptor signaling pathway in the JR *vs* JC group, the intestinal immune network for IgA production and hematopoietic cell lineage in all three groups (**Figures 4D–F**, **Supplementary Table 3**).

Validation of Differentially Expressed circRNAs

To further verify the reliability of the RNA sequencing results, six circRNAs with high fold changes and a high number of junctions from high-throughput sequencing were randomly selected for qRT-PCR. The qRT-PCR results suggested that circRNA expression using qRT-PCR was consistent with the RNA sequencing results (**Figure 5**).

The Interaction Network of Differentially Expressed circRNA-mRNA Networks

To reveal the function of circRNAs, a coexpression network map between differentially expressed circRNAs and mRNAs was constructed using the *P*-value of hypergeometric distribution. In the top 100 coexpressed circRNA-mRNA network maps, a total of 32 circRNAs and 74 mRNAs were identified in the JS *vs* JC group (**Figure 6A**, **Supplementary Table 4**). Eighteen circRNAs and 55 mRNAs in the JR *vs* JC group were coexpressed in the cecums of *E. tenella*-infected chickens (**Figure 6B**, **Supplementary Table 5**), and 30 circRNAs and 79 mRNAs were coexpressed in the JR *vs* JS group (**Figure 6C**, **Supplementary Table 6**). Among them, in the JS *vs* JC group, circRNA2202 and circRNA0759 were positively correlated with *DTX1* expression. Moreover, circRNA6300 was positively correlated with the expression of *RORC* and *CD101*. CircRNA4338 was coexpressed with *VPREB3* and *CXCL13L3* in the JR *vs* JC group, and circRNA2612 was coexpressed with *IL8L1* and *F2RL2* in the JR *vs* JS group.

DISCUSSION

Research on the selection of broiler chicken breeds or strains naturally resistant to coccidiosis has been on the way. Johnson and Edgar (1982) reported early that the genetic variability of chickens could affect the resistance and susceptibility to acute cecal coccidiosis (ACC) and confirmed that resistant and susceptible lines of Auburn Strain Leghorn resulted in a sixfold difference in the ACC mortality rate. Later, Quist et al. (1993) showed that coccidia infection in the host cells of the Auburn Strain Leghorn-resistant line was more serious than in the host cells of the resistant line *in vitro*. In addition, *Marek's* disease and *Necrotizing Enteritis*-resistant and -susceptible strains have been reported (Heidari et al., 2020; Pham et al., 2020). Therefore, the resistance of chickens to pathogens are related to genetic variability. Swaggerty et al. (2011) selected broiler lines with strong innate immunity and showed stronger natural resistance to coccidia, as demonstrated by lower lesion scores and higher weight gain. The coccidial resistance of chickens also depend on the immune capacity of the host. In this study, the chicken groups that are naturally resistant and susceptible to *E. tenella* were selected from different families to explore the molecular mechanism of the differences between susceptible groups and resistant groups.

CircRNAs not only participate in the posttranscriptional regulation of genes functioning as miRNA molecular sponges but also interact with RNA binding proteins (Du et al., 2016). Although the functions of most circRNAs remain largely unexplored, as circRNA functions are being gradually revealed, it is becoming increasingly important to study the circRNA

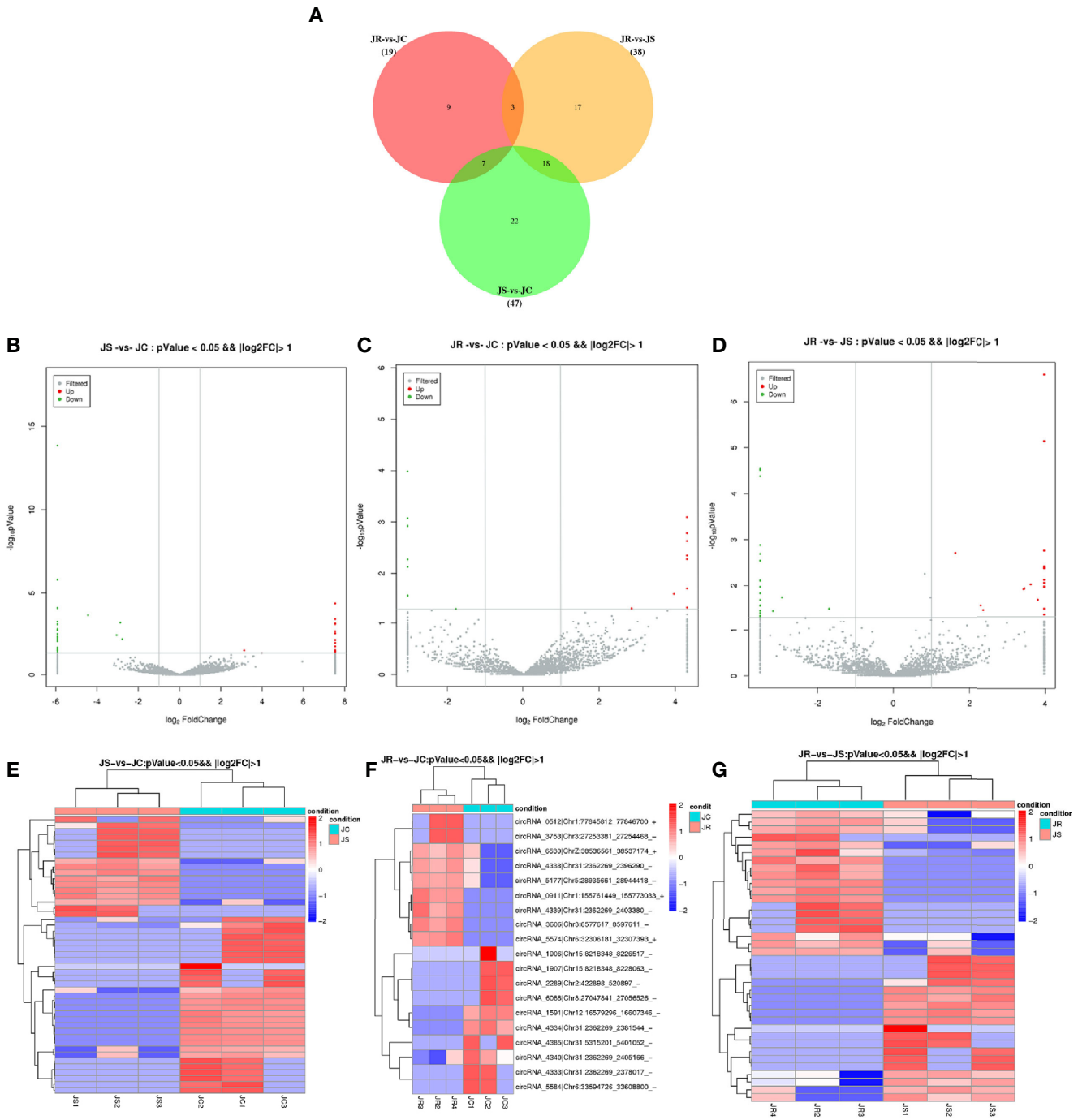

FIGURE 3 | Expression profiles of differentially expressed circRNAs in chicken cecal tissues of different groups during *E. tenella* infection. **(A)** Venn diagram of differentially expressed circRNAs. **(B–D)** Volcano plots of differentially expressed circRNAs in the JS *vs* JC group **(B)**, JR *vs* JC group **(C)**, and JR *vs* JS group **(D)**. **(E–G)** Hierarchical clustering plots of differentially expressed circRNAs in the JS *vs* JC group **(E)**, JR *vs* JC group **(F)**, and JR *vs* JS group **(G)**.

mechanisms in infection and diseases. In previous studies, the expression pattern and regulation of circRNA have been described in porcine endemic diarrhea virus (PEDV) (Chen et al., 2019b), bovine viral diarrhea virus (BVDV) (Li et al., 2019), and crucian carp *Carassius auratus gibelio* (Hu et al., 2019). In poultry, Chen et al. (2019a) found that five differentially expressed circRNAs were upregulated in chicken ammonia poisoning. Liu et al. (2020) reported that 27 differentially expressed circRNAs were involved in the immune response to infectious bursal infection in chickens. Fan et al. (2020)

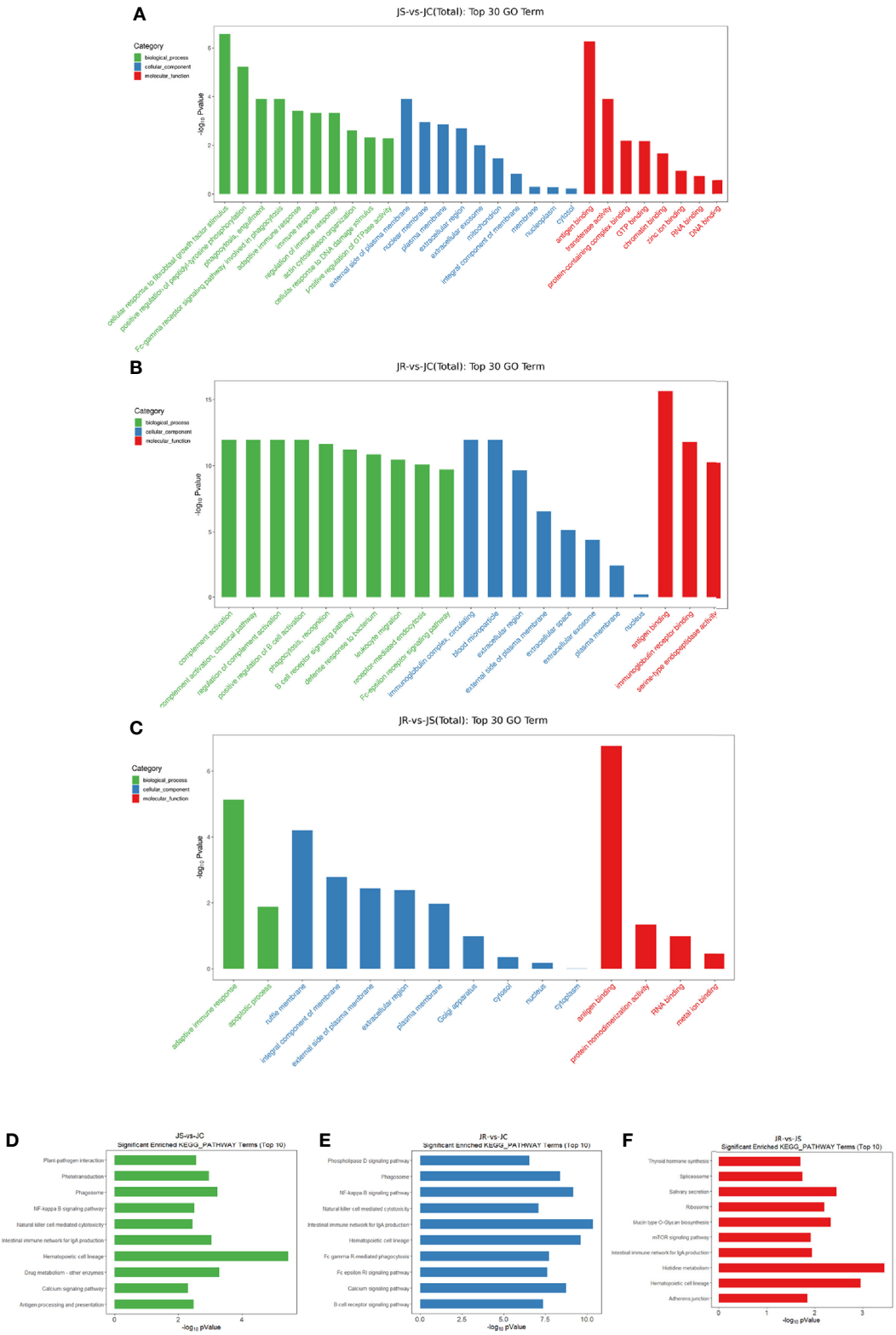

FIGURE 4 | Functional enrichment analysis of differentially expressed circRNAs in chicken cecal tissues of different groups during *E. tenella* infection. **(A–C)** GO term analysis of differentially expressed circRNAs in the JS *vs* JC group **(A)**, JR *vs* JC group **(B)**, and JR *vs* JS group **(C)**. **(D–F)** KEGG pathway analysis of differentially expressed circRNAs in the JS *vs* JC group **(D)**, JR *vs* JC group **(E)**, and JR *vs* JS group **(F)**.

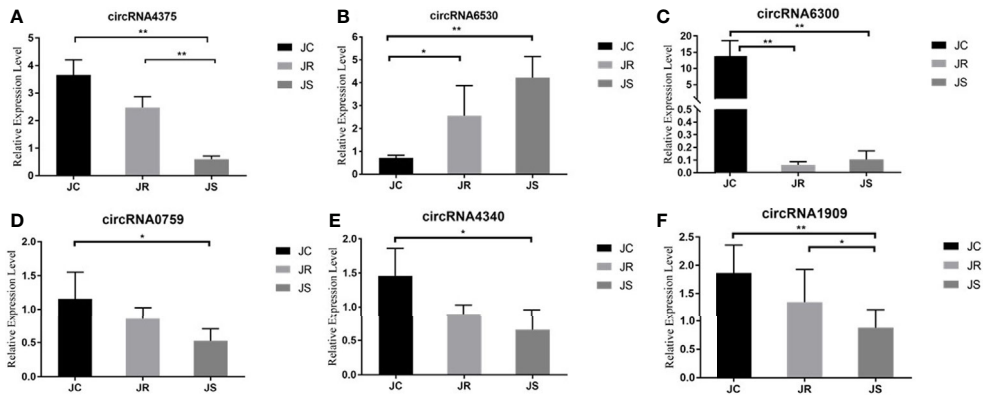

FIGURE 5 | Validation of differentially expressed circRNAs in chicken cecal tissues of different groups during E. tenella infection. Six circRNAs are in the following order: circRNA4375 **(A)**, circRNA6530 **(B)**, circRNA6300 **(C)**, circRNA0759 **(D)**, circRNA4340 **(E)** and circRNA1909 **(F)**. Values are the mean ± SD (n = 3 per group), and qRT-PCR analysis was conducted in triplicate. $^{*}P < 0.05$, $^{**}P < 0.01$.

performed transcriptome sequencing on the small intestine tissues of chickens infected with *E. necatrix*. and showed that 13 differentially expressed circRNAs, such as circRNA2673, circRNA3106, and circRNA1579, played an important role in the process of *E. necatrix* infection. In this study, *E. tenella* infection induced the significant alteration of these circRNAs expression. Further, we found that the functional enrichment of these differentially expressed circRNAs were significantly enriched in the adaptive immune response and the B cell receptor signaling pathways. Adaptive immunity is specific and regulates the antigen-specific immune responses to prevent colonization and growth of the pathogen inside the host and the adaptive immune response plays a dominant role in anticoccidial protective immunity (Kim et al., 2019). B cells are the important components of adaptive immune responses in birds (Girard et al., 1997). When coccidia begins to infect the host, B lymphocytes can express antigen-specific surface immunoglobulin molecules that bind to the antigen, and then B cells with the same surface immunoglobulin continue to proliferate and differentiate to participate in host immunity (Lillehoj, 1998). In addition, the natural killer cell-mediated cytotoxicity was the pathway that differentially expressed circRNAs significantly were enriched. Studies have shown that natural killer (NK) cells are involved in defense against invasion of the gut mucosa by coccidia and associated with the innate immunity of coccidial infection (Lillehoj, 1998; Min et al., 2013). Additionally, this study also revealed the potential role of NF-kappa B signaling and the intestinal immune network for IgA production pathways in the process of coccidia infection. These results indicated that these circRNAs are involved in the coccidial infection through affecting chicken innate and adaptive immune response.

To date, a large number of circRNAs have been identified in various species. However, the ways of most circRNAs function are various. Construction of a circRNA-mRNA coexpression network is an effective method to predict circRNA function. In this study, we analyzed the network of circRNA-mRNA coexpression. In the JS *vs* JC group, circRNA2202 and circRNA0759 were positively correlated with the expression of Deltex1 (*DTX1*). DTX1 is an important Notch signaling target and participates in T cell anergy (Matsuno et al., 1998). DTX1 lack enhances T cell activation, enhances autoantibody production, and promotes inflammation (Hsiao et al., 2009). Moreover, DTX1 controls the stability of Tregs at another level *in vivo* by maintaining the protein expression of Foxp3 in Tregs (Hsiao et al., 2015). Therefore, circRNA2202 and circRNA0759 would participate in the immune response of coccidia infection by regulating the *DTXI* gene. In the JR *vs* JC group, circRNA4338 was positively coexpressed with *VPREB3* and *CXCL13L3*. CXCL13 is a member of the chemokine superfamily CXC subtype and is also known as a B cell chemokine 1 or B lymphocyte chemotactic agent (Gunn et al., 1998). VPREB3 belongs to the immunoglobulin (Ig) superfamily and regulates the assembly of the light chain proteins VPREB1 and IGLL1 to form the pre-B-cell receptor (pre-BCR) (Rosnet et al., 2004). The complete pre-BCR plays a vital role in the development of mammalian B lymphocytes (Rodig et al., 2010). Felizola et al. (2015) showed that VPREB3 is expressed in B cell differentiation and mature B lymphocyte subsets. Therefore, circRNA4338 would be involved in the immune response to coccidia infection. In the JR *vs* JS group, circRNA2612 was coexpressed with *IL8L1* and *F2RL2*. Interleukin-8 (IL-8), known as chemokine CX-CL8 (CXCL8), is a proinflammatory factor closely related to the occurrence and development of various inflammatory diseases. IL-8 exerts various biological functions by binding to the receptors CXCR1 and CXCR2, including pro-inflammatory cell chemotaxis, inducing neutrophils to release lysosomal enzymes to eliminate pathogens (Coussens and Werb, 2002), activating immune responses and promoting infected tissue healing (Wang et al., 2020). As a G-protein-coupled protease-activated receptor, F2RL2 plays an important role in the coagulation cascade (Kaufmann and Hollenberg, 2012). Research by Liu et al. (2019) showed that the expression level of *F2RL2* was downregulated during infection with BVDV, suggesting that the complement system may play a key role in BVDV infection. In this study, circRNA2612 would participate in

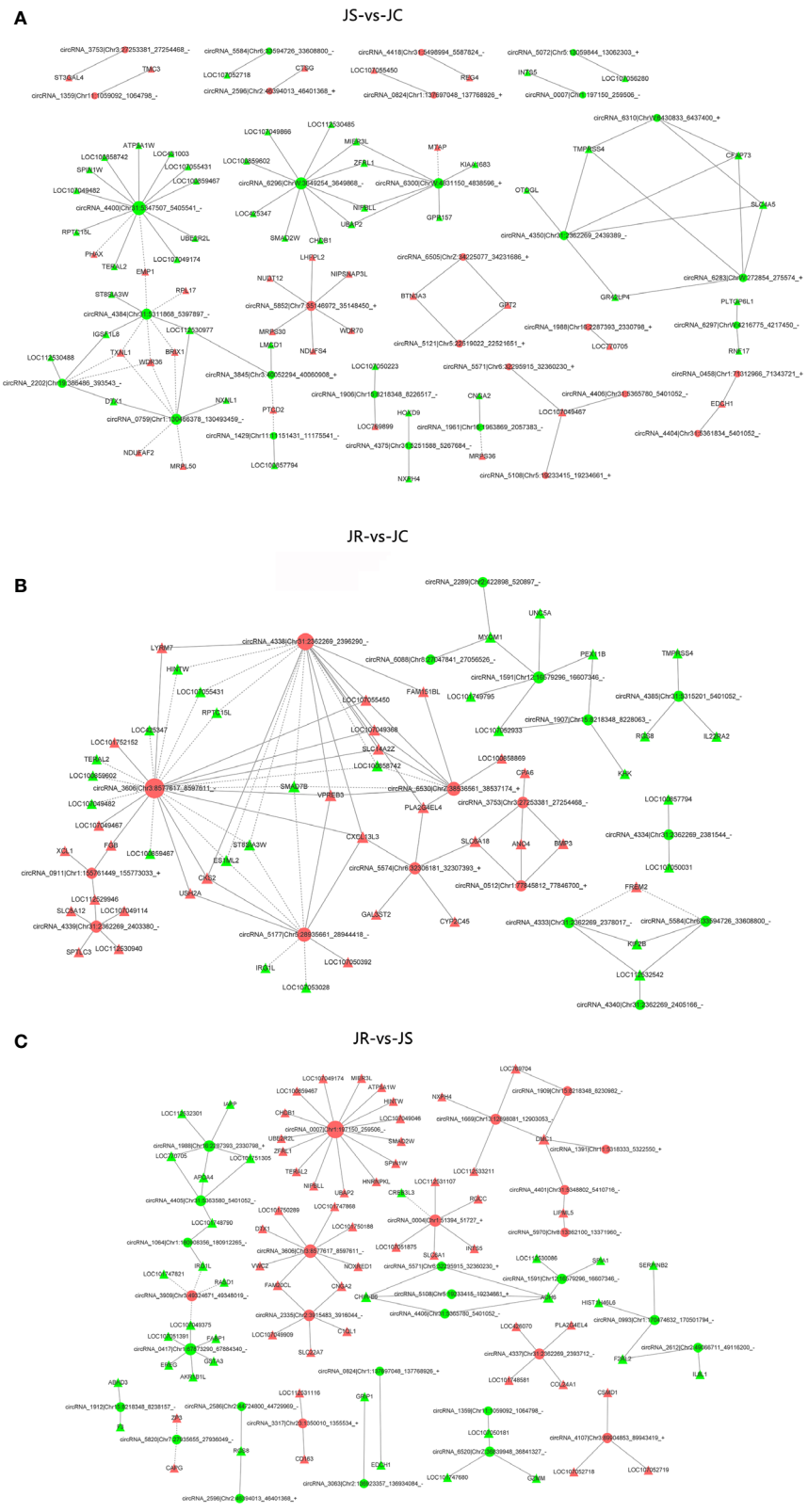

FIGURE 6 | The coexpression network of differentially expressed circRNAs-mRNAs. **(A)** JS *vs* JC group. **(B)** JR *vs* JC group. **(C)** JR *vs* JS group. The red and green represent upregulated and downregulated circRNAs, respectively, while the circles represent the circRNAs, and the triangles represent the mRNAs.

the immune response of the chicken host against *E. tenella* infection by associating with *IL8L1* and *F2RL2*. At present, there are related reports on the functional verification of circRNAs involved in disease and the inflammatory response through regulatory genes (Ma et al., 2018; Zhang et al., 2019). However, few studies have been reported on the functional test of circRNA regulatory genes involved in the immune response to coccidiosis. Therefore, functional verification experiments on the screened circRNAs *in vivo* and *in vitro* are the next research work of our group.

In conclusion, the results of this study demonstrate for the first time that circRNAs are differentially expressed in the cecal tissues of chickens infected with *E. tenella* and may be involved in host responses to *E. tenella* infection in chickens. These findings also provide valuable data for understanding the circRNA complex mechanisms of *E. tenella* resistance and susceptibility in chickens. However, the action mechanisms of circRNAs and mRNAs remain to be clarified.

DATA AVAILABILITY STATEMENT

The datasets presented in this study can be found in online repositories. The names of the repository/repositories and accession number(s) can be found below: NCBI; PRJNA678759.

ETHICS STATEMENT

The animal study was reviewed and approved by the Animal Welfare Committee of Yangzhou University.

AUTHOR CONTRIBUTIONS

HY and GD designed the study and wrote the manuscript. HY, CM, and QW performed the experiments and analyzed the data. HY and WZ performed the transcriptome data and prepared the figures. TZ, GZ, KX, HS, and JW reviewed the manuscript. All authors contributed to the article and approved the submitted version.

FUNDING

This research was supported by the Jiangsu Agricultural Industry Technology System (JATS[2020]437), the National Sci-Tech Support Plan (2014BAD13B02), the Priority Academic Program Development of Jiangsu Higher Education Institutions (PAPD), and the China Agriculture Research System (CARS-41-G23).

ACKNOWLEDGMENTS

The authors would like to thank all members of this work for their advice and technical assistance.

SUPPLEMENTARY MATERIAL

The Supplementary Material for this article can be found online at: https://www.frontiersin.org/articles/10.3389/fcimb.2021.628667/full#supplementary-material

REFERENCES

Anders, S., Pyl, P. T., and Huber, W. (2015). HTSeq–a Python framework to work with high-throughput sequencing data. *Bioinformatics* 31, 166–169. doi: 10.1093/bioinformatics/btu638

Blake, D. P., and Tomley, F. M. (2014). Securing poultry production from the ever-present Eimeria challenge. *Trends Parasitol.* 30, 12–19. doi: 10.1016/j.pt.2013.10.003

Cervera-Carles, L., Dols-Icardo, O., Molina-Porcel, L., Alcolea, D., Cervantes-Gonzalez, A., Muñoz-Llahuna, L., et al. (2020). Assessing circular RNAs in Alzheimer's disease and frontotemporal lobar degeneration. *Neurobiol. Aging* 92, 7–11. doi: 10.1016/j.neurobiolaging.2020.03.017

Chen, D., Miao, Z., Peng, M., Xing, H., Zhang, H., and Teng, X. (2019a). The co-expression of circRNA and mRNA in the thymuses of chickens exposed to ammonia. *Ecotoxicol. Environ. Saf.* 176, 146–152. doi: 10.1016/j.ecoenv.2019.03.076

Chen, J., Wang, H., Jin, L., Wang, L., Huang, X., Chen, W., et al. (2019b). Profile analysis of circRNAs induced by porcine endemic diarrhea virus infection in porcine intestinal epithelial cells. *Virology* 527, 169–179. doi: 10.1016/j.virol.2018.11.014

Coussens, L. M., and Werb, Z. (2002). Inflammation and cancer. *Nature* 420, 860–867. doi: 10.1038/nature01322

Du, W. W., Yang, W., Liu, E., Yang, Z., Dhaliwal, P., and Yang, B. B. (2016). Foxo3 circular RNA retards cell cycle progression via forming ternary complexes with p21 and CDK2. *Nucleic Acids Res.* 44, 2846–2858. doi: 10.1093/nar/gkw027

Fan, X. C., Liu, T. L., Wang, Y., Wu, X. M., Wang, Y. X., Lai, P., et al. (2020). Genome-wide analysis of differentially expressed profiles of mRNAs, lncRNAs and circRNAs in chickens during Eimeria necatrix infection. *Parasites Vectors* 13, 167. doi: 10.1186/s13071-020-04047-9

Felizola, S. J. A., Katsu, K., Ise, K., Nakamura, Y., Arai, Y., Satoh, F., et al. (2015). Pre-B lymphocyte protein 3 (VPREB3) expression in the adrenal cortex: precedent for non-immunological roles in normal and neoplastic human tissues. *Endocr. Pathol.* 26, 119–128. doi: 10.1007/s12022-015-9366-7

Gao, Y., Wang, J., and Zhao, F. (2015). CIRI: an efficient and unbiased algorithm for de novo circular RNA identification. *Genome Biol.* 16, 4. doi: 10.1186/s13059-014-0571-3

Girard, F., Fort, G., Yvore, P., and Quere, P. (1997). Kinetics of specific immunoglobulin A, M and G production in the duodenal and caecal mucosa of chickens infected with Eimeria acervulina or Eimeria tenella. *Int. J. Parasitol.* 27, 803–809. doi: 10.1016/S0020-7519(97)00044-1

Gunn, M. D., Ngo, V. N., Ansel, K. M., Ekland, E. H., Cyster, J. G., and Williams, L. T. (1998). A B-cell-homing chemokine made in lymphoid follicles activates Burkitt's lymphoma receptor-1. *Nature* 391, 799–803. doi: 10.1038/35876

Hansen, T. B., Jensen, T. I., Clausen, B. H., Bramsen, J. B., Finsen, B., Damgaard, C. K., et al. (2013). Natural RNA circles function as efficient microRNA sponges. *Nature* 495, 384–388. doi: 10.1038/nature11993

Heidari, M., Zhang, L., and Zhang, H. (2020). MicroRNA profiling in the bursae of Marek's disease virus-infected resistant and susceptible chicken lines. *Genomics* 112, 2564–2571. doi: 10.1016/j.ygeno.2020.02.009

Hsiao, H. W., Liu, W. H., Wang, C. J., Lo, Y. H., Wu, Y. H., Jiang, S. T., et al. (2009). Deltex1 is a target of the transcription factor NFAT that promotes T cell energy. *Immunity* 31, 72–83. doi: 10.1016/j.immuni.2009.04.017

Hsiao, H. W., Hsu, T. S., Liu, W. H., Hsieh, W. C., Chou, T. F., Wu, Y. J., et al. (2015). Deltex1 antagonizes HIF-1α and sustains the stability of regulatory T cells in vivo. *Nat. Commun.* 6, 6353. doi: 10.1038/ncomms7353

Hu, X., Dai, Y., Zhang, X., Dai, K., Liu, B., Yuan, R., et al. (2019). Identification and characterization of novel type of RNAs, circRNAs in crucian carp Carassius auratus gibelio. *Fish Shellfish Immunol.* 94, 50–57. doi: 10.1016/j.fsi.2019.08.070

Jeck, W. R., Sorrentino, J. A., Wang, K., Slevin, M. K., Burd, C. E., Liu, J., et al. (2013). Circular RNAs are abundant, conserved, and associated with ALU repeats. *RNA (New York N.Y.)* 19, 141–157. doi: 10.1261/rna.035667.112

Jiao, J., Yang, Y., Liu, M., Li, J., Cui, Y., Yin, S., et al. (2018). Artemisinin and Artemisia annua leaves alleviate Eimeria tenella infection by facilitating apoptosis of host cells and suppressing inflammatory response. *Vet. Parasitol.* 254, 172–177. doi: 10.1016/j.vetpar.2018.03.017

Johnson, L. W., and Edgar, S. A. (1982). Responses to prolonged selection for resistance and susceptibility to acute cecal coccidiosis in the auburn strain single comb white leghorn. *Poult. Sci.* 61, 2344–2355. doi: 10.3382/ps.0612344

Johnson, J., and Reid, W. M. (1970). Anticoccidial drugs: lesion scoring techniques in battery and floor-pen experiments with chickens. *Exp. Parasitol.* 28, 30–36. doi: 10.1016/0014-4894(70)90063-9

Kaufmann, R., and Hollenberg, M. D. (2012). "Proteinase-activated receptors (PARs) and calcium signaling in cancer," in *Calcium Signaling*. Ed. M. S. Islam (Springer: Dordrecht, Netherlands), 979–1000.

Kim, D. K., Kim, C. H., Lamont, S. J., Keeler, C. L., and Lillehoj, H. S. (2009). Gene expression profiles of two B-complex disparate, genetically inbred Fayoumi chicken lines that differ in susceptibility to Eimeria maxima. *Poult. Sci.* 88, 1565–1579. doi: 10.3382/ps.2009-00012

Kim, D., Langmead, B., and Salzberg, S. L. (2015). HISAT: a fast spliced aligner with low memory requirements. *Nat. Methods* 12, 357–360. doi: 10.1038/nmeth.3317

Kim, W. H., Chaudhari, A. A., and Lillehoj, H. S. (2019). Involvement of T cell immunity in avian coccidiosis. *Front. Immunol.* 10, 2732. doi: 10.3389/fimmu.2019.02732

Li, X., Swaggerty, C. L., Kogut, M. H., Chiang, H., Wang, Y., Genovese, K. J., et al. (2008). The paternal effect of campylobacter jejuni colonization in ceca in broilers. *Poult. Sci.* 87, 1742–1747. doi: 10.3382/ps.2008-00136

Li, P., Chen, S., Chen, H., Mo, X., Li, T., Shao, Y., et al. (2015). Using circular RNA as a novel type of biomarker in the screening of gastric cancer. *Clin. Chim. Acta* 444, 132–136. doi: 10.1016/j.cca.2015.02.018

Li, X., Liu, C. X., Xue, W., Zhang, Y., Jiang, S., Yin, Q. F., et al. (2017). Coordinated circRNA biogenesis and function with NF90/NF110 in viral infection. *Mol. Cell* 67, 214–227.e217. doi: 10.1016/j.molcel.2017.05.023

Li, X., Yang, L., and Chen, L. (2018). The Biogenesis, Functions, and Challenges of Circular RNAs. *Mol. Cell.* 71, 428–442. doi: 10.1016/j.molcel.2018.06.034

Li, C., Li, X., Hou, X., Ni, W., Zhang, M., Li, H., et al. (2019). Comprehensive analysis of circRNAs expression profiles in different periods of MDBK cells infected with bovine viral diarrhea virus. *Res. Vet. Sci.* 125, 52–60. doi: 10.1016/j.rvsc.2019.05.005

Lillehoj, H. S. (1998). Role of T lymphocytes and cytokines in coccidiosis. *Int. J. Parasitol.* 28, 1071–1081. doi: 10.1016/S0020-7519(98)00075-7

Liu, C., Liu, Y., Liang, L., Cui, S., and Zhang, Y. (2019). RNA-Seq based transcriptome analysis during bovine viral diarrhoea virus (BVDV) infection. *BMC Genom.* 20, 774. doi: 10.1186/s12864-019-6120-4

Liu, X., Song, J., Liu, X., and Shan, H. (2020). Research Note: Circular RNA expressing in different developmental stages of the chicken bursa of Fabricius. *Poult. Sci.* 99, 3846–3852. doi: 10.1016/j.psj.2020.04.026

Livak, K. J., and Schmittgen, T. D. (2001). Analysis of relative gene expression data using real-time quantitative PCR and the 2(-Delta Delta C(T)) method. *Methods* 25, 402–408. doi: 10.1006/meth.2001.1262

Ma, X., Zhao, X., Zhang, Z., Guo, J., Guan, L., Li, J., et al. (2018). Differentially expressed non-coding RNAs induced by transmissible gastroenteritis virus potentially regulate inflammation and NF-κB pathway in porcine intestinal epithelial cell line. *BMC Genom.* 19, 747. doi: 10.1186/s12864-018-5128-5

Matsuno, K., Eastman, D., Mitsiades, T., Quinn, A. M., Carcanciu, M. L., Ordentlich, P., et al. (1998). Human deltex is a conserved regulator of Notch signalling. *Nat. Genet.* 19, 74–78. doi: 10.1038/ng0598-74

Memczak, S., Jens, M., Elefsinioti, A., Torti, F., Krueger, J., Rybak, A., et al. (2013). Circular RNAs are a large class of animal RNAs with regulatory potency. *Nature* 495, 333–338. doi: 10.1038/nature11928

Min, W., Kim, W. H., Lillehoj, E. P., and Lillehoj, H. S. (2013). Recent progress in host immunity to avian coccidiosis: IL-17 family cytokines as sentinels of the intestinal mucosa. *Dev. Compar. Immunol.* 41, 418–428. doi: 10.1016/j.dci.2013.04.003

Morehouse, N. F., and Baron, R. R. (1970). Coccidiosis: evaluation of coccidiostats by mortality, weight gains, and fecal scores. *Exp. Parasitol.* 28, 25–29. doi: 10.1016/0014-4894(70)90062-7

Pham, T. T., Ban, J., Hong, Y., Lee, J., Vu, T. H., Truong, A. D., et al. (2020). MicroRNA gga-miR-200a-3p modulates immune response via MAPK signaling pathway in chicken afflicted with necrotic enteritis. *Vet. Res.* 51:8. doi: 10.1186/s13567-020-0736-x

Quist, K. L., Taylor, R.L. Jr., Johnson, L. W., and Strout, R. G. (1993). Comparative development of Eimeria tenella in primary chick kidney cell cultures derived from coccidia-resistant and -susceptible chickens. *Poult. Sci.* 72, 82–87. doi: 10.3382/ps.0720082

Roberts, A., Trapnell, C., Donaghey, J., Rinn, J. L., and Pachter, L. (2011). Improving RNA-Seq expression estimates by correcting for fragment bias. *Genome Biol.* 12, R22. doi: 10.1186/gb-2011-12-3-r22

Rodig, S. J., Kutok, J. L., Paterson, J. C., Nitta, H., Zhang, W., Chapuy, B., et al. (2010). The pre-B-cell receptor associated protein VpreB3 is a useful diagnostic marker for identifying c-MYC translocated lymphomas. *Haematologica* 95, 2056–2062. doi: 10.3324/haematol.2010.025767

Rose, M. E., and Hesketh, P. (1976). Immunity to coccidiosis: stages of the life-cycle of Eimeria maxima which induce, and are affected by, the response of the host. *Parasitology* 73, 25–37. doi: 10.1017/S0031182000051295

Rosnet, O., Blanco-Betancourt, C., Grivel, K., Richter, K., and Schiff, C. (2004). Binding of free immunoglobulin light chains to VpreB3 inhibits their maturation and secretion in chicken B cells. *J. Biol. Chem.* 279, 10228–10236. doi: 10.1074/jbc.m312169-a200

Sharman, P. A., Smith, N. C., Wallach, M. G., and Katrib, M. (2010). Chasing the golden egg: vaccination against poultry coccidiosis. *Parasite Immunol.* 32, 590–598. doi: 10.1111/j.1365-3024.2010.01209.x

Shirley, M. W., and Lillehoj, H. S. (2012). The long view: a selective review of 40 years of coccidiosis research. *Avian Pathol.* 41, 111–121. doi: 10.1080/03079457.2012.666338

Swaggerty, C. L., Ferro, P. J., Pevzner, I. Y., and Kogut, M. H. (2005). Heterophils are associated with resistance to systemic Salmonella enteritidisinfections in genetically distinct chicken lines. *FEMS Immunol. Med. Microbiol.* 43, 149–154. doi: 10.1016/j.femsim.2004.07.013

Swaggerty, C. L., Genovese, K. J., He, H., Duke, S. E., Pevzner, I. Y., and Kogut, M. H. (2011). Broiler breeders with an efficient innate immune response are more resistant to Eimeria tenella. *Poult. Sci.* 90, 1014–1019. doi: 10.3382/ps.2010-01246

Swaggerty, C. L., Pevzner, I. Y., and Kogut, M. H. (2015). Selection for pro-inflammatory mediators produces chickens more resistant to Eimeria tenella. *Poult. Sci.* 94, 37–42. doi: 10.3382/ps/peu053

Trapnell, C., Williams, B. A., Pertea, G., Mortazavi, A., Kwan, G., van Baren, M. J., et al. (2010). Transcript assembly and quantification by RNA-Seq reveals unannotated transcripts and isoform switching during cell differentiation. *Nat. Biotechnol.* 28, 511–515. doi: 10.1038/nbt.1621

Wang, X. H., Yu, H. L., Zou, W. B., Mi, C. H., Dai, G. J., Zhang, T., et al. (2020). Study of the relationship between polymorphisms in the IL-8 gene promoter region and coccidiosis resistance index in Jinghai Yellow Chickens. *Genes* 11, 476–488. doi: 10.3390/genes11050476

Xie, Y., Huang, B., Xu, L., Zhao, Q., Zhu, S., Zhao, H., et al. (2020). Comparative transcriptome analyses of drug-sensitive and drug-resistant strains of Eimeria tenella by RNA -sequencing. *J. Eukaryot. Microbiol.* 67, 406–416. doi: 10.1111/jeu.12790

Yu, H., Zou, W., Xin, S., Wang, X., Mi, C., Dai, G., et al. (2019). Association analysis of single nucleotide polymorphisms in the 5' regulatory region of the IL-6 gene with Eimeria tenella resistance in Jinghai Yellow Chickens. *Genes* 10, 890–897. doi: 10.3390/genes10110890

Zhang, Z., Zhang, T., Feng, R., Huang, H., Xia, T., and Sun, C. (2019). CircARF3 alleviates mitophagy-mediated inflammation by targeting miR-103/TRAF3 in mouse adipose tissue. *Mol. Ther.: Nucleic Acids* 14, 192–203. doi: 10.1016/j.omtn.2018.11.014

Conflict of Interest: HS was employed by Jiangsu Jinghai Poultry Group Co. Ltd.

The remaining authors declare that the research was conducted in the absence of any commercial or financial relationships that could be construed as a potential conflict of interest.

frontiers in Microbiology

ORIGINAL RESEARCH
published: 11 March 2021
doi: 10.3389/fmicb.2021.619335

PLK:Δ*gra9* Live Attenuated Strain Induces Protective Immunity Against Acute and Chronic Toxoplasmosis

*Jixu Li[1,2,3], Eloiza May Galon[3], Huanping Guo[3], Mingming Liu[3], Yongchang Li[3], Shengwei Ji[3], Iqra Zafar[3], Yang Gao[3], Weiqing Zheng[3,4], Paul Franck Adjou Moumouni[3], Mohamed Abdo Rizk[3,5], Maria Agnes Tumwebaze[3], Byamukama Benedicto[3], Aaron Edmond Ringo[3], Tatsunori Masatani[6] and Xuenan Xuan[3]**

[1] State Key Laboratory of Plateau Ecology and Agriculture, Qinghai University, Xining, China, [2] College of Agriculture and Animal Husbandry, Qinghai University, Xining, China, [3] National Research Center for Protozoan Diseases, Obihiro University of Agriculture and Veterinary Medicine, Obihiro, Japan, [4] The Collaboration Unit for Field Epidemiology of State Key Laboratory for Infectious Disease Prevention and Control, Jiangxi Provincial key Laboratory of Animal-origin and Vector-borne Diseases, Nanchang Center for Disease Control and Prevention, Nanchang, China, [5] Department of Internal Medicine and Infectious Diseases, Faculty of Veterinary Medicine, Mansoura University, Mansoura, Egypt, [6] Transboundary Animal Diseases Research Center, Joint Faculty of Veterinary Medicine, Kagoshima University, Kagoshima, Japan

OPEN ACCESS

Edited by:
Hong-Juan Peng, Southern Medical University, China

Reviewed by:
Si-Yang Huang, Yangzhou University, China
Dong-Hui Zhou, Fujian Agriculture and Forestry University, China

***Correspondence:**
Xuenan Xuan
gen@obihiro.ac.jp

Specialty section:
This article was submitted to Infectious Diseases, a section of the journal Frontiers in Microbiology

Received: *20 October 2020*
Accepted: *19 February 2021*
Published: *11 March 2021*

Citation:
Li J, Galon EM, Guo H, Liu M, Li Y, Ji S, Zafar I, Gao Y, Zheng W, Adjou Moumouni PF, Rizk MA, Tumwebaze MA, Benedicto B, Ringo AE, Masatani T and Xuan X (2021) PLK:Δgra9 Live Attenuated Strain Induces Protective Immunity Against Acute and Chronic Toxoplasmosis. Front. Microbiol. 12:619335. doi: 10.3389/fmicb.2021.619335

Toxoplasmosis is a zoonotic parasitic disease caused by the obligate intracellular protozoa *Toxoplasma gondii*, which threatens a range of warm-blooded mammals including humans. To date, it remains a challenge to find safe and effective drug treatment or vaccine against toxoplasmosis. In this study, our results found that the development of a mutant strain based on gene disruption of dense granule protein 9 (gra9) in type II PLK strain decreased parasite replication *in vivo*, severely attenuated virulence in mice, and significantly reduced the formation of cysts in animals. Hence, we developed an immunization scheme to evaluate the protective immunity of the attenuated strain of Δ*gra9* in type II PLK parasite as a live attenuated vaccine against toxoplasmosis in the mouse model. Δ*gra9* vaccination-induced full immune responses characterized by significantly high levels of pro-inflammatory cytokine interferon gamma (IFN-γ) and interleukin-12 (IL-12), maintained the high *T. gondii*-specific immunoglobulin G (IgG) level, and mixed high IgG1/IgG2a levels. Their levels provided the complete protective immunity which is a combination of cellular and humoral immunity in mouse models against further infections of lethal doses of type I RH, type II PLK wild-type tachyzoites, or type II PLK cysts. Results showed that Δ*gra9* vaccination proved its immunogenicity and potency conferring 100% protection against acute and chronic *T. gondii* challenges. Together, Δ*gra9* vaccination provided safe and efficient immune protection against challenging parasites, suggesting that *PLK*:Δ*gra9* is a potentially promising live attenuated vaccine candidate.

Keywords: *Toxoplasma gondii*, toxoplasmosis, live attenuated vaccine, *PLK*:Δ*gra9*, protective immunity

INTRODUCTION

Toxoplasmosis is a zoonotic parasitic disease caused by the obligate intracellular protozoan *Toxoplasma gondii* (Montoya and Liesenfeld, 2004; Saadatnia and Golkar, 2012). *T. gondii* has the ability to infect all nucleated cells, and thus, has a broad host range of warm-blooded mammals, including humans (Loh et al., 2019). One-third of the global population is estimated

to have *T. gondii* infection, most of which are asymptomatic in immunocompetent people, but causes severe complications in immunocompromised individuals and pregnant women (Tenter et al., 2000; Innes, 2010; Robert-Gangneux and Darde, 2012; Le Roux et al., 2020). Additionally, reproductive problems, i.e., abortion and stillbirth, induced by *T. gondii* infection in livestock presents a grave challenge to the animal industry (Robert-Gangneux and Darde, 2012; Wang et al., 2019). The ensuing public health problems and agricultural economic losses necessitate the search for and development of safe and effective drug treatments and vaccines against toxoplasmosis in humans and animals.

Despite unsparing research efforts in recent decades, treatment and vaccine options against toxoplasmosis are still limited, owing to the unique characteristics of *T. gondii*. For instance, *Toxoplasma* infection has multiple routes of transmission in humans or animals. One route is ingestion of raw or undercooked meat containing tissue cysts with bradyzoites which transmits the parasite to humans. Although a combination of pyrimethamine and sulfadiazine or other compounds has been used to treat active toxoplasmosis in animals or humans (Alday and Doggett, 2017; Dunay et al., 2018), there is no significant therapeutic efficiency on the bradyzoite residing within tissue cysts. Furthermore, *T. gondii* develops complex population structures, in which North America and Europe strains are classified into three major clonal lineages, type I, II, and III (Howe and Sibley, 1995; Loh et al., 2019). The composition of these complex strains will inevitably bring new challenges to the control of toxoplasmosis because of the different proliferative ability and degree of pathogenicity in mouse models. Therefore, due to the current unsatisfactory status in drug treatment of toxoplasmosis, such as the inability of eliminating tissue cysts, the development of a vaccine to control *Toxoplasma* infections caused by different strains and contracted through multiple routes has been a priority.

Several studies on *T. gondii* vaccines have been done and reported in animal models. Although compared with nucleic acid vaccines (Li et al., 2015; Zhang et al., 2015; Lu et al., 2017) and recombinant protein vaccines (El Bissati et al., 2014; Tanaka et al., 2014; Wang et al., 2014a,b), the higher protection against acute or chronic *T. gondii* infection provided by live attenuated vaccines (Fox and Bzik, 2015; Lagal et al., 2015; Abdelbaset et al., 2017; Wang et al., 2017, 2018; Xia et al., 2018b; Yang et al., 2019; Liang et al., 2020) was highlighted both in short- and long-term vaccination using different strains in the mouse model. However, the safeness of these mutants still needs to be tested in animal models. With the advent of the genomic era, the widespread application of the CRISPR/Cas9 system has permitted precise and efficient genetic manipulations in *T. gondii*, such as gene editing and gene deletion resulting in attenuated strains which can be functionally selected (Shen et al., 2017). Advantages of this system facilitate the development of a live attenuated vaccine with reduced virulence but retaining its ability for limited replication in order to induce an immune response, which is considered as the ideal vaccine for resisting toxoplasmosis (Wang et al., 2019).

Dense granule proteins (GRAs) play major functions within the structural formation of the parasitophorous vacuole (PV) and the cyst wall of *T. gondii* (Guevara et al., 2019). One of the GRAs, the dense granule protein 9 (GRA9), has been characterized in *T. gondii*. Recent studies reported that GRA9 was investigated as one of the intravacuolar-network-associated GRAs during cyst development *in vitro*, and loss of gra9 in type II Prugniaud (Pru) strain induced severe defects in the development of chronic-stage cysts *in vivo* (Fox et al., 2019; Guevara et al., 2019). More so, our previous study revealed that disruption of gra9 gene in *T. gondii* type II PLK strain significantly reduced the growth of tachyzoites *in vitro* (Guo et al., 2019). In the current study, we confirmed that the development of a mutant strain based on gene disruption of gra9 in type II PLK strain decreased parasite replication *in vivo*, severely attenuated virulence in mice, and significantly reduced the formation of cysts in animals. These suggest that Δ*gra9* could be considered a vaccine candidate. Hence, we developed an immunization scheme to evaluate the protective immunity of the attenuated strain of Δ*gra9* in type II PLK parasite as a live attenuated vaccine against toxoplasmosis in the mouse model. Results showed that Δ*gra9* vaccination proved its immunogenicity and potency with 100% protection against acute and chronic *T. gondii* challenge infections.

MATERIALS AND METHODS

Animals and Parasite Strains

The recommendations in the Guide for the Care and Use of Laboratory Animals of Obihiro University of Agriculture and Veterinary Medicine, Japan were strictly followed. The protocol of this study was approved by the Committee on the Ethics of Animal Experiments at the Obihiro University of Agriculture and Veterinary Medicine, Japan (permission numbers: 190246). Six-week-old female BALB/c mice were purchased from Clea Japan. All animals were housed in the animal facility of the National Research Center for Protozoan Diseases, Obihiro University of Agriculture and Veterinary Medicine, with adequate temperature (25 ± 2°C) and luminosity (12-h light and 12-h dark) under specific pathogen-free conditions, and free access to food and water. All animals were used at least one week after habituation.

All procedures of pathogen experiments were carried out according to the guidelines of Obihiro University of Agriculture and Veterinary Medicine (permission number: 2018728). In this study, *T. gondii* type I (RH strain with hypoxanthine-xanthine-guanine phosphoribosyl transferase deficiency), and type II (PLK, which is a clone of ME49 strain) strain (Kirkman et al., 2001) were used. Mutant *PLK*:Δ*gra9* attenuated strain with green fluorescent protein (GFP) was generated and cultured in our laboratory, which has been passed for more than 250 generations (Guo et al., 2019). All parasites were cultured in human foreskin fibroblast (HFF) cells maintained in Dulbecco's modified Eagle's medium (DMEM, Sigma), as previously described (Li et al., 2020).

Bradyzoite Differentiation *in vitro* of Δ*gra9* Strain

Toxoplasma gondii PLK wild-type (WT) or *PLK*:Δ*gra9* parasites were cultured in RPMI 1640 medium supplemented with 50 mM HEPES and 1% fetal bovine serum, pH 8.2, ambient

CO_2 for 4 days, as previously described (Xia et al., 2018a). The parasites (2×10^5 per well) forced to egress were allowed to invade cell monolayer (1×10^5 per well) for 3 h, then washed, and each culture was allowed to grow under bradyzoite-inducing conditions for 24, 48, 72, and 96 h, as described above. Subsequently, samples were fixed by 4% paraformaldehyde. After permeabilizing with 0.3% Triton X-100/phosphate-buffered saline (PBS), samples were incubated with rabbit anti-SAG1 polyclonal antibody diluted to 1:500. The Alexa Fluor 594-conjugated goat anti-rabbit IgG (Life Technologies, Inc., United States) and *Dolichos biflorus Agglutinin*, FITC Conjugate (DBA-FITC) (Vector Laboratories, United States) were used to detect primary antibody and cyst wall. Samples were examined using the All-in-one Fluorescence Microscope (BZ-900, Keyence, Japan). Conversion rates were counted in at least 100 vacuoles, wherein DBA-FITC (green) was used for cyst wall staining and anti-SAG1 (red) antibody was used for tachyzoite marker. All assays were conducted in triplicate and repeated at least three times.

Mutant Δ*gra9* Parasite Infection Tests in Mice

To determine the virulence of *PLK*:Δ*gra9* in animals, six BALB/c mice were injected with a lethal dose (freshly egressed tachyzoites, 1×10^5 per mouse) by intraperitoneal injection (i.p.). Daily observations of body weight and clinical signs were noted. Clinical scores ranged from 0 to 10, denoting presence of no signs or all signs, respectively. Evaluated clinical signs included hunching, piloerection, worm-seeking, behavior, ptosis, sunken eyes, ataxia, the latency of movement, deficient evacuation and touch reflexes, and lying on belly (Leesombun et al., 2016). Surviving mice were monitored for 30 days and blood was drawn at day 30 to confirm infection by an ELISA. Tissues were collected to determine parasite burdens through an examination of *TgB1* gene by quantitative PCR (qPCR). *T. gondii* PLK strain was used as control.

To test the cyst formation in animals, 10^3 tachyzoites of *PLK*:Δ*gra9* was used to infect four 7-week-old female BALB/c mice by i.p. Mice were monitored for 35 days, and sera from the blood samples were tested to confirm infection by ELISA. Fresh brain cysts were isolated from each positive mouse brain homogenates, and the number of cysts was estimated by DBA-FITC staining, as previously described (Huskinson-Mark et al., 1991). *T. gondii* PLK WT strain was used as control.

To test the difference in immune response between PLK and *PLK*:Δ*gra9*-infected mice, the different doses of parasites including 10^3, 10^4, or 10^5 were used to infect mice and clinical signs or *T. gondii*-specific IgG levels were noted. Moreover, sera of 10^3 *T. gondii* PLK or *PLK*:Δ*gra9*-injected mice as above, were collected at day 7 or 30 post-infection to determine *T. gondii*-specific IgG levels using 0.5 μg/ml soluble PLK tachyzoite antigens coated by ELISA assay, and cytokine productions such as interleukin 12 (IL-12), interleukin 10 (IL-10), and interferon-gamma (IFN-γ) were tested using ELISA kits (Thermo Fisher Scientific, United States) according to the manufacturer's recommendations. Furthermore, the difference in cytokine productions by splenocytes after *T. gondii* antigen stimulation was determined in infected mice with PLK or *PLK*:Δ*gra9* parasite at day 35 post-infection, as follows.

Vaccination of Mice and Immunogenicity Measurements

Mice were either vaccinated once with 10^3 freshly harvested *PLK*:Δ*gra9* tachyzoites or mock-vaccinated in a total of 200 μl PBS i.p. 30 and 70 days post-infection (dpi), then, sera were collected to test total *T. gondii*-specific IgG and IgG subclasses (IgG1 and IgG2a) levels. Briefly, the 96-well ELISA plates were coated with 0.5 μg/ml soluble tachyzoite antigens of PLK parasites diluted in coating buffer (0.05 M Carbonate-Bicarbonate, pH 9.6) and incubated at 4°C overnight. The ELISA plates were washed by PBS-T (0.05% Tween-20) three times, and then blocked with 3% BSA, then washed once. Collected sera were diluted by 1:50 and incubated for 1 h at 37°C. The plates were washed with PBS-T six times, the HRP conjugated goat anti-mouse IgG, IgG1 and IgG2a secondary antibodies were added and incubated for another 1 h at 37°C. After washing six times, ABTS (2, 2′-Azinobis [3-ethylbenzothiazoline-6-sulfonic acid]-diammonium salt) substrate was used to develop the reaction and measure the results at OD 415 nm. All samples were analyzed three times. Meanwhile, cytokine productions IL-12, IL-10, and IFN-γ were determined using ELISA kits according to the manufacturer's recommendations, as above.

Cytokine Productions of Splenocytes by *T. gondii* Antigens Stimulation After Vaccination

Vaccinated mouse spleens were isolated to test stimulating cytokine productions of splenocytes at 70 days post-vaccination (dpv), and unvaccinated mouse spleens were also collected to use as controls. In brief, the splenocytes were washed three times with RPMI 1640 (Sigma, United States), and hemolyzed in a lysing buffer (0.83% NH_4Cl and 0.01 M Tris-HCl, pH 7.2) for 5 min, then washed with RPMI 1640. The viability of the splenocytes was determined by trypan blue staining. A total of 3×10^5 viable splenocytes each well of 96-well cell culture plates were plated and cultured in RPMI 1640 supplemented with 20% FBS maintained 24 h. The final concentration of 50 μg/ml of *T. gondii* soluble antigens (TSA) of PLK parasites were used to stimulate cytokine productions for 3 days. Then supernatants from each well were harvested for cytokine level measurements, as above. For negative and positive controls, the same number of splenocytes was also plated into 96-well cell culture plates at the same time and stimulated with RPMI 1640 with 20% FBS only or 5 μg/ml concanavalin A (Sigma, United States) for 3 days, respectively. Each spleen-harvested splenocytes were plated in at least three wells for TSA, negative and positive control, and each supernatant sample was tested three times.

Protective Immunity Against *T. gondii* Challenges

BALB/c mice were vaccinated with 10^3 tachyzoites of *PLK*:Δ*gra9* through i.p. At 70 dpv, mice were challenged with 10^3 type I

RH or 10^5 type II PLK tachyzoites by i.p., or 50 PLK cysts by oral administration (six mice for each group). Unvaccinated mice with same ages and numbers were used as control and infected with the same doses and routes. All challenged mice were monitored for another 30 days for tachyzoite-challenge or 35 days for cyst-challenge infections to record daily body weights, clinical signs, and survival rates in detail. Meanwhile, at 7 days tachyzoite post-challenges or 14 days cyst post-challenges, peritoneal fluid and serum samples of all experimental mice were collected to test cytokine productions. Parasite burdens were examined in peritoneal fluids during acute challenges at day 7 post-challenges. Furthermore, for chronic infection, the number of cysts in survival mouse brains was detected as above at 35 days cyst post-challenges.

Passive Immunization Test of Δ*gra9*-Vaccinated Sera

BALB/c mice were infected with 10^5 type II PLK tachyzoites through i.p. At the day 0 and 3 post-infection, the 100 μl sera from naïve mice or the day 70 after *PLK*:Δ*gra9*-vaccinated per mouse were administered into WT parasite infected mice by intraperitonea injection, which includes four mice for naïve sera as negative control, and five mice for *PLK*:Δ*gra9*-vaccinated sera as test group. Survival rates were recorded. Parasite burdens were examined in peritoneal fluids at day 5 or 7 post-infection by qPCR as follows to evaluate parasite growth under passive immunization.

DNA Isolation and Quantitative PCR (qPCR) Detection of Parasite Burdens in Infected Mice

DNA was extracted from the tissues or peritoneal fluid of parasite-challenged mice by DNeasy Blood & Tissue Kit (Qiagen, Germany), according to the manufacturer's instructions. The 50 ng DNA was then amplified with primers specific to the *T. gondii* B1 gene (forward primer 5′-AAC GGG CGA GTA GCA CCT GAG GAG-3′ and reverse primer 5′-TGG GTC TAC GTC GAT GGC ATG ACA AC-3′) by qPCR, as previously described (Li et al., 2020). A standard curve was constructed using 10-fold serial dilutions of *T. gondii* DNA extracted from 10^5 parasites; thus, the curve ranged from 0.01 to 10,000 parasites. The parasite number was calculated from the standard curve.

Statistical Analysis

To graph and analyze the data, GraphPad Prism 7 software (GraphPad Software Inc., United States) was used. In this study, statistical analyses were performed using unpaired Student's *t*-test, Tukey's Multiple Comparison Test, and one-way ANOVA plus Tukey-Kramer *post hoc* analysis. Data represent the mean ± Standard Error of Mean. Survival curves were generated using the Kaplan–Meier method and statistical comparisons were made by the log-rank method. A P value < 0.05 was considered statistically significant.

RESULTS

Δ*gra9* Generation in Type II PLK Strain Markedly Reduces Cyst Formation *in vitro* and *in vivo*

Our previous study revealed that (Guo et al., 2019). To see whether a single mutant of Δ*gra9* affects bradyzoite differentiation from tachyzoite, WT or Δ*gra9* (with GFP) tachyzoites were cultured under bradyzoite-inducing conditions to count the conversion rates. Both strains formed cysts, as cysts were stained by DBA-FITC (green) (**Figure 1A**). However, compared with the cyst differentiation rate of WT parasites, Δ*gra9* reduced by 74.19, 94.04, 63.07, and 41.52% at 24, 48, 72, and 96 h post-induction, respectively (**Figure 1B**). *In vivo*, with the dose of 10^3 tachyzoites infections, no mortalities were recorded until day 35 in mice infected with parasites either strains (data not shown), while as shown in **Figure 1C**, the cyst number in the brain of mice with Δ*gra9* infection significantly reduced by 73.68% compared with that of the PLK. Collectively, the loss of gra9 in type II PLK strain, did not abolish, but markedly reduced cyst formation *in vitro* and *in vivo*.

Δ*gra9* Generation in Type II PLK Strain Severely Attenuates Virulence in Mice

To evaluate the virulence of Δ*gra9*, a lethal dose of 10^5 parasites was infected into mice by i.p., with body weight and clinical signs monitored for 30 days. The parental PLK strain caused 100% mortality (**Figure 2A**) with severe body weight losses (**Figure 2B**) and clinical symptoms (**Figure 2C**), whereas infection with the mutant strain surprisingly proved to be unfatal to mice (**Figure 2A**), indicating that Δ*gra9* generation in type II PLK strain severely attenuated virulence in mice.

Δ*gra9* Infection Shows Different Cytokine Productions and Relatively High *T. gondii*-Specific IgG Levels Compared With Wild-Type Infection in Mice

Lethal type II strain infections are associated with extremely elevated pro-inflammatory cytokine levels in the serum, including IFN-γ and IL-12 (Mordue et al., 2001). In order to elucidate the differences in immune response caused by infection with Δ*gra9* or WT strains, mice were infected with a non-lethal dose of 10^3 parasites. Sera were collected at 7 or 30 dpi to measure the changes in immune response. Levels of pro-inflammatory cytokines IFN-γ and IL-12, as well as anti-inflammatory cytokine IL-10, were significantly elevated at 7 and 30 dpi in both Δ*gra9* and WT infections compared with control (**Supplementary Figures S1A–C**). However, Δ*gra9*-infected mice showed 39.17–54.05% lower serum cytokine levels compare with WT infections at 7 dpi, although not statistically significant (**Supplementary Figures S1A–C**). This suggests that loss of gra9 in PLK parasites led to milder cytokine productions resulting in complete mouse survival. Conversely, similarly high *T. gondii*-specific IgG levels were induced at 30 dpi after either PLK or mutant parasite

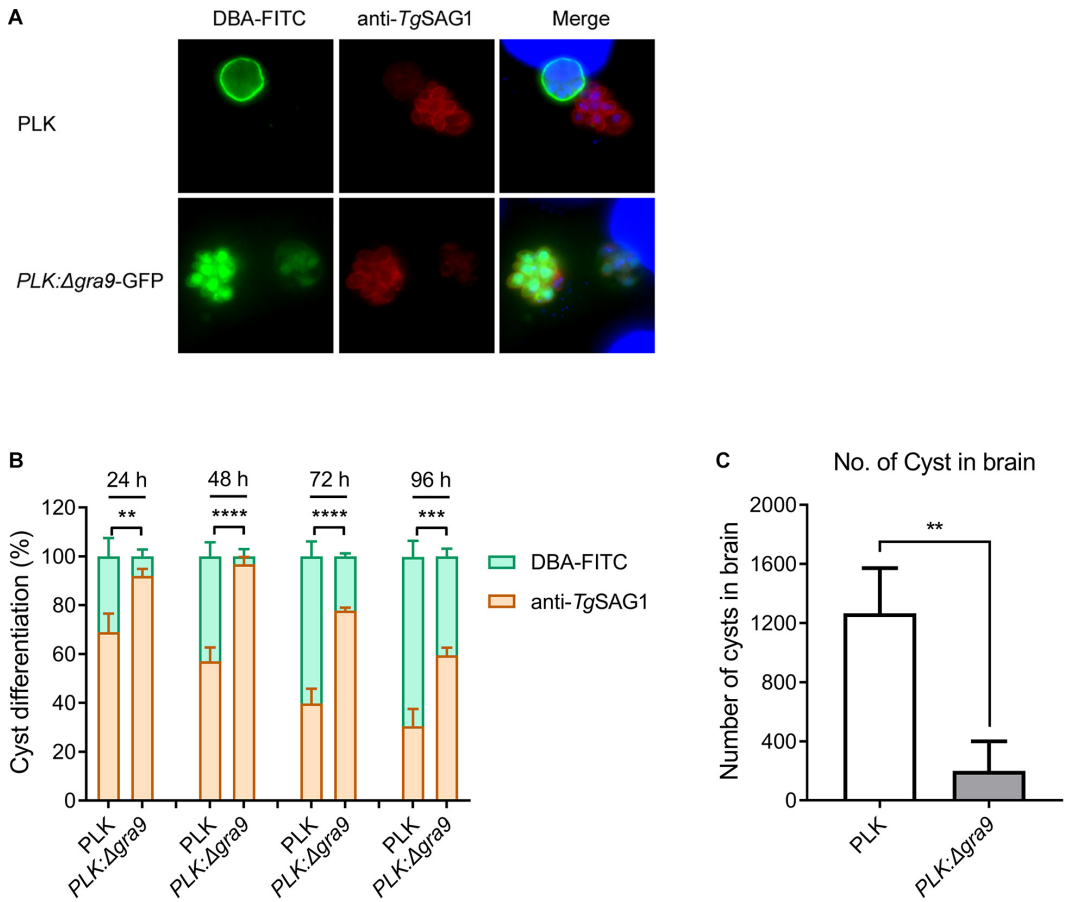

FIGURE 1 | Disruption of gra9 in type II PLK strain reduces cyst formation *in vitro* and *in vivo*. **(A)** The bradyzoite differentiation from wild-type or Δ*gra9* with GFP tachyzoites under bradyzoite-inducing conditions *in vitro*. DBA-FITC (green) was used for cyst wall staining and anti-SAG1 (red) antibody was used for tachyzoite marker. Both strains formed cysts, as cysts were stained by DBA-FITC. The blue fluorescence showed the nuclear DNA staining by DAPI. **(B)** Conversion rates *in vitro*. Bradyzoite differentiation rates were counted in at least 100 vacuoles at 24, 48, 72, and 96 post-induced hours. The data are presented as the mean ± SEM of at least three independent experiments (***P* < 0.01; ****P* < 0.001; *****P* < 0.0001; one-way ANOVA plus Dunnett's multiple comparisons test). **(C)** The cyst number in the mouse brains of Δ*gra9* infection. The dose of 10^3 WT or Δ*gra9* tachyzoites were injected each mouse and were monitored for 35 days, and then the number of cysts in survival mouse brains were determined (*n* = 4; ***P* < 0.01; Student's *t*-test).

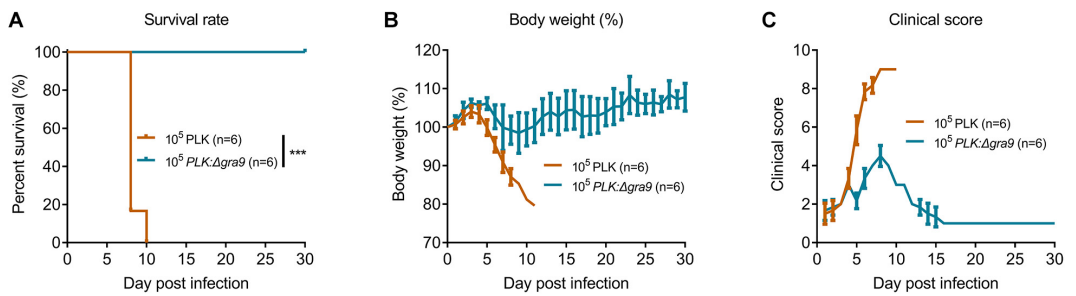

FIGURE 2 | Δ*gra9* generation in PLK strain severely attenuates the virulence in mice. A lethal dose of 10^5 parasites of wild-type or Δ*gra9* were infected into female BALB/c mice by intraperitoneal injection (*n* = 6), and mice were monitored for 30 days to note daily observations of body weight and clinical signs. **(A)** Survival rates (****P* < 0.001; Log-rank (Mantel-Cox) test). **(B)** Body weight%. **(C)** Clinical scores. The scores varied from 0 (no signs) to 10 (all signs).

infection (**Supplementary Figure S1D**). At the cellular level, cytokine productions by splenocytes after *T. gondii* antigen stimulation was determined at 35 dpi, found that high levels of cytokine IFN-γ and IL-10 in Δ*gra9*-infected splenocytes were induced quickly, which were slightly higher than the WT (**Supplementary Figures S1E,F**). Together, these results suggest

that Δ*gra9* infection induces balanced cytokine productions and relatively high *T. gondii*-specific IgG levels compared with WT infection in mice, which relates to the severely attenuated virulence of Δ*gra9* strain.

Δ*gra9* Vaccination Induces Full *T. gondii*-Specific Immune Response

The above findings reveal the fact that Δ*gra9* strain attenuated acute virulence and affected the formation of cysts. To evaluate the potential as a good vaccine of this mutant strain and test the immunogenicity derived from Δ*gra9* vaccination, we designed an immunization scheme within 105 days using mouse models (**Figure 3A**). At the outset, the chosen immune dose was 10^3 Δ*gra9* tachyzoites each mouse by i.p. Results of our preliminary experiments showed that the lowly clinical score was observed in 10^3 Δ*gra9*-infected mice, whereas 10^4 and 10^5 Δ*gra9*-infected or 10^3, 10^4, and 10^5 PLK-infected mice showed severe clinical signs (**Supplementary Figure S2**). At 30 dpi, induced *T. gondii*-specific IgG in sera of 10^3, 10^4, and 10^5 Δ*gra9*- or 10^3 and 10^4 PLK-infected mice were of similarly high levels (**Supplementary Figure S3**). These represent similar immunogenicity and suggest that Δ*gra9* vaccination of 10^3 tachyzoites was a safe and effective immune dose. After vaccination of 10^3 Δ*gra9* tachyzoites, the immunogenicity of Δ*gra9* was tested through detection of specific anti-*T. gondii* IgG and IgG subclasses (IgG1 and IgG2a) levels in vaccinated mouse sera at 30 and 70 dpv. Unvaccinated (naïve) mice were used as control. The ELISA results showed that Δ*gra9* vaccination induced a significantly higher *T. gondii*-specific IgG level at 30 dpv, and maintained a similarly high level at 70 dpv (**Figure 3B**). Nest study was to test the levels of IgG subclasses, the results showed that compared to unvaccinated mice, the level of IgG2a in vaccinated mice was significantly higher at 30 and 70 dpv (**Figure 3B**). To test IgG1 level in mice, although the level was lower at 30 dpv compared with 70 dpv, it was also increased to significantly higher in the vaccinated mice both 30 and 70 dpv than unvaccinated mice (**Figure 3B**). These suggest that Δ*gra9* vaccination elicits a mixed Th1/Th2 immune response both 30 and 70 dpv. Opposite to the stable IgG levels, cytokine levels changed over time. Relatively higher levels of pro-inflammatory IFN-γ and IL-12, or anti-inflammatory IL-10 were recorded from vaccinated mice compared with unvaccinated mice at 30 dpv, while levels decreased at 70 dpv (**Figures 3C–E**). Collectively, these results reveal that Δ*gra9* vaccination provided a benign humoral and cellular immune response in mice and proved to induce effective immunogenicity.

To assess the immunological memory in Δ*gra9* vaccinated mice, splenocytes were harvested from vaccinated or unvaccinated mice at 70 dpv, and stimulated with total *Toxoplasma* soluble antigen (TSA) prepared from fresh wild-type (PLK) tachyzoites. As shown in **Figures 4A,B**, the significantly high levels of pro-inflammatory cytokine IFN-γ, as well as anti-inflammatory cytokine IL-10, were stimulated by TSA compared with no stimulation or no vaccination. Interestingly, although the significantly decreased levels of stimulated IFN-γ (16,787.5 pg/ml) and IL-10 (5,347.5 pg/ml) at 70 dpv were observed compared with their levels of IFN-γ (207,667.7 pg/ml) and IL-10 (10,210.4 pg/ml) at 30 dpv in the Δ*gra9* vaccinated splenocytes (**Supplementary Figures S1E,F**), there were obviously high levels at both time points. These suggest that Δ*gra9* vaccination could activate the ability of the immune cells to quickly and specifically recognize the *Toxoplasma* antigen to produce corresponding immune cytokines in short-term and long-term immunization.

Δ*gra9* Vaccination Confers Potent for Protection Against Acute and Chronic *T. gondii* Challenges

Based on the findings that Δ*gra9* has strong immunogenicity and immunological memory, we then preformed the second challenges with 10^3 type I (RH) or 10^5 type II (PLK) tachyzoites by i.p. or 50 cysts (PLK) by oral administration to vaccinated mice at 70 dpv. All challenged mice were monitored for another 30 days for tachyzoite or 35 days for cyst infections, and recorded daily body weights, clinical signs, and survival rates. For both RH (**Figure 5A**) and PLK (**Figure 5B**) tachyzoite challenges, Δ*gra9* vaccination elicited strong protection following 100% survival rates of mice and no obvious signs or body weight changes were observed during the 30-day challenge period (**Supplementary Figure S4**). However, for unvaccinated mice challenged with the lethal dose of RH or PLK tachyzoites, the clinical signs and body weight changes were initially observed at day 4 of RH or day 2 of PLK infections until the signs developed to most severe at 6-8 days (**Supplementary Figure S4**), resulting in 100% mortality rates for unvaccinated mice within 8 days post-challenges (**Figures 5A,B**). As expected, all Δ*gra9*-vaccinated mice survived when infected with 50 cysts (PLK strain), whereas only 50% of unvaccinated mice survived (**Figure 5C**). While the 50 cysts-challenges to vaccinated or unvaccinated mice led to decreased body weights (%) in both groups during the whole period of 35 days, clinical signs were observed only in unvaccinated mice starting from day 8 post-challenge infection (**Supplementary Figure S4**). Altogether, Δ*gra9* vaccination confers strong protective immunity against acute and chronic toxoplasmosis.

Δ*gra9* Vaccination Rapidly Clears Challenging Parasites and Blocks Cyst Formation in New Challenges

To further understand how Δ*gra9* vaccination provided strong protection in mice suffering both acute and chronic *T. gondii* challenges, peritoneal fluids and sera in challenged mice were collected at 7 days tachyzoite post-challenges or 14 days cyst post-challenges (time-points when we observed the most serious signs in unvaccinated mice) to determine cytokine productions, as well as parasite burdens in peritoneal fluids. In naïve mice, RH infections resulted in rapid proliferation with 87,305 parasites in 50 ng DNA, whereas PLK infections caused higher parasite burdens of 2.74×10^7 at 7 days post-challenge infection (**Figure 6A**). However, we could not detect any parasites using a qPCR test in both RH- and PLK- challenged Δ*gra9*-vaccinated mice, suggesting that Δ*gra9* vaccination promoted the activity to rapidly clear infecting parasites. Meanwhile, for chronic

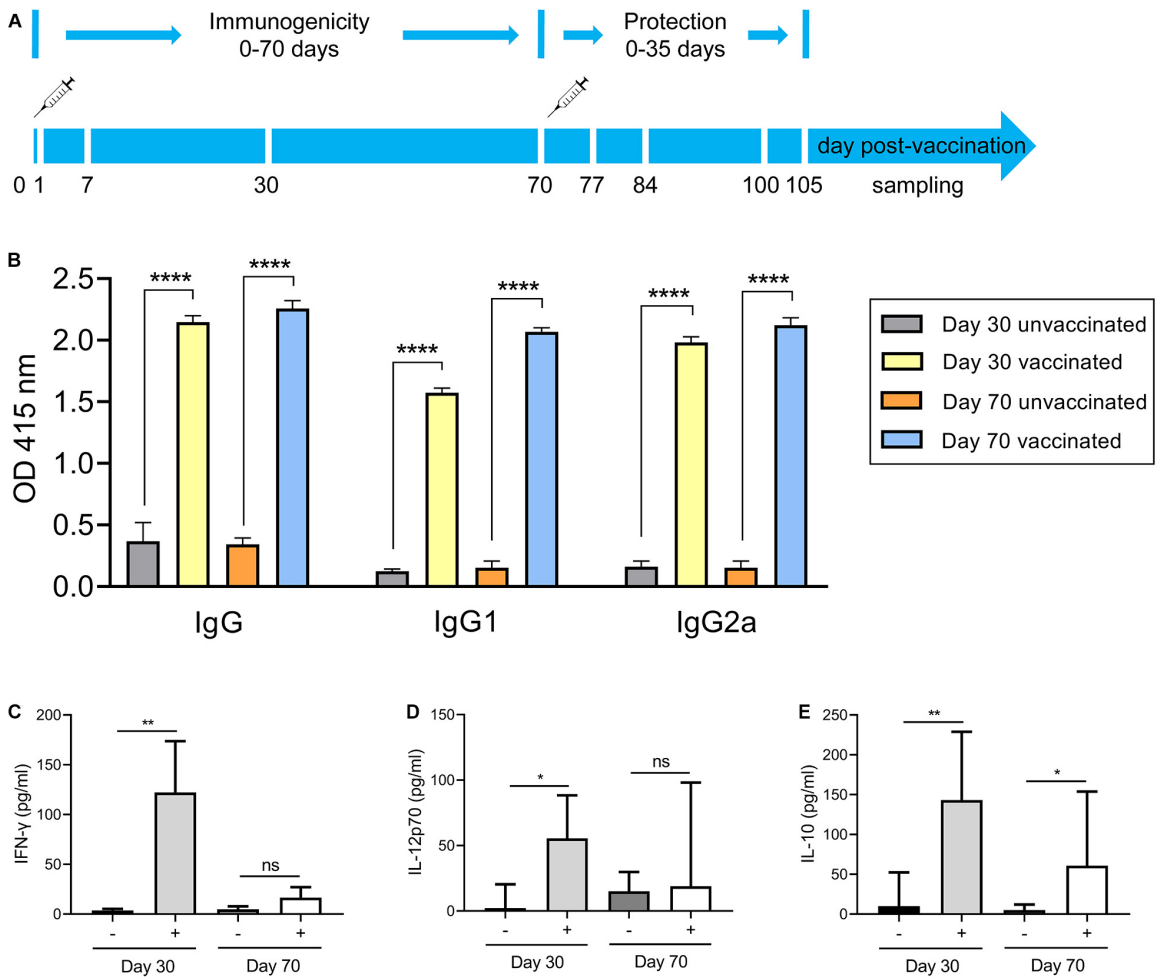

FIGURE 3 | Immunization scheme and study design. **(A)** Immunization scheme. The immune dose of 10^3 Δ*gra9* tachyzoites each mouse was injected into female BALB/c mice (n = 6 each group) by intraperitoneal injection and that day was designated as 0 day post-vaccination. The immunogenicity of Δ*gra9* vaccination was tested via the detection of specific anti-*T. gondii* IgG levels and cytokine productions in sera at 30 and 70 dpv. At 70 dpv, vaccinated or unvaccinated mice were secondly challenged by acute or chronic *T. gondii* infection to assess the protection. Within the vaccination and challenge period of total 105 days, the daily body weights, clinical signs, and survival rates of all mice were recorded in detail, and peritoneal fluid or serum samples were collected to evaluate immune response at the limited sampling periods as shown in **(A)**. **(B)** The specific anti-*T. gondii* IgG and IgG subclasses (IgG1 and IgG2a) levels in vaccinated mice at 30 or 70 dpv. Unvaccinated naïve mice with the same ages were used as control (****$P < 0.0001$; Student's t-test). **(C–E)** Cytokine productions in sera at 30 and 70 dpv. The levels of IFN-γ **(C)**, IL-12p70 **(D)**, or IL-10 **(E)** were determined by ELISA kits. –, unvaccinated mice; +, vaccinated mice (*$P < 0.05$; **$P < 0.01$; ns, not significant; Student's t-test).

toxoplasmosis, parasites were not detected in any mice peritoneal fluid at 14 dpi (data not shown), but markedly reduced number of cysts in vaccinated survival mouse brain was noted by day 35 compared with unvaccinated mice (**Figure 6B**), which are similar to that level of cyst formation of vaccinated but no cyst challenged mice (**Figure 1C**). This suggests that Δ*gra9* vaccination blocks cyst formation in new challenged cysts.

Subsequently, the immune responses were also tested during the limited time-points, levels of cytokines (IFN-γ, IL-12, and IL-10) in both peritoneal fluid and serum were substantially induced in unvaccinated mice relative to the extremely low levels in Δ*gra9*-vaccinated mice, especially the IFN-γ levels (**Figure 7A**). More importantly, all mice remained with high levels of *T. gondii*-specific IgG (**Figure 7B**). Taken together, Δ*gra9* vaccination provided efficient and safe immune protection to kill challenging parasites, resulting in host survival.

A Special Protection Against *T. gondii* Infection Is Provided by the Sera of Δ*gra9*-Vaccinated Mice

Δ*gra9* vaccination induced a significantly high *T. gondii*-specific IgG level with low cytokine levels at 70 dpv in mouse sera as shown above. In this study, the sera from *PLK*:Δ*gra9*-vaccinated mice were administered into parasites infected mice with lethal dose, survival rates were recorded and parasite burdens were determined in peritoneal fluids at day 5 and 7 post-infection to evaluate parasite growth under passive immunization. The

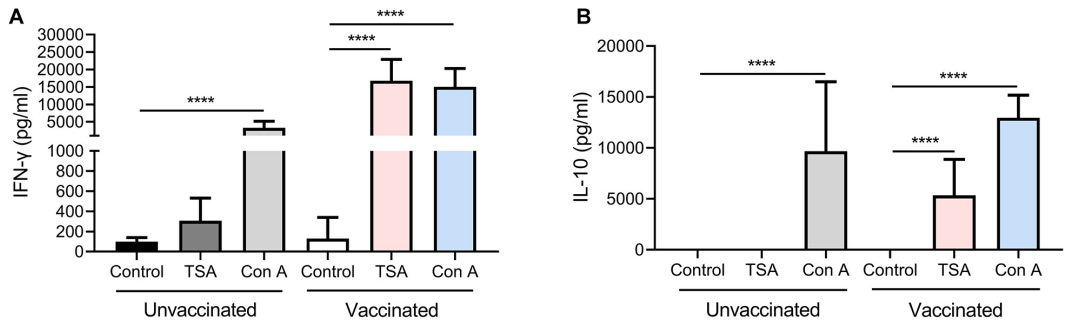

FIGURE 4 | Δ*gra9* vaccination activates the ability of the splenocytes to rapidly and specifically recognize the *Toxoplasma* antigen to induce high-level cytokines, compared with unvaccinated. Immunological memory of mice in Δ*gra9* vaccination was evaluated at 70 dpv via stimulated splenocytes by total *Toxoplasma* soluble antigen resulting in the production of cytokines IFN-γ **(A)** or IL-10 **(B)**. RPMI 1640 with 20% FBS only or 5 μg/ml concanavalin A were used as negative or positive controls, respectively. The data are presented as the mean ± SEM of at least three repeats each sample (****$P < 0.0001$; Student's *t*-test).

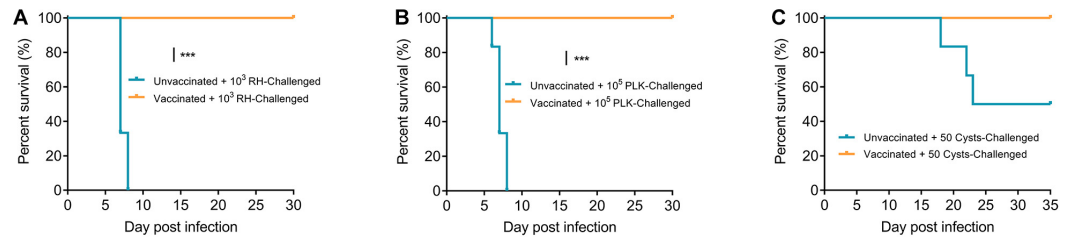

FIGURE 5 | Δ*gra9* vaccination protects mice against *T. gondii* infections. Vaccinated or unvaccinated mice were challenged with 10^3 type I RH **(A)** or 10^5 type II PLK **(B)** tachyzoites by intraperitoneal injection or 50 PLK cysts **(C)** by oral administration at 70 dpv, and monitored for another 30 days for tachyzoite or 35 days for cyst infections to note survival rates (***$P < 0.001$; Log-rank (Mantel-Cox) test).

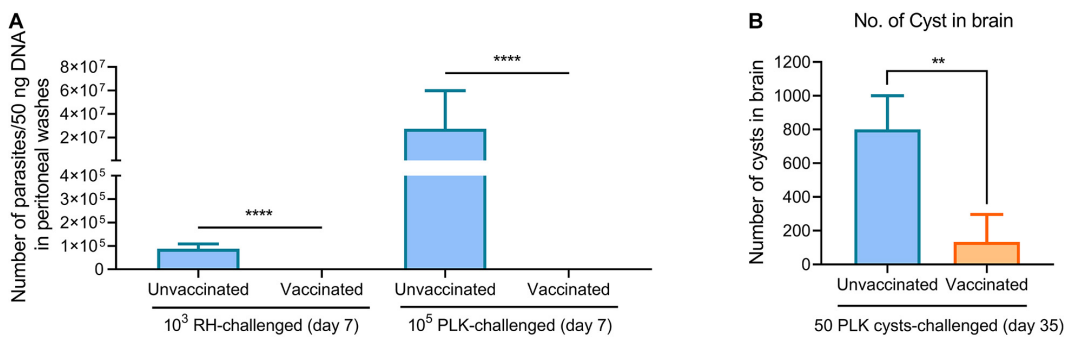

FIGURE 6 | Δ*gra9* vaccination rapidly clears challenging parasites and blocks cyst formation in new challenges. **(A)** Parasite burdens in peritoneal fluids of RH or PLK tachyzoites-challenged vaccinated mice. A quantitative PCR of the *Tg*B1 gene using 50 ng extracted DNA from peritoneal fluids was used to confirm parasite proliferation in vaccinated mice at 7 days post-challenge infection, compared with unvaccinated challenged mice (****$P < 0.0001$; Student's *t*-test). **(B)** No. of cyst in brain in PLK cysts-challenged vaccinated mice. At day 35 post-challenges, the brains were isolated from survival mice of 50 cysts challenges to estimate cyst numbers by DBA-FITC staining (**$P < 0.01$; Student's *t*-test).

results showed that vaccinated sera gave 40% survival rates ($n = 5$, **Figure 8A**) and led to significantly lower parasite burdens in peritoneal fluids of WT parasites-infected mice both 5 and 7 dpi, compared with naïve sera (**Figure 8B**). As shown in **Figure 8B**, the numbers of parasite in control mice at 5 or 7 day post-infection were resulted in 5 or 4 times of mice injected with vaccinated sera, respectively. These suggest that the sera of Δ*gra9*-vaccinated mice with high IgG and low cytokine levels are able to reduce parasite propagation in mice.

DISCUSSION

In recent years, active immunization is considered to be the ideal and long-term strategy to induce the host immune response against acute and chronic *T. gondii* infections (Loh et al., 2019). One means is to develop live attenuated vaccines, a whole parasite-based vaccine, which is the live strain with reduced replication and attenuated virulence but retaining the ability to induce an immune response against a variety of wild-type strain

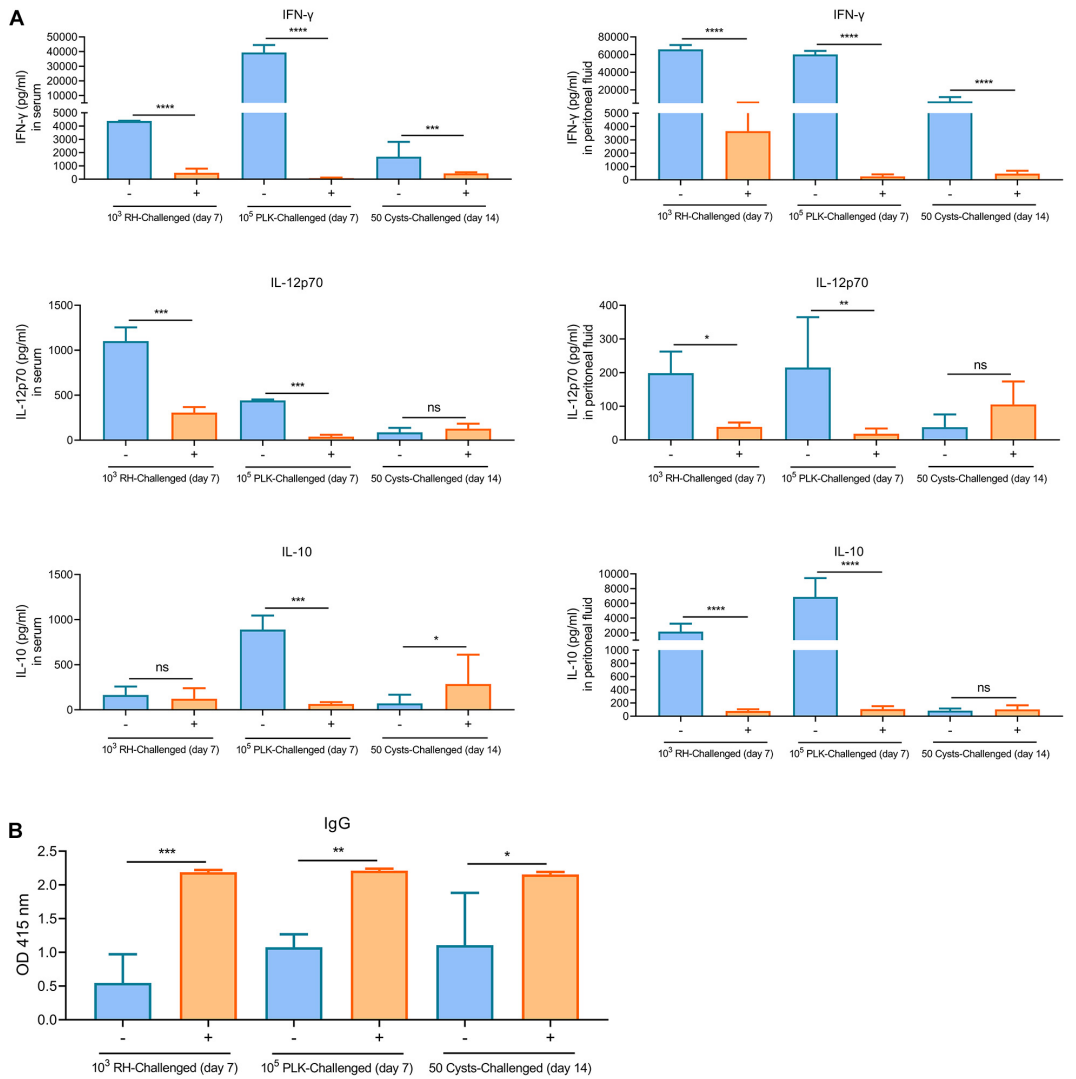

FIGURE 7 | Δ*gra9* vaccination provides safe and effective immune protection. The peritoneal fluids and sera in challenged mice were collected at 7 days tachyzoite post-challenges or 14 days cyst post-challenges to determine cytokine productions and *T. gondii* specific IgG, compared with unvaccinated but secondly challenged mouse samples. **(A)** IFN-γ, IL-12p70, or IL-10 levels in serum or peritoneal fluid samples. –, unvaccinated; +, vaccinated (*$P < 0.05$; **$P < 0.01$; ***$P < 0.001$; ****$P < 0.0001$; ns, not significant; Student's *t*-test). **(B)** The levels of *T. gondii* specific IgG. IgG levels in vaccinated challenged or unvaccinated challenged mice at 7 days tachyzoite post-challenges or 14 days cyst post-challenges were determined by an ELISA test. –, unvaccinated, +, vaccinated (*$P < 0.05$; **$P < 0.01$; ***$P < 0.001$; Student's *t*-test).

and multiple stages of parasite infections (Wang et al., 2017, 2018; Xia et al., 2018b; Yang et al., 2019; Liang et al., 2020). In this study, *PLK*:Δ*gra9* vaccination induced a high level of immune response and resisted the infections of tachyzoites from type I or type II strains and cysts from type II strain.

Our previous study reported that the generation of mutant Δ*gra9* strain in PLK parasites not only significantly reduced the growth of tachyzoites *in vitro* but also changed replication in mice resulting in severely attenuated virulence (Guo et al., 2019), which consistent with the current result of 100% survival rate in mice during challenge infection with 10^5 Δ*gra9* parasites which have been passed for more than 250 generations in culture cells. This suggests that the attenuated *Toxoplasma* strain did not revert back to virulent form in animals at least 250 cell passages under confirmed loss of gra9 gene. Importantly, GRAs have been investigated with playing the major structural roles within the PV and the cyst wall of *T. gondii* (Guevara et al., 2019). Current results demonstrate that loss of gra9 in type II strain (PLK), reduced the formation of cysts *in vitro* and *in vivo*, which corroborates gra9 protein as one of the intravacuolar-network-associated dense GRAs involved during cyst development (Fox et al., 2019; Guevara et al., 2019). To test the virulence of cysts, we isolated and injected 50 cysts of Δ*gra9* were into three mice which resulted in no mice deaths (data not shown), suggesting the possibility that the loss of gra9 in type II PLK strain might reduce the virulence of cysts, although there was limited little

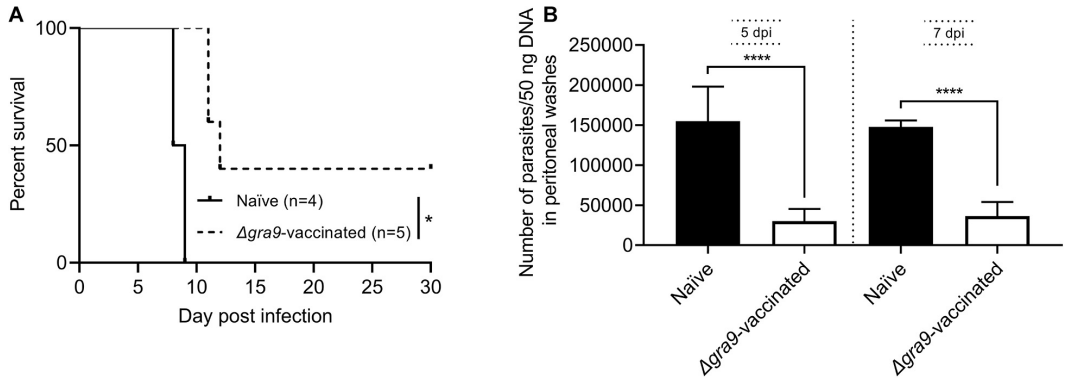

FIGURE 8 | The sera from Δ*gra9*-vaccinated mice are able to reduce parasite propagation in mice. The sera from *PLK*:Δ*gra9*-vaccinated mice were administered into 10^5 PLK parasites infected mice at 0 and 3 day post-infection, survival rates were noted and parasite burdens were determined in peritoneal fluids at day 5 and 7 post-infection to evaluate parasite growth under passive immunization. The four mice for naïve sera as negative control, and five mice for *PLK*:Δ*gra9*-vaccinated sera as test group. **(A)** Survival rates (*$P < 0.05$; Log-rank (Mantel-Cox) test). **(B)** Parasite burdens (****$P < 0.0001$; Student's *t*-test).

number of mouse model. Δ*gra9* strain's inability to form cysts or significantly reduce cyst formation and the lack of virulence from the type II parasites are good indicators that the produced strain could be utilized as a candidate vaccine. On the other hand, compared with the severe immune response after wild-type parasite infection, Δ*gra9*-infected mice produced moderate immune response which represents a balance between inducing pro-inflammatory and anti-inflammatory cytokines, denoting its safety as a live attenuated vaccine. Furthermore, it is worthy of attention that the chosen immune dose was 10^3 Δ*gra9* tachyzoites each mouse, since mice with 10^3 Δ*gra9* infection observed the high specific anti-*T. gondii* IgG levels and no significantly clinical symptoms compared with naïve mice, suggesting that the vaccination with 10^3 Δ*gra9* tachyzoites was effective and safe immune dose.

In the two phases of the entire experiment, the generation of immunogenicity and the second challenge of protection, we recorded in detail the changes in the levels of cytokines and antibodies in mice. Compared with unimmunized mice, the vaccinated mice showed significantly higher levels of the pro-inflammatory cytokines IFN-γ and IL-12 and the anti-inflammatory cytokine IL-10 at 30 dpv and dropped to low levels at 70 dpv. In the subsequent challenge infection, cytokine levels of vaccinated mice at 7 days post-challenge infection surprisingly remained at similar levels as before being challenged, suggesting the second challenges did not cause severe immune responses in vaccinated mice. Importantly, the specific anti-*T. gondii* IgG was maintained at a similarly high level throughout the process. While to test the levels of IgG subclasses, the results confirmed that both IgG1 and IgG2a in vaccinated mice was significantly higher levels at challenged time-point compared with unvaccinated mice. These suggest that Δ*gra9* vaccination elicits a mixed Th1/Th2 immune response at this time-point. On the other hand, the passive immunization test was observed that the sera from vaccinated mice could reduce parasite propagation. Hence, we consider that the Δ*gra9* vaccination-induced full protective immunity was a cellular immunity-based immune response combined with humoral immunity. At 70 dpv, Δ*gra9* vaccination induced a Th1-biased inflammatory response to produce IFN-γ and IL-12 which are two pro-inflammatory cytokines crucial for activation of cell-mediated immunity against *T. gondii* infection (Pifer and Yarovinsky, 2011; Hunter and Sibley, 2012; Yarovinsky, 2014). Meanwhile, the anti-inflammatory cytokine IL-10 was also highly produced suggesting that the balanced level of cytokines was maintained in Δ*gra9*-vaccinated mice. This balance was also proved by the splenocytes stimulation test, which rapidly and specifically produced significantly high levels of pro-inflammatory cytokine IFN-γ and anti-inflammatory cytokine IL-10. When vaccinated mice are secondly challenged with wild-type parasites, the immune system rapidly recognizes and produces high levels of IFN-γ and other pro-inflammatory cytokines to activate cellular immune responses, and simultaneously, the high level of *T. gondii*-specific IgG antibodies hinders the parasite attachment and invasion to host cells and activates the classical complement pathway to clear secondary infections efficiently in cooperation (Sayles et al., 2000; Spellberg and Edwards, 2001; Pifer and Yarovinsky, 2011; Hunter and Sibley, 2012). These are consistent with our results that Δ*gra9* vaccination rapidly blocks challenging parasite tachyzoites and new cyst formation.

In the present mouse models, noteworthy is the lack of any obvious signs or body weight changes in vaccinated mice during challenge periods, signifying that infecting parasites are strongly inhibited from replication and killed quickly by the rapid immune response during tachyzoite challenges. This might also explain why the increased levels of cytokine productions were not observed at day 7 post-challenge. In contrast, we noted significantly high parasite burden and the high levels of pro-inflammatory or anti-inflammatory cytokines with severe clinical symptoms and significant weight loss resulting in 100% mortality in naïve mice challenge infected with a lethal dose of tachyzoites. On the other hand, the Δ*gra9*-vaccination-induced full immune response was not only observed against type I RH and type II PLK wild-type tachyzoite acute infections but also against type

II cyst challenge and reduction of cyst formation. Interestingly, IFN-γ was cytokine which had significantly different levels between vaccinated and unvaccinated mice at day 14 post-cyst-challenge, suggesting that IFN-γ is also central to the development of immunity against *T. gondii* cyst infection, consistent with Δ*gra9*-vaccination-induced immune response for protection of cyst challenge.

CONCLUSION

In conclusion, the present study demonstrated that loss of gra9 in type II PLK strain dramatically attenuated virulence and significantly reduced the formation of cysts in animals. Δ*gra9* vaccination effectively elicited immune responses which conferred absolute protection from subsequent lethal type I RH, type II PLK wild-type tachyzoites or type II PLK cysts challenge infections in mice, suggesting that the mutant Δ*gra9* of *T. gondii* type II PLK strain is a potential live-attenuated vaccine candidate against acute and chronic toxoplasmosis. However, the current study is limited to the mouse model; thus, the effectiveness and safety should likewise be extensively investigated in animals of veterinary and economic importance, including but not limited to definitive hosts cats, susceptible sheep and pigs and other meat-producing animals. Future studies should assess its effectiveness against other *Toxoplasma* strains, particularly infections with local endemic strains.

DATA AVAILABILITY STATEMENT

The raw data supporting the conclusions of this article will be made available by the authors, without undue reservation.

ETHICS STATEMENT

The animal study was reviewed and approved by the Committee on the Ethics of Animal Experiments at the Obihiro University of Agriculture and Veterinary Medicine, Japan (permission numbers: 190246).

AUTHOR CONTRIBUTIONS

JL and XX conceived and designed the experiments. JL, EG, HG, ML, YL, and SJ performed the experiments. JL, IZ, YG, and WZ analyzed the data and wrote the manuscript. PA, MR, MT, BB, AR, and TM critically revised the manuscript. All authors read and approved the final version of the manuscript.

FUNDING

This study was supported by a Grant-in-Aid for Scientific Research (19K22354) from the Ministry of Education, Culture, Sports and Technology, Japan.

ACKNOWLEDGMENTS

We would like to thank all the people who were involved in making this project a success.

SUPPLEMENTARY MATERIAL

The Supplementary Material for this article can be found online at: https://www.frontiersin.org/articles/10.3389/fmicb.2021.619335/full#supplementary-material

Supplementary Figure 1 | Δ*gra9* infection induces mild cytokine productions and relatively high *T. gondii*-specific IgG levels in mice compared with Wild-type PLK infection. A non-lethal dose of 10^3 parasites was chosen to infect BALB/c mice, and the sera were collected at day 7 or 30 post-infection to measure immune response. Naïve mouse sera were used as controls. The levels of pro-inflammatory cytokines IFN-γ **(A)** and IL-12p70 **(B)** or anti-inflammatory cytokine IL-10 **(C)** were assessed by an ELISA test ($n = 4$; $^*P < 0.05$; $^{**}P < 0.01$; $^{***}P < 0.001$; $^{****}P < 0.0001$, Control vs parental or Δ*gra9* at 7 dpi; $^{\#}P < 0.05$, control vs parental or Δ*gra9* at 30 dpi; one-way ANOVA plus Tukey-Kramer *post hoc* analysis). **(D)** The *T. gondii*-specific IgG levels were measured at day 7 or 30 post-infection compared with naïve mice ($^{****}P < 0.0001$; Student's *t*-test). **(E,F)** Cytokine productions by splenocytes after *T. gondii* antigen stimulation. At 35 dpi, the splenocytes were harvested from parental or Δ*gra9* infected mouse spleens, and 3×10^5 viable splenocytes were cultured *in vitro* and stimulated by *T. gondii* antigen to induce cytokine IFN-γ **(E)** or IL-10 **(F)** productions. For the negative and positive controls, the same number of splenocytes was cultured at same time and stimulated with RPMI 1640 with 20% FBS only or 5 μg/ml concanavalin A, respectively ($^{****}P < 0.0001$; Student's *t*-test).

Supplementary Figure 2 | Clinical symptoms of mice during parasite infection. The different dose of 10^3, 10^4, and 10^5 Δ *gra9*- or 10^3, 10^4, and 10^5 PLK-parasites were injected into mice, and clinical signs of infected mice were noted within 30 days post-infection. The clinical scores varied from 0 (no signs) to 10 (all signs). No-infected mice were used as control.

Supplementary Figure 3 | *T. gondii*-specific IgG in sera from *Toxoplasma* infected-mice. The different dose of 10^3, 10^4, and 10^5 Δ*gra9*- or 10^3 and 10^4 PLK-parasites were injected into mice, at 30 dpi, induced *T. gondii*-specific IgG in sera were detected by ELISA tests. No-infected sera and PBS only were used as control ($^{****}P < 0.0001$; Student's *t*-test).

Supplementary Figure 4 | Δ*gra9* vaccination protects mice against *T. gondii* infections. Vaccinated or unvaccinated mice were challenged with 10^3 type I RH or 10^5 type II tachyzoites by intraperitoneal injection or 50 PLK cysts by oral administration at 70 dpv, and monitored for another 30 days for tachyzoite or 35 days for cyst infections to note daily body weights **(A–C)** and clinical signs **(D–F)** in detail.

REFERENCES

Abdelbaset, A. E., Fox, B. A., Karram, M. H., Abd Ellah, M. R., Bzik, D. J., and Igarashi, M. (2017). Lactate dehydrogenase in *Toxoplasma gondii* controls virulence, bradyzoite differentiation, and chronic infection. *PLoS One* 12:e0173745. doi: 10.1371/journal.pone.0173745

Alday, P. H., and Doggett, J. S. (2017). Drugs in development for toxoplasmosis: advances, challenges, and current status. *Drug Des. Devel. Ther.* 11, 273–293.

Dunay, I. R., Gajurel, K., Dhakal, R., Liesenfeld, O., and Montoya, J. G. (2018). Treatment of toxoplasmosis: historical perspective, animal models, and current clinical practice. *Clin. Microbiol. Rev.* 31:e0057-17. doi: 10.1128/CMR.00057-17

El Bissati, K., Zhou, Y., Dasgupta, D., Cobb, D., Dubey, J. P., Burkhard, P., et al. (2014). Effectiveness of a novel immunogenic nanoparticle platform for

Toxoplasma peptide vaccine in HLA transgenic mice. *Vaccine* 32, 3243–3248. doi: 10.1016/j.vaccine.2014.03.092

Fox, B. A., and Bzik, D. J. (2015). Nonreplicating, cyst-defective type II *Toxoplasma gondii* vaccine strains stimulate protective immunity against acute and chronic infection. *Infect. Immun.* 83, 2148–2155. doi: 10.1128/IAI.02756-14

Fox, B. A., Guevara, R. B., Rommereim, L. M., Falla, A., Bellini, V., Pétre, G., et al. (2019). *Toxoplasma gondii* parasitophorous vacuole membrane-associated dense granule proteins orchestrate chronic infection and GRA12 underpins resistance to host gamma interferon. *mBio* 10:e0589-19.

Guevara, R. B., Fox, B. A., Falla, A., and Bzik, D. J. (2019). *Toxoplasma gondii* intravacuolar-network-associated dense granule proteins regulate maturation of the cyst matrix and cyst wall. *mSphere* 4:e0487-19. doi: 10.1128/mSphere.00487-19

Guo, H., Gao, Y., Jia, H., Moumouni, P. F. A., Masatani, T., Liu, M., et al. (2019). Characterization of strain-specific phenotypes associated with knockout of dense granule protein 9 in *Toxoplasma gondii*. *Mol. Biochem. Parasitol.* 229, 53–61.

Howe, D. K., and Sibley, L. D. (1995). *Toxoplasma gondii* comprises three clonal lineages: correlation of parasite genotype with human disease. *J. Infect. Dis.* 172, 1561–1566. doi: 10.1093/infdis/172.6.1561

Hunter, C. A., and Sibley, L. D. (2012). Modulation of innate immunity by *Toxoplasma gondii* virulence effectors. *Nat. Rev. Microbiol.* 10, 766–778. doi: 10.1038/nrmicro2858

Huskinson-Mark, J., Araujo, F. G., and Remington, J. S. (1991). Evaluation of the effect of drugs on the cyst form of *Toxoplasma gondii*. *J. Infect. Dis.* 164, 170–171. doi: 10.1093/infdis/164.1.170

Innes, E. A. (2010). A brief history and overview of *Toxoplasma gondii*. *Zoonoses Public Health* 57, 1–7. doi: 10.1111/j.1863-2378.2009.01276.x

Kirkman, L. A., Weiss, L. M., and Kim, K. (2001). Cyclic nucleotide signaling in *Toxoplasma gondii* bradyzoite differentiation. *Infect. Immun.* 69, 148–153.

Lagal, V., Dinis, M., Cannella, D., Bargieri, D., Gonzalez, V., Andenmatten, N., et al. (2015). AMA1-deficient *Toxoplasma gondii* parasites transiently colonize mice and trigger an innate immune response that leads to long-lasting protective immunity. *Infect. Immun.* 83, 2475–2486. doi: 10.1128/IAI.02606-14

Le Roux, D., Djokic, V., Morisse, S., Chauvin, C., Doré, V., Lagrée, A. C., et al. (2020). Evaluation of immunogenicity and protection of the Mic1-3 knockout *Toxoplasma gondii* live attenuated strain in the feline host. *Vaccine* 38, 1457–1466.

Leesombun, A., Boonmasawai, S., Shimoda, N., and Nishikawa, Y. (2016). Effects of extracts from Thai Piperaceae plants against infection with *Toxoplasma gondii*. *PLoS One* 11:e0156116. doi: 10.1371/journal.pone.0156116

Li, J., Guo, H., Galon, E. M., Gao, Y., Lee, S. H., Liu, M., et al. (2020). Hydroxylamine and carboxymethoxylamine can inhibit *Toxoplasma gondii* growth through an aspartate aminotransferase-independent pathway. *Antimicrob. Agents Chemother.* 64:e01889-19.

Li, X. Z., Wang, X. H., Xia, L. J., Weng, Y. B., Hernandez, J. A., Tu, L. Q., et al. (2015). Protective efficacy of recombinant canine adenovirus type-2 expressing *Tg*ROP18 (CAV-2-ROP18) against acute and chronic *Toxoplasma gondii* infection in mice. *BMC Infect. Dis.* 15:114. doi: 10.1186/s12879-015-0815-1

Liang, Q. L., Sun, L. X., Elsheikha, H. M., Cao, X. Z., Nie, L. B., Li, T. T., et al. (2020). *RH*Δ*gra17*Δ*npt1* strain of *Toxoplasma gondii* elicits protective immunity against acute, chronic and congenital toxoplasmosis in mice. *Microorganisms* 8:E352.

Loh, F. K., Nathan, S., Chow, S. C., and Fang, C. M. (2019). Vaccination challenges and strategies against long-lived *Toxoplasma gondii*. *Vaccine* 37, 3989–4000. doi: 10.1016/j.vaccine.2019.05.083

Lu, G., Zhou, J., Zhou, A., Han, Y., Guo, J., Song, P., et al. (2017). SAG5B and SAG5C combined vaccine protects mice against *Toxoplasma gondii* infection. *Parasitol. Int.* 66, 596–602.

Montoya, J. G., and Liesenfeld, O. (2004). Toxoplasmosis. *Lancet* 363, 1965–1976. doi: 10.1016/S0140-6736(04)16412-X

Mordue, D. G., Monroy, F., La Regina, M., Dinarello, C. A., and Sibley, L. D. (2001). Acute toxoplasmosis leads to lethal overproduction of Th1 cytokines. *J. Immunol.* 167, 4574–4584.

Pifer, R., and Yarovinsky, F. (2011). Innate responses to *Toxoplasma gondii* in mice and humans. *Trends Parasitol.* 27, 388–393. doi: 10.1016/j.pt.2011.03.009

Robert-Gangneux, F., and Darde, M. L. (2012). Epidemiology of and diagnostic strategies for toxoplasmosis. *Clin. Microbiol. Rev.* 25, 264–296.

Saadatnia, G., and Golkar, M. (2012). A review on human toxoplasmosis. *Scand. J. Infect. Dis.* 44, 805–814. doi: 10.3109/00365548.2012.693197

Sayles, P. C., Gibson, G. W., and Johnson, L. L. (2000). B cells are essential for vaccination-induced resistance to virulent *Toxoplasma gondii*. *Infect. Immun.* 68, 1026–1033.

Shen, B., Brown, K., Long, S., and Sibley, L. D. (2017). Development of CRISPR/Cas9 for efficient genome editing in *Toxoplasma gondii*. *Methods Mol. Biol.* 1498, 79–103. doi: 10.1007/978-1-4939-6472-7_6

Spellberg, B., and Edwards, J. E. Jr. (2001). Type 1/type 2 immunity in infectious diseases. *Clin. Infect. Dis.* 32, 76–102. doi: 10.1086/317537

Tanaka, S., Kuroda, Y., Ihara, F., Nishimura, M., Hiasa, J., Kojima, N., et al. (2014). Vaccination with profilin encapsulated in oligomannose-coated liposomes induces significant protective immunity against *Toxoplasma gondii*. *Vaccine* 32, 1781–1785. doi: 10.1016/j.vaccine.2014.01.095

Tenter, A. M., Heckeroth, A. R., and Weiss, L. M. (2000). *Toxoplasma gondii*: from animals to humans. *Int. J. Parasitol.* 30, 1217–1258.

Wang, H. L., Pang, M., Yin, L. T., Zhang, J. H., Meng, X. L., Yu, B. F., et al. (2014a). Intranasal immunisation of the recombinant *Toxoplasma gondii* receptor for activated C kinase 1 partly protects mice against *T. gondii* infection. *Acta. Trop.* 137, 58–66.

Wang, H. L., Zhang, T. E., Yin, L. T., Pang, M., Guan, L., Liu, H. L., et al. (2014b). Partial protective effect of intranasal immunization with recombinant *Toxoplasma gondii* rhoptry protein 17 against toxoplasmosis in mice. *PLoS One* 9:e108377. doi: 10.1371/journal.pone.0108377

Wang, J. L., Elsheikha, H. M., Zhu, W. N., Chen, K., Li, T. T., Yue, D. M., et al. (2017). Immunization with *Toxoplasma gondii* GRA17 deletion mutant induces partial protection and survival in challenged mice. *Front. Immunol.* 8:730. doi: 10.3389/fimmu.2017.00730

Wang, J. L., Li, T. T., Elsheikha, H. M., Chen, K., Cong, W., Yang, W. B., et al. (2018). Live attenuated *Pru:*Δ*cdpk2* strain of *Toxoplasma gondii* protects against acute, chronic, and congenital toxoplasmosis. *J. Infect. Dis.* 218, 768–777.

Wang, J. L., Zhang, N. Z., Li, T. T., He, J. J., Elsheikha, H. M., and Zhu, X. Q. (2019). Advances in the development of anti-*Toxoplasma gondii* vaccines: Challenges, opportunities, and perspectives. *Trends Parasitol.* 35, 239–253.

Xia, N., Yang, J., Ye, S., Zhang, L., Zhou, Y., Zhao, J., et al. (2018a). Functional analysis of *Toxoplasma* lactate dehydrogenases suggests critical roles of lactate fermentation for parasite growth in vivo. *Cell Microbiol.* 20:10.

Xia, N., Zhou, T., Liang, X., Ye, S., Zhao, P., Yang, J., et al. (2018b). A lactate fermentation mutant of *Toxoplasma* stimulates protective immunity against acute and chronic toxoplasmosis. *Front. Immunol.* 9:1814. doi: 10.3389/fimmu.2018.01814

Yang, W. B., Wang, J. L., Gui, Q., Zou, Y., Chen, K., Liu, Q., et al. (2019). Immunization with a live-attenuated *RH:*Δ*NPT1* strain of *Toxoplasma gondii* induces strong protective immunity against toxoplasmosis in mice. *Front. Microbiol.* 10:1875. doi: 10.3389/fmicb.2019.01875

Yarovinsky, F. (2014). Innate immunity to *Toxoplasma gondii* infection. *Nat. Rev. Immunol.* 14, 109–121. doi: 10.1038/nri3598

Zhang, N. Z., Xu, Y., Wang, M., Petersen, E., Chen, J., Huang, S. Y., et al. (2015). Protective efficacy of two novel DNA vaccines expressing *Toxoplasma gondii* rhomboid 4 and rhomboid 5 proteins against acute and chronic toxoplasmosis in mice. *Expert. Rev. Vacc.* 14, 1289–1297. doi: 10.1586/14760584.2015.1061938

Conflict of Interest: The authors declare that the research was conducted in the absence of any commercial or financial relationships that could be construed as a potential conflict of interest.

frontiers in Cellular and Infection Microbiology

REVIEW
published: 07 April 2021
doi: 10.3389/fcimb.2021.660415

Transcription Factors Interplay Orchestrates the Immune-Metabolic Response of *Leishmania* Infected Macrophages

Haifa Bichiou[1,2], *Cyrine Bouabid*[1,2], *Imen Rabhi*[1,3] *and Lamia Guizani-Tabbane*[1*]

[1] Laboratory of Medical Parasitology, Biotechnology and Biomolecules (PMBB), Institut Pasteur de Tunis, Tunis, Tunisia, [2] Faculty of Sciences of Tunis, Université de Tunis El Manar, Tunis, Tunisia, [3] Biotechnology Department, Higher Institute of Biotechnology at Sidi-Thabet (ISBST), Biotechpole Sidi-Thabet- University of Manouba, Tunis, Tunisia

Leishmaniasis is a group of heterogenous diseases considered as an important public health problem in several countries. This neglected disease is caused by over 20 parasite species of the protozoa belonging to the *Leishmania* genus and is spread by the bite of a female phlebotomine sandfly. Depending on the parasite specie and the immune status of the patient, leishmaniasis can present a wide spectrum of clinical manifestations. As an obligate intracellular parasite, *Leishmania* colonize phagocytic cells, mainly the macrophages that orchestrate the host immune response and determine the fate of the infection. Once inside macrophages, *Leishmania* triggers different signaling pathways that regulate the immune and metabolic response of the host cells. Various transcription factors regulate such immune-metabolic responses and the associated leishmanicidal and inflammatory reaction against the invading parasite. In this review, we will highlight the most important transcription factors involved in these responses, their interactions and their impact on the establishment and the progression of the immune response along with their effect on the physiopathology of the disease.

Keywords: ***Leishmania*, macrophages, transcription factor, immune response, metabolic response**

OPEN ACCESS

Edited by:
Yongliang Zhang,
National University of Singapore, Singapore

Reviewed by:
Saikat Majumder,
University of Pittsburgh, United States
Lucas P. Carvalho,
Gonçalo Moniz Institute (IGM), Brazil

***Correspondence:**
Lamia Guizani-Tabbane
lamia.guizani@Pasteur.rns.tn

Specialty section:
This article was submitted to Parasite and Host, a section of the journal Frontiers in Cellular and Infection Microbiology

Received: *29 January 2021*
Accepted: *22 March 2021*
Published: *07 April 2021*

Citation:
Bichiou H, Bouabid C, Rabhi I and Guizani-Tabbane L (2021) Transcription Factors Interplay Orchestrates the Immune-Metabolic Response of Leishmania Infected Macrophages. Front. Cell. Infect. Microbiol. 11:660415. doi: 10.3389/fcimb.2021.660415

INTRODUCTION

Leishmania spp. are protozoan parasites that affects millions of people around the world. They are the causative agent of leishmaniasis, a group of heterogeneous diseases endemic in various countries. Depending on the parasite specie, and the immune status of the patient, leishmaniasis can present a spectrum of clinical manifestations. In the mammalian host, this parasite targets the immune cells that represent the first line of defense against infections and uses macrophage as a final host making *Leishmania*-macrophages interactions central to the outcome of the disease.

Different *Leishmania* species trigger distinct immune responses and macrophage polarization, upon their infection by the parasite, highly impact the infection outcome.

In the site of infection, recruited monocytes differentiate into macrophages that show extensive plasticity, depending on converging signals delivered by the numerous factors (microbial products, cytokines (IFNγ, TNFα) and growth factors, present in the local tissue environment. Macrophages

would then adopt a spectrum of distinct polarization states, among which the M1 inflammatory and the M2 anti-inflammatory cells are the extremes (Xue et al., 2014).

The « classically activated » or M1 macrophages polarization are important for the control of infections by intracellular pathogens. They are characterized by the production of proinflammatory cytokines such as TNFα, IL-1β, IL-6, IL-12, IL-18, IL-23, and Type 1 IFN, but also by the generation of reactive oxygen and nitrogen species that ensure efficient microbial killing. The « alternatively activated" M2 macrophages are elicited by type 2 cytokines (IL-4, IL-10, IL-13) and are inflammation-resolving macrophages with anti-parasitic and tissue repair functions (Murray, 2017).

These macrophage polarization phenotypes are also characterized by two distinct metabolic signatures. Indeed, in resting macrophages, glucose is metabolized to pyruvate which is transported into the mitochondria where it is oxidized into acetyl coenzyme A (acetyl-CoA) to fuel the tricarboxylic acid (TCA) cycle. The latter generates NADH, which provides electrons to the mitochondrial electron transport chain so that oxidative phosphorylation (OXPHOS) can progress and generate ATP. Upon infection, the metabolic profile switches from oxidative phosphorylation to aerobic glycolysis and the macrophages rely on glycolysis for the production of ATP (Kelly and O'Neill, 2015). Glycolysis provides the glucose-6-phosphate, an enhancer of the Pentose Phosphate Pathway (PPP) and a booster of NADPH production. This latter is then used by the NADPH oxidase for ROS and nitric oxide generation, two pathogens-killing agents. Metabolism reprogramming embraces also different other metabolism including lipid, and M1 macrophages have been shown to drive fatty acid synthesis (Zhu et al., 2015). By contrast, M2 macrophages rely on fatty acid oxidation in the mitochondria to generate acetyl-CoA, NADH, and FADH2 used to produce ATP through OXPHOS, assuring the long-term need in energy of these macrophages.

Along with this role in energy generation, cellular metabolism is emerging as an important determinant of the functional phenotype acquired by macrophages and a key regulator of macrophage immune response and inflammation (Kelly and O'Neill, 2015; Zhu et al., 2015). For instance, the role of L-arginine metabolism in regulating the microbicidal activity of macrophages through the production of nitric oxide or the generation of ornithine and polyamines is well documented and was one of the first characteristics used to define macrophage subsets (Muxel et al., 2017).

Progress has been made in defining the molecular pathways that underlie M2 versus M1 polarization and the different signaling molecules and transcription factors involved in regulating macrophage metabolic profiles, polarization and function.

Functional control of macrophages largely occurs at the transcriptional level and different transcription factors have been implicated in the polarization and activation of macrophages in response to infection. Signal transducers and activators of transcription (STATs) (STAT1), interferon regulatory factors (IRF) and nuclear factor kappa B (NF-κB) together with hypoxia-Inducible Factor (HIFα), are major players in inflammation and in the M1 polarization of macrophage during infection whereas IRF4, STAT6 and Peroxisome proliferator-activated receptor (PPAR) activated by IL-4, control M2 gene expression (Murray, 2017).

In this review we will summarize key mechanisms of *Leishmania*-macrophage interactions, focusing on the contribution of transcription factors (**Table 1**) to macrophage responses and to the physiopathology of the disease.

TRANSCRIPTOMIC SIGNATURE OF *LEISHMANIA* INFECTED MACROPHAGES

When infecting macrophages, microbes induce marked changes in gene expression programme and shape the phenotype and function of the infected cell. These changes have been investigated for different intracellular pathogens and the macrophagic transcriptomic signature identified for various bacteria, viruses and parasites. Different genes expression profiles have been compared and pathogens-mediated signaling have been shown to share a common host-transcriptional-response (Jenner and Young, 2005), which includes the group of genes that activate immune response, genes encoding inflammatory cytokines and chemokines and those stimulated by Interferon. This common host transcriptional-response is also shared by the transcriptomic profile of *Leishmania* infected macrophages (Buates and Matlashewski, 2001; Chaussabel et al., 2003; Rodriguez et al., 2004;

TABLE 1 | Key transcription factors that modulate macrophages response to *Leishmania* infection.

Transcription Factors	upstream regulators	Biological Effects	References
IRFs	TLR	Macrophage polarization	(Honda et al., 2005; Negishi et al., 2005)
NF-κB	TLR/TNFα/IL-1Rc-TRAF-IKK	Immune response-Inflammation	(Reinhard et al., 2012)
HIF-1α	Hypoxia, TLR	Increases Glycolysis-Inflammatory, immune responses	(Schatz et al., 2018)
NF-AT	TLR2-PI3K-PLC-Calcineurin	Immune response	(Bhattacharjee et al., 2016)
SREBP	PI3K/Akt/mTOR	cholesterol biosynthesis and lipid homeostasis	(Mesquita et al., 2020)
NRF2	PI3K/Akt/PKR…	Response to oxidative stress	(Vivarini and Lopes 2019)
PPAR	Oxidized fatty acids and their derivatives	Macrophage polarization	(Bouhlel et al., 2007; Díaz-Gandarilla et al., 2013)
LXR	Oxysterols	Decreased fatty acids and cholesterol synthesis	(Leopold Wager et al., 2019)

Osorio y Fortea et al., 2009) except for the IFNγ activated genes involved in the development of the microbicidal activities and promoted by the Janus kinase signal transducer and activator of transcription (JAK/STAT) pathway.

Interferon gamma receptor ligation induces the activation of JAK1 and JAK2 tyrosine kinases, constitutively associated to the receptor. These kinases phosphorylate, on the receptor, specific tyrosine residues that serve as a docking site for STATI transcription factor which is also a target of JAKs. Once phosphorylated by JAKs, STATI form dimers and translocate to the nucleus to bind the gamma interferon activation site (GAS) elements, present on different promoters of several genes including those encoding for NOS2, the MHC class II transactivator (CIITA) and IL-12 cytokine.

Leishmania-infected macrophages fail to respond to IFNγ a key cytokine that empower macrophages to clear the parasite and this failure is the result of the IFNγ signaling pathway inhibition. Indeed, in both differentiated U-937 cells and human monocytes infected by *Leishmania donovani*, the tyrosine phosphorylation, Jakl and Jak2 activation and Statl phosphorylation normally induced by IFNγ, were selectively impaired (Nandan and Reiner, 1995). Similar response was observed when macrophages were infected by other *Leishmania* species. Several mechanisms have been proposed to explain the inhibition of JAK-STAT pathway during *Leishmania* infection. This IFNγ signaling pathway inhibition was suggested to be the result of a decreased expression of IFN-gamma R-alpha protein after infection (Ray et al., 2000). The co-immunoprecipitation of JAK2 with the *Leishmania* induced-tyrosine phosphatase (P'TP) SHP-1, suggests that this phosphatase may be at the origin of the IFN-gamma-inducible JAK2 unresponsiveness (Blanchette et al., 1999). However, additional mechanisms must participate to the inhibition of IFNγ signaling as *Leishmania* parasite retains its capability to inhibit STATI activation in SHP-1-deficient macrophages suggesting a SHP-1 independent mechanism (Forget et al., 2006). *Leishmania* induced STATI inactivation could be also the consequence of proteasome-mediated degradation of this transcription factor since proteasome inhibitors rescued STAT1 nuclear translocation and restored STAT1 protein level (Forget et al., 2005). It could also be the result of a defective nuclear translocation of STATI due to a compromised IFN-induced STAT1 association with the nuclear transport adaptor importin-5 as described for *L. donovani* amastigote (Matte and Descoteaux, 2010).

The suppressor of cytokine signaling (SOCS) proteins by binding to JAK or cytokine receptors and suppressing STAT phosphorylation are one of the crucial negative regulators of JAK/STAT signaling pathways. SOCS have been reported to be activated in response to different parasites (Bullen et al., 2003a; Zimmermann et al., 2006; Dalpke et al., 2008) and to play a role in regulating immune response in various infectious disease including leishmaniasis (Bullen et al., 2003b). Indeed, *Leishmania* LPG, an agonist of TLR2 (de Veer et al., 2003) and *L. donovani* parasites have been shown to induce SOCS3 and SOCS1 expression in macrophages (Bertholet et al., 2003). The early and transient expression of SOCS3 may suppress the reactive oxygen species-mediated apoptotic signaling cascade (Srivastav et al., 2014) while the stable and robust expression of SOCS1 could inhibit phosphorylation of STAT1 and induce the down-regulation the IL-12 cytokine level in infected macrophages (Chandrakar et al., 2020).

Hence, in response to *Leishmania* infection, several mechanisms, acting at various steps of the JAK-STAT pathway might potentially cooperate to coordinately shutdown JAK-STAT pathway, crucial for macrophage-T cells cross talk.

TRANSCRIPTION FACTORS UNDERLYING *LEISHMANIA*-INDUCED INFLAMMATORY RESPONSE

Macrophages sense protozoan parasites using different surface receptors that participate in the course of infection and have different effect on macrophage-*Leishmania* interaction. Among these, the Toll like receptors (TLRs), activated by various parasites surface molecules, play a crucial role in initiating host innate immune responses and directing adaptive immune responses against invading pathogens. TLRs localize variously as TLR1, -2, -4, -5, and 6, are expressed on the cell membrane, whereas TLR3, -7, -8, -9, are expressed in the endosome. Once activated adaptor molecules, such as MyD88 (myeloid differentiation primary-response protein 88) shared by all TLRs except for TLR3, TRIF (TIR-domain-containing adaptor protein inducing beta interferon (IFN-β), unique to TLR3 and TLR4 signaling, TIRAP (TIR-domain-containing adaptor protein) that mediates the activation of signaling downstream of TLR2 and TLR4, or TRAM (TIR-domain-containing adaptor molecule) unique to TLR4, are recruited to the receptor (Satoh and Akira, 2016).

Different TLRs such as TLR2, TLR4 (Kropf et al., 2004) and TLR9 have been involved in providing protection against *Leishmania* spp infection (Liese et al., 2007; Gurung and Kanneganti, 2015). It was therefore not surprising that mice deficient for MyD88, the common adaptor acting downstream of almost all the TLRs, were highly susceptible to *L. major* infections (de Veer et al., 2003; Debus et al., 2003; Muraille et al., 2003).

The interaction between the *Leishmania* ligands and TLRs induce the recruitment of different adaptor molecules that transduce TLRs intracellular signals and lead to the activation of various transcription factors, including NF-κB and IRFs which play a key role in defining functional phenotype of macrophages (Colonna, 2007).

Indeed, MyD88 adaptor has been shown to form a multimolecular complex consisting of IRAKI, IRAK4, TRAF6, IRF-5, and IRF-7. IRF7 is a master regulator of type I IFN genes (Honda et al., 2005) whereas IRF5 is implicated in TLR-dependent induction of pro-inflammatory cytokines, such as interleukin-6 (L-6), IL-12p40 and tumour-necrosis factor-alpha (TNFα) as confirmed by IRF5 deficient mice (Takaoka et al., 2005). IRF-5 that play an essential role in M1 macrophages

polarization, compete with IRF4 for binding to MyD88 (Ferrante and Leibovich, 2012). This negative regulator of MyD88 signaling is crucial for M2 polarization and IRF4 and IRF5 competition for binding to MyD88 plays a key role in choosing whether macrophage polarization goes toward M1 or M2 phenotype (Negishi et al., 2005).

The TRIF-dependent pathway, restricted to TLR-3 and TLR-4, recruits IRF3 to induce type I IFN responses, particularly IFN-beta (Sharma et al., 2003).

IRF1, highly induced by IFNγ, directly interacts with and is activated by MyD88 upon TLR9 activation (Schmitz et al., 2007) and the TLR9-mediated IRF1 activation, as confirmed in IRF1-deficient cells, is required for optimal regulation of a specific gene subset that includes IFNβ, inducible NO synthase (iNOS) and IL-12p35 (Negishi et al., 2006).

Hence multiple TLR pathways require either IRF-1, IRF-3 or IRF-7 for type I IFN-induction. IRF-1 and IRF-7 are recruited and activated through MyD88, which simultaneously triggers IRF-5 and a parallel signaling pathway for NF-κB activation leading to secretion of proinflammatory cytokines (Colonna, 2007).

IRF-1 (Lohoff et al., 1997), IRF-2 (Lohoff et al., 2000) and IRF-8 (Giese et al., 1997) knockout mice fail to mount a protective Th1 response and are thus highly susceptible to *L. major* infection. However, a defect in IRF1 expression is also observed in *Leishmania* infected macrophages treated with IFNγ (Matte and Descoteaux, 2010). This defect may be due to the inhibition of STAT1 activation by *Leishmania* infection. Indeed, IRF1 expression is mediated by STAT1 and NF-κB transcription factors, a finding confirmed by the data showing that IFN-induced expression of IRF-1 mRNA was completely abolished in STATl deficient cells (Meraz et al., 1996). Similarly, IRF5 was shown to be required for the development of host-protective Th1 responses in response to *Leishmania donovani*. However, in IRF5-/- mice (Paun et al., 2011) and in myeloïd CD11c specific IRF5-/- mice, *Leishmania* failed to induce splenomegaly which seems to be detrimental to the host (Mai et al., 2019).

Besides IRFs, the TLR MyD88/TIRAP signaling pathways culminate in activation of the transcription factor nuclear factor-kappaB (NF-κB) *via* either classical pathway engaging the IKK-related kinases TBK1 (TRAF family member-associated NF-κB activator (TANK) binding kinase-1) downstream of TRAF6 or alternative pathways (Kawai and Akira, 2007).

NF-κB transcription factor family has five different members: NF-κB1(p50), NF-κB2 (p52) (formed from a larger precursor, respectively p105 et p102), p65 relA, c-rel and rel-B. They are all able to operate as a homo- or hetero-dimers and potentially yield to 15 different NF-κB complexes. These NF-κB dimers bind an inhibitory protein "inhibitor of κB" (IκB) and are trapped in the cytoplasm. The phosphorylation of IκB induces its ubiquitination and degradation and result in the release and the nuclear translocation of this master transcription factor that regulates hundred of genes. A large bulk of these genes are involved in both immediate and delayed expression of inflammatory mediators making NF-κB transcription factor a key regulator of proinflammatory pathway (Reinhard et al., 2012), NADPH oxidase expression and mitochondrial activity.

NF-κB pathway plays a crucial role in host protection against *Leishmania* infection and the deficiencies in different NF-κB family members in mice result in high susceptibility to *Leishmania* infection. Indeed, a defect in relB induces a multi-organ inflammation in mice, underlying the inhibitory effect of relB protein (Weih et al., 1995). Similarly, NF-κB2 deficient mice, with resistant background, develop chronic non healing lesions associated with uncontrolled parasite replication as a result of a reduced CD40-induced IL-12 production by macrophages (Speirs et al., 2002). RelA deficiency is fatal and induces the death of mice during the fetal life. However, RelA-/- chimeric mice present defects in macrophage function and show a reduced production of NO and an inability to control parasite replication and to clear infection (Mise-Omata et al., 2009). While relA is implicated in the regulation of iNOS expression, c-rel seems to regulate IL-12 production and c-Rel-deficient mice were unable to resolve *Leishmania* infection in the absence of IL-12 recombinant treatment (Grigoriadis et al., 1996; Sanjabi et al., 2000; Abu-Dayyeh et al., 2010).

In macrophages, *Leishmania* parasite seems to be unable to activate p65 NF-κB subunit. Indeed, *Leishmania Mexicana* promastigotes induce the cleavage of p65 relA subunit and generate a smaller p35 protein whereas the amastigote form fully degrades relA (Abu-Dayyeh et al., 2010). *Leishmania amazoniensis* induces the p50/p50 repressor complex which leads to a reduced activation of nitric oxide synthase (iNOS) (Calegari-Silva et al., 2015). From his side, *Leishmania major* down-regulates relA containing complexes but induces a c-rel containing complexes that retain the ability to strengthen the innate immune response of the host through the regulation of proinflammatory cytokines expression (Guizani-Tabbane et al., 2004).

NF-κB regulates the expression of myriads of cytokines and chemokines including IL-1β that play crucial role in cellular defense. This cytokine is produced as pro-IL-1β which is processed and released by the NLRP3 inflammasome activated caspase1. Different species of *Leishmania* have been reported to induce NLRP3 inflammasome, that have been shown to play a key role in restricting *Leishmania* replication in macrophages (Lefèvre et al., 2013; Lima-Junior et al., 2013) although detrimental effects have been reported for certain *Leishmania* strains such *L. major* Seidman strain or *L. braziliensis* for which disease severity is associated to IL-1β production (Charmoy et al., 2016; Santos et al., 2018). It is therefore consistent that several *Leishmania* species actively inhibit inflammasome formation and have developed different strategies to inhibit NF-κB-dependent inflammatory response. This was achieved in part by targeting the cytosolic inducible protein A20, also known as TNFα-induced protein 3 that de-ubiquitinates TRAF6 to inhibit IκB degradation and hence NF-κB activation reducing the extend of NLRP3 inflammasome activation (Boone et al., 2004; Gupta et al., 2017). Recent study highlights a key role for epigenetic modifications at the promoter of NF-κB-regulated genes that dampen inflammasome activation (Lecoeur et al., 2020). Indeed, *Leishmania amazoniensis* amastigotes effector molecules, target histone H3 post-translational acetylation, to

reduce expression of positive regulators of the NF-κB pathway and upregulate transcripts of anti-inflammatory molecules and known inhibitors of NF-κB activation, leading to the inhibition of NF-κB-NLRP3 axis.

TRANSCRIPTION FACTOR HIF-1α AND *LEISHMANIA*-INDUCED METABOLIC REPROGRAMING

Since a decade, the importance of metabolic reprogramming in macrophages fighting microbes has emerged (Chauhan and Saha, 2018; Wang et al., 2019). Indeed, low oxygen levels have been described in the areas of myeloid cell activity and site of inflammation. Studies extending back almost a century have demonstrated that macrophages in these areas are highly dependent on anaerobic glycolysis for the production of ATP. This glycolysis surge and reduced glucose mitochondrial oxidation have been shown to depend on HIF-α transcription factor, which plays a key role in assisting macrophage to adapt to hypoxic conditions and achieve their microbicidal function (Marín-Hernández et al., 2009).

Under hypoxia, the inactivation of the oxygen-sensitive enzymes prolylhydroxylases (PHDs) allows HIFα (one of the HIF-α isoforms: HIF-1α or HIF-2α) to escape proteosomal degradation. HIF-α accumulates and translocates to the nucleus where it forms a heterodimer with the constitutively expressed HIF-1ß subunit. The HIFα/β heterodimer binds to the hypoxia response elements (HREs) and drive then the expression of different genes (Ke and Costa, 2006). HIF-1α is a direct transcriptional activator of glucose transporters genes involved in glucose uptake as well as keys glycolytic and gluconeogenesis enzymes. It also decreases mitochondrial respiration and thus oxygen consumption by upregulating the expression of pyruvate dehydrogenase kinase (PDK) (Bishop and Ratcliffe, 2014) that limit the formation of acetyl-CoA. Glycolysis even less efficient than oxidative phosphorylation for ATP generation can be promptly ramped up to sustain ATP production and meet the rapid energy requirement of macrophages (Nagao et al., 2019).

Similarly to other site of infection, *Leishmania* infected skin has been demonstrated to be hypoxic. This low oxygen level has been described for *L. amazonensis* and *L. major* infected tissue (Araujo et al., 2013) and resolution of the wound was reported to correlate with reoxygenation (Mahnke et al., 2014).

HIF-lα expression can also occur in an oxygen-independent manner in myeloid cells fighting pathogens, driving metabolic reprogramming to modulate oxygen consumption and modulating innate immunity (Jantsch and Schödel, 2015; Devraj et al., 2017; Stothers et al., 2018; Knight and Stanley, 2019). *Leishmania* parasite also induces HIF-1α activation (Charpentier et al., 2016; Schatz et al., 2018). Indeed, the HIF-lα has been detected in the cutaneous lesions of Balb/c mice (Arrais-Silva et al., 2005) and in the nucleus of *L. amazonensis* infected mouse peritoneal macrophages and human MDM (Degrossoli et al., 2007). HIF-1α also accumulates in *L. donovani* infected macrophagic cell lines (Singh et al., 2012) under normoxic conditions. In our hand, *L. major* induces the accumulation of HIF-la in BMDM cells as assessed by confocal microscopy (unpublished data). A more recent study has however shown that *L. major* infection induces HIF-lα accumulation in the macrophage-rich cutaneous *Leishmania* lesions of mice and humans, but needs, *in vitro*, additional stimulation such IFNγ (Schatz et al., 2016).

Moreover, different HIF1α target genes including glucose transporters assuring glucose uptake, glycolytic enzymes and pyruvate dehydrogenase kinase 1 (PDK1) leading to inactivation of the TCA cycle are induced in *Leishmania* infected macrophages (Rabhi et al., 2012; Moreira et al., 2015). These allow the metabolic reprogramming of infected macrophages toward aerobic glycolysis and hence increased glucose uptake, activation of the pentose phosphate pathway (PPP) that fuels NADPH to activate NADPH oxidase for ROS generation, enhanced lactate production and decreased mitochondrial oxygen consumption.

Activation of HIF1α has contrasting effects on the pathogen survival. Unlike for bacterial and for some viral infections (Devraj et al., 2017), HIF-lα activation during several parasitic infections could promote the intracellular survival of parasites. Indeed, HIF-la stabilization is required for the survival of *Toxoplasma gondii* (Wiley et al., 2010); Similarly, *Theileria annulata* induces hif1-α transcription and drive host cell toward aerobic glycolysis limiting the production of H202 and hence protecting the parasites in infected macrophages (Metheni et al., 2014).

The impact of HIF1α on *Leishmania* parasite survival has been addressed in several studies and has yielded contrasting results. Indeed, Singh et al., using macrophagic cell lines, show that knockdown of HIF-lα inhibited intracellular growth whereas over expression of this TF promotes intracellular growth of *L. donovani* parasites (Singh et al., 2012). However, different other studies show that HIF-1 alpha is a host protective factor against infection by *Leishmania* parasites. Indeed, silencing of HIF-lα in macrophages, using RNA interference, inhibited LPS/IFNy-induced NO release in response to *L. major* and abolished the leishmanicidal activity of macrophages showing that HIF-lα expression by myeloid cells contributes to the control of *L. major* parasites *in vitro* and *in vivo* (Schatz et al., 2016). Finally, the viability of *L. donovani* is enhanced in myeloïd-restricted HIF-1-/- mice (mHIF-1-/-) and in macrophages from mHIF-1-/-. This increased intracellular growth both *in vitro* and *in vivo*, was the result of enhanced lipid synthesis induced by a defect in the expression of BNIP3 that allows the activation of the mTOR/SREBPlc axis (Mesquita et al., 2020).

Thus, besides carbohydrates metabolism regulation, HIF1α, by regulating mTOR signaling pathway, controls lipid metabolism.

HIF-1 is also linked to inflammatory response and microbicidal activities of myeloid cells. Indeed, the relationship between the hypoxic and inflammatory responses is tightly controlled and cross talk between HIF1α and NF-κB, the two main molecular players involved in hypoxia and innate immunity, has been demonstrated (Palazon et al., 2014; D'Ignazio et al., 2016). Different studies have underlined the

importance of HIF-1 in regulating inflammatory cytokines. Mice with HIF-1α myeloid-specific deletion showed impaired inflammatory responses, underlining the importance of HIF1α and the high glycolytic rates and energy generation for basic myeloid cell activities (Cramer et al., 2003). Both HIFs are able to regulate a number of pro-inflammatory cytokines and chemokines directly, further contributing to the inflammation response (D'Ignazio et al., 2016) and NF-κB is critical transcriptional activator of HIF1α (Rius et al., 2008; van Uden et al., 2008).

Hypoxic response is also tightly connected to innate immune response and HIF1 and NF-κB synergistically respond against pathogens. Indeed, hypoxia and bacterial infections increased NF-kB activity in phagocytes, leading to the increase in HIF-1a mRNA transcription (Rius et al., 2008). Moreover, bacteria-infected macrophages are characterized by a defective HIF-1α expression following ablation of Iκκb, an essential regulator of NF-κB activity (Rius et al., 2008).

Hence, *Leishmania* infection, by inducing NF-κB and HIF1 transcription factor, provides a bridge for regulating immune response and ignite inflammation by glucose fueling (**Figure 1**).

INTERPLAY BETWEEN TRANSCRIPTION FACTORS AND ENERGY SENSORS IN *LEISHMANIA*-INFECTED MACROPHAGES

One target gene of NFκB is SIRT1 whose promoter sequence contains several putative NF-kB binding sites (Voelter-Mahlknecht and Mahlknecht, 2006; Mahlknecht and Voelter-Mahlknecht, 2009). Sirt1 belong to the Sirtuins family of nicotinamide nucleotide dinucleotide NAD(+)-dependent protein deacetylases that contain seven enzymatic activities in mammals (SIRT1–SIRT7) with different subcellular localisation that function to suppress gene transcription by epigenetic

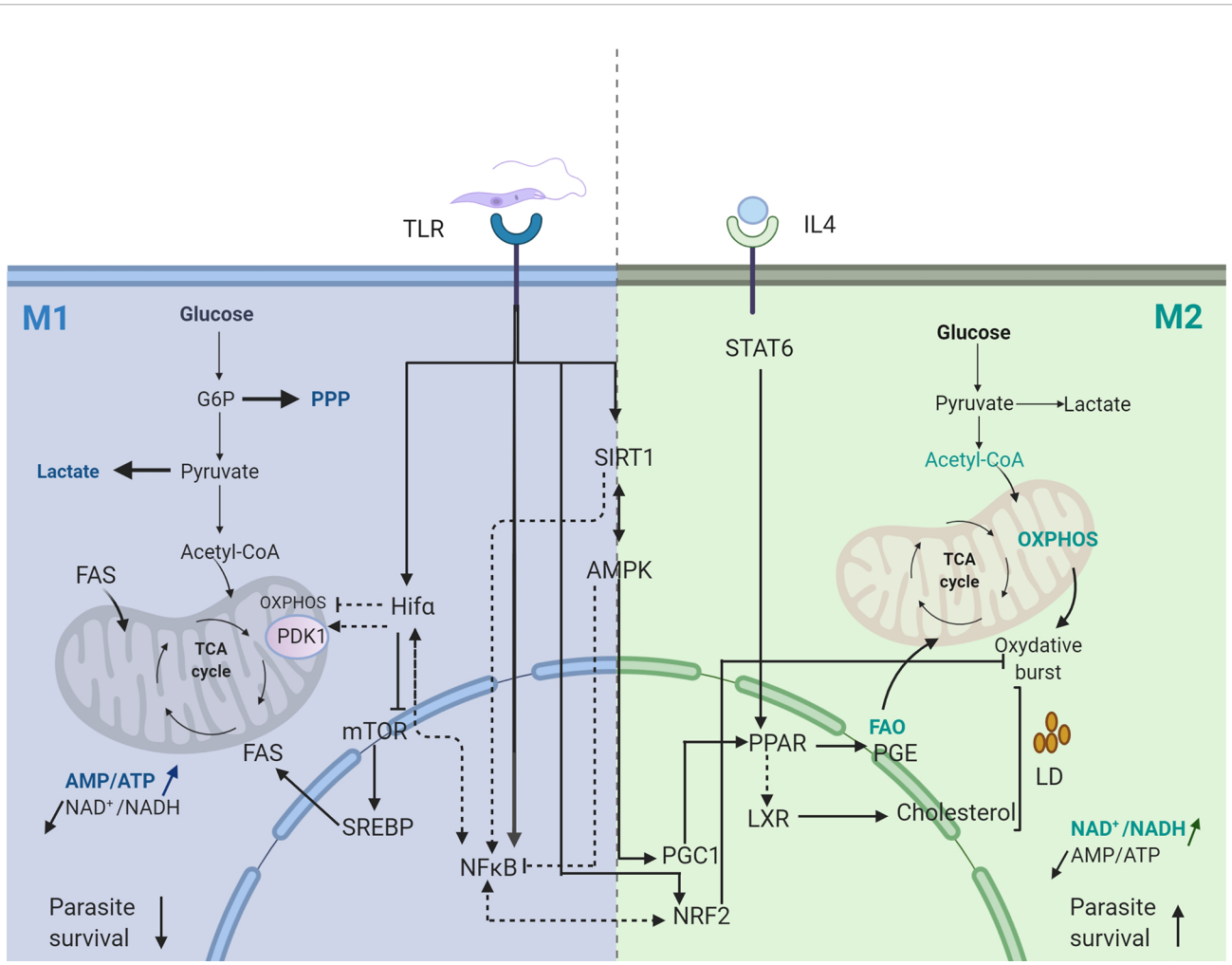

FIGURE 1 | Transcriptional signature of *Leishmania* infected macrophage. Dotted arrows represent pathways not validated in *Leishmania* infected macrophages. Straight arrows represent pathways validated in *Leishmania* infected macrophages. FAS, Fatty Acid Synthesis; FAO, Fatty Acid Oxydation; PGE, Prostaglandine E; PPP, Pentose Phosphate Pathway; OXPHOS, Oxidative Phosphorylation. Created with BioRender.com.

mechanisms. A second energy sensor, the adenosine 5'-monophosphate (AMP)-activated protein kinase (AMPK) is a key player in preserving cellular ATP.

During the early pro-inflammatory phase relying on glycolysis, decreases in ATP production and later on in NADH formation, increase the ratios of AMP/ATP, and NAD^+/NADH. The increased AMP/ATP ratio induces AMPK while the enhanced cellular NAD+ activates SIRT proteins. These two pathways, can act in concert to reinforce one another in order to ensure the metabolic homeostasis of the cell. Indeed, On one hand SIRT1 protein has been described as an upstream activator of the AMPK through LKB1 (the kinase that mediates the phosphorylation of AMPK) deacetylation (Lan et al., 2008) and on the other hand has been considered as a downstream target of AMPK, becoming activated by the AMPK-induced increased levels of NAD+ (Cantó et al., 2010). Moreover, SIRT1 and AMPK proteins share several downstream targets such as PGC-1α (Rodgers et al., 2005) and PPARα (Purushotham et al., 2009).

SirT1 directly interacts with and deacetylates NFκB p65 (Yeung et al., 2004) inhibiting its transactivation capacity and suppressing the transcription of NF-κB dependent genes expression (Natoli, 2009). This antagonistic cross talk between NF-κB signaling pathway and SIRT1 pathways, bridge energy metabolism with innate immunity and have crucial role in the termination of NF-κB driven inflammatory response (Kauppinen et al., 2013; Vachharajani et al., 2016).

SIRT1 also deacetylates another key player in the regulation of energy metabolism/promoting mitochondrial biogenesis, the peroxisome proliferator activated receptor γ (PPARγ) coactivator 1 (PGC1) α, upregulating its activity which is further enhanced by AMK-mediated phosphorylation (Cantó et al., 2010). PGC-1α promotes the metabolic switch toward M2 profile. Indeed, the overexpression of PGC-1 reduces the transcriptional activity of NF-κB and suppressed the expression of proinflammatory cytokines and free fatty acids (Eisele et al., 2013). PGC-1α cooperates with the peroxisome proliferator-activated receptor alpha (PPARα) to control the transcription of genes encoding mitochondrial fatty acid oxidation enzymes shifting the fuel usage from glucose to fatty acids (Vega et al., 2000). Moreover, PGC1α is also a coactivator of a wide variety of transcription factors including Forkhead box-containing protein type O 1 (FOXO1), nuclear respiratory factors (NRF)1 and NRF2, many of which are involved in the transcriptional control of mitochondrial proteins and thus in mitochondrial biogenesis (Feige and Auwerx, 2007).

Hence, these energy sensors have emerged as key regulators of inflammation and metabolic switches, playing a crucial role in macrophage metabolic reprogramming toward M2 macrophages profile during the progression of inflammatory response.

These energy sensors have been shown to play an important role in the polarization of parasite infected macrophages. Indeed, the intracellular growth of *Trypanosoma cruzi* was recently shown to rely predominantly on energy production, nucleotide metabolism and fatty acid oxidation of the host and silencing of AMPK catalytic or regulatory subunits, favors intracellular *T. cruzi* growth (Caradonna et al., 2013). Similarly, activation of the host AMPK signaling inhibits the intracellular growth of *Plasmodium falciparum* parasite (Ruivo et al., 2016). The initial transient aerobic glycolytic phase induced by *Leishmania* parasites has been shown to be followed by a metabolic shift towards mitochondrial metabolism, allowing the metabolic recovery of the host cell (Moreira et al., 2015). This metabolic switch to oxidative phosphorylation and β-oxidation, is associated with an increase in PGC-1α levels and a significant increase in the AMP/ATP ratio. This metabolic reprogramming requires the activation of AMPK downstream to SIRT1 and LKB1 and ultimately contributes to parasite survival *in vitro* and *in vivo* (Moreira et al., 2015). Hence targeting the SIRT-AMPK axis may explain how the *Leishmania* parasite subverts the host metabolism to insure its persistence and replication (**Figure 1**).

MICROENVIRONMENT IMPACT ON ACTIVITY OF PGC1 CO-ACTIVATOR

Microenvironment play a role, *in vivo*, in the metabolic reprograming of *Leishmania* infected macrophages and their shift from M1to M2. Indeed, the significantly raised plasma levels of IL-4/IL-13 and IL-10 in VL patients suggested a microenvironment conducive for alternative activation of monocytes/macrophages (Roy et al., 2015). Indeed, both IL-4 and IL-13 cytokines induced the expression of the two metabolic regulators, Pparγ, Pparδ and of the coactivator protein PGC-1β, through the activation of STAT6.

The Peroxisome proliferator-activated receptors (PPARs) but also the Liver X Receptors (LXRs) nuclear receptors are two transcription factors families implicated in the regulation of macrophage lipids metabolism. Both ligand-dependent transcription factors heterodimerize with the retinoid X receptor (RXR).

The peroxisome proliferator-activated receptor-γ (PPARγ) is a master regulator that assures fatty acid homeostasis. It binds mono- and polyunsaturated fatty acids and derivatives such as eicosanoids to regulate the transcription of various genes that control lipid metabolism and fine-tune immune function. Indeed, a peroxisome proliferator response element (PRE) have been identified in all the genes that encode the rate limiting steps in the transport, synthesis, storage, mobilization, activation and oxidation of fatty acids but also in the promoter region of arginase I (Odegaard et al., 2007) and in the promoters region of phospholipase A2 (cPLA2) and cyclooxygenase-2 (COX-2), two enzymes regulating the prostaglandin production that have been often associated with anti-inflammatory activities. Phospholipase A2 (cPLA2) and cyclooxygenase-2 (COX-2) have been also reported to be activated upon TLR2 stimulation; whereas the increased macrophage cPLA2 activity induced by *Leishmania* infection is regulated at the post transcriptional level, *Leishmania*-driven COX2 induction was regulated by calcineurin and calcineurin-dependent NFAT transcription factor (Bhattacharjee et al., 2016). PPARγ inhibits the induction of a broad subset of inflammatory genes, suggesting that transrepression might be a primary mechanism responsible for the anti-inflammatory action of PPARγ.

PPARγ deficient macrophages show reduced rates of β-oxidation of fatty acids and blunted mitochondrial biogenic response and are hence unable to induce oxidative phosphorylation, showing that PPARy plays a crucial role in the differentiation of circulating monocytes toward anti-inflammatory M2 macrophages, both in humans and mice (Bouhlel et al., 2007; Odegaard et al., 2007). Similarly, the overexpression of the PPARγ transcriptional coactivators PGC-1β primes macrophages for alternative activation and prevents an M1 inflammatory response following stimulation with LPS and IFNγ (Vats et al., 2006). Indeed, the two PPAR subtypes expressed in macrophages have been implicated in the negative regulation of inflammatory responses as they inhibit pro-inflammatory gene expression including IL1β, IL6, TNFα, IL12 and iNOS (Delerive et al., 2001; Kostadinova et al., 2005).

PPARγ also activates a cholesterol efflux by inducing the Liver X receptor-alpha (LXR) expression either directly or through the induction of CYP27, which is capable of generating 27-hydroxycholesterol, an endogenous LXR activator.

Endogenous agonists binding to LXR induces conformational changes that trigger co-repressor release and co-activators recruitment, leading to transcriptional regulation of the target genes. These include those encoding the sterol regulatory element binding protein 1 (SREBPlc), the other master transcriptional regulator of fatty acid synthesis (Repa et al., 2000) but also the ATP binding cassette transporters ABCAl and ABCG1 as well as the gene encoding apolipoprotein E (APOE) (Repa et al., 2002), the cholesterol transporters that promote cholesterol efflux. LXR activation also leads to an increase in the levels of long chain polyunsaturated fatty acids (PUFAs) and triglyceride synthesis.

The Liver X Receptors, (LXRs) also play a crucial role in the macrophage anti inflammatory response promoting alternative (M2) macrophage activation. Two LXR subtypes, LXRα and LXRβ are expressed in hematopoietic cells with LXRα being restricted to the myeloid lineage. The deficient regulation of both isoforms of LXRs activity can lead to chronic inflammatory conditions. Indeed, several LXR regulated genes are targets of NF-κB and LXR agonist treatment can limit the transcriptional up-regulation of inflammatory genes such as tumor necrosis factor alpha (TNFα), cyclooxygenase 2 (COX2), inducible nitric oxide synthase (NOS2) and matrix metalloprotease 9 (MMP9) (Castrillo et al., 2003; Joseph et al., 2003).

Several mechanisms, have been proposed to explain LXR capacity to inhibit inflammation including the trans-repression of NF-κB (Ghisletti et al., 2009) and regulation of genes encoding enzymes involved in the synthesis of long chain PUFAS with known anti-inflammatory activity (Repa et al., 2000). Moreover, together with fatty acids, LXR regulates expression of LPCAT3 an enzyme that controls Fatty acyl-chain remodeling in phospholipid (Hashidate-Yoshida et al., 2015). These changes in phospholipid composition can reduce inflammation both by modulating kinase activation through changes in membrane composition and by affecting substrate availability for inflammatory mediator production (Rong et al., 2013).

Nuclear receptors (NRs) are emerging as key players in infectious diseases and targeting NRs as a novel host-directed treatment approach to infectious diseases appears to be a valid solution (Leopold Wager et al., 2019).

LXR deficiency in mice leads to reduced control of the intracellular *Mycobacterium tuberculosis* growth (Korf et al., 2009) and increased susceptibility to *Listeria monocytogenes* (Joseph et al., 2004). By contrast, mice deficient for LXR and challenged with the visceralizing species *Leishmania chagasi/infantum* had significantly decreased parasite burdens compared to C57Bl6 wild-type mice and enhanced NO production showing enhanced resistance of LXR-deficient mice to *Leishmania* infection (Ghisletti et al., 2009).

Regardless of PPARs subtypes induced by *Trypanosoma cruzi* (i.e., PPARy in murine peritoneal macrophage and PPARα in BMdM and Raw 264.7 macrophagic cell line), PPAR is involved in the *in vitro* M2 polarization of macrophages isolated from *T. cruzi*-infected mice and have a protective role in *T. cruzi* infection (Penas et al., 2015; Koo et al., 2018). In *Leishmania* infection the rôle of PPAR is controversial. PPAR agonists treatment of *L. mexicana* infected macrophages induced M1 polarization through IL-10 downregulation, cPLA2-COX-2 prostaglandins pathway deactivation and increased ROS production that control parasite burden in murine macrophages (Díaz-Gandarilla et al., 2013). By contrast, PPARy is activated by *L. donovani* both *in vivo* and *in vitro* and have been shown to promote the parasite survival, whereas the inhibition of PPAR-y facilitates *Leishmania* clearance in C57B16 peritoneal macrophages (Chan et al., 2012), suggesting that *Leishmania* parasites harness PPARγ to sustain the M2 phenotype and increase dissemination of the infection. PPARγ knockout Balb/c mice had significantly less footpad swelling 5-7 weeks after injection of *L. major* promastigotes than wild type mice, suggesting that absence of PPARγ delay disease progression in Balb/c mice (Odegaard et al., 2007). In lipid loaded *Leishmania*-infected BMDM, PPAR ligands promote *L. major* amastigote growth in an arginase-dependent manner (Gallardo-Soler et al., 2008).

Like other trypanosomatid parasites, *Leishmania* depend on their hosts for several nutrients necessary for their replication and survival. While carbohydrates have been proposed as the primary source of carbon for various parasites, including *Leishmania* (Naderer et al., 2010) various other sources have been suggested. Lipids would be a potential source especially since the infection induces the production of intracellular lipid droplets which rapidly localized in close association with the parasites (Rabhi et al., 2012; Rabhi et al., 2016).

Hence, like different other pathogens *Leishmania* parasite target metabolic pathway to scavenge nutrients to ensure its survival and to subvert the host immune response feeding two birds with one scone.

NRF2 ANTIOXIDANT PATHWAY

The metabolic reprogramming toward aerobic glycolysis attenuates the activities of the respiratory chain, allowing reactive-oxygen species (ROS) production. The respiratory

burst or ROS, generated by the NADPH oxydase and the mitochondrial electron transport chain after the phagocytosis of pathogens, has been recognized since decades as an essential mechanism of microbial killing. To avoid detrimental side effects and oxidative damage, host cells produce antioxidants enzymes in order to deplete ROS and RNS. The transcription of phase II defense gene including detoxifying enzymes, such as genes involved in the regeneration of glutathione (GSH), genes encoding proteins involved in sequestration of iron ions (ferritine, heme oxygenase (HO-1), genes encoding proteins responsible for the production of NADPH and anti-oxidant genes (e.g., SODs, GPx, GSH reductase), is orchestrated by the master transcription (nuclear factor (erythroid-derived 2)-like 2 (NRF2) (Suzuki and Yamamoto, 2015).

Upon cell activation, NRF2 oxidative sensor is released from its inhibitor Kelch-like ECH-associated protein-1 (Keap-1), phosphorylated by different kinases including the MAPK, phosphatidylinositol-3 Kinase (Kang et al., 2002) and double-stranded RNA-dependent protein kinase R (PKR) (Vivarini et al., 2017) and translocated to the nucleus where it binds, once associated with small Maf proteins, to the antioxidant response elements (AREs) present in the promoter region of target genes (Jung and Kwak, 2010; Ding et al., 2019; Ingram et al., 2019). This master transcription factor orchestrates the regulation of about 200 genes, working in a network to regulate various functions.

NRF2 is a key player regulating inflammation; Indeed, Nrf2 knock-out mice shows increased expression of cytokines, chemokines, and adhesion molecules and sustains the development of different inflammatory disorders (Thimmulappa et al., 2006; Kim et al., 2010). Cross talk between NRF2 and NF-κB is essential to resolve inflammatory response of the cell. Indeed, NFκB can directly regulate the induction of Nrf2 transcription, but can also by interacting with Keap1 suppress the Nrf2-ARE pathway, resulting in the repression of various genes (Wardyn et al., 2015; Bellezza et al., 2018). This inhibitory effect on macrophage inflammatory response may be also indirect, induced by NRF2-activated anti-oxidant genes. Among the antioxidative stress genes whose expression is regulated by NRF2, the Heme oxygenase 1 (HO-1) has received considerable attention. HO-1 is the rate limiting enzyme that catalysis the degradation of heme into carbon monoxide (CO) and iron and biliverdin to bilirubin. NRF2-mediated HO-1 expression, inhibited NF-κB signaling preventing the expression of inflammasome components such IL-1β and nlrp3 induced by LPS (Vitali et al., 2020). Similarly to NRF2 knockout mouse, HO-1 knockout mouse displayed chronic inflammatory disorders, are highly vulnerable to experimental sepsis induced by the classical pro-inflammatory mediator endotoxin (Wiesel et al., 2000). Human cases of genetic HO-1 deficiency are similar to those observed in HO-1 knockout mice (Kawashima et al., 2002) confirming the anti-inflammatory role of HO-1 (Paine et al., 2010). Moreover, Nrf2 expression but also HO-1 induction have been identified as a key mediator of polarization to a novel macrophage phenotype (Mox), that develops in response to oxidative tissue damage (Kadl et al., 2010). This M2 phenotype has redox and antioxidant potential and induces the expression of the anti-inflammatory and antiapoptotic Cox2, IL1β, HO-1, VEGF, and Nrf2.

Thus, the complex network of protective mechanisms against the oxidative burst orchestrated by NRF2 and the NRF2-HO-1 axis implicated in the resolution of inflammation, modulates the function and phenotype of macrophages driving macrophages polarization towards M2 phenotype (Naito et al., 2014).

The effect of NRF2 on mitochondria biogenesis may also play a role during infection. Indeed, four AREs were identified in the NRF1 (nuclear respiratory factors 1) gene promoter and were capable of Nrf2 binding (Piantadosi et al., 2008). NRF1 through TFAM (transcription factor A mitochondrial), is involved in the mitochondrial DNA replication. Moreover, crosstalk between PGC1a and NRF2 has been also recently reported highlighting a link between cellular redox and mitochondrial homeostasis.

The NRF2 pathway orchestrates the expression of anti-oxidant and cytoprotective genes. Its activity is induced upon exposure to oxidative stress to protect cell from environmental insults and to adapt to endogenous stressors.

However, it is not clear to what extend oxidative stress is crucial for pathogens clearance as several microorganisms seem to be able to survive and even thrive in an oxidative environment (Paiva and Bozza, 2014). Indeed, different bacteria and parasites can thrive in oxidative environments while antioxidants promote their clearance. *Trypanosoma cruzi* infected mice treated with several Nrf2 inducers, including cobalt protoporphyrin (CoPP), sulforaphane, N-acetyl-cysteine (NAC), or pterostilbene, had a decreased parasite burden. The inhibition of Nrf2 activity with SnPP or the promotion of oxidative stress with paraquat or H202 treatment increased *T. cruzi* parasitism, suggesting that oxidative stress fuels *Trypanosoma cruzi* infection in mice (Paiva et al., 2012). During the malaria-induced inflammatory processes, the treatment of macrophages with NRF2 inducers enhances the CD36 expression and CD36-mediated Plasmodium phagocytosis and thus the control of severe malaria through parasite clearance (Olagnier et al., 2011). Nrf2 participates in infections by other protozoan microorganisms and different study show that various parasites such *Toxoplasma gondii*, activates Nrf2 signaling pathway that is required for parasites replication (Pang et al., 2019).

The potential role of NRF2 signaling in *Leishmania* infection outcomes has been recently reviewed (Vivarini and Lopes, 2019). NRF2 antioxidant pathway is activated in response to different *Leishmania* species even if differences are observed between species. Indeed, *Leishmania amazoniensis* but also *Leishmania brasiliensis*, induce *in vitro*, NRF2 expression, *via* protein kinase R signaling (Barreto-de-Souza et al., 2015; Vivarini et al., 2017), a result confirmed in skin biopsies from *Leishmania* infected patients. Treatment of *L. major* infected BALB/c mice with NAC, a Nrf2 inducer, reduces the parasitism in their footpads (Rocha-Vieira et al., 2003), whereas depletion of glutathione, increases the burden in the footpads of C57BL/6 mice infected with *L. major* (Cruz et al., 2008). However, for *L. amazoniensis*, the Nrf2 knockdown that promotes oxidative stress, impairs parasite survival in macrophages (Vivarini et al., 2017).

Whereas NRF2-induced anti-oxidant genes, HO-1, is required for protection against *Toxoplasma gondii* (Araujo et al., 2013), antioxidative enzymes such SOD1 and HO-1, favor the establishment of *Leishmania* infection. Indeed, *L. pifanoi* amastigotes and *L. chagasi* infection induce in macrophages an increased expression of HO-1 that promotes *Leishmania* persistence (Pham et al., 2005; Luz et al., 2012). Moreover, in mouse peritoneal and human macrophages lineages, infection by *L. amazonensis* leads to the increase of SOD1 expression in a PKR/Nrf2-dependent manner (Vivarini et al., 2017). SOD1 reduces the *Leishmania* oxidative stress and may promote the parasite survival and affect the outcome of the infection (Khouri et al., 2009; Khouri et al., 2010).

CONCLUSION AND PERSPECTIVES

In recent years much progress has been made in immunometabolism and there is a growing understanding of how metabolic pathways are regulated to support or direct functional changes in immune cells, controlling immunity and inflammation. Metabolic signature of immune cells including macrophages is now known to change depending on stages of development, activation state and pathological conditions. A better understanding of the metabolic mechanisms and metabolic needs of immune cells, as well as the interactions that underlie the complex metabolic and immune networks, is essential to develop promising drugs with effective metabolic interventions that enhance immune cell response.

In the context of anticancer immunotherapy, drugs targeting cancer metabolism might synergistically enhance immunotherapy *via* metabolic reprogramming of the tumor microenvironment. Different combinations of metabolic agents and immunotherapies are already in clinical trials (Li et al., 2019). Deciphering the intricate interaction existent between metabolic reprogramming and immune response has also promising therapeutic application for inflammatory and autoimmune diseases. Different small molecules targeting metabolic processes in immune cells as a strategy to limit inflammation and change the outcome of inflammatory and autoimmune diseases are currently in use clinically (Pålsson-McDermott and O'Neill, 2020). Hence, the majority of available or under development anti-rheumatic drugs, target various metabolites in immune cells belonging to purine, pyrimidine or GSH metabolism (Piranavan et al., 2020). The host directed therapies includes different promising treatment strategies targeting macrophages' polarization to the M2 phenotype that have been found associated with atherosclerosis regression and different compound are being tested to develop more efficient antiatherosclerosis therapy (Bi et al., 2019). Infectious diseases are more complex pathologies given the additional interactions that take place between the host cell and the pathogen. Host directed therapy (HDT) targeting metabolic pathway could represent new therapeutic strategies to fight infectious diseases in the face of emergence of antimicrobial resistance or compromised host immunity. Indeed, recent studies suggest that foamy macrophages, the major contributors to Tuberculosis pathogenesis, and lipid metabolism are promising targets for HDT against Tuberculosis (Shim et al., 2020). Macrophage polarization is also an important tool in the physiopathology of leishmaniasis (Tomiotto-Pellissier et al., 2018) and targeting metabolic pathway, once a better understanding of the balance required to develop a protective response is gained, might potentially change the outcome of the infection.

Targeting transcription factors could be another promising therapeutic strategy. Indeed, deregulation of transcription factors is a common feature to the majority of human cancers and is involved in a large number of human diseases (Papavassiliou and Papavassiliou, 2016). A better understanding of the pathologies, of the mechanisms of transcriptional regulation and their precise function as well as the development of new technologies (Hagenbuchner and Ausserlechner, 2016; Hecker and Wagner, 2017; Becskei, 2020), has allowed the development of novel therapeutic strategies that target transcription factors. Different small molecules that interact in various way with transcription factors to modulate their expression, degradation, interaction with DNA or other proteins, are actually used or evaluated for cancer treatment (Lambert et al., 2018). Agents targeting transcription factors for the treatment of chronic kidney disease are under clinical trial (Hishikawa et al., 2018). Transcription factors induced in response to *Leishmania* infection play crucial role in regulating immune and metabolic responses and hence macrophage polarization. Almost all the transcription factors involved in the macrophage immune and metabolic response to *Leishmania* infection have been described as therapeutic target in different diseases including infectious ones. These includes HIF that couple immunity with metabolism (Bhandari and Nizet, 2014; Santos and Andrade, 2017), nuclear receptors in metabolic, inflammatory and infectious diseases (Rudraiah et al., 2016; Wang et al., 2017; Mirza et al., 2019) and NRF2 in cancer (Lu et al., 2016). Despite the challenges that remain to be overcome (delivery methods, compensatory and pleiotropic effects), targeting transcription factors could represent new therapeutic strategies to reprogram the macrophage response in order to amplify the microbicidal activity that should allow the fight against infectious diseases while preventing an exacerbated immune response leading to a worsening of the lesions.

AUTHOR CONTRIBUTIONS

All authors contributed to the article and approved the submitted version.

ACKNOWLEDGMENTS

Continuous support by the Tunisian Ministry of higher Education is gratefully acknowledged. Our warmest thanks to Dr. R. Herwig and Dr. M. Essefi for their critical reading of the manuscript.

REFERENCES

Abu-Dayyeh, I., Hassani, K., Westra, E. R., Mottram, J. C., and Olivier, M. (2010). Comparative study of the ability of Leishmania mexicana promastigotes and amastigotes to alter macrophage signaling and functions. *Infect. Immun.* 78, 2438–2445. doi: 10.1128/IAI.00812-09

Araujo, E. C. B., Barbosa, B. F., Coutinho, L. B., Barenco, P. V. C., Sousa, L. A., Milanezi, C. M., et al. (2013). Heme oxygenase-1 activity is involved in the control of Toxoplasma gondii infection in the lung of BALB/c and C57BL/6 and in the small intestine of C57BL/6 mice. *Vet. Res.* 44, 89. doi: 10.1186/1297-9716-44-89

Arrais-Silva, W. W., Paffaro, V. A., Yamada, A. T., and Giorgio, S. (2005). Expression of hypoxia-inducible factor-1alpha in the cutaneous lesions of BALB/c mice infected with Leishmania amazonensis. *Exp. Mol. Pathol.* 78, 49–54. doi: 10.1016/j.yexmp.2004.09.002

Barreto-de-Souza, V., Ferreira, P. L. C., Vivarini, A. C., Calegari-Silva, T., Soares, D. C., Regis, E. G., et al. (2015). IL-27 enhances Leishmania amazonensis infection via ds-RNA dependent kinase (PKR) and IL-10 signaling. *Immunobiology* 220, 437–444. doi: 10.1016/j.imbio.2014.11.006

Becskei, A. (2020). Tuning up Transcription Factors for Therapy. *Molecules Basel Switz* 25, 1902. doi: 10.3390/molecules25081902

Bellezza, I., Giambanco, I., Minelli, A., and Donato, R. (2018). Nrf2-Keap1 signaling in oxidative and reductive stress. *Biochim. Biophys. Acta Mol. Cell Res.* 1865, 721–733. doi: 10.1016/j.bbamcr.2018.02.010

Bertholet, S., Dickensheets, H. L., Sheikh, F., Gam, A. A., Donnelly, R. P., and Kenney, R. T. (2003). Leishmania donovani-induced expression of suppressor of cytokine signaling 3 in human macrophages: a novel mechanism for intracellular parasite suppression of activation. *Infect. Immun.* 71, 2095–2101. doi: 10.1128/iai.71.4.2095-2101.2003

Bhandari, T., and Nizet, V. (2014). Hypoxia-Inducible Factor (HIF) as a Pharmacological Target for Prevention and Treatment of Infectious Diseases. *Infect. Dis. Ther.* 3, 159–174. doi: 10.1007/s40121-014-0030-1

Bhattacharjee, A., Majumder, S., Das, S., Ghosh, S., Biswas, S., and Majumdar, S. (2016). Leishmania donovani-Induced Prostaglandin E2 Generation Is Critically Dependent on Host Toll-Like Receptor 2-Cytosolic Phospholipase A2 Signaling. *Infect. Immun.* 84, 2963–2973. doi: 10.1128/IAI.00528-16

Bi, Y., Chen, J., Hu, F., Liu, J., Li, M., and Zhao, L. (2019). M2 Macrophages as a Potential Target for Antiatherosclerosis Treatment. *Neural Plast.* 2019:6724903. doi: 10.1155/2019/6724903

Bishop, T., and Ratcliffe, P. J. (2014). Signaling hypoxia by hypoxia-inducible factor protein hydroxylases: a historical overview and future perspectives. *Hypoxia Auckl NZ* 2, 197–213. doi: 10.2147/HP.S47598

Blanchette, J., Racette, N., Faure, R., Siminovitch, K. A., and Olivier, M. (1999). Leishmania-induced increases in activation of macrophage SHP-1 tyrosine phosphatase are associated with impaired IFN-gamma-triggered JAK2 activation. *Eur. J. Immunol.* 29, 3737–3744. doi: 10.1002/(SICI)1521-4141(199911)29:11<3737::AID-IMMU3737>3.0.CO;2-S

Boone, D. L., Turer, E. E., Lee, E. G., Ahmad, R.-C., Wheeler, M. T., Tsui, C., et al. (2004). The ubiquitin-modifying enzyme A20 is required for termination of Toll-like receptor responses. *Nat. Immunol.* 5, 1052–1060. doi: 10.1038/ni1110

Bouhlel, M. A., Derudas, B., Rigamonti, E., Dièvart, R., Brozek, J., Haulon, S., et al. (2007). PPARgamma activation primes human monocytes into alternative M2 macrophages with anti-inflammatory properties. *Cell Metab.* 6, 137–143. doi: 10.1016/j.cmet.2007.06.010

Buates, S., and Matlashewski, G. (2001). General Suppression of Macrophage Gene Expression During *Leishmania donovani* Infection. *J. Immunol.* 166, 3416–3422. doi: 10.4049/jimmunol.166.5.3416

Bullen, D. V. R., Hansen, D. S., Siomos, M.-A. V., Schofield, L., Alexander, W. S., and Handman, E. (2003a). The lack of suppressor of cytokine signalling-1 (SOCS1) protects mice from the development of cerebral malaria caused by Plasmodium berghei ANKA. *Parasite Immunol.* 25, 113–118. doi: 10.1046/j.1365-3024.2003.00616.x

Bullen, D. V. R., Baldwin, T. M., Curtis, J. M., Alexander, W. S., and Handman, E. (2003b). Persistence of lesions in suppressor of cytokine signaling-1-deficient mice infected with Leishmania major. *J. Immunol. Baltim Md 1950* 170, 4267–4272. doi: 10.4049/jimmunol.170.8.4267

Calegari-Silva, T. C., Vivarini, Á. C, Miqueline, M., Dos Santos, G. R. R. M., Teixeira, K. L., Saliba, A. M., et al. (2015). The human parasite Leishmania amazonensis downregulates iNOS expression via NF-κB p50/p50 homodimer: role of the PI3K/Akt pathway. *Open Biol.* 5, 150118. doi: 10.1098/rsob.150118

Cantó, C., Jiang, L. Q., Deshmukh, A. S., Mataki, C., Coste, A., Lagouge, M., et al. (2010). Interdependence of AMPK and SIRT1 for metabolic adaptation to fasting and exercise in skeletal muscle. *Cell Metab.* 11, 213–219. doi: 10.1016/j.cmet.2010.02.006

Caradonna, K. L., Engel, J. C., Jacobi, D., Lee, C.-H., and Burleigh, B. A. (2013). Host metabolism regulates intracellular growth of Trypanosoma cruzi. *Cell Host Microbe* 13, 108–117. doi: 10.1016/j.chom.2012.11.011

Castrillo, A., Joseph, S. B., Marathe, C., Mangelsdorf, D. J., and Tontonoz, P. (2003). Liver X receptor-dependent repression of matrix metalloproteinase-9 expression in macrophages. *J. Biol. Chem.* 278, 10443–10449. doi: 10.1074/jbc.M213071200

Chan, M. M., Adapala, N., and Chen, C. (2012). Peroxisome Proliferator-Activated Receptor-γ-Mediated Polarization of Macrophages in Leishmania Infection. *PPAR Res.* 2012, 796235. doi: 10.1155/2012/796235

Chandrakar, P., Parmar, N., Descoteaux, A., and Kar, S. (2020). Differential Induction of SOCS Isoforms by Leishmania donovani Impairs Macrophage-T Cell Cross-Talk and Host Defense. *J. Immunol. Baltim Md 1950* 204, 596–610. doi: 10.4049/jimmunol.1900412

Charmoy, M., Hurrell, B. P., Romano, A., Lee, S. H., Ribeiro-Gomes, F., Riteau, N., et al. (2016). The Nlrp3 inflammasome, IL-1β, and neutrophil recruitment are required for susceptibility to a nonhealing strain of Leishmania major in C57BL/6 mice. *Eur. J. Immunol.* 46, 897–911. doi: 10.1002/eji.201546015

Charpentier, T., Hammami, A., and Stäger, S. (2016). Hypoxia inducible factor 1α: A critical factor for the immune response to pathogens and Leishmania. *Cell Immunol.* 309, 42–49. doi: 10.1016/j.cellimm.2016.06.002

Chauhan, P., and Saha, B. (2018). Metabolic regulation of infection and inflammation. *Cytokine* 112, 1–11. doi: 10.1016/j.cyto.2018.11.016

Chaussabel, D., Semnani, R. T., McDowell, M. A., Sacks, D., Sher, A., and Nutman, T. B. (2003). Unique gene expression profiles of human macrophages and dendritic cells to phylogenetically distinct parasites. *Blood* 102, 672–681. doi: 10.1182/blood-2002-10-3232

Colonna, M. (2007). TLR pathways and IFN-regulatory factors: to each its own. *Eur. J. Immunol.* 37, 306–309. doi: 10.1002/eji.200637009

Cramer, T., Yamanishi, Y., Clausen, B. E., Förster, I., Pawlinski, R., Mackman, N., et al. (2003). HIF-1alpha is essential for myeloid cell-mediated inflammation. *Cell* 112, 645–657. doi: 10.1016/s0092-8674(03)00154-5

Cruz, K. K., Fonseca, S. G., Monteiro, M. C., Silva, O. S., Andrade, V. M., Cunha, F. Q., et al. (2008). The influence of glutathione modulators on the course of Leishmania major infection in susceptible and resistant mice. *Parasite Immunol.* 30, 171–174. doi: 10.1111/j.1365-3024.2007.01014.x

Dalpke, A., Heeg, K., Bartz, H., and Baetz, A. (2008). Regulation of innate immunity by suppressor of cytokine signaling (SOCS) proteins. *Immunobiology* 213, 225–235. doi: 10.1016/j.imbio.2007.10.008

de Veer, M. J., Curtis, J. M., Baldwin, T. M., DiDonato, J. A., Sexton, A., McConville, M. J., et al. (2003). MyD88 is essential for clearance of Leishmania major: possible role for lipophosphoglycan and Toll-like receptor 2 signaling. *Eur. J. Immunol.* 33, 2822–2831. doi: 10.1002/eji.200324128

Debus, A., Gläsner, J., Röllinghoff, M., and Gessner, A. (2003). High levels of susceptibility and T helper 2 response in MyD88-deficient mice infected with Leishmania major are interleukin-4 dependent. *Infect. Immun.* 71, 7215–7218. doi: 10.1128/iai.71.12.7215-7218.2003

Degrossoli, A., Bosetto, M. C., Lima, C. B. C., and Giorgio, S. (2007). Expression of hypoxia-inducible factor 1alpha in mononuclear phagocytes infected with Leishmania amazonensis. *Immunol. Lett.* 114, 119–125. doi: 10.1016/j.imlet.2007.09.009

Delerive, P., Fruchart, J. C., and Staels, B. (2001). Peroxisome proliferator-activated receptors in inflammation control. *J. Endocrinol.* 169, 453–459. doi: 10.1677/joe.0.1690453

Devraj, G., Beerlage, C., Brüne, B., and Kempf, V. A. J. (2017). Hypoxia and HIF-1 activation in bacterial infections. *Microbes Infect.* 19, 144–156. doi: 10.1016/j.micinf.2016.11.003

Díaz-Gandarilla, J. A., Osorio-Trujillo, C., Hernández-Ramírez, V. I., and Talamás-Rohana, P. (2013). PPAR activation induces M1 macrophage polarization via cPLA$_2$-COX-2 inhibition, activating ROS production against

Leishmania mexicana. *BioMed. Res. Int.* 2013:215283. doi: 10.1155/2013/215283

Ding, L., Yuan, X., Yan, J., Huang, Y., Xu, M., Yang, Z., et al. (2019). Nrf2 exerts mixed inflammation and glucose metabolism regulatory effects on murine RAW264.7 macrophages. *Int. Immunopharmacol.* 71, 198–204. doi: 10.1016/j.intimp.2019.03.023

D'Ignazio, L., Bandarra, D., and Rocha, S. (2016). NF-κB and HIF crosstalk in immune responses. *FEBS J.* 283, 413–424. doi: 10.1111/febs.13578

Eisele, P. S., Salatino, S., Sobek, J., Hottiger, M. O., and Handschin, C. (2013). The peroxisome proliferator-activated receptor γ coactivator 1α/β (PGC-1) coactivators repress the transcriptional activity of NF-κB in skeletal muscle cells. *J. Biol. Chem.* 288, 2246–2260. doi: 10.1074/jbc.M112.375253

Feige, J. N., and Auwerx, J. (2007). Transcriptional coregulators in the control of energy homeostasis. *Trends Cell Biol.* 17, 292–301. doi: 10.1016/j.tcb.2007.04.001

Ferrante, C. J., and Leibovich, S. J. (2012). Regulation of Macrophage Polarization and Wound Healing. *Adv. Wound Care* 1, 10–16. doi: 10.1089/wound.2011.0307

Forget, G., Gregory, D. J., and Olivier, M. (2005). Proteasome-mediated degradation of STAT1alpha following infection of macrophages with Leishmania donovani. *J. Biol. Chem.* 280, 30542–30549. doi: 10.1074/jbc.M414126200

Forget, G., Gregory, D. J., Whitcombe, L. A., and Olivier, M. (2006). Role of host protein tyrosine phosphatase SHP-1 in Leishmania donovani-induced inhibition of nitric oxide production. *Infect. Immun.* 74, 6272–6279. doi: 10.1128/IAI.00853-05

Gallardo-Soler, A., Gómez-Nieto, C., Campo, M. L., Marathe, C., Tontonoz, P., Castrillo, A., et al. (2008). Arginase I induction by modified lipoproteins in macrophages: a peroxisome proliferator-activated receptor-gamma/delta-mediated effect that links lipid metabolism and immunity. *Mol. Endocrinol. Baltim Md* 22, 1394–1402. doi: 10.1210/me.2007-0525

Ghisletti, S., Huang, W., Jepsen, K., Benner, C., Hardiman, G., Rosenfeld, M. G., et al. (2009). Cooperative NCoR/SMRT interactions establish a corepressor-based strategy for integration of inflammatory and anti-inflammatory signaling pathways. *Genes Dev.* 23, 681–693. doi: 10.1101/gad.1773109

Giese, N. A., Gabriele, L., Doherty, T. M., Klinman, D. M., Tadesse-Heath, L., Contursi, C., et al. (1997). Interferon (IFN) consensus sequence-binding protein, a transcription factor of the IFN regulatory factor family, regulates immune responses in vivo through control of interleukin 12 expression. *J. Exp. Med.* 186, 1535–1546. doi: 10.1084/jem.186.9.1535

Grigoriadis, G., Zhan, Y., Grumont, R. J., Metcalf, D., Handman, E., Cheers, C., et al. (1996). The Rel subunit of NF-kappaB-like transcription factors is a positive and negative regulator of macrophage gene expression: distinct roles for Rel in different macrophage populations. *EMBO J.* 15, 7099–7107. doi: 10.1002/j.1460-2075.1996.tb01101.x

Guizani-Tabbane, L., Ben-Aissa, K., Belghith, M., Sassi, A., and Dellagi, K. (2004). Leishmania major amastigotes induce p50/c-Rel NF-kappa B transcription factor in human macrophages: involvement in cytokine synthesis. *Infect. Immun.* 72, 2582–2589. doi: 10.1128/iai.72.5.2582-2589.2004

Gupta, A. K., Ghosh, K., Palit, S., Barua, J., Das, P. K., and Ukil, A. (2017). Leishmania donovani inhibits inflammasome-dependent macrophage activation by exploiting the negative regulatory proteins A20 and UCP2. *FASEB J.* 31, 5087–5101. doi: 10.1096/fj.201700407R

Gurung, P., and Kanneganti, T.-D. (2015). Innate immunity against Leishmania infections. *Cell Microbiol.* 17, 1286–1294. doi: 10.1111/cmi.12484

Hagenbuchner, J., and Ausserlechner, M. J. (2016). Targeting transcription factors by small compounds–Current strategies and future implications. *Biochem. Pharmacol.* 107, 1–13. doi: 10.1016/j.bcp.2015.12.006

Hashidate-Yoshida, T., Harayama, T., Hishikawa, D., Morimoto, R., Hamano, F., Tokuoka, S. M., et al. (2015). Fatty acid remodeling by LPCAT3 enriches arachidonate in phospholipid membranes and regulates triglyceride transport. *eLife* 4, e06328. doi: 10.7554/eLife.06328

Hecker, M., and Wagner, A. H. (2017). Transcription factor decoy technology: A therapeutic update. *Biochem. Pharmacol.* 144, 29–34. doi: 10.1016/j.bcp.2017.06.122

Hishikawa, A., Hayashi, K., and Itoh, H. (2018). Transcription Factors as Therapeutic Targets in Chronic Kidney Disease. *Molecules Basel Switz* 23, 1123. doi: 10.3390/molecules23051123

Honda, K., Yanai, H., Negishi, H., Asagiri, M., Sato, M., Mizutani, T., et al. (2005). IRF-7 is the master regulator of type-I interferon-dependent immune responses. *Nature* 434, 772–777. doi: 10.1038/nature03464

Ingram, S., Mengozzi, M., Sacre, S., Mullen, L., and Ghezzi, P. (2019). Differential induction of nuclear factor-like 2 signature genes with toll-like receptor stimulation. *Free Radic. Biol. Med.* 135, 245–250. doi: 10.1016/j.freeradbiomed.2019.03.018

Jantsch, J., and Schödel, J. (2015). Hypoxia and hypoxia-inducible factors in myeloid cell-driven host defense and tissue homeostasis. *Immunobiology* 220, 305–314. doi: 10.1016/j.imbio.2014.09.009

Jenner, R. G., and Young, R. A. (2005). Insights into host responses against pathogens from transcriptional profiling. *Nat. Rev. Microbiol.* 3, 281–294. doi: 10.1038/nrmicro1126

Joseph, S. B., Castrillo, A., Laffitte, B. A., Mangelsdorf, D. J., and Tontonoz, P. (2003). Reciprocal regulation of inflammation and lipid metabolism by liver X receptors. *Nat. Med.* 9, 213–219. doi: 10.1038/nm820

Joseph, S. B., Bradley, M. N., Castrillo, A., Bruhn, K. W., Mak, P. A., Pei, L., et al. (2004). LXR-dependent gene expression is important for macrophage survival and the innate immune response. *Cell* 119, 299–309. doi: 10.1016/j.cell.2004.09.032

Jung, K.-A., and Kwak, M.-K. (2010). The Nrf2 system as a potential target for the development of indirect antioxidants. *Molecules Basel Switz* 15, 7266–7291. doi: 10.3390/molecules15107266

Kadl, A., Meher, A. K., Sharma, P. R., Lee, M. Y., Doran, A. C., Johnstone, S. R., et al. (2010). Identification of a novel macrophage phenotype that develops in response to atherogenic phospholipids via Nrf2. *Circ. Res.* 107, 737–746. doi: 10.1161/CIRCRESAHA.109.215715

Kang, K. W., Lee, S. J., Park, J. W., and Kim, S. G. (2002). Phosphatidylinositol 3-kinase regulates nuclear translocation of NF-E2-related factor 2 through actin rearrangement in response to oxidative stress. *Mol. Pharmacol.* 62, 1001–1010. doi: 10.1124/mol.62.5.1001

Kauppinen, A., Suuronen, T., Ojala, J., Kaarniranta, K., and Salminen, A. (2013). Antagonistic crosstalk between NF-κB and SIRT1 in the regulation of inflammation and metabolic disorders. *Cell Signal* 25, 1939–1948. doi: 10.1016/j.cellsig.2013.06.007

Kawai, T., and Akira, S. (2007). TLR signaling. *Semin. Immunol.* 19, 24–32. doi: 10.1016/j.smim.2006.12.004

Kawashima, A., Oda, Y., Yachie, A., Koizumi, S., and Nakanishi, I. (2002). Heme oxygenase-1 deficiency: the first autopsy case. *Hum. Pathol.* 33, 125–130. doi: 10.1053/hupa.2002.30217

Ke, Q., and Costa, M. (2006). Hypoxia-inducible factor-1 (HIF-1). *Mol. Pharmacol.* 70, 1469–1480. doi: 10.1124/mol.106.027029

Kelly, B., and O'Neill, L. A. (2015). Metabolic reprogramming in macrophages and dendritic cells in innate immunity. *Cell Res.* 25, 771–784. doi: 10.1038/cr.2015.68

Khouri, R., Bafica, A., Silva M da, P. P., Noronha, A., Kolb, J.-P., Wietzerbin, J., et al. (2009). IFN-beta impairs superoxide-dependent parasite killing in human macrophages: evidence for a deleterious role of SOD1 in cutaneous leishmaniasis. *J. Immunol. Baltim Md 1950* 182, 2525–2531. doi: 10.4049/jimmunol.0802860

Khouri, R., Novais, F., Santana, G., de Oliveira, C. I., Vannier dos Santos, M. A., Barral, A., et al. (2010). DETC induces Leishmania parasite killing in human in vitro and murine in vivo models: a promising therapeutic alternative in Leishmaniasis. *PloS One* 5, e14394. doi: 10.1371/journal.pone.0014394

Kim, J., Cha, Y.-N., and Surh, Y.-J. (2010). A protective role of nuclear factor-erythroid 2-related factor-2 (Nrf2) in inflammatory disorders. *Mutat. Res.* 690, 12–23. doi: 10.1016/j.mrfmmm.2009.09.007

Knight, M., and Stanley, S. (2019). HIF-1α as a central mediator of cellular resistance to intracellular pathogens. *Curr. Opin. Immunol.* 60, 111–116. doi: 10.1016/j.coi.2019.05.005

Koo, S.-J., Szczesny, B., Wan, X., Putluri, N., and Garg, N. J. (2018). Pentose Phosphate Shunt Modulates Reactive Oxygen Species and Nitric Oxide Production Controlling Trypanosoma cruzi in Macrophages. *Front. Immunol.* 9:202. doi: 10.3389/fimmu.2018.00202

Korf, H., Vander Beken, S., Romano, M., Steffensen, K. R., Stijlemans, B., Gustafsson, J.-A., et al. (2009). Liver X receptors contribute to the protective immune response against Mycobacterium tuberculosis in mice. *J. Clin. Invest.* 119, 1626–1637. doi: 10.1172/JCI35288

Kostadinova, R., Wahli, W., and Michalik, L. (2005). PPARs in diseases: control mechanisms of inflammation. *Curr. Med. Chem.* 12, 2995–3009. doi: 10.2174/092986705774462905

Kropf, P., Freudenberg, N., Kalis, C., Modolell, M., Herath, S., Galanos, C., et al. (2004). Infection of C57BL/10ScCr and C57BL/10ScNCr mice with Leishmania major reveals a role for Toll-like receptor 4 in the control of parasite replication. *J. Leukoc. Biol.* 76, 48–57. doi: 10.1189/jlb.1003484

Lambert, M., Jambon, S., Depauw, S., and David-Cordonnier, M.-H. (2018). Targeting Transcription Factors for Cancer Treatment. *Molecules Basel Switz* 23, 1479. doi: 10.3390/molecules23061479

Lan, F., Cacicedo, J. M., Ruderman, N., and Ido, Y. (2008). SIRT1 modulation of the acetylation status, cytosolic localization, and activity of LKB1. Possible role in AMP-activated protein kinase activation. *J. Biol. Chem.* 283, 27628–27635. doi: 10.1074/jbc.M805711200

Lecoeur, H., Prina, E., Rosazza, T., Kokou, K., N'Diaye, P., Aulner, N., et al. (2020). Targeting Macrophage Histone H3 Modification as a Leishmania Strategy to Dampen the NF-κB/NLRP3-Mediated Inflammatory Response. *Cell Rep.* 30, 1870–1882.e4. doi: 10.1016/j.celrep.2020.01.030

Lefèvre, L., Lugo-Villarino, G., Meunier, E., Valentin, A., Olagnier, D., Authier, H., et al. (2013). The C-type lectin receptors dectin-1, MR, and SIGNR3 contribute both positively and negatively to the macrophage response to Leishmania infantum. *Immunity* 38, 1038–1049. doi: 10.1016/j.immuni.2013.04.010

Leopold Wager, C. M., Arnett, E., and Schlesinger, L. S. (2019). Macrophage nuclear receptors: Emerging key players in infectious diseases. *PloS Pathog.* 15, e1007585. doi: 10.1371/journal.ppat.1007585

Li, X., Wenes, M., Romero, P., Huang, S. C.-C., Fendt, S.-M., and Ho, P.-C. (2019). Navigating metabolic pathways to enhance antitumour immunity and immunotherapy. *Nat. Rev. Clin. Oncol.* 16, 425–441. doi: 10.1038/s41571-019-0203-7

Liese, J., Schleicher, U., and Bogdan, C. (2007). TLR9 signaling is essential for the innate NK cell response in murine cutaneous leishmaniasis. *Eur. J. Immunol.* 37, 3424–3434. doi: 10.1002/eji.200737182

Lima-Junior, D. S., Costa, D. L., Carregaro, V., Cunha, L. D., Silva, A. L. N., Mineo, T. W. P., et al. (2013). Inflammasome-derived IL-1β production induces nitric oxide-mediated resistance to Leishmania. *Nat. Med.* 19, 909–915. doi: 10.1038/nm.3221

Lohoff, M., Ferrick, D., Mittrucker, H. W., Duncan, G. S., Bischof, S., Rollinghoff, M., et al. (1997). Interferon regulatory factor-1 is required for a T helper 1 immune response in vivo. *Immunity* 6, 681–689. doi: 10.1016/s1074-7613(00)80444-6

Lohoff, M., Duncan, G. S., Ferrick, D., Mittrücker, H. W., Bischof, S., Prechtl, S., et al. (2000). Deficiency in the transcription factor interferon regulatory factor (IRF)-2 leads to severely compromised development of natural killer and T helper type 1 cells. *J. Exp. Med.* 192, 325–336. doi: 10.1084/jem.192.3.325

Lu, M.-C., Ji, J.-A., Jiang, Z.-Y., and You, Q.-D. (2016). The Keap1-Nrf2-ARE Pathway As a Potential Preventive and Therapeutic Target: An Update. *Med. Res. Rev.* 36, 924–963. doi: 10.1002/med.21396

Luz, N. F., Andrade, B. B., Feijó, D. F., Araújo-Santos, T., Carvalho, G. Q., Andrade, D., et al. (2012). Heme oxygenase-1 promotes the persistence of Leishmania chagasi infection. *J. Immunol. Baltim Md 1950* 188, 4460–4467. doi: 10.4049/jimmunol.1103072

Mahlknecht, U., and Voelter-Mahlknecht, S. (2009). Chromosomal characterization and localization of the NAD+-dependent histone deacetylase gene sirtuin 1 in the mouse. *Int. J. Mol. Med.* 23, 245–252. doi: 10.3892/ijmm_00000123

Mahnke, A., Meier, R. J., Schatz, V., Hofmann, J., Castiglione, K., Schleicher, U., et al. (2014). Hypoxia in Leishmania major skin lesions impairs the NO-dependent leishmanicidal activity of macrophages. *J. Invest. Dermatol.* 134, 2339–2346. doi: 10.1038/jid.2014.121

Mai, L. T., Smans, M., Silva-Barrios, S., Fabié, A., and Stäger, S. (2019). IRF-5 Expression in Myeloid Cells Is Required for Splenomegaly in L. donovani Infected Mice. *Front. Immunol.* 10:3071. doi: 10.3389/fimmu.2019.03071

Marín-Hernández, A., Gallardo-Pérez, J. C., Ralph, S. J., Rodríguez-Enríquez, S., and Moreno-Sánchez, R. (2009). HIF-1alpha modulates energy metabolism in cancer cells by inducing over-expression of specific glycolytic isoforms. *Mini Rev. Med. Chem.* 9, 1084–1101. doi: 10.2174/138955709788922610

Matte, C., and Descoteaux, A. (2010). Leishmania donovani Amastigotes Impair Gamma Interferon-Induced STAT1α Nuclear Translocation by Blocking the Interaction between STAT1α and Importin-α5. *Infect. Immun.* 78, 3736–3743. doi: 10.1128/IAI.00046-10

Meraz, M. A., White, J. M., Sheehan, K. C., Bach, E. A., Rodig, S. J., Dighe, A. S., et al. (1996). Targeted disruption of the Stat1 gene in mice reveals unexpected physiologic specificity in the JAK-STAT signaling pathway. *Cell* 84, 431–442. doi: 10.1016/s0092-8674(00)81288-x

Mesquita, I., Ferreira, C., Moreira, D., Kluck, G. E. G., Barbosa, A. M., Torrado, E., et al. (2020). The Absence of HIF-1α Increases Susceptibility to Leishmania donovani Infection via Activation of BNIP3/mTOR/SREBP-1c Axis. *Cell Rep.* 30, 4052–4064.e7. doi: 10.1016/j.celrep.2020.02.098

Metheni, M., Echebli, N., Chaussepied, M., Ransy, C., Chéreau, C., Jensen, K., et al. (2014). The level of H_2O_2 type oxidative stress regulates virulence of Theileria-transformed leukocytes. *Cell Microbiol.* 16, 269–279. doi: 10.1111/cmi.12218

Mirza, A. Z., Althagafi, I. I., and Shamshad, H. (2019). Role of PPAR receptor in different diseases and their ligands: Physiological importance and clinical implications. *Eur. J. Med. Chem.* 166, 502–513. doi: 10.1016/j.ejmech.2019.01.067

Mise-Omata, S., Kuroda, E., Sugiura, T., Yamashita, U., Obata, Y., and Doi, T. S. (2009). The NF-kappaB RelA subunit confers resistance to Leishmania major by inducing nitric oxide synthase 2 and Fas expression but not Th1 differentiation. *J. Immunol. Baltim Md 1950* 182, 4910–4916. doi: 10.4049/jimmunol.0800967

Moreira, D., Rodrigues, V., Abengozar, M., Rivas, L., Rial, E., Laforge, M., et al. (2015). Leishmania infantum modulates host macrophage mitochondrial metabolism by hijacking the SIRT1-AMPK axis. *PloS Pathog.* 11, e1004684. doi: 10.1371/journal.ppat.1004684

Muraille, E., De Trez, C., Brait, M., De Baetselier, P., Leo, O., and Carlier, Y. (2003). Genetically resistant mice lacking MyD88-adapter protein display a high susceptibility to Leishmania major infection associated with a polarized Th2 response. *J. Immunol. Baltim Md 1950* 170, 4237–4241. doi: 10.4049/jimmunol.170.8.4237

Murray, P. J. (2017). Macrophage Polarization. *Annu. Rev. Physiol.* 79, 541–566. doi: 10.1146/annurev-physiol-022516-034339

Muxel, S. M., Aoki, J. I., Fernandes, J. C. R., Laranjeira-Silva, M. F., Zampieri, R. A., Acuña, S. M., et al. (2017). Arginine and Polyamines Fate in Leishmania Infection. *Front. Microbiol.* 8:2682. doi: 10.3389/fmicb.2017.02682

Naderer, T., Heng, J., and McConville, M. J. (2010). Evidence that intracellular stages of Leishmania major utilize amino sugars as a major carbon source. *PloS Pathog.* 6, e1001245. doi: 10.1371/journal.ppat.1001245

Nagao, A., Kobayashi, M., Koyasu, S., Chow, C. C. T., and Harada, H. (2019). HIF-1-Dependent Reprogramming of Glucose Metabolic Pathway of Cancer Cells and Its Therapeutic Significance. *Int. J. Mol. Sci.* 20, 238. doi: 10.3390/ijms20020238

Naito, Y., Takagi, T., and Higashimura, Y. (2014). Heme oxygenase-1 and anti-inflammatory M2 macrophages. *Arch. Biochem. Biophys.* 564, 83–88. doi: 10.1016/j.abb.2014.09.005

Nandan, D., and Reiner, N. E. (1995). Attenuation of gamma interferon-induced tyrosine phosphorylation in mononuclear phagocytes infected with Leishmania donovani: selective inhibition of signaling through Janus kinases and Stat1. *Infect. Immun.* 63, 4495–4500. doi: 10.1128/IAI.63.11.4495-4500.1995

Natoli, G. (2009). When sirtuins and NF-kappaB collide. *Cell* 136, 19–21. doi: 10.1016/j.cell.2008.12.034

Negishi, H., Ohba, Y., Yanai, H., Takaoka, A., Honma, K., Yui, K., et al. (2005). Negative regulation of Toll-like-receptor signaling by IRF-4. *Proc. Natl. Acad. Sci. U.S.A.* 102, 15989–15994. doi: 10.1073/pnas.0508327102

Negishi, H., Fujita, Y., Yanai, H., Sakaguchi, S., Ouyang, X., Shinohara, M., et al. (2006). Evidence for licensing of IFN-gamma-induced IFN regulatory factor 1 transcription factor by MyD88 in Toll-like receptor-dependent gene induction program. *Proc. Natl. Acad. Sci. U.S.A.* 103, 15136–15141. doi: 10.1073/pnas.0607181103

Odegaard, J. I., Ricardo-Gonzalez, R. R., Goforth, M. H., Morel, C. R., Subramanian, V., Mukundan, L., et al. (2007). Macrophage-specific PPARgamma controls alternative activation and improves insulin resistance. *Nature* 447, 1116–1120. doi: 10.1038/nature05894

Olagnier, D., Lavergne, R.-A., Meunier, E., Lefèvre, L., Dardenne, C., Aubouy, A., et al. (2011). Nrf2, a PPARγ alternative pathway to promote CD36 expression on inflammatory macrophages: implication for malaria. *PloS Pathog.* 7, e1002254. doi: 10.1371/journal.ppat.1002254

Osorio y Fortea, J., de La Llave, E., Regnault, B., Coppee, J.-Y., Milon, G., Lang, T., et al. (2009). Transcriptional signatures of BALB/c mouse macrophages housing multiplying Leishmania amazonensis amastigotes. *BMC Genomics* 10:119. doi: 10.1186/1471-2164-10-119

Paine, A., Eiz-Vesper, B., Blasczyk, R., and Immenschuh, S. (2010). Signaling to heme oxygenase-1 and its anti-inflammatory therapeutic potential. *Biochem. Pharmacol.* 80, 1895–1903. doi: 10.1016/j.bcp.2010.07.014

Paiva, C. N., and Bozza, M. T. (2014). Are reactive oxygen species always detrimental to pathogens? *Antioxid. Redox Signal* 20, 1000–1037. doi: 10.1089/ars.2013.5447

Paiva, C. N., Feijó, D. F., Dutra, F. F., Carneiro, V. C., Freitas, G. B., Alves, L. S., et al. (2012). Oxidative stress fuels Trypanosoma cruzi infection in mice. *J. Clin. Invest.* 122, 2531–2542. doi: 10.1172/JCI58525

Palazon, A., Goldrath, A. W., Nizet, V., and Johnson, R. S. (2014). HIF Transcription Factors, Inflammation, and Immunity. *Immunity* 41, 518–528. doi: 10.1016/j.immuni.2014.09.008

Pålsson-McDermott, E. M., and O'Neill, L. A. J. (2020). Targeting immunometabolism as an anti-inflammatory strategy. *Cell Res.* 30, 300–314. doi: 10.1038/s41422-020-0291-z

Pang, Y., Zhang, Z., Chen, Y., Cao, S., Yang, X., and Jia, H. (2019). The Nrf2 pathway is required for intracellular replication of Toxoplasma gondii in activated macrophages. *Parasite Immunol.* 41, e12621. doi: 10.1111/pim.12621

Papavassiliou, K. A., and Papavassiliou, A. G. (2016). Transcription Factor Drug Targets. *J. Cell Biochem.* 117, 2693–2696. doi: 10.1002/jcb.25605

Paun, A., Bankoti, R., Joshi, T., Pitha, P. M., and Stäger, S. (2011). Critical role of IRF-5 in the development of T helper 1 responses to Leishmania donovani infection. *PloS Pathog.* 7, e1001246. doi: 10.1371/journal.ppat.1001246

Penas, F., Mirkin, G. A., Vera, M., Cevey, Á., González, C. D., Gómez, M. I., et al. (2015). Treatment in vitro with PPARα and PPARγ ligands drives M1-to-M2 polarization of macrophages from T. cruzi-infected mice. *Biochim. Biophys. Acta* 1852, 893–904. doi: 10.1016/j.bbadis.2014.12.019

Pham, N.-K., Mouriz, J., and Kima, P. E. (2005). Leishmania pifanoi amastigotes avoid macrophage production of superoxide by inducing heme degradation. *Infect. Immun.* 73, 8322–8333. doi: 10.1128/IAI.73.12.8322-8333.2005

Piantadosi, C. A., Carraway, M. S., Babiker, A., and Suliman, H. B. (2008). Heme oxygenase-1 regulates cardiac mitochondrial biogenesis via Nrf2-mediated transcriptional control of nuclear respiratory factor-1. *Circ. Res.* 103, 1232–1240. doi: 10.1161/01.RES.0000338597.71702.ad

Piranavan, P., Bhamra, M., and Perl, A. (2020). Metabolic Targets for Treatment of Autoimmune Diseases. *Immunometabolism* 2, e200012. doi: 10.20900/immunometab20200012

Purushotham, A., Schug, T. T., Xu, Q., Surapureddi, S., Guo, X., and Li, X. (2009). Hepatocyte-specific deletion of SIRT1 alters fatty acid metabolism and results in hepatic steatosis and inflammation. *Cell Metab.* 9, 327–338. doi: 10.1016/j.cmet.2009.02.006

Rabhi, I., Rabhi, S., Ben-Othman, R., Rasche, A., Daskalaki, A., Trentin, B., et al. (2012). Transcriptomic signature of Leishmania infected mice macrophages: a metabolic point of view. *PloS Negl. Trop. Dis.* 6, e1763. doi: 10.1371/journal.pntd.0001763

Rabhi, S., Rabhi, I., Trentin, B., Piquemal, D., Regnault, B., Goyard, S., et al. (2016). Lipid Droplet Formation, Their Localization and Dynamics during Leishmania major Macrophage Infection. *PloS One* 11, e0148640. doi: 10.1371/journal.pone.0148640

Ray, M., Gam, A. A., Boykins, R. A., and Kenney, R. T. (2000). Inhibition of Interferon-γ Signaling by *Leishmania donovani*. *J. Infect. Dis.* 181, 1121–1128. doi: 10.1086/315330

Reinhard, K., Huber, M., Lohoff, M., and Visekruna, A. (2012). The role of NF-κB activation during protection against Leishmania infection. *Int. J. Med. Microbiol.* 302, 230–235. doi: 10.1016/j.ijmm.2012.07.006

Repa, J. J., Liang, G., Ou, J., Bashmakov, Y., Lobaccaro, J. M., Shimomura, I., et al. (2000). Regulation of mouse sterol regulatory element-binding protein-1c gene (SREBP-1c) by oxysterol receptors, LXRalpha and LXRbeta. *Genes Dev.* 14, 2819–2830. doi: 10.1101/gad.844900

Repa, J. J., Berge, K. E., Pomajzl, C., Richardson, J. A., Hobbs, H., and Mangelsdorf, D. J. (2002). Regulation of ATP-binding cassette sterol transporters ABCG5 and ABCG8 by the liver X receptors alpha and beta. *J. Biol. Chem.* 277, 18793–18800. doi: 10.1074/jbc.M109927200

Rius, J., Guma, M., Schachtrup, C., Akassoglou, K., Zinkernagel, A. S., Nizet, V., et al. (2008). NF-kappaB links innate immunity to the hypoxic response through transcriptional regulation of HIF-1alpha. *Nature* 453, 807–811. doi: 10.1038/nature06905

Rocha-Vieira, E., Ferreira, E., Vianna, P., De Faria, D. R., Gaze, S. T., Dutra, W. O., et al. (2003). Histopathological outcome of Leishmania major-infected BALB/c mice is improved by oral treatment with N-acetyl-l-cysteine. *Immunology* 108, 401–408. doi: 10.1046/j.1365-2567.2003.01582.x

Rodgers, J. T., Lerin, C., Haas, W., Gygi, S. P., Spiegelman, B. M., and Puigserver, P. (2005). Nutrient control of glucose homeostasis through a complex of PGC-1alpha and SIRT1. *Nature* 434, 113–118. doi: 10.1038/nature03354

Rodriguez, N. E., Chang, H. K., and Wilson, M. E. (2004). Novel program of macrophage gene expression induced by phagocytosis of Leishmania chagasi. *Infect. Immun.* 72, 2111–2122. doi: 10.1128/iai.72.4.2111-2122.2004

Rong, X., Albert, C. J., Hong, C., Duerr, M. A., Chamberlain, B. T., Tarling, E. J., et al. (2013). LXRs regulate ER stress and inflammation through dynamic modulation of membrane phospholipid composition. *Cell Metab.* 18, 685–697. doi: 10.1016/j.cmet.2013.10.002

Roy, S., Mukhopadhyay, D., Mukherjee, S., Ghosh, S., Kumar, S., Sarkar, K., et al. (2015). A Defective Oxidative Burst and Impaired Antigen Presentation are Hallmarks of Human Visceral Leishmaniasis. *J. Clin. Immunol.* 35, 56–67. doi: 10.1007/s10875-014-0115-3

Rudraiah, S., Zhang, X., and Wang, L. (2016). Nuclear Receptors as Therapeutic Targets in Liver Disease: Are We There Yet? *Annu. Rev. Pharmacol. Toxicol.* 56, 605–626. doi: 10.1146/annurev-pharmtox-010715-103209

Ruivo, M. T. G., Vera, I. M., Sales-Dias, J., Meireles, P., Gural, N., Bhatia, S. N., et al. (2016). Host AMPK Is a Modulator of Plasmodium Liver Infection. *Cell Rep.* 16, 2539–2545. doi: 10.1016/j.celrep.2016.08.001

Sanjabi, S., Hoffmann, A., Liou, H. C., Baltimore, D., and Smale, S. T. (2000). Selective requirement for c-Rel during IL-12 P40 gene induction in macrophages. *Proc. Natl. Acad. Sci. U.S.A.* 97, 12705–12710. doi: 10.1073/pnas.230436397

Santos, D., Campos, T. M., Saldanha, M., Oliveira, S. C., Nascimento, M., Zamboni, D. S., et al. (2018). IL-1β Production by Intermediate Monocytes Is Associated with Immunopathology in Cutaneous Leishmaniasis. *J. Invest. Dermatol.* 138, 1107–1115. doi: 10.1016/j.jid.2017.11.029

Santos, S. A. D., and Andrade, DR de (2017). HIF-1alpha and infectious diseases: a new frontier for the development of new therapies. *Rev. Inst. Med. Trop. Sao Paulo* 59, e92. doi: 10.1590/S1678-9946201759092

Satoh, T., and Akira, S. (2016). Toll-Like Receptor Signaling and Its Inducible Proteins. *Microbiol. Spectr.* 4, 6. doi: 10.1128/microbiolspec.MCHD-0040-2016

Schatz, V., Strüssmann, Y., Mahnke, A., Schley, G., Waldner, M., Ritter, U., et al. (2016). Myeloid Cell-Derived HIF-1α Promotes Control of Leishmania major. *J. Immunol. Baltim Md 1950* 197, 4034–4041. doi: 10.4049/jimmunol.1601080

Schatz, V., Neubert, P., Rieger, F., and Jantsch, J. (2018). Hypoxia, Hypoxia-Inducible Factor-1α, and Innate Antileishmanial Immune Responses. *Front. Immunol.* 9:216. doi: 10.3389/fimmu.2018.00216

Schmitz, F., Heit, A., Guggemoos, S., Krug, A., Mages, J., Schiemann, M., et al. (2007). Interferon-regulatory-factor 1 controls Toll-like receptor 9-mediated IFN-beta production in myeloid dendritic cells. *Eur. J. Immunol.* 37, 315–327. doi: 10.1002/eji.200636767

Sharma, S., tenOever, B. R., Grandvaux, N., Zhou, G.-P., Lin, R., and Hiscott, J. (2003). Triggering the interferon antiviral response through an IKK-related pathway. *Science* 300, 1148–1151. doi: 10.1126/science.1081315

Shim, D., Kim, H., and Shin, S. J. (2020). Mycobacterium tuberculosis Infection-Driven Foamy Macrophages and Their Implications in Tuberculosis Control as Targets for Host-Directed Therapy. *Front. Immunol.* 11:910. doi: 10.3389/fimmu.2020.00910

Singh, A. K., Mukhopadhyay, C., Biswas, S., Singh, V. K., and Mukhopadhyay, C. K. (2012). Intracellular pathogen Leishmania donovani activates hypoxia inducible factor-1 by dual mechanism for survival advantage within macrophage. *PloS One* 7, e38489. doi: 10.1371/journal.pone.0038489

Speirs, K., Caamano, J., Goldschmidt, M. H., Hunter, C. A., and Scott, P. (2002). NF-kappa B2 is required for optimal CD40-induced IL-12 production but dispensable for Th1 cell Differentiation. *J. Immunol. Baltim Md 1950* 168, 4406–4413. doi: 10.4049/jimmunol.168.9.4406

Srivastav, S., Basu Ball, W., Gupta, P., Giri, J., Ukil, A., and Das, P. K. (2014). Leishmania donovani prevents oxidative burst-mediated apoptosis of host

macrophages through selective induction of suppressors of cytokine signaling (SOCS) proteins. *J. Biol. Chem.* 289, 1092–1105. doi: 10.1074/jbc.M113.496323

Stothers, C. L., Luan, L., Fensterheim, B. A., and Bohannon, J. K. (2018). Hypoxia-inducible factor-1α regulation of myeloid cells. *J. Mol. Med. Berl Ger* 96, 1293–1306. doi: 10.1007/s00109-018-1710-1

Suzuki, T., and Yamamoto, M. (2015). Molecular basis of the Keap1-Nrf2 system. *Free Radic. Biol. Med.* 88, 93–100. doi: 10.1016/j.freeradbiomed.2015.06.006

Takaoka, A., Yanai, H., Kondo, S., Duncan, G., Negishi, H., Mizutani, T., et al. (2005). Integral role of IRF-5 in the gene induction programme activated by Toll-like receptors. *Nature* 434, 243–249. doi: 10.1038/nature03308

Thimmulappa, R. K., Lee, H., Rangasamy, T., Reddy, S. P., Yamamoto, M., Kensler, T. W., et al. (2006). Nrf2 is a critical regulator of the innate immune response and survival during experimental sepsis. *J. Clin. Invest.* 116, 984–995. doi: 10.1172/JCI25790

Tomiotto-Pellissier, F., Bortoleti BT da, S., Assolini, J. P., Gonçalves, M. D., Carloto, A. C. M., Miranda-Sapla, M. M., et al. (2018). Macrophage Polarization in Leishmaniasis: Broadening Horizons. *Front. Immunol.* 9:2529. doi: 10.3389/fimmu.2018.02529

Vachharajani, V. T., Liu, T., Wang, X., Hoth, J. J., Yoza, B. K., and McCall, C. E. (2016). Sirtuins Link Inflammation and Metabolism. *J. Immunol. Res.* 2016:8167273. doi: 10.1155/2016/8167273

van Uden, P., Kenneth, N. S., and Rocha, S. (2008). Regulation of hypoxia-inducible factor-1alpha by NF-kappaB. *Biochem. J.* 412, 477–484. doi: 10.1042/BJ20080476

Vats, D., Mukundan, L., Odegaard, J. I., Zhang, L., Smith, K. L., Morel, C. R., et al. (2006). Oxidative metabolism and PGC-1beta attenuate macrophage-mediated inflammation. *Cell Metab.* 4, 13–24. doi: 10.1016/j.cmet.2006.05.011

Vega, R. B., Huss, J. M., and Kelly, D. P. (2000). The coactivator PGC-1 cooperates with peroxisome proliferator-activated receptor alpha in transcriptional control of nuclear genes encoding mitochondrial fatty acid oxidation enzymes. *Mol. Cell Biol.* 20, 1868–1876. doi: 10.1128/mcb.20.5.1868-1876.2000

Vitali, S. H., Fernandez-Gonzalez, A., Nadkarni, J., Kwong, A., Rose, C., Mitsialis, S. A., et al. (2020). Heme oxygenase-1 dampens the macrophage sterile inflammasome response and regulates its components in the hypoxic lung. *Am. J. Physiol. Lung Cell Mol. Physiol.* 318, L125–L134. doi: 10.1152/ajplung.00074.2019

Vivarini, A. C., and Lopes, U. G. (2019). The Potential Role of Nrf2 Signaling in Leishmania Infection Outcomes. *Front. Cell Infect. Microbiol.* 9:453. doi: 10.3389/fcimb.2019.00453

Vivarini, Á. C., Calegari-Silva, T. C., Saliba, A. M., Boaventura, V. S., França-Costa, J., Khouri, R., et al. (2017). Systems Approach Reveals Nuclear Factor Erythroid 2-Related Factor 2/Protein Kinase R Crosstalk in Human Cutaneous Leishmaniasis. *Front. Immunol.* 8:1127. doi: 10.3389/fimmu.2017.01127

Voelter-Mahlknecht, S., and Mahlknecht, U. (2006). Cloning, chromosomal characterization and mapping of the NAD-dependent histone deacetylases gene sirtuin 1. *Int. J. Mol. Med.* 17, 59–67. doi: 10.3892/ijmm.17.1.59

Wang, Z., Schaffer, N. E., Kliewer, S. A., and Mangelsdorf, D. J. (2017). Nuclear receptors: emerging drug targets for parasitic diseases. *J. Clin. Invest.* 127, 1165–1171. doi: 10.1172/JCI88890

Wang, S., Liu, R., Yu, Q., Dong, L., Bi, Y., and Liu, G. (2019). Metabolic reprogramming of macrophages during infections and cancer. *Cancer Lett.* 452, 14–22. doi: 10.1016/j.canlet.2019.03.015

Wardyn, J. D., Ponsford, A. H., and Sanderson, C. M. (2015). Dissecting molecular cross-talk between Nrf2 and NF-κB response pathways. *Biochem. Soc. Trans.* 43, 621–626. doi: 10.1042/BST20150014

Weih, F., Carrasco, D., Durham, S. K., Barton, D. S., Rizzo, C. A., Ryseck, R. P., et al. (1995). Multiorgan inflammation and hematopoietic abnormalities in mice with a targeted disruption of RelB, a member of the NF-kappa B/Rel family. *Cell* 80, 331–340. doi: 10.1016/0092-8674(95)90416-6

Wiesel, P., Patel, A. P., DiFonzo, N., Marria, P. B., Sim, C. U., Pellacani, A., et al. (2000). Endotoxin-induced mortality is related to increased oxidative stress and end-organ dysfunction, not refractory hypotension, in heme oxygenase-1-deficient mice. *Circulation* 102, 3015–3022. doi: 10.1161/01.cir.102.24.3015

Wiley, M., Sweeney, K. R., Chan, D. A., Brown, K. M., McMurtrey, C., Howard, E. W., et al. (2010). Toxoplasma gondii activates hypoxia-inducible factor (HIF) by stabilizing the HIF-1alpha subunit via type I activin-like receptor kinase receptor signaling. *J. Biol. Chem.* 285, 26852–26860. doi: 10.1074/jbc.M110.147041

Xue, J., Schmidt, S. V., Sander, J., Draffehn, A., Krebs, W., Quester, I., et al. (2014). Transcriptome-based network analysis reveals a spectrum model of human macrophage activation. *Immunity* 40, 274–288. doi: 10.1016/j.immuni.2014.01.006

Yeung, F., Hoberg, J. E., Ramsey, C. S., Keller, M. D., Jones, D. R., Frye, R. A., et al. (2004). Modulation of NF-kappaB-dependent transcription and cell survival by the SIRT1 deacetylase. *EMBO J.* 23, 2369–2380. doi: 10.1038/sj.emboj.7600244

Zhu, L., Zhao, Q., Yang, T., Ding, W., and Zhao, Y. (2015). Cellular Metabolism and Macrophage Functional Polarization. *Int. Rev. Immunol.* 34, 82–100. doi: 10.3109/08830185.2014.969421

Zimmermann, S., Murray, P. J., Heeg, K., and Dalpke, A. H. (2006). Induction of suppressor of cytokine signaling-1 by Toxoplasma gondii contributes to immune evasion in macrophages by blocking IFN-gamma signaling. *J. Immunol. Baltim Md 1950* 176, 1840–1847. doi: 10.4049/jimmunol.176.3.1840

Conflict of Interest: The authors declare that the research was conducted in the absence of any commercial or financial relationships that could be construed as a potential conflict of interest.

frontiers in Cellular and Infection Microbiology

REVIEW
published: 16 April 2021
doi: 10.3389/fcimb.2021.669079

Comparative Analysis of Virulence Mechanisms of Trypanosomatids Pathogenic to Humans

Artur Leonel de Castro Neto, José Franco da Silveira and Renato Arruda Mortara*

Departamento de Microbiologia, Imunologia e Parasitologia, Escola Paulista de Medicina, Universidade Federal de São Paulo, São Paulo, Brazil

Trypanosoma brucei, *Leishmania* spp., and *T. cruzi* are flagellate protozoans of the family Trypanosomatidae and the causative agents of human African trypanosomiasis, leishmaniasis, and Chagas disease, respectively. These diseases affect humans worldwide and exert a significant impact on public health. Over the course of evolution, the parasites associated with these pathologies have developed mechanisms to circumvent the immune response system throughout the infection cycle. In cases of human infection, this function is undertaken by a group of proteins and processes that allow the parasites to propagate and survive during host invasion. In *T. brucei*, antigenic variation is promoted by variant surface glycoproteins and other proteins involved in evasion from the humoral immune response, which helps the parasite sustain itself in the extracellular milieu during infection. Conversely, *Leishmania* spp. and *T. cruzi* possess a more complex infection cycle, with specific intracellular stages. In addition to mechanisms for evading humoral immunity, the pathogens have also developed mechanisms for facilitating their adhesion and incorporation into host cells. In this review, the different immune evasion strategies at cellular and molecular levels developed by these human-pathogenic trypanosomatids have been discussed, with a focus on the key molecules responsible for mediating the invasion and evasion mechanisms and the effects of these molecules on virulence.

Keywords: *Trypanosoma brucei*, *Leishmania* spp., *Trypanosoma cruzi*, virulence factors, immune system evasion, host-parasite interaction

OPEN ACCESS

Edited by:
Hong-Juan Peng, Southern Medical University, China

Reviewed by:
Santuza Maria Ribeiro Teixeira, Federal University of Minas Gerais, Brazil
Claudia Masini d'Avila-Levy, Oswaldo Cruz Foundation (Fiocruz), Brazil

****Correspondence:***
Artur Leonel de Castro Neto
artur.leonel@gmail.com

Specialty section:
This article was submitted to Parasite and Host, a section of the journal Frontiers in Cellular and Infection Microbiology

Received: *17 February 2021*
Accepted: *30 March 2021*
Published: *16 April 2021*

Citation:
de Castro Neto AL, da Silveira JF and Mortara RA (2021) Comparative Analysis of Virulence Mechanisms of Trypanosomatids Pathogenic to Humans. Front. Cell. Infect. Microbiol. 11:669079. doi: 10.3389/fcimb.2021.669079

INTRODUCTION

Trypanosomatids are flagellate protozoans that can infect several types of hosts, including insects and vertebrates from different orders, in their monoxenous and dixenous forms, respectively (Nussbaum et al., 2010; Kaufer et al., 2017). Certain members of the genera *Trypanosoma* and *Leishmania* from the family Trypanosomatidae are causative agents of serious diseases in humans and have been associated with severe effects on public health globally. *Trypanosoma brucei* and *T. cruzi* cause human African trypanosomiasis (HAT) and Chagas disease, respectively. *Leishmania* parasites cause visceral and cutaneous leishmaniasis (Nussbaum et al., 2010; Kaufer et al., 2017; Mitra and Mawson, 2017).

While visceral or cutaneous leishmaniasis affects individuals worldwide (Africa, Asia, Europe, and America), Chagas disease has been primarily reported in the Americas (Central, South, and North America, and mostly in Mexico), whereas HAT has been mostly reported in African countries. Since the endemic regions may overlap, it is not uncommon to find cases of co-infection by these parasites (Mitra and Mawson, 2017; Winkler et al., 2018). The parasites are mainly dixenous and transmitted by hematophagous insects in a zoonotic or anthroponotic life cycle. Depending on the parasite species, the site of infection and development in vertebrate and invertebrate hosts will influence the severity of the disease and the virulence status (Cupolillo et al., 2000; Kaufer et al., 2017). Since these parasites must persist in insect and mammalian hosts, they develop mechanisms to infect, propagate, and survive in different environments. In insects infection, the surface proteins play a role in cell attachment and survival (Kamhawi et al., 2004; Maslov et al., 2013), whereas in mammals, the parasites produce a group of proteins and initiate processes that provide assistance during host invasion by helping the parasite evade the host immune system components (Geiger et al., 2016). Despite sharing the same evolutionary origin, *T. cruzi*, *T. brucei*, and *Leishmania* spp. adopt different methods for establishing and maintaining infection owing to the differences in the mechanisms underlying the invasion of mammalian hosts. *T. brucei* is an extracellular parasite during its life cycle (Ponte-Sucre, 2016) whereas *T. cruzi* can invade nucleated cells (Fernandes and Andrews, 2012) and *Leishmania* can only infect phagocytic cells (Walker et al., 2014). After the early invasion step, there are multiple methods which these parasites use that can modulate both innate (during the extracellular stage) and adaptive (during the intracellular stage) immune responses and induce their own growth (Zambrano-Villa et al., 2002). These include methods of host cell invasion and evasion of innate and adaptive host immune responses, which are mediated by various virulence factors, such as proteins, glycoproteins, and carbohydrates, which may be present on the cell surface or inside vesicles, or may be released by the parasite, as discussed in the subsequent sections.

This review aims to discuss the different invasion and survival mechanisms at cellular and molecular levels adopted by trypanosomatids pathogenic to humans. The components that play central roles during the invasion and evasion cycles and their influence on virulence have also been discussed.

T. BRUCEI

Among the trypanosomatids, *T. brucei* does not have intracellular stages in its life cycle and is exposed to constant attacks by antibody-mediated immune responses. This parasite can cause infections in humans and animals, depending on the subspecies that are inoculated by the insect vector. HAT, also known as sleeping sickness, is caused by *T. brucei gambiense* and *T. brucei rhodesiense*, whereas *T. brucei brucei* is known to cause infections in domestic and wild animals (Franco et al., 2014; Kaufer et al., 2017).

The entry of the parasites into the host is followed by the induction of innate immune responses, secretion of inflammatory cytokine and chemokines, and activation of myeloid cells for the elimination of the parasite (Ponte-Sucre, 2016; Stijlemans et al., 2016). To prevent prompt elimination, trypanosomes evade immune system attacks. One of the first lines of defense involves limiting the production of tumor necrosis factor alpha (TNF-α) by myeloid cells. This is mediated by adenylyl cyclases on the trypanosome plasma membrane, which are activated when the parasite is phagocytosed (Salmon et al., 2012; Pays et al., 2014).

The parasites encounter multiple types of host molecules associated with the humoral immune response; some of the common molecules belong to a group of high-density lipoproteins that determine the susceptibility or resistance to infection. These proteins are classified into two subsets, namely trypanolytic factors 1 and 2 (TLF1 and TLF2), which are present in human serum. There is limited information available about their levels and mode of action, besides the fact that apolipoprotein-L1 (apoL-I) is present in both complexes and is probably the primary lytic factor. In case of infection by *T. b. brucei*, apoL-I will promote parasite lysis mediated by the formation of pores in the intracellular membranes (Perez-Morga, 2005; Field et al., 2007; Wheeler, 2010; Geiger et al., 2016; Ponte-Sucre, 2016). However, the human pathogens *T. b. gambiense* and *T. b. rhodesiense* possess mechanisms that confer resistance to TLF1 and TLF2 complexes. Several processes appear to be associated with resistance in *T. b. gambiense*; these include: (1) reduction in TLF1 uptake owing to polymorphisms in its binding receptor, (2) resistance to apoL-I lysis through the expression of a truncated variant surface glycoprotein (VSG) (TgsGP), and (3) apoL-I degradation by cysteine proteases (Uzureau et al., 2013; Capewell et al., 2015). A serum resistance-associated gene encoding a truncated VSG that is actively expressed in cells resistant to human serum has been identified in the genome of *T. b. rhodesiense* (Capewell et al., 2015; Ponte-Sucre, 2016).

Once the parasites effectively counter the attack by the serum lytic system in the humoral immune response, VSG expression is another evasion mechanism used against the adaptive immune response. VSGs are highly antigenic proteins present on the surface of the parasite composed of a highly variable N-terminal domain that is exposed to the extracellular environment and a C-terminal domain that is bound to the cell membrane by a glycosylphosphatidylinositol (GPI) anchor (Ferguson et al., 1988). Before the parasites infect the human host, the expression of these proteins is activated in the salivary glands of the insect host. Following infection, VSGs help evade host responses throughout the infection cycle in the bloodstream. When these parasites are re-ingested by the tsetse fly during a blood meal, the VSGs are removed from the parasite membrane in the midgut of the insect (Pays et al., 2014; Ponte-Sucre, 2016).

Approximately 10^7 VSGs are organized into dimers and form a protective coat on the surface of the whole cell, which shields

the parasite and other membrane proteins from complement-mediated lysis by the host immune system. To elicit a protective role, the majority of the *T. brucei* population expresses the same VSG variant from a repertoire of approximately 1,000–2,000 different VSG genes (McConville et al., 2002; Geiger et al., 2016). During infection, VSGs induce an antibody response by the host immune system against the variant expressed at the moment. To reduce parasitemia, the host produces anti-VSG specific antibodies, which opsonize and lyse these parasites. However, some parasites that do not express the same variant will avoid immediate detection by the host immune system and expand their population. This mechanism confers constant antigenic variation to the parasite and allows it to sustain itself for long durations in the host bloodstream (Zambrano-Villa et al., 2002; Ponte-Sucre, 2016; Reis-Cunha et al., 2017).

Besides the major antigenic variation mechanisms described above, there are other mechanisms by which VSGs may be used by the parasite to evade the immune system of the mammalian host. Although anti-VSG antibodies can effectively eliminate the parasite, studies have shown that at a low antibody titer, the trypanosome may remove the antibodies from the cell surface through endocytosis, which occurs in the flagellar pocket, followed by the degradation of the complex in the lysosomes (McConville et al., 2002; Rudenko, 2005; Field et al., 2007; Stijlemans et al., 2016). This is possible owing to the hydrodynamic drag force resulting from directional swimming by the parasite, which pushes the VSG-bound antibodies toward the flagellar pocket and helps remove the complex *via* endocytosis (Overath and Engstler, 2004; Engstler et al., 2007; Krüger and Engstler, 2015). In addition to endocytosis in the flagellar pocket, new VSG variants are transported to the extracellular surface. Collectively, these events constitute the VSG recycling system, with constant renewal of the VSG cargo through endocytosis and exocytosis (Bangs et al., 1986; Silverman and Bangs, 2012) and a complete turnover of the entire VSG pool expressed on the cell surface within 12 min (Engstler et al., 2004).

VSGs can also be released extracellularly in a soluble form (sVSG) and eliminate bound IgGs from the surface of the parasite (Stijlemans et al., 2016). Since they are bound to the membrane by a GPI anchor, they can be cleaved upon the activation of phospholipase C (PLC), which is present in abundance in the parasite. Upon cleavage, the released VSGs carry the glycosylinositolphosphate moiety of the GPI anchor, whereas the lipid moiety (dimyristoyl glycerol) remains attached to the membrane of the parasite (Magez et al., 2002; Morrison, 2011; Geiger et al., 2016). The release of sVSG fractions during early infection has been associated with the modulation of the host immune response by the induction of a Th1 cell response and IFN-γ production. In the chronic stage of the infection, the release of these proteins have been shown to inhibit intracellular signaling and activation of macrophages (Geiger et al., 2016), elimination of preformed circulating antibodies, and formation of immune complexes (Moreno et al., 2019). Although PLC plays an important role in VSG cleavage, a previous study showed that deletions in PLC genes did not lead to a significant loss in virulence (Leal et al., 2001), which implies that antigenic variation is the primary immune escape mechanism adopted by African trypanosomes during infection (Magez et al., 2002; Morrison, 2011; Geiger et al., 2016).

VSG function is of vital importance in host-parasite interactions throughout the infection period. The variations in the sequence, expression, and release of VSGs contributes to the exhaustion of the immune system and completion of the cycle through parasite survival in the host followed by transmission back to the vector (Ponte-Sucre, 2016; Stijlemans et al., 2016).

LEISHMANIA SPP

Leishmania spp. have evolved in environments different from those in which *T. brucei* has evolved. Infections caused by *Leishmania* spp. have widespread incidence worldwide. They are associated with a broad range of clinical and pathological manifestations (visceral and cutaneous leishmaniasis) depending on the parasite species causing the infection and the host immune response. In Africa, Asia, and Europe, *Leishmania major* is considered the primary causative agent of cutaneous leishmaniasis, and *Leishmania donovani* is mostly associated with visceral cases of the disease. In the Americas, *Leishmania braziliensis* and *Leishmania infantum* are considered the primary causative species of the cutaneous and visceral forms of the disease, respectively (Steverding, 2017; Torres-Guerrero et al., 2017).

Although this group of parasites diverged approximately 500 million years ago and evolved in different habitats worldwide (Akhoundi et al., 2016), their host-parasite interaction mechanisms appear to be conserved, with a few differences in the number and sequence of the proteins involved in this process (Reis-Cunha et al., 2017). Unlike *T. brucei*, in which the VSG variation system is the primary immune evasion tool, *Leishmania* species mediate evasion *via* various virulence factors, including proteins and carbohydrates. Glycosylinositol phospholipids (GIPLs), lipophosphoglycans (LPGs), proteophosphoglycans (PPGs), and the glycoprotein gp63 are the primary representative molecules of this group of factors that promote the invasion and maintenance of chronic infection (Franco et al., 2012; Gupta et al., 2013).

The molecules mentioned are present on the parasite membrane, and most are attached through a GPI anchor. Among these molecules, LPGs are considered the major surface glycoconjugates of the glycocalyx that cover the entire cell surface in *Leishmania*. They are present in large numbers in the promastigote form of *Leishmania*, and a significant reduction in their content is observed in the amastigote form. This molecule is composed of four distinct domains: a GPI anchor, a glycan core (carbohydrate moiety), a linear phosphoglycan chain, and a terminal neutral oligosaccharide cap. Its structure and number may vary depending on the species and stage of the parasite life cycle (Ilg et al., 1992; Ferguson, 1999; Valente et al., 2019). LPGs are one of the first targets of the immune system when the metacyclic form of *Leishmania* infects a vertebrate host. LPGs act as barriers that cause steric hindrance in the

attachment of complement molecules to the surface of the parasite. This is enabled by the elongation of LPGs upon differentiation from the promastigote to the metacyclic form, which involves the doubling of linear phosphoglycan (PG) units compared to that in the promastigote (Franco et al., 2012; Gupta et al., 2013; Forestier et al., 2015). LPG also facilitates parasite attachment to and phagocytosis by macrophages, which is beneficial for *Leishmania*, since macrophages are the primary resident cells for *Leishmania*, in which the parasite replicates and differentiates during the infection process. These actions may be mediated *via* different mechanisms, such as direct binding to the macrophage receptors or through indirect interaction with proteins that contribute to the internalization of the parasite (Anversa et al., 2018). This virulence factor is associated with several other mechanisms, such as evasion of complement lysis, invasion, and survival within macrophages, as reported by Franco et al. (2012).

There is limited knowledge about the effects exerted by GIPLs on virulence, besides the fact that they are present in both cellular forms of the parasite (promastigote and amastigote) and inhibit nitric oxide (NO) synthesis by macrophages, which protects the parasite from damage (Franco et al., 2012). GIPLs have also been reported to impair the protein kinase C (PKC) pathway (Chawla and Vishwakarma, 2003). This favors parasite survival and is also associated with the activity of other virulence factors such as LPGs and gp63, although each factor adopts a different inhibitory mechanism (Gupta et al., 2013).

PPGs are mucin-like glycoproteins with a structure resembling that of LPGs; PPGs are present on the surface of *Leishmania* promastigotes and amastigotes. PPGs can also be released in abundance in the extracellular milieu by amastigotes once they move inside the parasitophorous vacuole (Ilg, 2000; Živanović et al., 2018). PPGs have been implicated in the binding of the parasite to macrophages, facilitation of parasite internalization, and modulation of the host response to the parasite. In the early stages of infection, PPGs can impair the synthesis of cytokines, such as TNF-α, and induce the onset of the invasion. Nonetheless, when macrophages are activated by T-cell cytokines, similar to LPGs, they stimulate the production of NO, which contributes to parasite destruction (Piani et al., 1999). PPGs have also been reported to suppress proteolytic activity in the serum and prevent opsonization of the parasite. However, PPGs also activate the complement system, which contributes to disease development (Peters et al., 1997). Collectively, PPGs help the amastigote survive in host macrophages, owing to its production at high levels in the amastigote and its extracellular release (Franco et al., 2012).

gp63 is a zinc-dependent metalloendopeptidase bound to the parasite membrane by a GPI anchor. Despite being attached to the membrane, the protein has been shown to be released in the extracellular milieu, either outside vesicles or inside them. It is considered one of the major virulence factors owing to its wide range of functions and its contribution to infection onset and maintenance (Isnard et al., 2012). Briefly, gp63 was reported to inactivate the complement cascade by inhibiting the C3b factor. This was reported to prevent the formation of the membrane attack complex (MAC) and enable the opsonization of the parasite, which facilitated its phagocytosis (Isnard et al., 2012; Shao et al., 2019). gp63 has also been shown to facilitate the binding of the parasite to macrophages through fibronectin receptors. It also exhibits protease activity by cleaving proteins from the extracellular matrix of the host, which provides *Leishmania* rapid entry into macrophages (Olivier et al., 2012).

Among other functions, gp63 affects the internal metabolism of macrophages by suppressing the production of cytokines (TNF-α and IL-12) and other cellular products (e.g., NO) that contribute in parasite elimination (Podinovskaia and Descoteaux, 2015). The inhibitory effect of this protein is also potentialized by the inactivation of mTOR kinase, which impairs the formation of an efficient translation initiation complex. Thereafter, the host macrophages become susceptible to parasite multiplication (Jaramillo et al., 2011).

During *Leishmania* infection, the virulence factors ensure parasite survival, maintenance, and proliferation inside the host, as mentioned earlier in this review. However, these factors are not restricted to immune evasion mechanisms and interactions with the immune system. There are multiple other proteins that are considered virulence factors, such as those involved in acquiring nutrients for the survival of the parasite when it is present inside the parasitophorous vacuole in macrophages (Liu and Uzonna, 2012). This acquisition is performed by parasite proteins that compete with components of host cell nutrition mechanisms, such as LIT1 and LIT2 (involved in iron sequestration) and arginase. These factors help acquire nutrients that are essential for parasite growth, and consequently, inhibit NO production by the host cell, since both processes require arginine as a basic component. Rab7 and LAMP-1 are involved in the impairment of phagosome-lysosome fusion *via* the inhibition of endosome maturation (Gupta et al., 2013).

Other proteins, such as A2, are involved in the transition of the extracellular promastigote to amastigote, which facilitates the internalization of the parasite into host cells (McCall et al., 2013). The parasite may also interact with the host cell membranes *via* amastins, a group of proteins classified into four classes (α, β, γ, and δ). The knockdown of the δ amastin gene subset was shown to impair the interaction between the parasite and the macrophage membrane, decrease amastigote viability, and attenuate the expression of the disease phenotype (de Paiva et al., 2015).

Notably, despite the fact that a parasite possesses numerous virulence factors, it is difficult to identify the most critical molecule among these, which is indispensable to the effective induction of infection by the parasite. Different studies have described knockout or knockdown experiments of the cited molecules. However, the results obtained were divergent. LPGs were shown to be critical virulence factors in *L. major* infections, but not in *L. mexicana* infections. Other studies have shown that the parasites induced an infection and were not eliminated by the immune system even in the absence of LPG or GIPL expression (Zhang and Beverley, 2010; Franco et al., 2012). In contrast, deletions in gp63 rendered the parasite significantly sensitive to

complement-mediated lysis (Joshi et al., 2002; Isnard et al., 2012). A2 downregulation decreased visceralization in mouse liver cells (McCall et al., 2013), whereas amastin knockdown impaired parasite growth and attenuated the effects of the disease (de Paiva et al., 2015).

Although these results indicate that certain virulence factors may be more important for parasite survival and maintenance of infection than others, it is difficult to find a factor as important as VSG is for *T. brucei*. Possibly, in *Leishmania*, these factors take up a complementary role and work synergistically to achieve the same result. This can be easily observed in LPGs, gp63, GIPLs (39), and amastins (de Paiva et al., 2015). These are implicated in the same macrophage adhesion function; however, the molecules exhibit different modes of action and interact with different macrophage receptors. LPGs, gp63, and GIPLs also inactivate the PKC pathway during infection, which is responsible for the production of oxidative products that lead to parasite destruction (Gupta et al., 2013).

T. CRUZI

Unlike other trypanosomatids discussed in this review, *T. cruzi* is present at several cellular stages throughout the infection process, with the parasite at each stage infecting different classes of host cells using an appropriate virulence mechanism. Here, we have focused on three major mechanisms: resistance to oxidative damage, evasion of the humoral immune response, and cell invasion. Upon infection, metacyclic trypomastigotes (MTs) actively infect cells at the point of entrance (fibroblasts and surrounding tissue cells) and may be phagocytized by macrophages and dendritic cells, where they essentially need to resist oxidative stress (Osorio et al., 2012; Mesías et al., 2019).

The antioxidant mechanisms adopted by *T. cruzi* are crucial for the inactivation of reactive oxygen and nitrogen species produced by the host cells during infection initiation. To achieve this, the parasite produces several peroxidases that act on different substrates from the cellular oxidative pathway. For instance, TcGPXI and TcGPXII are glutathione peroxidases that inactivate exogenous hydroperoxides and lipid-hydroperoxides, respectively (Piacenza et al., 2013; Mesías et al., 2019); similarly, TcAPX (ascorbate-dependent heme peroxidase) disables H_2O_2 in conjunction with TcCPX and TcMPX, which are tryparedoxin peroxidases that also inactivate small-chain organic hydroperoxides. FeSOD (from the iron superoxide dismutase group) counters O_2 toxicity (Piacenza et al., 2013). Proteins from the *T. cruzi* antioxidative network were found to be present at higher levels in MTs than in epimastigotes, and the expression of individual proteins such as TcCPX and TcMPX was directly correlated with cell stage differentiation (Piacenza et al., 2009).

Before escaping from the insect as an MT and after the parasite multiplies inside the host cell and egresses by disrupting the membrane as bloodstream trypomastigotes (BTs), the surface proteins of the parasite undergo extensive changes to develop mechanisms to endure complement-mediated lysis upon host infection. This evasion mechanism is mediated by the trypomastigote glycoproteins that confer resistance to the different complement pathways [classical pathway (CP), alternative pathway (AP), and lectin pathway (LP)] at these stages in the life cycle of the parasite (Osorio et al., 2012; Lidani et al., 2017).

Numerous proteins can interact with different complement pathway components. Some of these are common components of CP, AP, and LP that impair MAC formation (Cestari and Ramirez, 2010). The trypomastigote decay-accelerating factor (T-DAF) is one such component that inhibits the activation of CP and AP, and even of LP, by regulating C3 convertase expression. The *T. cruzi* complement regulatory protein (CRP), also known as gp160, blocks the same complement pathways *via* different mechanisms. T-DAF and CRP are trans-sialidase-like glycoproteins that belong to the same subfamily of the trans-sialidase superfamily of *T. cruzi* (Frasch et al., 1991; Schenkman et al., 1994). CRP is bound to the surface of the parasite through a GPI anchor and can also be released in soluble form in the extracellular milieu. Both proteins follow the same mode of action, i.e., interaction with C4b and C3b, which impairs C3b formation in CP, AP, and LP (Beucher et al., 2003; Lidani et al., 2017).

Calreticulin (TcCRT) is a calcium-binding protein that inhibits CP *via* interaction with C1q (essential for CP initiation). It also binds to a group of lectins, such as ficolins and mannose-binding lectins, which are responsible for LP activation (Ramírez-Toloza and Ferreira, 2017; Shao et al., 2019). *Trypanosoma cruzi* complement C2 receptor inhibitor tri-spanning protein (TcCRIT) impairs CP and LP activation *via* the cleavage of C2, which is a common component present in both pathways, and its interaction with C4 impairs the formation of C3 convertase (Lidani et al., 2017; Ramírez-Toloza and Ferreira, 2017; Shao et al., 2019). gp58/68 is a fibronectin/collagen receptor present on the surface of trypomastigotes that blocks AP by inhibiting the formation of C3 convertase (Fischer et al., 1988).

Following the initial host cell rupture and complement lysis evasion, the parasites enter a new cycle of infection by differentiating into extracellular amastigotes (EAs) and actively invade new host cells. With the support of adhesion and invasion molecules, the EAs attach to the surface of host cells, possibly through carbohydrate interactions (Bonfim-Melo et al., 2018). Proteins released by EAs (e.g., P21 and TcMVK) were shown to positively modulate host cell invasion. P21 reorganizes the host actin filaments in addition to inducing phagocytosis and actin polymerization (da Silva et al., 2009; Rodrigues et al., 2012). In contrast, TcMVK is attached to the host cell membrane and stimulates its uptake in HeLa cells (Ferreira et al., 2016).

Other proteins (e.g., trans-sialidases (TS), trans-sialidase-like proteins gp82 and gp85, mucins (gp35/50), and the proteases cruzipain and gp63) also exhibit virulence at different stages of the cell cycle; these proteins will be discussed in brief in this review. gp82 is one of the primary surface proteins detected in the metacyclic stage of *T. cruzi*. It is responsible for host cell adhesion and Ca^{2+} signaling cascade activation, which lead to the internalization of the parasite (Ramirez et al., 1993; Maeda et al.,

2012). Experiments in mice showed that gp82 plays a major role in infection through the oral route by conferring resistance to pepsin degradation in the gastric mucosal epithelium (Yoshida, 2009).

TS are essential to *T. cruzi* virulence (Schenkman et al., 1994; Freire-De-Lima et al., 2015). Active TS belong to group I of the TS superfamily, which includes proteins that can be linked by a GPI anchor to the cell membrane or released by the parasite upon the action of PLC on the GPI anchor, which helps modulate the host immune response (Freitas et al., 2011). These molecules can be categorized into two major groups based on the presence or absence of catalytic domains. Proteins with catalytic domains participate in the transfer of sialic acid residues (present on the surface of mammalian cells) to other cell-surface glycoconjugates in the host and to mucin-like molecules present on the membrane of the parasite. The proteins lacking the catalytic domains required for the aforementioned transfer participate in the adhesion and invasion processes by binding to host cell receptors (Schenkman et al., 1994; Freire-De-Lima et al., 2015). gp85 is another surface glycoprotein of the TS superfamily (group II) present on the surface of BTs. It contributes to cell invasion *via* a conserved FLY domain. This epitope exhibits tropism for endothelial cells, especially in the heart vessels, *via* the activation of extracellular signal-regulated kinases (Magdesian et al., 2001).

Mucins are acceptors of sialic acid residues transferred from the host donor by TS. They comprise a group of glycoconjugates present on the surface of the parasite and are classified into two groups: 1) those present only in the mammalian host (TcMUC) and providing protection against the immune system; 2) those that protect the parasite in the insect vector (TcSMUG). As protective molecules, mucins in the mammalian host receive sialic acid from TS, which is used in adhesion, immunomodulation of host defense, and complement evasion (Almeida et al., 1999; Acosta-Serrano et al., 2001). In insect vectors, mucins protect the parasite from digestive proteases, besides contributing to adhesion events (Herreros-Cabello et al., 2020).

Mucin-associated surface proteins (MASPs), which exhibit structural similarities with TcMUC, constitute a large group of proteins primarily found in the parasites in infectious stages (MTs and BTs); these proteins contribute to invasion by facilitating endocytosis (dos Santos et al., 2012), and also contribute to the survival and multiplication of intracellular amastigotes (Bartholomeu et al., 2009). gp35/50 is a mucin-like protein complex that is also present in MTs; it plays a role considerably similar to that of gp82 and promotes the internalization of MTs in the host cell using Ca^{2+} (Maeda et al., 2012).

In addition to these proteins, cysteine endopeptidases have also been implicated in the virulence of several parasites. In *T. cruzi*, cruzipain is the best-characterized protein from this group. It is expressed in the major stages of the parasite life cycle and is primarily present in lysosome-associated organelles, besides being present on the membrane in amastigotes (Alvarez et al., 2012). Cruzipain contributes to the proteolytic degradation of host tissues, host cell invasion, and immune evasion, possibly through the degradation of human IgG moieties (McKerrow et al., 2006; Osorio et al., 2012). Several other cell invasion-associated proteins have been identified, and their functions have been discussed in detail in earlier publications (Osorio et al., 2012; Leiria Campo et al., 2016; Horta et al., 2020).

Similar to that in *Leishmania*, gp63 proteases are also present in *T. cruzi*. The genes encoding these proteins undergo expansion, similar to the genes encoding TS and TS-like glycoproteins, mucins, and MASPs; this suggests that the proteins may be involved in host immune system evasion by the parasite (Garcia et al., 2007). There are two types of gp63 proteases: gp63-I and gp63-II. gp63-I is known for its metalloprotease activity and membrane attachment *via* GPI anchoring, and is detected in the three cellular stages of the parasite. Certain proteins in the gp63-I group are glycosylated, whereas others are non-glycosylated. The glycosylated forms are present on the membrane of the amastigote and epimastigote, whereas the non-glycosylated forms are present intracellularly, located close to the kinetoplast and flagellum pocket in the metacyclic trypomastigote. Compared to what is known about gp63-II proteins, there is limited information available on the functions and location of gp63-I proteins, besides the fact that they do not contain the GPI anchor domain sequence (Pech-Canul et al., 2017).

CONCLUDING REMARKS

Despite sharing a close evolutionary relationship and exhibiting similarities in terms of morphology and genetic composition, the different clinical presentations of the diseases caused by *Leishmania* and trypanosomes and the differences between the host environments clearly indicate the existence of specific virulence mechanisms in the different parasites. Since *T. brucei* is predominantly extracellular, its mechanisms are mostly focused on escaping the humoral immune response and neutralizing the lytic effects of the complement and antibody attacks. These actions (escape from the complement and lytic systems) are well conserved among the three trypanosomatids, despite being mediated by different sets of proteins, as shown in **Figure 1**. Unlike *T. brucei*, both *Leishmania* and *T. cruzi* have intracellular stages in their life cycles, which are associated with complex mechanisms typical to the particular infection stage; however, there are a few important differences between the intracellular stages in the two parasites. *Leishmania* amastigotes are generally present inside macrophages and immune system cells that phagocytose the parasite; therefore, they tend to induce their own opsonization and bind to immune cell receptors to stimulate and facilitate their incorporation into these cells. These actions are also performed by *T. cruzi* during the initial stages of infection. However, through evolution, *T. cruzi* has acquired methods to actively infect host cells even when it is absent from the immune system, which confers the ability to avoid detection even in cases of acute infection and results in the detection of the parasite years after the infection, when the health of the host organs is significantly compromised.

Notably, the virulence mechanisms described in the review and illustrated on **Figure 1** (e.g., complement system evasion, adhesion, and host cell invasion) are mediated by a group of

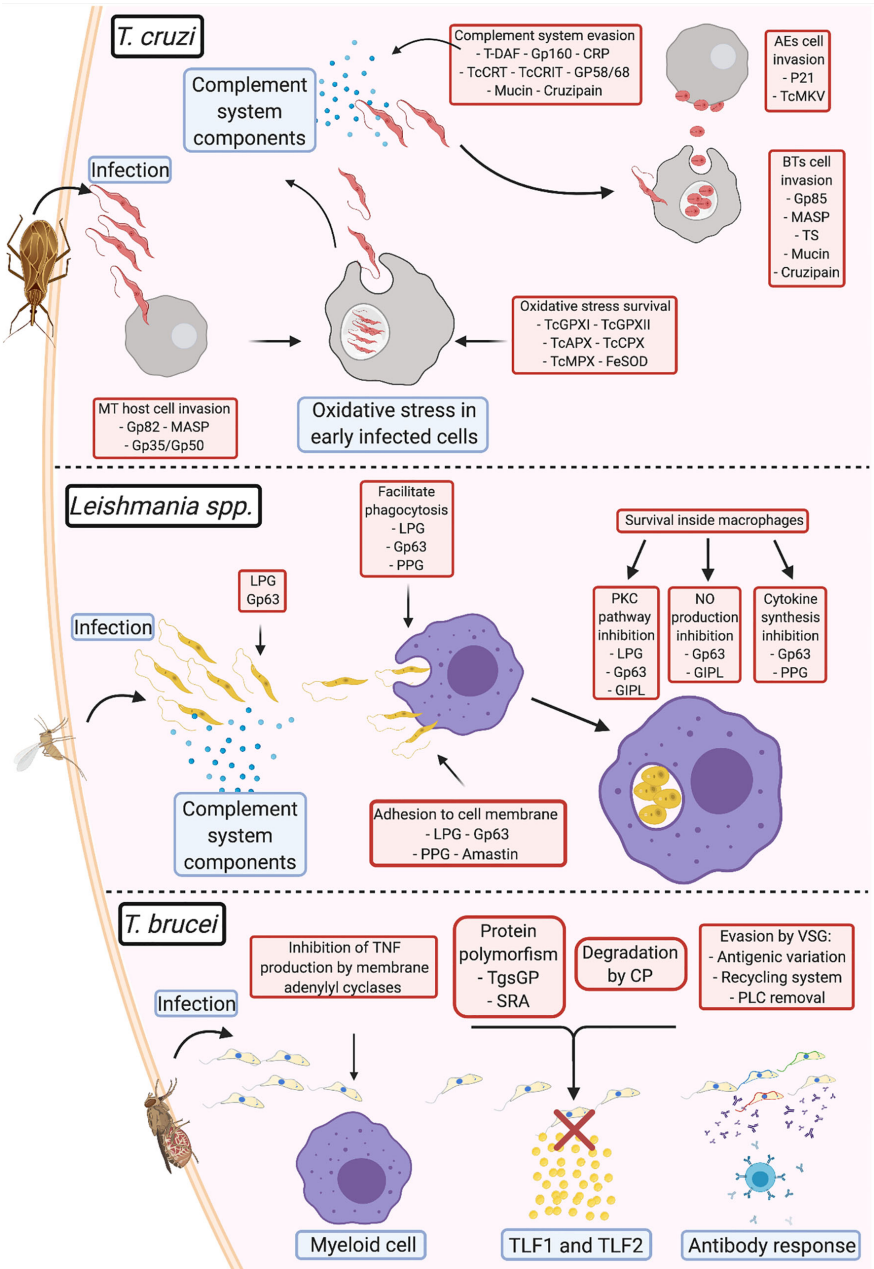

FIGURE 1 | Comparison of virulence strategies adopted by human pathogenic trypanosomatids ***Trypanosoma cruzi***: During infection, the metacyclic trypomastigotes invade cells at the site of entrance aided by gp82, MASP, and gp35/gp50; once inside the cell, TcGPXI TcGPXII, TcAPX, TcCPX, TcMPX, and FeSOD protect the parasite from the oxidative stress response; after multiplication and return to the extracellular milieu, *T. cruzi* evades the complement system (using T-DAF, gp160, CRP, TcCRT, TcCRIT, gp58/68, mucin, and cruzipain) until they invade new cells *via* membrane adhesion (using gp85, MASP, TS, mucin, and cruzipain). After a fresh round of multiplication and egression from the infected cell, if the parasite exits as an extracellular amastigote, it can directly infect new cells using surface protein adhesion (P21 and TcMKV). ***Leishmania* spp.**: Complement system evasion in *Leishmania* is primarily mediated by gp63 and lipophosphoglycans (LPGs). This interaction opsonizes the parasites and facilitates adhesion to the membrane of phagocytic cells, with assistance from proteophosphoglycans (PPGs) and amastins. Upon entry into the parasitophorous vacuole, gp63, LPGs, glycosylinositol phospholipids, and PPGs block the pathways that produce components that damage *Leishmania* and promote parasite survival and multiplication. *T. brucei*: To prevent immediate elimination, the parasite suppresses TNF-α production from the membrane adenylyl cyclases in myeloid cells. Evasion from TLF1 and TLF2 by *T. b. gambiense* is mediated *via* cysteine proteases and polymorphisms in the TgsGP receptor; *T. b. rhodesiense* prevents interaction with the same lytic factors using the serum resistance-associated proteins present on the membrane. In *T. brucei*, variant surface glycoproteins (VSGs) are primarily responsible for antibody response evasion. This involves: (1) prevention of the binding of antibodies to the cell membrane *via* antigenic variation, (2) elimination of antibodies bound to VSG by endocytosis of the VSG-antibody complex in the VSG recycling system, or (3) cleavage of the antigen-antibody complex by phospholipase C (PLC).

different parasite molecules that eventually achieve the same result. Therefore, it is difficult to determine the proteins responsible for the progression of each evasion process, since host-parasite interactions appear to occur stochastically, depending on the strain of the parasite, the virulence factor, and the availability of its receptor during infection. In case a virulence factor is blocked or unavailable, others that mediate the same function would play the role, perhaps with different efficiencies. However, further studies are required to confirm this. This observation also draws attention to the potential of virulence factors as targets for drug-based therapy, immunotherapy, or vaccine development. Since most studies in this area of research only tend to focus on single targets, studies on the identification of multiple targets may help improve the efficiency in preventing infection.

AUTHOR CONTRIBUTIONS

AC wrote the manuscript and prepared the figure. JS and RM reviewed and edited the manuscript and figure. All authors contributed to the article and approved the submitted version.

ACKNOWLEDGMENTS

We would like to thank Fundação de Amparo a Pesquisa do Estado de São Paulo (FAPESP) (Grant: 2016/15000-4 and fellowship: 2019/23302-9) for their financial support. The figure was created with BioRender.com.

REFERENCES

Acosta-Serrano, A., Almeida, I. C., Freitas-Junior, L. H., Yoshida, N., and Schenkman, S. (2001). The mucin-like glycoprotein super-family of Trypanosoma cruzi: Structure and biological roles. *Mol. Biochem. Parasitol.* 114, 143–150. doi: 10.1016/S0166-6851(01)00245-6

Akhoundi, M., Kuhls, K., Cannet, A., Votýpka, J., Marty, P., Delaunay, P., et al. (2016). A Historical Overview of the Classification, Evolution, and Dispersion of Leishmania Parasites and Sandflies. *PloS Negl. Trop. Dis.* 10, 1–40. doi: 10.1371/journal.pntd.0004349

Almeida, I. C., Gazzinelli, R., Ferguson, M. A. J., and Travassos, L. R. (1999). Trypanosoma cruzi Mucins: Potential Functions of a Complex Structure. *Mem. Inst. Oswaldo Cruz* 94, 173–176. doi: 10.1590/S0074-02761999000700023

Alvarez, V. E., Niemirowicz, G. T., and Cazzulo, J. J. (2012). The peptidases of Trypanosoma cruzi: Digestive enzymes, virulence factors, and mediators of autophagy and programmed cell death. *Biochim. Biophys. Acta - Proteins Proteomics* 1824, 195–206. doi: 10.1016/j.bbapap.2011.05.011

Anversa, L. S., Tiburcio, M. G. S., Richini-Pereira, V. B., and Ramirez, L. E. (2018). Human leishmaniasis in Brazil: A general review. *Rev. Assoc. Med. Bras.* 64, 281–289. doi: 10.1590/1806-9282.64.03.281

Bangs, J. D., Andrews, N. W., Hart, G. W., and Englund, P. T. (1986). Posttranslational modification and intracellular transport of a trypanosome variant surface glycoprotein. *J. Cell Biol.* 103, 255–263. doi: 10.1083/jcb.103.1.255

Bartholomeu, D. C., Cerqueira, G. C., Leão, A. C. A., daRocha, W. D., Pais, F. S., Macedo, C., et al. (2009). Genomic organization and expression profile of the mucin-associated surface protein (masp) family of the human pathogen Trypanosoma cruzi. *Nucleic Acids Res.* 37, 3407–3417. doi: 10.1093/nar/gkp172

Beucher, M., Meira, W. S. F., Zegarra, V., Galvão, L. M. C., Chiari, E., and Norris, K. A. (2003). Expression and purification of functional, recombinant Trypanosoma cruzi complement regulatory protein. *Protein Expr. Purif.* 27, 19–26. doi: 10.1016/S1046-5928(02)00562-4

Bonfim-Melo, A., Ferreira, E. R., Florentino, P. T. V., and Mortara, R. A. (2018). Amastigote Synapse: The Tricks of Trypanosoma cruzi Extracellular Amastigotes. *Front. Microbiol.* 9, 1341. doi: 10.3389/fmicb.2018.01341

Capewell, P., Cooper, A., Clucas, C., Weir, W., and MacLeod, A. (2015). A co-evolutionary arms race: Trypanosomes shaping the human genome, humans shaping the trypanosome genome. *Parasitology* 142, S108–S119. doi: 10.1017/S0031182014000602

Cestari, I., and Ramirez, M. I. (2010). Inefficient complement system clearance of Trypanosoma cruzi metacyclic trypomastigotes enables resistant strains to invade eukaryotic cells. *PloS One* 5, 1–11. doi: 10.1371/journal.pone.0009721

Chawla, M., and Vishwakarma, R. A. (2003). Alkylacylglycerolipid domain of GPI molecules of Leishmania is responsible for inhibition of PKC-mediated c-fos expression. *J. Lipid Res.* 44, 594–600. doi: 10.1194/jlr.M200296-JLR200

Cupolillo, E., Medina-Acosta, E., Noyes, H., Momen, H., and Grimaldi, G. (2000). A revised classification for Leishmania and Endotrypanum. *Parasitol. Today* 16, 142–144. doi: 10.1016/S0169-4758(99)01609-9

da Silva, C. V., Kawashita, S. Y., Probst, C. M., Dallagiovanna, B., Cruz, M. C., da Silva, E. A., et al. (2009). Characterization of a 21kDa protein from Trypanosoma cruzi associated with mammalian cell invasion. *Microbes Infect.* 11, 563–570. doi: 10.1016/j.micinf.2009.03.007

de Paiva, R. M. C., Grazielle-Silva, V., Cardoso, M. S., Nakagaki, B. N., Mendonça-Neto, R. P., Canavaci, A. M. C., et al. (2015). Amastin Knockdown in Leishmania braziliensis Affects Parasite-Macrophage Interaction and Results in Impaired Viability of Intracellular Amastigotes. *PloS Pathog.* 11, 1–24. doi: 10.1371/journal.ppat.1005296

dos Santos, S. L., Freitas, L. M., Lobo, F. P., Rodrigues-Luiz, G. F., Mendes, T. A., de, O., et al. (2012). The MASP Family of Trypanosoma cruzi: Changes in Gene Expression and Antigenic Profile during the Acute Phase of Experimental Infection. *PloS Negl. Trop. Dis.* 6, 1–14. doi: 10.1371/journal.pntd.0001779

Engstler, M., Thilo, L., Weise, F., Grünfelder, C. G., Schwarz, H., Boshart, M., et al. (2004). Kinetics of endocytosis and recycling of the GPI-anchored variant surface glycoprotein in Trypanosoma brucei. *J. Cell Sci.* 117, 1105–1115. doi: 10.1242/jcs.00938

Engstler, M., Pfohl, T., Herminghaus, S., Boshart, M., Wiegertjes, G., Heddergott, N., et al. (2007). Hydrodynamic Flow-Mediated Protein Sorting on the Cell Surface of Trypanosomes. *Cell* 131, 505–515. doi: 10.1016/j.cell.2007.08.046

Ferguson, M. A. J., Homans, S. W., Dwek, R. A., and Rademacher, T. W. (1988). Glycosyl-phosphatidylinositol moiety that anchors Trypanosoma brucei variant surface glycoprotein to the membrane. *Science (80-)* 239, 753–759. doi: 10.1126/science.3340856

Ferguson, M. A. J. (1999). The structure, biosynthesis and functions of glycosylphosphatidylinositol anchors, and the contributions of trypanosome research. *J. Cell Sci.* 112, 2799–2809.

Fernandes, M. C., and Andrews, N. W. (2012). Host cell invasion by Trypanosoma cruzi : a unique strategy that promotes persistence. *FEMS Microbiol. Rev.* 36, 734–747. doi: 10.1111/j.1574-6976.2012.00333.x

Ferreira, É. R., Horjales, E., Bonfim-Melo, A., Cortez, C., Da Silva, C. V., De Groote, M., et al. (2016). Unique behavior of Trypanosoma cruzi mevalonate kinase: A conserved glycosomal enzyme involved in host cell invasion and signaling. *Sci. Rep.* 6, 1–13. doi: 10.1038/srep24610

Field, M. C., Natesan, S. K. A., Gabernet-Castello, C., and Lila Koumandou, V. (2007). Intracellular trafficking in the trypanosomatids. *Traffic* 8, 629–639. doi: 10.1111/j.1600-0854.2007.00558.x

Fischer, E., Ouaissi, M. A., Velge, P., Cornette, J., and Kazatchkine, M. D. (1988). gp 58/68, a parasite component that contributes to the escape of the trypomastigote form of T. cruzi from damage by the human alternative complement pathway. *Immunology* 65, 299–303.

Forestier, C., Gao, Q., and Boons, G. (2015). Leishmania lipophosphoglycan : how to establish structure-activity relationships for this highly complex and multifunctional glycoconjugate? *Front. Cell. Infect. Microbiol.* 4, 193. doi: 10.3389/fcimb.2014.00193

Franco, L. H., Beverley, S. M., and Zamboni, D. S. (2012). Innate immune activation and subversion of mammalian functions by Leishmania lipophosphoglycan. *J. Parasitol. Res.* 2012, 1–11. doi: 10.1155/2012/165126

Franco, J. R., Simarro, P. P., Diarra, A., and Jannin, J. G. (2014). Epidemiology of human African trypanosomiasis. *Clin. Epidemiol.* 6, 257–275. doi: 10.2147/CLEP.S39728

Frasch, A. C. C., Cazzulo, J. J., Åslund, L., and Pettersson, U. (1991). Comparison of genes encoding Trypanosoma cruzi antigens. *Parasitol. Today* 7, 148–151. doi: 10.1016/0169-4758(91)90284-U

Freire-De-Lima, L., Fonseca, L. M., Oeltmann, T., Mendonça-Previato, L., and Previato, J. O. (2015). The trans-sialidase, the major Trypanosoma cruzi virulence factor: Three decades of studies. *Glycobiology* 25, 1142–1149. doi: 10.1093/glycob/cwv057

Freitas, L. M., dos Santos, S. L., Rodrigues-Luiz, G. F., Mendes, T. A. O., Rodrigues, T. S., Gazzinelli, R. T., et al. (2011). Genomic analyses, gene expression and antigenic profile of the trans-sialidase superfamily of trypanosoma cruzi reveal an undetected level of complexity. *PloS One* 6, 1–14. doi: 10.1371/journal.pone.0025914

Garcia, E. S., Ratcliffe, N. A., Whitten, M. M., Gonzalez, M. S., and Azambuja, P. (2007). Exploring the role of insect host factors in the dynamics of Trypanosoma cruzi-Rhodnius prolixus interactions. *J. Insect Physiol.* 53, 11–21. doi: 10.1016/j.jinsphys.2006.10.006

Geiger, A., Bossard, G., Sereno, D., Pissarra, J., Lemesre, J. L., Vincendeau, P., et al. (2016). Escaping deleterious immune response in their hosts: Lessons from Trypanosomatids. *Front. Immunol.* 7, 212. doi: 10.3389/fimmu.2016.00212

Gupta, G., Oghumu, S., and Satoskar, A. R. (2013). "Mechanisms of Immune Evasion in Leishmaniasis," in. *Adv. Appl. Microbiol.*, 82, 155–184. doi: 10.1016/B978-0-12-407679-2.00005-3

Herreros-Cabello, A., Callejas-Hernández, F., Gironès, N., and Fresno, M. (2020). Trypanosoma Cruzi Genome: Organization, Multi-Gene Families, Transcription, and Biological Implications. *Genes (Basel)* 11, 1–26. doi: 10.3390/genes11101196

Horta, M. F., Andrade, L. O., Martins-Duarte, É. S., and Castro-Gomes, T. (2020). Cell invasion by intracellular parasites - the many roads to infection. *J. Cell Sci.* 133, 1–15. doi: 10.1242/jcs.232488

Ilg, T., Etges, R., Overath, P., McConville, M. J., Thomas-Oates, J., Thomas, J., et al. (1992). Structure of Leishmania mexicana lipophosphoglycan. *J. Biol. Chem.* 267, 6834–6840. doi: 10.1016/S0021-9258(19)50502-6

Ilg, T. (2000). Proteophosphoglycans of Leishmania. *Parasitol. Today* 16, 489–497. doi: 10.1016/S0169-4758(00)01791-9

Isnard, A., Shio, M. T., and Olivier, M. (2012). Impact of Leishmania metalloprotease GP63 on macrophage signaling. *Front. Cell. Infect. Microbiol.* 2, 72. doi: 10.3389/fcimb.2012.00072

Jaramillo, M., Gomez, M. A., Larsson, O., Shio, M. T., Topisirovic, I., Contreras, I. I., et al. (2011). Leishmania repression of host translation through mTOR cleavage is required for parasite survival and infection. *Cell Host Microbe* 9, 331–341. doi: 10.1016/j.chom.2011.03.008

Joshi, P. B., Kelly, B. L., Kamhawi, S., Sacks, D. L., and McMaster, W. R. (2002). Targeted gene deletion in Leishmania major identifies leishmanolysin (GP63) as a virulence factor. *Mol. Biochem. Parasitol.* 120, 33–40. doi: 10.1016/S0166-6851(01)00432-7

Kamhawi, S., Ramalho-Ortigao, M., Van, M. P., Kumar, S., Lawyer, P. G., Turco, S. J., et al. (2004). A role for insect galectins in parasite survival. *Cell* 119, 329–341. doi: 10.1016/j.cell.2004.10.009

Kaufer, A., Ellis, J., Stark, D., and Barratt, J. (2017). The evolution of trypanosomatid taxonomy. *Parasites Vectors* 10, 1–17. doi: 10.1186/s13071-017-2204-7

Krüger, T., and Engstler, M. (2015). Flagellar motility in eukaryotic human parasites. *Semin. Cell Dev. Biol.* 46, 113–127. doi: 10.1016/j.semcdb.2015.10.034

Leal, S., Acosta-Serrano, A., Morita, Y. S., Englund, P. T., Böhme, U., and Cross, G. A. M. (2001). Virulence of Trypanosoma brucei strain 427 is not affected by the absence of glycosylphosphatidylinositol phospholipase C. *Mol. Biochem. Parasitol.* 114, 245–247. doi: 10.1016/S0166-6851(01)00257-2

Leiria Campo, V., Braga Martins-Teixeira, M., and Carvalho, I. (2016). Trypanosoma cruzi Invasion into Host Cells: A Complex Molecular Targets Interplay. *Mini-Rev. Med. Chem.* 16, 1084–1097. doi: 10.2174/1389557516666160607230238

Lidani, K. C. F., Bavia, L., Ambrosio, A. R., and de Messias-Reason, I. J. (2017). The complement system: A prey of Trypanosoma cruzi. *Front. Microbiol.* 8, 607. doi: 10.3389/fmicb.2017.00607

Liu, D., and Uzonna, J. E. (2012). The early interaction of Leishmania with macrophages and dendritic cells and its influence on the host immune response. *Front. Cell. Infect. Microbiol.* 2, 83. doi: 10.3389/fcimb.2012.00083

Maeda, F. Y., Cortez, C., and Yoshida, N. (2012). Cell signaling during Trypanosoma cruzi invasion. *Front. Immunol.* 3, 361. doi: 10.3389/fimmu.2012.00361

Magdesian, M. H., Giordano, R., Ulrich, H., Juliano, M. A., Juliano, L., Schumacher, R. I., et al. (2001). Infection by Trypanosoma cruzi. *J. Biol. Chem.* 276, 19382–19389. doi: 10.1074/jbc.M011474200

Magez, S., Stijlemans, B., Baral, T., and De Baetselier, P. (2002). VSG-GPI anchors of African trypanosomes: Their role in macrophage activation and induction of infection-associated immunopathology. *Microbes Infect.* 4, 999–1006. doi: 10.1016/S1286-4579(02)01617-9

Maslov, D. A., Votýpka, J., Yurchenko, V., and Lukeš, J. (2013). Diversity and phylogeny of insect trypanosomatids: All that is hidden shall be revealed. *Trends Parasitol.* 29, 43–52. doi: 10.1016/j.pt.2012.11.001

McCall, L. I., Zhang, W. W., and Matlashewski, G. (2013). Determinants for the Development of Visceral Leishmaniasis Disease. *PloS Pathog.* 9, 1–7. doi: 10.1371/journal.ppat.1003053

McConville, M. J., Mullin, K. A., Ilgoutz, S. C., and Teasdale, R. D. (2002). Secretory Pathway of Trypanosomatid Parasites. *Microbiol. Mol. Biol. Rev.* 66, 122–154. doi: 10.1128/mmbr.66.1.122-154.2002

McKerrow, J. H., Caffrey, C., Kelly, B., Loke, P., and Sajid, M. (2006). Proteases in Parasitic Diseases. *Annu. Rev. Pathol. Mech. Dis.* 1, 497–536. doi: 10.1146/annurev.pathol.1.110304.100151

Mesías, A. C., Garg, N. J., and Zago, M. P. (2019). Redox Balance Keepers and Possible Cell Functions Managed by Redox Homeostasis in Trypanosoma cruzi. *Front. Cell. Infect. Microbiol.* 9, 1–20. doi: 10.3389/fcimb.2019.00435

Mitra, A. K., and Mawson, A. R. (2017). Neglected tropical diseases: Epidemiology and global burden. *Trop. Med. Infect. Dis.* 2, 1–15. doi: 10.3390/tropicalmed2030036

Moreno, C. J. G., Temporão, A., Torres, T., and Silva, M. S. (2019). Trypanosoma brucei interaction with host: Mechanism of VSG release as target for drug discovery for african trypanosomiasis. *Int. J. Mol. Sci.* 20, 1–10. doi: 10.3390/ijms20061484

Morrison, L. J. (2011). Parasite-driven pathogenesis in Trypanosoma brucei infections. *Parasite Immunol.* 33, 448–455. doi: 10.1111/j.1365-3024.2011.01286.x

Nussbaum, K., Honek, J., C.v.C. Cadmus, C., and Efferth, T. (2010). Trypanosomatid Parasites Causing Neglected Diseases. *Curr. Med. Chem.* 17, 1594–1617. doi: 10.2174/092986710790979953

Olivier, M., Atayde, V. D., Isnard, A., Hassani, K., and Shio, M. T. (2012). Leishmania virulence factors: Focus on the metalloprotease GP63. *Microbes Infect.* 14, 1377–1389. doi: 10.1016/j.micinf.2012.05.014

Osorio, L., Ríos, I., Gutiérrez, B., and González, J. (2012). Virulence factors of Trypanosoma cruzi: Who is who? *Microbes Infect.* 14, 1390–1402. doi: 10.1016/j.micinf.2012.09.003

Overath, P., and Engstler, M. (2004). Endocytosis, membrane recycling and sorting of GPI-anchored proteins: Trypanosoma brucei as a model system. *Mol. Microbiol.* 53, 735–744. doi: 10.1111/j.1365-2958.2004.04224.x

Pays, E., Vanhollebeke, B., Uzureau, P., Lecordier, L., and Pérez-Morga, D. (2014). The molecular arms race between African trypanosomes and humans. *Nat. Rev. Microbiol.* 12, 575–584. doi: 10.1038/nrmicro3298

Pech-Canul, Á. D. L. C., Monteón, V., and Solís-Oviedo, R.-L. (2017). A Brief View of the Surface Membrane Proteins from Trypanosoma cruzi. *J. Parasitol. Res.* 2017, 1–13. doi: 10.1155/2017/3751403

Perez-Morga, D. (2005). Apolipoprotein L-I Promotes Trypanosome Lysis by Forming Pores in Lysosomal Membranes. *Science (80-)* 309, 469–472. doi: 10.1126/science.1114566

Peters, C., Kawakami, M., Kaul, M., Ilg, T., Overath, P., and Aebischer, T. (1997). Secreted proteophosphoglycan of Leishmania mexicana amastigotes activates complement by triggering the mannan binding lectin pathway. *Eur. J. Immunol.* 27, 2666–2672. doi: 10.1002/eji.1830271028

Piacenza, L., Zago, M. P., Peluffo, G., Alvarez, M. N., Basombrio, M. A., and Radi, R. (2009). Enzymes of the antioxidant network as novel determiners of Trypanosoma cruzi virulence. *Int. J. Parasitol.* 39, 1455–1464. doi: 10.1016/j.ijpara.2009.05.010

Piacenza, L., Peluffo, G., Alvarez, M. N., Martínez, A., and Radi, R. (2013). Trypanosoma cruzi antioxidant enzymes as virulence factors in chagas disease. *Antioxid. Redox Signal.* 19, 723–734. doi: 10.1089/ars.2012.4618

Piani, A., Ilg, T., Elefanty, A. G., Curtis, J., and Handman, E. (1999). Leishmania major proteophosphoglycan is expressed by amastigotes and has an immunomodulatory effect on macrophage function. *Microbes Infect.* 1, 589–599. doi: 10.1016/S1286-4579(99)80058-6

Podinovskaia, M., and Descoteaux, A. (2015). *Leishmania* and the macrophage: a multifaceted interaction. *Future Microbiol.* 10, 111–129. doi: 10.2217/fmb.14.103

Ponte-Sucre, A. (2016). An overview of trypanosoma brucei infections: An intense host-parasite interaction. *Front. Microbiol.* 7, 2126. doi: 10.3389/fmicb.2016.02126

Ramirez, M. I., De Cassia Ruiz, R., Araya, J. E., Da Silveira, J. F., and Yoshida, N. (1993). Involvement of the stage-specific 82-kilodalton adhesion molecule of Trypanosoma cruzi metacyclic trypomastigotes in host cell invasion. *Infect. Immun.* 61, 3636–3641. doi: 10.1128/iai.61.9.3636-3641.1993

Ramírez-Toloza, G., and Ferreira, A. (2017). Trypanosoma cruzi evades the complement system as an efficient strategy to survive in the mammalian host: The specific roles of host/parasite molecules and Trypanosoma cruzi calreticulin. *Front. Microbiol.* 8, 1667. doi: 10.3389/fmicb.2017.01667

Reis-Cunha, J. L., Valdivia, H. O., and Bartholomeu, D. C. (2017). Gene and Chromosomal Copy Number Variations as an Adaptive Mechanism Towards a Parasitic Lifestyle in Trypanosomatids. *Curr. Genomics* 19, 87–97. doi: 10.2174/1389202918666170911161311

Rodrigues, A. A., Clemente, T. M., dos Santos, M. A., Machado, F. C., Gomes, R. G. B., Moreira, H. H. T., et al. (2012). A Recombinant Protein Based on Trypanosoma cruzi P21 Enhances Phagocytosis. *PloS One* 7, 1–9. doi: 10.1371/journal.pone.0051384

Rudenko, G. (2005). Maintaining the protective variant surface glycoprotein coat of African trypanosomes. *Biochem. Soc. Trans.* 33, 981. doi: 10.1042/BST20050981

Salmon, D., Vanwalleghem, G., Morias, Y., Denoeud, J., Krumbholz, C., Lhommé, F., et al. (2012). Adenylate cyclases of Trypanosoma brucei inhibit the innate immune response of the host. *Science (80-)* 337, 463–466. doi: 10.1126/science.1222753

Schenkman, S., Eichinger, D., Pereira, M. E. A., and Nussenzweig, V. (1994). Structural and functional properties of Trypanosoma trans-sialidase. *Annu. Rev. Microbiol.* 48, 499–523. doi: 10.1146/annurev.mi.48.100194.002435

Shao, S., Sun, X., Chen, Y., Zhan, B., and Zhu, X. (2019). Complement evasion: An effective strategy that parasites utilize to survive in the host. *Front. Microbiol.* 10, 532. doi: 10.3389/fmicb.2019.00532

Silverman, J. S., and Bangs, J. D. (2012). Form and function in the trypanosomal secretory pathway. *Curr. Opin. Microbiol.* 15, 463–468. doi: 10.1016/j.mib.2012.03.002

Steverding, D. (2017). The history of leishmaniasis. *Parasitol. Vectors* 10, 1–10. doi: 10.1186/s13071-017-2028-5

Stijlemans, B., Caljon, G., Van Den Abbeele, J., Van Ginderachter, J. A., Magez, S., and De Trez, C. (2016). Immune evasion strategies of Trypanosoma brucei within the mammalian host: Progression to pathogenicity. *Front. Immunol.* 7, 1–14. doi: 10.3389/fimmu.2016.00233

Torres-Guerrero, E., Quintanilla-Cedillo, M. R., Ruiz-Esmenjaud, J., and Arenas, R. (2017). Leishmaniasis: a review. *F1000Research* 6, 750. doi: 10.12688/f1000research.11120.1

Uzureau, P., Uzureau, S., Lecordier, L., Fontaine, F., Tebabi, P., Homblé, F., et al. (2013). Mechanism of Trypanosoma brucei gambiense resistance to human serum. *Nature* 501, 430–434. doi: 10.1038/nature12516

Valente, M., Castillo-Acosta, V. M., Vidal, A. E., and González-Pacanowska, D. (2019). Overview of the role of kinetoplastid surface carbohydrates in infection and host cell invasion: Prospects for therapeutic intervention. *Parasitology* 146, 1743–1754. doi: 10.1017/S0031182019001355

Walker, D. M., Oghumu, S., Gupta, G., McGwire, B. S., Drew, M. E., and Satoskar, A. R. (2014). Mechanisms of cellular invasion by intracellular parasites. *Cell. Mol. Life Sci.* 71, 1245–1263. doi: 10.1007/s00018-013-1491-1

Wheeler, R. J. (2010). The trypanolytic factor-mechanism, impacts and applications. *Trends Parasitol.* 26, 457–464. doi: 10.1016/j.pt.2010.05.005

Winkler, A. S., Klohe, K., Schmidt, V., Haavardsson, I., Abraham, A., Prodjinotho, U. F., et al. (2018). Neglected tropical diseases - the present and the future. *Tidsskr. den Nor. Laegeforening* 138, 1–7. doi: 10.4045/tidsskr.17.0678

Yoshida, N. (2009). Molecular mechanisms of Trypanosoma cruzi infection by oral route. *Mem. Inst. Oswaldo Cruz* 104, 101–107. doi: 10.1590/S0074-02762009000900015

Zambrano-Villa, S., Rosales-Borjas, D., Carrero, J. C., and Ortiz-Ortiz, L. (2002). How protozoan parasites evade the immune response. *Trends Parasitol.* 18, 272–278. doi: 10.1016/S1471-4922(02)02289-4

Zhang, K., and Beverley, S. M. (2010). Phospholipid and sphingolipid metabolism in Leishmania. *Mol. Biochem. Parasitol.* 170, 55–64. doi: 10.1016/j.molbiopara.2009.12.004

Živanović, V., Semini, G., Laue, M., Drescher, D., Aebischer, T., and Kneipp, J. (2018). Chemical Mapping of Leishmania Infection in Live Cells by SERS Microscopy. *Anal. Chem.* 90, 8154–8161. doi: 10.1021/acs.analchem.8b01451

Conflict of Interest: The authors declare that the research was conducted in the absence of any commercial or financial relationships that could be construed as a potential conflict of interest.

frontiers in Microbiology

ORIGINAL RESEARCH
published: 28 April 2021
doi: 10.3389/fmicb.2021.630682

Immunization With a DNA Vaccine Encoding the *Toxoplasma gondii*' s GRA39 Prolongs Survival and Reduce Brain Cyst Formation in a Murine Model

Yuchao Zhu[1†], Yanan Xu[2†], Lu Hong[1], Chunxue Zhou[3] and Jia Chen[1,2*]*

[1] Department of Radiology, The Affiliated Hospital of Medical School of Ningbo University, Ningbo, China, [2] The Ningbo Women and Children's Hospital, Ningbo, China, [3] Department of Pathogen Biology, School of Basic Medical Sciences, Cheeloo College of Medicine, Shandong University, Jinan, China

OPEN ACCESS

Edited by:
Axel Cloeckaert,
Le Nouvel Institut National de Recherche sur l'Agriculture, l'Alimentation et l'Environnement en France INRAE, France

Reviewed by:
Kai Li,
Harbin Veterinary Research Institute, Chinese Academy of Agricultural Sciences, China
Shawn Babiuk,
National Centre for Foreign Animal Disease (NCFAD), Canada
Ricardo Wagner Portela,
Federal University of Bahia, Brazil
Jorge Enrique Gómez Marín,
University of Quindío, Colombia

***Correspondence:**
Jia Chen
chenjia@nbu.edu.cn
Chunxue Zhou
zhouchunxue23@163.com

[†] These authors have contributed equally to this work

Specialty section:
This article was submitted to Infectious Diseases, a section of the journal Frontiers in Microbiology

Received: 18 November 2020
Accepted: 29 March 2021
Published: 28 April 2021

Citation:
Zhu Y, Xu Y, Hong L, Zhou C and Chen J (2021) Immunization With a DNA Vaccine Encoding the Toxoplasma gondii' s GRA39 Prolongs Survival and Reduce Brain Cyst Formation in a Murine Model. Front. Microbiol. 12:630682. doi: 10.3389/fmicb.2021.630682

Toxoplasma gondii, an obligate intracellular protozoan parasite, can cause infect almost all warm-blooded animals and humans. To evaluate the immunogenicity and protective efficacy of *T. gondii* GRA39 (TgGRA39) in mice by using DNA immunization, we constructed a recombinant eukaryotic plasmid pVAX-TgGRA39. The specific immune responses in immunized mice were analyzed by serum antibody and cytokine measurements, lymphocyte proliferation assays and flow cytometry of T lymphocyte subclasses. Also, protective efficacy against acute and chronic *T. gondii* infection was assessed by observing the survival time after challenge with the highly virulent *T. gondii* RH strain (Genotype I) and counting the number of cyst-forming in brain at 4 weeks post-infection with the cyst-forming PRU strain of *T. gondii* (Genotype II), respectively. Our results showed that DNA immunization with pVAX-GRA39 via intramuscular injection three times, at 2-week intervals could elicit humoral and cellular immune response, indicated by enhanced levels of IgG and IgG2a antibodies (a slightly elevated IgG2a to IgG1 ratio), and increased levels of cytokines IFN-γ, IL-2, IL-12, IL-17A, IL-17F, IL-22 and IL-23 and percentages of CD3+ CD4+ CD8- and CD3+ CD8+ CD4– T cells, in contrast to non-immunized mice. The significant increase in the expression levels of IL-6, TGF-β1, IL-1β, and the transcription factor factors RORγt, RORα, and STAT3 involved in the activation and pathway of Th17 and Tc17 cells, were also observed. However, no significant difference was detected in level of IL-4 and IL-10 ($p > 0.05$). These effective immune responses had mounted protective immunity against *T. gondii* infection, with a prolonged survival time (16.80 ± 3.50 days) and reduced cyst numbers (44.5%) in comparison to the control mice. Our data indicated that pVAX-TgGRA39 could induce effective humoral, and Th1-type, Th17, and Tc17 cellular immune responses, and may represent a promising vaccine candidate against both acute and chronic *T. gondii* infection.

Keywords: ***Toxoplasma gondii*, GRA39, DNA vaccine, toxoplasmosis, Th1**

INTRODUCTION

Toxoplasma gondii is an obligate intracellular protozoan parasite that infects a broad range of warm-blooded vertebrates, including humans and birds (Gangneux and Dardé, 2012; Hakimi et al., 2017; Kochanowsky and Koshy, 2018). As a ubiquitous human and veterinary pathogen, it has a global distribution, and it is estimated that 30% of the global human population may be infected (Wang et al., 2017d). *T. gondii* infection is usually asymptomatic or subclinical in immunocompetent individuals, while in immunocompromised individuals (e.g., AIDS, patients receiving organ transplants or undergoing cancer treatment, developing fetuses), severe and potentially lethal toxoplasmosis may be developed (Petersen et al., 2012; Wang et al., 2017c; Wohlfert et al., 2017). *T. gondii* infection in animals can cause abortion and neonatal death, particularly in sheep and goats, resulting in significant economic losses to animal production (Tenter et al., 2000).

Despite that some drugs could be used to treat acute *T. gondii* infections, no available drugs can eliminate the parasite cysts effectively (Wang et al., 2019). Immunoprophylaxis with effective vaccines would be of high priority to control *T. gondii* infection (Zhang et al., 2013, 2015a). Although a commercially licensed live-attenuated vaccine (Toxovax based on the S48 strain) is available for the veterinary industry in some countries, it was not used for humans and food-producing animals due to its side effects, including virulence reversion, as well as the potential pathogenicity in immune-compromised individuals, and inadequate efficacy (Jongert et al., 2009). Thus, it is imperative to develop safe, practical and effective vaccines against *T. gondii* infections in humans and animals.

DNA-based vaccines offer an alternative approach for immunization, with the ability of eliciting effective humoral and cell-mediated immunity against cellular pathogen invasions in animal models by an unique way of delivering the expressed protein as an endogenous antigen (Liu, 2011). In the past years, a number of antigens has been identified as DNA vaccine candidates, which mainly focused on some virulence factors of *T. gondii* (Li and Zhou, 2018). However, no any identified DNA vaccine candidates can induce complete protective immunity against *T. gondii* infection, so the screening of novel potential vaccine candidates against *T. gondii* infection will be important for DNA vaccination (Zhang et al., 2013; Li and Zhou, 2018). Thus, current studies of *T. gondii* vaccines have been focused on finding novel vaccine candidates and evaluating their protective immunity against toxoplasmosis in animal models.

The dense granule protein 39 (GRA39) was recently identified as a novel *T. gondii* virulence factor, which is critical for efficient replication within its host cell and plays a key role in pathogenesis (Nadipuram et al., 2016). Due to the critical biological roles of GRA39 in *T. gondii*, it could represent a potential vaccine candidate against *T. gondii* infection. However, no studies have evaluated the vaccine potentiality of GRA39 gene. Thus, the objective of this study was to determine the immunogenicity of TgGRA39 in a murine model and to assess protective effects of this DNA vaccine candidate.

MATERIALS AND METHODS

Mice and Parasite

Specific-pathogen-free (SPF) female Kunming mice of six to eight weeks old were purchased from Zhejiang Laboratory Animal Center, Hangzhou, China, which have been used as a proper model for *T. gondii* vaccine evaluation and challenge in previous studies (Chen et al., 2016; Zhang et al., 2018a; Zhu et al., 2020). All mice were maintained in strict accordance according to the Animal Ethics Procedures and Guidelines of the People's Republic of China. Animal experiments were approved by the ethical committee of Ningbo University [permission: SYXK(ZHE)2013-0190].

Tachyzoites of the highly virulent RH strain of *T. gondii* (Type I) and the brain cyst-forming of the PRU strain (Type II) were used for the *in vivo* challenge of mice. These two strains of *T. gondii* were propagated and harvested as described in our previous studies (Chen et al., 2016; Zhang et al., 2018a; Zhu et al., 2020). The obtained tachyzoites were also used for total RNA extraction (RNAprep Pure Tissue Kit, Sangon, China) and the preparation of *T. gondii* lysate antigen (TLA), as previously described (Chen et al., 2015).

Epitope Prediction

DNASTAR software (Madison, WI, United States) and its program of "Editseq" and "Protean" was operated and used to predict epitope and analyze the immunogenicity of *T. gondii* GRA39, including its antigenic index, hydrophilicity, flexible regions, and surface probability.

Construction of the Eukaryotic Expression Plasmid

The coding sequence of the TgGRA39 gene (ToxoDB: 289380\033840) was amplified by PCR from *T. gondii* strain RH DNA for constructing the pVAX-GRA39 plasmid, with a pair of oligonucleotide primers (forward primer, 5′-CGGGGTACC CCGATGGGGCACCCTACCTCTTTC-3′, and reverse primer, 5′-TGCTCTAGAGCATCACGTTTCCGGTGGTGGC-3′), and *Kpn*I and *Xba*I restriction sites were introduced. The obtained PCR product was ligated into the pMD-18 T Vector (TaKaRa, China), generating pMD-GRA39. The GRA39 fragment was cleaved by *Kpn*I/*Xba*I from pMD-GRA39 and then subcloned into pVAX I (Invitrogen, United States) which were cleaved by *Kpn*I/*Xba*I, then generated the plasmid pVAX-TgGRA39 using T4 DNA ligase. The recombinant plasmids were identified by PCR, double restriction enzyme digestion and sequencing. DNASTAR software (Madison, WI, United States) was used to predict the potential epitopes and to analyze the biochemical indexes of GRA39, such as antigenic index, hydrophilicity, as well as flexible regions, and surface probability.

The positive plasmids were purified from transformed *Escherichia coli* DH5α cells by anion exchange chromatography (EndoFree plasmid giga kit, Qiagen Sciences, MD, United States) according to the manufacturer's instructions. The concentrations of plasmids were determined by spectrophotometer at OD260 and OD280, and then dissolved in sterile phosphate-buffered

saline (PBS) with a final concentration of 1 mg/mL and stored at −20°C until use.

Expression of pVAX-GRA39 Plasmid *in vitro*

The Lipofectamine 2000 reagent (Invitrogen) was used for transfection of pVAX-GRA39 into Marc-145 cells, according to the manufacturer's instructions, as described previously (Chen et al., 2016). In brief, 48 h post-transfection, the cells were fixed with cool acetone for 30 min and expression of pVAX-GRA39 was examined using the indirect immunofluorescence assay (IFA) followed by anti-*T. gondii* polyclonal antiserum (1:50) and a FITC-labeled donkey-anti-goat IgG (Proteintech Group Inc., Chicago, IL, United States; 1:1000). The monolayers binding marker were covered with glycerine and examined for specific fluorescence under a Zeiss Axioplan fluorescence microscope (Carl Zeiss, Germany). Marc-145 cells transfected with empty pVAX I were used as the negative control.

Expression of pVAX-GRA39 in the transfected cells was then examined by western blotting. Briefly, the Marc-145 cells transfected with pVAX-GRA39 were lysed by freezing and thawing for five times, and then the lysates were subjected to SDS-PAGE. Thereafter, the nitrocellulose (NC) membrane (Sigma, United States) was incubated with 5% bovine serum albumin (BSA) in PBST (PBS with 0.05% Tween-20) at room temperature (RT) for 1 h to block the non-specific binding sites followed by electrotransfer. After washing for three times with PBST, the membrane was cultured with pVAX-GRA39-vaccinated mouse sera (diluted in 1:500) at RT for 1 h, which was collected at 2 weeks after the third immunization. The membrane was washed for 3 times with PBST and was then incubated with goat anti-mouse IgG-HRP antibody (diluted at 1:3000, Sigma, United States) for 1 h at RT. The enhanced chemiluminescence chromogenic substrate was quantified by densitometry using ImageJ (NIH, United States). The specific band was visualized with Clarity™ Western ECL Blotting Substrates (Bio-Rad, United States) according to the manufacturer's protocol. Mouse sera from PBS-treated mice were used as the negative control.

Immunization and Challenge

A total of 100 female Kunming mice were randomly divided into four groups of 25 mice each. As described in our previous studies (Chen et al., 2016; Zhu et al., 2020), each mouse was injected with 100 μl (1 μg/μl) pVAX-GRA39 plasmid, PBS, empty plasmid pVAX I vector, respectively, and those with no treatment served as blank controls. Blood samples were collected from the tail vein from 25 mice in each group at weeks 0, 2, 4, 6, and stored at −20°C until use.

As described in our previous studies (Chen et al., 2016; Zhang et al., 2018a; Zhu et al., 2020), 2 weeks after the last immunization, 10 mice in all groups were challenged with 10^3 tachyzoites of the highly virulent *T. gondii* RH strain intraperitoneally and the survival periods were recorded daily until all mice were dead. Meanwhile, the other six mice of each group were orally inoculated with 10 PRU tissue cysts and the mouse brains were removed and homogenized in 1 ml of PBS, and then cysts were morphologically identified and the mean brain cyst loadings were counted under a microscope (40 × objective) on three aliquots of 20 μl, at 4 weeks after the challenge. All samples were counted in triplicate.

Two weeks after the last immunization, a total of nine mice per group were sacrificed and splenocytes were aseptically harvested for flow cytometric analysis (three mice), lymphoproliferation assay (three mice), and cytokine measurements (another three mice).

Detection of Total *T. gondii* IgG and IgG Subclass Titers

T. gondii-specific serum antibody levels were measured by SBA Clonotyping System-HRP Kit (Southern Biotech Co., Ltd, Birmingham, United Kingdom) according to the manufacture's instruction, as described previously (Chen et al., 2016). Briefly, the 96-well plates were coated with 100 μl (10 μg/ml) TLA diluted in PBS overnight at 4°C. The plates were washed with PBST and blocked PBS containing 1% BSA for 1 h at RT. Mouse serum samples (diluted 1:100 with PBS) were added to the wells and incubated at RT for 1 h. After washing, the wells were incubated with 100 μl of HRP conjugated anti-mouse IgG, anti-mouse IgG1, and IgG2a for 1h. Binding was visualized by incubating with 100 μl substrate solution (pH4.0; 1.05% citrate substrate buffer, 1.5% ABTS, 0.03% H_2O_2) for 30 min. The absorbance was measured at 450 nm using an ELISA reader (Bio-TekEL × 800, United States). The highest dilution factor that gives an OD 450 of twice that of the naïve sample at the dilution was designated as the antibody end point titer. All samples were running in triplicate.

Lymphoproliferation Assay

Splenocyte suspensions from three mice of each group were prepared by pushing the spleens through a wire mesh, and then purified by removing the red blood cells using RBC erythrocyte lysis buffer, and re-suspended in DMEM medium supplemented with 10% fetal calf serum (FCS). In brief, 3×10^6 cells per well were cultured in 96-well plates and cultured with different stimuli, TLA (10 or 5 μg/ml), concanavalin A (ConA; 5 μg/ml; Sigma) as positive control, or medium alone as negative control at 37°C under 5% CO_2 for 72 h. Then, 10 μl of 3-(4,5-dimethylthylthiazol-2-yl)-2,5-diphenyltetrazolium bromide (MTT, 5 mg/ml, Sigma, Sangon, China) was added to each well and incubated for 4 h. The stimulation index (SI) was calculated as the ratio of the average OD450 value of wells containing antigen-stimulated cells to the average OD450 value of wells containing only cells with medium. All measurements were performed in triplicate.

Flow Cytometry Analysis

The percentages of CD4+ and CD8+ T lymphocytes were determined by using the flow cytometry analysis, according to our previously described method (Chen et al., 2016; Zhang et al., 2018a). Briefly, splenocyte suspensions were stained with fluorochrome-labeled mAbs including PE-CD3, APC-CD4 and FITC-CD8 (eBioscience) at 4°C for 30 min in the dark, and then

fixed with FACScan buffer (PBS containing 1% FCS and 0.1% Sodium azide), and 2% paraformaldehyde. The samples were analyzed for fluorescence profiles on a FACScan flow cytometer (BD Bio-sciences) by SYSTEM II software (Coulter).

Cytokine Assays

The obtained spleen cells were co-cultured with TLA, ConA (positive control) and medium alone (negative control) in 96-well microtiter plates. Cell-free supernatants were harvested and assayed for IL-2, IL-4 and IL-12p40 at 24 h, for IL-22 activity at 48 h, for IL-10, IL-17A, IL-17F, and IL-23 activity at 72 h, and for gamma interferon (IFN-γ) and IL-12p70 activity at 96 h using commercial ELISA kits according to the manufacturer's instructions (Biolegend, United States). The analyses were performed in triplicate.

Quantitative Real-Time PCR

In an effort to determine the pathway mediating the increased production of Th17 and Tc17 responses, the expression of IL-6, TGF-β1, IL-1β, RORγt, RORα, and STAT3 were analyzed by qRT-PCR. Total RNA was isolated from three purified splenocytes of mice in each group by using Trizol reagent (Invitrogen, United States), as per the manufacturer's instructions. RNAs were dissolved in RNase-free ddH2O (TaKaRa, China) and the cDNA was synthesized using a GoScript^{TM} Reverse Transcription System (Promega, Madison, WI, United States), which were used as templates for quantitative real-time polymerase chain reaction (qRT-PCR). qRT-PCR was performed using the Light Cycler 480 SYBR Green I Master (Roche, Switzerland). The primers used for amplification are listed in **Supplementary Materials**. qRT-PCR analysis was performed on the Light Cycler 480 (Roche, Switzerland) and data were calculated using the comparative cycle threshold (CT) method ($2^{-\Delta\Delta CT}$).

Statistical Analysis

All statistical analyses were conducted using Graph Pad Prism 5.0 and SPSS17.0 Data Editor (SPSS, Inc, IL, United States). The differences of antibody responses, lympho-proliferation assays, cytokine production, and percentage of CD4+ and CD8+ T cells between all the groups were compared by one-way ANOVA. Survival results are represented by Kaplan–Meier curves and were compared using log rank test. The level of significant difference in comparisons between groups was considered significantly different if $p < 0.05$.

RESULTS

Epitope Analysis

DNASTAR was used to predict the potential epitopes of the TgGRA39 protein, including surface probability, antigenic index, hydrophilic plot, as well as flexible region. As shown in **Figure 1**, most regions of TgGRA39 protein were hydrophilicity plots and flexible regions, and TgGRA39 exhibited ideal surface probability and antigenic index, indicating a potentiality of constructing DNA vaccine with it.

Identification of the GRA39 Gene Expression *in vitro*

Under the fluorescence microscope, specific green fluorescence was observed in the Marc-145 cells transfected with pVAX-GRA39, while no fluorescence was observed in cells transfected with the empty pVAX I (**Figure 2A**). The western blotting results revealed a single band of about 100 kDa, which was consistent with the expected molecular size, indicating that pVAX-GRA39 was expressed in Marc-145 cells (**Figure 2B**). On the contrary, no protein band was detected in cells transfected with the empty pVAX1 vector. These results indicated that the GRA39 protein was expressed by pVAX-GRA39 in Marc-145 cells.

Antibody Detection

The antibody titers of IgG and subclasses IgG (IgG1 and IgG2a) in experimental group and the three control groups were detected by standard ELISA. As shown in **Figure 3A**, the statistically significantly higher levels of endpoint titers of IgG were detected in the sera of mice immunized with pVAX-GRA39, and total antibody levels significantly increased with the continuous immunization, while no increase of antibody titers occurred among the three control groups.

As shown in **Figure 3B**, the levels of IgG1 and IgG2a endpoint titers were significantly increased in mice immunized with pVAX-GRA39 ($p < 0.001$), in contrast to the three control groups (blank control, PBS, and pVAX I) ($p < 0.05$). In the meanwhile, the ratios of IgG2a/IgG1 were higher in mice immunized with pVAX-GRA39 in comparison with the controls.

Splenocyte Proliferation

To analyze the proliferation of splenocytes, the assay was carried out by stimulation of splenocytes with TLA or ConA at two weeks after last immunization. As shown in **Figure 4**, the proliferative response of lymphocytes was observed on spleen cells, and the proliferation stimulation index (SI) measured at OD450nm in mice immunized with pVAX-GRA39 was significantly higher than in the three controls. However, the three control groups showed no significant difference ($p > 0.05$).

Flow Cytometry Analysis of Lymphocytes Subpopulations

As shown in **Figure 5**, the percentage of CD3+ CD8+ CD4- T lymphocyte subsets (14.78 ± 0.32) in mice immunized with pVAX-GRA39 were much higher than those in the blank (7.34 ± 0.20), PBS (7.41 ± 0.17), pVAX I control (7.40 ± 0.15) group ($p < 0.05$). Also, pVAX-GRA39 group ($p < 0.05$) showed the higher percentage of CD3+ CD4+ CD8-T lymphocyte subsets (26.88 ± 0.35) than that in controls. The ratio of CD8+/CD4+ T cells showed higher level in the group of mice immunized with pVAX-GRA39 in comparison with that of the three control groups.

Cytokines and Transcription Factors Production

The levels of IL-2, IL-4, IL-10, IL-12p70, IL-12p40, IFN-γ, IL-17A, IL-17F, IL-22, and IL-23 were detected in the mice of

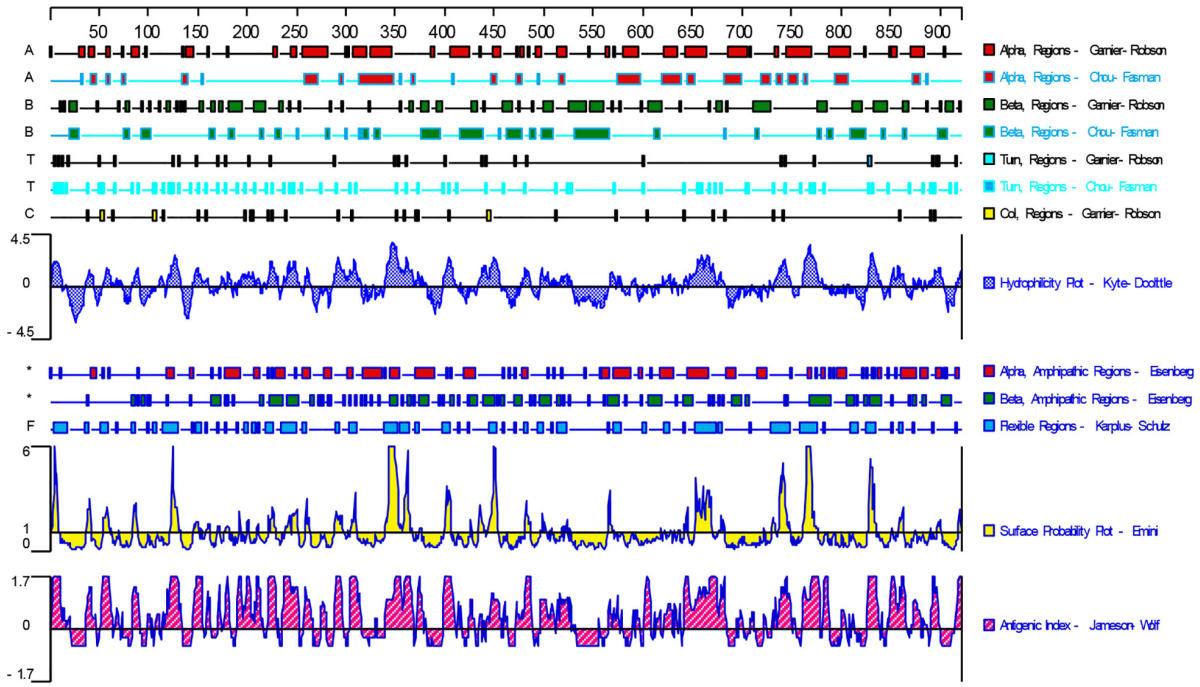

FIGURE 1 | Plot of the DNASTAR-predicted hydrophilicity, flexible regions, antigenic index, and surface probability plot of the linear-B cell epitopes of GRA39.

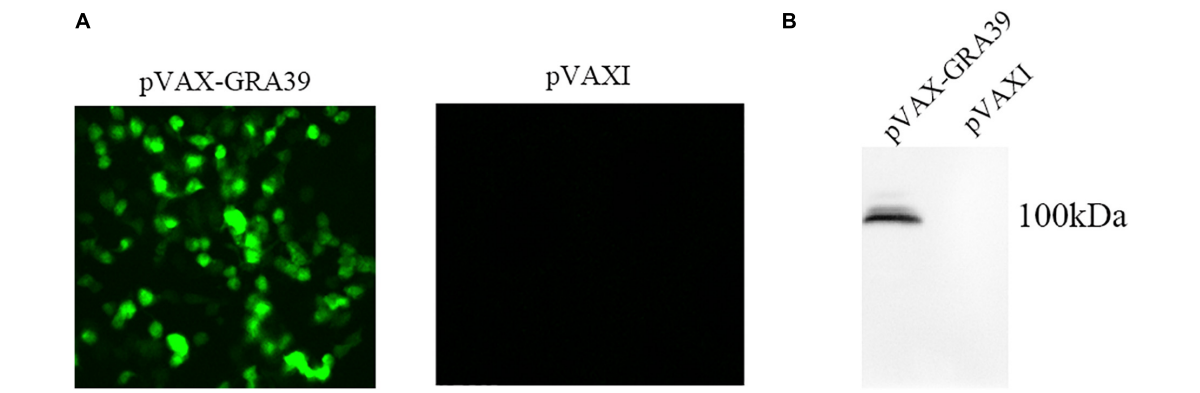

FIGURE 2 | Expression of pVAX-GRA39 in Marc-145 cell. **(A)** Immunofluorescence assay for the recombinant GRA39 protein expressed in Marc-145 cells. **(B)** Western blotting analysis of the expression of GRA39 in Marc-145 cell lysates and empty pVAX I.

experimental group and three controls. As shown in **Figure 6**, the productions of IFN-γ, IL-2, IL-12p70, and IL-12p40 in the mice immunized with pVAX-GRA39 were significantly higher than that in controls. Besides, increased levels of IL-17A, IL-17F, IL-22, and IL-23 were also detected in mice of experimental group compared to the control groups ($p < 0.05$). The levels of IL-4 and IL-10 cytokines showed no statistically differences to that in three controls ($p > 0.05$).

Expression levels of cytokine gene, IL-6, TGF-β1, and IL-1β, as well as the transcription factors RORγt, RORα, and STAT3 were detected using RT-PCR. We examined the difference in the mRNA level of cytokine genes and transcription factors between control mice and pVAX-GRA39-immunized mice. The expression of IL-6, TGF-β1 and IL-1β, RORγt, RORα, and STAT3 was significantly higher in pVAX-GRA39-immunized mice than in the control group ($p < 0.05$) (**Figure 7**). These results indicated that increased expression of IL-6, TGF-β1 and IL-1β, RORγt, RORα and STAT3 followed by pVAX1-GRA39 immunization could activate Th17 responses.

Protective Efficacy of Vaccinated Mice

Mortality was observed daily after intraperitoneal challenge with RH strain (1×10^3 tachyzoites) until all the mice of controls and experimental group were dead. As shown in **Figure 8A**, the mice in the group immunized with pVAX-TgGRA39 significantly prolonged survival time (16.8 ± 3.5) compared to mice in

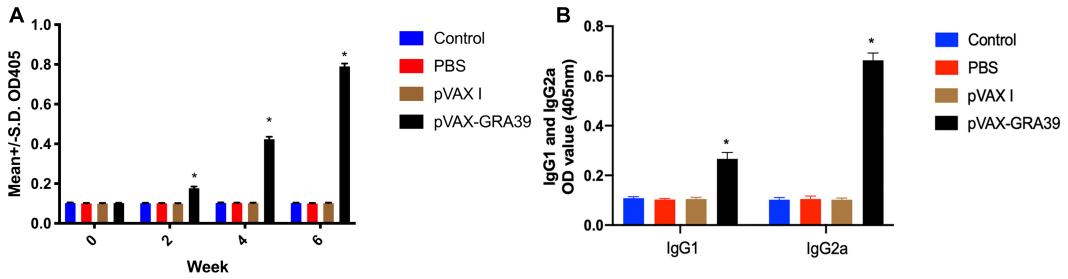

FIGURE 3 | Detection the levels of total IgG, IgG1 and IgG2a antibodies in the sera of Kunming mice. **(A)** Determination of IgG titers induced by DNA immunization at weeks 0, 2, 4, 6. **(B)** Determination of IgG1 and IgG2a titers in the sera of mice two weeks after the last immunization. The results were expressed as means ± SD ($n = 3$) with respect to absorbance at OD450 and statistical differences ($p < 0.05$) are indicated by (*). The bars represented the levels of IgG, IgG1, and IgG2a in the serum of mice.

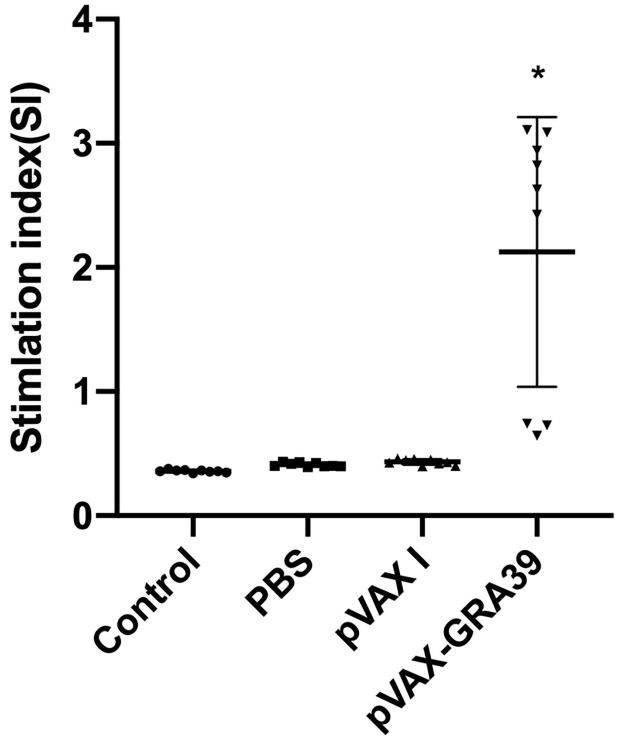

FIGURE 4 | Splenocyte proliferation assay. Two weeks after the last immunization, spleen lymphocytes were collected from vaccinated mice. The proliferative response was evaluated by MTT assay. The results are expressed as the stimulation index (SI) ± SD ($n = 3$). Statistical differences are represented by * ($p < 0.05$).

groups of PBS, blank and pVAX I control. While the mice of three control groups died within 6 days after challenge with RH strain, there is no significant difference among the three control groups ($p > 0.05$).

To evaluate the protective efficacy against chronic infection with *T. gondii* PRU strain, tissue cyst loads were examined in brains of the experimental mice and controls at 4 weeks after the third immunization. As shown in **Figure 8B**, there was a significant reduction (44.5%) in the number of tissue cysts in the brain of the mice immunized with pVAX-TgGRA39 compared to that in three controls ($p > 0.05$).

DISCUSSION

In recent years, some alternatives have been carried out on vaccines against *T. gondii* in animal models, such as attenuated vaccines (Wang et al., 2017a, 2018), subunit vaccines (Zheng et al., 2013; Ching et al., 2016; Sonaimuthu et al., 2016; Wang et al., 2017b; Gatkowska et al., 2018), exosome vaccines (Beauvillain et al., 2009; Li and Zhou, 2018), DNA vaccines (Zhang et al., 2015b), and other types of vaccines (Lee et al., 2018; Zhang et al., 2018a). Due to the their low production cost and thermal stability, as well as their ability to induce cellular and humoral immune responses, DNA vaccines have become promising method used for defending against *T. gondii* infection in animal models (Cao et al., 2015; Li and Zhou, 2018). Prior to evaluating the potentiality of DNA vaccine candidate, bioinformatics has been widely used as an experimental methodology, and also been used to predict gene structures, functions, and epitopes, or to design new vaccine candidates. Among those epitopes, some molecules in the studies of *T. gondii* DNA vaccines have been predicted by the immunogenicity of some molecules, including SAG4 (Zhou and Wang, 2017), ROP21 (Zhang et al., 2018c), TgDOC2C (Zhang et al., 2018b), GRA24 (Zheng et al., 2019), etc. In the present study, the bioinformatics analysis of TgGRA39 protein showed that most regions of the TgGRA39 protein hydrophilicity plots and flexible regions, suggesting an excellent antigenic index and surface probability, which is indicative of a promising vaccine candidate.

In previous studies, some DNA vaccine candidates encoding GRA protein of *T. gondii*, such as GRA6, GRA7, GRA2, GRA15, GRA16, GRA24, and GRA25, have demonstrated some efficacy against *T. gondii* infection, with their ability of eliciting immunity, particularly cellular immune responses, which is critical for defending against acute and chronic toxoplasmosis in animal models (Chen et al., 2015; Hu et al., 2017; Xu et al., 2019; Zheng et al., 2019). In the present study, we constructed a DNA vaccine expressing TgGRA39, and evaluated its immunogenicity and protective efficacy against infection with the highly virulent

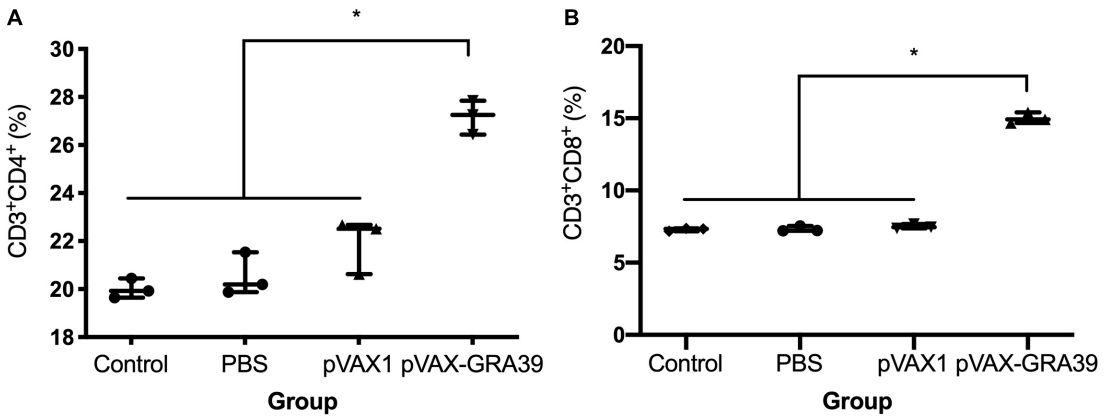

FIGURE 5 | DNA immunization augmented the frequency of antigen-specific T cells in mice. **(A)** Total numbers of CD3+ CD4+ CD8– T lymphocytes per spleen. **(B)** Total numbers of CD3+ CD8+ CD4– T lymphocytes per spleen. Data are mean ± SDs (representative of three experiments). $^{*}p < 0.05$, compared with the control groups.

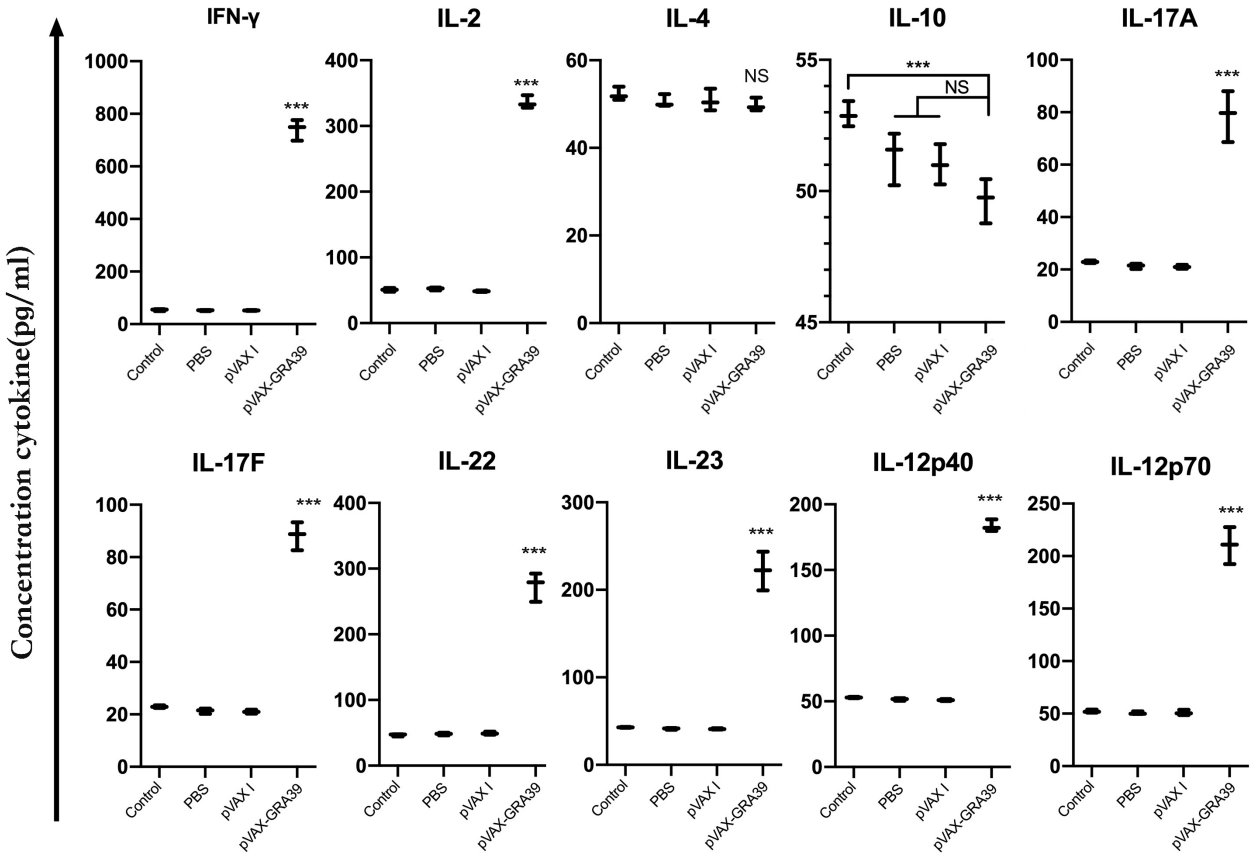

FIGURE 6 | Cytokine production by splenocytes of immunized Kunming mice after stimulation with toxoplasma lysate antigen (TLA). Each bar represents the mean pg/ml (±SE, $n = 3$). $^{***}p < 0.001$, compared with the control groups. NS: no significant.

T. gondii RH strain and the chronic *T. gondii* PRU strain. Our results revealed that immunization with pVAX-GRA39 can evoke specific humoral and cellular immune responses, resulting in effective protective immunity against acute and chronic toxoplasmosis in Kunming mice.

Th1-type immune response is considered to play a crucial role in resistance against *T. gondii* infection (Gigley et al., 2009). IFN-γ, the cytokine of the Th1-type lymphocytes, is confirmed to induce inflammatory response and thus to control *T. gondii* load during early stages of infection (Silva et al., 2009). IL-2, another

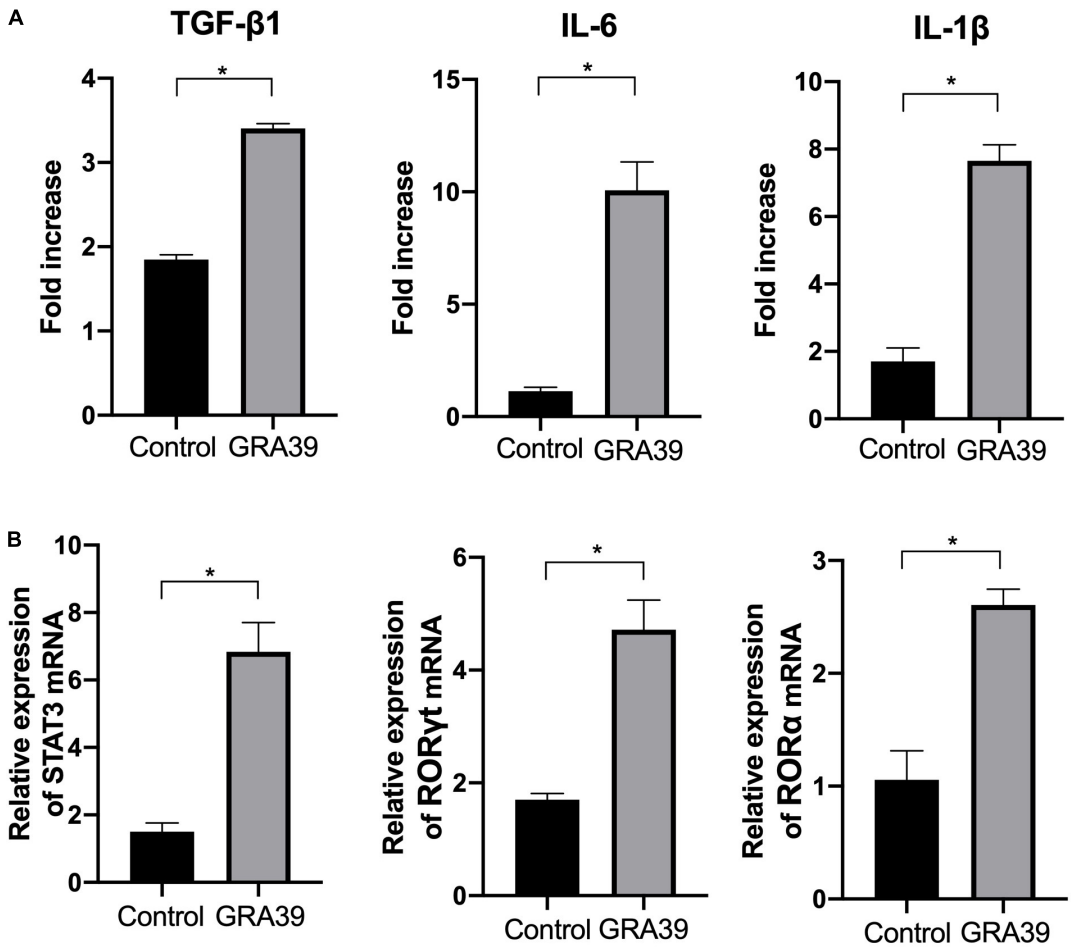

FIGURE 7 | Expression of the cytokines IL-1β, IL-6 and TGF-β1 and transcription factors RORγt, RORα and STAT3. mRNA expression levels of IL-1β, IL-6, TGF-β1, RORγt, RORα and STAT3 were measured in spleens from mice immunized with pVAX-GRA39, and expressed as fold increase over control. **(A)** The mRNA levels of IL-1β, IL-6, TGF-β1; **(B)** The mRNA levels of RORγt, RORα and STAT3. Statistical differences are represented by *($p < 0.05$).

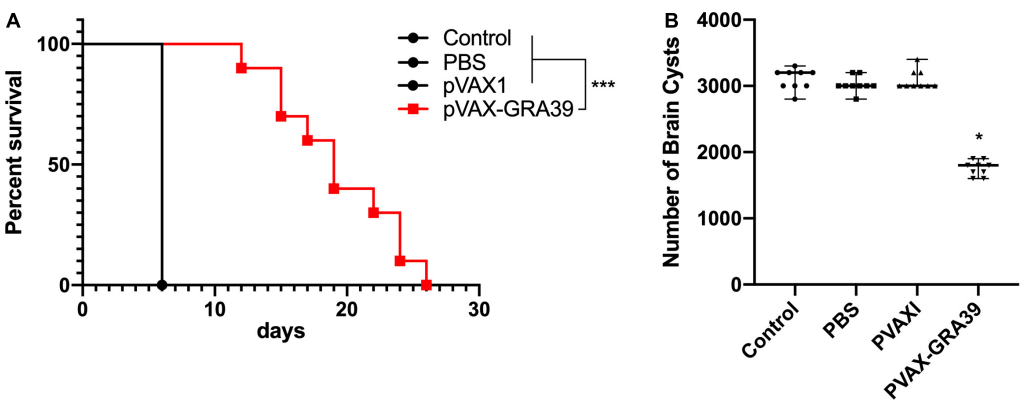

FIGURE 8 | Protective efficacy of mice immunized with pVAX-GRA39 **(A)** Survival curves of Kunming mice after challenge of *T. gondii* RH strain. The mice (10 per group) in all groups were challenged with 1×10^3 tachyzoites of the virulent *T. gondii* RH strain intraperitoneally. Three control groups (PBS, pVAX I and blank control) had 0% survival at day 6. Immunized groups have prolonged survival time of mice. **(B)** Protection against chronic toxoplasmosis in immunized mice two weeks after the last booster immunization. The bars represented the mean cyst burden per mouse brain after oral challenge with a dose of 10 cysts of the Pru strain. Cyst load was counted from whole brain homogenates of mice 4 weeks after challenge. Data are mean ± SDs (representative of three experiments). *$p < 0.05$, ***$p < 0.001$ compared with the control groups.

important Th1-biased cytokine, could regulate the proliferation and activities of CTLs, which are important for resistance against *T. gondii* infection (Karna et al., 2009). IL-12 (IL-12p70) is the determinant of Th1 cells immune response, which could promote the production of Th1-biased cytokine, such as IFN-γ, effectively (LaRosa et al., 2008). Besides, IL-12p40 could also promote the proliferation of T cells including memory T cells and the generation of IFN-γ (Karna et al., 2009). In the present study, significantly increased levels of IFN-γ, IL-12p70, IL-12p40, and IL-2 were detected in the group of mice immunized with pVAX-GRA39, suggesting that Th1-type mediated immunity was elicited by pVAX-GRA39 injection in mice successfully, which are essential for the prolonged survival and reduced brain cysts in the immunized mice. In contrast, as marker cytokines for Th2 cells, IL-4, and IL-10 secreted from the group of mice immunized with pVAX-GRA39 was not significantly higher than that in the control groups, which is an indicative of a more pronounced Th1 response than a Th2 response. However, the absence of a IL-4 and IL-10 response followed by DNA immunization with pVAX-GRA39 may be harmful for the *T. gondii* infective process, which is ascribed to their regulatory role of an extreme Th1 response, involved in limiting the inflammation and inhibiting CD4+ T cell-mediated severe immunopathology (Dupont et al., 2012).

Apart from Th1 cytokines, Th17-mediated protective cellular immunity induced by vaccine have been demonstrated to play a critical role in defending against some pathogens, including *Mycobacterium tuberculosis*, *Helicobacter pylori*, *Pseudomonas aeruginosa* (Khader et al., 2007; Priebe et al., 2008; DeLyria et al., 2009). Th17 cells, this new lineage of T helper cells, were recognized for producing pro-inflammatory cytokines, including IL-17, IL-22, and IL-23 (Ghosh et al., 2013; Sacramento et al., 2014). Among these cytokines, IL-17A produced by CD4+ Th17 cells was found to play a protective role against the intracellular pathogen *Trypanosoma cruzi*, *Leishmania donovani*, and *Leishmania infantum* (Banerjee et al., 2016; Cai et al., 2016). However, evaluation of Th17 responses during immunization trials against *T. gondii* received less attention compared to Th1 and Th2 responses. In our study, after DNA immunization with pVAX-GRA39, a significant increase of IL-17A, IL-17F, IL-22, and IL-23 was detected, suggesting the activated Th17 responses, which is in accordance with some previous studies on immune responses induced by *L. donovani* and *M. tuberculosis* vaccines (Khader et al., 2007; Priebe et al., 2008; DeLyria et al., 2009).

Currently, IL-6, TGF-β1, IL-1β have been considered to be Th17-inducing cytokines, which could prime naive T cell (Th0) differentiation toward Th1/Th2/Treg/Th17 phenotype, and play important roles in the differentiation, proliferation, and maintenance of Th17 cells (Mills, 2008; Korn et al., 2009). Both IL-6 and TGF-β1 could prime naïve CD8+ T cells toward Tc17 cells, thereby, express hallmark molecules, such as retinoic acid receptor-related orphan receptor (ROR)gammat, RORalpha and IL-21 (Yen et al., 2009; Srenathan et al., 2016). Also, the development of Tc17 cell is indispensably dependent on STAT3 and can be augmented by increased expression of RORγt (Huber et al., 2009). In the present study, a significant increase in the expression level of IL-6, TGF-β1, IL-1β, and the transcription factor factors RORγt, RORα, and STAT3 was observed in mice immunized with pVAX-GRA39 compared to mice in the control group, indicating that Tc17 cells responses were activated in CD8+ T cells through RORγt and STAT3 following DNA immunization with pVAX-GRA39. Our findings indicated that pVAX-GRA39 was capable of evoking Th17 and Tc17 differentiation, resulting in a pro-inflammatory protective immunity. A distinct subset of IL–17–producing CD8+ T cells had been identified and designated as Tc17 cells, which are recognized as playing a protective role in host against vaccinia and influenza virus infections (Yeh et al., 2010; Hamada et al., 2013), and are also indispensable for protective immunity against fungal pneumonia (Nanjappa et al., 2015). Recently, it has been established that Tc17 cells could secrete IL-17F and IL-22, and express IL-23R, along with Th17 lineage-specific transcription factors RORγ and RORα (Stritesky et al., 2008; Glosson et al., 2014). These encouraging results in combination with our findings have emphasized that Th17- and Tc17-associated responses induced by DNA immunization with pVAX-GRA39 may play an important role in host defending against *T. gondii* infection.

During the *T. gondii* invasion, T-cell-mediated immunity is also dominant in the process of host immune response for mediating resistance to *T. gondii* infection (Jongert et al., 2010; Zhang et al., 2015a). Especially, CD8+ T cells are specialized cytotoxic T lymphocyte cell that mediate lysis of *T. gondii* by the production of IFN-γ or perforin-mediated cytolysis, in synergy with CD4+ T cells (Gigley et al., 2009; Dupont et al., 2012). The data in the present study was consistent with some previous reports, underlying the protective effects of those vaccines (Xu et al., 2014; Zhang et al., 2014), with the activated proliferative response of lymphocytes and significant increase of both CD8+ and CD4+ T cells in immunized mice. These increased levels of CD4+ and CD8+ T cells further emphasized that T cell-associated immune responses hold a position in resistance against *T. gondii* infection followed by pVAX-GRA39 immunization.

Humoral responses were well known to play an important role in immunity against *T. gondii*, especially, specific antibodies can attached the parasite to the host cell receptors or to the complement molecular, involving in antibody-mediated activation of the classical pathways of complement (Sayles et al., 2000). Augmented levels of IgG were detected in immunized group by ELISA assay, suggesting that DNA immunization pVAX-GRA39 activated humoral immune response effectively, which may be beneficial to opsonize the parasite for phagocytosis and block invasion (Sayles et al., 2000). In addition, pVAX-GRA39 immunization has induced a significant high ratio of IgG2a to IgG1 titers, a characteristic of the Th1-type response in contrast to three control groups.

Similar with previous studies (Chen et al., 2013, 2017; Gao et al., 2018), DNA immunization with a single antigen of TgGRA39 could only induce partial protective immunity in Kunming mice, due to its limited lymphocyte binding sites, leading to a difficulty of mounting an efficient immune response against *T. gondii* (Donnelly et al., 2005). Although this single DNA immunization with pVAX-GRA39 has elicited similar or different effective immunity in comparison with some other single DNA vaccine candidates, such as TgGRA24, TgGRA25 and

TgGRA16 (Hu et al., 2017; Xu et al., 2019; Zheng et al., 2019), this DNA immunization has evoked Th17 responses, which are commonly directly correlated with mucosa protection, and also considered to be beneficial in limiting the host infection via the gastrointestinal tract (Gaffen and Moutsopoulos, 2020). However, in those previous studies on *T. gondii* vaccines, detection of Th17 responses was rarely found. So, these effective responses induced by DNA immunization with pVAX-GRA39 could limit the infection with *T. gondii* via the gastrointestinal tract, leading to the reduction of brain cysts and prolonged survival time in mice models in combination with activated Th1-responses. In addition, the challenge dose of *T. gondii* has been recognized as an important impact factor in analyzing the immune protective effect (Li and Zhou, 2018). Especially, the vaccine could elicit the protective immunity, but it is unable to fight too high a dosage of the lethal *T. gondii* parasite strain RH, resulting in failing observation of a longer survival time due to high the dosage (Yan et al., 2012). So, the low-virulence strain PRU may be more suitable to study survival after challenge, and further study can be explored to 80 cysts of strain PRU per mouse were administered intragastrically in order to study survival after challenge, according to some previous studies (Yan et al., 2012). Moreover, further studies should also evaluate the role of limited lymphocyte binding sites of TgGRA39 by adding immunotargeting molecules to the antigen, and also the immunity against *T. gondii* infection with TgGRA39-based multiantigenic vaccine, and even electroporation can be further used to enhance the protective immune responses, associated with the increased duration of survival and/or fewer cysts.

In conclusion, our work demonstrated that TgGRA39 is a DNA vaccine candidate in Kunming mice model, with ability of eliciting humoral immune responses and Th1-biased, Th17 and Tc17 responses. This potential vaccine candidate can prolong the survival time in mice infected with RH strain and reduce the number of cysts in mice infected with PRU strain, providing a foundation for further multi-epitope vaccine design based on TgGRA39.

DATA AVAILABILITY STATEMENT

The original contributions presented in the study are included in the article/**Supplementary Material**, further inquiries can be directed to the corresponding authors.

ETHICS STATEMENT

The animal study was reviewed and approved by the Ethical Committee of Ningbo University [permission: SYXK(ZHE)2013-0190].

AUTHOR CONTRIBUTIONS

JC, CZ, and YZ were involved in the final development of the project and manuscript preparation. YX analyzed the data. YZ and LH performed most of the experiments. All authors contributed to the article and approved the submitted version.

FUNDING

The project support was provided by the National Natural Science Foundation of China (Grant No. 31402190), the China Postdoctoral Science Foundation (Grant No. 132764), and the Ningbo Public Welfare Science and Technology Project (202002N3153).

SUPPLEMENTARY MATERIAL

The Supplementary Material for this article can be found online at: https://www.frontiersin.org/articles/10.3389/fmicb.2021.630682/full#supplementary-material

REFERENCES

Banerjee, A., Bhattacharya, P., Joshi, A. B., Ismail, N., Dey, R., and Nakhasi, H. L. (2016). Role of pro-inflammatory cytokine IL-17 in *Leishmania* pathogenesis and in protective immunityby *Leishmania* vaccines. *Cell Immunol.* 309, 37–41. doi: 10.1016/j.cellimm.2016.07.004

Beauvillain, C., Juste, M. O., Dion, S., Pierre, J., and Poisson, I. D. (2009). Exosomes are an effective vaccine against congenital toxoplasmosis in mice. *Vaccine* 27, 1750–1757. doi: 10.1016/j.vaccine.2009.01.022

Cai, C. W., Blase, J. R., Zhang, X., Eickhoff, C. S., and Hoft, D. F. (2016). Th17 cells are more protective than Th1 cells against the intracellular parasite *Trypanosoma cruzi*. *PLoS Pathog.* 12:e1005902. doi: 10.1371/journal.ppat.1005902

Cao, A., Liu, Y., Wang, J., Li, X., Wang, S., Zhao, Q., et al. (2015). *Toxoplasma gondii*: vaccination with a DNA vaccine encoding T- and B-cell epitopes of SAG1, GRA2, GRA7 and ROP16 elicits protection against acute toxoplasmosis in mice. *Vaccine* 33, 6757–6762. doi: 10.1016/j.vaccine.2015.10.077

Chen, J., Huang, S. Y., Zhou, D. H., Li, Z. Y., Petersen, E., Song, H. Q., et al. (2013). DNA immunization with eukaryotic initiation factor-2α of *Toxoplasma gondii* induces protective immunity against acute and chronic toxoplasmosis in mice. *Vaccine* 31, 6225–6231. doi: 10.1016/j.vaccine.2013.10.034

Chen, J., Li, Z. Y., Petersen, E., Huang, S. Y., Zhou, D. H., and Zhu, X. Q. (2015). DNA vaccination with genes encoding *Toxoplasma gondii* antigens ROP5 and GRA15 induces protective immunity against toxoplasmosis in Kunming mice. *Expert. Rev. Vaccines* 14, 617–624. doi: 10.1586/14760584.2015.1011133

Chen, J., Li, Z. Y., Petersen, E., Liu, W. G., and Zhu, X. Q. (2016). Co-administration of interleukins 7 and 15 with DNA vaccine improves protective immunity against *Toxoplasma gondii*. *Exp. Parasitol.* 162, 18–23. doi: 10.1016/j.exppara.2015.12.013

Chen, K., Wang, J. L., Huang, S. Y., Yang, W. B., Zhu, W. N., and Zhu, X. Q. (2017). Immune responses and protection after DNA vaccination against *Toxoplasma gondii* calcium-dependent protein kinase 2 (TgCDPK2). *Parasite* 24:41. doi: 10.1051/parasite/2017045

Ching, X. T., Fong, M. Y., and Lau, Y. L. (2016). Evaluation of immunoprotection conferred by the subunit vaccines of GRA2 and GRA5 against acute toxoplasmosis in BALB/c mice. *Front. Microbiol.* 7:609. doi: 10.3389/fmicb.2016.00609

DeLyria, E. S., Redline, R. W., and Blanchard, T. G. (2009). Vaccination of mice against H pylori induces a strong Th-17 response and immunity that is neutrophil dependent. *Gastroenterology* 136, 247–256. doi: 10.1053/j.gastro.2008.09.017

Donnelly, J. J., Wahren, B., and Liu, M. A. (2005). DNA vaccines: progress and challenges. *J. Immunol.* 175, 633–639. doi: 10.4049/jimmunol.175.2.633

Dupont, C. D., Christian, D. A., and Hunter, C. A. (2012). Immune response and immunopathology during toxoplasmosis. *Semin Immunopathol.* 34, 793–813. doi: 10.1007/s00281-012-0339-3

Gaffen, S. L., and Moutsopoulos, N. M. (2020). Regulation of host-microbe interactions at oral mucosal barriers by type 17 immunity. *Sci. Immunol.* 5:eaau4594. doi: 10.1126/sciimmunol.aau4594

Gangneux, F. R., and Dardé, M. L. (2012). Epidemiology of and diagnostic strategies for toxoplasmosis. *Clin. Microbiol. Rev.* 25, 264–296. doi: 10.1128/CMR.05013-11

Gao, Q., Zhang, N. Z., Zhang, F. K., Wang, M., Hu, L. Y., and Zhu, X. Q. (2018). Immune response and protective effect against chronic *Toxoplasma gondii* infection induced by vaccination with a DNA vaccine encoding profilin. *BMC Infect Dis.* 18:117. doi: 10.1186/s12879-018-3022-z

Gatkowska, J., Wieczorek, M., Dziadek, B., Dzitko, K., Dziadek, J., and Długońska, H. (2018). Assessment of the antigenic and neuroprotective activity of the subunit anti-toxoplasma vaccine in *T. gondii* experimentally infected mice. *Vet. Parasitol.* 254, 82–94. doi: 10.1016/j.vetpar.2018.02.043

Ghosh, K., Sharma, G., Saha, A., Kar, S., Das, P. K., and Ukil, A. (2013). Successful therapy of visceral leishmaniasis with curdlan involves T-helper 17 cytokines. *J. Infect. Dis.* 207, 1016–1025. doi: 10.1093/infdis/jis771

Gigley, J. P., Fox, B. A., and Bzik, D. J. (2009). Cell-mediated immunity to *Toxoplasma gondii* develops primarily by local Th1 host immune responses in the absence of parasite replication. *J. Immunol.* 182, 1069–1078. doi: 10.4049/jimmunol.182.2.1069

Glosson, B. N. L., Sehra, S., and Kaplan, M. H. (2014). STAT4 is required for IL-23 responsiveness in Th17 memory cells and NKT cells. *JAKSTAT* 3:e955393. doi: 10.4161/21623988.2014.955393

Hakimi, M., Olias, P., and Sibley, L. D. (2017). *Toxoplasma* effectors targeting host signaling and transcription. *Clin. Microbiol. Rev.* 30, 615–645. doi: 10.1128/CMR.00005-17

Hamada, H., Bassity, E., Flies, A., Strutt, T. M., Garcia, H., Mde, L., et al. (2013). Multiple redundant effector mechanisms of CD8+ T cells protect against influenza infection. *J. Immunol.* 190, 296–306. doi: 10.4049/jimmunol.1200571

Hu, L. Y., Zhang, N. Z., Zhang, F. K., Wang, M., Gao, Q., Wang, J. L., et al. (2017). Resistance to chronic *Toxoplasma gondii* infection induced by a DNA vaccine expressing GRA16. *Biomed. Res. Int.* 2017:1295038. doi: 10.1155/2017/1295038

Huber, M., Heink, S., Grothe, H., Guralnik, A., Reinhard, K., Elflein, K., et al. (2009). A Th17-like developmental process leads to CD8(+) Tc17 cells with reduced cytotoxic activity. *Eur. J. Immunol.* 39, 1716–1725. doi: 10.1002/eji.200939412

Jongert, E., Lemiere, A., Ginderachter, J. V., Craeye, S. D., Huygen, K., and D'Souza, S. (2010). Functional characterization of in vivo effector CD4(+) and CD8(+) T cell responses in acute Toxoplasmosis: an interplay of IFN-gamma and cytolytic T cells. *Vaccine* 28, 2556–2564. doi: 10.1016/j.vaccine.2010.01.031

Jongert, E., Roberts, C. W., Gargano, N., Waldl, E. F., and Petersen, E. (2009). Vaccines against *Toxoplasma gondii*: challenges and opportunities. *Mem. Inst. Oswaldo Cruz.* 104, 252–266. doi: 10.1590/s0074-02762009000200019

Karna, J. M., Piekarska, V. D., and Kemona, H. (2009). Does *Toxoplasma gondii* infection affect the levels of IgE and cytokines (IL-5, IL-6, IL-10, IL-12, and TNF-alpha)? *Clin. Dev. Immunol.* 2009:374696.

Khader, S. A., Bell, G. K., Pearl, J. E., Fountain, J. J., Moreno, J. R., Cilley, G. E., et al. (2007). IL-23 and IL-17 in the establishment of protective pulmonary $CD4^+$ T cell responses after vaccination and during Mycobacterium tuberculosis challenge. *Nat. Immunol.* 8, 369–377. doi: 10.1038/ni1449

Kochanowsky, J. A., and Koshy, A. A. (2018). *Toxoplasma gondii*. *Curr. Biol.* 23, R770–R771. doi: 10.1016/j.cub.2018.05.035

Korn, T., Bettelli, E., Oukka, M., and Kuchroo, V. K. (2009). IL-17 and Th17 Cells. *Annu. Rev. Immunol.* 27, 485–517. doi: 10.1146/annurev.immunol.021908.132710

LaRosa, D. F., Stumhofer, J. S., Gelman, A. E., Rahman, A. H., Taylor, D. K., Hunter, C. A., et al. (2008). T cell expression of MyD88 is required for resistance to *Toxoplasma gondii*. *Proc. Natl. Acad. Sci. U.S.A.* 105, 3855–3860. doi: 10.1073/pnas.0706663105

Lee, S. H., Kang, H. J., Lee, D. H., Kang, S. M., and Quan, F. S. (2018). Virus-like particle vaccines expressing *Toxoplasma gondii* rhoptry protein 18 and microneme protein 8 provide enhanced protection. *Vaccine* 36, 5692–5700. doi: 10.1016/j.vaccine.2018.08.016

Li, Y., and Zhou, H. (2018). Moving towards improved vaccines for *Toxoplasma gondii*. *Expert. Opin. Biol. Ther.* 18, 273–280. doi: 10.1080/14712598.2018.1413086

Liu, M. A. (2011). DNA vaccines: an historical perspective and view to the future. *Immunol. Rev.* 239, 62–84. doi: 10.1111/j.1600-065X.2010.00980.x

Mills, K. H. G. (2008). Induction, function and regulation of IL-17-producing T cells. *Eur. J. Immunol.* 38, 2636–2649. doi: 10.1002/eji.200838535

Nadipuram, S. M., Kim, E. K., Vashisht, A. A., Lin, A. H., Bell, H. N., Coppens, I., et al. (2016). In vivo biotinylation of the *Toxoplasma* parasitophorous vacuole reveals novel dense granule proteins important for parasite growth and pathogenesis. *mBio* 7:e808-16. doi: 10.1128/mBio.00808-16

Nanjappa, S. G., Hernández, S. N., Galles, K., Wüthrich, M., Suresh, M., and Klein, B. S. (2015). Intrinsic MyD88-Akt1-mTOR signaling coordinates disparate Tc17 and Tc1 responses during vaccine immunity against fungal pneumonia. *PLoS Pathog.* 11:e1005161. doi: 10.1371/journal.ppat.1005161

Petersen, E., Kijlstra, A., and Stanford, M. (2012). Epidemiology of ocular toxoplasmosis. *Ocul. Immunol. Inflamm.* 20, 68–75. doi: 10.3109/09273948.2012.661115

Priebe, G. P., Walsh, R. L., Cederroth, T. A., Kamei, A., Sledge, Y. S. C., Goldberg, J. B., et al. (2008). IL-17 is a critical component of vaccine-induced protection against lung infection by lipopolysaccharide-heterologous strains of *Pseudomonas aeruginosa*. *J. Immunol.* 181, 4965–4975. doi: 10.4049/jimmunol.181.7.4965

Sacramento, L. A., Cunha, F. Q., Almeida, R. P. D., Silva, J. S. D., and Carregaro, V. (2014). Protective role of 5-lipoxigenase during *Leishmania* infantum infection is associated with Th17 subset. *Biomed. Res. Int.* 2014:264270. doi: 10.1155/2014/264270

Sayles, P. C., Gibson, G. W., and Johnson, L. L. (2000). B cells are essential for vaccination-induced resistance to virulent *Toxoplasma gondii*. *Infect. Immun.* 68, 1026–1033. doi: 10.1128/iai.68.3.1026-1033.2000

Silva, N. M., Vieira, J. C. M., Carneiro, C. M., and Tafuri, W. L. (2009). *Toxoplasma gondii*: the role of IFN-gamma, TNFRp55 and iNOS in inflammatory changes during infection. *Exp. Parasitol.* 123, 65–72. doi: 10.1016/j.exppara.2009.05.011

Sonaimuthu, P., Ching, X. Y., and Fong, M. Y., Kalyanasundaram, R., and Lau, Y. L. (2016). Induction of protective immunity against toxoplasmosis in BALB/c mice vaccinated with *Toxoplasma*. *Front. Microbiol.* 7:808. doi: 10.3389/fmicb.2016.00808

Srenathan, U., Steel, K., and Taams, L. S. (2016). IL-17^+ $CD8^+$ T cells: differentiation, phenotype and role in inflammatory disease. *Immunol. Lett.* 178, 20–26. doi: 10.1016/j.imlet.2016.05.001

Stritesky, G. L., Yeh, N., and Kaplan, M. H. (2008). IL-23 promotes maintenance but not commitment to the Th17 lineage. *J. Immunol.* 181, 5948–5955. doi: 10.4049/jimmunol.181.9.5948

Tenter, A. M., Heckeroth, A. R., and Weiss, L. M. (2000). *Toxoplasma gondii*: from animals to humans. *Int. J. Parasitol.* 30, 1217–1258. doi: 10.1016/s0020-7519(00)00124-7

Wang, J. L., Elsheikha, H. M., Zhu, W. N., Chen, K., Li, T. T., Yue, D. M., et al. (2017a). Immunization with *Toxoplasma gondii* GRA17 deletion mutant induces partial protection and survival in challenged mice. *Front. Immunol.* 8:730. doi: 10.3389/fimmu.2017.00730

Wang, S., Zhang, Z., Wang, Y., Gadahi, J. A., Xu, L., Yan, R., et al. (2017b). *Toxoplasma gondii* elongation factor 1-Alpha (TgEF-1α) is a novel vaccine candidate antigen against toxoplasmosis. *Front. Microbiol.* 8:168. doi: 10.3389/fmicb.2017.00168

Wang, Z. D., Liu, H. H., Ma, Z. X., Ma, H. Y., Li, Z. Y., Yang, Z. B., et al. (2017c). *Toxoplasma gondii* infection in immunocompromised patients: a systematic review and meta-analysis. *Front. Microbiol.* 8:389. doi: 10.3389/fmicb.2017.00389

Wang, Z. D., Wang, S. C., Liu, H. H., Ma, H. Y., Li, Z. Y., Wei, F., et al. (2017d). Prevalence and burden of Toxoplasma gondii infection in HIV-infected people: a systematic review and meta-analysis. *Lancet HIV* 4, e177–e188. doi: 10.1016/S2352-3018(17)30005-X

Wang, J. L., Li, T. T., Elsheikha, H. M., Chen, K., Cong, W., Yang, W. B., et al. (2018). Live attenuated Pru:Δcdpk2 Strain of *Toxoplasma gondii* protects against acute, chronic, and congenital toxoplasmosis. *J. Infect. Dis.* 218, 768–777. doi: 10.1093/infdis/jiy211

Wang, J. L., Zhang, N. Z., Li, T. T., He, J. J., Elsheikha, H. M., and Zhu, X. Q. (2019). Advances in the development of anti-*Toxoplasma gondii* vaccines: challenges, opportunities, and perspectives. *Trends Parasitol.* 35, 239–253. doi: 10.1016/j.pt.2019.01.005

Wohlfert, E. A., Blader, I. J., and Wilson, E. H. (2017). Brains and brawn: toxoplasma infections of the central nervous system and skeletal muscle. *Trends Parasitol.* 33, 519–531. doi: 10.1016/j.pt.2017.04.001

Xu, X. P., Liu, W. G., Xu, Q. M., Zhu, X. Q., and Chen, J. (2019). Evaluation of immune protection against *Toxoplasma gondii* infection in mice induced by a multi-antigenic DNA vaccine containing TgGRA24, TgGRA25 and TgMIC6. *Parasite* 26:58. doi: 10.1051/parasite/2019050

Xu, Y., Zhang, N. Z., Tan, Q. D., Chen, J., Lu, J., Xu, Q. M., et al. (2014). Evaluation of immuno-efficacy of a novel DNA vaccine encoding *Toxoplasma gondii* rhoptry protein 38 (TgROP38) against chronic toxoplasmosis in a murine model. *BMC Infect. Dis.* 14:525. doi: 10.1186/1471-2334-14-525

Yan, H. Z., Yuan, Z. G., Song, H. Q., Petersen, E., Zhou, Y., Ren, D., et al. (2012). Vaccination with a DNA vaccine coding for perforin-like protein 1 and MIC6 induces significant protective immunity against *Toxoplasma gondii*. *Clin. Vaccine Immunol.* 19, 684–689. doi: 10.1128/CVI.05578-11

Yeh, N., Glosson, N. L., Wang, N., Guindon, L., McKinley, C., Hamada, H., et al. (2010). Tc17 cells are capable of mediating immunity to vaccinia virus by acquisition of a cytotoxicphenotype. *J. Immunol.* 185, 2089–2098. doi: 10.4049/jimmunol.1000818

Yen, H. R., Harris, T. J., Wada, S., Grosso, J. F., Getnet, D., Goldberg, M. V., et al. (2009). Tc17 CD8 T cells: functional plasticity and subset diversity. *J. Immunol.* 183, 7161–7168. doi: 10.4049/jimmunol.0900368

Zhang, N. Z., Chen, J., Wang, M., Petersen, E., and Zhu, X. Q. (2013). Vaccines against *Toxoplasma gondii*: new developments and perspectives. *Expert. Rev. Vaccines.* 12, 1287–1299. doi: 10.1586/14760584.2013.844652

Zhang, N. Z., Gao, Q., Wang, M., Elsheikha, H. M., Wang, B., Wang, J. L. et al. (2018a). Immunization with a DNA vaccine cocktail encoding TgPF, TgROP16, TgROP18, TgMIC6, and TgCDPK3 genes protects mice against chronic toxoplasmosis. *Front. Immunol.* 9:1505. doi: 10.3389/fimmu.2018.01505

Zhang, N. Z., Gao, Q., Wang, M., Hou, J. L., Zhang, F. K., Hu, L. Y., et al. (2018b). Protective efficacy against acute and chronic *Toxoplasma gondii* infection induced by immunization with the DNA Vaccine TgDOC2C. *Front. Microbiol.* 9:2965. doi: 10.3389/fmicb.2018.02965

Zhang, Z., Li, Y., Wang, M., Xie, Q., Li, P., Zuo, S., et al. (2018c). Immune protection of rhoptry protein 21 (ROP21) of *Toxoplasma gondii* as a DNA vaccine against toxoplasmosis. *Front. Microbiol.* 9:909. doi: 10.3389/fmicb.2018.00909

Zhang, N. Z., Huang, S. Y., Xu, Y., Chen, J., Wang, J. L., Tian, W. P., et al. (2014). Evaluation of immune responses in mice after DNA immunization with putative *Toxoplasma gondii* calcium-dependent protein kinase 5. *Clin. Vaccine Immunol.* 21, 924–929. doi: 10.1128/CVI.00059-14

Zhang, N. Z., Wang, M., Xu, Y., Petersen, E., and Zhu, X. Q. (2015a). Recent advances in developing vaccines against *Toxoplasma gondii*: an update. *Expert. Rev. Vaccines.* 14, 1609–1621. doi: 10.1586/14760584.2015.1098539

Zhang, N. Z., Xu, Y., Wang, M., Petersen, E., Chen, J., Huang, S. Y., et al. (2015b). Protective efficacy of two novel DNA vaccines expressing *Toxoplasma gondii* rhomboid 4 and rhomboid 5 proteins against acute and chronic toxoplasmosis in mice. *Expert. Rev. Vaccines* 14, 1289–1297. doi: 10.1586/14760584.2015.1061938

Zheng, B., Lou, D., Ding, J., Zhuo, X., Ding, H., Kong, Q., et al. (2019). GRA24-based DNA vaccine prolongs survival in mice challenged with a virulent *Toxoplasma gondii* Strain. *Front. Immunol.* 10:418. doi: 10.3389/fimmu.2019.00418

Zheng, B., Lu, S., Tong, Q., Kong, Q., and Lou, D. (2013). The virulence-related rhoptry protein 5 (ROP5) of *Toxoplasma Gondii* is a novel vaccine candidate against toxoplasmosis in mice. *Vaccine* 31, 4578–4584. doi: 10.1016/j.vaccine.2013.07.058

Zhou, J., and Wang, L. (2017). SAG4 DNA and peptide vaccination provides partial protection against *T. gondii* Infection in BALB/c Mice. *Front. Microbiol.* 8:1733. doi: 10.3389/fmicb.2017.01733

Zhu, Y. C., He, Y., Liu, J. F., and Chen, J. (2020). Adjuvantic cytokine IL-33 improves the protective immunity of cocktailed DNA vaccine of ROP5 and ROP18 against *Toxoplasma gondii* infection in mice. *Parasite* 27:26. doi: 10.1051/parasite/2020021

Conflict of Interest: The authors declare that the research was conducted in the absence of any commercial or financial relationships that could be construed as a potential conflict of interest.

frontiers in Microbiology

REVIEW
published: 30 April 2021
doi: 10.3389/fmicb.2021.670775

Whole-Killed Blood-Stage Vaccine: Is It Worthwhile to Further Develop It to Control Malaria?

Jingjing Cai[1†], Suilin Chen[1,2,3†], Feng Zhu[1,2,3], Xiao Lu[4], Taiping Liu[1,2,3] and Wenyue Xu[1,2,3*]*

[1]College of Basic Medicine, Army Medical University (Third Military Medical University), Chongqing, China, [2]Department of Pathogenic Biology, Army Medical University (Third Military Medical University), Chongqing, China, [3]Key Laboratory of Extreme Environmental Medicine, Ministry of Education of China, Chongqing, China, [4]Department of Thoracic Surgery, Xinqiao Hospital, Army Medical University (Third Military Medical University), Chongqing, China

Major challenges have been encountered regarding the development of highly efficient subunit malaria vaccines, and so whole-parasite vaccines have regained attention in recent years. The whole-killed blood-stage vaccine (WKV) is advantageous as it can be easily manufactured and efficiently induced protective immunity against a blood-stage challenge, as well as inducing cross-stage protection against both the liver and sexual-stages. However, it necessitates a high dose of parasitized red blood cell (pRBC) lysate for immunization, and this raises concerns regarding its safety and low immunogenicity. Knowledge of the major components of WKV that can induce or evade the host immune response, and the development of appropriate human-compatible adjuvants will greatly help to optimize the WKV. Therefore, we argue that the further development of the WKV is worthwhile to control and potentially eradicate malaria worldwide.

Keywords: malaria parasite, whole-killed blood-stage vaccine, liver stage, sexual-stage, blood stage

OPEN ACCESS

Edited by:
Karl Kuchler,
Medical University of Vienna, Austria

Reviewed by:
Yang Cheng,
Jiangnan University, China
Jun-Hu Chen,
National Institute of Parasitic Diseases, China
Alberto Moreno,
Emory University, United States

***Correspondence:**
Wenyue Xu
xuwenyue@tmmu.edu.cn
Taiping Liu
liutaiping@tmmu.edu.cn

[†]These authors have contributed equally to this work

Specialty section:
This article was submitted to Infectious Diseases, a section of the journal Frontiers in Microbiology

Received: *22 February 2021*
Accepted: *08 April 2021*
Published: *30 April 2021*

Citation:
Cai J, Chen S, Zhu F, Lu X, Liu T and Xu W (2021) Whole-Killed Blood-Stage Vaccine: Is It Worthwhile to Further Develop It to Control Malaria? Front. Microbiol. 12:670775. doi: 10.3389/fmicb.2021.670775

INTRODUCTION

Malaria remains a potentially fatal public health problem, resulting in high morbidity and mortality in tropical and subtropical regions. Recently, malaria control interventions, such as artemisinin-based combination therapy (ACT), insecticide-treated bed nets (ITNs), and other mosquito vector control strategies, have greatly reduced the incidence of malaria all over the world (O'Meara et al., 2010). However, the emergence of artemisinin derivative-resistant malaria parasites (Phyo et al., 2012; Uwimana et al., 2020) and insecticide-resistant mosquitoes (Ranson et al., 2011) has greatly hampered the effectiveness of ACTs and ITNs. Therefore, the development of a highly efficient malaria vaccine has been regarded as the most cost-effective tool for malaria control and elimination, and potentially even eradication (Crompton et al., 2010).

Malaria is caused by the infections of species in the *Plasmodium* genus. There are four human malaria parasites, namely, *Plasmodium vivax* (*P. vivax*), *P. falciparum*, *P. ovale*, and *P. malariae*. Of these, *P. falciparum* is the deadliest. A *Plasmodium* infection is initiated by sporozoite inoculation into the host skin by an infected female *Anopheles* mosquito. The sporozoites travel to the liver and infect a small number of hepatocytes, with a single sporozoite giving rise to tens of thousands of merozoites. Next, merozoites are released into the bloodstream when merosomes bud from an infected hepatocyte, and they invade red blood cells (RBCs), initiating blood-stage development. A merozoite can multiply up to 20-fold every 1–3 days in

cycles of invasion, replication, and RBC rupture, which releases many infectious merozoites. Some of the asexual blood stages transform into sexual forms called as gametocytes, which can eventually move into the midgut of a blood-feeding mosquito and then develop into sporozoites in the salivary gland. The blood-feeding mosquito then injects these sporozoites into another human, thereby initiating a new human infection (**Figure 1**).

Thus, the *Plasmodium* life cycle involves the liver stage (pre-erythrocytic stage) and blood stage in mammals and the sexual-stage in its vector. The blood stage is the main cause of the clinical manifestations (ranging from mild to severe malaria), and a blood-stage vaccine aims to reduce mortality and morbidity in malaria patients. In contrast, the liver stage is clinically silent, and a liver-stage vaccine is promising for preventing malaria infection (Smith et al., 2012). The development of the parasite in mosquitoes is essential for malaria transmission. Therefore, a sexual-stage vaccine aims to block malaria transmission (Acquah et al., 2019; **Figure 1**). For each stage, two kinds of vaccines, namely subunit and whole-parasite vaccines, are being explored. As major challenges have been encountered regarding subunit malaria vaccines, whole-parasite vaccines have recently been regaining attention. Here, we discuss promising aspects regarding the development of a whole-killed blood-stage vaccine (WKV) that protects against all stages and perspectives on its optimization in the future.

MAJOR CHALLENGES HAVE BEEN ENCOUNTERED IN THE DEVELOPMENT OF A HIGHLY EFFICIENT SUBUNIT MALARIA VACCINE

In the past three decades, great efforts have been made to develop efficient subunit vaccines against the pre-erythrocytic, blood, and sexual-stages, but major challenges have been encountered. The dominant protective antigen of the pre-erythrocytic stage is the main surface protein of sporozoites,

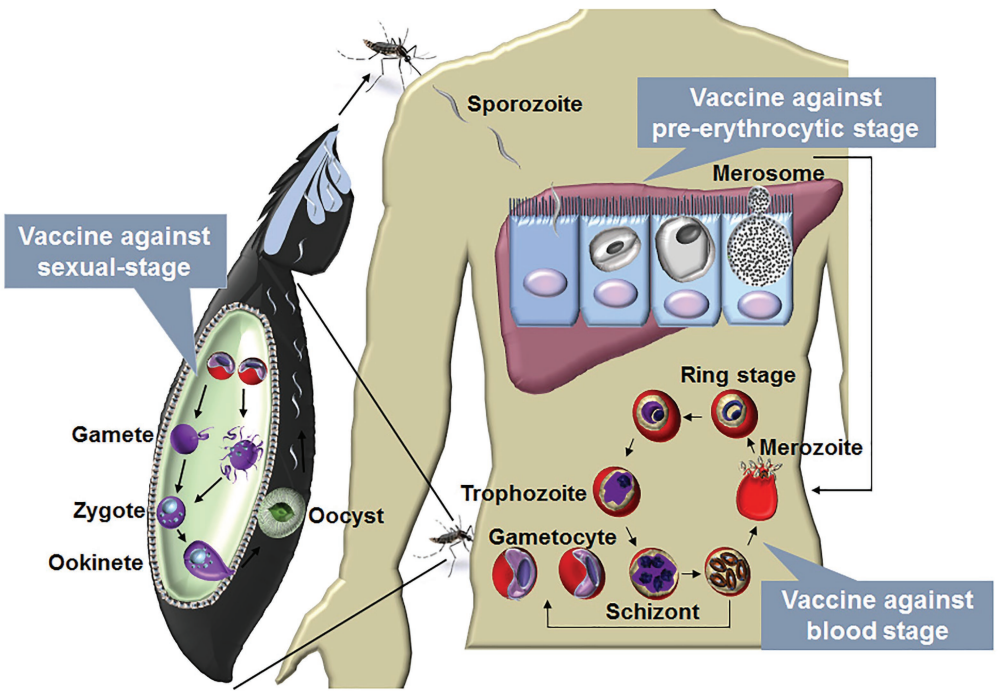

FIGURE 1 | The life cycle of malaria parasite and vaccines designed against each stage. The life cycle of *Plasmodium* includes liver stage and blood stage in human and sexual-stage in the mosquito vector. A *Plasmodium* infection begins when an infected female *Anopheles* mosquito takes a blood meal and injects a small number of sporozoites into a human host. The sporozoites enter blood vessels and invade target hepatocytes, with a single sporozoite giving rise to tens of thousands of merozoites. Next, merozoites are budded from an infected hepatocyte by the merosomes and rupture to release thousands of merozoites into the bloodstream. In the bloodstream, the merozoites invade RBCs, initiating blood-stage development. A merozoite, which subsequently develop into ring, trophozoite, and schizont stage parasites, can multiply up to 20-fold every 1 to 3 days in cycles of invasion, replication, and RBC rupture. New daughter merozoites are released and rapidly invade the non-infected erythrocytes. Within erythrocytes, some of the merozoites differentiate into sexual forms of the parasite, which are called as male or female gametocytes. When male and female gametocytes are picked up by a female *Anopheles* mosquito during a blood meal, they develop further into mature sexual stages called as gametes. Fertilization happens between the male and female gametes, giving rise to a zygote. The developing zygotes transform into elongated motile ookinetes, which invade through the midgut wall of the mosquito and form oocysts on the exterior surface. Once the oocysts have matured, they eventually burst, releasing thousands of sporozoites that migrate to the mosquito salivary glands ready to infect another human host during the next mosquito blood meal (Julien and Wardemann, 2019). A vaccine against the blood stage aims to reduce the mortality and morbidity of malaria patients, and vaccine against the liver stage is a promising method to prevent malaria infection. The development of the parasite in the vector is essential for transmission, a vaccine against the sexual-stage aims, therefore, to block transmission of malaria parasites.

circumsporozoite protein (CSP), which plays an important role in sporozoite invasion of hepatocytes (Dame et al., 1984; Rathore et al., 2002; Kumar et al., 2006). The most advanced CSP-based subunit malaria vaccine is RTS,S/AS01. This vaccine consists of a large part of the CSP fused with hepatitis B virus surface antigen (HBV-S Ag) particle formulated with the potent liposomal adjuvant AS01 (Cohen, 1996; Casares et al., 2010). Phase 3 clinical trials showed that the vaccine's protection efficacy was 50.4% against the first clinical episode of malaria and 45.1% against severe malaria in young children, but only 30.1% in infants (Agnandji et al., 2011, 2012). In 2015, the European Medicines Agency announced the adoption of a positive scientific opinion regarding the use of RTS,S in regions outside of the European Union, where malaria is a major problem (EMA, 2015). In 2019, the World Health Organization (WHO) recommended the large-scale pilot implementations of routine use of RTS,S in real-life settings, involving moderate-to-high malaria transmission in order to assess its protective benefits and safety (WHO, 2019). However, RTS,S/AS01 still does not meet the criteria for a licensable first-generation vaccine (50% efficacy lasting for ≥1 year; Crompton et al., 2010), as the vaccine efficacy was dropped to 28 and 18% at 3–4 years post-vaccination in children and young infants, respectively (Rts, 2015). Therefore, the main challenge of the use of RTS,S is to sustain high antibody concentrations to mediate durable protection.

Most blood-stage candidate antigens are essential invasion proteins of merozoites such as merozoite surface protein (MSP1) and MSP3, apical membrane antigen 1 (AMA1), and erythrocyte-binding antigen 175 (EBA-175). These blood stage malaria vaccine candidates seek to induce high titers of plasmodium specific antibody that inhibit erythrocyte invasion by merozoites or limit parasite replication in red blood cells. However, most of the vaccine candidates exhibit extensive polymorphism between malaria strains from different geographical regions, and immunization with these vaccines only led to partial protection against vaccine-like strains (Bull et al., 1998; Sutherland, 2007; Fowkes et al., 2010). In addition, the RBC invasion pathways of merozoite exhibit redundancy, with the blockade of one invasion pathway failing to confer protection against challenge (Ogutu et al., 2009; Sagara et al., 2009; Sirima et al., 2011). The leading vaccine candidates AMA1 did not provide significant protection against clinical malaria in vaccine trials, and an MSP3 vaccine in Burkinabe children also demonstrated short-term protection (Sirima et al., 2011; Thera et al., 2011). At present, the most promising blood-stage candidate antigen is *P. falciparum* reticulocyte-binding protein homolog 5 (PfRH5), which interacts with basigin (CD147) on the RBC surface during merozoite invasion (Wright et al., 2014). PfRH5 exhibits limited polymorphism, and PfRH5/basigin is essential for merozoite invasion of RBCs (Weiss et al., 2015; Volz et al., 2016). Pre-clinical studies showed that PfRH5 induced cross-strain neutralizing antibody (Douglas et al., 2011) and confers nearly complete protection against challenge with heterologous *Plasmodium* strains in Aotus monkeys (Douglas et al., 2015). Recent study has defined that the neutralizing and non-neutralizing epitopes of PfRH5 are both essential for red blood cell invasion by the merozoites, which will optimize the designation of PfRH5-based vaccine (Alanine et al., 2019). However, protection in monkeys required a high level of anti-PfRH5 IgG (an estimated 200 μg/ml), and there was modest or no boosting of vaccine-induced antibody by infection of the monkeys (Douglas et al., 2015). This may limit the efficacy and duration of protection conferred by a PfRH5-based subunit vaccine.

Leading candidate antigens related to the malaria sexual-stage, include *P. falciparum* Pfs230 and Pfs48/45, which are expressed by gametocytes, and Pfs25, which is exclusively expressed by zygotes and ookinetes. In phase 1 clinical trials, vaccines based on Pfs25 and its *P. vivax* ortholog Pvs25 have induced antibodies that block mosquito infection (Wu et al., 2008). However, substantial antibody levels were only achieved after four doses, and antibody levels rapidly waned after the final dose (Sagara et al., 2018). In addition, these antigens are cysteine-rich with multiple 6-cys domains and/or epidermal growth factor (EGF)-like domains, and it is difficult to prepare the properly folded recombinant protein (Barr et al., 1991).

The major issue regarding the current subunit malaria vaccines is that they always contain only a single or a small number of antigens, which do not induce broad-spectrum long-lasting immune responses. It is well known that *Plasmodium* encodes approximately 5,300 proteins, but only a few candidate antigens have been identified (Gardner et al., 2002; Doolan et al., 2003). Therefore, it is currently difficult to design highly efficient subunit malaria vaccines.

PROMISING MALARIA VACCINE: WHOLE-PARASITE BLOOD-STAGE VACCINE

In contrast to the narrow antigen spectrum related to subunit vaccines, whole-parasite vaccines maximize the spectrum of antigens, greatly enhancing protective immunity, and they have attracted more attention in recent years (Tarun et al., 2008; Ting et al., 2008; Moorthy and Ballou, 2009; Aly et al., 2010; Demarta-Gatsi et al., 2016; Mordmuller et al., 2017; **Table 1**). Attenuated sporozoites are the most promising vaccines against the pre-erythrocytic stage. It has been reported that either irradiation-, genetic-, or chemo-attenuated sporozoites (also called as chemoprophylaxis with sporozoites, CPS) could induce sterilizing protective immunity against homologous sporozoite challenge in both mice and humans (Nussenzweig et al., 1967; Mueller et al., 2005; Roestenberg et al., 2009; Epstein et al., 2011; Bijker et al., 2013; Seder et al., 2013). An irradiation-attenuated sporozoite vaccine could also induce a strain-transcending T cell response and durable protection against heterologous controlled human malaria infection (CHMI; Lyke et al., 2017). PfSPZ vaccine was confirmed to be extremely well tolerated and showed the significant protection in Mali adults against *P falciparum* infection in phase 1 trial (Sissoko et al., 2017). Furthermore, in the recent study by Roestenberg et al. (2020) in phase 1/2a trial, genetically attenuated malaria vaccine PfSPZ-GA1 also showed the modest protective immunity

TABLE 1 | The time table of the development of whole parasite vaccines.

Parasite stage and vaccine candidate	Time	Current status
Pre-erythrocytic stage		
Radiation-attenuated sporozoite vaccine (rodent)	1967 (Nussenzweig et al., 1967)	Preclinical
Chemically attenuated sporozoite vaccine	2009 (Roestenberg et al., 2009)	Phase 2
Genetically attenuated sporozoite vaccine	2005 (Mueller et al., 2005)	Phase 1
Radiation-attenuated sporozoite vaccine (human)	2011 (Clyde et al., 1973; Clyde, 1975; Epstein et al., 2011b)	Phase 2
Blood stage		
Whole-killed blood-stage vaccine	1948 (Freund et al., 1948)	Preclinical
Genetic-attenuated whole-parasite blood-stage vaccines	2008 (Ting et al., 2008)	Preclinical
Chemically attenuated whole-parasite blood-stage vaccines	2018 (Stanisic et al., 2018)	Phase 1

Pre-erythrocytic and blood-stage whole parasite vaccines are being evaluated in clinical trials (denoted as phases 1–4) or are being tested in rodent or non-human primate models (preclinical research).

to mosquito-bite challenge. However, safety remains a great concern because the breakthrough of genetically attenuated sporozoites has been reported (Vaughan et al., 2010; Spring et al., 2013). Meanwhile, sporozoites can only be developed in mosquitoes, and sourcing and delivering aseptic, purified, and cryopreserved sporozoites limit the broad application of sporozoite vaccines (Prinz et al., 2018).

Compared to the sourcing of sporozoites, the culture of the *Plasmodium falciparum* blood stage is a well-established process, so whole-parasite blood-stage vaccines can easily be manufactured. Therefore, efforts have been made to develop genetically or chemically attenuated whole-parasite blood-stage vaccines. Attenuated *P. yoelii* (*Plasmodium yoelii*) with purine nucleoside phosphorylase (PNP), nucleoside transporter 1 (NT1), or histamine-releasing factor (HRF) deficiency confer complete sterile protection against both homologous and heterologous blood-stage challenge (Ting et al., 2008; Aly et al., 2010; Demarta-Gatsi et al., 2016). Regarding chemical attenuation, the blood stage can be chemically attenuated both *in vivo* and *in vitro*. *In vivo*, this has been achieved by creating a persistent subpatent blood-stage infection using a low dose of malaria parasite followed by treatment with anti-malaria drugs, which induces sterile protection against both high-dose homologous and heterologous blood-stage challenge (Pombo et al., 2002; Elliott et al., 2005). *In vitro*, several approaches have been used to chemically attenuate the blood stage, such as treatment with the parasite DNA-binding drugs centanamycin (CM; Good et al., 2013) and tafuramycin-A (TF-A; Stanisic et al., 2018), or the delayed death-causing drugs doxycycline or azithromycin (Low et al., 2019). The vaccination of *in vitro* chemically attenuated blood stage has also been reported to induce protective immunity against both homologous and heterologous blood-stage challenges (Good et al., 2013; Raja et al., 2016; Low et al., 2019). However, safety concerns regarding the breakthrough of genetically or chemically attenuated blood stages remains unavoidable. In contrast, a WKV, which is an inactive vaccine prepared by several cycles of freezinge/thawing of pRBCs (mostly containing schizonts), is theoretically much safer than other forms of whole-parasite blood-stage vaccine. Furthermore, our previous study and other research have demonstrated that the WKV induced strong protective immunity against both homologous and heterologous blood-stage challenge (Liu et al., 2013; Lu et al., 2017).

Most importantly, the protection brought about by genetically or chemically attenuated blood-stage vaccines involved both antibodies and $CD4^+$ T cell responses (Good et al., 2013; Raja et al., 2016; Low et al., 2019). However, WKV with CpG as the adjuvant is dependent on $CD4^+$ T cell responses, which might target the antigens that are conserved across strains (Pinzon-Charry et al., 2010). Thus, whole-parasite blood-stage vaccines, such as WKV, induce strong $CD4^+$ T cell responses against universal epitopes, allowing them to confer species-transcending protection, unlike most subunit malaria vaccines against the polymorphic B cell epitopes.

It is thought that a subunit vaccine developed to induce a response against a certain stage of the malaria parasite induces stage-specific, but not cross-stage, immunity. In contrast, whole-parasite vaccines against the pre-erythrocytic stage, such as chemically and genetically attenuated sporozoites, have been shown to induce cross-stage protection against the blood stage (Nahrendorf et al., 2015b; Sack et al., 2015). Although the protection induced by chemically attenuated blood-stage *P. yoelii* parasites was stage specific as immunized mice were not protected against intravenous or mosquito bite sporozoite challenges (Raja et al., 2016), our study showed that the WKV not only conferred the cross-stage immunity against sporozoite challenge but also blocked parasite development in mosquitoes (**Figure 2**; Lu et al., 2017; Zhu et al., 2017). Therefore, the WKV not only prevents malarial infection and reduces mortality and morbidity among malaria patients but also blocks malaria transmission. Compared to the genetically or chemically attenuated blood-stage vaccines, the WKV is more acceptable and easily manufactured and shows promise regarding controlling and even eradicating malaria worldwide.

OPTIMIZATION OF THE WKV

The main limitation of the WKV is the high dose required per vaccine due to its low immunogenicity. The immunization dose of WKV typically needs to be at least 1.5×10^7 parasites or parasite equivalents per vaccine dose (Liu et al., 2013). Therefore, it is a significant challenge due to the difficulties in vaccine manufacture, which involves the human red blood cells. The use of human blood products may also have the possibility to contaminate the vaccine with infectious adventitious agents in the manufacturing process. In the final WKV formulation, an appropriate human-compatible adjuvant is required to induce protection with the lowest dose of parasite. Up to now, all the whole-parasite blood-stage vaccines are at a very early stage of clinical evaluation, and there is no WKV enters clinical trial for the assessment of safety and

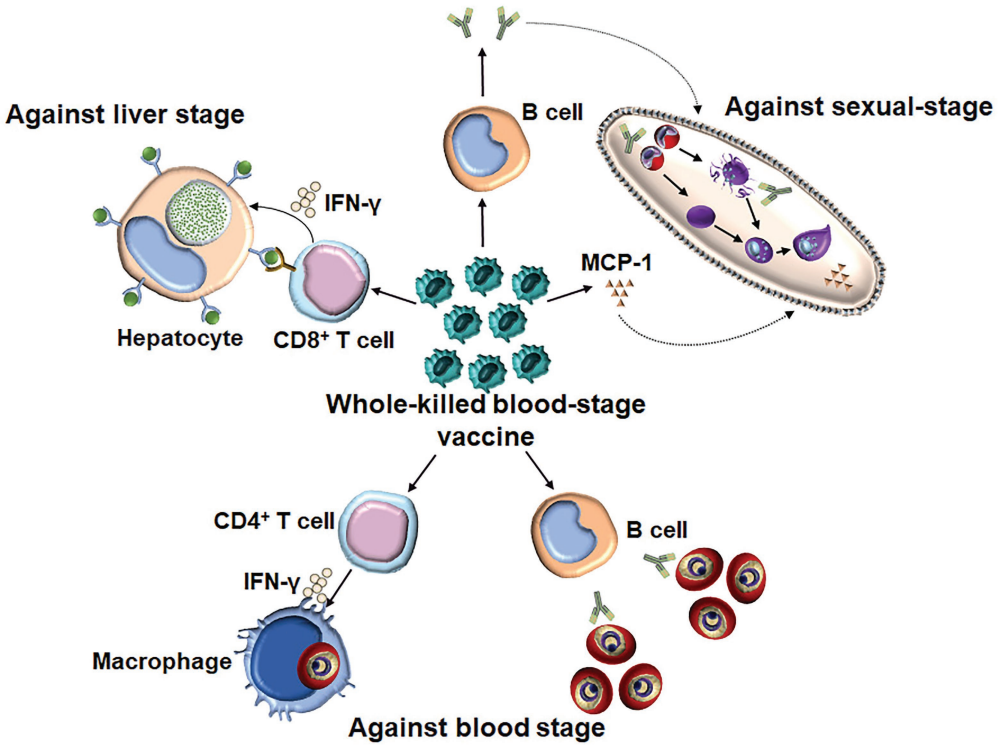

FIGURE 2 | The underlying mechanism of WKV against all three stages. WKV (an inactivate vaccine) could not only efficiently induce a protection against a blood-stage challenge but also confer the cross-stage protection against both liver stage and sexual-stage. The protective immunity against blood stage is dependent on both parasite-specific antibody and $CD4^+$ T cells, which might enhance the capacity of macrophages to kill the intracellular parasite through the secretion of IFN-γ. WKV could also provide cross-protection against liver stage through priming parasite-specific $CD8^+$ T cells, although the target antigen of which is still needed to be defined. In contrast, the protective immunity induced by WKV against sexual-stage is largely dependent on parasite-specific antibody and MCP-1, the non-specific effect of latter might explain the species-transcending protection against sexual-stage.

immunogenicity (Stanisic et al., 2018). Hence, the clinical evaluation of WKV remains a significant challenge. Additionally, the safety concerns regarding the WKV should also be considered, as the parasite is grown in human RBCs, and immunization with pRBCs may induce anti-RBC antibodies and possibly lead to autoimmunity following immunization (Good, 2011). Although no adverse events have been reported, the immunogenicity of the current WKV still needs to be improved. One way to potentially do this is to gain further understanding into the underlying mechanisms of the WKV against each of the three stages, and another is to develop human-compatible adjuvants.

Understanding the Mechanisms of the WKV Against All Three Stages

Knowledge of the mechanisms of the WKV against all stages would guide the optimization of its formulation. Regarding the protective immunity induced by the WKV against the blood stage, several studies have demonstrated that it is dependent on both humoral and $CD4^+$ T cell responses (Pinzon-Charry et al., 2010). Although the purine salvage enzyme HGXPT (hypoxanthine guanine xanthine phosphoribosyl transferase) has been identified as a major potential target antigen for $CD4^+$ T cell responses against the blood stage (Makobongo et al., 2003; Woodberry et al., 2009), the protective B cell antigens of WKV still need to be defined. We found that the WKV could greatly increase the frequency of $CD8\alpha^{low}CD11a^{high}$ T cells, which are representative malaria parasite-specific $CD8^+$ T cells (Rai et al., 2009). A T cell depletion assay demonstrated that the protective immunity induced by the WKV against the liver stage is mainly dependent on $CD8^+$ T cell responses, but not $CD4^+$ T cell responses (Lu et al., 2017). Cytotoxic $CD8^+$ T cells were previously thought to have no role against the blood stages because RBCs generally do not express human leukocyte antigen class I (HLA I). However, a recent study showed that *P. vivax*-infected reticulocytes express HLA I and circulating $CD8^+$ T cells in malaria patients can recognize the *P. vivax*-infected reticulocytes in a HLA-dependent manner and kill the intracellular parasites (Junqueira et al., 2018). Despite this, the relative importance of the role of parasite-specific $CD8^+$ T cells regarding the protective immunity induced by the WKV against the *Plasmodium*, which cannot infect reticulocytes, remains unclear. In contrast to protective immunity against the blood and liver stages, we found that $CD4^+$ T effector cells are dispensable for the cross-protection induced by the WKV against the sexual-stage (Zhu et al., 2017). Instead, this cross-protection is mainly dependent on malaria parasite-specific

antibodies and monocyte chemoattractant protein (MCP)-1, but not interferon (IFN)-γ (Zhu et al., 2017). Although the exact mechanism of MCP-1 against the sexual-stage in this context is unknown, its non-specific effect might interpret the cross-species protection induced by the WKV against sexual-stage.

Interestingly, the cellular and humoral immune responses induced by the WKV are critical for its cross-protection against the liver and sexual-stage, respectively (Liu et al., 2013; Lu et al., 2017). Therefore, the investigation of underlying mechanisms for the activation of cellular and humoral immune responses may help us to optimize the WKV against all stages. It has been shown that the activation of malaria parasite-specific immune responses during WKV immunization involves malarial hemozoin triggering TLR9 (Toll-like receptor 9; Coban et al., 2010). Our previous data also indicated that the C5a/C5aR signaling pathway in dendritic cells (DCs) was activated during immunization and is essential for the optimal induction of the malaria parasite-specific $CD4^+$ T cell response (Liu et al., 2013). However, the investigation of the critical components of the WKV responsible for the upregulation of protective immune responses has only just begun.

In addition to the positive regulatory components, the identification and genetic deletion of the components that negatively regulate the protective immune response is also critical for vaccine optimization. In humans, the malaria parasite induces DC apoptosis and thereby inhibits parasite-specific $CD4^+$ T cell responses to facilitate its survival (Woodberry et al., 2012; Pinzon-Charry et al., 2013), along with downregulating costimulatory molecules on DCs (Urban et al., 1999). Additionally, Tr27 cells, which are IL-27-producing $CD4^+$ T cells, are induced by the malaria parasite to regulate $CD4^+$ T cell responses against the infection (Kimura et al., 2016). The expansion of $CD4^+CD25^+$ regulatory T cells during malaria infection suppresses T helper cell responses and follicular T helper (TFH)-B cell interactions in germinal centers *via* secretion of CTLA-4 (**Figure 3**; Kurup et al., 2017). This has been confirmed by the findings that the protection efficacy induced by several whole-parasite vaccines is much lower in malaria-exposed African individuals than in malaria-naïve United States and European individuals, and the malaria blood stage infection also suppresses both the humoral and cellular immune responses against sporozoites (Ocana-Morgner et al., 2003; Keitany et al., 2016). Furthermore, durable immunity was also difficult to be induced in African individuals, potentially because malaria inhibits the vaccine-induced formation of long-lived plasma cells (LLPCs) and high-affinity memory B cells (MBCs). Multiple mechanisms have been postulated to explain the insufficient induction of LLPCs and MBCs, including preferential expansion of $CXCR3^+$ (TH1-like) TFH cells (Obeng-Adjei et al., 2015), regulatory T cells (Kurup et al., 2017), and atypical MBCs (Weiss et al., 2009; Obeng-Adjei et al., 2017), as well as the dysregulation of chemokines and cytokines (Ryg-Cornejo et al., 2016) and the induction of immune checkpoints (Butler et al., 2011), which may delay or impair the acquisition of humoral immunity against malaria. In addition, a recent study revealed that the metabolic hyperactivity of plasmablasts resulted in nutrient deprivation that affects the germinal center reaction, limiting the generation of MBC and LLPC responses against malaria parasites (Vijay et al., 2020). The limited duration of the host protective immunity against the malaria parasite may also be explained by the parasite, inducing the apoptosis of LLPCs, MBCs, and activated $CD4^+$ T cells (**Figure 3**; Hirunpetcharat and Good, 1998; Wipasa et al., 2001; Xu et al., 2002; Wykes et al., 2005). Lastly, the immune evasion mechanisms established by the malaria blood stage also include the parasite antigen variation, sequestration, and rosetting (Niang et al., 2014; Wahlgren et al., 2017; Belachew, 2018).

The identification of cross-protective antigens shared by all three stages could also help to optimize the multi-stage effects of the WKV and facilitate the development of a multi-stage malaria subunit vaccine. Several recent studies have reported cross-stage protection between the blood and liver stages (Nahrendorf et al., 2015b; Sack et al., 2015), and the identification of cross-protective antigens has attracted more attention (Nahrendorf et al., 2015a). Although no cross-protective antigens have yet been identified, it should be feasible to screen for the overlapping antigens by comparing the transcriptional profiles between two stages. Additionally, the proteome-wide screening of antibody and T cell reactivity between protected and unprotected individuals (immunomics) may also help to characterize the cross-protective antigens (Doolan, 2011; Davies et al., 2015; Schussek et al., 2017). Concurrently, further research is needed on WKV components that may downregulate host protective immune responses.

Development of an Appropriate Human-Compatible Adjuvant

Developing an appropriate human-compatible adjuvant to enhance the immunogenicity of the WKV is an urgent issue. Aluminum-containing adjuvants are the most widely used clinical adjuvants, which have been demonstrated not only to directly trigger the NALP3 inflammasome but also to indirectly activate the host innate immune response by inducing the release of the endogenous danger signal uric acid (Lambrecht et al., 2009). However, we found that alum only slightly improved the immunogenicity of pRBC lysate (Fu et al., 2020). Although CpG has been reported to be able to significantly enhance the malaria parasite-specific $CD4^+$ T responses and reduce the vaccine dose from 10^8 to 10^3 (Pinzon-Charry et al., 2010), the use of CpG as an adjuvant in humans has not been approved.

The immunomodulatory role of chloroquine has been known for approximately 30 years. Early *ex vivo* studies claimed that chloroquine had a direct suppressive effect on several immune cells, such as T cells and natural killer cells (Bygbjerg et al., 1986, 1987; Goldman et al., 2000). However, chloroquine was found to greatly promote $CD8^+$ T cell responses against soluble antigens *in vivo*, through inhibiting the degradation of internalized soluble antigen in endosomes by increasing the pH of the endosomes (Accapezzato et al., 2005). Interestingly, we found that low-dose antimalarial chloroquine along with alum synergistically improved the immunogenicity of pRBC lysates by enhancing the humoral response, although

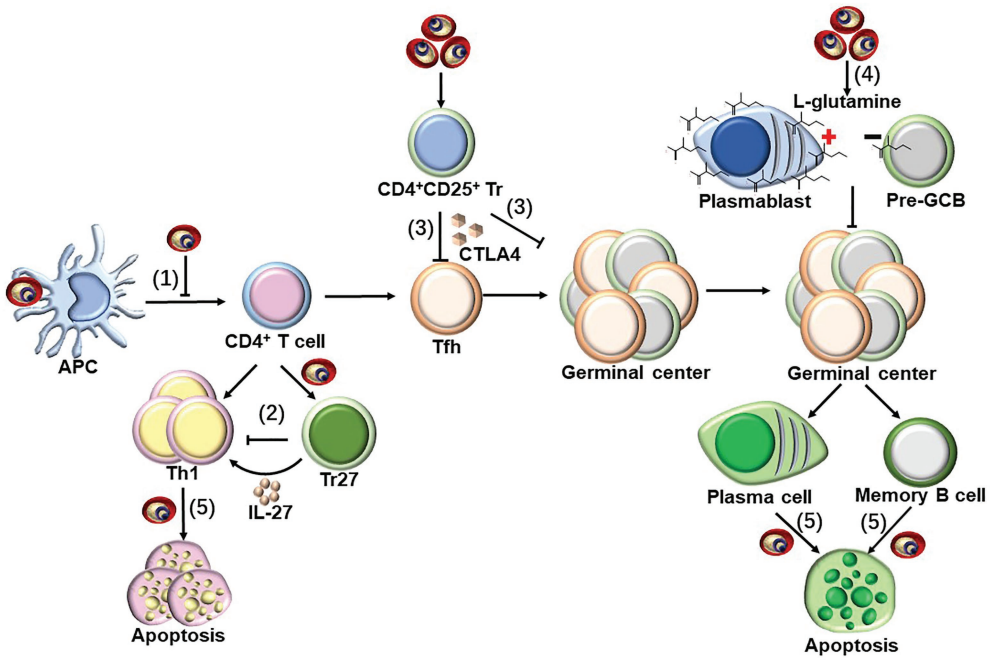

FIGURE 3 | Strategies to suppress host immune response by blood-stage malaria parasites. Parasite-specific CD4+ T cells are essential for host protective immunity against blood stage, as which can not only directly clear parasite through secretion Th1 cytokines but also provide help for B cells to produce antibody. However, malaria parasites have evolved to evade host immune response through following strategies. (1) pRBCs could inhibit the maturation of DCs, and subsequently suppress the CD4+ T cell activation (Urban et al., 1999; Woodberry et al., 2012; Pinzon-Charry et al., 2013). (2) Tr27 cells, the IL-27-producing CD4+ T cells, have also been reported to be activated during malaria infection, which reciprocally suppresses CD4+ T cells activation through the secretion of IL-27 (Kimura et al., 2016). (3) Malaria infection also induce the expansion of CD4+CD25+ regulatory T cells, which interfere T helper cell responses and follicular T helper (TFH)-B cell interactions in germinal centers through secretion of CTLA-4 (Kurup et al., 2017). (4) The early differentiation of parasite-specific B cells into short-lived plasmablasts consumes a large amount of L-glutamine during malaria blood-stage infection, resulting in the nutrient deprivation of GCB, limiting the generation of MBC and LLPC responses against malaria parasites (Vijay et al., 2020). (5) The infection of malaria parasite could even induce the apoptosis of the activated CD4+ T cells dependent on IFN-γ, but both LLPCs and MBCs are deleted by an unknown mechanism (Hirunpetcharat and Good, 1998; Wipasa et al., 2001; Xu et al., 2002; Wykes et al., 2005).

chloroquine alone only had a slight effect (Fu et al., 2020). As chloroquine has been approved as safe for humans, we strongly suggest that the use of low-dose chloroquine, along with alum, should be explored to enhance the immunogenicity of WKV.

CONCLUDING REMARKS AND FUTURE PERSPECTIVES

Although the burden of malaria has been greatly reduced by control measures in the past decades, a highly efficient and safe vaccine is a high priority to ultimately control and even eradicate malaria around the world. *Plasmodium* is a complicated organism, encoding more than 5,000 proteins, but only a few protective antigens have been identified. Therefore, the current subunit vaccine strategy has encountered major challenges, as these vaccines can only induce narrow immune responses, and the future development of malaria subunit vaccine is not optimistic. Although multi-stage or multi-antigen vaccines are theoretically promising to control malaria, it is dependent on the identification of protective antigens. In contrast, the immune responses induced by whole-parasite vaccines are broad, sparking a renewed interest in these vaccines. Owing to the difficulties in sourcing and delivering cryopreserved sporozoites, whole-parasite blood-stage vaccine manufacturing is more feasible, as the culture of *P. falciparum* blood stage is a well-established process. Furthermore, the *Plasmodium* life cycle is very complicated, with three developmental stages, each of which has different antigens. An ideal vaccine would confer cross-stage immunity against all three stages, and WKV, an inactive whole-parasite vaccine, is safe and can induce cross-protection against both the liver and sexual-stages.

However, the immunogenicity of WKV is low and needs to be improved. To optimize WKV, two major elements should be identified: (1) malaria parasite components that positively regulate the host immune responses and (2) the mechanisms and parasite components that suppress or evade the host immune responses, which would affect the magnitude and duration of the protective immune response induced by WKV. With this knowledge, negative regulatory components could be removed and positively components could be strengthened from the parasite by genetic manipulation to greatly improve the immunogenicity and protective efficacy of the WKV.

AUTHOR CONTRIBUTIONS

WX and TL: conceptualization, writing-review and editing, and funding acquisition. JC, SC, XL, and FZ: writing-original draft. All authors contributed to the article and approved the submitted version.

FUNDING

This work was supported by the State Key Program of the National Natural Science Foundation of China (Nos. 81830067 and 82072299).

REFERENCES

Accapezzato, D., Visco, V., Francavilla, V., Molette, C., Donato, T., Paroli, M., et al. (2005). Chloroquine enhances human $CD8^+$ T cell responses against soluble antigens in vivo. *J. Exp. Med.* 202, 817–828. doi: 10.1084/jem.20051106

Acquah, F. K., Adjah, J., Williamson, K. C., and Amoah, L. E. (2019). Transmission-blocking vaccines: old friends and new prospects. *Infect. Immun.* 87, e00775–e00818. doi: 10.1128/IAI.00775-18

Agnandji, S. T., Lell, B., Fernandes, J. F., Abossolo, B. P., Methogo, B. G., Kabwende, A. L., et al. (2012). A phase 3 trial of RTS,S/AS01 malaria vaccine in African infants. *N. Engl. J. Med.* 367, 2284–2295. doi: 10.1056/NEJMoa1208394

Agnandji, S. T., Lell, B., Soulanoudjingar, S. S., Fernandes, J. F., Abossolo, B. P., Conzelmann, C., et al. (2011). First results of phase 3 trial of RTS,S/AS01 malaria vaccine in African children. *N. Engl. J. Med.* 365, 1863–1875. doi: 10.1056/NEJMoa1102287

Alanine, D. G. W., Quinkert, D., Kumarasingha, R., Mehmood, S., Donnellan, F. R., Minkah, N. K., et al. (2019). Human antibodies that slow erythrocyte invasion potentiate malaria-neutralizing antibodies. *Cell* 178, 216.e221–228.e221. doi: 10.1016/j.cell.2019.05.025

Aly, A. S., Downie, M. J., Mamoun, C. B., and Kappe, S. H. (2010). Subpatent infection with nucleoside transporter 1-deficient Plasmodium blood stage parasites confers sterile protection against lethal malaria in mice. *Cell. Microbiol.* 12, 930–938. doi: 10.1111/j.1462-5822.2010.01441.x

Barr, P. J., Green, K. M., Gibson, H. L., Bathurst, I. C., Quakyi, I. A., and Kaslow, D. C. (1991). Recombinant Pfs25 protein of *Plasmodium falciparum* elicits malaria transmission-blocking immunity in experimental animals. *J. Exp. Med.* 174, 1203–1208. doi: 10.1084/jem.174.5.1203

Belachew, E. B. (2018). Immune response and evasion mechanisms of *Plasmodium falciparum* parasites. *J. Immunol. Res.* 2018:6529681. doi: 10.1155/2018/6529681

Bijker, E. M., Bastiaens, G. J., Teirlinck, A. C., van Gemert, G. J., Graumans, W., van de Vegte-Bolmer, M., et al. (2013). Protection against malaria after immunization by chloroquine prophylaxis and sporozoites is mediated by preerythrocytic immunity. *Proc. Natl. Acad. Sci. U. S. A.* 110, 7862–7867. doi: 10.1073/pnas.1220360110

Bull, P. C., Lowe, B. S., Kortok, M., Molyneux, C. S., Newbold, C. I., and Marsh, K. (1998). Parasite antigens on the infected red cell surface are targets for naturally acquired immunity to malaria. *Nat. Med.* 4, 358–360. doi: 10.1038/nm0398-358

Butler, N. S., Moebius, J., Pewe, L. L., Traore, B., Doumbo, O. K., Tygrett, L. T., et al. (2011). Therapeutic blockade of PD-L1 and LAG-3 rapidly clears established blood-stage Plasmodium infection. *Nat. Immunol.* 13, 188–195. doi: 10.1038/ni.2180

Bygbjerg, I. C., Svenson, M., Theander, T. G., and Bendtzen, K. (1987). Effect of antimalarial drugs on stimulation and interleukin 2 production of human lymphocytes. *Int. J. Immunopharmacol.* 9, 513–519. doi: 10.1016/0192-0561(87)90027-0

Bygbjerg, I. C., Theander, T. G., Andersen, B. J., Flachs, H., Jepsen, S., and Larsen, P. B. (1986). In vitro effect of chloroquine, mefloquine and quinine on human lymphocyte proliferative responses to malaria antigens and other antigens/mitogens. *Trop. Med. Parasitol.* 37, 245–247.

Casares, S., Brumeanu, T. D., and Richie, T. L. (2010). The RTS,S malaria vaccine. *Vaccine* 28, 4880–4894. doi: 10.1016/j.vaccine.2010.05.033

Clyde, D. F. (1975). Immunization of man against falciparum and vivax malaria by use of attenuated sporozoites. *Am. J. Trop. Med. Hyg.* 24, 397–401. doi: 10.4269/ajtmh.1975.24.397

Clyde, D. F., McCarthy, V. C., Miller, R. M., and Hornick, R. B. (1973). Specificity of protection of man immunized against sporozoite-induced falciparum malaria. *Am. J. Med. Sci.* 266, 398–403. doi: 10.1097/00000441-197312000-00001

Coban, C., Igari, Y., Yagi, M., Reimer, T., Koyama, S., Aoshi, T., et al. (2010). Immunogenicity of whole-parasite vaccines against *Plasmodium falciparum* involves malarial hemozoin and host TLR9. *Cell Host Microbe* 7, 50–61. doi: 10.1016/j.chom.2009.12.003

Cohen, J. (1996). *Vaccine Composition Against Malaria*. U.S. patent.

Crompton, P. D., Pierce, S. K., and Miller, L. H. (2010). Advances and challenges in malaria vaccine development. *J. Clin. Invest.* 120, 4168–4178. doi: 10.1172/JCI44423

Dame, J. B., Williams, J. L., McCutchan, T. F., Weber, J. L., Wirtz, R. A., Hockmeyer, W. T., et al. (1984). Structure of the gene encoding the immunodominant surface antigen on the sporozoite of the human malaria parasite *Plasmodium falciparum*. *Science* 225, 593–599. doi: 10.1126/science.6204383

Davies, D. H., Duffy, P., Bodmer, J. L., Felgner, P. L., and Doolan, D. L. (2015). Large screen approaches to identify novel malaria vaccine candidates. *Vaccine* 33, 7496–7505. doi: 10.1016/j.vaccine.2015.09.059

Demarta-Gatsi, C., Smith, L., Thiberge, S., Peronet, R., Commere, P. H., Matondo, M., et al. (2016). Protection against malaria in mice is induced by blood stage-arresting histamine-releasing factor (HRF)-deficient parasites. *J. Exp. Med.* 213, 1419–1428. doi: 10.1084/jem.20151976

Doolan, D. L. (2011). Plasmodium immunomics. *Int. J. Parasitol.* 41, 3–20. doi: 10.1016/j.ijpara.2010.08.002

Doolan, D. L., Southwood, S., Freilich, D. A., Sidney, J., Graber, N. L., Shatney, L., et al. (2003). Identification of *Plasmodium falciparum* antigens by antigenic analysis of genomic and proteomic data. *Proc. Natl. Acad. Sci. U. S. A.* 100, 9952–9957. doi: 10.1073/pnas.1633254100

Douglas, A. D., Baldeviano, G. C., Lucas, C. M., Lugo-Roman, L. A., Crosnier, C., Bartholdson, S. J., et al. (2015). A PfRH5-based vaccine is efficacious against heterologous strain blood-stage *Plasmodium falciparum* infection in aotus monkeys. *Cell Host Microbe* 17, 130–139. doi: 10.1016/j.chom.2014.11.017

Douglas, A. D., Williams, A. R., Illingworth, J. J., Kamuyu, G., Biswas, S., Goodman, A. L., et al. (2011). The blood-stage malaria antigen PfRH5 is susceptible to vaccine-inducible cross-strain neutralizing antibody. *Nat. Commun.* 2:601. doi: 10.1038/ncomms1615

Elliott, S. R., Kuns, R. D., and Good, M. F. (2005). Heterologous immunity in the absence of variant-specific antibodies after exposure to subpatent infection with blood-stage malaria. *Infect. Immun.* 73, 2478–2485. doi: 10.1128/IAI.73.4.2478-2485.2005

EMA (2015). First Malaria Vaccine Receives Positive Scientific Opinion From EMA. Available at: https://www.ema.europa.eu/en/news/first-malaria-vaccine-receives-positive-scientificopinion-ema (Accessed January 10, 2021).

Epstein, J. E., Tewari, K., Lyke, K. E., Sim, B. K., Billingsley, P. F., Laurens, M. B., et al. (2011). Live attenuated malaria vaccine designed to protect through hepatic CD8 T cell immunity. *Science* 334, 475–480. doi: 10.1126/science.1211548

Fowkes, F. J., Richards, J. S., Simpson, J. A., and Beeson, J. G. (2010). The relationship between anti-merozoite antibodies and incidence of *Plasmodium falciparum* malaria: a systematic review and meta-analysis. *PLoS Med.* 7:e1000218. doi: 10.1371/journal.pmed.1000218

Freund, J., Thomson, K. J., Sommer, H. E., Walter, A. W., and Pisani, T. M. (1948). Immunization of monkeys against malaria by means of killed parasites with adjuvants. *Am. J. Trop. Med. Hyg.* 28, 1–22. doi: 10.4269/ajtmh.1948.s1-28.1

Fu, Y., Lu, X., Zhu, F., Zhao, Y., Ding, Y., Ye, L., et al. (2020). Improving the immunogenicity and protective efficacy of a whole-killed malaria blood-stage vaccine by chloroquine. *Parasite Immunol.* 42:e12682. doi: 10.1111/pim.12682

Gardner, M. J., Hall, N., Fung, E., White, O., Berriman, M., Hyman, R. W., et al. (2002). Genome sequence of the human malaria parasite *Plasmodium falciparum*. *Nature* 419, 498–511. doi: 10.1038/nature01097

Goldman, F. D., Gilman, A. L., Hollenback, C., Kato, R. M., Premack, B. A., and Rawlings, D. J. (2000). Hydroxychloroquine inhibits calcium signals in T cells: a new mechanism to explain its immunomodulatory properties. *Blood* 95, 3460–3466. doi: 10.1182/blood.V95.11.3460

Good, M. F. (2011). A whole parasite vaccine to control the blood stages of *Plasmodium*—the case for lateral thinking. *Trends Parasitol.* 27, 335–340. doi: 10.1016/j.pt.2011.03.003

Good, M. F., Reiman, J. M., Rodriguez, I. B., Ito, K., Yanow, S. K., El-Deeb, I. M., et al. (2013). Cross-species malaria immunity induced by chemically attenuated parasites. *J. Clin. Invest.* 123, 3353–3362. doi: 10.1172/JCI66634

Hirunpetcharat, C., and Good, M. F. (1998). Deletion of *Plasmodium berghei*-specific $CD4^+$ T cells adoptively transferred into recipient mice after challenge with homologous parasite. *Proc. Natl. Acad. Sci. U. S. A.* 95, 1715–1720. doi: 10.1073/pnas.95.4.1715

Julien, J. P., and Wardemann, H. (2019). Antibodies against *Plasmodium falciparum* malaria at the molecular level. *Nat. Rev. Immunol.* 19, 761–775. doi: 10.1038/s41577-019-0209-5

Junqueira, C., Barbosa, C. R. R., Costa, P. A. C., Teixeira-Carvalho, A., Castro, G., Sen Santara, S., et al. (2018). Cytotoxic CD8(+) T cells recognize and kill *Plasmodium vivax*-infected reticulocytes. *Nat. Med.* 24, 1330–1336. doi: 10.1038/s41591-018-0117-4

Keitany, G. J., Kim, K. S., Krishnamurty, A. T., Hondowicz, B. D., Hahn, W. O., Dambrauskas, N., et al. (2016). Blood stage malaria disrupts humoral immunity to the pre-erythrocytic stage circumsporozoite protein. *Cell Rep.* 17, 3193–3205. doi: 10.1016/j.celrep.2016.11.060

Kimura, D., Miyakoda, M., Kimura, K., Honma, K., Hara, H., Yoshida, H., et al. (2016). Interleukin-27-producing CD4(+) T cells regulate protective immunity during malaria parasite infection. *Immunity* 44, 672–682. doi: 10.1016/j.immuni.2016.02.011

Kumar, K. A., Sano, G., Boscardin, S., Nussenzweig, R. S., Nussenzweig, M. C., Zavala, F., et al. (2006). The circumsporozoite protein is an immunodominant protective antigen in irradiated sporozoites. *Nature* 444, 937–940. doi: 10.1038/nature05361

Kurup, S. P., Obeng-Adjei, N., Anthony, S. M., Traore, B., Doumbo, O. K., Butler, N. S., et al. (2017). Regulatory T cells impede acute and long-term immunity to blood-stage malaria through CTLA-4. *Nat. Med.* 23, 1220–1225. doi: 10.1038/nm.4395

Lambrecht, B. N., Kool, M., Willart, M. A., and Hammad, H. (2009). Mechanism of action of clinically approved adjuvants. *Curr. Opin. Immunol.* 21, 23–29. doi: 10.1016/j.coi.2009.01.004

Liu, T., Xu, G., Guo, B., Fu, Y., Qiu, Y., Ding, Y., et al. (2013). An essential role for C5aR signaling in the optimal induction of a malaria-specific $CD4^+$ T cell response by a whole-killed blood-stage vaccine. *J. Immunol.* 191, 178–186. doi: 10.4049/jimmunol.1201190

Low, L. M., Ssemaganda, A., Liu, X. Q., Ho, M. F., Ozberk, V., Fink, J., et al. (2019). Controlled infection immunization using delayed death drug treatment elicits protective immune responses to blood-stage malaria parasites. *Infect. Immun.* 87, e00587–e00618. doi: 10.1128/IAI.00587-18

Lu, X., Liu, T., Zhu, F., Chen, L., and Xu, W. (2017). A whole-killed, blood-stage lysate vaccine protects against the malaria liver stage. *Parasite Immunol.* 39:e12386. doi: 10.1111/pim.12386

Lyke, K. E., Ishizuka, A. S., Berry, A. A., Chakravarty, S., DeZure, A., Enama, M. E., et al. (2017). Attenuated PfSPZ vaccine induces strain-transcending T cells and durable protection against heterologous controlled human malaria infection. *Proc. Natl. Acad. Sci. U. S. A.* 114, 2711–2716. doi: 10.1073/pnas.1615324114

Makobongo, M. O., Riding, G., Xu, H., Hirunpetcharat, C., Keough, D., de Jersey, J., et al. (2003). The purine salvage enzyme hypoxanthine guanine xanthine phosphoribosyl transferase is a major target antigen for cell-mediated immunity to malaria. *Proc. Natl. Acad. Sci. U. S. A.* 100, 2628–2633. doi: 10.1073/pnas.0337629100

Moorthy, V. S., and Ballou, W. R. (2009). Immunological mechanisms underlying protection mediated by RTS,S: a review of the available data. *Malar. J.* 8:312. doi: 10.1186/1475-2875-8-312

Mordmuller, B., Surat, G., Lagler, H., Chakravarty, S., Ishizuka, A. S., Lalremruata, A., et al. (2017). Sterile protection against human malaria by chemoattenuated PfSPZ vaccine. *Nature* 542, 445–449. doi: 10.1038/nature21060

Mueller, A. K., Labaied, M., Kappe, S. H., and Matuschewski, K. (2005). Genetically modified *Plasmodium* parasites as a protective experimental malaria vaccine. *Nature* 433, 164–167. doi: 10.1038/nature03188

Nahrendorf, W., Scholzen, A., Sauerwein, R. W., and Langhorne, J. (2015a). Cross-stage immunity for malaria vaccine development. *Vaccine* 33, 7513–7517. doi: 10.1016/j.vaccine.2015.09.098

Nahrendorf, W., Spence, P. J., Tumwine, I., Levy, P., Jarra, W., Sauerwein, R. W., et al. (2015b). Blood-stage immunity to *Plasmodium chabaudi* malaria following chemoprophylaxis and sporozoite immunization. *eLife* 4:e05165. doi: 10.7554/eLife.05165

Niang, M., Bei, A. K., Madnani, K. G., Pelly, S., Dankwa, S., Kanjee, U., et al. (2014). STEVOR is a *Plasmodium falciparum* erythrocyte binding protein that mediates merozoite invasion and rosetting. *Cell Host Microbe* 16, 81–93. doi: 10.1016/j.chom.2014.06.004

Nussenzweig, R. S., Vanderberg, J., Most, H., and Orton, C. (1967). Protective immunity produced by the injection of x-irradiated sporozoites of *Plasmodium berghei*. *Nature* 216, 160–162. doi: 10.1038/216160a0

Obeng-Adjei, N., Portugal, S., Holla, P., Li, S., Sohn, H., Ambegaonkar, A., et al. (2017). Malaria-induced interferon-gamma drives the expansion of Tbethi atypical memory B cells. *PLoS Pathog.* 13:e1006576. doi: 10.1371/journal.ppat.1006576

Obeng-Adjei, N., Portugal, S., Tran, T. M., Yazew, T. B., Skinner, J., Li, S., et al. (2015). Circulating Th1-cell-type Tfh cells that exhibit impaired B cell help are preferentially activated during acute malaria in children. *Cell Rep.* 13, 425–439. doi: 10.1016/j.celrep.2015.09.004

Ocana-Morgner, C., Mota, M. M., and Rodriguez, A. (2003). Malaria blood stage suppression of liver stage immunity by dendritic cells. *J. Exp. Med.* 197, 143–151. doi: 10.1084/jem.20021072

Ogutu, B. R., Apollo, O. J., McKinney, D., Okoth, W., Siangla, J., Dubovsky, F., et al. (2009). Blood stage malaria vaccine eliciting high antigen-specific antibody concentrations confers no protection to young children in Western Kenya. *PLoS One* 4:e4708. doi: 10.1371/journal.pone.0004708

O'Meara, W. P., Mangeni, J. N., Steketee, R., and Greenwood, B. (2010). Changes in the burden of malaria in sub-Saharan Africa. *Lancet Infect. Dis.* 10, 545–555. doi: 10.1016/S1473-3099(10)70096-7

Phyo, A. P., Nkhoma, S., Stepniewska, K., Ashley, E. A., Nair, S., McGready, R., et al. (2012). Emergence of artemisinin-resistant malaria on the western border of Thailand: a longitudinal study. *Lancet* 379, 1960–1966. doi: 10.1016/S0140-6736(12)60484-X

Pinzon-Charry, A., McPhun, V., Kienzle, V., Hirunpetcharat, C., Engwerda, C., McCarthy, J., et al. (2010). Low doses of killed parasite in CpG elicit vigorous $CD4^+$ T cell responses against blood-stage malaria in mice. *J. Clin. Invest.* 120, 2967–2978. doi: 10.1172/JCI39222

Pinzon-Charry, A., Woodberry, T., Kienzle, V., McPhun, V., Minigo, G., Lampah, D. A., et al. (2013). Apoptosis and dysfunction of blood dendritic cells in patients with falciparum and vivax malaria. *J. Exp. Med.* 210, 1635–1646. doi: 10.1084/jem.20121972

Pombo, D. J., Lawrence, G., Hirunpetcharat, C., Rzepczyk, C., Bryden, M., Cloonan, N., et al. (2002). Immunity to malaria after administration of ultra-low doses of red cells infected with *Plasmodium falciparum*. *Lancet* 360, 610–617. doi: 10.1016/S0140-6736(02)09784-2

Prinz, H., Sattler, J. M., Roth, A., Ripp, J., Adams, J. H., and Frischknecht, F. (2018). Immunization efficacy of cryopreserved genetically attenuated *Plasmodium berghei* sporozoites. *Parasitol. Res.* 117, 2487–2497. doi: 10.1007/s00436-018-5937-0

Rai, D., Pham, N. L., Harty, J. T., and Badovinac, V. P. (2009). Tracking the total CD8 T cell response to infection reveals substantial discordance in magnitude and kinetics between inbred and outbred hosts. *J. Immunol.* 183, 7672–7681. doi: 10.4049/jimmunol.0902874

Raja, A. I., Cai, Y., Reiman, J. M., Groves, P., Chakravarty, S., McPhun, V., et al. (2016). Chemically attenuated blood-stage *Plasmodium yoelii* parasites induce long-lived and strain-transcending protection. *Infect. Immun.* 84, 2274–2288. doi: 10.1128/IAI.00157-16

Ranson, H., N'Guessan, R., Lines, J., Moiroux, N., Nkuni, Z., and Corbel, V. (2011). Pyrethroid resistance in African anopheline mosquitoes: what are the implications for malaria control? *Trends Parasitol.* 27, 91–98. doi: 10.1016/j.pt.2010.08.004

Rathore, D., Sacci, J. B., de la Vega, P., and McCutchan, T. F. (2002). Binding and invasion of liver cells by *Plasmodium falciparum* sporozoites. Essential involvement of the amino terminus of circumsporozoite protein. *J. Biol. Chem.* 277, 7092–7098. doi: 10.1074/jbc.M106862200

Roestenberg, M., McCall, M., Hopman, J., Wiersma, J., Luty, A. J., van Gemert, G. J., et al. (2009). Protection against a malaria challenge by

sporozoite inoculation. *N. Engl. J. Med.* 361, 468–477. doi: 10.1056/NEJMoa0805832

Roestenberg, M., Walk, J., van der Boor, S. C., Langenberg, M. C. C., Hoogerwerf, M. A., Janse, J. J., et al. (2020). A double-blind, placebo-controlled phase 1/2a trial of the genetically attenuated malaria vaccine PfSPZ-GA1. *Sci. Transl. Med.* 12:eaaz5629. doi: 10.1126/scitranslmed.aaz5629

Rts, S. C. T. P. (2015). Efficacy and safety of RTS,S/AS01 malaria vaccine with or without a booster dose in infants and children in Africa: final results of a phase 3, individually randomised, controlled trial. *Lancet* 386, 31–45. doi: 10.1016/S0140-6736(15)60721-8

Ryg-Cornejo, V., Ioannidis, L. J., Ly, A., Chiu, C. Y., Tellier, J., Hill, D. L., et al. (2016). Severe malaria infections impair germinal center responses by inhibiting T follicular helper cell differentiation. *Cell Rep.* 14, 68–81. doi: 10.1016/j.celrep.2015.12.006

Sack, B. K., Keitany, G. J., Vaughan, A. M., Miller, J. L., Wang, R., and Kappe, S. H. (2015). Mechanisms of stage-transcending protection following immunization of mice with late liver stage-arresting genetically attenuated malaria parasites. *PLoS Pathog.* 11:e1004855. doi: 10.1371/journal.ppat.1004855

Sagara, I., Dicko, A., Ellis, R. D., Fay, M. P., Diawara, S. I., Assadou, M. H., et al. (2009). A randomized controlled phase 2 trial of the blood stage AMA1-C1/Alhydrogel malaria vaccine in children in Mali. *Vaccine* 27, 3090–3098. doi: 10.1016/j.vaccine.2009.03.014

Sagara, I., Healy, S. A., Assadou, M. H., Gabriel, E. E., Kone, M., Sissoko, K., et al. (2018). Safety and immunogenicity of Pfs25H-EPA/alhydrogel, a transmission-blocking vaccine against *Plasmodium falciparum*: a randomised, double-blind, comparator-controlled, dose-escalation study in healthy Malian adults. *Lancet Infect. Dis.* 18, 969–982. doi: 10.1016/S1473-3099(18)30344-X

Schussek, S., Trieu, A., Apte, S. H., Sidney, J., Sette, A., and Doolan, D. L. (2017). Novel *Plasmodium* antigens identified via genome-based antibody screen induce protection associated with polyfunctional T cell responses. *Sci. Rep.* 7:15053. doi: 10.1038/s41598-017-15354-0

Seder, R. A., Chang, L. J., Enama, M. E., Zephir, K. L., Sarwar, U. N., Gordon, I. J., et al. (2013). Protection against malaria by intravenous immunization with a nonreplicating sporozoite vaccine. *Science* 341, 1359–1365. doi: 10.1126/science.1241800

Sirima, S. B., Cousens, S., and Druilhe, P. (2011). Protection against malaria by MSP3 candidate vaccine. *N. Engl. J. Med.* 365, 1062–1064. doi: 10.1056/NEJMc1100670

Sissoko, M. S., Healy, S. A., Katile, A., Omaswa, F., Zaidi, I., Gabriel, E. E., et al. (2017). Safety and efficacy of PfSPZ vaccine against *Plasmodium falciparum* via direct venous inoculation in healthy malaria-exposed adults in Mali: a randomised, double-blind phase 1 trial. *Lancet Infect. Dis.* 17, 498–509. doi: 10.1016/S1473-3099(17)30104-4

Smith, T., Ross, A., Maire, N., Chitnis, N., Studer, A., Hardy, D., et al. (2012). Ensemble modeling of the likely public health impact of a pre-erythrocytic malaria vaccine. *PLoS Med.* 9:e1001157. doi: 10.1371/journal.pmed.1001157

Spring, M., Murphy, J., Nielsen, R., Dowler, M., Bennett, J. W., Zarling, S., et al. (2013). First-in-human evaluation of genetically attenuated *Plasmodium falciparum* sporozoites administered by bite of *Anopheles* mosquitoes to adult volunteers. *Vaccine* 31, 4975–4983. doi: 10.1016/j.vaccine.2013.08.007

Stanisic, D. I., Fink, J., Mayer, J., Coghill, S., Gore, L., Liu, X. Q., et al. (2018). Vaccination with chemically attenuated *Plasmodium falciparum* asexual blood-stage parasites induces parasite-specific cellular immune responses in malaria-naive volunteers: a pilot study. *BMC Med.* 16:184. doi: 10.1186/s12916-018-1173-9

Sutherland, C. (2007). A challenge for the development of malaria vaccines: polymorphic target antigens. *PLoS Med.* 4:e116. doi: 10.1371/journal.pmed.0040116

Tarun, A. S., Peng, X., Dumpit, R. F., Ogata, Y., Silva-Rivera, H., Camargo, N., et al. (2008). A combined transcriptome and proteome survey of malaria parasite liver stages. *Proc. Natl. Acad. Sci. U. S. A.* 105, 305–310. doi: 10.1073/pnas.0710780104

Thera, M. A., Doumbo, O. K., Coulibaly, D., Laurens, M. B., Ouattara, A., Kone, A. K., et al. (2011). A field trial to assess a blood-stage malaria vaccine. *N. Engl. J. Med.* 365, 1004–1013. doi: 10.1056/NEJMoa1008115

Ting, L. M., Gissot, M., Coppi, A., Sinnis, P., and Kim, K. (2008). Attenuated *Plasmodium yoelii* lacking purine nucleoside phosphorylase confer protective immunity. *Nat. Med.* 14, 954–958. doi: 10.1038/nm.1867

Urban, B. C., Ferguson, D. J., Pain, A., Willcox, N., Plebanski, M., Austyn, J. M., et al. (1999). *Plasmodium falciparum*-infected erythrocytes modulate the maturation of dendritic cells. *Nature* 400, 73–77. doi: 10.1038/21900

Uwimana, A., Legrand, E., Stokes, B. H., Ndikumana, J. M., Warsame, M., Umulisa, N., et al. (2020). Emergence and clonal expansion of in vitro artemisinin-resistant *Plasmodium falciparum* kelch13 R561H mutant parasites in Rwanda. *Nat. Med.* 26, 1602–1608. doi: 10.1038/s41591-020-1005-2

Vaughan, A. M., Wang, R., and Kappe, S. H. (2010). Genetically engineered, attenuated whole-cell vaccine approaches for malaria. *Hum. Vaccin.* 6, 107–113. doi: 10.4161/hv.6.1.9654

Vijay, R., Guthmiller, J. J., Sturtz, A. J., Surette, F. A., Rogers, K. J., Sompallae, R. R., et al. (2020). Infection-induced plasmablasts are a nutrient sink that impairs humoral immunity to malaria. *Nat. Immunol.* 21, 790–801. doi: 10.1038/s41590-020-0678-5

Volz, J. C., Yap, A., Sisquella, X., Thompson, J. K., Lim, N. T., Whitehead, L. W., et al. (2016). Essential role of the PfRh5/PfRipr/CyRPA complex during *Plasmodium falciparum* invasion of erythrocytes. *Cell Host Microbe* 20, 60–71. doi: 10.1016/j.chom.2016.06.004

Wahlgren, M., Goel, S., and Akhouri, R. R. (2017). Variant surface antigens of *Plasmodium falciparum* and their roles in severe malaria. *Nat. Rev. Microbiol.* 15, 479–491. doi: 10.1038/nrmicro.2017.47

Weiss, G. E., Crompton, P. D., Li, S., Walsh, L. A., Moir, S., Traore, B., et al. (2009). Atypical memory B cells are greatly expanded in individuals living in a malaria-endemic area. *J. Immunol.* 183, 2176–2182. doi: 10.4049/jimmunol.0901297

Weiss, G. E., Gilson, P. R., Taechalertpaisarn, T., Tham, W. H., de Jong, N. W., Harvey, K. L., et al. (2015). Revealing the sequence and resulting cellular morphology of receptor-ligand interactions during *Plasmodium falciparum* invasion of erythrocytes. *PLoS Pathog.* 11:e1004670. doi: 10.1371/journal.ppat.1004670

WHO (2019). MVIP Countries: Ghana, Kenya, and Malawi. Available at: https://www.who.int/immunization/diseases/malaria/malaria_vaccine_implementation_programme/pilot_countries_ghana_kenya_malawi/en/ (Accessed January 10, 2021).

Wipasa, J., Xu, H., Stowers, A., and Good, M. F. (2001). Apoptotic deletion of Th cells specific for the 19-kDa carboxyl-terminal fragment of merozoite surface protein 1 during malaria infection. *J. Immunol.* 167, 3903–3909. doi: 10.4049/jimmunol.167.7.3903

Woodberry, T., Minigo, G., Piera, K. A., Amante, F. H., Pinzon-Charry, A., Good, M. F., et al. (2012). Low-level *Plasmodium falciparum* blood-stage infection causes dendritic cell apoptosis and dysfunction in healthy volunteers. *J. Infect. Dis.* 206, 333–340. doi: 10.1093/infdis/jis366

Woodberry, T., Pinzon-Charry, A., Piera, K. A., Panpisutchai, Y., Engwerda, C. R., Doolan, D. L., et al. (2009). Human T cell recognition of the blood stage antigen *Plasmodium* hypoxanthine guanine xanthine phosphoribosyl transferase (HGXPRT) in acute malaria. *Malar. J.* 8:122. doi: 10.1186/1475-2875-8-122

Wright, K. E., Hjerrild, K. A., Bartlett, J., Douglas, A. D., Jin, J., Brown, R. E., et al. (2014). Structure of malaria invasion protein RH5 with erythrocyte basigin and blocking antibodies. *Nature* 515, 427–430. doi: 10.1038/nature13715

Wu, Y., Ellis, R. D., Shaffer, D., Fontes, E., Malkin, E. M., Mahanty, S., et al. (2008). Phase 1 trial of malaria transmission blocking vaccine candidates Pfs25 and Pvs25 formulated with montanide ISA 51. *PLoS One* 3:e2636. doi: 10.1371/journal.pone.0002636

Wykes, M. N., Zhou, Y. H., Liu, X. Q., and Good, M. F. (2005). *Plasmodium yoelii* can ablate vaccine-induced long-term protection in mice. *J. Immunol.* 175, 2510–2516. doi: 10.4049/jimmunol.175.4.2510

Xu, H., Wipasa, J., Yan, H., Zeng, M., Makobongo, M. O., Finkelman, F. D., et al. (2002). The mechanism and significance of deletion of parasite-specific CD4(+) T cells in malaria infection. *J. Exp. Med.* 195, 881–892. doi: 10.1084/jem.20011174

Zhu, F., Liu, T., Zhao, C., Lu, X., Zhang, J., and Xu, W. (2017). Whole-killed blood-stage vaccine-induced immunity suppresses the development of malaria parasites in mosquitoes. *J. Immunol.* 198, 300–307. doi: 10.4049/jimmunol.1600979

Conflict of Interest: The authors declare that the research was conducted in the absence of any commercial or financial relationships that could be construed as a potential conflict of interest.

frontiers in Cellular and Infection Microbiology

MINI REVIEW
published: 25 May 2021
doi: 10.3389/fcimb.2021.689401

The Mucosal Innate Immune Response to *Cryptosporidium parvum*, a Global One Health Issue

Charles K. Crawford and Amir Kol *

Department of Pathology, Microbiology, & Immunology, School of Veterinary Medicine, University of California, Davis, Davis, CA, United States

Cryptosporidium parvum is an apicomplexan parasite that infects the intestinal epithelium of humans and livestock animals worldwide. Cryptosporidiosis is a leading cause of diarrheal-related deaths in young children and a major cause of economic loss in cattle operations. The disease is especially dangerous to infants and immunocompromised individuals, for which there is no effective treatment or vaccination. As human-to-human, animal-to-animal and animal-to-human transmission play a role in cryptosporidiosis disease ecology, a holistic 'One Health' approach is required for disease control. Upon infection, the host's innate immune response restricts parasite growth and initiates the adaptive immune response, which is necessary for parasite clearance and recovery. The innate immune response involves a complex communicative interplay between epithelial and specialized innate immune cells. Traditional models have been used to study innate immune responses to *C. parvum* but cannot fully recapitulate natural host-pathogen interactions. Recent shifts to human and bovine organoid cultures are enabling deeper understanding of host-specific innate immunity response to infection. This review examines recent advances and highlights research gaps in our understanding of the host-specific innate immune response to *C. parvum*. Furthermore, we discuss evolving research models used in the field and potential developments on the horizon.

Keywords: *Cryptosporidium parvum*, innate immune response, One Health, intestinal parasite, intestinal epithelium

OPEN ACCESS

Edited by:
Jian Du,
Anhui Medical University, China

Reviewed by:
Rui Zhou,
Wuhan University, China
Jan Mead,
Emory University, United States

***Correspondence:**
Amir Kol
akol@ucdavis.edu

Specialty section:
This article was submitted to Parasite and Host, a section of the journal Frontiers in Cellular and Infection Microbiology

Received: *31 March 2021*
Accepted: *07 May 2021*
Published: *25 May 2021*

Citation:
Crawford CK and Kol A (2021) The Mucosal Innate Immune Response to Cryptosporidium parvum, a Global One Health Issue. Front. Cell. Infect. Microbiol. 11:689401. doi: 10.3389/fcimb.2021.689401

INTRODUCTION

Cryptosporidium parvum is an apicomplexan parasite that causes potentially life-threatening infectious diarrhea in infants and neonate calves with no available FDA-approved vaccine (Abrahamsen et al., 2004; Abubakar et al., 2007). Nitazoxanide is approved for use in adult, immunocompetent patients, but is not effective or approved for use in the most vulnerable populations: infants and immunocompromised patients (Abubakar et al., 2007). Infected hosts (humans and cows) shed billions of highly infectious and environmentally stable parasites (Nydam et al., 2001; Zambriski et al., 2013). The parasite is transmitted zoonotically and between humans worldwide (Bouzid et al., 2013; Ryan et al., 2016; Hatam-Nahavandi et al., 2019), and it contaminates drinking water sources (Chique et al., 2020), recreational swimming sites (Li et al., 2019), soils (Nag et al., 2020), and aquaculture environments (Marquis et al., 2015). Wildlife is further impacted by cryptosporidiosis (Ziegler et al., 2007). As such, a comprehensive and

interdisciplinary research approach is required to eliminate this significant source of global disease burden. Cryptosporidiosis is one of three etiologies responsible for the most global diarrheal deaths in children younger than five years of age (Checkley et al., 1997; Ong et al., 2005; Gormley et al., 2011; Kotloff et al., 2013; Khalil et al., 2018). In the U.S. *C. parvum* caused the largest waterborne pathogen outbreak in American history (Corso et al., 2003), and 444 outbreaks of cryptosporidiosis were reported from 2009-2017, leading to an estimated 750,000 individual cases per year (Scallan et al., 2011; Gharpure et al., 2019). *Cryptosporidium* has even been included as a relevant biological threat agent by the CDC (Rotz et al., 2002).

While the role of $CD4^+$ T cells in clearing infection is well studied, the role of the innate immune response within the parasite's natural hosts (i.e. human and cattle) is not fully understood. We will succinctly review current advances in our understanding of the mucosal innate immune response to *C. parvum*, and innovative models that have the potential to elucidate such responses within clinically relevant hosts. We will highlight key knowledge gaps and future research opportunities.

INNATE IMMUNE RESPONSE

The intestinal innate immune system, comprised of the gut epithelium and specialized innate immune cells, is the first line of defense against *C. parvum* infection. Innate immunity restricts the expansion and growth of the parasite and initiates the adaptive response. Understanding the innate immune response to *C. parvum* infection in its native hosts is critical in building a 'One Health' strategy to limit *Cryptosporidium's* devastating impact on global health, agriculture, and the environment (Ziegler et al., 2007; Laurent and Lacroix-Lamande, 2017; Ivanova et al., 2019).

Intestinal Epithelial Cells

Intestinal epithelial cells that line the gut epithelium create a physical barrier between luminal content and internal tissues.

Because *C. parvum* infects intestinal epithelial cells and does not invade deeper tissues, the epithelium is particularly important regarding the immune response to *C. parvum*.

Primary bovine intestinal epithelial cell infection by *C. parvum* leads to activation of the inflammatory transcription factor NF-κB; this increases expression of the long noncoding RNA NR_045064 (Li et al., 2018) and induces the transcription of numerous inflammatory mediators, primarily CXCL8 (aka IL-8) and TNFα, a response primarily mediated by Toll-like receptor-2 (TLR2) and TLR4 (Yang et al., 2015). *C. parvum* infection induces an increase in TLR4 expression, regulated by suppression of the noncoding miRNA, *let-7i* (Chen et al., 2007). TLR2 and TLR4 activation by *C. parvum* and subsequent NF-κB nuclear translocation induces the release of antimicrobial peptides LL-37 and β-defensin-2 (Chen et al., 2005). Despite this, TLR2 and TLR4 deficiency did not increase parasite load in neonatal mice; however, direct comparisons are difficult given the different models and experimental designs (Lantier et al., 2014).

Evidence suggests that intracellular recognition of *C. parvum* via NOD-like receptors (NLR) and subsequent activation of the inflammasome complex is an important innate response to infection. IL-18, a product of the inflammasome complex, is elevated in human epithelial cell lines following *C.* parvum infection (McDonald et al., 2006); moreover, IL-18 knockout and inflammasome components caspase-1 or ASC knockout mice are more susceptible to *Cryptosporidium* infection than control mice (Ehigiator et al., 2005; McNair et al., 2018; Sateriale et al., 2021). IL-1β, the second key product of inflammasome activation, was not increased post-infection, nor was there an effect on infection susceptibility in IL-1β knockout mice (McNair et al., 2018). The latter findings are corroborated by the fact that parasite shedding was strongly increased in mice lacking NLRP6, which induces IL-18 secretion, but not in mice lacking other inflammasome-forming NLRs including NLRP3, NLRP1b, Aim2, and NLRc4 that primarily induce IL-1β secretion (Sateriale et al., 2021).

Antimicrobial peptides include small positively-charged polypeptides that elicit antimicrobial effects against a variety of pathogens including bacteria, fungi, viruses, and protozoan parasites (Mahlapuu et al., 2016). Phospholipases (Carryn et al., 2012) and the antimicrobial peptides β-defensin-1, β-defensin-2, and LL-37 can kill *C. parvum* (Giacometti et al., 1999). Part of the TLR signal response by epithelial cells includes the release of LL-37 and β-defensin-2, and these antimicrobial peptides bind to free *C. parvum* to directly enact their effects (Chen et al., 2005). LL-37 and α-defensin-2 are increased in response to the rise in the inflammasome product, IL-18, in human cell lines (McDonald et al., 2006). However, *C. parvum* influences epithelial cells by inhibiting the production of other antimicrobial peptides including β-defensin-1 by an undiscovered mechanism (Zaalouk et al., 2004), and CCL20 by a *C. parvum*-induced rise in miR21 (Guesdon et al., 2015).

C. parvum infection is restricted to a parasitophorous vacuole on the apical side of the intestinal epithelium, therefore chemokine and cytokine release from infected epithelial cells is critical in the recruitment of specialized immune cells that facilitate parasite clearance (Laurent et al., 1999). Activation of TLRs by *C. parvum* induces the NF-κB signaling pathway causing the basolateral release of Growth Regulated Oncogene-α (GRO-α) (Yang et al., 2015) and CXCL8, which are key neutrophil chemoattractant molecules (Laurent et al., 1997). Additionally, in the neonatal mouse model, several chemokines including CCL2, CCL5, CXCL10, and CXCL9 are released, which recruit various immune cells to the infection site (Lacroix-Lamande et al., 2002; Auray et al., 2007; Lantier et al., 2013). Chemokine-induced immune cell recruitment is critical in the response to *C. parvum*, as evidenced by the increased susceptibility to infection of mice deficient in chemokine receptors, even in spite of redundancy in immune cell recruitment processes (Lacroix-Lamande et al., 2008; Lantier et al., 2013).

Another defense against intracellular pathogens is apoptosis of the host cell, and infection by *C. parvum* initiates apoptosis of infected and surrounding epithelial cells through Fas and Fas-L

interactions (Chen et al., 1999). However, within hours post-infection, *C. parvum* in one life stage, the trophozoite, inhibits apoptosis, likely to facilitate growth within the host cell, by inducing the production of anti-apoptotic factors BCL-2 (Mele et al., 2004), survivin (Liu et al., 2009), and osteoprotegerin (McCole et al., 2000; Castellanos-Gonzalez et al., 2008). Later in infection, in a different part of the *C. parvum* life cycle known as the sporozoite and merozoite life stages, inhibition is removed and apoptosis of the host cell is promoted (Mele et al., 2004; Liu et al., 2009).

Interferons (IFNs)

IFNs are an essential component to the host response to *C. parvum*. The importance of **IFN-γ** is shown by an increased susceptibility to *C. parvum* infection in IFN-$\gamma^{-/-}$ mice (Mead and You, 1998; Lacroix-Lamande et al., 2002) and wild-type neonate mice treated with anti-IFN-γ-antibodies (McDonald et al., 2013). Adult mice with a disrupted IFN-γ gene shed more parasites, experience extensive damage to the intestinal mucosa, and die within weeks of infection (Theodos et al., 1997). Severe combined immunodeficiency (SCID) mice, which are deficient in T and B cells, experience reduced *C. parvum* infection compared to SCID IFN-$\gamma^{-/-}$ mice, showing that protective IFN-γ during *C. parvum* infection is derived, at least in part, from non-T or B cells (Hayward et al., 2000). In addition to increased IFN-γ, *in vivo* piglet infection and *in vitro* experiments show that intestinal epithelial cells secrete abundant **IFN-λ3** (a type-III IFN) independently of specialized immune cells (Ferguson et al., 2019). Historically, type III IFNs have been associated with local epithelial defense from viruses (Zhou et al., 2018). More recently, IFN-λ was shown to mediate the gut epithelium defense against non-viral pathogens via TLRs (Odendall et al., 2017). Neutralization of IFN-λ3 leads to increased villus blunting and fecal shedding of infective *C. parvum* in neonate mice, and when intestinal epithelial cells are primed with recombinant IFN-λ3 they show reduced barrier disruption and increased cellular defense against *C. parvum* (Ferguson et al., 2019).

Specialized Immune Cells

Natural Killer (NK) Cells

NK cells contribute to the innate immune response to *C. parvum* through IFN-γ production and cytolysis of infected epithelial cells. *In vivo*, treating immunocompetent or immunodeficient mice with the NK cell activator, IL-12, leads to a protective effect against *C. parvum* associated with a concomitant rise in intestinal IFN-γ (Urban et al., 1996); *in vitro*, human NK cells lyse infected intestinal epithelial cells in response to IL-15 and presentation of MHC class I-related protein A and B (Dann et al., 2005). Mice lacking NK cells experience increased severity of infection and excrete more oocysts compared to mice with NK cells, but when treated with anti-IFN-γ antibodies the infection of NK positive mice was heavily exacerbated, thus implying a protective role of NK cells that is connected to IFN-γ (Barakat et al., 2009). Despite the increased morbidity in mice without NK cells, they produced IFN-γ after infection, meaning that NK cells are one, but not the only source of IFN-γ in response to *C. parvum*. The number of NK cells localized in the gut is increased within days following *C. parvum* exposure in lambs (Olsen et al., 2015). Activation of the NK cell receptor, NKG2D, is involved in NK cell-mediated protection, via its ligand, MICA, which is upregulated in the intestinal epithelium of infected humans (Dann et al., 2005). The role that other innate-like lymphocytes play during *C. parvum* infection is poorly understood and future investigations are warranted.

Dendritic Cells (DCs)

DCs exposed to *C. parvum* secrete numerous cytokines including IL-6, IL-1β, IL-12, IL-18, TNFα, and type I interferons via TLR4 receptor activation (Barakat et al., 2009; Bedi and Mead, 2012; Perez-Cordon et al., 2014). DCs also capture *C. parvum* antigens in the gut mucosa and migrate to draining lymph nodes where they present these antigens and facilitate the adaptive immune response (Auray et al., 2007; Perez-Cordon et al., 2014). DCs may acquire such antigens by directly capturing luminal organisms or phagocytizing apoptotic infected epithelial cells (Farache et al., 2013). Macrophages may further engulf free *C. parvum* and transfer the parasite to DCs for migration (Marcial and Madara, 1986). One hypothesis for the increased infection susceptibility of neonatal mice compared to adults is that neonates have fewer intestinal DCs, and injecting neonates with Flt3L – which induces DC differentiation from progenitor cells – increases the number of DCs as well as resistance to infection (Lantier et al., 2013). Furthermore, adult mice devoid of DCs are more susceptible to infection and excrete more parasites, and adoptive transfer of DCs pre-exposed to *C. parvum* reduces the parasite load (Bedi et al., 2014).

Macrophages

Macrophages develop from the same bone marrow precursor cells as DCs and are found in most organ systems and epithelial barriers, including the gut (Verschoor et al., 2012; Kumar, 2019). Following *C. parvum* infection in neonatal mice, macrophages accumulate in the lamina propria (de Sablet et al., 2016) and are associated with intact and digested parasites in Payer's patches in guinea pigs (Marcial and Madara, 1986). Macrophages' contribution to *C. parvum* clearance appears to be primarily as a secondary source of IFN-γ. Infected Rag2$^{-/-}\gamma_c^{-/-}$ mice, which lack T and B lymphocytes and NK cells, still produce IFN-γ, suggesting an IFN-γ source alternative to T cells and NK cells (Barakat et al., 2009). When treated with clodronate-liposomes to deplete macrophages, the mice were less resistant to *C. parvum* and could not produce IFN-γ (Barakat et al., 2009). IFN-γ production by macrophages is promoted by IL-18 when Rag2$^{-/-}\gamma_c^{-/-}$ mice are infected by *C. parvum* (Choudhry et al., 2012), and IFN-$\gamma^{-/-}$ mice have fewer macrophages and T cells recruited to the gut accompanying an inability to recover from infection (Lacroix-Lamande et al., 2002).

Neutrophils

Neutrophils infiltrate the intestinal mucosa during *C. parvum* infection (Goodgame et al., 1995), and preventing mucosal recruitment of neutrophils increases *C. parvum*-related barrier

dysfunction as measured by transepithelial electrical resistance (Zadrozny et al., 2006). Inhibiting neutrophil recruitment does not influence mortality or infection severity, nor does it affect *C. parvum*-mediated villous atrophy and diarrhea (Zadrozny et al., 2006). With no influence on mortality or infection severity, it does not appear that neutrophils are directly protective in the context of *C. parvum*.

As research models advance, the multi-dimensional innate immune response grows more complex but better understood (**Figure 1**). However, questions regarding the relevancy of these data to the natural hosts of *C. parvum* remain, provided the use of models that do not fully recapitulate the environment of human or ruminant intestines. New biotechnological advances, such as the development of bovine and human organoids, may provide the models necessary to confirm what is currently inferred about the innate immune response to *C. parvum* in these hosts.

CRYPTOSPORIDIUM RESEARCH MODELS

The potential to fully understand *C. parvum*'s pathogenesis and develop therapeutics is dependent on the models used to research the host-pathogen interactions it induces within its natural and clinically relevant hosts (i.e. human and cattle). Traditional *in vitro C. parvum* infection models can only be maintained for several days at a time and do not fully recapitulate native intestinal tissue, and *In vivo* mouse models are sub-optimal, as mice are not a natural host of *C. parvum*. Innovative models and advancing technologies are necessary to advance this field.

In Vivo Models

In vivo animal models are foundational to host-pathogen interaction research, but the nature of *C. parvum* complicates the application of traditional animal models. The natural and clinically

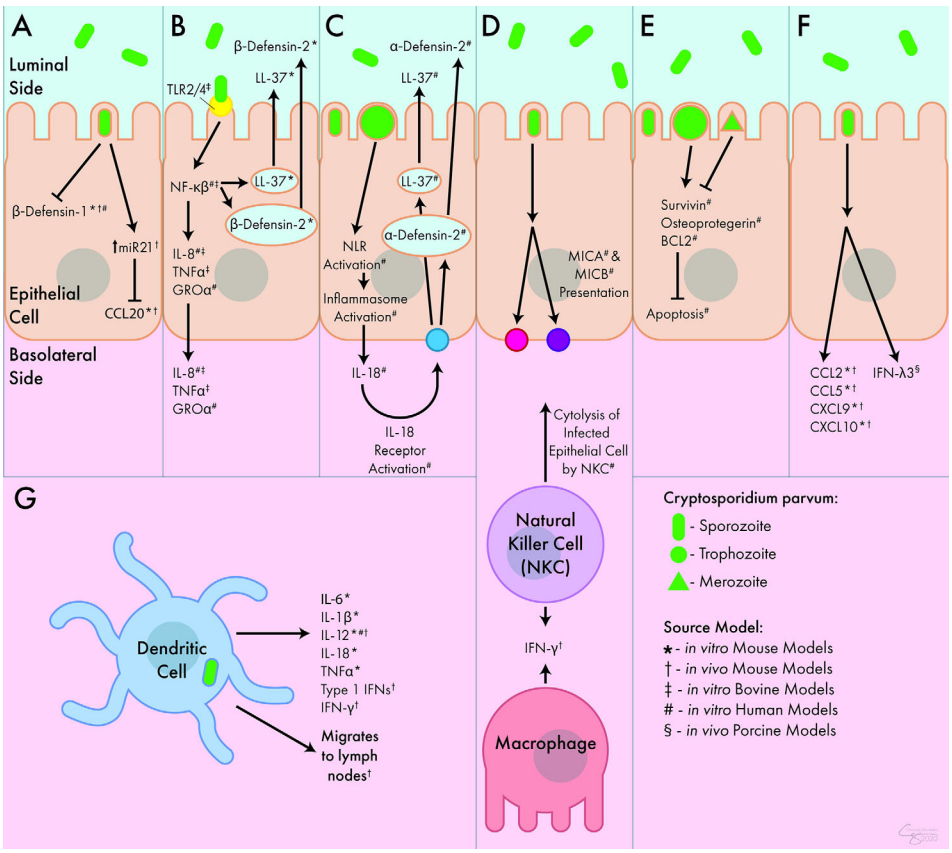

FIGURE 1 | Innate Immune Response to *C. parvum*. **(A)** *C. parvum* inhibits the release of the antimicrobial peptides β-defensin-1 and CCL20. **(B)** Activation of TLR receptors by *C. parvum* leads to the luminal secretion of antimicrobial peptides β-defensin-2 and LL-37 as well as the basolateral secretion of IL-8, TNFα, and GROα. **(C)** Inflammasome activation by *C. parvum* leads to the basolateral release of IL-18, which causes the luminal secretion of α -defensin-2 and LL-37. **(D)** *C. parvum*-mediated presentation of MICA and MICB lead to cytolysis of infected epithelial cells by NK cells. NK cells and macrophages both act as sources of IFN-γ during infection. **(E)** *C. parvum* trophozoites stimulate apoptosis, but merozoites inhibit apoptosis, mediated through survivin, osteoprotegerin, and BCL2. **(F)** In response to *C. parvum*, intestinal epithelial cells release numerous chemokines and cytokines including CCL2, CCL5, CXCL9, CXCL10, and IFN-λ3. **(G)** DCs respond to *C. parvum* by releasing IL-6, IL-1β, IL-12, IL-18, TNFα, and type I interferons. They can also migrate to lymph nodes following parasite exposure. Interferon (IFN), Interleukin (IL-), Tumor Necrosis Factor (TNF), C-C Chemokine Ligand (CCL), C-X-C Chemokine Ligand (CXCL), Growth Regulated Oncogene (GRO), Toll-Like Receptor (TLR), Nod-Like Receptor (NLR), MicroRNA 21 (miR21), Nuclear Factor (NF), Cathelicidin (LL-37), Major Histocompatibility Complex Class I Chain-Related Protein (MIC), B-Cell Lymphoma 2-Apoptosis Regulator (BCL2), Natural Killer Cell (NKC).

relevant hosts for *C. parvum* are humans and ruminants; mice can sustain *C. parvum* infection but only when severely immunocompromised (Mead et al., 1991; Petry et al., 1995; Griffiths et al., 1998). Given that humans and ruminants are the primary natural hosts, calves, lambs, and non-human primates have been used to investigate cryptosporidiosis in naturally infected species (Tzipori, 1998). However, housing and maintaining large animal species requires significant funds and specialized facilities, equipment, and training. Moreover, many of the genetic and molecular research tools that are available for mice models are not available for large animal models such as cows or sheep.

Adult mice, a preferred animal model in terms of costs and availably of reagents, are resistant to *C. parvum* but are susceptible to infection by the related species, *C. muris*; however, *C. muris* differs from *C. parvum* in phylogeny, biochemical nature of infection, and infection site (*C. muris* infects the stomach mucosa) (Sateriale et al., 2019). Mice can become susceptible to *C. parvum* through chemical or genetic immunosuppression, such as the previously discussed SCID (Mead et al., 1991), IFN-$\gamma^{-/-}$ (Griffiths et al., 1998), and Rag2$^{-/-}$ mice, which, in addition to neonate mice, have provided established murine platforms for *C. parvum* research (Petry et al., 1995). Unfortunately, mouse models have limited translatability for natural hosts such as humans and cattle. This has been elucidated through bovine-specific responses to *C. parvum* that are absent in mice, such as differences in NK cell receptor activation (Allan et al., 2015), recruitment of γδ T cells (Guzman et al., 2012), and developed resistance in adulthood (Sateriale et al., 2019). More recently, *C. tyzzeri* was identified as a natural mouse pathogen that mirrors aspects of *C. parvum's* pathogenesis and host response in mice (Sateriale et al., 2019).

In Vitro Models

The allure of primary intestinal epithelium cells lies in the morphological and species-specific accuracy compared to immortalized cell lines. Primary human (Castellanos-Gonzalez et al., 2013) and bovine intestinal epithelial cells have been successfully infected with *C. parvum* (Hashim et al., 2006). Unfortunately, primary intestinal cells have limitations involving their availability, obsoletion, and difficulty in long-term propagation (Varughese et al., 2014).

Most *in vitro* models for *C. parvum* host-pathogen interaction research include cancer-derived transformed or immortalized human cell lines including HCT-8, Caco-2, and HT29 cells, which are all derived from colorectal adenocarcinomas (Karanis and Aldeyarbi, 2011). Other non-colorectal cancer cell lines have also been used: RL95-2 (human endometrial carcinoma) (Rasmussen et al., 1993), Madin-Darby bovine kidney cells (Upton et al., 1994), MRC-5 (lung fibroblast) (Dawson et al., 2004), FHs 74 Int cells (non-cancer, immortalized human small intestinal epithelium) (Varughese et al., 2014), and BS-C-1 (African green monkey kidney) cells (Deng and Cliver, 1998). None of these lines maintained infection longer than six days except for HT29 cells, which could maintain infection for thirteen days but only for the asexual life stages of *C. parvum*. One non-intestinal cell line, COLO-680N, is human esophageal squamous carcinoma-derived and can propagate infective parasites continually for eight weeks, but applications to host-pathogen interaction are questionable given that the esophagus is not the natural niche for *C. parvum* (Miller et al., 2018).

Early attempts to utilize three-dimensional structures for *C. parvum* research involved low-shear microgravity cultures where HCT-8 cells seeded onto submucosa grafts formed structures that maintained *C. parvum* infection; however, parasites decreased after 48 hours (Alcantara Warren et al., 2008). Later, a hollow fiber bioreactor system was used to infect three-dimensional HCT-8 cell structures for over six months, which is far longer than two-dimensional HCT-8 infection, while producing significantly more oocysts/day/mL (Morada et al., 2016). Silk fiber scaffolding has also been utilized to induce three-dimensional culture of Caco-2 and HT29 cells, maintaining infection for two weeks (DeCicco RePass et al., 2017).

While these cell lines are useful tools, they are susceptible to genetic variation, most cannot maintain all phases of the *C. parvum* life cycle, and most cannot maintain and propagate *C. parvum* infection for extended periods of time (Bhalchandra et al., 2018). This, in addition to the fact that these cell lines do not recapitulate the native intestinal epithelial tissue of *C. parvum* hosts, encourages the search for increasingly accurate models of study.

Enteroids

Intestinal organoids (aka enteroids) circumvent shortcomings exhibited by cell lines and primary epithelial cells while also introducing a three-dimensional culture model. Enteroids are composed of a polarized single layer of epithelium with crypt and villus domains containing the various intestinal epithelial cells such as stem cells, enterocytes, enteroendocrine cells, goblet cells, etc., thus recapitulating the microanatomy and functionality of native intestinal epithelial tissue (**Figure 2**) (Zachos et al., 2016).

Stem cell-derived organoids allow long-term three-dimensional culture while maintaining the morphological relevance of native tissue. Isolated crypts from neonatal and immunocompromised mice were exposed to *C. parvum* upon plating, resulting in inhibited organoid propagation and budding, decreased expression of intestinal stem cell markers, and increased cell senescence (Zhang et al., 2016). In another study, human enteroids were infected with *C. parvum* by microinjection and the parasite was able to complete its entire life cycle within these organoids (Heo et al., 2018). Though bovine enteroids have been described, they have not yet been used to study *C. parvum* infection (Powell and Behnke, 2017; Hamilton et al., 2018; Derricott et al., 2019).

Organoid technology for *C. parvum* research is in its relative infancy, but the benefits of the culture model are enticing and allow questions that were not possible to investigate with previous models.

DISCUSSION

C. parvum is a parasite of international clinical importance across human and animal healthcare. Because of its high infectivity, resistance to water treatment, and the danger it poses to immunocompromised individuals, understanding the responses it induces in its host is a high priority endeavor to allow the creation of

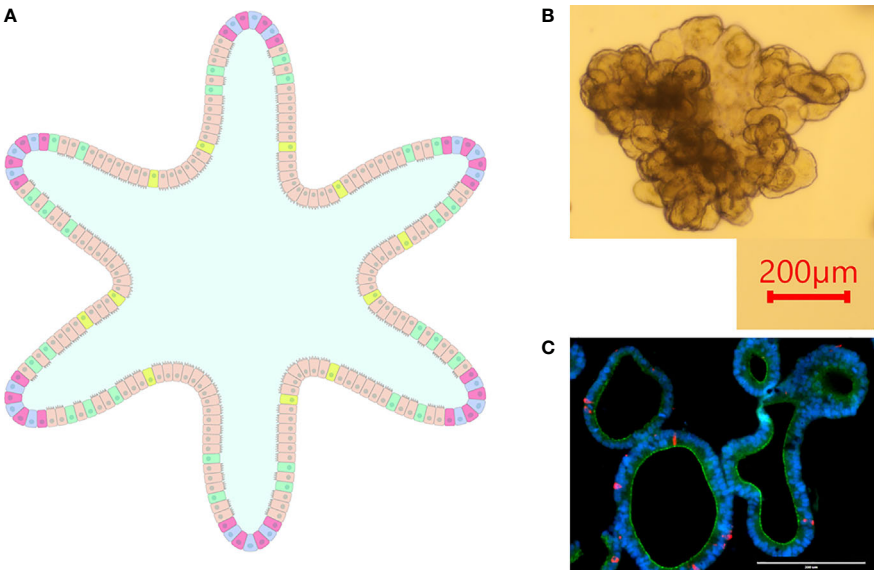

FIGURE 2 | Intestinal Organoids. **(A)** graphical representation of an intestinal organoid. The inside of the organoid corresponds to the luminal side, and the outside of the organoid corresponds to the basolateral side. Blue: intestinal stem cells, Red: Paneth cells, Tan: enterocytes, Green: goblet cells, Yellow: enteroendocrine cells. **(B)** Bovine intestinal organoid 6 days post-plating. Numerous folds and budding structures are noted, indicating crypt and villi-like domains. **(C)** Sectioned ovine intestinal organoid illustrating nuclei (DAPI), apical junctional protein ZO-1 (green), and chromogranin-A (red) indicating enteroendocrine cell differentiation.

effective preventative measures and therapies. The innate immune response is multifaceted and involves the intestinal epithelium, innate immune cells, and a complex interplay of cytokine signaling. To discover this, various models have been utilized. These include natural host species such as calves as well as more specialized models like immunocompromised mice, and *in vitro* models such as primary cell explants and immortalized cell lines. A relatively recent shift to three-dimensional cultures and the expanding use of organoids opens new avenues to study the parasite and its host-pathogen interaction.

As research in the field continues, attention must be brought to handling *C. parvum* from a 'One Health' perspective. New models must increase the relevant understanding of the parasite in bovine and human hosts and drive the discovery of innate mechanisms of resistance that can be utilized for management. Improved knowledge of the innate defenses against *C. parvum* in both ruminant and human hosts will hopefully lead to treatments to augment host natural innate defense and act as transient preventative measures to reduce environmental transmission of *C. parvum* between and within host species.

AUTHOR CONTRIBUTIONS

CC performed writing – original draft preparation. CC and AK performed writing – review and editing. AK performed project administration and supervision. All authors contributed to the article and approved the submitted version.

FUNDING

The work presented here was supported by funding from The Center for Food and Animal Health of The National Institute of Food and Agriculture, grant number: CALV-RIVAS-0060.

ACKNOWLEDGMENTS

We thank Chrisoula Toupadakis Skouritakis, PhD for assistance in the development of **Figures 1**, **2**.

REFERENCES

Abrahamsen M. S., Templeton T. J., Enomoto S., Abrahante J. E., Zhu G., Lancto C. A., et al. (2004). Complete Genome Sequence of the Apicomplexan, Cryptosporidium Parvum. *Science* 304 (5669), 441–445. doi: 10.1126/science.1094786

Abubakar I., Aliyu S. H., Arumugam C., Hunter P. R., and Usman N. K. (2007). Prevention and Treatment of Cryptosporidiosis in Immunocompromised Patients. *Cochrane Database Syst. Rev.* 1 (1), CD004932. doi: 10.1002/14651858.CD004932.pub2

Alcantara Warren C., Destura R. V., Sevilleja J. E., Barroso L. F., Carvalho H., Barrett L. J., et al. (2008). Detection of Epithelial-Cell Injury, and Quantification of Infection, in the HCT-8 Organoid Model of Cryptosporidiosis. *J. Infect. Dis.* 198 (1), 143–149. doi: 10.1086/588819

Allan A. J., Sanderson N. D., Gubbins S., Ellis S. A., and Hammond J. A. (2015). Cattle NK Cell Heterogeneity and the Influence of MHC Class I. *J. Immunol.* 195 (5), 2199–2206. doi: 10.4049/jimmunol.1500227

Auray G., Lacroix-Lamande S., Mancassola R., Dimier-Poisson I., and Laurent F. (2007). Involvement of Intestinal Epithelial Cells in Dendritic Cell Recruitment During C. Parvum Infection. *Microbes Infect.* 9 (5), 574–582. doi: 10.1016/j.micinf.2007.01.026

Barakat F. M., McDonald V., Di Santo J. P., and Korbel D. S. (2009). Roles for NK Cells and an NK Cell-Independent Source of Intestinal Gamma Interferon for

Innate Immunity to Cryptosporidium Parvum Infection. *Infect. Immun.* 77 (11), 5044–5049. doi: 10.1128/IAI.00377-09

Barakat F. M., McDonald V., Foster G. R., Tovey M. G., and Korbel D. S. (2009). Cryptosporidium Parvum Infection Rapidly Induces a Protective Innate Immune Response Involving Type I Interferon. *J. Infect. Dis.* 200 (10), 1548–1555. doi: 10.1086/644601

Bedi B., McNair N. N., and Mead J. R. (2014). Dendritic Cells Play a Role in Host Susceptibility to Cryptosporidium Parvum Infection. *Immunol. Lett.* 158 (1-2), 42–51. doi: 10.1016/j.imlet.2013.11.015

Bedi B., and Mead J. R. (2012). Cryptosporidium Parvum Antigens Induce Mouse and Human Dendritic Cells to Generate Th1-enhancing Cytokines. *Parasite Immunol.* 34 (10), 473–485. doi: 10.1111/j.1365-3024.2012.01382.x

Bhalchandra S., Cardenas D., and Ward H. D. (2018). Recent Breakthroughs and Ongoing Limitations in Cryptosporidium Research. *F1000Res* 7, 1–9. doi: 10.12688/f1000research.15333.1

Bouzid M., Hunter P. R., Chalmers R. M., and Tyler K. M. (2013). Cryptosporidium Pathogenicity and Virulence. *Clin. Microbiol. Rev.* 26 (1), 115–134. doi: 10.1128/CMR.00076-12

Carryn S., Schaefer D. A., Imboden M., Homan E. J., Bremel R. D., and Riggs M. W. (2012). Phospholipases and Cationic Peptides Inhibit Cryptosporidium Parvum Sporozoite Infectivity by Parasiticidal and non-Parasiticidal Mechanisms. *J. Parasitol* 98 (1), 199–204. doi: 10.1645/GE-2822.1

Castellanos-Gonzalez A., Cabada M. M., Nichols J., Gomez G., and White A. C.Jr. (2013). Human Primary Intestinal Epithelial Cells as an Improved In Vitro Model for Cryptosporidium Parvum Infection. *Infect. Immun.* 81 (6), 1996–2001. doi: 10.1128/IAI.01131-12

Castellanos-Gonzalez A., Yancey L. S., Wang H. C., Pantenburg B., Liscum K. R., Lewis D. E., et al. (2008). Cryptosporidium Infection of Human Intestinal Epithelial Cells Increases Expression of Osteoprotegerin: A Novel Mechanism for Evasion of Host Defenses. *J. Infect. Dis.* 197 (6), 916–923. doi: 10.1086/528374

Checkley W., Gilman R. H., Epstein L. D., Suarez M., Diaz J. F., Cabrera L., et al. (1997). Asymptomatic and Symptomatic Cryptosporidiosis: Their Acute Effect on Weight Gain in Peruvian Children. *Am. J. Epidemiol.* 145 (2), 156–163. doi: 10.1093/oxfordjournals.aje.a009086

Chen X. M., Gores G. J., Paya C. V., and LaRusso N. F. (1999). Cryptosporidium Parvum Induces Apoptosis in Biliary Epithelia by a Fas/Fas Ligand-Dependent Mechanism. *Am. J. Physiol.* 277 (3), G599–G608. doi: 10.1152/ajpgi.1999.277.3.G599

Chen X. M., O'Hara S. P., Nelson J. B., Splinter P. L., Small A. J., Tietz P. S., et al. (2005). Multiple TLRs are Expressed in Human Cholangiocytes and Mediate Host Epithelial Defense Responses to Cryptosporidium Parvum Via Activation of NF-Kappab. *J. Immunol.* 175 (11), 7447–7456. doi: 10.4049/jimmunol.175.11.7447

Chen X. M., Splinter P. L., O'Hara S. P., and LaRusso N. F. (2007). A Cellular micro-RNA, let-7i, Regulates Toll-like Receptor 4 Expression and Contributes to Cholangiocyte Immune Responses Against Cryptosporidium Parvum Infection. *J. Biol. Chem.* 282 (39), 28929–28938. doi: 10.1074/jbc.M702633200

Chique C., Hynds P. D., Andrade L., Burke L., Morris D., Ryan M. P., et al. (2020). Cryptosporidium Spp. in Groundwater Supplies Intended for Human Consumption - A Descriptive Review of Global Prevalence, Risk Factors and Knowledge Gaps. *Water Res.* 176:115726. doi: 10.1016/j.watres.2020.115726

Choudhry N., Petry F., van Rooijen N., and McDonald V. (2012). A Protective Role for Interleukin 18 in Interferon Gamma-Mediated Innate Immunity to Cryptosporidium Parvum That is Independent of Natural Killer Cells. *J. Infect. Dis.* 206 (1), 117–124. doi: 10.1093/infdis/jis300

Corso P. S., Kramer M. H., Blair K. A., Addiss D. G., Davis J. P., and Haddix A. C. (2003). Cost of Illness in the 1993 Waterborne Cryptosporidium Outbreak, Milwaukee, Wisconsin. *Emerg. Infect. Dis.* 9 (4), 426–431. doi: 10.3201/eid0904.020417

Dann S. M., Wang H. C., Gambarin K. J., Actor J. K., Robinson P., Lewis D. E., et al. (2005). Interleukin-15 Activates Human Natural Killer Cells to Clear the Intestinal Protozoan Cryptosporidium. *J. Infect. Dis.* 192 (7), 1294–1302. doi: 10.1086/444393

Dawson D. J., Samuel C. M., Scrannage V., and Atherton C. J. (2004). Survival of Cryptosporidium Species in Environments Relevant to Foods and Beverages. *J. Appl. Microbiol.* 96 (6), 1222–1229. doi: 10.1111/j.1365-2672.2004.02281.x

DeCicco RePass M. A., Chen Y., Lin Y., Zhou W., Kaplan D. L., and Ward H. D. (2017). Novel Bioengineered Three-Dimensional Human Intestinal Model for Long-Term Infection of Cryptosporidium Parvum. *Infect. Immun.* 85 (3), 1–11. doi: 10.1128/IAI.00731-16

Deng M. Q., and Cliver D. O. (1998). Cryptosporidium Parvum Development in the BS-C-1 Cell Line. *J. Parasitol* 84 (1), 8–15. doi: 10.2307/3284519

Derricott H., Luu L., Fong W. Y., Hartley C. S., Johnston L. J., Armstrong S. D., et al. (2019). Developing a 3D Intestinal Epithelium Model for Livestock Species. *Cell Tissue Res.* 375 (2), 409–424. doi: 10.1007/s00441-018-2924-9

de Sablet T., Potiron L., Marquis M., Bussiere F. I., Lacroix-Lamande S., and Laurent F. (2016). Cryptosporidium Parvum Increases Intestinal Permeability Through Interaction With Epithelial Cells and IL-1beta and TNFalpha Released by Inflammatory Monocytes. *Cell Microbiol.* 18 (12), 1871–1880. doi: 10.1111/cmi.12632

Ehigiator H. N., Romagnoli P., Borgelt K., Fernandez M., McNair N., Secor W. E., et al. (2005). Mucosal Cytokine and Antigen-Specific Responses to Cryptosporidium Parvum in IL-12p40 KO Mice. *Parasite Immunol.* 27 (1-2), 17–28. doi: 10.1111/j.1365-3024.2005.00736.x

Farache J., Koren I., Milo I., Gurevich I., Kim K. W., Zigmond E., et al. (2013). Luminal Bacteria Recruit CD103+ Dendritic Cells Into the Intestinal Epithelium to Sample Bacterial Antigens for Presentation. *Immunity* 38 (3), 581–595. doi: 10.1016/j.immuni.2013.01.009

Ferguson S. H., Foster D. M., Sherry B., Magness S. T., Nielsen D. M., and Gookin J. L. (2019). Interferon-Lambda3 Promotes Epithelial Defense and Barrier Function Against Cryptosporidium Parvum Infection. *Cell Mol. Gastroenterol. Hepatol* 8 (1), 1–20. doi: 10.1016/j.jcmgh.2019.02.007

Gharpure R., Perez A., Miller A. D., Wikswo M. E., Silver R., and Hlavsa M. C. (2019). Cryptosporidiosis Outbreaks - United States, 2009-2017. *MMWR Morb Mortal Wkly Rep.* 68 (25), 568–572. doi: 10.15585/mmwr.mm6825a3

Giacometti A., Cirioni O., Barchiesi F., Caselli F., and Scalise G. (1999). In-Vitro Activity of Polycationic Peptides Against Cryptosporidium Parvum, Pneumocystis Carinii and Yeast Clinical Isolates. *J. Antimicrob. Chemother.* 44 (3), 403–406. doi: 10.1093/jac/44.3.403

Goodgame R. W., Kimball K., Ou C. N., White A. C.Jr., Genta R. M., Lifschitz C. H., et al. (1995). Intestinal Function and Injury in Acquired Immunodeficiency Syndrome-Related Cryptosporidiosis. *Gastroenterology* 108 (4), 1075–1082. doi: 10.1016/0016-5085(95)90205-8

Gormley F. J., Little C. L., Chalmers R. M., Rawal N., and Adak G. K. (2011). Zoonotic Cryptosporidiosis From Petting Farms, England and Wales, 1992-2009. *Emerg. Infect. Dis.* 17 (1), 151–152. doi: 10.3201/eid1701.100902

Griffiths J. K., Theodos C., Paris M., and Tzipori S. (1998). The Gamma Interferon Gene Knockout Mouse: A Highly Sensitive Model for Evaluation of Therapeutic Agents Against Cryptosporidium Parvum. *J. Clin. Microbiol.* 36 (9), 2503–2508. doi: 10.1128/JCM.36.9.2503-2508.1998

Guesdon W., Auray G., Pezier T., Bussiere F. I., Drouet F., Le Vern Y., et al. (2015). Ccl20 Displays Antimicrobial Activity Against Cryptosporidium Parvum, But Its Expression Is Reduced During Infection in the Intestine of Neonatal Mice. *J. Infect. Dis.* 212 (8), 1332–1340. doi: 10.1093/infdis/jiv206

Guzman E., Price S., Poulsom H., and Hope J. (2012). Bovine Gammadelta T Cells: Cells With Multiple Functions and Important Roles in Immunity. *Vet. Immunol. Immunopathol.* 148 (1-2), 161–167. doi: 10.1016/j.vetimm.2011.03.013

Hamilton C. A., Young R., Jayaraman S., Sehgal A., Paxton E., Thomson S., et al. (2018). Development of In Vitro Enteroids Derived From Bovine Small Intestinal Crypts. *Vet. Res.* 49 (1):54. doi: 10.1186/s13567-018-0547-5

Hashim A., Mulcahy G., Bourke B., and Clyne M. (2006). Interaction of Cryptosporidium Hominis and Cryptosporidium Parvum With Primary Human and Bovine Intestinal Cells. *Infect. Immun.* 74 (1), 99–107. doi: 10.1128/IAI.74.1.99-107.2006

Hatam-Nahavandi K., Ahmadpour E., Carmena D., Spotin A., Bangoura B., and Xiao L. (2019). Cryptosporidium Infections in Terrestrial Ungulates With Focus on Livestock: A Systematic Review and Meta-Analysis. *Parasit Vectors* 12 (1), 453. doi: 10.1186/s13071-019-3704-4

Hayward A. R., Chmura K., and Cosyns M. (2000). Interferon-Gamma is Required for Innate Immunity to Cryptosporidium Parvum in Mice. *J. Infect. Dis.* 182 (3), 1001–1004. doi: 10.1086/315802

Heo I., Dutta D., Schaefer D. A., Iakobachvili N., Artegiani B., Sachs N., et al. (2018). Modelling Cryptosporidium Infection in Human Small Intestinal and Lung Organoids. *Nat. Microbiol.* 3 (7), 814–823. doi: 10.1038/s41564-018-0177-8

Ivanova D. L., Denton S. L., Fettel K. D., Sondgeroth K. S., Munoz Gutierrez J., Bangoura B., et al. (2019). Innate Lymphoid Cells in Protection, Pathology, and Adaptive Immunity During Apicomplexan Infection. *Front. Immunol.* 10, 196. doi: 10.3389/fimmu.2019.00196

Karanis P., and Aldeyarbi H. M. (2011). Evolution of Cryptosporidium In Vitro Culture. *Int. J. Parasitol* 41 (12), 1231–1242. doi: 10.1016/j.ijpara.2011.08.001

Khalil I. A., Troeger C., Rao P. C., Blacker B. F., Brown A., Brewer T. G., et al. (2018). Morbidity, Mortality, and Long-Term Consequences Associated With Diarrhoea From Cryptosporidium Infection in Children Younger Than 5 Years: A Meta-Analyses Study. *Lancet Glob Health* 6 (7), e758–e768. doi: 10.1016/S2214-109X(18)30283-3

Kotloff K. L., Nataro J. P., Blackwelder W. C., Nasrin D., Farag T. H., Panchalingam S., et al. (2013). Burden and Aetiology of Diarrhoeal Disease in Infants and Young Children in Developing Countries (the Global Enteric Multicenter Study, GEMS): A Prospective, Case-Control Study. *Lancet* 382 (9888), 209–222. doi: 10.1016/S0140-6736(13)60844-2

Kumar V. (2019). "Macrophages: The Potent Immunoregulatory Innate Immune Cells," in *Macrophage Activation - Biology and Disease*. Ed. K. H. Bhat (London, UK: IntechOpen).

Lacroix-Lamande S., Mancassola R., Auray G., Bernardet N., and Laurent F. (2008). CCR5 is Involved in Controlling the Early Stage of Cryptosporidium Parvum Infection in Neonates But is Dispensable for Parasite Elimination. *Microbes Infect.* 10 (4), 390–395. doi: 10.1016/j.micinf.2007.12.020

Lacroix-Lamande S., Mancassola R., Naciri M., and Laurent F. (2002). Role of Gamma Interferon in Chemokine Expression in the Ileum of Mice and in a Murine Intestinal Epithelial Cell Line After Cryptosporidium Parvum Infection. *Infect. Immun.* 70 (4), 2090–2099. doi: 10.1128/iai.70.4.2090-2099.2002

Lantier L., Drouet F., Guesdon W., Mancassola R., Metton C., Lo-Man R., et al. (2014). Poly(I:C)-Induced Protection of Neonatal Mice Against Intestinal Cryptosporidium Parvum Infection Requires an Additional TLR5 Signal Provided by the Gut Flora. *J. Infect. Dis.* 209 (3), 457–467. doi: 10.1093/infdis/jit432

Lantier L., Lacroix-Lamande S., Potiron L., Metton C., Drouet F., Guesdon W., et al. (2013). Intestinal CD103+ Dendritic Cells are Key Players in the Innate Immune Control of Cryptosporidium Parvum Infection in Neonatal Mice. *PloS Pathog.* 9 (12), e1003801. doi: 10.1371/journal.ppat.1003801

Laurent F., Eckmann L., Savidge T. C., Morgan G., Theodos C., Naciri M., et al. (1997). Cryptosporidium Parvum Infection of Human Intestinal Epithelial Cells Induces the Polarized Secretion of C-X-C Chemokines. *Infect. Immun.* 65 (12), 5067–5073. doi: 10.1128/IAI.65.12.5067-5073.1997

Laurent F., and Lacroix-Lamande S. (2017). Innate Immune Responses Play a Key Role in Controlling Infection of the Intestinal Epithelium by Cryptosporidium. *Int. J. Parasitol* 47 (12), 711–721. doi: 10.1016/j.ijpara.2017.08.001

Laurent F., McCole D., Eckmann L., and Kagnoff M. F. (1999). Pathogenesis of Cryptosporidium Parvum Infection. *Microbes Infect.* 1 (2), 141–148. doi: 10.1016/s1286-4579(99)80005-7

Li X., Chase J. A., Bond R. F., Lor P., Fernandez K., Nguyen T. H., et al. (2019). Microbiological Safety of Popular Recreation Swimming Sites in Central California. *Environ. Monit Assess.* 191 (7), 456. doi: 10.1007/s10661-019-7601-2

Li M., Gong A. Y., Zhang X. T., Wang Y., Mathy N. W., Martins G. A., et al. (2018). Induction of a Long Noncoding RNA Transcript, NR_045064, Promotes Defense Gene Transcription and Facilitates Intestinal Epithelial Cell Responses Against Cryptosporidium Infection. *J. Immunol.* 201 (12), 3630–3640. doi: 10.4049/jimmunol.1800566

Liu J., Deng M., Lancto C. A., Abrahamsen M. S., Rutherford M. S., and Enomoto S. (2009). Biphasic Modulation of Apoptotic Pathways in Cryptosporidium Parvum-Infected Human Intestinal Epithelial Cells. *Infect. Immun.* 77 (2), 837–849. doi: 10.1128/IAI.00955-08

Mahlapuu M., Hakansson J., Ringstad L., and Bjorn C. (2016). Antimicrobial Peptides: An Emerging Category of Therapeutic Agents. *Front. Cell Infect. Microbiol.* 6, 194. doi: 10.3389/fcimb.2016.00194

Marcial M. A., and Madara J. L. (1986). Cryptosporidium: Cellular Localization, Structural Analysis of Absorptive Cell-Parasite Membrane-Membrane Interactions in Guinea Pigs, and Suggestion of Protozoan Transport by M Cells. *Gastroenterology* 90 (3), 583–594. doi: 10.1016/0016-5085(86)91112-1

Marquis N. D., Record N. R., and Robledo J. A. (2015). Survey for Protozoan Parasites in Eastern Oysters (Crassostrea Virginica) From the Gulf of Maine Using PCR-based Assays. *Parasitol Int.* 64 (5), 299–302. doi: 10.1016/j.parint.2015.04.001

McCole D. F., Eckmann L., Laurent F., and Kagnoff M. F. (2000). Intestinal Epithelial Cell Apoptosis Following Cryptosporidium Parvum Infection. *Infect. Immun.* 68 (3), 1710–1713. doi: 10.1128/iai.68.3.1710-1713.2000

McDonald V., Korbel D. S., Barakat F. M., Choudhry N., and Petry F. (2013). Innate Immune Responses Against Cryptosporidium Parvum Infection. *Parasite Immunol.* 35 (2), 55–64. doi: 10.1111/pim.12020

McDonald V., Pollok R. C., Dhaliwal W., Naik S., Farthing M. J., and Bajaj-Elliott M. (2006). A Potential Role for interleukin-18 in Inhibition of the Development of Cryptosporidium Parvum. *Clin. Exp. Immunol.* 145 (3), 555–562. doi: 10.1111/j.1365-2249.2006.03159.x

McNair N. N., Bedi C., Shayakhmetov D. M., Arrowood M. J., and Mead J. R. (2018). Inflammasome Components Caspase-1 and Adaptor Protein Apoptosis-Associated Speck-Like Proteins are Important in Resistance to Cryptosporidium Parvum. *Microbes Infect.* 20 (6), 369–375. doi: 10.1016/j.micinf.2018.04.006

Mead J. R., Arrowood M. J., Sidwell R. W., and Healey M. C. (1991). Chronic Cryptosporidium Parvum Infections in Congenitally Immunodeficient SCID and Nude Mice. *J. Infect. Dis.* 163 (6), 1297–1304. doi: 10.1093/infdis/163.6.1297

Mead J. R., and You X. (1998). Susceptibility Differences to Cryptosporidium Parvum Infection in Two Strains of Gamma Interferon Knockout Mice. *J. Parasitol* 84 (5), 1045–1048. doi: 10.2307/3284643

Mele R., Gomez Morales M. A., Tosini F., and Pozio E. (2004). Cryptosporidium Parvum At Different Developmental Stages Modulates Host Cell Apoptosis In Vitro. *Infect. Immun.* 72 (10), 6061–6067. doi: 10.1128/IAI.72.10.6061-6067.2004

Miller C. N., Josse L., Brown I., Blakeman B., Povey J., Yiangou L., et al. (2018). A Cell Culture Platform for Cryptosporidium That Enables Long-Term Cultivation and New Tools for the Systematic Investigation of its Biology. *Int. J. Parasitol* 48 (3-4), 197–201. doi: 10.1016/j.ijpara.2017.10.001

Morada M., Lee S., Gunther-Cummins L., Weiss L. M., Widmer G., Tzipori S., et al. (2016). Continuous Culture of Cryptosporidium Parvum Using Hollow Fiber Technology. *Int. J. Parasitol* 46 (1), 21–29. doi: 10.1016/j.ijpara.2015.07.006

Nag R., Whyte P., Markey B. K., O'Flaherty V., Bolton D., Fenton O., et al. (2020). Ranking Hazards Pertaining to Human Health Concerns From Land Application of Anaerobic Digestate. *Sci. Total Environ.* 710, 136297. doi: 10.1016/j.scitotenv.2019.136297

Nydam D. V., Wade S. E., Schaaf S. L., and Mohammed H. O. (2001). Number of Cryptosporidium Parvum Oocysts or Giardia Spp Cysts Shed by Dairy Calves After Natural Infection. *Am. J. Vet. Res.* 62 (10), 1612–1615. doi: 10.2460/ajvr.2001.62.1612

Odendall C., Voak A. A., and Kagan J. C. (2017). Type III Ifns Are Commonly Induced by Bacteria-Sensing Tlrs and Reinforce Epithelial Barriers During Infection. *J. Immunol.* 199 (9), 3270–3279. doi: 10.4049/jimmunol.1700250

Olsen L., Akesson C. P., Storset A. K., Lacroix-Lamande S., Boysen P., Metton C., et al. (2015). The Early Intestinal Immune Response in Experimental Neonatal Ovine Cryptosporidiosis is Characterized by an Increased Frequency of Perforin Expressing NCR1(+) NK Cells and by NCR1(-) CD8(+) Cell Recruitment. *Vet. Res.* 46, 28. doi: 10.1186/s13567-014-0136-1

Ong C. S., Li A. S., Priest J. W., Copes R., Khan M., Fyfe M. W., et al. (2005). Enzyme Immunoassay of Cryptosporidium-specific Immunoglobulin G Antibodies to Assess Longitudinal Infection Trends in Six Communities in British Columbia, Canada. *Am. J. Trop. Med. Hyg* 73 (2), 288–295. doi: 10.4269/ajtmh.2005.73.288

Perez-Cordon G., Yang G., Zhou B., Nie W., Li S., Shi L., et al. (2014). Interaction of Cryptosporidium Parvum With Mouse Dendritic Cells Leads to Their Activation and Parasite Transportation to Mesenteric Lymph Nodes. *Pathog. Dis.* 70 (1), 17–27. doi: 10.1111/2049-632X.12078

Petry F., Robinson H. A., and McDonald V. (1995). Murine Infection Model for Maintenance and Amplification of Cryptosporidium Parvum Oocysts. *J. Clin. Microbiol.* 33 (7), 1922–1924. doi: 10.1128/JCM.33.7.1922-1924.1995

Powell R. H., and Behnke M. S. (2017). WRN Conditioned Media is Sufficient for In Vitro Propagation of Intestinal Organoids From Large Farm and Small Companion Animals. *Biol. Open* 6 (5), 698–705. doi: 10.1242/bio.021717

Rasmussen K. R., Larsen N. C., and Healey M. C. (1993). Complete Development of Cryptosporidium Parvum in a Human Endometrial Carcinoma Cell Line. *Infect. Immun.* 61 (4), 1482–1485. doi: 10.1128/IAI.61.4.1482-1485.1993

Rotz L. D., Khan A. S., Lillibridge S. R., Ostroff S. M., and Hughes J. M. (2002). Public Health Assessment of Potential Biological Terrorism Agents. *Emerg. Infect. Dis.* 8 (2), 225–230. doi: 10.3201/eid0802.010164

Ryan U., Zahedi A., and Paparini A. (2016). Cryptosporidium in Humans and Animals-a One Health Approach to Prophylaxis. *Parasite Immunol.* 38 (9), 535–547. doi: 10.1111/pim.12350

Sateriale A., Gullicksrud J. A., Engiles J. B., McLeod B. I., Kugler E. M., Henao-Mejia J., et al. (2021). The Intestinal Parasite Cryptosporidium is Controlled by an Enterocyte Intrinsic Inflammasome That Depends on NLRP6. *Proc. Natl. Acad. Sci. U.S.A.* 118 (2), 1–8. doi: 10.1073/pnas.2007807118

Sateriale A., Slapeta J., Baptista R., Engiles J. B., Gullicksrud J. A., Herbert G. T., et al. (2019). A Genetically Tractable, Natural Mouse Model of Cryptosporidiosis Offers Insights Into Host Protective Immunity. *Cell Host Microbe* 26 (1), 135–146.e135. doi: 10.1016/j.chom.2019.05.006

Scallan E., Hoekstra R. M., Angulo F. J., Tauxe R. V., Widdowson M. A., Roy S. L., et al. (2011). Foodborne Illness Acquired in the United States–Major Pathogens. *Emerg. Infect. Dis.* 17 (1), 7–15. doi: 10.3201/eid1701.P11101

Theodos C. M., Sullivan K. L., Griffiths J. K., and Tzipori S. (1997). Profiles of Healing and Nonhealing Cryptosporidium Parvum Infection in C57BL/6 Mice With Functional B and T Lymphocytes: The Extent of Gamma Interferon Modulation Determines the Outcome of Infection. *Infect. Immun.* 65 (11), 4761–4769. doi: 10.1128/IAI.65.11.4761-4769.1997

Tzipori S. (1998). Cryptosporidiosis: Laboratory Investigations and Chemotherapy. *Adv. Parasitol* 40, 187–221. doi: 10.1016/s0065-308x(08)60121-9

Upton S. J., Tilley M., and Brillhart D. B. (1994). Comparative Development of Cryptosporidium Parvum (Apicomplexa) in 11 Continuous Host Cell Lines. *FEMS Microbiol. Lett.* 118 (3), 233–236. doi: 10.1111/j.1574-6968.1994.tb06833.x

Urban J. F. Jr., Fayer R., Chen S. J., Gause W. C., Gately M. K., and Finkelman F. D. (1996). Il-12 Protects Immunocompetent and Immunodeficient Neonatal Mice Against Infection With Cryptosporidium Parvum. *J. Immunol.* 156 (1), 263–268.

Varughese E. A., Bennett-Stamper C. L., Wymer L. J., and Yadav J. S. (2014). A New In Vitro Model Using Small Intestinal Epithelial Cells to Enhance Infection of Cryptosporidium Parvum. *J. Microbiol. Methods* 106, 47–54. doi: 10.1016/j.mimet.2014.07.017

Verschoor C. P., Puchta A., and Bowdish D. M. (2012). The Macrophage. *Methods Mol. Biol.* 844, 139–156. doi: 10.1007/978-1-61779-527-5_10

Yang Z., Fu Y., Gong P., Zheng J., Liu L., Yu Y., et al. (2015). Bovine TLR2 and TLR4 Mediate Cryptosporidium Parvum Recognition in Bovine Intestinal Epithelial Cells. *Microb. Pathog.* 85, 29–34. doi: 10.1016/j.micpath.2015.05.009

Zaalouk T. K., Bajaj-Elliott M., George J. T., and McDonald V. (2004). Differential Regulation of Beta-Defensin Gene Expression During Cryptosporidium Parvum Infection. *Infect. Immun.* 72 (5), 2772–2779. doi: 10.1128/iai.72.5.2772-2779.2004

Zachos N. C., Kovbasnjuk O., Foulke-Abel J., In J., Blutt S. E., de Jonge H. R., et al. (2016). Human Enteroids/Colonoids and Intestinal Organoids Functionally Recapitulate Normal Intestinal Physiology and Pathophysiology. *J. Biol. Chem.* 291 (8), 3759–3766. doi: 10.1074/jbc.R114.635995

Zadrozny L. M., Stauffer S. H., Armstrong M. U., Jones S. L., and Gookin J. L. (2006). Neutrophils do Not Mediate the Pathophysiological Sequelae of Cryptosporidium Parvum Infection in Neonatal Piglets. *Infect. Immun.* 74 (10), 5497–5505. doi: 10.1128/IAI.00153-06

Zambriski J. A., Nydam D. V., Wilcox Z. J., Bowman D. D., Mohammed H. O., and Liotta J. L. (2013). Cryptosporidium Parvum: Determination of ID(5)(0) and the Dose-Response Relationship in Experimentally Challenged Dairy Calves. *Vet. Parasitol* 197 (1-2), 104–112. doi: 10.1016/j.vetpar.2013.04.022

Zhang X. T., Gong A. Y., Wang Y., Chen X., Lim S. S., Dolata C. E., et al. (2016). Cryptosporidium Parvum Infection Attenuates the Ex Vivo Propagation of Murine Intestinal Enteroids. *Physiol. Rep.* 4 (24), 1–13. doi: 10.14814/phy2.13060

Zhou J. H., Wang Y. N., Chang Q. Y., Ma P., Hu Y., and Cao X. (2018). Type III Interferons in Viral Infection and Antiviral Immunity. *Cell Physiol. Biochem.* 51 (1), 173–185. doi: 10.1159/000495172

Ziegler P. E., Wade S. E., Schaaf S. L., Stern D. A., Nadareski C. A., and Mohammed H. O. (2007). Prevalence of Cryptosporidium Species in Wildlife Populations Within a Watershed Landscape in Southeastern New York State. *Vet. Parasitol* 147 (1-2), 176–184. doi: 10.1016/j.vetpar.2007.03.024

Conflict of Interest: The authors declare that the research was conducted in the absence of any commercial or financial relationships that could be construed as a potential conflict of interest.

frontiers in Cellular and Infection Microbiology

REVIEW
published: 03 August 2021
doi: 10.3389/fcimb.2021.685239

Lessons Learned for Pathogenesis, Immunology, and Disease of Erythrocytic Parasites: *Plasmodium* and *Babesia*

Vitomir Djokic[1], *Sandra C. Rocha*[2] *and Nikhat Parveen*[2]*

[1] Department for Bacterial Zoonozes, Laboratory for Animal Health, French Agency for Food, Environmental and Occupational Health & Safety, UPEC, University Paris-Est, Maisons-Alfort, France, [2] Department of Microbiology, Biochemistry and Molecular Genetics, Rutgers New Jersey Medical School, Newark, NJ, United States

OPEN ACCESS

Edited by:
Yongliang Zhang,
National University of Singapore, Singapore

Reviewed by:
Benoit Malleret,
National University of Singapore, Singapore
Rajesh Chandramohanadas,
National University of Singapore, Singapore

***Correspondence:**
Nikhat Parveen
parveeni@njms.rutgers.edu

Specialty section:
This article was submitted to Parasite and Host, a section of the journal Frontiers in Cellular and Infection Microbiology

Received: 25 March 2021
Accepted: 15 July 2021
Published: 03 August 2021

Citation:
Djokic V, Rocha SC and Parveen N (2021) Lessons Learned for Pathogenesis, Immunology, and Disease of Erythrocytic Parasites: Plasmodium and Babesia. Front. Cell. Infect. Microbiol. 11:685239. doi: 10.3389/fcimb.2021.685239

Malaria caused by *Plasmodium* species and transmitted by *Anopheles* mosquitoes affects large human populations, while *Ixodes* ticks transmit *Babesia* species and cause babesiosis. Babesiosis in animals has been known as an economic drain, and human disease has also emerged as a serious healthcare problem in the last 20–30 years. There is limited literature available regarding pathogenesis, immunity, and disease caused by *Babesia* spp. with their genomes sequenced only in the last decade. Therefore, using previous studies on *Plasmodium* as the foundation, we have compared similarities and differences in the pathogenesis of *Babesia* and host immune responses. Sexual life cycles of these two hemoparasites in their respective vectors are quite similar. An adult *Anopheles* female can take blood meal several times in its life such that it can both acquire and transmit Plasmodia to hosts. Since each tick stage takes blood meal only once, transstadial horizontal transmission from larva to nymph or nymph to adult is essential for the release of *Babesia* into the host. The initiation of the asexual cycle of these parasites is different because *Plasmodium* sporozoites need to infect hepatocytes before egressed merozoites can infect erythrocytes, while *Babesia* sporozoites are known to enter the erythrocytic cycle directly. *Plasmodium* metabolism, as determined by its two- to threefold larger genome than different *Babesia*, is more complex. *Plasmodium* replication occurs in parasitophorous vacuole (PV) within the host cells, and a relatively large number of merozoites are released from each infected RBC after schizogony. The *Babesia* erythrocytic cycle lacks both PV and schizogony. Cytoadherence that allows the sequestration of Plasmodia, primarily *P. falciparum* in different organs facilitated by prominent adhesins, has not been documented for *Babesia* yet. Inflammatory immune responses contribute to the severity of malaria and babesiosis. Antibodies appear to play only a minor role in the resolution of these diseases; however, cellular and innate immunity are critical for the clearance of both pathogens. Inflammatory immune responses affect the severity of both diseases. Macrophages facilitate the resolution of both infections and also offer cross-protection against related protozoa. Although the immunosuppression of

adaptive immune responses by these parasites does not seem to affect their own clearance, it significantly exacerbates diseases caused by coinfecting bacteria during coinfections.

Keywords: *Plasmodium*, malaria, *Babesia*, babesiosis, pathogenesis, immune responses, vector borne protozoa, hemoparasite

INTRODUCTION

Apicomplexan protozoa, *Plasmodium*, and *Babesia* species are described as erythrocyte-dwelling hemoparasites that cause serious morbidity in humans and animals alike (Allred, 1995; Springer et al., 2015), and are evolutionary-related organisms with overlapping life cycles, disease manifestations, and immune responses (Clark and Allison, 1974; Frolich et al., 2012). Out of 60 species, *P. falciparum, P. vivax, P. ovale, P. malariae*, *P. knowlesi, P. cynomolgi*, and *P. simium* infect humans to cause malaria (Milner, 2018; Garrido-Cardenas et al., 2019), while four others, *P. chabaudi, P. berghei, P. vinckei*, and *P. yoelii*, infect rodents (De Niz and Heussler, 2018). Similarly, out of over 100 *Babesia* spp. known, only *B. microti, B. duncani*, *B. divergens*, and *B. venatorum* are documented to infect humans in North America and Europe (Lobo et al., 2020), while others are identified more as infections of different animals (Lobo, 2005). Both protozoa are transmitted by vectors. *Anopheles* female mosquitoes transmit *Plasmodium*, and *Ixodes* species are vectors for *Babesia* transmission. While malaria is a very well-known disease, babesiosis has long been recognized as an economically important disease of cattle and other animals and has emerged as a reportable human disease in the United States only in 2011 (Lobo, 2005). Another major healthcare problem associated with babesiosis is that *Babesia* spp. can also be transmitted by blood transfusion; however, donated blood is usually not tested for this parasite. As a result, babesiosis is one of the most important pathogenic diseases transmitted by blood transfusion in the United States. It can also be transmitted vertically from mother to child during pregnancy (Wormser et al., 2015; Saetre et al., 2018) like *P. falciparum*. The proof for efficacy of blood screening was already proven some 40 years ago on *Plasmodium* spp., lowering its transmission greatly throughout the world. Screening of donated blood, once implemented for antibodies against, or DNA from *B. microti* showed association with a decrease in the risk of transfusion-transmitted babesiosis (Moritz et al., 2016). *P. falciparum* strain 3D7 genome of 22.8 Mb is distributed among 14 chromosomes ranging in size from approximately 0.643 to 3.29 Mb (Gardner et al., 2002). In comparison, *B. microti* possesses the smallest nuclear genome of 6.4 Mb among apicomplexan parasites with four chromosomes, thus limiting its metabolic functions (Cornillot et al., 2012), while the *B. divergens* genome size is ~10.7 Mb (Cuesta et al., 2014), indicating that more complex gene expression and regulatory systems are present in *Plasmodium* than *Babesia*.

Transmissibility of *Babesia* species from animals to humans and vice versa allows through vector the involvement of wildlife as reservoirs. Therefore, understanding this hemoparasite transmission patterns can provide an insight into elevated disease risks, especially in the light of climate change, disappearance of wildlife species risks, and human disruption of natural ecosystems (Springer et al., 2015). Despite the involvement of different vectors, the sexual life cycle of both *Plasmodium* and *Babesia* species is completed in their respective vectors and shows significant overlapping stages (**Figure 1**). They start with gametogenesis in the midgut and end with sporozoites release in the salivary glands of the vector to allow the transmission to the hosts during blood meal with *Babesia* transmission mechanism resembling other hard tick-transmitted infections (Khan and Waters, 2004; Steere et al., 2016; Stewart and Rosa, 2018). A major difference in the transmission cycle of these protozoa is that all developmental stages of *Plasmodium* occur in adult *Anopheles* female mosquitoes, which are able to take multiple blood meals (Norris et al., 2010), while horizontal transfer from larvae to nymph or nymph to adult stages (transstadial transmission) is required for the completion of the *Babesia* sexual cycle in ticks. This is because each developmental stage of ticks takes blood meal only once, such that if a larva acquires the gametocytes of *Babesia* during initial blood meal, nymph will transmit sporozoites to the host during its blood meal to cause infection. Rarely, *Babesia* spp. also perpetuate in ticks by transovarial transmission (Stewart and Rosa, 2018; Jalovecka et al., 2019). Furthermore, the parasite transmission rates differ because mosquitoes use tube-like mouthparts called proboscis that can penetrate the host skin and suck up blood within seconds; however, ticks blood meal from the host is demonstrated to be slow and requires approximately 36 h during which the transmission of parasite occurs from the infected ticks.

Plasmodium begins its asexual cycle in the host by infection of liver hepatocytes by sporozoites delivered by the mosquito in the dermis [**Figure 1**, and (Gowda and Wu, 2018)], while *Babesia* appears to start its asexual cycle by direct invasion of erythrocytes by its sporozoites. Infection of the liver or any other organ by these protozoan sporozoites has not been documented. In the liver, *Plasmodium* undergoes a single round of replication producing ~10,000 merozoites in *P. vivax*/*P. ovale* and up to 30,000 in *P. falciparum* that are released by the lysis of hepatocytes (Antinori et al., 2012). Some *Plasmodium* spp. that infect primates, such as *P. vivax* and *P. ovale*, also form long-lived dormant parasites called hypnozoite (Markus, 2011) and often result in the relapse of malaria. This latent stage of *Plasmodium* can remain in the liver for more than a year (Vaughan and Kappe, 2017; Venugopal et al., 2020).

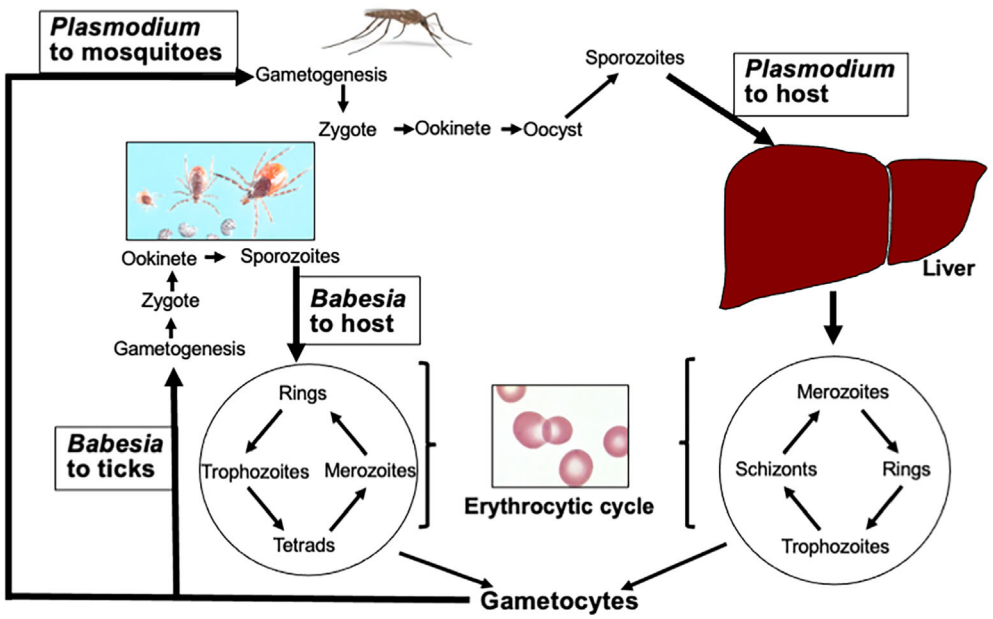

FIGURE 1 | Life cycles of *Plasmodium* and *Babesia* species. After acquiring *Plasmodium* gametocytes from infected hosts, gametogenesis followed by fusion of gametes to produce zygote occurs in the midgut of Anopheles females. Ookinete passes through the midgut wall, and sporozoites are released from the oocyte into salivary glands that are transmitted to the host during blood meal. Similar steps are followed by *Babesia* species in ticks except it requires transstadial horizontal transmission of parasites from one stage of the tick developmental cycle to the next. After deposition in skin dermis, the haploid sporozoites of *Plasmodium* travel to the liver through blood and infect hepatocytes. After a single replication cycle, the merozoites released from hepatocytes enter the erythrocytic cycle. Invasion of hepatocytes is absent in the *Babesia* cycle. In addition, the *Babesia* cycle in RBCs differs from *Plasmodium* because unlike *Plasmodium*, it does not replicate in the parasitophorous vacuole, lacks PTEX secretion apparatus, and does not undergo schizogony. (Image of different stages of *Ixodes scapularis* ticks was generously provided by James Occi of Rutgers University at New Brunswick, NJ, USA.)

The obligatory intracellular life cycle in vertebrates enables both of these parasites to hide from the host immune system during most of their asexual reproductive stages. At this stage, the host immune response can only target the changed surface of the infected erythrocyte (Allred, 1995). In immunocompetent individuals, protective humoral and cellular immune responses together with innate immune response eliminate most of the parasites, but in the cases of immune deprivation, the infection can have dire consequences especially when not diagnosed and treated in a timely manner. In this review, using *Plasmodium* as a model system, because a significant body of literature is available for this parasite, we have compared the erythrocytic cycle of both pathogens in the hosts and summarized known differences and similarities in host immune responses during infection. We have also summarized in brief the mechanisms of immune evasion by *Plasmodium* species and the consequence of immunosuppression by both parasites on other pathogens.

PATHOGENESIS

Invasion of Erythrocytes

The name for apicomplexans comes from the characteristic apical complex of secretory organelles that are discharged in a tightly controlled and highly regulated order. In mature merozoites of both protozoa, different protein populations localize in the rhoptry bulb and neck, but the functions of many of these proteins still remain unknown. Rhoptries are twinned, club-shaped structures with a body or bulb region that tapers to a narrow neck as it meets the apical prominence of the merozoite. One group of such proteins called rhoptry-associated membrane antigen (RAMA) is indispensable for blood-stage parasite survival. RAMA is not required for the trafficking of all rhoptry bulb proteins but are essential for the invasion of red blood cells (RBCs) and do not induce cell membrane changes in target RBCs especially in the malaria parasite (Sherling et al., 2019). After emerging from the liver, *Plasmodium* merozoites invade RBCs. On the other hand, after tick bite, *Babesia* sporozoites appear to directly invade the erythrocytes, but proteins with function similar to RAMA are not shown in these parasites (Herwaldt et al., 2003).

Invasion of erythrocytes is an integral and essential component of both *Plasmodium* and *Babesia* life cycles. The intercellular adhesion molecule ICAM-4 is expressed on the surface of RBCs, and *P. falciparum* merozoites use it as one of their anchor points (Bhalla et al., 2015). At the same time, parasites secrete a subtilisin-like serine protease from their dense granules in order to modify the erythrocyte's membrane and prepare it for invasion (Blackman et al., 1998). No evidence exists of *Babesia* using ICAM receptors; however, *B. divergens* uses neuraminidase- and trypsin-sensitive receptors such as glycophorins for cell invasion (Lobo, 2005). Bovine

erythrocytes become rigid and adhere to vascular endothelial cells when infected with *B. bovis*. These modifications result in the appearance of ridge-like structures on the erythrocyte surface, similar to the knob-like structures observed on the surface of *P. falciparum* infected human RBCs, but they are morphologically and biochemically distinct (Hutchings et al., 2007). Interestingly, *P. vivax* and *P. ovale* prefer infecting reticulocytes (immature RBCs), which limits their replication and levels of parasitemia development (Lim et al., 2017; Kanjee et al., 2018; Pasini and Kocken, 2020), while *P. falciparum* infects both reticulocytes and mature erythrocytes (Pasvol et al., 1980; Srivastava et al., 2015) similar to that observed in canine pathogen *B. gibsoni*, which results in a high level of parasitic burden in blood and causes more severe disease. On the other hand, *P. malariae* prefers old erythrocytes, and human pathogen *B. microti* also exhibits a higher tropism for mature RBCs (Borggraefe et al., 2006). Nevertheless, these cellular and physiological changes are related to the virulence of both *Plasmodium* and *Babesia* (Hutchings et al., 2007).

Intraerythrocytic Multiplication, Egress, and Re-Infection

Many host protein receptors have been shown to facilitate the adhesion and invasion of parasites; however, host molecules involved in interactions with the parasites during intracellular development remain poorly explored (Hentzschel et al., 2020). Even lesser is known about the *Babesia* interaction with RBCs. There are several differences in the erythrocytic cycle of *Plasmodium* and *Babesia*. Once the invasion of erythrocytes occurs, parasites rely on various host factors to grow and replicate. Repeated cycles of replication depicting different stages of infection: ring, trophozoites, and schizonts for *Plasmodium*, occur while schizogony has not been known for *Babesia* spp. (**Figures 1**, **2**). Despite the growing importance of this tick-borne disease, investigation of the basic biology of *Babesia* species that infect humans remains somewhat neglected. Its highly unusual variable intra-erythrocytic life cycle forms; the life span of each population of infected cells and the time required for the generation of the different stages of parasite have been documented to some extent. Unlike repeated replication cycles during schizogony to produce a large number of merozoites from a single RBC (~6-36/iRBC depending on *Plasmodium* species) (Antinori et al., 2012), only one to three *Babesia* replication cycles are reported to occur producing different morphological forms: paired figures, multiple trophozoites, pyriform, figure eight, Maltese Cross, etc. [**Figure 2** and (Cursino-Santos et al., 2016)]. Importantly, the choice of developmental pathway of these parasites is determined by the availability of RBCs for infection and nutritional environment present. Thus, parasites respond swiftly to the availability of uninfected RBCs for invasion and nutritional components needed (Cursino-Santos et al., 2016).

Interestingly, malaria parasites replicate within the non-phagosomal parasitophorous vacuole (PV) and retain *Plasmodium* Translocon for Exported Proteins (PTEX) inserted in the parasitophorous vacuole membrane (PVM) to both release molecules into the erythrocytic cytoplasm and import nutrients (Ho et al., 2018). PTEX is used to export proteins in the RBC cytoplasm that remodels erythrocytes to facilitate the uptake of nutrients and the disposal of waste products (de Koning-Ward et al., 2016; Kalanon et al., 2016). In addition, PTEX is also involved in the modification of the erythrocyte membrane and the insertion of *Plasmodium* virulence proteins and adhesins, such as the highly variable *P. falciparum* erythrocyte membrane protein 1 (PfEMP1) in knob-like protrusion and ring-infected erythrocyte surface antigen (RESA) and different chaperons into the erythrocyte membrane. Although the parasite-derived multicopy variant erythrocyte surface antigen (VESA) proteins of *B. divergens, B. bigemina*, and *B. bovis* are also displayed on the surface of iRBCs, only three similar genes are present in *B. microti* and it is not known if they are even present on the infected erythrocytes surface (Cornillot et al., 2012; Jackson et al., 2014). Another major difference between *Plasmodium* and *Babesia* is their reaction to heme, a product of hemoglobin destruction that occurs during the invasion of RBCs. Heme is toxic for *Plasmodium* but has no effect on *Babesia* parasites. Heme is transported to the digestive vacuole of the *Plasmodium* where, by still an unclear mechanism, it is transformed into the hemozoin crystal, the characteristic pigment of this protozoan (Kapishnikov et al., 2021).

During rigorous asexual multiplication cycles, the rupture of PVM occurs and ultimately mature schizonts burst open the erythrocytic membrane to facilitate *Plasmodium* merozoites egress. The replicative cycle of *P. falciparum* followed by full development of invasive parasites is synchronized with their egress. Using inhibitors of known proteases, several parasite proteases have been identified as key effectors of the egress process for the blood stage as reviewed previously (Singh and Chitnis, 2017), in addition to perforin-like proteins with homology with mammalian perforins (PfPLP) and the subtilisin-like protease, PfSub1, that are located in micronemes and exonemes, respectively. These enzymes cause the disruption of the RBC cytoskeleton and the rupture of different membranes (Salmon et al., 2001; Millholland et al., 2011). Several of these effectors are localized in the apical organelles of apicomplexan protozoa and are secreted systematically to initiate the egress of merozoites. Furthermore, phosphoproteomic analysis of merozoites with a cGMP-dependent kinase inhibitor, compound 1, suggests the involvement of this enzyme in regulating the key processes of the invasion and egress of *P. falciparum* merozoites (Alam et al., 2015).

Although the *B. microti* egress mechanism has not been well documented until now, the release of *B. divergens* merozoites starts by establishing contacts with the plasma membrane of the erythrocyte from inside before they exit the cell (Sevilla et al., 2018). The merozoites released from iRBCs are ready for invasion of new erythrocytes and repeat multiplication cycle. In both protozoa, a small proportion of parasites commit to produce sexual progeny represented by gametocytes. Such commitment levels vary between species within the same genus and are affected by genetic, epigenetic, and environmental

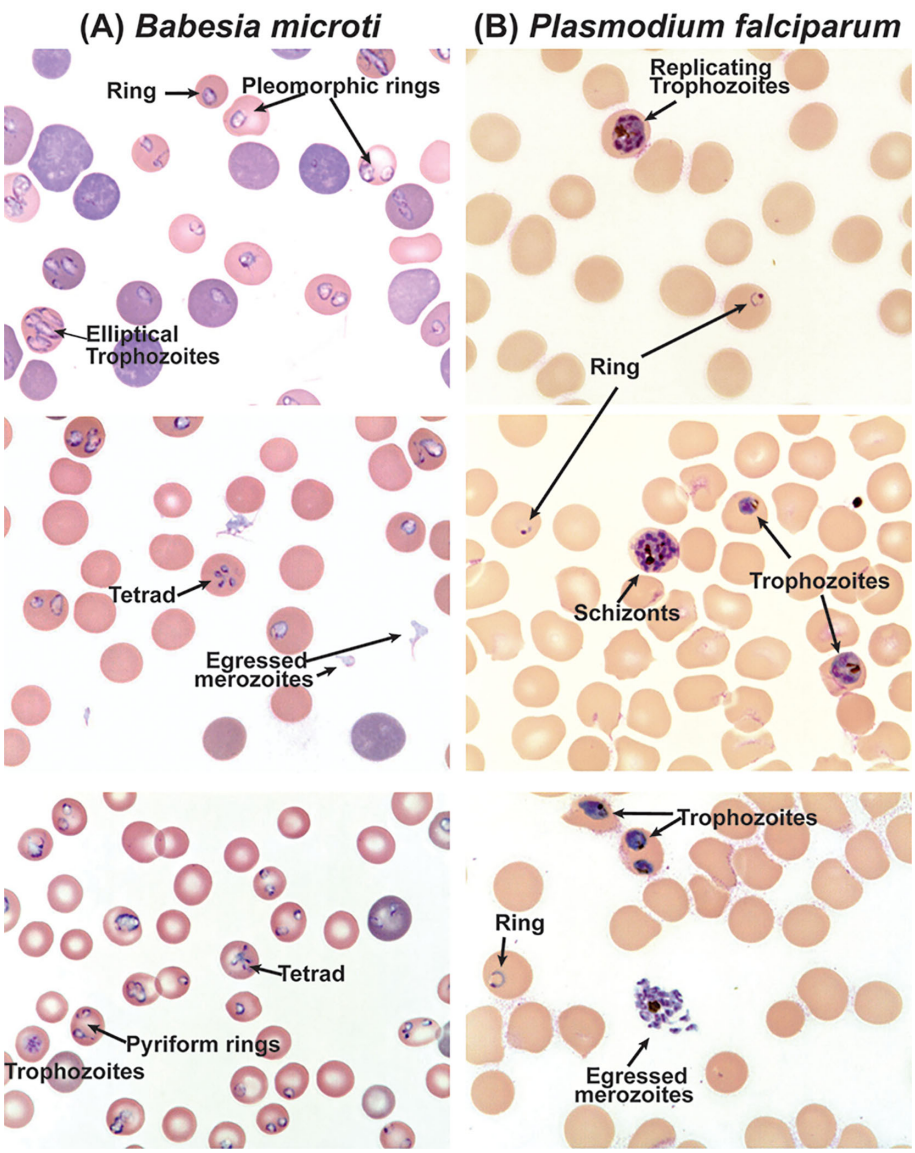

FIGURE 2 | Differential morphological forms of *B. microti* during replication in RBCs of C3H mouse and *in vitro* culture of *P. falciparum*. **(A)** Clearly defined rings, pleomorphic trophozoites and pyriforms, and tetrads are observed during the replication of *B. microti*, while **(B)** rings, trophozoites, and schizonts are clearly observed during the erythrocytic cycle of *P. falciparum*.

conditions. Once matured, these gametocytes are ready by the vectors to take up to start the sexual cycle in the midgut of the respective vectors.

IMMUNITY AGAINST THESE TWO PROTOZOAN PATHOGENS

During the infection of hosts with parasites, a tug of war ensues to determine if a person gets seriously sick or recovers. Using the rodent malaria parasite *P. chabaudi* as a model system, Wale and coworkers presented three components of the immune response on distinct effects on parasites and disease (Wale et al., 2019). According to them, the host deploys a strategy in which it destroys RBCs early in infection to restrict erythrocyte supply for invasion. They attributed the loss of total RBCs to the indiscriminate removal of both iRBCs and uninfected RBCs causing anemia. This phenomenon of immunopathology appeared to be beneficial to the host by restricting the *Plasmodium* population. Late in the infection, the accelerated turnover of RBCs allowed mice to recover from anemia while simultaneously limiting *P. chabaudi* invasion and proliferation in erythrocytes. Ultimately, by returning of the components of the host response with respect to the resupply of reticulocytes and indiscriminate killing to the initial phase and infections taking different trajectories, heightened targeted killing response to

iRBCs resulted in the decrease in parasite numbers to undetectable levels (Wale et al., 2019). A somewhat similar response was also observed when *B. microti* infected C3H mice (Djokic et al., 2018a; Djokic et al., 2019).

Innate Immune Response

Plasmodium spp. challenge the mammalian immune system with a delicate balancing act. These parasites have acquired immune escape mechanisms that prevent the development of sterile immunity. During the past two decades, there has been a significant progress in understanding the molecular and cellular mechanisms of host–parasite interactions and the associated signaling of immune responses to the malaria parasite. Soon after infection, both the liver and blood stage parasites are sensed by various receptors involved in the host innate immune system resulting in the activation of signaling pathways and the production of cytokines and chemokines. Similar to other pathogens, innate immunity is the first line of defense against *Plasmodium* infection and starts during the initiation of the host–parasite contact. In the mouse model, *Plasmodium* sporozoites injection into the dermis recruits mast cells at the site of infection (Wilainam et al., 2015). Sporozoites make their entrance into liver hepatocytes by passing through blood circulation where liver resident Natural Killer (NK) and NKT cells are activated. During this stage, *Plasmodium* RNA likely stimulates pro-inflammatory type I interferon (IFN-I) in an interferon-α/β receptor-dependent manner and also stimulates the production of IFN-γ to facilitate phagocytosis by macrophages (Liehl et al., 2014).

Appropriately regulated innate immune response and pro-inflammatory cytokine production are required both for generating protective immunity and stimulation of adaptive immune response. Although in the early erythrocytic cycle, dendritic cells (DCs) and macrophages are key responders, macrophages have been known to become immunosuppressive after the phagocytosis of *Plasmodium* iRBCs while DCs continue to produce pro-inflammatory cytokines and chemokines to promote innate and adaptive immune responses (Schwarzer et al., 2003; Wu et al., 2015). In addition to producing a wide range of pro-inflammatory cytokines, including TNFα, IL-12, and IL-6, and chemokines, such as CXCL1, CXCL2, CCL2, CCL5, CXCL9, and CXCL10, during the *Plasmodium* erythrocytic cycle, DCs also contribute significantly for immunity development and pathogenesis of the parasite (Gowda and Wu, 2018; Wu et al., 2018). For example, DCs produce IL-12 that activates NK cells to induce the production of IFN-γ, which primes macrophages and neutrophils to enhance phagocytosis and promotes Th1 and effector T cell responses connecting innate to adaptive immune responses against the malaria parasite (Walsh and Mills, 2013; King and Lamb, 2015). During the *Plasmodium* infection, DC function is compromised to some extent that results in the reduction of immune responses against the parasite as well as against heterologous antigens.

Babesia susceptible C3H mice show several human-like disease manifestations and are ideal to study the pathogenesis of this protozoan. In the immunocompetent C3H mice, peak *B. microti* parasitemia of >40% was associated with a significant decrease in the hemoglobin level (Djokic et al., 2019). Splenomegaly and destruction of the marginal zone in spleen, and lysed erythrocytes and released *B. microti* life forms were also observed in these mice. After undetectable parasitemia was achieved, a significant increase in splenic macrophages levels was observed in *B. microti* infected mice suggesting a role of these phagocytes in disease resolution. The severe combined immunodeficient (SCID) mice as well as IFNγ-deficient mice with chronic *B. microti* infections demonstrated protective responses comparable to those of fully immunocompetent animals (Li et al., 2012). Furthermore, NK cell depletion *in vivo* did not significantly impair the protective responses. Conversely, macrophage depletion resulted in increased susceptibility to *B. rodhaini* infection that was associated with changes in their antibody and cytokine profiles, indicating a crucial role of macrophages in the protection against the challenge infection (Li et al., 2012).

Bastos et al. (2007) characterized peripheral blood monocyte-derived DC from *B. bovis* infected cattle, and myeloid DC from afferent lymph, but not resident DC from other bovine tissues (Bastos et al., 2007). For the hemoprotozoan infections like in babesiosis, the spleen as a secondary lymphoid organ is central to the innate and acquired immune response. The authors examined the phenotypic profile of myeloid DC from spleen and another myeloid cell population with monocyte features represented by the CD13+CD172a+/-CD14-CD11a-CD11b+/-CD11c+ and CD13+/-CD172a+CD14+CD11a-CD11b+/-CD11c+, respectively. (Bastos et al., 2007). The CD13+ population was obtained only from the spleen; however, they obtained the same percentage of CD172a+ population from the spleen and peripheral blood. The myeloid splenic DCs exhibited immature state. Early interactions of cells of the innate immune system including DCs and NK cells can influence the development and ability of the adaptive immune response to reduce/eliminate intracellular pathogens. Upregulation of MHCII, CD80, and CD86 in activated DCs during infection suggested that mature *Babesia*-activated CD13(+) splenic DCs were required for the stimulation of bovine NK cells (Bastos et al., 2008).

Plasmodium glycosylphosphatidylinositol (GPI) used to anchor several proteins into the merozoite membrane are structurally heterogeneous lipid molecules based upon differences in length and extent of unsaturated acyl residue presence and location of acyl components in the phosphatidylinositol moiety. GPI has been shown to induce the production of pro-inflammatory cytokines by macrophages primarily through recognition by TLR2-TLR1 heterodimer depending on GPI composition and by participation of TLR4 to somewhat lesser extent (Mockenhaupt et al., 2006; Gowda, 2007; Seixas et al., 2009; Zhu et al., 2011). This signaling likely occurs due to the burst of release of a large number of merozoites (up to 36/iRBC) of *Plasmodium* during the active erythrocytic cycle making GPI anchored proteins easy access to TLR2 and TLR4. Other TLRs, including TLR7 and TLR9, are also involved in signaling by RNA, DNA, and other molecules of the malaria parasite to produce pro-inflammatory cytokines and IFN-I (Gowda and Wu, 2018). Only limited information is available for GPI anchored merozoite proteins of *Babesia* species, and it was

reported not to induce the stimulation of pro-inflammatory cytokines (Delbecq et al., 2002; Debierre-Grockiego et al., 2019; Nathaly Wieser et al., 2019). Unlike *Plasmodium* species, the composition of GPI in *B. microti* proteins has not been described yet, such that the contribution of TLR2 and TLR4 remains to be investigated to understand the influence of the signaling mechanisms during infection of the host defective in the specific TLRs. The role of TLR4 in *B. microti* pathogenesis is unknown, but its GPI anchors were suggested to possibly activate TLR4 and TLR2 (Campos et al., 2001; Debierre-Grockiego et al., 2007). Other TLRs, including TLR7 and TLR9, are also involved in signaling by RNA, DNA, and other molecules of the malaria parasite to produce pro-inflammatory cytokines and IFN-I (Gowda and Wu, 2018). Using TLR2 and TLR4 transfected human embryonic kidney (HEK) 293 cells, we observed the lack of production of pro-inflammatory IL-8 and TNFα cytokines when *B. microti* infected mouse blood or released parasites were used for stimulation (Akoolo et al., 2021). Different structure of GPI, the absence of *Babesia* GPI proteins display on the iRBCs surface, and a small number of released merozoites (2-8/iRBC) could all account for the absence of TLR2/TLR4 stimulation by *B. microti* merozoites/iRBCs. Lyme disease causing *Borrelia burgdorferi*, which is also transmitted by ticks, expresses large amounts of TLR2 ligand lipoproteins. This treatment served as a control to show the stimulation of TLR2 and to less extent TLR4 to increase pro-inflammatory cytokine IL-8 and TNFα production significantly (Akoolo et al., 2021). The involvement of host TLR2 during Babesia infection is not yet examined.

Adaptive: Cellular Immune Response

Adaptive immune response is also dependent on the *Plasmodium* stage of the life cycle. Although antibodies appear to be important during erythrocytic infection, T cells are the major immune modulators in the liver and erythrocytic stages of infection. CD8+ cells specific for *Plasmodium* antigens eliminate the intracellular parasite in hepatocytes by NO and IFNγ-dependent and independent mechanisms (Doolan and Martinez-Alier, 2006; Chakravarty et al., 2008; Kelemen et al., 2019). Involvement of $CD8^+$ T cells was also shown during the *P. vivax* erythrocytic cycle (Burel et al., 2016; Junqueira et al., 2018). During both cellular and humoral immune responses, CD4+ cells carry out their traditional helper function (Perez-Mazliah and Langhorne, 2014; Soon and Haque, 2018). Inflammatory CD4+ T-cells that produce IFNγ and TNFα have been implicated in conferring protection from malaria in adults by preventing *P. falciparum* infection or its replication such that higher parasitemia and clinical malaria are diminished (Boyle et al., 2015). In a study involving children in Uganda that is endemic for *P. falciparum* infection, Boyle and coworkers showed that although all children exhibited similar percentage of CD4+ cells as adults and uninfected children, somewhat lower levels of *P. falciparum* specific CD4+ T cells producing IFNγ, IL-10, and TNFα cytokines were present in infected children's blood with asymptomatic malaria (Boyle et al., 2017). IL-10 secretion by CD4+ cells diminished with the age of the individuals. They also showed a high positive correlation between parasite burden and the frequencies of *P. falciparum*-specific IL-10 producing CD4+ T cells but not with IFNγ or TNFα producing CD4+ cells; however, these cells could not prevent infection prospectively. Importantly, IL-10 exerted quantitatively stronger regulatory effects on innate and CD4+ T cell responses during primary and secondary infections, respectively. The durability of IL-10-producing CD4+ T cells post-infection demonstrated how this cytokine may contribute to optimizing the control of parasites and prevent immunity-mediated pathology during recurrent malaria infections (Villegas-Mendez et al., 2016).

Cell-mediated immunity appears to be critical in preventing severe blood-stage malaria. IFNγ, but not IL-2, was shown to play an essential role in the cell-mediated immunity against *P. chabaudi adami* infections (Batchelder et al., 2003). The inability to generate protective immune response against *Plasmodium* spp. and inadequate T-cell responses could help persistent blood-stage infection and malaria. The lack of effective protection against malaria albeit production of highly inflammatory cytokines during infection suggests the absence of adequate memory T cells development to confer immunity. The *Plasmodium* ortholog of the macrophage migration inhibitory factor was found to enhance inflammatory cytokines production and also induced antigen-exposed CD4+ T cells to mature into short-lived effector cells and not into precursor cells for memory development. These findings indicate that the parasite actively interferes with immunological memory development and could have helped maintain the conserved orthologs of the parasite macrophage migration inhibitory factor during evolution (Sun et al., 2012). The lack of immunological memory could account for failure of various vaccine candidates to confer protection against malaria.

B. microti strain KR-1 was isolated from a Connecticut resident with babesiosis. The inoculation of this strain in SCID mice and TCRαβ knockouts resulted in the sustenance of severe but nonlethal parasitemia averaging 35% to 45% infected erythrocytes (Clawson et al., 2002). IFNγ-deficient mice developed a less severe parasitemia and were able to clear infection. In contrast, in six of eight JHD-null mice (B-cell deficient), the levels of parasitemia were indistinguishable from those in the wild-type animals. To summarize, these results indicate that cellular immunity is critical for the clearance of *B. microti* in BALB/c mice and that disease resolution can occur even in the absence of IFNγ (Clawson et al., 2002).

Depletion of CD25+ Treg cells significantly reversed the inhibition of CD4+ T-cell proliferation and IL-2 production, indicating that this cell population contributes to the suppression of T-cell function during malaria (Nie et al., 2007; Wammes et al., 2013). Moreover, depletion of Treg cells prevented the development of parasite-specific Th1 cells involved in the induction of cerebral malaria during a secondary parasitic challenge, demonstrating a regulatory role for this cell population in the control of pathogenic responses that otherwise lead to fatal disease. As mentioned above, immune responses against *Plasmodium* protozoan are unable to inhibit the establishment of its infection and can even contribute to the severity of disease. Individuals who survive multiple infections

show some level of protective immunity where primed immune responses inhibit severe disease manifestations by limiting inflammation. CD4+ T cells play critical roles in the immunoregulatory pathways established during malaria by priming for phagocytosis mediated killing of parasitized RBCs, and by helping B cell differentiation to produce functional anti-*Plasmodium* antibodies (Kumar et al., 2020). In malaria-endemic areas, a segment of population that shows minimal clinical signs, if any, could become chronic carriers of Plasmodia. The Tregs activation marker TNFRII expression was shown to increase during the infection of these individuals but diminished after treatment. This TNFRII expression showed positive correlation with TNFα in response to *P. falciparum*-infected RBCs, but this association disappeared after treatment. Asymptomatic malaria also appeared to be associated with increased TNFRII expression on Tregs, together with Th2 cytokine responses suppression, which could facilitate the survival of the parasites in *Plasmodium* carriers (Wammes et al., 2013). The apparent suppression of IL-13 secretion in response to *P. falciparum*-infected erythrocytes also recovered after the treatment of individuals for malaria.

Immunocompetent mice mount a very strong adaptive immune response against *B. microti*, with features including the following: (i) a robust germinal center induction; (ii) follicular helper T cell development that accounts for ~30% of splenic CD4+ T cells; and (iii) an increase in effector T-cell cytokine levels, including IL-21 and IFNγ together with enhanced secretion of specific antibodies (Yi et al., 2018). Interestingly, parasitemia of *B. microti* was significantly lower in the Towns sickle cell disease mouse strain. Although splenic architecture is highly disorganized before infection in these mice, they elicited a surprisingly robust adaptive immune response, including comparable levels of germinal center B cells, follicular helper T cells, and effector cytokines, and higher immunoglobulin G responses against potential immunogenic epitopes of two *Babesia*-specific proteins.

B. microti infected C3H mice also showed significantly higher concentration of CD4+ cells secreted cytokines such as IL-2 and IFNγ in plasma, while the increase of cytokines such as IL-4, IL-5 and IL-13 secreted by CD8+ cells was not always significant. (Djokic et al., 2019). Thus, Th1 cells-mediated immunity appears to be important in the clearance of this intracellular pathogen. A significant increase in IL-6, which induces Th17 cell differentiation, was observed; however, it led to only a moderate change in Th17 cell secreted cytokines, IL-17A, IL-17F, IL-21, and IL-22. A similar immune response to *Trypanosoma* infection was reported to affect the clearance of this parasite, as well as of coinfecting pathogen(s) (Hoft et al., 2000; Santamaria and Corral, 2013; Cai et al., 2016). At the acute stage of *B. microti* infection, splenic cells exhibited Th1 polarization in young mice with an increase in IFNγ and TNFα producing T cells and a simultaneous increase in the Tregs/Th17 ratio. These changes likely help in the clearance of infection in young mice and also prevent mortality that occurs due to the infection of mice with *B. duncani* WA-1 strain that stimulates potent inflammatory response infection in mice (Djokic et al., 2018b).

The role of T cell subpopulations in protective cellular immunity development at the early stage of infection with *B. microti* and *B. rodhaini* was depicted by the changes in the course of infection and delayed type hypersensitivity (DTH) response against parasites (Shimada et al., 1996). Lyt-2+ and L3T4+ T cells showed opposite effects on *B. microti* and *B. rodhaini*. Depletion of Lyt-2+ T cells increased resistance to *B. microti* and susceptibility to *B. rodhaini* infection. In contrast, depletion of L3T4+ T cells enhanced susceptibility to *B. microti* infection but led to increased resistance to *B. rodhaini* infection. The DTH response to *B. microti* in infected mice was exacerbated by depletion of Lyt-2+ T cells but reduced significantly after L3T4+ T cell depletion. A self-limiting infection of *B. microti* in mice still makes them resistant to reinfection. Anti-CD4 monoclonal antibody (MAb) treatment of immune mice restricted the protective immune response against challenge infection; however, anti-CD8 MAb treatment did not affect protection. Supporting these results, the transfer of CD4+ T-cell-depleted spleen cells resulted in higher parasitemia than when CD8+ T-cell-depleted spleen cells were injected. An increase in IFNγ production by CD4+ T cells was observed in the culture supernatant of spleen cells from immune mice. Treatment of immune mice with anti-IFNγ MAb reduced their protection from *B. microti* infection to some extent. Furthermore, protection against challenge infection was not observed in IFNγ-deficient mice. On the other hand, treatment of immune mice with MAbs against IL-2, IL-4, or TNFα did not affect protective immunity. Although parasitemia of *B. microti* declined in CD4-deficient mice, these mice maintained parasites for more than a month (Skariah et al., 2017). Treatment of mice with anti-CD4 MAbs and transfer of naïve mice with $CD4^+$-depleted spleen cells showed significantly higher parasitemia after challenge infection (Igarashi et al., 1999). These combined results suggest the essential requirements for CD4+ T cells and IFNγ in protective immunity against challenge infection with *B. microti*.

Infection with *B. duncani* strain WA1 is fatal in mice, whereas *B. microti* parasitemia gets resolved and the latter infection is not fatal. Mortality due to WA1 inoculation is associated with the stimulation of high levels of TNFα production, whereas the resolution of *B. microti* infections was associated with an increase in IL-10 and IL-4 production. The contribution of excessive TNFα production was further emphasized by using TNFRp55-/- mice that exhibited a 90% survival rate due to the disruption of the TNFα−stimulation pathway resulting in diminished pathology associated with WA1 infection. Thus, a high level of TNFα produced by mice is an important mediator of the WA1 pathogenesis (Hemmer et al., 2000). WA1 infection in T-$\gamma\delta^{-/-}$ cells and wild-type mice also resulted in fatality. CD4+ T cells participate in parasite elimination during *Babesia* infection, while CD8+ T cells may also contribute to the disease manifestations by the WA1 strain.

DCs are the bridge between innate and adaptive immunity such that interactions between antigen-presenting DCs and inducible T cells are necessary for the stimulation of an adaptive immune response. During *Plasmodium* infection, DC function is

attenuated due to hemozoin released from engulfed iRBCs resulting in the reduction in immune responses against both parasitic and heterologous antigens. These results suggest that the suppression of both DC costimulatory activity and functional T cell responses reduces the immunity against *Plasmodium* (Millington et al., 2007; Hisaeda et al., 2008; Yap et al., 2019). Supporting this premise, TLR9(-/-) mice infected with *P. yoelii* were somewhat resistant to fatal infection through limited activation of Tregs that impaired effector T cell development (Hisaeda et al., 2008). Additionally, DCs of humans inflicted with malaria mediated strong immunosuppression through the induction of Indoleamine 2,3-Dioxygenase 1(IDO1) and Lymphocyte Activation Gene 3 (LAG3), which attenuates inflammatory response by decreasing class II antigen presentation (Vallejo et al., 2018). Furthermore, *P. vivax* downregulates three G-protein coupled receptors, CXCR1, CXCR2, and CSF3R, that induces the depletion of neutrophil populations. While the immunosuppressive signaling has been reported during infection with different *Plasmodium* spp., such a response to *P. falciparum* was significantly more pronounced (Vallejo et al., 2018). CD40 responses to merozoites and pro-inflammatory cytokine production by DCs were impaired in the presence of freshly isolated *P. falciparum* infected RBCs (Yap et al., 2019). Similarly, after *P. berghei* ANKA infection clearance, robust immunological memory against malaria parasites was reported, albeit the splenic DCs had significantly decreased the capacity of cytokine production as well as lower surface expression of MHC Class II molecules (Adachi and Tamura, 2020).

Compared to replication-deficient parasites, immunization with replication-competent parasites confers better protection and also induces an IFN-I response, but whether this response has beneficial or adverse effects on vaccine-induced adaptive immunity is not known. When mice deficient in IFN-I signaling were immunized with replication-competent sporozoites of rodent parasite *P. yoelii*, they demonstrated superior protection against infection (Minkah et al., 2019). Strong CD8+ T cell memory response development (also in liver) showed correlation with this protection. In a complementary experiment, the adoptive transfer of memory CD8+ T cells recovered from the livers of IFN-I signaling-deficient immunized mice offered increased protection specifically against liver stage parasites. Overall, these results demonstrate that hepatic CD8+ T cell memory development is impaired by IFN-I signaling stimulated by the liver stage parasites. On the other hand, innate, cellular, and humoral immune responses conferred by IFNγ and Th1 type responses were documented to play critical roles in controlling blood-stage malarial disease. Inflammatory responses help the resolution of infection. In contrast, anti-inflammatory immunomodulators, TGFβ, and IL-10 were considered important in reducing inflammation and pathology during malaria (Drewry and Harty, 2020). The specific mechanisms and pathway involved in which TGFβ helps in offering protection against severity of malaria remain to be investigated.

During the murine modeling of severe malaria, conventional DCs (cDCs) lose the ability to phagocytose and present parasitic antigens when the burden of pathogen increases resulting in the suppression of CD4+ T cell responses. IFN-I signaling adversely affects cDC function, such that they are unable to fully prime Th1 cells that produce IFNγ cytokine. IFN-I signaling was shown to modulate all subsets of splenic cDCs; however, CD8-lacking cDCs were found to be most susceptible such that type I IFNs reduced their phagocytic and Th1 responses. In response to *P. berghei* infection, IFN-I signaling of cDCs resulted in rapid and substantial IFNα production, which also suppressed the Th1 response. Overall, results from Haque and coworkers suggest that the elimination of IFN-I signaling in CD8-negative splenic cDCs results in increased Th1 responses against *Plasmodium* and also against other pathogens that induce IFN-I signal (Haque et al., 2014).

Adaptive: Humoral Immune Response

Pre-erythrocytic stage antigens are good targets for the elimination of *Plasmodium* species by vaccines because the parasitic population is small, and the chance of generation of escape mutants is low. Several targets for antibodies include sporozoites circumsporozoite protein (CSP), LSA1, TRAP, and Apical Membrane Antigen-1 (AMA-1) (Marsh and Kinyanjui, 2006). The AMA-1 molecule is involved in the invasion of RBCs and has also been described as an excellent vaccine candidate. Interestingly, antibody production against the extracellular domain of *B. divergens* AMA-1 is weak and produced late, usually between 1 and 5 months of parasites post-inoculation even though both IgG1 and IgG2 were induced (Moreau et al., 2015). Human IgG antibodies to *P. falciparum* antigens PfEMP1 and RIFIN are sufficient to activate antibody-dependent cellular cytotoxicity by primary human NK cells, which highly selectively lyse iRBCs and inhibit parasite growth (Arora et al., 2018). However, mouse IgG against *P. yoelii* and *P. chabaudi chabaudi* bound poorly to the surface of parasitized RBCs and did not affect their clearance, despite the continuation of inflammation, albeit antibodies prevented the infection of the next RBC generation. Compared to other parasitic infections, while a direct role for IgA in malaria infection has not been investigated, IgG, IgE, and IgM were shown to contribute to the adverse pathology in the rodent model. Malaria parasites induce the development of specific IgA secreting B cells among individuals who had multiple episodes of infection (Deore et al., 2019). Optimal function of *Plasmodium*-specific IgG antibody, which strongly bound to surface molecules of merozoites released from the erythrocyte, needed contributions of splenic macrophages and dendritic cells for parasitic elimination (Akter et al., 2019). CD4+ T cell subtypes were reported to be associated with immune functions and production of different antibody isotypes (Oakley et al., 2014). T-bet can suppress *Plasmodium*-induced apoptosis or stimulate the proliferation of T cells and thus may be responsible for T-bet-dependent antibody isotype switching and lower parasite burden. Interestingly, during *P. vivax* infection, children develop higher levels of IgM but not IgG antibodies, while IgG3 are more prevalent in adults (Oyong et al., 2019).

Antibody participation is not essential for offering cross-protection against other hemoparasites. Infection of mice with

B. microti could protect mice against a follow-up fatal infection by *B. rodhaini* (Efstratiou et al., 2020) by reducing parasitemia levels. Surprisingly, significant reduction in the level of antibodies was observed in the protected mice, and levels of cytokines including IFNγ, IL-2, IL-8, IL-10, and IL-12, and of nitric oxide after infection with *B. rodhaini* also diminished. Mice immunized with dead *B. microti* were not protected from *B. rodhaini* infection, although high antibody responses were induced indicating a minor role played by antibodies for protection against death. Inoculation with live *B. microti* also protected against subsequent fatal malarial infections in mice and primates. Unexpectedly, immunization with dead *B. microti* led to lethal *P. chabaudi* infection despite the induction of high antibody responses, which means that other products of parasite metabolism, not just the antigens, play an important role in the development of generalized immune response against these two apicomplexans. Notably, cross-protection was also observed in mice lacking functional B and T lymphocytes. On examination of the other innate immune effector cells, mice depleted of NK cells showing chronic *B. microti* infection were also protected from *P. chabaudi* infection (Efstratiou et al., 2020). In contrast, *in vivo* depletion of macrophages in mice made them susceptible to *P. chabaudi*. These results show that the cross-protection offered by one protozoan, *B. microti*, against another, *P. chabaudi*, is dependent on innate immune response and appears to rely mainly upon the macrophage function.

The molecules of *Plasmodium* driving humoral immunity include CD4+ T cells, B cells, and IL-21 together with the T cell costimulator. In *P. chabaudi chabaudi* AS infection, early IL-6 stimulation resulted in *Plasmodium*-specific IgM but not IgG production. IL-6, rather than germinal center B-cell differentiation, induced the splenic CD138+ plasmablast development. IL-6 also induced the T cell costimulator in CD4+ T cells causing their localization adjacent to splenic B cells. In addition, IL-6 promoted the control of parasitemia and induced IgM and IgG production, T cell costimulator expression by Tfh cells, and germinal center B-cell development. This cytokine also promoted the stimulation of CD4+ T cell and B cell responses during the erythrocytic cycle of *Plasmodium* that facilitated the production of protozoan-specific antibodies (Sebina et al., 2017).

To evade the host immune responses, *P. vivax* disrupts the function of the B cell subsets. Some antibodies produced during infection have the potential to block *Plasmodium* invasion as well as its dissemination into the host. The prevalence of antibodies to *P. vivax* merozoite surface protein-8 (PvMSP8) was reported to be high during and after infection. The anti-PvMSP8 antibody responses could be detected for 4 years in some patients who had recovered from an infection suggesting that persistence of long-term humoral immune response occurs against PvMSP8 (Kochayoo et al., 2019); however, no correlation of this response was observed with the presence of titer of circulating antibodies.

IL-10 is a pleiotropic cytokine expressed during malaria and is essential for anti-*Plasmodium* humoral immunity. Germinal center B cell reactions, isotype-switched antibody responses, parasite control, and host survival require B cell-intrinsic IL-10 signaling. IL-10 also indirectly supported humoral immunity by suppressing excessive IFNγ, which induces T-bet expression in B cells. B cell-produced IL-10 increased, whereas IFNγ and T-bet from B cells suppressed germinal center B cell responses and anti-*Plasmodium* humoral immunity (Guthmiller et al., 2017). *Plasmodium* infection-induced IFN-I limited T follicular helper accumulation and constrained malaria-specific humoral immunity. CD4 T cell associated IFN-I signal stimulated T-bet and Blimp-1 expression and induced T regulatory 1 responses. Secreted IL-10 and IFNγ cytokines of T regulatory 1 cells together restricted the accumulation of T follicular helper cells, restricted specific antibody production, and allowed the persistence of parasites. The authors suggested that IFN-I-mediated Blimp-1 induction that caused the expansion of T regulatory 1 cells is a systemic, inflammatory response to viral and parasitic infections and accompany humoral immune response suppression (Zander et al., 2016).

The effects of *P. falciparum* infection on peripheral B-cell subsets have been investigated, but limited information is available for *P. vivax*. In a prospective study with malaria patients to determine peripheral B cell profiles, the authors reported a temporary increase in atypical memory B cells and B cell-activating factor (BAFF)-independent percentage of total and activated immature B cells in malaria patients. An increase in TLR4 expression occurred in naive B cells from malaria patients. During acute infection, total IgM levels remained steady; however, a significant increase in these antibodies was observed at the recovery stage. Persistence of serum IgM antibodies specific to parasite proteins was observed during the recovery of patients (Patgaonkar et al., 2018).

B. microti infection resulted in high levels of IL-10 production due to increased frequency of IL-10-producing regulatory B cell and T cell presence. In contrast, the absence of B cells in B cell-deficient mice demonstrated increased susceptibility of these mice to *B. microti* infection (Jeong et al., 2012). The ability of immunized rats to resist challenge with *B. divergens* was suggested to be splenic independent (Ben Musa and Dawoud, 2004). The uptake of infected erythrocytes by the liver was suggested not to happen in immune rats. Rather the clearing of parasitemia in rats could depend upon antibody inhibition of merozoite invasion. Histological studies on livers collected from immune rats showed that lymphocytes are accumulated in the liver, and these consisted of B and T cells. Liver leukocytes might therefore be very important in the development of acquired immunity to *B. divergens* in splenectomized rats.

Immune Evasion and Immunosuppression

Human complement is the first line of defense against invading pathogens, including the *Plasmodium* and *Babesia* parasites. The complement represents a particular threat for the clinically relevant blood stages of the parasites such that this protozoan has evolved to overcome its effects. To evade complement-mediated destruction, the parasites bind host factor H (FH) to FH-related protein 1 (FHR-1) or the specific receptors on their surface, thus competing host cells for binding, and thus resulting in the prevention of complement-mediated opsonophagocytosis.

These proteins accumulate differentially on the surface of intraerythrocytic schizonts versus free merozoites. The purpose of two proteins (FHR-1 and specific receptor) displaying the same activity is poorly understood as the mechanisms involving both proteins target the same FH-mediated human immune response and facilitate similar evasion of complement-mediated killing (Reiss et al., 2018).

Erythrocytic rosetting is a mechanism involved in avoiding phagocytosis-mediated elimination of iRBCs. The surface of *Plasmodium*-infected RBCs is decorated with parasitic proteins, which are targeted by monocytes. Some of the parasitic proteins displayed on the iRBCs make them stickier. Type I rosetting is accomplished by direct interaction of ligands on iRBC with uninfected RBC receptors. Thus, the infected erythrocytes get surrounded by a protective cage of uninfected RBCs, which results in a formation called "rosettes." Insulin like growth factor-binding protein 7 (IGFBP7), a protein secreted by monocytes in response to parasitic infection, stimulates rosette formation by *P. falciparum* and *P. vivax* infected erythrocytes. IGFBP7-mediated type II rosette formation was observed to be fast albeit a reversible process (Lee et al., 2020) and required von Willebrand factor and thrombospondin-1 serum factors. The interaction of these factors with IGFBP7 promotes rosette formation by the iRBC. Engulfment of iRBC by host phagocytes was reported to be hampered by the IGFBP7-induced type II rosette formation.

Although infection by *B. microti* is usually asymptomatic in immunocompetent young individual, persons aged >40 years often experience serious manifestations, and elderly exhibit life-threatening disease (Krause et al., 2003; Akoolo et al., 2017) because persistent parasitemia increases with the age of individuals and often their immune status is somewhat compromised. Since susceptible mice exhibit many symptoms similar to those observed in humans, they serve as a model system to investigate pathogenesis, immune response, and babesiosis disease. BALB/c and C57BL/6 mice were found to be resistant, regardless of age, which indicates that the genotype of mice determines the resistance to *B. microti* (Vannier et al., 2004). Unlike immunocompetent mice, SCID mice, which retain an innate immune system but lack the lymphocytes needed for adaptive immunity, were shown to develop high and persistent parasitemia. Of importance, mice also showed age-associated loss of protection such that when spleen cells were transferred from older immunocompetent mouse strain (18 months old), cells from BALB/c mice, but not DBA mice, were able to control persistent parasitemia in SCID mice. Thus, the age (as observed in humans) and genetic make-up of the donor of splenic cells determined the adequate building up of the protective immune response in young recipient SCID mice, and hence, cells from older mice adversely affected the control of persistent parasitemia in immunocompromised mice (Vannier et al., 2004).

During their asexual stages in vertebrate hosts, *Plasmodium* parasites mainly hide in the hematopoietic colonies of the bone marrow (Venugopal et al., 2020). For infection, *P. malariae* shows preference for mature erythrocytes and *P. vivax* to immature RBCs. *Babesia* species also prefer the invasion of the mature RBCs (Borggraefe et al., 2006). Sequestration of *P. falciparum*-infected RBCs by cytoadherence helps in immune evasion and prevents their clearance by spleen. Different variants of the *P. falciparum* protein PfEMP1 that are displayed on iRBCs facilitate their binding to various receptors including CD36 on endothelial cells causing the sequestration of parasites in different organs. Furthermore, host endothelial receptors ICAM1 and endothelial protein C receptor (EPCR) are used for sequestration in the brain and cause cerebral malaria (Smith et al., 2000), whereas chondroitin sulfate A binding by some variants (Var2CsA) facilitates placenta binding (Fried and Duffy, 1996). This sequestration allows parasites to hide in the brain, lungs, liver, intestine, dermal tissues, and placenta, thereby avoiding splenic clearance of iRBCs. Adherence-mediated sequestration could also cause persistence of infection with potential for fatal consequences due to cerebral malaria and as a result of single and multiple organ failure of kidneys, liver and lungs. Cerebral malaria has been reported to occur due to iRBC sequestration within the brain blood vessels and is exacerbated by inflammation caused by the stimulation of the effector cells including T lymphocytes and the production of pro-inflammatory cytokines in the host. Sequestration of *Plasmodium* spp. by adherence to chondroitin sulfate 4 present on placental cells could result in congenital malaria (Fried and Duffy, 1996; Nunes and Scherf, 2007; Fried and Duffy, 2017; Fried et al., 2017).

The suppression of the host immune system by parasites plays critical roles on the persistence of infection. During acute malaria infection with both *P. falciparum* and *P. vivax*, significant reduction in lymphocyte counts was observed in the peripheral blood in Ethiopia [**Table 1**; (Kassa et al., 2006)]. This diminished immune status could make a patient susceptible to other infections that may occur simultaneously with malaria resulting in serious consequences. In fact, coinfection of mice with *P. berghei* and relapsing fever spirochete *B. duttonii* led to decreased malaria parasite burden but enhanced levels of relapsing fever spirochetes and an increased death rate (Lundqvist et al., 2010). Since C3H mice are susceptible to *B. microti* and show symptoms like parasitemia, anemia, splenomegaly, and hepatomegaly, suppressive impact on splenic lymphocytes (**Table 1**) could be extrapolated to also occur during infection of humans (Krause et al., 1996). In fact, coinfection of *B. microti* with Lyme spirochete, *Borrelia burgdorferi*, in C3H mice resulted in a significant increase in the burden of spirochetes in different organs and resulted in the persistence of inflammatory Lyme disease manifestations (Djokic et al., 2019) similar to that observed during *Plasmodium–Borrelia* coinfections. **Table 1** shows that *B. microti* subverted the splenic immune response, and a marked decrease in splenic B and T cells also resulted in the reduction of the levels of antibodies and hence diminished functional humoral immunity. Furthermore, increased *B. burgdorferi* burden in organs and severe inflammatory Lyme disease manifestations resulted due to immunosuppression by *B. microti* in coinfected mice showed an association with enhanced Lyme disease manifestations (Djokic et al., 2019). A similar response was also reported with

TABLE 1 | Suppression of adaptive immune response during *Plasmodium* and *Babesia* infection.

Cell Type	Absolute count/μl of blood (Mean ± SD) in humans[a]		
	Control (N=46)	***P. vivax* (N=69)**	***P. falciparum* (N=7)**
Lymphocytes	1,815 ± 729	1,078 ± 583	940 ± 472
T cells (CD3+)	1,379 ± 607	819 ± 404	701 ± 378
CD4+ cells	691 ± 234	455 ± 240	387 ± 206
CD8+ cells	643 ± 482	336 ± 200	297 ± 203
B cells (CD19+)	192 ± 98	86 ± 56 (N=43)	61 ± 39 (N=26)
	Mean splenocytes count in young C3H mice infected with *B. microti*[b]		
	Control	***B. microti* (acute phase)**	***B. microti* (after parasitemia resolution)**
T cells (CD3+)	9,220/8,710	14,250 ± 670	8,590 ± 1,160
CD4+ cells	4,900/4,900	4,920 ± 300	1,880 ± 180
CD8+ cells	3,900/3,200	1,139 ± 140	480 ± 280
B cells (CD19+)	18,150/19,610	27,910 ± 1,070	12,590 ± 2,680

P. falciparum shows severe disease compared to P. vivax and has more pronounced effect on adaptive immune response of humans during infection.
[a]*(Kassa et al., 2006).*
[b]*(Djokic et al., 2019).*

respect to *Mycobacterium tuberculosis* coinfection with rodent malaria parasite *P. yoeli* (Blank et al., 2016).

DISEASE AND SYMPTOMS

In addition to HIV/AIDS and tuberculosis, malaria is considered as one of the three major fatal diseases in the world (Medaglini and Hoeveler, 2003). Therefore, WHO Global Malaria Programme, with active participation of NIH and Gates Foundation, provides technical support to malaria-endemic countries to attain the goals of reducing malaria cases and mortality by 90% in 2030. Malaria is primarily a tropical disease, and symptoms associated with the erythrocytic cycle of *Plasmodium* spp. usually occur during rainy season when mosquitoes are active. A symptomatic malaria patient could exhibit cough, rapid heart rate and breathing, fatigue, and overall malaise in addition to usual fever, chills (despite high surrounding temperature), headache, etc. Persistence of infection during asymptomatic malaria was reported to occur in Mali where only transmission season shows association with the symptomatic malaria (Andrade et al., 2020). During the dry season, PCR positive individuals showed subclinical *P. falciparum* infection that was more pronounced in older children and young adults than young children. Protozoa isolated during the dry season were transcriptionally and metabolically distinguishable from those recovered from persons with febrile malaria during the rainy, active transmission season, and the host immune cells and inflammation markers in these asymptomatic individuals were similar to those in uninfected controls. The parasites during the dry season also showed poor cytoadherence allowing increased splenic clearance (Andrade et al., 2020).

Cerebral malaria is the most severe complication of human infection with *P. falciparum*, but the mechanisms involved are still not fully understood. Pro-inflammatory immune responses are required for the control of blood-stage malaria infection but are also implicated in the pathogenesis of severe cerebral malaria. A fine balance between pro- and anti-inflammatory immune responses is required for parasite clearance without the induction of host pathology. The most accepted experimental model to study human cerebral malaria is *P. berghei* ANKA (PbANKA) strain infection in C57BL/6 mice that leads to the development of a complex neurological syndrome, which shares many characteristics with the human disease. In a study by Blank and coworkers, *M. tuberculosis* coinfection did not change the clinical trajectory of PbANKA-induced experimental cerebral malaria (Blank et al., 2016). In fact, the immunological environments in spleen and brain were similar in singly infected and coinfected mice. Overall levels of cytokine production and T cell responses in coinfected mice were also similar to PbANKA infected animals when inoculated alone. Another rodent parasite, *P. yoelii* coinfection with *M. tuberculosis*, resulted in a slight increase in *M. tuberculosis* burden detected by measuring lung CFU in coinfected mice and exacerbation of tuberculosis manifestation that also coincided with elevated levels of both pro-inflammatory (levels of IFNγ, IL-6, TNFα) and anti-inflammatory (IL-10) responses. Enhanced T cell responses in coinfected mice likely contributed to increased cytokine production (Blank et al., 2016). Malaria parasite immunosuppressive effects may also play a role on enhancing the severity of *M. tuberculosis*-induced pathology in mice, similar to that observed during *B. microti–B. burgdorferi* and *P. berghei–B. duttonii* coinfections.

Pregnant women and children below 5 years of age remain most susceptible to malaria because *Plasmodium* is capable of vertical transplacental transmission from mother to child. As a result, another devastating consequence of *P. falciparum* infection in pregnant women is congenital malaria that remains a major global problem especially in the endemic regions (Bilal et al., 2020; Danwang et al., 2020). Congenital malaria is defined as the presence of intraerythrocytic malaria parasites in the cord blood and/or the peripheral blood of an infant within the first week of birth, independent of display of the clinical symptoms (Omer et al., 2020). Infected newborns often show nonspecific, sepsis-like clinical manifestations in which early treatment can result in diminished risk of complicated malaria. Based upon the meta-analysis of 1,961 studies, the

congenital malaria level was reported to be ~40%, and difference between prevalence of cases in continent of Africa and outside Africa was not statistically significant (Danwang et al., 2020). In some newborns, clinical malaria was observed within 7 days of birth (40/1,000); however, a few showed disease until 28 days of birth (10/1,000). Relatively lower prevalence of malaria in newborns was attributed to the presence of high concentration of fetal hemoglobin in neonatal red blood cell that provided unfavorable conditions for *Plasmodium* replication and growth, with transfer of maternal immunity also playing a role in protection. Placental *Plasmodium* infections were found to show significant association with the risk of perinatal morbidity and mortality such as preterm birth, low birth weight, and intrauterine fetal loss (Osungbade and Oladunjoye, 2012). The prevalence rate of congenital malaria is usually significantly higher in non-endemic regions (Quinn et al., 1982; Bilal et al., 2020). Using *P. falciparum* infected placental samples, Duffy et al. described that iRBCs obtained from placenta bound to purified chondroitin sulfate A (Fried and Duffy, 1996) and also that placental malaria was often associated with the expression of the Var2CsA variant of PfEMP1, although other *var* genes were also transcribed at the same time (Duffy et al., 2006). In fact, the design of vaccine based upon fragments of Var2CsA has been attempted to inhibit placental colonization by *Plasmodium* and thus prevent congenital malaria (Fried and Duffy, 2015)

The severity of babesiosis ranges from mild, self-limited, febrile illness accompanied by nonspecific subjective symptoms to even life-threatening infection in immunocompromised individuals that is associated with severe hemolytic anemia, disseminated intravascular coagulation leading to acute respiratory distress syndrome, and even renal or hepatic failure. Hepatomegaly and splenomegaly are often observed in babesiosis patients, and a life-threatening complication of severe *B. microti* infection is spontaneous splenic rupture (Froberg et al., 2008; El Khoury et al., 2011; Farber et al., 2015; Dumic et al., 2018; Li et al., 2018; Patel et al., 2019) similar to fatal outcomes reported for malaria (Imbert et al., 2009; Chang et al., 2018; Elizalde-Torrent et al., 2018). Depending on the stage and severity of babesiosis, the marginal zone of spleen is eliminated, and white and red pulp regions merge. Since the red pulp region macrophages need to remove increased numbers of dead and infected RBCs, enlargement of the red pulp region is often observed. The elasticity of the splenic membrane plays a key role in patient survival as sometimes the organ can be up to five times its normal size, as is the case during malaria. Recently, Kho et al. described the accumulation of biomass due to medium to high $CD71^+$ expressing reticulocytes as well as non-phagocytosed parasites, thus providing another shelter for the parasite's survival and replication, contributing to splenomegaly (Kho et al., 2021). We also demonstrated the presence of free parasites in the spleens during the murine model of *B. microti* infection (Djokic et al., 2018a); however, neither RBC aggregations nor biomass accumulation was observed (Srivastava et al., 2015). Human architecture details for spleen involvement are scarce for babesiosis such that it is difficult to draw any conclusions. Transfusion transmitted babesiosis in already immunocompromised recipients with a variety of underlying medical conditions results in complicated disease such that death can occur in all age group patients (Herwaldt et al., 2011; Fang and McCullough, 2016; Gray and Herwaldt, 2019). Transmission of babesiosis can also occur through infected solid organ transplantation (Herwaldt et al., 2011; Gray and Herwaldt, 2019). Overall, severe babesiosis is more of a health problem in elderly, splenectomized, and immunocompromised individuals, while *Plasmodium* species, particularly *P. falciparum*, can cause brain hemorrhage and death even in immunocompetent young persons.

DISCUSSION

Plasmodium and *Babesia* are two parasites that belong to the class Apicomplexa and are erythrocyte-infecting protozoa. The life cycles of these two protozoa overlap greatly despite their difference as modes of transmission. *Plasmodium* spp. are transmitted by adult infected *Anopheles* female mosquitoes during their quick blood meals, while *Babesia*-transmitting ticks take days to imbibe blood during both the acquisition of this pathogen from one vertebrate host and during its transmission to another. Adult *Anopheles* female mosquitoes are able to acquire gametocytes from hosts, which then undergo sexual cycle, and then these mosquitoes transmit sporozoites during the next blood meal. In contrast, different developmental stages of hard ticks are responsible for acquisition and transmission of *Babesia* species because each stage takes blood meal only once. Thus, if the larvae of ticks acquire *Babesia* gametocytes during blood meal from the infected host, after sexual cycle completion, only nymphs that develop after molting will be able to transmit sporozoites to the next host during their blood meal. The sporozoites infection of hepatocytes that occurs during the *Plasmodium* asexual cycle in the host has not been reported to occur during the *Babesia* infection cycle. Since donated blood is not widely tested for *Babesia* presence, transfusion-transmitted babesiosis, and not malaria, remains a significant healthcare problem. Both parasites can also exhibit transplacental transmission from a pregnant mother to her child. The major differences in their asexual cycle are that *Plasmodium* species replicate in the PV inside the host cells surrounded by PVM in which PTEX insertion allows the secretion and uptake of molecules (Ho et al., 2018). This parasite also undergoes schizogony to produce a large number (~6-36/iRBC) of merozoites (Antinori et al., 2012). In contrast, *Babesia* species multiplies within the host erythrocyte cytoplasm, undergo only one to three replication cycles, and lack schizogony. Unlike *Plasmodium* species, *Babesia* is not susceptible to heme produced as a result of the degradation of hemoglobin during infection.

Innate immune response during the early stages of infection by malaria parasites in the liver is mediated by NK and NKT cells. At the same time, *Plasmodium* RNA is suggested to cause pro-inflammatory IFN-I stimulation through an interferon-α/β

receptor-dependent manner that acts together with IFN-γ production (Liehl et al., 2014). This partnership results in phagocytosis-mediated killing by macrophages. The role of IFN-I is not explored yet for babesiosis likely because the liver stage is absent for this pathogen. Depletion of NK cells in mice did not impair the clearance of *B. microti* parasitemia, while macrophage depletion made mice susceptible to *B. rodhaini*, emphasizing the role of these phagocytes in the hemoparasites (Li et al., 2012). DCs produce pro-inflammatory cytokines and play a crucial role during the immunity and pathogenesis of the malaria parasite. They provide a link between innate and adaptive immune responses. For example, IL-12 produced by DCs activates NK cells to induce the production of IFNγ, which primes macrophages and neutrophils to enhance phagocytosis (Walsh and Mills, 2013; King and Lamb, 2015). Macrophages both act as antigen-presenting cells to induce adaptive immune response and promote Th1 and effector T cell responses. During the erythrocytic cycle, the host macrophages play a critical role in the resolution of parasitemia during both malaria and babesiosis, and together with cellular immunity also offer cross-protection against other related hemoparasites. In fact, *B. microti* in the susceptible mouse model of infection showed the importance of macrophages in the resolution of parasitemia (Djokic et al., 2018a; Djokic et al., 2018b; Djokic et al., 2019).

Both cellular and humoral immune responses are significantly induced during *Babesia* and *Plasmodium* infection. Antibodies block *Plasmodium* merozoite invasion of erythrocytes; however, they do not appear to significantly promote opsonophagocytosis of iRBCs of either *Babesia* or *Plasmodium* (Moreau et al., 2015; Arora et al., 2018; Akter et al., 2019; Kochayoo et al., 2019; Oyong et al., 2019; Efstratiou et al., 2020). Therefore, humoral immunity appears to play a minor role in resolving the parasitemia of these parasites. CD8+ cells are involved in the clearance of *Plasmodium* in hepatocytes by producing NO and IFNγ and also contributing immune cells during the *P. vivax* erythrocytic cycle (Doolan and Martinez-Alier, 2006; Chakravarty et al., 2008; Kelemen et al., 2019). CD4+ cells play the traditional helper cells role for cellular and humoral immune responses. Th1 response plays a critical role in the clearance of both protozoa and the resolution of both malaria and babesiosis. Inflammatory CD4+ T cells offer protection against malaria by producing IFNγ and TNFα such that *P. falciparum* infection or its replication is inhibited, thus preventing severe malaria (Boyle et al., 2015). Interestingly, this phenomenon is more prominent in adults than children (Boyle et al., 2017). On the other hand, IL-10 producing CD4+ cells show a correlation with parasite burden and likely regulate immune response such that immunopathology is restricted (Drewry and Harty, 2020). Similarly, pronounced inflammatory response to *B. duncani* WA1 strain infection results in mouse fatality due to excessive inflammatory cytokine, such as TNFα production (Hemmer et al., 2000), while IL-10 producing CD4+ cells play effector roles during *B. microti* infection in mice that show high parasitemia and anemia, but infection does not result in death (Djokic et al., 2018b; Djokic et al., 2019). The crucial roles of CD4+ cells during *B. microti* infection are also demonstrated experimentally since treatment of mice with anti-CD4 MAbs diminished protection against challenge infection. In addition, CD4 cell deficient mice failed to completely clear parasitemia, and the transfer of CD4 depleted spleen cells to naïve mice challenged with *B. microti* failed to resolve parasitemia efficiently (Igarashi et al., 1999; Skariah et al., 2017).

Both immunosuppression and immune evasion occur during infection with *Babesia*, and more prominently during *Plasmodium* infections (Fried and Duffy, 1996; Smith et al., 2000; Kassa et al., 2006; Nunes and Scherf, 2007; Fried and Duffy, 2017; Fried et al., 2017; Reiss et al., 2018; Djokic et al., 2019; Lee et al., 2020). Suppression of adaptive immune response by both of these parasites does not seem to affect their own clearance; however, it exacerbates diseases caused by bacteria that may coinfect the hosts with these protozoa. Both parasites result in splenomegaly and even hepatomegaly. Cytoadherence-mediated sequestration of iRBCs in different organs during malaria infection is a hallmark of immune evasion demonstrated by *P. falciparum*, while latent hypnozoites forms of *P. vivax* can survive hiding in the liver of patients for a long time and can result in the relapse of malaria. Cerebral malaria is the most serious consequence of *P. falciparum* infection and sequestration, while placental sequestration results in congenital malaria. Sequestration of *Babesia* species in organs has not been carefully investigated until now. Although the general symptoms of babesiosis are similar to malaria and congenital transmission has also been reported (Wormser et al., 2015; Saetre et al., 2018), the most serious disease-causing mortality due to *Babesia* infection occurs in immunocompromised, splenectomized, and elderly patients due to multi-organ failure. While severe malaria occurs even in immunocompetent humans of different ages, healthy individuals usually remain asymptomatic after *Babesia* infection.

The summary of general immune responses extracted from studies on infection with different species of *Plasmodium* and *Babesia* individually is provided in **Figure 3**. This cartoon figure depicts the major mechanisms reported for clearance of parasites, excessive inflammation mediated killing of the host(s), and immunosuppression relative to uninfected individuals or animal controls, protozoan sequestration, and immune evasion that facilitate their long-term survival in their respective hosts. Overall, this review summarizes the similarities and differences between *Plasmodium* and *Babesia* species infection cycles, the immune responses they generate, the immune evasion mechanisms employed by *P. falciparum* and *P. vivax*, and the immunosuppression caused by these two *Plasmodium* species as well as by *B. microti*. The impact of suppression of primarily adaptive immunity by these parasites on coinfecting bacterial pathogens is also summarized. Generally, the immunosuppression caused by these parasites is only mild; however, the attenuation of adaptive immunity exacerbates disease manifestations by coinfecting bacterial pathogens, which become more persistent and result in more severe diseases (Nordstrand et al., 2007; Lundqvist et al., 2010; Blank et al., 2016a; Blank et al., 2016b; Djokic et al., 2019) irrespective of the pathogenic species involved. This relatively poorly examined healthcare problem will need more attention in the future because it could result in more fit pathogen evolution due

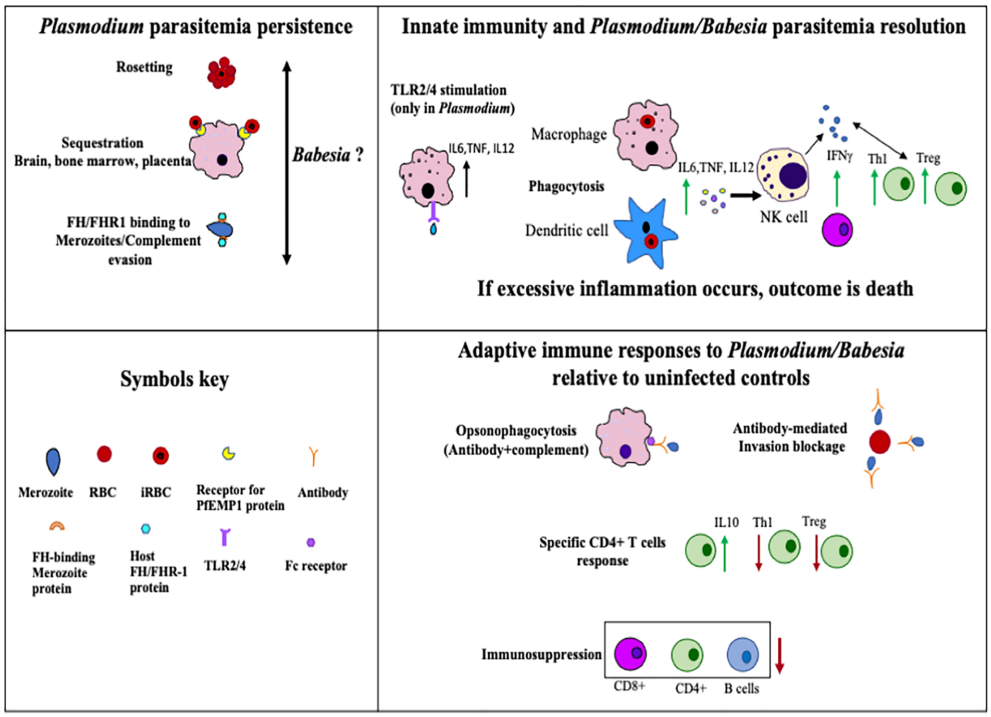

FIGURE 3 | Summary of host immune responses stimulated during *Plasmodium* and *Babesia* species infection that help in the clearance of parasites, cause death of the host due to excessive inflammation, or allow protozoan survival in the host for long periods of time. Uninfected individuals or animals were included as controls for comparison in various previous studies that formed the foundation of this figure.

to the selection of the bacterial mutants that could accumulate during coinfections.

AUTHOR CONTRIBUTIONS

VD and NP wrote the initial draft of this review. SR generated data for **Figure 2**, and all three authors edited and read the final version. NP also prepared figures and table. All authors contributed to the article and approved the submitted version.

FUNDING

This publication is supported by the National Institutes of Health (R01 AI137425) grant to NP.

REFERENCES

Adachi, R., and Tamura, T. (2020). Plasmodium Infection Cure Cycles Induce Modulation of Conventional Dendritic Cells. *Microbiol. Immunol.* 64, 377–386. doi: 10.1111/1348-0421.12783

Akoolo, L., Djokic, V., Rocha, S. C., and Parveen, N. (2021). Pathogenesis of Borrelia Burgdorferi and Babesia Microti in TLR4-Competent and TLR4-Dysfunctional C3H Mice. *Cell Microbiol.* e13350. doi: 10.1111/cmi.13350

Akoolo, L., Schlachter, S., Khan, R., Alter, L., Rojtman, A. D., Gedroic, K., et al. (2017). A Novel Quantitative PCR Detects *Babesia* Infection in Patients Not Identified by Currently Available Non-Nucleic Acid Amplification Tests. *BMC Microbiol.* 17, 16. doi: 10.1186/s12866-017-0929-2

Akter, J., Khoury, D. S., Aogo, R., Lansink, L. I. M., SheelaNair, A., Thomas, B. S., et al. (2019). Plasmodium-Specific Antibodies Block *In Vivo* Parasite Growth Without Clearing Infected Red Blood Cells. *PloS Pathog.* 15, e1007599. doi: 10.1371/journal.ppat.1007599

Alam, M. M., Solyakov, L., Bottrill, A. R., Flueck, C., Siddiqui, F. A., Singh, S., et al. (2015). Phosphoproteomics Reveals Malaria Parasite Protein Kinase G as a Signalling Hub Regulating Egress and Invasion. *Nat. Commun.* 6, 7285. doi: 10.1038/ncomms8285

Allred, D. R. (1995). Immune Evasion by *Babesia Bovis* and *Plasmodium Falciparum*: Cliff-Dwellers of the Parasite World. *Parasitol. Today* 11, 100–105. doi: 10.1016/0169-4758(95)80166-9

Andrade, C. M., Fleckenstein, H., Thomson-Luque, R., Doumbo, S., Lima, N. F., Anderson, C., et al. (2020). Increased Circulation Time of *Plasmodium Falciparum* Underlies Persistent Asymptomatic Infection in the Dry Season. *Nat. Med.* 26, 1929–1940. doi: 10.1038/s41591-020-1084-0

Antinori, S., Galimberti, L., Milazzo, L., and Corbellino, M. (2012). Biology of Human Malaria Plasmodia Including Plasmodium Knowlesi. *Mediterr. J. Hematol. Infect. Dis.* 4, e2012013. doi: 10.4084/mjhid.2012.013

Arora, G., Hart, G. T., Manzella-Lapeira, J., Doritchamou, J. Y., Narum, D. L., Thomas, L. M., et al. (2018). NK Cells Inhibit *Plasmodium Falciparum* Growth in Red Blood Cells *via* Antibody-Dependent Cellular Cytotoxicity. *Elife* 7, e36806. doi: 10.7554/eLife.36806

Bastos, R. G., Johnson, W. C., Brown, W. C., and Goff, W. L. (2007). Differential Response of Splenic Monocytes and DC From Cattle to Microbial Stimulation

With *Mycobacterium Bovis* BCG and *Babesia Bovis* Merozoites. *Vet. Immunol. Immunopathol.* 115, 334–345. doi: 10.1016/j.vetimm.2006.11.001

Bastos, R. G., Johnson, W. C., Mwangi, W., Brown, W. C., and Goff, W. L. (2008). Bovine NK Cells Acquire Cytotoxic Activity and Produce IFN-Gamma After Stimulation by *Mycobacterium Bovis* BCG- or *Babesia Bovis*-Exposed Splenic Dendritic Cells. *Vet. Immunol. Immunopathol.* 124, 302–312. doi: 10.1016/j.vetimm.2008.04.004

Batchelder, J. M., Burns, J. M.Jr., Cigel, F. K., Lieberg, H., Manning, D. D., Pepper, B. J., et al. (2003). *Plasmodium Chabaudi Adami:* Interferon-Gamma But Not IL-2 is Essential for the Expression of Cell-Mediated Immunity Against Blood-Stage Parasites in Mice. *Exp. Parasitol.* 105, 159–166. doi: 10.1016/j.exppara.2003.12.003

Ben Musa, N., and Dawoud, H. A. (2004). Immunity of *Babesia Divergens* in the Rat. Histology of the Infected Liver and its Possible Role in Removing PRBC's. *J. Egypt. Soc. Parasitol.* 34, 791–806.

Bhalla, K., Chugh, M., Mehrotra, S., Rathore, S., Tousif, S., Prakash Dwivedi, V., et al. (2015). Host ICAMs Play a Role in Cell Invasion by *Mycobacterium Tuberculosis* and Plasmodium Falciparum. *Nat. Commun.* 6, 6049. doi: 10.1038/ncomms7049

Bilal, J. A., Malik, E. E., Al-Nafeesah, A., and Adam, I. (2020). Global Prevalence of Congenital Malaria: A Systematic Review and Meta-Analysis. *Eur. J. Obstet. Gynecol. Reprod. Biol.* 252, 534–542. doi: 10.1016/j.ejogrb.2020.06.025

Blackman, M. J., Fujioka, H., Stafford, W. H., Sajid, M., Clough, B., Fleck, S. L., et al. (1998). A Subtilisin-Like Protein in Secretory Organelles of *Plasmodium Falciparum* Merozoites. *J. Biol. Chem.* 273, 23398–23409. doi: 10.1074/jbc.273.36.23398

Blank, J., Behrends, J., Jacobs, T., and Schneider, B. E. (2016a). *Mycobacterium Tuberculosis* Coinfection Has No Impact on *Plasmodium Berghei* ANKA-Induced Experimental Cerebral Malaria in C57BL/6 Mice. *Infect. Immun.* 84, 502–510. doi: 10.1128/IAI.01290-15

Blank, J., Eggers, L., Behrends, J., Jacobs, T., and Schneider, B. E. (2016b). One Episode of Self-Resolving *Plasmodium Yoelii* Infection Transiently Exacerbates Chronic *Mycobacterium Tuberculosis* Infection. *Front. Microbiol.* 7, 152. doi: 10.3389/fmicb.2016.00152

Borggraefe, I., Yuan, J., Telford, S. R.3rd, Menon, S., Hunter, R., Shah, S., et al. (2006). *Babesia Microti* Primarily Invades Mature Erythrocytes in Mice. *Infect. Immun.* 74, 3204–3212. doi: 10.1128/IAI.01560-05

Boyle, M. J., Jagannathan, P., Bowen, K., McIntyre, T. I., Vance, H. M., Farrington, L. A., et al. (2015). Effector Phenotype of *Plasmodium Falciparum*-Specific CD4+ T Cells Is Influenced by Both Age and Transmission Intensity in Naturally Exposed Populations. *J. Infect. Dis.* 212, 416–425. doi: 10.1093/infdis/jiv054

Boyle, M. J., Jagannathan, P., Bowen, K., McIntyre, T. I., Vance, H. M., Farrington, L. A., et al. (2017). The Development of *Plasmodium Falciparum*-Specific IL10 CD4 T Cells and Protection From Malaria in Children in an Area of High Malaria Transmission. *Front. Immunol.* 8, 1329. doi: 10.3389/fimmu.2017.01329

Burel, J. G., Apte, S. H., McCarthy, J. S., and Doolan, D. L. (2016). *Plasmodium Vivax* But Not *Plasmodium Falciparum* Blood-Stage Infection in Humans Is Associated With the Expansion of a CD8+ T Cell Population With Cytotoxic Potential. *PloS Negl. Trop. Dis.* 10, e0005031. doi: 10.1371/journal.pntd.0005031

Cai, C. W., Blase, J. R., Zhang, X., Eickhoff, C. S., and Hoft, D. F. (2016). Th17 Cells Are More Protective Than Th1 Cells Against the Intracellular Parasite Trypanosoma Cruzi. *PloS Pathog.* 12, e1005902. doi: 10.1371/journal.ppat.1005902

Campos, M. A., Almeida, I. C., Takeuchi, O., Akira, S., Valente, E. P., Procopio, D. O., et al. (2001). Activation of Toll-Like Receptor-2 by Glycosylphosphatidylinositol Anchors From a Protozoan Parasite. *J. Immunol.* 167, 416–423. doi: 10.4049/jimmunol.167.1.416

Chakravarty, S., Baldeviano, G. C., Overstreet, M. G., and Zavala, F. (2008). Effector CD8+ T Lymphocytes Against Liver Stages of *Plasmodium Yoelii* do Not Require Gamma Interferon for Antiparasite Activity. *Infect. Immun.* 76, 3628–3631. doi: 10.1128/IAI.00471-08

Chang, C. Y., Pui, W. C., Kadir, K. A., and Singh, B. (2018). Spontaneous Splenic Rupture in *Plasmodium Knowlesi* Malaria. *Malar. J.* 17, 448. doi: 10.1186/s12936-018-2600-2

Clark, I. A., and Allison, A. C. (1974). Babesia Microti and Plasmodium Berghei Yoelii Infections in Nude Mice. *Nature* 252, 328–329. doi: 10.1038/252328a0

Clawson, M. L., Paciorkowski, N., Rajan, T. V., La Vake, C., Pope, C., La Vake, M., et al. (2002). Cellular Immunity, But Not Gamma Interferon, is Essential for Resolution of *Babesia Microti* Infection in BALB/c Mice. *Infect. Immun.* 70, 5304–5306. doi: 10.1128/IAI.70.9.5304-5306.2002

Cornillot, E., Hadj-Kaddour, K., Dassouli, A., Noel, B., Ranwez, V., Vacherie, B., et al. (2012). Sequencing of the Smallest Apicomplexan Genome From the Human Pathogen Babesia Microti. *Nucleic Acids Res.* 40, 9102–9114. doi: 10.1093/nar/gks700

Cuesta, I., Gonzalez, L. M., Estrada, K., Grande, R., Zaballos, A., Lobo, C. A., et al. (2014). High-Quality Draft Genome Sequence of *Babesia Divergens*, the Etiological Agent of Cattle and Human Babesiosis. *Genome Announc.* 2 (6), e01194–14. doi: 10.1128/genomeA.01194-14

Cursino-Santos, J. R., Singh, M., Pham, P., Rodriguez, M., and Lobo, C. A. (2016). Babesia Divergens Builds a Complex Population Structure Composed of Specific Ratios of Infected Cells to Ensure a Prompt Response to Changing Environmental Conditions. *Cell Microbiol.* 18, 859–874. doi: 10.1111/cmi.12555

Danwang, C., Bigna, J. J., Nzalie, R. N. T., and Robert, A. (2020). Epidemiology of Clinical Congenital and Neonatal Malaria in Endemic Settings: A Systematic Review and Meta-Analysis. *Malar. J.* 19, 312. doi: 10.1186/s12936-020-03373-8

Debierre-Grockiego, F., Campos, M. A., Azzouz, N., Schmidt, J., Bieker, U., Resende, M. G., et al. (2007). Activation of TLR2 and TLR4 by Glycosylphosphatidylinositols Derived From Toxoplasma Gondii. *J. Immunol.* 179, 1129–1137. doi: 10.4049/jimmunol.179.2.1129

Debierre-Grockiego, F., Smith, T. K., Delbecq, S., Ducournau, C., Lantier, L., Schmidt, J., et al. (2019). *Babesia Divergens* Glycosylphosphatidylinositols Modulate Blood Coagulation and Induce Th2-Biased Cytokine Profiles in Antigen Presenting Cells. *Biochimie* 167, 135–144. doi: 10.1016/j.biochi.2019.09.007

de Koning-Ward, T. F., Dixon, M. W., Tilley, L., and Gilson, P. R. (2016). *Plasmodium* Species: Master Renovators of Their Host Cells. *Nat. Rev. Microbiol.* 14, 494–507. doi: 10.1038/nrmicro.2016.79

Delbecq, S., Precigout, E., Vallet, A., Carcy, B., Schetters, T. P., and Gorenflot, A. (2002). *Babesia Divergens*: Cloning and Biochemical Characterization of Bd37. *Parasitology* 125, 305–312. doi: 10.1017/S0031182002002160

De Niz, M., and Heussler, V. T. (2018). Rodent Malaria Models: Insights Into Human Disease and Parasite Biology. *Curr. Opin. Microbiol.* 46, 93–101. doi: 10.1016/j.mib.2018.09.003

Deore, S., Kumar, A., Kumar, S., Mittal, E., Lotke, A., and Musti, K. (2019). Erythrocyte Binding Ligand Region VI Specific IgA Confers Tissue Protection in Malaria Infection. *Mol. Biol. Rep.* 46, 3801–3808. doi: 10.1007/s11033-019-04822-7

Djokic, V., Akoolo, L., Primus, S., Schlachter, S., Kelly, K., Bhanot, P., et al. (2019). Protozoan Parasite *Babesia Microti* Subverts Adaptive Immunity and Enhances Lyme Disease Severity. *Front. Microbiol.* 10, 1596. doi: 10.3389/fmicb.2019.01596

Djokic, V., Primus, S., Akoolo, L., Chakraborti, M., and Parveen, N. (2018b). Age-Related Differential Stimulation of Immune Response by Babesia Microti and Borrelia Burgdorferi During Acute Phase of Infection Affects Disease Severity. *Front. Immunol.* 9, 2891. doi: 10.3389/fimmu.2018.02891

Djokic, V., Akoolo, L., and Parveen, N. (2018a). *Babesia Microti* Infection Changes Host Spleen Architecture and Is Cleared by a Th1 Immune Response. *Front. Microbiol.* 9, 1–11. doi: 10.3389/fmicb.2018.00085

Doolan, D. L., and Martinez-Alier, N. (2006). Immune Response to Pre-Erythrocytic Stages of Malaria Parasites. *Curr. Mol. Med.* 6, 169–185. doi: 10.2174/156652406776055249

Drewry, L. L., and Harty, J. T. (2020). Balancing in a Black Box: Potential Immunomodulatory Roles for TGF-Beta Signaling During Blood-Stage Malaria. *Virulence* 11, 159–169. doi: 10.1080/21505594.2020.1726569

Duffy, M. F., Caragounis, A., Noviyanti, R., Kyriacou, H. M., Choong, E. K., Boysen, K., et al. (2006). Transcribed Var Genes Associated With Placental Malaria in Malawian Women. *Infect. Immun.* 74, 4875–4883. doi: 10.1128/IAI.01978-05

Dumic, I., Patel, J., Hart, M., Niendorf, E. R., Martin, S., and Ramanan, P. (2018). Splenic Rupture as the First Manifestation of *Babesia Microti* Infection: Report of a Case and Review of Literature. *Am. J. Case Rep.* 19, 335–341. doi: 10.12659/AJCR.908453

Efstratiou, A., Galon, E. M. S., Wang, G., Umeda, K., Kondoh, D., Terkawi, M. A., et al. (2020). Babesia Microti Confers Macrophage-Based Cross-Protective Immunity Against Murine Malaria. *Front. Cell Infect. Microbiol.* 10, 193. doi: 10.3389/fcimb.2020.00193

Elizalde-Torrent, A., Val, F., Azevedo, I. C. C., Monteiro, W. M., Ferreira, L. C. L., Fernandez-Becerra, C., et al. (2018). Sudden Spleen Rupture in a *Plasmodium*

Vivax-Infected Patient Undergoing Malaria Treatment. *Malar. J.* 17, 79. doi: 10.1186/s12936-018-2228-2

El Khoury, M. Y., Gandhi, R., Dandache, P., Lombardo, G., and Wormser, G. P. (2011). Non-Surgical Management of Spontaneous Splenic Rupture Due to *Babesia Microti* Infection. *Ticks Tick Borne Dis.* 2, 235–238. doi: 10.1016/j.ttbdis.2011.08.001

Fang, D. C., and McCullough, J. (2016). Transfusion-Transmitted Babesia Microti. *Transfus. Med. Rev.* 30, 132–138. doi: 10.1016/j.tmrv.2016.04.002

Farber, F. R., Muehlenbachs, A., and Robey, T. E. (2015). Atraumatic Splenic Rupture From *Babesia*: A Disease of the Otherwise Healthy Patient. *Ticks Tick Borne Dis.* 6, 649–652. doi: 10.1016/j.ttbdis.2015.05.010

Fried, M., and Duffy, P. E. (1996). Adherence of *Plasmodium Falciparum* to Chondroitin Sulfate A in the Human Placenta. *Science* 272, 1502–1504. doi: 10.1126/science.272.5267.1502

Fried, M., and Duffy, P. E. (2015). Designing a VAR2CSA-Based Vaccine to Prevent Placental Malaria. *Vaccine* 33, 7483–7488. doi: 10.1016/j.vaccine.2015.10.011

Fried, M., and Duffy, P. E. (2017). Malaria During Pregnancy. *Cold Spring Harb. Perspect. Med.* 7 (6), a025551. doi: 10.1101/cshperspect.a025551

Fried, M., Kurtis, J. D., Swihart, B., Pond-Tor, S., Barry, A., Sidibe, Y., et al. (2017). Systemic Inflammatory Response to Malaria During Pregnancy Is Associated With Pregnancy Loss and Preterm Delivery. *Clin. Infect. Dis.* 65, 1729–1735. doi: 10.1093/cid/cix623

Froberg, M. K., Dannen, D., Bernier, N., Shieh, W. J., Guarner, J., and Zaki, S. (2008). Case Report: Spontaneous Splenic Rupture During Acute Parasitemia of Babesia Microti. *Ann. Clin. Lab. Sci.* 38, 390–392.

Frolich, S., Entzeroth, R., and Wallach, M. (2012). Comparison of Protective Immune Responses to Apicomplexan Parasites. *J. Parasitol. Res.* 2012, 852591. doi: 10.1155/2012/852591

Gardner, M. J., Hall, N., Fung, E., White, O., Berriman, M., Hyman, R. W., et al. (2002). Genome Sequence of the Human Malaria Parasite Plasmodium Falciparum. *Nature* 419, 498–511. doi: 10.1038/nature01097

Garrido-Cardenas, J. A., Gonzalez-Ceron, L., Manzano-Agugliaro, F., and Mesa-Valle, C. (2019). Plasmodium Genomics: An Approach for Learning About and Ending Human Malaria. *Parasitol. Res.* 118, 1–27. doi: 10.1007/s00436-018-6127-9

Gowda, D. C. (2007). TLR-Mediated Cell Signaling by Malaria GPIs. *Trends Parasitol.* 23, 596–604. doi: 10.1016/j.pt.2007.09.003

Gowda, D. C., and Wu, X. (2018). Parasite Recognition and Signaling Mechanisms in Innate Immune Responses to Malaria. *Front. Immunol.* 9, 3006. doi: 10.3389/fimmu.2018.03006

Gray, E. B., and Herwaldt, B. L. (2019). Babesiosis Surveillance - United States, 2011-2015. *MMWR Surveill. Summ.* 68, 1–11. doi: 10.15585/mmwr.ss6806a1

Guthmiller, J. J., Graham, A. C., Zander, R. A., Pope, R. L., and Butler, N. S. (2017). Cutting Edge: IL-10 Is Essential for the Generation of Germinal Center B Cell Responses and Anti-Plasmodium Humoral Immunity. *J. Immunol.* 198, 617–622. doi: 10.4049/jimmunol.1601762

Haque, A., Best, S. E., Montes de Oca, M., James, K. R., Ammerdorffer, A., Edwards, C. L., et al. (2014). Type I IFN Signaling in CD8- DCs Impairs Th1-Dependent Malaria Immunity. *J. Clin. Invest.* 124, 2483–2496. doi: 10.1172/JCI70698

Hemmer, R. M., Ferrick, D. A., and Conrad, P. A. (2000). Role of T Cells and Cytokines in Fatal and Resolving Experimental Babesiosis: Protection in TNFRp55-/- Mice Infected With the Human Babesia WA1 Parasite. *J. Parasitol.* 86, 736–742. doi: 10.1645/0022-3395(2000)086[0736:ROTCAC]2.0.CO;2

Hentzschel, F., Obrova, K., and Marti, M. (2020). No Evidence for Ago2 Translocation From the Host Erythrocyte Into the Plasmodium Parasite. *Wellcome Open Res.* 5, 92. doi: 10.12688/wellcomeopenres.15852.2

Herwaldt, B. L., Caccio, S., Gherlinzoni, F., Aspock, H., Slemenda, S. B., Piccaluga, P., et al. (2003). Molecular Characterization of a non-*Babesia Divergens* Organism Causing Zoonotic Babesiosis in Europe. *Emerg. Infect. Dis.* 9, 942–948. doi: 10.3201/eid0908.020748

Herwaldt, B. L., Linden, J. V., Bosserman, E., Young, C., Olkowska, D., and Wilson, M. (2011). Transfusion-Associated Babesiosis in the United States: A Description of Cases. *Ann. Internal Med.* 155, 509–519. doi: 10.7326/0003-4819-155-8-201110180-00362

Hisaeda, H., Tetsutani, K., Imai, T., Moriya, C., Tu, L., Hamano, S., et al. (2008). Malaria Parasites Require TLR9 Signaling for Immune Evasion by Activating Regulatory T Cells. *J. Immunol.* 180, 2496–2503. doi: 10.4049/jimmunol.180.4.2496

Ho, C. M., Beck, J. R., Lai, M., Cui, Y., Goldberg, D. E., Egea, P. F., et al. (2018). Malaria Parasite Translocon Structure and Mechanism of Effector Export. *Nature* 561, 70–75. doi: 10.1038/s41586-018-0469-4

Hoft, D. F., Schnapp, A. R., Eickhoff, C. S., and Roodman, S. T. (2000). Involvement of CD4(+) Th1 Cells in Systemic Immunity Protective Against Primary and Secondary Challenges With Trypanosoma Cruzi. *Infect. Immun.* 68, 197–204. doi: 10.1128/IAI.68.1.197-204.2000

Hutchings, C. L., Li, A., Fernandez, K. M., Fletcher, T., Jackson, L. A., Molloy, J. B., et al. (2007). New Insights Into the Altered Adhesive and Mechanical Properties of Red Blood Cells Parasitized by Babesia Bovis. *Mol. Microbiol.* 65, 1092–1105. doi: 10.1111/j.1365-2958.2007.05850.x

Igarashi, I., Suzuki, R., Waki, S., Tagawa, Y., Seng, S., Tum, S., et al. (1999). Roles of CD4(+) T Cells and Gamma Interferon in Protective Immunity Against *Babesia Microti* Infection in Mice. *Infect. Immun.* 67, 4143–4148. doi: 10.1128/IAI.67.8.4143-4148.1999

Imbert, P., Rapp, C., and Buffet, P. A. (2009). Pathological Rupture of the Spleen in Malaria: Analysis of 55 Cases (1958-2008). *Travel Med. Infect. Dis.* 7, 147–159. doi: 10.1016/j.tmaid.2009.01.002

Jackson, A. P., Otto, T. D., Darby, A., Ramaprasad, A., Xia, D., Echaide, I. E., et al. (2014). The Evolutionary Dynamics of Variant Antigen Genes in Babesia Reveal a History of Genomic Innovation Underlying Host-Parasite Interaction. *Nucleic Acids Res.* 42, 7113–7131. doi: 10.1093/nar/gku322

Jalovecka, M., Sojka, D., Ascencio, M., and Schnittger, L. (2019). Babesia Life Cycle - When Phylogeny Meets Biology. *Trends Parasitol.* 35, 356–368. doi: 10.1016/j.pt.2019.01.007

Jeong, Y. I., Hong, S. H., Cho, S. H., Lee, W. J., and Lee, S. E. (2012). Induction of IL-10-Producing CD1dhighCD5+ Regulatory B Cells Following *Babesia Microti*-Infection. *PloS One* 7, e46553. doi: 10.1371/journal.pone.0046553

Junqueira, C., Barbosa, C. R. R., Costa, P. A. C., Teixeira-Carvalho, A., Castro, G., Sen Santara, S., et al. (2018). Cytotoxic CD8(+) T Cells Recognize and Kill Plasmodium Vivax-Infected Reticulocytes. *Nat. Med.* 24, 1330–1336. doi: 10.1038/s41591-018-0117-4

Kalanon, M., Bargieri, D., Sturm, A., Matthews, K., Ghosh, S., Goodman, C. D., et al. (2016). The Plasmodium Translocon of Exported Proteins Component EXP2 is Critical for Establishing a Patent Malaria Infection in Mice. *Cell Microbiol.* 18, 399–412. doi: 10.1111/cmi.12520

Kanjee, U., Rangel, G. W., Clark, M. A., and Duraisingh, M. T. (2018). Molecular and Cellular Interactions Defining the Tropism of Plasmodium Vivax for Reticulocytes. *Curr. Opin. Microbiol.* 46, 109–115. doi: 10.1016/j.mib.2018.10.002

Kapishnikov, S., Hempelmann, E., Elbaum, M., Als-Nielsen, J., and Leiserowitz, L. (2021). Malaria Pigment Crystals, the Achilles Heel of the Malaria Parasite. *ChemMedChem.* 16 (10), 1515–1532. doi: 10.1002/cmdc.202000895

Kassa, D., Petros, B., Mesele, T., Hailu, E., and Wolday, D. (2006). Characterization of Peripheral Blood Lymphocyte Subsets in Patients With Acute P*lasmodium Falciparum* and P. Vivax Malaria Infections at Wonji Sugar Estate, Ethiopia. *Clin. Vaccine Immunol.* 13, 376–379. doi: 10.1128/CVI.13.3.376-379.2006

Kelemen, R. K., Rajakaruna, H., Cockburn, I. A., and Ganusov, V. V. (2019). Clustering of Activated CD8 T Cells Around Malaria-Infected Hepatocytes Is Rapid and Is Driven by Antigen-Specific Cells. *Front. Immunol.* 10, 2153. doi: 10.3389/fimmu.2019.02153

Khan, S. M., and Waters, A. P. (2004). Malaria Parasite Transmission Stages: An Update. *Trends Parasitol.* 20, 575–580. doi: 10.1016/j.pt.2004.10.001

Kho, S., Qotrunnada, L., Leonardo, L., Andries, B., Wardani, P. A. I., Fricot, A., et al. (2021). Evaluation of Splenic Accumulation and Colocalization of Immature Reticulocytes and Plasmodium Vivax in Asymptomatic Malaria: A Prospective Human Splenectomy Study. *PloS Med.* 18, e1003632. doi: 10.1371/journal.pmed.1003632

King, T., and Lamb, T. (2015). Interferon-Gamma: The Jekyll and Hyde of Malaria. *PloS Pathog.* 11, e1005118. doi: 10.1371/journal.ppat.1005118

Kochayoo, P., Kittisenachai, N., Changrob, S., Wangriatisak, K., Muh, F., Chootong, P., et al. (2019). The Acquisition of Long-Lived Memory B Cell Responses to Merozoite Surface Protein-8 in Individuals With *Plasmodium Vivax* Infection. *Malar. J.* 18, 188. doi: 10.1186/s12936-019-2821-z

Krause, P. J., McKay, K., Gadbaw, J., Christianson, D., Closter, L., Lepore, T., et al. (2003). Increasing Health Burden of Human Babesiosis in Endemic Sites. *Am. J. Trop. Med. Hyg.* 68, 431–436. doi: 10.4269/ajtmh.2003.68.431

Krause, P. J., Telford, S. R.3rd, Spielman, A., Sikand, V., Ryan, R., Christianson, D., et al. (1996). Concurrent Lyme Disease and Babesiosis. Evidence for Increased Severity and Duration of Illness. *JAMA* 275, 1657–1660. doi: 10.1001/jama.1996.03530450047031

Kumar, R., Loughland, J. R., Ng, S. S., Boyle, M. J., and Engwerda, C. R. (2020). The Regulation of CD4(+) T Cells During Malaria. *Immunol. Rev.* 293, 70–87. doi: 10.1111/imr.12804

Lee, W. C., Russell, B., Sobota, R. M., Ghaffar, K., Howland, S. W., Wong, Z. X., et al. (2020). Plasmodium-Infected Erythrocytes Induce Secretion of IGFBP7 to Form Type II Rosettes and Escape Phagocytosis. *Elife* 9, ee51546. doi: 10.7554/eLife.51546

Liehl, P., Zuzarte-Luis, V., Chan, J., Zillinger, T., Baptista, F., Carapau, D., et al. (2014). Host-Cell Sensors for Plasmodium Activate Innate Immunity Against Liver-Stage Infection. *Nat. Med.* 20, 47–53. doi: 10.1038/nm.3424

Li, S., Goyal, B., Cooper, J. D., Abdelbaki, A., Gupta, N., and Kumar, Y. (2018). Splenic Rupture From Babesiosis, an Emerging Concern? A Systematic Review of Current Literature. *Ticks Tick Borne Dis.* 9, 1377–1382. doi: 10.1016/j.ttbdis.2018.06.004

Lim, C., Dankwa, S., Paul, A. S., and Duraisingh, M. T. (2017). Host Cell Tropism and Adaptation of Blood-Stage Malaria Parasites: Challenges for Malaria Elimination. *Cold Spring Harb. Perspect. Med.* 7. doi: 10.1101/cshperspect.a025494

Li, Y., Terkawi, M. A., Nishikawa, Y., Aboge, G. O., Luo, Y., Ooka, H., et al. (2012). Macrophages are Critical for Cross-Protective Immunity Conferred by *Babesia Microti* Against *Babesia Rodhaini* Infection in Mice. *Infect. Immun.* 80, 311–320. doi: 10.1128/IAI.05900-11

Lobo, C. A. (2005). *Babesia Divergens* and *Plasmodium Falciparum* Use Common Receptors, Glycophorins A and B, to Invade the Human Red Blood Cell. *Infect. Immun.* 73, 649–651. doi: 10.1128/IAI.73.1.649-651.2005

Lobo, C. A., Singh, M., and Rodriguez, M. (2020). Human Babesiosis: Recent Advances and Future Challenges. *Curr. Opin. Hematol.* 27, 399–405. doi: 10.1097/MOH.0000000000000606

Lundqvist, J., Larsson, C., Nelson, M., Andersson, M., Bergstrom, S., and Persson, C. (2010). Concomitant Infection Decreases the Malaria Burden But Escalates Relapsing Fever Borreliosis. *Infect. Immun.* 78, 1924–1930. doi: 10.1128/IAI.01082-09

Markus, M. B. (2011). Malaria: Origin of the Term "Hypnozoite". *J. Hist. Biol.* 44, 781–786. doi: 10.1007/s10739-010-9239-3

Marsh, K., and Kinyanjui, S. (2006). Immune Effector Mechanisms in Malaria. *Parasite Immunol.* 28, 51–60. doi: 10.1111/j.1365-3024.2006.00808.x

Medaglini, D., and Hoeveler, A. (2003). The European Research Effort for HIV/AIDS, Malaria and Tuberculosis. *Vaccine* 21 Suppl 2, S116–S120. doi: 10.1016/S0264-410X(03)00212-3

Millholland, M. G., Chandramohanadas, R., Pizzarro, A., Wehr, A., Shi, H., Darling, C., et al. (2011). The Malaria Parasite Progressively Dismantles the Host Erythrocyte Cytoskeleton for Efficient Egress. *Mol. Cell Proteomics* 10 (12), M111.010678. doi: 10.1074/mcp.M111.010678

Millington, O. R., Gibson, V. B., Rush, C. M., Zinselmeyer, B. H., Phillips, R. S., Garside, P., et al. (2007). Malaria Impairs T Cell Clustering and Immune Priming Despite Normal Signal 1 From Dendritic Cells. *PloS Pathog.* 3, 1380–1387. doi: 10.1371/journal.ppat.0030143

Milner, D. A. Jr. (2018). Malaria Pathogenesis. *Cold Spring Harb. Perspect. Med.* 8 (1), a025569. doi: 10.1101/cshperspect.a025569

Minkah, N. K., Wilder, B. K., Sheikh, A. A., Martinson, T., Wegmair, L., Vaughan, A. M., et al. (2019). Innate Immunity Limits Protective Adaptive Immune Responses Against Pre-Erythrocytic Malaria Parasites. *Nat. Commun.* 10, 3950. doi: 10.1038/s41467-019-11819-0

Mockenhaupt, F. P., Cramer, J. P., Hamann, L., Stegemann, M. S., Eckert, J., Oh, N. R., et al. (2006). Toll-Like Receptor (TLR) Polymorphisms in African Children: Common TLR-4 Variants Predispose to Severe Malaria. *Proc. Natl. Acad. Sci. U.S.A.* 103, 177–182. doi: 10.1073/pnas.0506803102

Moreau, E., Bonsergent, C., Al Dybiat, I., Gonzalez, L. M., Lobo, C. A., Montero, E., et al. (2015). *Babesia Divergens* Apical Membrane Antigen-1 (BdAMA-1): A Poorly Polymorphic Protein That Induces a Weak and Late Immune Response. *Exp. Parasitol.* 155, 40–45. doi: 10.1016/j.exppara.2015.04.024

Moritz, E. D., Winton, C. S., Tonnetti, L., Townsend, R. L., Berardi, V. P., Hewins, M. E., et al. (2016). Screening for *Babesia Microti* in the U.S. Blood Supply. *N Engl. J. Med.* 375, 2236–2245. doi: 10.1056/NEJMoa1600897

Nathaly Wieser, S., Schnittger, L., Florin-Christensen, M., Delbecq, S., and Schetters, T. (2019). Vaccination Against Babesiosis Using Recombinant GPI-Anchored Proteins. *Int. J. Parasitol.* 49, 175–181. doi: 10.1016/j.ijpara.2018.12.002

Nie, C. Q., Bernard, N. J., Schofield, L., and Hansen, D. S. (2007). CD4+ CD25+ Regulatory T Cells Suppress CD4+ T-Cell Function and Inhibit the Development of *Plasmodium Berghei*-Specific TH1 Responses Involved in Cerebral Malaria Pathogenesis. *Infect. Immun.* 75, 2275–2282. doi: 10.1128/IAI.01783-06

Nordstrand, A., Bunikis, I., Larsson, C., Tsogbe, K., Schwan, T. G., Nilsson, M., et al. (2007). Tickborne Relapsing Fever Diagnosis Obscured by Malaria, Togo. *Emerg. Infect. Dis.* 13, 117–123. doi: 10.3201/eid1301.060670

Norris, L. C., Fornadel, C. M., Hung, W. C., Pineda, F. J., and Norris, D. E. (2010). Frequency of Multiple Blood Meals Taken in a Single Gonotrophic Cycle by Anopheles Arabiensis Mosquitoes in Macha, Zambia. *Am. J. Trop. Med. Hyg.* 83, 33–37. doi: 10.4269/ajtmh.2010.09-0296

Nunes, M. C., and Scherf, A. (2007). *Plasmodium Falciparum* During Pregnancy: A Puzzling Parasite Tissue Adhesion Tropism. *Parasitology* 134, 1863–1869. doi: 10.1017/S0031182007000133

Oakley, M. S., Sahu, B. R., Lotspeich-Cole, L., Majam, V., Thao Pham, P., Sengupta Banerjee, A., et al. (2014). T-Bet Modulates the Antibody Response and Immune Protection During Murine Malaria. *Eur. J. Immunol.* 44, 2680–2691. doi: 10.1002/eji.201344437

Omer, S. A., Adam, I., Noureldien, A., Elhaj, H., Guerrero-Latorre, L., Silgado, A., et al. (2020). Congenital Malaria in Newborns Delivered to Mothers With Malaria-Infected Placenta in Blue Nile State, Sudan. *J. Trop. Pediatr.* 66, 428–434. doi: 10.1093/tropej/fmz083

Osungbade, K. O., and Oladunjoye, O. O. (2012). Prevention of Congenital Transmission of Malaria in Sub-Saharan African Countries: Challenges and Implications for Health System Strengthening. *J. Trop. Med.* 2012, 648456. doi: 10.1155/2012/648456

Oyong, D. A., Wilson, D. W., Barber, B. E., William, T., Jiang, J., Galinski, M. R., et al. (2019). Induction and Kinetics of Complement-Fixing Antibodies Against *Plasmodium Vivax* Merozoite Surface Protein 3alpha and Relationship With Immunoglobulin G Subclasses and Immunoglobulin M. *J. Infect. Dis.* 220, 1950–1961. doi: 10.1093/infdis/jiz407

Pasini, E. M., and Kocken, C. H. M. (2020). Parasite-Host Interaction and Pathophysiology Studies of the Human Relapsing Malarias Plasmodium Vivax and Plasmodium Ovale Infections in Non-Human Primates. *Front. Cell Infect. Microbiol.* 10, 614122. doi: 10.3389/fcimb.2020.614122

Pasvol, G., Weatherall, D. J., and Wilson, R. J. (1980). The Increased Susceptibility of Young Red Cells to Invasion by the Malarial Parasite Plasmodium Falciparum. *Br. J. Haematol.* 45, 285–295. doi: 10.1111/j.1365-2141.1980.tb07148.x

Patel, K. M., Johnson, J. E., Reece, R., and Mermel, L. A. (2019). Babesiosis-Associated Splenic Rupture: Case Series From a Hyperendemic Region. *Clin. Infect. Dis.* 69, 1212–1217. doi: 10.1093/cid/ciy1060

Patgaonkar, M., Herbert, F., Powale, K., Gandhe, P., Gogtay, N., Thatte, U., et al. (2018). Vivax Infection Alters Peripheral B-Cell Profile and Induces Persistent Serum IgM. *Parasite Immunol.* 40, e12580. doi: 10.1111/pim.12580

Perez-Mazliah, D., and Langhorne, J. (2014). CD4 T-Cell Subsets in Malaria: TH1/TH2 Revisited. *Front. Immunol.* 5, 671. doi: 10.3389/fimmu.2014.00671

Quinn, T. C., Jacobs, R. F., Mertz, G. J., Hook, E. W.3rd, and Locklsey, R. M. (1982). Congenital Malaria: A Report of Four Cases and a Review. *J. Pediatr.* 101, 229–232. doi: 10.1016/S0022-3476(82)80128-5

Reiss, T., Rosa, T. F. A., Blaesius, K., Bobbert, R. P., Zipfel, P. F., Skerka, C., et al. (2018). Cutting Edge: FHR-1 Binding Impairs Factor H-Mediated Complement Evasion by the Malaria Parasite Plasmodium Falciparum. *J. Immunol.* 201, 3497–3502. doi: 10.4049/jimmunol.1800662

Saetre, K., Godhwani, N., Maria, M., Patel, D., Wang, G., Li, K. I., et al. (2018). Congenital Babesiosis After Maternal Infection With *Borrelia Burgdorferi* and Babesia Microti. *J. Pediatr. Infect. Dis. Soc.* 7, e1–e5. doi: 10.1093/jpids/pix074

Salmon, B. L., Oksman, A., and Goldberg, D. E. (2001). Malaria Parasite Exit From the Host Erythrocyte: A Two-Step Process Requiring Extraerythrocytic Proteolysis. *Proc. Natl. Acad. Sci. U.S.A.* 98, 271–276. doi: 10.1073/pnas.98.1.271

Santamaria, M. H., and Corral, R. S. (2013). Osteopontin-Dependent Regulation of Th1 and Th17 Cytokine Responses in Trypanosoma Cruzi-Infected C57BL/6 Mice. *Cytokine* 61, 491–498. doi: 10.1016/j.cyto.2012.10.027

Schwarzer, E., Kuhn, H., Valente, E., and Arese, P. (2003). Malaria-Parasitized Erythrocytes and Hemozoin Nonenzymatically Generate Large Amounts of Hydroxy Fatty Acids That Inhibit Monocyte Functions. *Blood* 101, 722–728. doi: 10.1182/blood-2002-03-0979

Sebina, I., Fogg, L. G., James, K. R., Soon, M. S. F., Akter, J., Thomas, B. S., et al. (2017). IL-6 Promotes CD4(+) T-Cell and B-Cell Activation During Plasmodium Infection. *Parasite Immunol.* 39, e12455. doi: 10.1111/pim.12455

Seixas, E., Moura Nunes, J. F., Matos, I., and Coutinho, A. (2009). The Interaction Between DC and *Plasmodium Berghei/Chabaudi*-Infected Erythrocytes in Mice Involves Direct Cell-to-Cell Contact, Internalization and TLR. *Eur. J. Immunol.* 39, 1850–1863. doi: 10.1002/eji.200838403

Sevilla, E., Gonzalez, L. M., Luque, D., Gray, J., and Montero, E. (2018). Kinetics of the Invasion and Egress Processes of *Babesia Divergens*, Observed by Time-Lapse Video Microscopy. *Sci. Rep.* 8, 14116. doi: 10.1038/s41598-018-32349-7

Sherling, E. S., Perrin, A. J., Knuepfer, E., Russell, M. R. G., Collinson, L. M., Miller, L. H., et al. (2019). The *Plasmodium Falciparum* Rhoptry Bulb Protein RAMA Plays an Essential Role in Rhoptry Neck Morphogenesis and Host Red Blood Cell Invasion. *PloS Pathog.* 15, e1008049. doi: 10.1371/journal.ppat.1008049

Shimada, T., Shikano, S., Hashiguchi, R., Matsuki, N., and Ono, K. (1996). Effects of Depletion of T Cell Subpopulations on the Course of Infection and Anti-Parasite Delayed Type Hypersensitivity Response in Mice Infected With *Babesia Microti* and Babesia Rodhaini. *J. Vet. Med. Sci.* 58, 343–347. doi: 10.1292/jvms.58.343

Singh, S., and Chitnis, C. E. (2017). Molecular Signaling Involved in Entry and Exit of Malaria Parasites From Host Erythrocytes. *Cold Spring Harb. Perspect. Med.* 7, a026815. doi: 10.1101/cshperspect.a026815

Skariah, S., Arnaboldi, P., Dattwyler, R. J., Sultan, A. A., Gaylets, C., Walwyn, O., et al. (2017). Elimination of *Babesia Microti* Is Dependent on Intraerythrocytic Killing and CD4+ T Cells. *J. Immunol.* 199, 633–642. doi: 10.4049/jimmunol.1601193

Smith, J. D., Craig, A. G., Kriek, N., Hudson-Taylor, D., Kyes, S., Fagan, T., et al. (2000). Identification of a *Plasmodium Falciparum* Intercellular Adhesion Molecule-1 Binding Domain: A Parasite Adhesion Trait Implicated in Cerebral Malaria. *Proc. Natl. Acad. Sci. U.S.A.* 97, 1766–1771. doi: 10.1073/pnas.040545897

Soon, M. S. F., and Haque, A. (2018). Recent Insights Into CD4(+) Th Cell Differentiation in Malaria. *J. Immunol.* 200, 1965–1975. doi: 10.4049/jimmunol.1701316

Springer, A., Fichtel, C., Calvignac-Spencer, S., Leendertz, F. H., and Kappeler, P. M. (2015). Hemoparasites in a Wild Primate: Infection Patterns Suggest Interaction of Plasmodium and Babesia in a Lemur Species. *Int. J. Parasitol. Parasites Wildl.* 4, 385–395. doi: 10.1016/j.ijppaw.2015.10.006

Srivastava, A., Creek, D. J., Evans, K. J., De Souza, D., Schofield, L., Muller, S., et al. (2015). Host Reticulocytes Provide Metabolic Reservoirs That can be Exploited by Malaria Parasites. *PloS Pathog.* 11, e1004882. doi: 10.1371/journal.ppat.1004882

Steere, A. C., Strle, F., Wormser, G. P., Hu, L. T., Branda, J. A., Hovius, J. W., et al. (2016). Lyme Borreliosis. *Nat. Rev. Dis. Primers* 2, 16090. doi: 10.1038/nrdp.2016.90

Stewart, P. E., and Rosa, P. A. (2018). Physiologic and Genetic Factors Influencing the Zoonotic Cycle of Borrelia Burgdorferi. *Curr. Top. Microbiol. Immunol.* 415, 63–82. doi: 10.1007/82_2017_43

Sun, T., Holowka, T., Song, Y., Zierow, S., Leng, L., Chen, Y., et al. (2012). A Plasmodium-Encoded Cytokine Suppresses T-Cell Immunity During Malaria. *Proc. Natl. Acad. Sci. U.S.A.* 109, E2117–E2126. doi: 10.1073/pnas.1206573109

Vallejo, A. F., Read, R. C., Arevalo-Herrera, M., Herrera, S., Elliott, T., and Polak, M. E. (2018). Malaria Systems Immunology: *Plasmodium Vivax* Induces Tolerance During Primary Infection Through Dysregulation of Neutrophils and Dendritic Cells. *J. Infect.* 77, 440–447. doi: 10.1016/j.jinf.2018.09.005

Vannier, E., Borggraefe, I., Telford, S. R.3rd, Menon, S., Brauns, T., Spielman, A., et al. (2004). Age-Associated Decline in Resistance to *Babesia Microti* is Genetically Determined. *J. Infect. Dis.* 189, 1721–1728. doi: 10.1086/382965

Vaughan, A. M., and Kappe, S. H. I. (2017). Malaria Parasite Liver Infection and Exoerythrocytic Biology. *Cold Spring Harb. Perspect. Med.* 7, a025486. doi: 10.1101/cshperspect.a025486

Venugopal, K., Hentzschel, F., Valkiunas, G., and Marti, M. (2020). Plasmodium Asexual Growth and Sexual Development in the Haematopoietic Niche of the Host. *Nat. Rev. Microbiol.* 18, 177–189. doi: 10.1038/s41579-019-0306-2

Villegas-Mendez, A., Inkson, C. A., Shaw, T. N., Strangward, P., and Couper, K. N. (2016). Long-Lived CD4+IFN-Gamma+ T Cells Rather Than Short-Lived CD4+IFN-Gamma+IL-10+ T Cells Initiate Rapid IL-10 Production To Suppress Anamnestic T Cell Responses During Secondary Malaria Infection. *J. Immunol.* 197, 3152–3164. doi: 10.4049/jimmunol.1600968

Wale, N., Jones, M. J., Sim, D. G., Read, A. F., and King, A. A. (2019). The Contribution of Host Cell-Directed vs. Parasite-Directed Immunity to the Disease and Dynamics of Malaria Infections. *Proc. Natl. Acad. Sci. U.S.A.* 116, 22386–22392. doi: 10.1073/pnas.1908147116

Walsh, K. P., and Mills, K. H. (2013). Dendritic Cells and Other Innate Determinants of T Helper Cell Polarisation. *Trends Immunol.* 34, 521–530. doi: 10.1016/j.it.2013.07.006

Wammes, L. J., Wiria, A. E., Toenhake, C. G., Hamid, F., Liu, K. Y., Suryani, H., et al. (2013). Asymptomatic Plasmodial Infection is Associated With Increased Tumor Necrosis Factor Receptor II-Expressing Regulatory T Cells and Suppressed Type 2 Immune Responses. *J. Infect. Dis.* 207, 1590–1599. doi: 10.1093/infdis/jit058

Wilainam, P., Nintasen, R., and Viriyavejakul, P. (2015). Mast Cell Activation in the Skin of *Plasmodium Falciparum* Malaria Patients. *Malar. J.* 14, 67. doi: 10.1186/s12936-015-0568-8

Wormser, G. P., Villafuerte, P., Nolan, S. M., Wang, G., Lerner, R. G., Saetre, K. L., et al. (2015). Neutropenia in Congenital and Adult Babesiosis. *Am. J. Clin. Pathol.* 144, 94–96. doi: 10.1309/AJCP2PHH4HBVHZFS

Wu, X., Gowda, N. M., and Gowda, D. C. (2015). Phagosomal Acidification Prevents Macrophage Inflammatory Cytokine Production to Malaria, and Dendritic Cells Are the Major Source at the Early Stages of Infection: IMPLICATION FOR MALARIA PROTECTIVE IMMUNITY DEVELOPMENT. *J. Biol. Chem.* 290, 23135–23147. doi: 10.1074/jbc.M115.671065

Wu, X., Gowda, N. M., Kawasawa, Y. I., and Gowda, D. C. (2018). A Malaria Protein Factor Induces IL-4 Production by Dendritic Cells *via* PI3K-Akt-NF-KappaB Signaling Independent of MyD88/TRIF and Promotes Th2 Response. *J. Biol. Chem.* 293, 10425–10434. doi: 10.1074/jbc.AC118.001720

Yap, X. Z., Lundie, R. J., Feng, G., Pooley, J., Beeson, J. G., and O'Keeffe, M. (2019). Different Life Cycle Stages of *Plasmodium Falciparum* Induce Contrasting Responses in Dendritic Cells. *Front. Immunol.* 10, 32. doi: 10.3389/fimmu.2019.00032

Yi, W., Bao, W., Rodriguez, M., Liu, Y., Singh, M., Ramlall, V., et al. (2018). Robust Adaptive Immune Response Against *Babesia Microti* Infection Marked by Low Parasitemia in a Murine Model of Sickle Cell Disease. *Blood Adv.* 2, 3462–3478. doi: 10.1182/bloodadvances.2018026468

Zander, R. A., Guthmiller, J. J., Graham, A. C., Pope, R. L., Burke, B. E., Carr, D. J., et al. (2016). Type I Interferons Induce T Regulatory 1 Responses and Restrict Humoral Immunity During Experimental Malaria. *PloS Pathog.* 12, e1005945. doi: 10.1371/journal.ppat.1005945

Zhu, J., Krishnegowda, G., Li, G., and Gowda, D. C. (2011). Proinflammatory Responses by Glycosylphosphatidylinositols (GPIs) of *Plasmodium Falciparum* are Mainly Mediated Through the Recognition of TLR2/TLR1. *Exp. Parasitol.* 128, 205–211. doi: 10.1016/j.exppara.2011.03.010

Conflict of Interest: The authors declare that the research was conducted in the absence of any commercial or financial relationships that could be construed as a potential conflict of interest.

Publisher's Note: All claims expressed in this article are solely those of the authors and do not necessarily represent those of their affiliated organizations, or those of the publisher, the editors and the reviewers. Any product that may be evaluated in this article, or claim that may be made by its manufacturer, is not guaranteed or endorsed by the publisher.

frontiers in Microbiology

ORIGINAL RESEARCH
published: 05 August 2021
doi: 10.3389/fmicb.2021.700892

Dynamic Expressions of TIGIT on Splenic T Cells and TIGIT-Mediated Splenic T Cell Dysfunction of Mice With Chronic *Toxoplasma gondii* Infection

Haoran Li[1], Jing Zhang[1], Changwei Su[1], Xiaowei Tian[1], Xuefang Mei[1], Zhenchao Zhang[1], Mingyong Wang[2], Xiangrui Li[1,3]* and Shuai Wang[1]**

[1]Xinxiang Key Laboratory of Pathogenic Biology, Department of Pathogenic Biology, School of Basic Medical Sciences, Xinxiang Medical University, Xinxiang, China, [2]Xinxiang Key Laboratory of Immunoregulation and Molecular Diagnostics, School of Laboratory Medicine, Xinxiang Medical University, Xinxiang, China, [3]MOE Joint International Research Laboratory of Animal Health and Food Safety, College of Veterinary Medicine, Nanjing Agricultural University, Nanjing, China

OPEN ACCESS

Edited by:
Hong-Juan Peng,
Southern Medical University, China

Reviewed by:
Jilong Shen,
Anhui Medical University, China
Dong-Hui Zhou,
Fujian Agriculture and Forestry University, China

***Correspondence:**
Shuai Wang
tongbaiws1003@163.com
Xiangrui Li
lixiangrui@njau.edu.cn
Mingyong Wang
wmy118@126.com

Specialty section:
This article was submitted to Infectious Diseases, a section of the journal Frontiers in Microbiology

Received: 27 April 2021
Accepted: 12 July 2021
Published: 05 August 2021

Citation:
Li H, Zhang J, Su C, Tian X, Mei X, Zhang Z, Wang M, Li X and Wang S (2021) Dynamic Expressions of TIGIT on Splenic T Cells and TIGIT-Mediated Splenic T Cell Dysfunction of Mice With Chronic Toxoplasma gondii Infection. Front. Microbiol. 12:700892. doi: 10.3389/fmicb.2021.700892

As an immunosuppressive receptor, T-cell immunoglobulin and immunoreceptor tyrosine-based inhibitory motif domain (TIGIT) play a critical part in cellular immune regulation mediated by pathogen infection. Whereas, TIGIT expression on splenic T cells in hosts infected with *Toxoplasma gondii* cysts has not been studied. In this study, we detected TIGIT expression and the changes of immune function in the spleen by flow cytometry and real-time PCR (RT-PCR). We found that TIGIT expression on splenic T cells increased significantly post infection. At the same time, splenic TIGIT$^+$T$_{CM}$ cells were activated and transformed into TIGIT$^+$T$_{EM}$ cells during the infection, and the cytotoxicity of TIGIT$^+$ T cells was reduced in the later stage of infection. This study shows that chronic *T. gondii* infection can upregulate TIGIT expression on the surface of T cells and affect immune cell function.

Keywords: TIGIT, *Toxoplasma gondii*, T cells, CD226, T$_{EM}$

INTRODUCTION

Toxoplasmosis caused by *Toxoplasma gondii* (*T. gondii*) infection has become an important zoonosis in the world, which is often transmitted *via* cysts in raw or under cooked meat or oocysts in cat feces (Fisch et al., 2019). Chronic *T. gondii* infection can lead to the formation of long-term and stable *T. gondii* cysts in multiple host tissues (Pinto-Ferreira et al., 2019). When host immune function is normal, *T. gondii* generally form long-term, stable cysts in infected tissues after 2–3 weeks of acute infection, which continuously stimulates the body to produce an immune response and results in chronic toxoplasmosis (Landrith et al., 2015). *T. gondii* cysts can survive for a long time. However, when the immune function of the host is impaired (such as patients with HIV/AIDS, cancer, or a transplanted organ), bradyzoites

in the cyst can escape from the cyst and cause acute infection, resulting in morbidity or death of the host (Montoya and Liesenfeld, 2004; Pinto-Ferreira et al., 2019). At present, there is no ideal drug to control and remove cysts during chronic *T. gondii* infection (Alday and Doggett, 2017). The long-term survival of tissue cysts mainly depends on the effective escape mechanism of *T. gondii* to host cellular immunity, so to explore the mechanism of *T. gondii* causing the failure of host T cells in the process of infection is the fundamental way to effectively removal cysts.

As the main immune organ of T cell immune response against pathogen infection, spleen controls *T. gondii* infection (Zorgi et al., 2016). Meanwhile, an important feature of intracellular pathogenic infection is that it causes the host spleen-specific T cells to proliferate rapidly and secrete a variety of functional cytokines. *T. gondii* infection often causes host T cell proliferation, mediates cytotoxicity and produces cytokines, such as TNF-α and IFN-γ, which plays an important part in anti-*T. gondii* infection (Landrith et al., 2015; Ochiai et al., 2016).

A growing number of studies have proven that high expression of immunosuppressive receptors PD-1 and TIM-3 in host spleen T cells during *T. gondii* infection is related to the inhibition of T cells effector function and reactivation of life-threatening toxoplasmic encephalitis (Bhadra et al., 2012; Wu et al., 2013). It was found that the expression of Tim-3 is positively correlated with IFN-γ, which plays a key part in the protective immunity against *T. gondii* infection (Berrocal Almanza et al., 2013). In addition, blocking PD-1 pathway can significantly restore T cell function and improve the survival rate of mice infected with *T. gondii* (Xiao et al., 2018). Therefore, to determine whether other immunosuppressive receptors are involved in the process of *T. gondii* infection and how they affect infection, it is very important to fully understand the mechanism of T cell immune function exhaustion caused by *T. gondii* infection. Identification of other immunosuppressive receptors is essential for understanding the correlation between T cell depletion and *T. gondii* infection.

TIGIT is a new member of the CD28 family, which can be expressed on almost all T cell subsets (except $CD4^+$ naive memory T cells) and NK cells (Solomon and Garrido-Laguna, 2018). TIGIT interacts with CD155 (PVR: poliovirus receptor), CD112 (PVRL2), CD113, and CD226 (DNAM-1) to regulate the immune responses of T cells and NK cells. As the main ligand of TIGIT, CD155 is expressed on the surface of non-hematopoietic cells and is a common ligand shared with the costimulatory molecule CD226. CD226 and TIGIT can competitively bind CD155, with TIGIT inhibiting the activation of T cells, and CD226 promoting the activation of T cells; thus, CD226 and TIGIT play opposite immunological functions and jointly regulate the dynamic balance of human immune function (Bottino et al., 2003; Johnston et al., 2014). Studies have shown that tumors, and viral and parasitic infections can upregulate the expression of TIGIT on T cells in the host spleen, which has a negative correlation with immune function (Johnston et al., 2014; Vendrame et al., 2020; Zhang et al., 2020; Wang et al., 2021). However, how chronic *T. gondii* infection regulates TIGIT expression on splenic T cells and its correlation with T cell function has not been reported.

In this study, our purpose was to study TIGIT expression on splenic T cells and the functional changes in spleen T cells during chronic *T. gondii* infection.

MATERIALS AND METHODS

Mice and Parasites

The PRU strain (type II, low virulence strain) of *T. gondii* used in this study was preserved by the Xinxiang Key Laboratory of Pathogenic Biology, Xinxiang Medical University (Henan, China). The *T. gondii* PRU strain was preserved in C57BL/6 mice by cyst passage. Male C57BL/6 mice (7–8 weeks old) were purchased from Beijing Vital River Experimental Animal Technology Co., Ltd. (Beijing, China) and kept in a specific pathogen-free facility.

T. gondii Infection

To detect the changes in TIGIT expression on and function in splenic T cells post infection, 280 mice were randomly divided into two groups. One group was challenged with 10 PRU cysts by oral administration (infection group), and the other group was treated with a phosphate-buffered saline (PBS) solution (control group).

Harvest and Preservation of the Spleen

Mice were sacrificed at 0, 1, 3, 6, 9, and 12 weeks post infection (n = 10 per group). Mouse spleens were removed aseptically to determine spleen index, and then five spleens were ground into powder by liquid nitrogen and frozen at −80°C for DNA and RNA acquisition. The other five spleens were fixed, sectioned and stained with hematoxylin and eosin (H&E), and then evaluated for the extent of tissue damage.

Splenic Mononuclear Cells Preparation

Our previous research procedure was applied to obtain splenic mononuclear cells (SMCs; Wang et al., 2021). The spleen was crushed and filtered through 200 mesh nylon net. Then use the lymphocyte separation solution to collect the middle lymphocytes at the interface, the lymphocytes were washed twice, counted and stored.

Flow Cytometry

SMCs were incubated with FcR Blocking Reagent to block non-specific immunoglobulin binding to Fc receptors, and then cell-surface molecules were stained. Next, the cells were fixed and permeabilized with the FIX&PERM Kit, and further intracellular staining was performed. Cells were incubated with specific antibodies or isotype controls, according to the manufacturer's guidelines. Antibodies for surface staining were consistent with those reported in our previous research (Wang et al., 2021). The antibodies for intracellular staining antibody were as follows: anti-Granzyme B (anti-human/mouse PE, BioLegend), anti-Perforin (anti-mouse PE, BioLegend), Granzyme B κ Isotype Ctrl (Mouse IgG1 PE, BioLegend), and Perforin κ Isotype Ctrl (Rat IgG2a PE, BioLegend).

The isotype controls were used to define positive cells and determine the corresponding gate. Under the same application settings, all flow cytometry samples were detected and analyzed on a CytoFLEX (Beckman Coulter, Brea, CA, United States) with CytExpert 2.1 software.

Quantitative Real-Time PCR

Total RNA or DNA was extracted from spleens using TRIzol reagent (Yi Fei Xue Biotechnology, Nanjing, China) or a Tissue DNA kit (OMEGA, Zhengzhou, China), and then RNA was converted into first-strand cDNA. The real-time PCR (RT-PCR) was run on a QuantStudio™ 5 (Applied Biosystems, Foster City, CA, United States) with SYBR qPCR Master Mix as described previously (Wang et al., 2021). The primer information used herein is shown in **Table 1**. The DNA samples were used for the detection of TgB1 gene represents the parasite load, which were normalized for the mouse beta-actin-1 primers (Bhadra et al., 2011). The mRNA expression levels of target genes, such as TIGIT, were normalized to those of the mouse beta-actin-2 primers. Relative expression levels were calculated by the $2^{-\triangle\triangle Ct}$ method.

Data Analysis

Statistical analysis was performed using SPSS 20 software for Windows (SPSS Inc., Chicago, IL, United States). The differences between the two groups were compared by Student's *t* test, and those among multiple groups were compared by one-way ANOVA. A value of $p < 0.05$ was considered as statistically significant.

RESULTS

Histopathological Changes in the Spleen Were Positively Correlated With the *T. gondii* Parasite Load

The relative expression of TgB1 in mice spleens increased sharply beginning in the 1st week post infection, until it was downregulated compared with the control group at the 6th week after infection (**Figure 1A**). Meanwhile, the spleen of mice rapidly enlarged from 1 week post infection, and the spleen index increased sharply and reached the peak at the 3rd week after infection (**Figure 1B**). Through H&E staining of spleen sections, we observed that there were no obvious

TABLE 1 | Sequences of the primers used in this study.

Gene	Primer sequence	Target gene length
TgB1		
Sense primer	5'TCCCCTCTGCTGGCGAAAAGT3'	97 bp
Antisense primer	5'AGCGTTCGTGGTCAACTATCGATTG3'	
Mouse beta-actin[#]		
Sense primer	5'TCACCCACACTGTGCCCATCTACGA3'	295 bp
Antisense primer	5'CAGCGGAACCGCTCATTGCCAATGG3'	
TIGIT		
Sense primer	5'GGCATGTCGCTTCAGTCTTC3'	139 bp
Antisense primer	5'CTCCCCTTGTAAATCCCACC3'	
CD226		
Sense primer	5'ACCACATGGCTTTCTTGCTC3'	112 bp
Antisense primer	5'CAGCATGAGAGTTGGACCAG3'	
IL-2		
Sense primer	5'CAAGCAGGCCACAGAATTGA 3'	80 bp
Antisense primer	5'GAGTCAAATCCAGAACATGCCG3'	
IL-12		
Sense primer	5'CTTAGCCAGTCCCGAAACCT3'	144 bp
Antisense primer	5'ACAGGTCTTCAATGTGCTGGT3'	
IFN-γ		
Sense primer	5'TCAAGTGGCATAGATGTGGAAGAA3'	267 bp
Antisense primer	5'CTGGACCTGTGGGTTGTTGA3'	
TNF-α		
Sense primer	5'AGCCGATGGGTTGTACCTTG3'	99 bp
Antisense primer	5'ATAGCAAATCGGCTGACGGT3'	
Perforin		
Sense primer	5'GAGAAGACCTATCAGGACCA3'	167 bp
Antisense primer	5'AGCCTGTGGTAAGCATG3'	
Granzyme B		
Sense primer	5'CCTCCTGCTACTGCTGAC 3'	174 bp
Antisense primer	5'GTCAGCACAAAGTCCTCTC3'	
Mouse beta-actin[##]		
Sense primer	5'GATGCAGAAGGAGATTACTG3'	91 bp
Antisense primer	5'ACCGATCCACACAGAGTA3'	

[#]*Indicates mouse beta-actin-1 primers in manuscript.*
[##]*Indicates mouse beta-actin-2 primers in manuscript.*

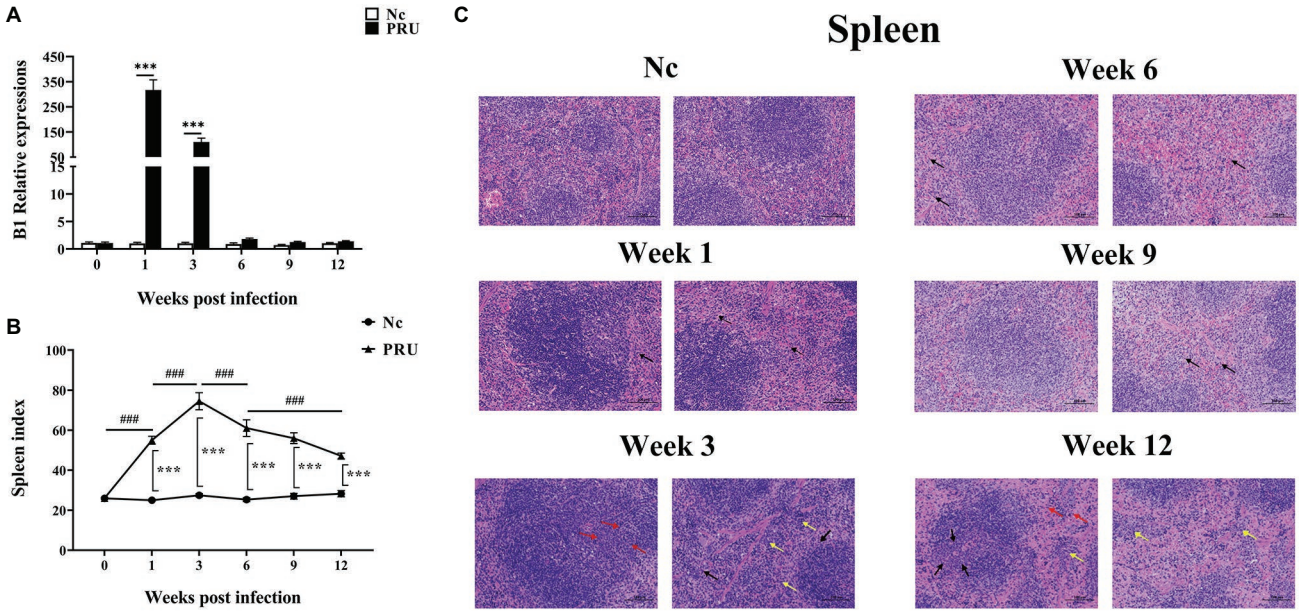

FIGURE 1 | Dynamic pathological changes in the spleen during chronic *Toxoplasma gondii* infection. **(A)** Relative expression of TgB1in the spleen at 0, 1, 3, 6, 9, and 12 weeks post infection in the spleen. **(B)** Spleen index values of the PRU and Nc groups. The results are representative of three independent experiments with five mice per group per experiment; with data denoting means ± SDs; **(C)** H&E staining of spleen sections at different time points post infection. $^{***,\#\#\#}p < 0.001$, *Indicates comparison with the control group. #Indicates comparison with other time points. The black arrow indicates neutrophil infiltration in the red pulp, the yellow arrow indicates extramedullary hematopoietic cell infiltration, and the red arrow indicates extramedullary hematopoietic cell proliferation.

pathological changes in the spleen in the 1st week post infection, only a small number of neutrophils were found in the red pulp, and at the 3rd week after infection, more neutrophils infiltration and a small number of extramedullary hematopoietic cells could be seen in the splenic red pulp. Local lymphocytes in white pulp decreased and extramedullary hematopoietic cells proliferated. At the 6th and 9th week after infection, the spleen returned to normal, with only a small number of neutrophils scattered in the red pulp, and at the 12th week after infection, the red and white pulp of the spleen was clearly demarcated, the number of lymphocytes in the red pulp decreased and the cells arranged loosely, and a small number of extramedullary hematopoietic cells were observed, and extramedullary hematopoietic cells eroded the white pulp, and a small number of neutrophils were scattered in the red pulp (**Figure 1C**). The results showed that *T. gondii* proliferated in the spleen during the first 3 weeks after infection, resulting in pathological enlargement of the spleen and immune function, thus eliminating *T. gondii*. At the 6th week after infection, *T. gondii* in the spleen was cleared and the spleen returned to normal.

TIGIT Expression on Splenic T Cells Was Specifically Upregulated by Chronic *T. gondii* Infection

As shown in **Figure 2**, compared with the Nc (normal control) group, TIGIT expression on splenic $CD4^+$ T cells of mice was significantly upregulated from the 1st week after PRU cyst infection to the 12th week after infection ($p < 0.01$). Similarly, the proportion of splenic $TIGIT^+CD8^+$ T cells of the infected group did not change significantly only at the 6th week after infection but was higher than that of the Nc group at other time points ($p < 0.01$).

CD226 Expression on Splenic T Cells Was Specifically Regulated by Chronic *T. gondii* Infection

CD226 expression on splenic T cells of mice was significantly downregulated in the 1st week after PRU cyst infection (**Figure 3A**). In addition, except that there was no prominent change in the proportion of $CD226^+CD4^+$ T cells at the 12th week after infection, CD226 expression on splenic T cells was notably higher than that of the control group since the 3rd week after infection (**Figure 3B**).

$TIGIT^+$ T_{EM} Cells Were Triggered by Chronic *T. gondii* Infection

Among the memory T cells, T_{CM} (central memory T cells) and T_{EM} (effector memory T cells) are important T cell subsets that play immune-protective roles in the host infected by intracellular pathogens. We labeled the surface of T cells with antibodies of against CD44 and CD62L and classified splenic memory T cells into four subtypes of T_{CM} ($CD44^+CD62L^+$), T_{EM} ($CD44^+CD62L^-$), T_{naive} ($CD44^-CD62L^+$), and T_{EMRA} ($CD44^-CD62L^-$). The subsets of splenic $TIGIT^+$ memory T cells were analyzed. As shown in **Figure 4**, the results were consistent with those of our previous studies on *T. gondii*

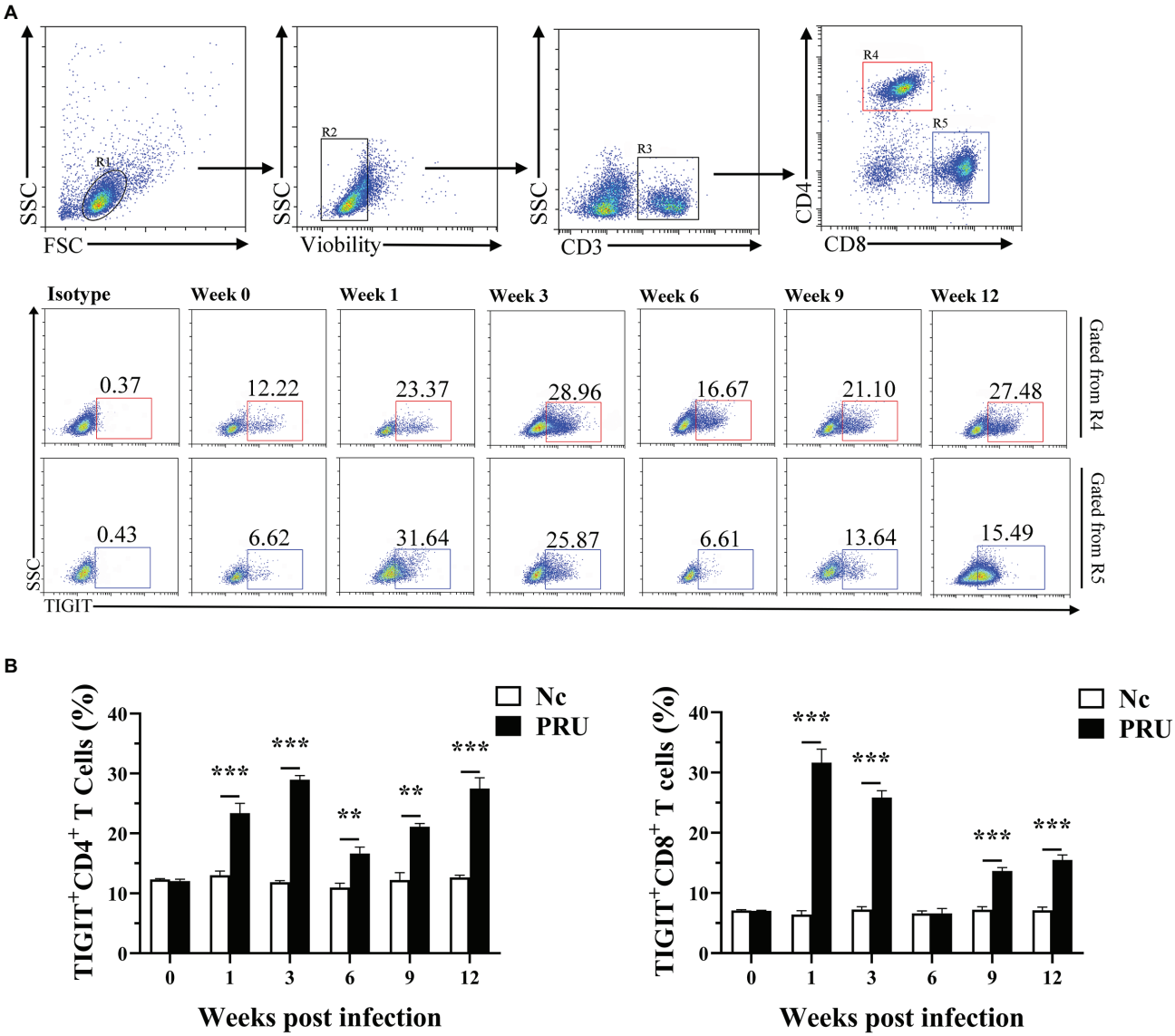

FIGURE 2 | Changes in TIGIT expression on T cells in spleen after *T. gondii* infection. **(A)** Proportions of TIGIT⁺ cells among CD4⁺ and CD8⁺ T cells in *T. gondii*-infected (PRU) and normal mice (Nc) after infection. **(B)** Dynamic changes in the percentages of TIGIT⁺ T cells at different time points. The results are representative of three independent experiments with five mice in each group per experiment, with data denoting means ± SDs. $^{**}p < 0.01$ and $^{***}p < 0.001$ (compared to the control).

infection with RH tachyzoites. The specific memory TIGIT⁺ T cell subsets in *T. gondii* infection were mainly T_{CM} and T_{EM} cells. Except for 6 weeks after infection, part of the specific TIGIT⁺CD4⁺ T cells of *T. gondii* in the spleen of the PRU group were activated and transformed into T_{EM}. Additionally, *T. gondii* specific memory TIGIT⁺CD8⁺ T cell subsets changed correspondingly at all the time points.

The Cytotoxicity of TIGIT⁺ T Cells Decreased During Chronic *T. gondii* Infection

As shown in **Figure 5**, the expression of Perforin (Prf1) and Granzyme B (Gzmb) in the spleen TIGIT⁺ T cells of mice infected with PRU cysts was significantly upregulated at the 1st week post infection ($p < 0.01$). The expression of both Prf1 and Gzmb in TIGIT⁺CD4⁺ T cells decreased from the 3rd week after infection to no significant difference from that in the Nc group, while Prf1 expression in TIGIT⁺CD8⁺ T cells was always higher than that in the Nc group ($p < 0.05$). Gzmb expression in TIGIT⁺CD8⁺ T cells remained higher than that in the control group until it returned to normal level at the 12th week after infection. The results showed that chronic toxoplasmosis is controlled by normal cytotoxicity of host T cells in the early stage, but the cytotoxic effect of TIGIT⁺T cells was weakened with persistent infection.

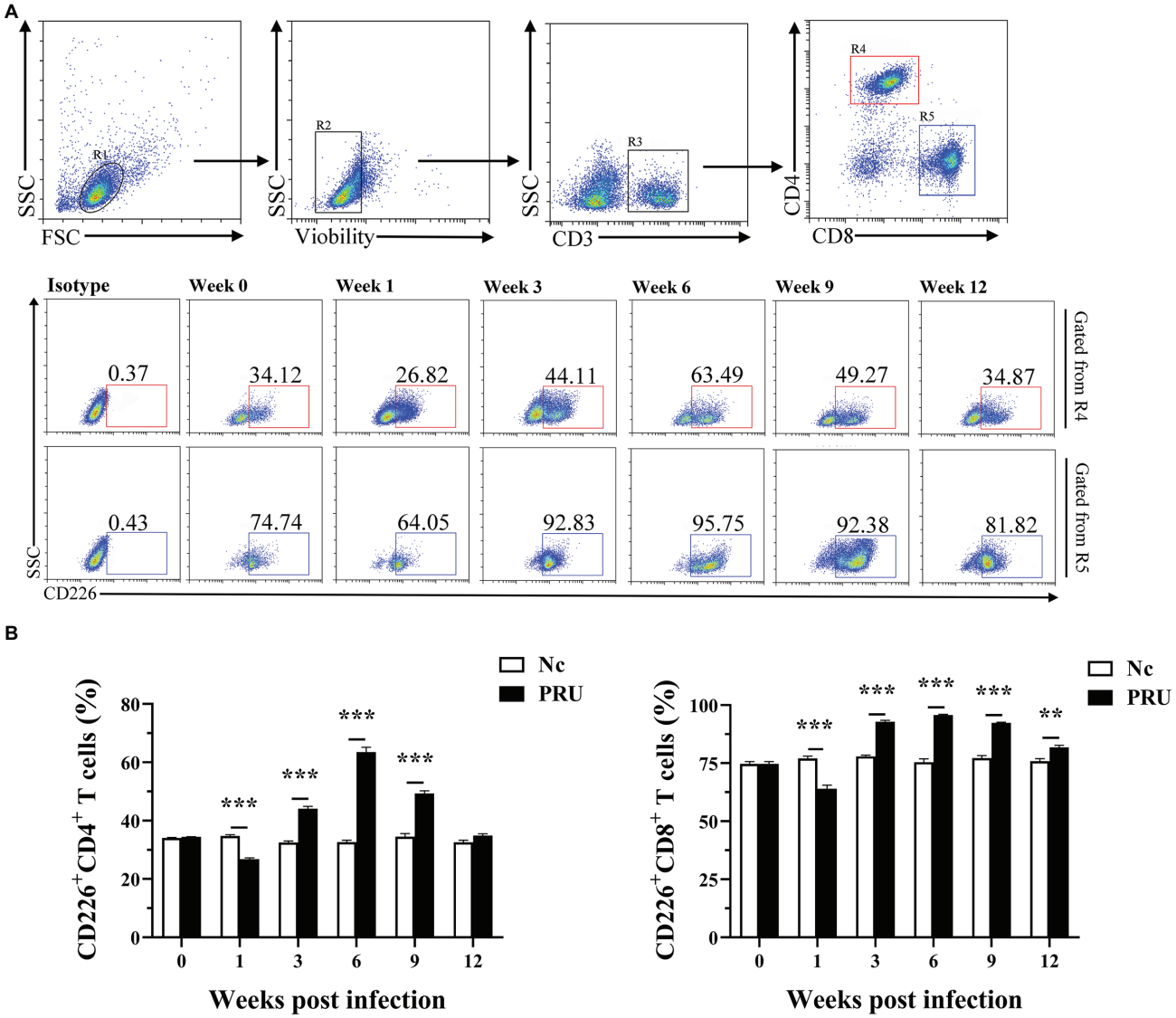

FIGURE 3 | Changes in CD226 expression on T cells in spleen after *T. gondii* infection. **(A)** Proportions of CD226$^+$ cells among CD4$^+$ and CD8$^+$ T cells in *T. gondii*-infected (PRU) and normal mice (Nc) after infection. **(B)** Dynamic changes in the percentages of CD226$^+$ T cells at different time points. The results are representative of three independent experiments with five mice in each group per experiment, with data denoting means ± SDs. $^{**}p < 0.01$ and $^{***}p < 0.001$ (compared to the control).

TIGIT, CD226, Perforin, Granzyme B, IL-2, IL-12, IFN-γ, and TNF-α mRNA Expression in the Spleen

As shown in **Figure 6**, compared with those in the control group, TIGIT mRNA expression in spleen was prominently upregulated at the 1st and 12th week post infection ($p < 0.01$), and the mRNA level of TIGIT was prominently downregulated at the 3rd and 9th week post infection ($p < 0.01$). Additionally, CD226 mRNA expression in spleen increased significantly in the 1st week post infection ($p < 0.01$) and decreased significantly at other time points ($p < 0.01$). On the contrary, Prf1 mRNA expression decreased significantly in the 1st week post infection ($p < 0.01$) and increased significantly at other time points ($p < 0.01$). Gzmb mRNA expression in spleen was significantly higher than that in the Nc group only at the 1st and 12th week after infection ($p < 0.01$), and markedly lower than that in the Nc group at other time points ($p < 0.01$). The expression of inflammatory factor IL-2 in spleen decreased significantly from 1 to 3 weeks post infection ($p < 0.01$), and the expression of IL-2 was markedly higher than that in Nc group at 6 and 12 weeks post infection ($p < 0.01$). IL-12 mRNA expression was markedly lower than that in the Nc group ($p < 0.01$) and remained until the 12th week after infection. The expression of IFN-γ was significantly downregulated from 1 to 9 weeks after infection and returned to normal at the 12th week after infection ($p < 0.01$). Furthermore, different from IFN-γ, the expression of TNF-α had no significant difference in the 1st week after infection.

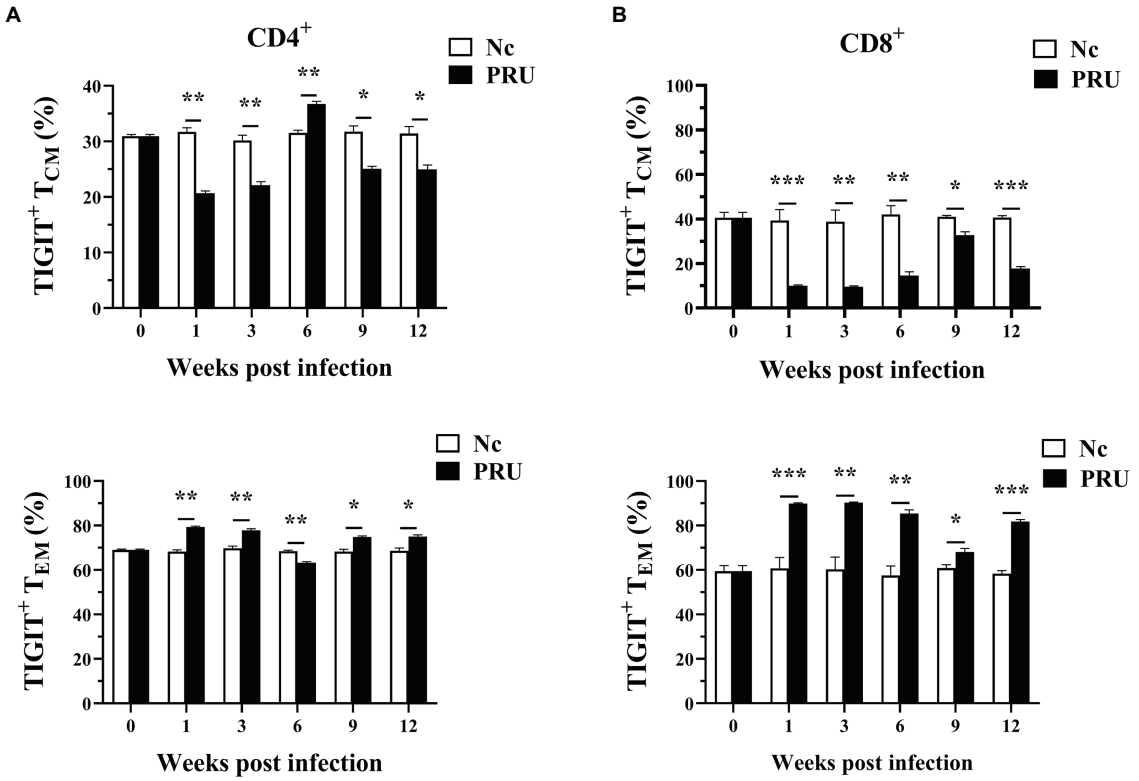

FIGURE 4 | Relative contributions of memory splenic T cell subsets to TIGIT⁺ T cells after *T. gondii* infection. **(A)** Dynamic changes in memory T cell subsets of TIGIT⁺CD4⁺ T cells in the spleen at different time points following PRU infection. **(B)** Dynamic changes in memory T cell subsets of TIGIT⁺CD8⁺ T cells in the spleen at different time points following PRU infection. The results are representative of three independent experiments with five mice in each group per experiment, with data denoting means ± SDs. *$p < 0.05$, **$p < 0.01$, and ***$p < 0.001$ (compared to the control).

DISCUSSION

TIGIT can participate in splenic immune responses induced in many chronic infectious diseases (Wykes and Lewin, 2018; Blazkova et al., 2021). Virological studies showed that the proportion of TIGIT⁺CD8⁺ T cells were increased significantly in HIV patients, which was positively correlated with plasma viral load and disease progression. After treatment with an anti-TIGIT monoclonal antibody, the secretion of IFN-γ from HIV-specific NK cells and CD8⁺ T cells was significantly increased. Double blockade of the TIGIT and PD-L1 pathways could significantly improve the ability of T cells to produce IL-2, thus prominently enhancing HIV-specific CD8⁺ T cell proliferation. It is suggested that TIGIT can be used as a potential target for immunotherapy in the treatment of HIV infection (Chew et al., 2016; Yin et al., 2018; Vendrame et al., 2020). Yasuma et al. found that the HBZ protein expressed by human T-cell leukemia virus type 1 (HTLV-1) can induce an increase in TIGIT expression and inhibit the transcription of the CD226 gene, which further enhances the inhibitory function of TIGIT. In addition, a large amount of TIGIT enhances the transcription of IL-10, allowing infected cells to escape being clearance by the immune system (Yasuma et al., 2016). The proportion of TIGIT⁺ T cells in peripheral blood of hepatitis B virus (HBV)-associated hepatocellular carcinoma (HBV-HCC) patients was significantly higher than that in healthy blood donors and hepatitis B virus (HBV)-associated liver cirrhosis (HBV-LC) patients, and the number of TIGIT⁺CD8⁺ T cells was positively correlated with tumor recurrence, tumor invasion and mortality of HBV-HCC, and higher frequency of TIGIT⁺CD8⁺ T cells was more closely related to poor prognosis of HBV-HCC than that of TIGIT⁺CD4⁺ T cells (Liu et al., 2019). In addition, TIGIT on T cell surface was found to be significantly upregulated in patients with lymphocytic choriomeningitis virus (LCMV) or human papilloma virus (HPV) infection (Gameiro et al., 2018; Schorer et al., 2020).

In the field of parasitology, Zhang et al. (2019b) proved that TIGIT expression on the surface of CD4⁺ and CD8⁺ T cells was upregulated in patients with alveolar echinococcosis, and that higher levels of Gzmb were present in TIGIT⁻CD8⁺ T cells rather than in TIGIT⁺CD8⁺ T cells. *Plasmodium yoelii* infection can induce an increase in TIGIT expression on splenic CD4⁺ T cells in mice (Villegas-Mendez et al., 2016). Additionally, blocking the TIM-3 pathway can lead to a compensatory increase in the expression of TIGIT in mice, resulting in the death of infected mice (Zhang et al., 2019a). *Schistosoma japonicum* egg antigen can increase TIGIT expression on CD4⁺ T cells, and the expression of TIGIT can enhance the proliferation of the Th2 cells, thus enhancing

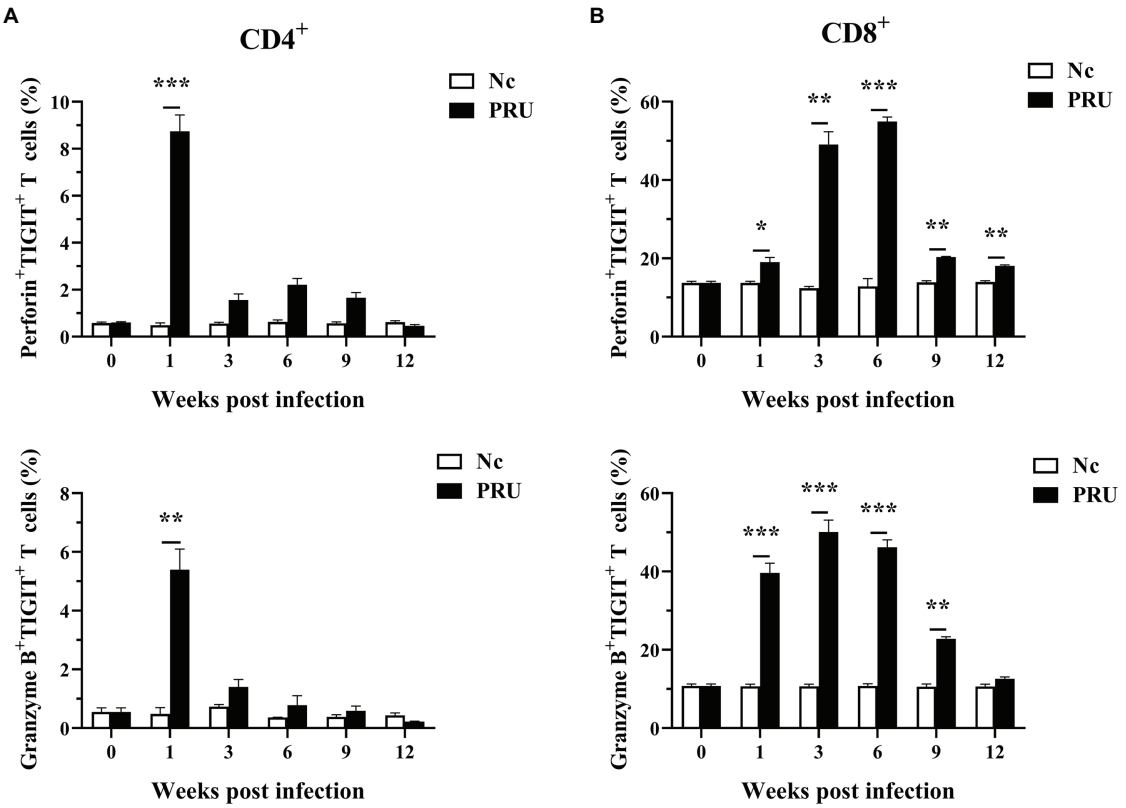

FIGURE 5 | Cytotoxic activity of TIGIT⁺ T cells in spleen after *T. gondii* infection. **(A)** Dynamic changes in TIGIT⁺CD4⁺ T cell cytotoxicity in the spleen of mice chronically infected with *T. gondii*. **(B)** Dynamic changes of TIGIT⁺CD8⁺ T cell cytotoxicity in the spleen of mice chronically infected with *T. gondii*. The results are representative of three independent experiments with five mice in each group per experiment, with data denoting means ± SDs. $^{*}p < 0.05$, $^{**}p < 0.01$, and $^{***}p < 0.001$ (compared to the control).

Th2 immune response in infected mice (Li-Na et al., 2018). In addition, our previous study showed that selective TIGIT expression on host splenic T cells could be induced by acute infection with *T. gondii* virulent strain (RH) tachyzoites, and that an increase in the proportion of T_{EM} subtypes in TIGIT⁺T cells could be observed (Wang et al., 2021). However, TIGIT expression on splenic immune cells of mice chronically infected with *T. gondii* cysts and its effect on immune function are not clearly characterized.

This study found that, different from our previous studies on acute *T. gondii* infection, *T. gondii* could be detected in the spleen from 1 to 3 weeks post infection, and TIGIT expression on T cells was significantly upregulated. However, with the formation of cysts in the tissue, the pathological sections showed that the spleen returned to normal at the 6th week after infection, and the spleen exerted its immune function and cleared the free *T. gondii* in the spleen. TIGIT expression on splenic CD8⁺ T cells returned to the normal level, but the expression of TIGIT in spleen increased again 9 weeks after infection, which may be related to the partial activation of *T. gondii* in mice. At the same time, compared with the control group, CD226 expression on splenic T cells was significantly downregulated only in the 1st week after infection, which was negatively correlated with the expression of TIGIT. However, with the formation of chronic toxoplasmosis, the immune system is gradually disordered, the mutual antagonism between them disappears, and the expression on T cells is significantly upregulated, which may be due to the existence of other modes of action between TIGIT and CD226 expressed during *T. gondii* infection, which need to be further studied.

The relative changes in T cell subsets in patients with pathogen infection affect T cell immune function and disease occurrence and development (Schlüter et al., 2002; Mueller et al., 2013). Research has shown that high expression of TIGIT in memory cell subsets of CD4⁺ T cells in patients with acute HCV infection, and the expression of TIGIT was the highest in effector memory T cells and the lowest in initial memory T cells, but TIGIT expression was relatively stable in T_{CM} and T_{EMRA} subsets (Ackermann et al., 2019). Therefore, we analyzed the changes of the proportions of specific TIGIT⁺ T cell subsets during *T. gondii* cysts infection by evaluating CD44 and CD62L. Similar to our previous studies, TIGIT⁺ T cells in mouse spleen were mainly divided into T_{CM} and T_{EM} after *T. gondii* cysts infection. Furthermore, studies have shown that continuous antigen stimulation can lead to the activation of T_{CM} cells to produce T_{EM} subsets during chronic parasite infection, and that long-term antigen stimulation

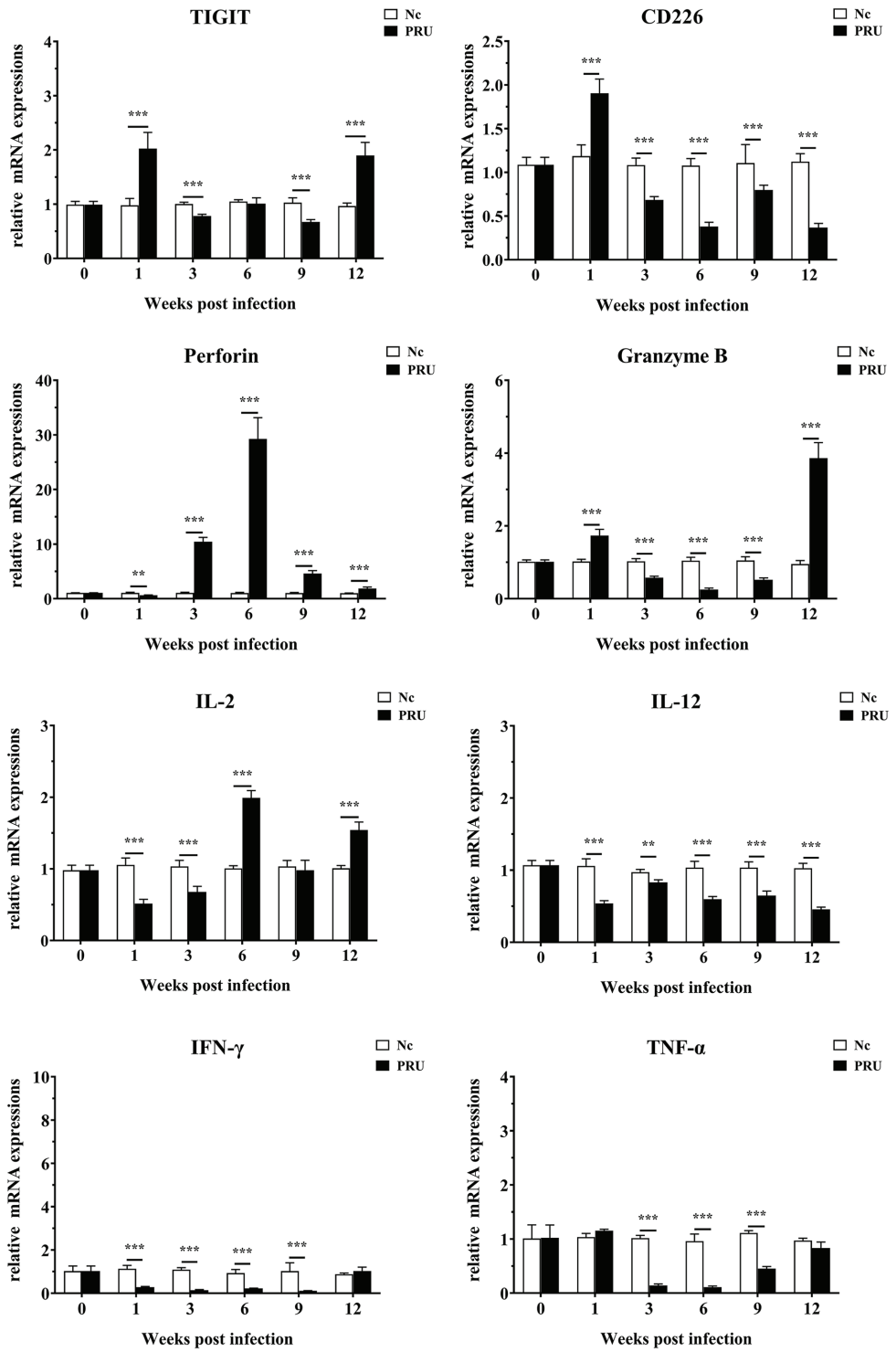

FIGURE 6 | mRNA expression of multiple transcripts in spleens from mice infected with the *T. gondii* PRU strain, as assessed by quantitative real-time PCR (qRT-PCR). Values are shown as the means of triplicate measurements, with data denoting means ± SDs; three independent experiments were performed with five mice per group. $^{**}p < 0.01$ and $^{***}p < 0.001$ (compared to the control).

keeps the working intensity of memory T cells at a high level, resulting in T cell functional exhaustion. In this study, spleen $CD8^+TIGIT^+$ T_{CM} cells was activated and transformed into $CD8^+TIGIT^+$ T_{EM} cells during infection. Similarly, except for the 6th week after infection, $CD4^+TIGIT^+$ T cells also had the same changes, indicating that *T. gondii* infection stimulated

the host TIGIT$^+$ T_{EM} cells to proliferate, migrate to the inflammatory surrounding tissue, and produce cytokines to control *T. gondii* infection.

Prf1 and Gzmb, as the main factors mediating the cytotoxicity of T cells, can kill infected cells from in a host and have an important effect on T cells defending against *T. gondii* infection (Yamada et al., 2011; Suzuki, 2020). In addition, the perforin dependent cytotoxic ability of T cell is involved in restricting the parasite to chronic state (Suzuki et al., 2010). Therefore, we detected the expression of Prf1 and Gzmb in TIGIT$^+$ T cells. The results showed that cytotoxicity of splenic TIGIT$^+$ T cells increased prominently in the early-stage infection of *T. gondii* cysts, but decreased in varying degrees after the stable existence of *T. gondii* cysts, indicating that the change of cytotoxicity of splenic TIGIT$^+$ T cells may be related to the formation and rupture of *T. gondii* cysts.

We further detected the changes in TIGIT gene transcriptional expression at the overall level in spleen during infection and found that it was significantly up-regulated in the 1st week after infection, then downregulated, and upregulated again in the 12th week after infection, when the spleen sections also showed abnormal pathological changes. At the same time, Gzmb also showed the same dynamic expression changes as TIGIT. However, the expressions of IL-12, IFN-γ, and TNF-α were not upregulated, suggesting the immune function has not been brought into full play. However, the effect of TIGIT on the proliferative activity of *T. gondii* specific T cells and its expression on other immune cells such as Treg and NK cells during *T. gondii* infection are not clear, and the changes of immune function of host splenic T cells by blocking the TIGIT pathway need to be further investigated.

CONCLUSION

This study shows that chronic infection of *T. gondii* cysts can increase the TIGIT expression in host splenic T cells, stimulate the host TIGIT$^+$ T_{EM} cells to proliferate, and weaken the cytotoxicity of TIGIT$^+$ T cells. Therefore, TIGIT is expected to be a therapeutic target for chronic *T. gondii* infection and provides new insights into prevention and treatment of *T. gondii* infection.

DATA AVAILABILITY STATEMENT

The raw data supporting the conclusions of this article will be made available by the authors, without undue reservation, to any qualified researcher.

ETHICS STATEMENT

All animal experiments were reviewed and approved by the Ethics Committee of Xinxiang Medical University.

AUTHOR CONTRIBUTIONS

SW, XL, and MW: conceptualization and methodology. HL, CS, and JZ: formal analysis and investigation. HL, XT, and JZ: data curation. HL, JZ, XT, and XM: data curation. HL: writing – original draft preparation. ZZ, MW, XL, and SW: writing – review and editing. MW, XL, and SW: funding acquisition. All authors contributed to the article and approved the submitted version.

FUNDING

The current work received the support from the National Natural Science Foundation of China (no. 81702025), the Science and Technology Planning Project of Henan Province (no. 212102310749), the Henan University Science and Technology Innovation Team Support Program (20IRTSTHN030), and the Outstanding Youth Project of Henan Natural Science Foundation (212300410013).

REFERENCES

Ackermann, C., Smits, M., Woost, R., Eberhard, J. M., Peine, S., Kummer, S., et al. (2019). HCV-specific CD4$^+$ T cells of patients with acute and chronic HCV infection display high expression of TIGIT and other co-inhibitory molecules. *Sci. Rep.* 9:10624. doi: 10.1038/s41598-019-47024-8

Alday, P. H., and Doggett, J. S. (2017). Drugs in development for toxoplasmosis: advances, challenges, and current status. *Drug Des. Devel. Ther.* 11, 273–293. doi: 10.2147/dddt.S60973

Berrocal Almanza, L. C., Muñoz, M., Kühl, A. A., Kamradt, T., Heimesaat, M. M., and Liesenfeld, O. (2013). Tim-3 is differently expressed in genetically susceptible C57BL/6 and resistant BALB/c mice during oral infection with *Toxoplasma gondii*. *Eur. J. Microbiol. Immunol.* 3, 211–221. doi: 10.1556/EuJMI.3.2013.3.10

Bhadra, R., Gigley, J. P., and Khan, I. A. (2012). PD-1-mediated attrition of polyfunctional memory CD8$^+$ T cells in chronic toxoplasma infection. *J. Infect. Dis.* 206, 125–134. doi: 10.1093/infdis/jis304

Bhadra, R., Gigley, J. P., Weiss, L. M., and Khan, I. A. (2011). Control of *Toxoplasma* reactivation by rescue of dysfunctional CD8$^+$ T-cell response via PD-1-PDL-1 blockade. *Proc. Natl. Acad. Sci. U. S. A.* 108, 9196–9201. doi: 10.1073/pnas.1015298108

Blazkova, J., Huiting, E. D., Boddapati, A. K., Shi, V., Whitehead, E. J., Justement, J. S., et al. (2021). TIGIT expression on CD8$^+$ T cells correlates with higher cytotoxic capacity. *J. Infect. Dis.* jiab155. doi: 10.1093/infdis/jiab155 [Epub ahead of print]

Bottino, C., Castriconi, R., Pende, D., Rivera, P., Nanni, M., Carnemolla, B., et al. (2003). Identification of PVR (CD155) and nectin-2 (CD112) as cell surface ligands for the human DNAM-1 (CD226) activating molecule. *J. Exp. Med.* 198, 557–567. doi: 10.1084/jem.20030788

Chew, G. M., Fujita, T., Webb, G. M., Burwitz, B. J., Wu, H. L., Reed, J. S., et al. (2016). TIGIT marks exhausted T cells, correlates with disease progression, and serves as a target for immune restoration in HIV and SIV infection. *PLoS Pathog.* 12:e1005349. doi: 10.1371/journal.ppat.1005349

Fisch, D., Clough, B., and Frickel, E. M. (2019). Human immunity to *Toxoplasma gondii*. *PLoS Pathog.* 15:e1008097. doi: 10.1371/journal.ppat.1008097

Gameiro, S. F., Ghasemi, F., Barrett, J. W., Koropatnick, J., Nichols, A. C., Mymryk, J. S., et al. (2018). Treatment-naïve HPV+ head and neck cancers display a T-cell-inflamed phenotype distinct from their HPV- counterparts that has implications for immunotherapy. *Onco. Targets. Ther.* 7:e1498439. doi: 10.1080/2162402X.2018.1498439

Johnston, R. J., Comps-Agrar, L., Hackney, J., Yu, X., Huseni, M., Yang, Y., et al. (2014). The immunoreceptor TIGIT regulates antitumor and antiviral CD8$^+$ T cell effector function. *Cancer Cell* 26, 923–937. doi: 10.1016/j.ccell.2014.10.018

Landrith, T. A., Harris, T. H., and Wilson, E. H. (2015). Characteristics and critical function of CD8+ T cells in the *Toxoplasma*-infected brain. *Semin. Immunopathol.* 37, 261–270. doi: 10.1007/s00281-015-0487-3

Li-Na, Z., Xiao-Fan, W., Qian-Qian, Q., Li-Yang, D., Lei, X., Ya-Nan, P., et al. (2018). Study on role of TIGIT signal in Th1/Th2 balance in *Schistosoma japonicum*-infected mice. *Zhongguo Xue Xi Chong Bing Fang Zhi Za Zhi* 30, 136–139. doi: 10.16250/j.32.1374.2017233

Liu, X., Li, M., Wang, X., Dang, Z., Jiang, Y., Wang, X., et al. (2019). PD-1$^+$ TIGIT$^+$ CD8$^+$ T cells are associated with pathogenesis and progression of patients with hepatitis B virus-related hepatocellular carcinoma. *Cancer Immunol. Immunother.* 68, 2041–2054. doi: 10.1007/s00262-019-02426-5

Montoya, J. G., and Liesenfeld, O. (2004). Toxoplasmosis. *Lancet* 363, 1965–1976. doi: 10.1016/S0140-6736(04)16412-X

Mueller, S. N., Gebhardt, T., Carbone, F. R., and Heath, W. R. (2013). Memory T cell subsets, migration patterns, and tissue residence. *Annu. Rev. Immunol.* 31, 137–161. doi: 10.1146/annurev-immunol-032712-095954

Ochiai, E., Sa, Q., Perkins, S., Grigg, M. E., and Suzuki, Y. (2016). CD8$^+$ T cells remove cysts of *Toxoplasma gondii* from the brain mostly by recognizing epitopes commonly expressed by or cross-reactive between type II and type III strains of the parasite. *Microbes Infect.* 18, 517–522. doi: 10.1016/j.micinf.2016.03.013

Pinto-Ferreira, F., Caldart, E. T., Pasquali, A. K. S., Mitsuka-Breganó, R., Freire, R. L., and Navarro, I. T. (2019). Patterns of transmission and sources of infection in outbreaks of human toxoplasmosis. *Emerg. Infect. Dis.* 25, 2177–2182. doi: 10.3201/eid2512.181565

Schlüter, D., Meyer, T., Kwok, L. Y., Montesinos-Rongen, M., Lütjen, S., Strack, A., et al. (2002). Phenotype and regulation of persistent intracerebral T cells in murine *Toxoplasma encephalitis*. *J. Immunol.* 169, 315–322. doi: 10.4049/jimmunol.169.1.315

Schorer, M., Rakebrandt, N., Lambert, K., Hunziker, A., Pallmer, K., Oxenius, A., et al. (2020). TIGIT limits immune pathology during viral infections. *Nat. Commun.* 11:1288. doi: 10.1038/s41467-020-15025-1

Solomon, B. L., and Garrido-Laguna, I. (2018). TIGIT: a novel immunotherapy target moving from bench to bedside. *Cancer Immunol. Immunother.* 67, 1659–1667. doi: 10.1007/s00262-018-2246-5

Suzuki, Y. (2020). The immune system utilizes two distinct effector mechanisms of T cells depending on two different life cycle stages of a single pathogen, *Toxoplasma gondii*, to control its cerebral infection. *Parasitol. Int.* 76:102030. doi: 10.1016/j.parint.2019.102030

Suzuki, Y., Wang, X., Jortner, B. S., Payne, L., Ni, Y., Michie, S. A., et al. (2010). Removal of *Toxoplasma gondii* cysts from the brain by perforin-mediated activity of CD8+ T cells. *Am. J. Pathol.* 176, 1607–1613. doi: 10.2353/ajpath.2010.090825

Vendrame, E., Seiler, C., Ranganath, T., Zhao, N. Q., Vergara, R., Alary, M., et al. (2020). TIGIT is upregulated by HIV-1 infection and marks a highly functional adaptive and mature subset of natural killer cells. *AIDS* 34, 801–813. doi: 10.1097/QAD.0000000000002488

Villegas-Mendez, A., Inkson, C. A., Shaw, T. N., Strangward, P., and Couper, K. N. (2016). Long-lived CD4$^+$IFN-γ^+ T cells rather than short-lived CD4$^+$IFN-γ^+IL-10$^+$ T cells initiate rapid IL-10 production to suppress anamnestic T cell responses during secondary malaria infection. *J. Immunol.* 197, 3152–3164. doi: 10.4049/jimmunol.1600968

Wang, S., Li, H., Zhang, F., Jiao, Y., Xie, Q., Zhang, Z., et al. (2021). Expression of TIGIT in splenic and circulatory T cells from mice acutely infected with *Toxoplasma gondii*. *Parasite* 28:13. doi: 10.1051/parasite/2021010

Wu, B., Huang, B., Chen, Y., Li, S., Yan, J., Zheng, H., et al. (2013). Upregulated expression of Tim-3 involved in the process of Toxoplasmic encephalitis in mouse model. *Parasitol. Res.* 112, 2511–2521. doi: 10.1007/s00436-013-3416-1

Wykes, M. N., and Lewin, S. R. (2018). Immune checkpoint blockade in infectious diseases. *Nat. Rev. Immunol.* 18, 91–104. doi: 10.1038/nri.2017.112

Xiao, J., Li, Y., Yolken, R. H., and Viscidi, R. P. (2018). PD-1 immune checkpoint blockade promotes brain leukocyte infiltration and diminishes cyst burden in a mouse model of *Toxoplasma* infection. *J. Neuroimmunol.* 319, 55–62. doi: 10.1016/j.jneuroim.2018.03.013

Yamada, T., Tomita, T., Weiss, L. M., and Orlofsky, A. (2011). *Toxoplasma gondii* inhibits granzyme B-mediated apoptosis by the inhibition of granzyme B function in host cells. *Int. J. Parasitol.* 41, 595–607. doi: 10.1016/j.ijpara.2010.11.012

Yasuma, K., Yasunaga, J., Takemoto, K., Sugata, K., Mitobe, Y., Takenouchi, N., et al. (2016). HTLV-1 bZIP factor impairs anti-viral immunity by inducing co-inhibitory molecule, T cell immunoglobulin and ITIM domain (TIGIT). *PLoS Pathog.* 12:e1005372. doi: 10.1371/journal.ppat.1005372

Yin, X., Liu, T., Wang, Z., Ma, M., Lei, J., Zhang, Z., et al. (2018). Expression of the inhibitory receptor TIGIT is up-regulated specifically on NK cells with CD226 activating receptor from HIV-infected individuals. *Front. Immunol.* 9:2341. doi: 10.3389/fimmu.2018.02341

Zhang, Y., Jiang, N., Zhang, T., Chen, R., Feng, Y., Sang, X., et al. (2019a). Tim-3 signaling blockade with α-lactose induces compensatory TIGIT expression in *Plasmodium berghei* ANKA-infected mice. *Parasit. Vectors* 12:534. doi: 10.1186/s13071-019-3788-x

Zhang, C., Lin, R., Li, Z., Yang, S., Bi, X., Wang, H., et al. (2020). Immune exhaustion of T cells in alveolar echinococcosis patients and its reversal by blocking checkpoint receptor TIGIT in a murine model. *Hepatology* 71, 1297–1315. doi: 10.1002/hep.30896

Zhang, C., Shao, Y., Yang, S., Bi, X., Li, L., Wang, H., et al. (2019b). Author correction: T-cell tolerance and exhaustion in the clearance of *Echinococcus multilocularis*: role of inoculum size in a quantitative hepatic experimental model. *Sci. Rep.* 9:3424. doi: 10.1038/s41598-019-39975-9

Zorgi, N. E., Galisteo, A. J. Jr., Sato, M. N., do Nascimento, N., and de Andrade, H. F. Jr. (2016). Immunity in the spleen and blood of mice immunized with irradiated *Toxoplasma gondii* tachyzoites. *Med. Microbiol. Immunol.* 205, 297–314. doi: 10.1007/s00430-015-0447-5

Conflict of Interest: The authors declare that the research was conducted in the absence of any commercial or financial relationships that could be construed as a potential conflict of interest.

Publisher's Note: All claims expressed in this article are solely those of the authors and do not necessarily represent those of their affiliated organizations, or those of the publisher, the editors and the reviewers. Any product that may be evaluated in this article, or claim that may be made by its manufacturer, is not guaranteed or endorsed by the publisher.

frontiers in Microbiology

ORIGINAL RESEARCH
published: 06 August 2021
doi: 10.3389/fmicb.2021.703804

Conservation of S20 as an Ineffective and Disposable IFNγ-Inducing Determinant of *Plasmodium* Sporozoites Indicates Diversion of Cellular Immunity

*Calvin Hon[1], Johannes Friesen[2,3], Alyssa Ingmundson[1,2], Diana Scheppan[2†], Julius C. R. Hafalla[4], Katja Müller[1,2] and Kai Matuschewski[1,2]**

[1] Department of Molecular Parasitology, Institute of Biology, Humboldt University, Berlin, Germany, [2] Parasitology Unit, Max Planck Institute for Infection Biology, Berlin, Germany, [3] Medical Care Unit Labor 28 GmbH, Berlin, Germany, [4] Department of Infection Biology, London School of Hygiene & Tropical Medicine, London, United Kingdom

OPEN ACCESS

Edited by:
Yongliang Zhang,
National University of Singapore,
Singapore

Reviewed by:
Sanjeev Kumar,
Assam University, India
Jessica N. McCaffery,
Centers for Disease Control and Prevention (CDC), United States
Rajesh Chandramohanadas,
National University of Singapore,
Singapore

***Correspondence:**
Kai Matuschewski
Kai.Matuschewski@hu-berlin.de

†Present address:
Diana Scheppan,
The Lübeck Institute of Experimental Dermatology, University Medical Center Schleswig-Holstein, Lübeck, Germany

Specialty section:
This article was submitted to Infectious Diseases, a section of the journal Frontiers in Microbiology

Received: 30 April 2021
Accepted: 07 July 2021
Published: 06 August 2021

Citation:
Hon C, Friesen J, Ingmundson A, Scheppan D, Hafalla JCR, Müller K and Matuschewski K (2021) Conservation of S20 as an Ineffective and Disposable IFNγ -Inducing Determinant of Plasmodium Sporozoites Indicates Diversion of Cellular Immunity. Front. Microbiol. 12:703804. doi: 10.3389/fmicb.2021.703804

Despite many decades of research to develop a malaria vaccine, only one vaccine candidate has been explored in pivotal phase III clinical trials. This candidate subunit vaccine consists of a portion of a single *Plasmodium* antigen, circumsporozoite protein (CSP). This antigen was initially identified in the murine malaria model and shown to contain an immunodominant and protective $CD8^+$ T cell epitope specific to the H-$2K^d$ (BALB/c)-restricted genetic background. A high-content screen for $CD8^+$ epitopes in the H$2K^b$/D^b (C57BL/6)-restricted genetic background, identified two distinct dominant epitopes. In this study, we present a characterization of one corresponding antigen, the *Plasmodium* sporozoite-specific protein *S20*. *Plasmodium berghei S20* knockout sporozoites and liver stages developed normally *in vitro* and *in vivo*. This potent infectivity of *s20*(-) sporozoites permitted comparative analysis of knockout and wild-type parasites in cell-based vaccination. Protective immunity of irradiation-arrested *s20*(-) sporozoites in single, double and triple immunizations was similar to irradiated unaltered sporozoites in homologous challenge experiments. These findings demonstrate the presence of an immunogenic *Plasmodium* pre-erythrocytic determinant, which is not essential for eliciting protection. Although *S20* is not needed for colonization of the mammalian host and for initiation of a blood infection, it is conserved amongst *Plasmodium* species. Malarial parasites express conserved, immunogenic proteins that are not required to establish infection but might play potential roles in diverting cellular immune responses.

Keywords: malaria, *Plasmodium*, sporozoite, whole organism vaccine, antigen, $CD8^+$ T cells, immunization, pre-erythrocytic stage

INTRODUCTION

Sustained anti-malaria therapy, exposure prophylaxis, and vector control have resulted in stable incidence and mortality rates in the tropics (World Health Organisation, 2020). To reduce global malaria burden and transmission of *Plasmodium* parasites, access to a safe and efficacious prophylactic vaccine will be needed. An established method to achieve lasting sterile protection

against natural *Plasmodium* sporozoite infection is intravenous administration of multiple doses of live γ-irradiation-attenuated sporozoites (γspz) (Nussenzweig et al., 1967; Clyde et al., 1973; Hoffman et al., 2002; Richie et al., 2015). Identification of immunogenic antigens and immune correlates of protection vs. sporozoite exposure remain research priorities to develop second-generation sporozoite vaccines.

Protective sporozoite-induced immunity is achieved by complementary humoral and cellular memory responses (Rodrigues et al., 1993; Hafalla et al., 2011). Previous studies using γspz vaccination in mice have revealed the pivotal role of circulating and liver-resident $CD8^+$ T cells in mediating protective immunity to the pre-erythrocytic stages of the parasite by cytolytic killing (Ferreira et al., 1986; Schofield et al., 1987; Weiss et al., 1988; Guebre-Xabier et al., 1999; Krzych et al., 2000; Schmidt et al., 2008). Antigen-specific, cytolytic $CD8^+$ T cells target infected hepatocytes, which present MHC I-restricted parasite peptides on the cell surface (Romero et al., 1989; Rodrigues et al., 1991). Upon peptide recognition by $CD8^+$ T cells, cytokines such as interferon-γ (IFNγ) (Schofield et al., 1987) and tumor necrosis factor (TNF) (Butler et al., 2010; Depinay et al., 2011) are released along with pro-apoptotic pore-forming lytic proteins, perforin and granzymes. The central role of $CD8^+$ T cells in pre-erythrocytic stage immunity has been further highlighted by several studies, where abrogation of immunity in γspz-immunized mice and non-human primates was observed after *in vivo* depletion of $CD8^+$ T cells (Schofield et al., 1987; Weiss et al., 1988; Doolan and Hoffman, 2000; Weiss and Jiang, 2012). $CD8^+$ T cells, however, are less likely to confer protection during the asexual parasite growth inside erythrocytes, simply because MHC I molecules are not found on the surface of mammalian erythrocytes. Accordingly, the key role of cytolytic $CD8^+$ T cells in sustained protection is largely restricted to the first obligate parasite expansion phase in the liver.

Despite decades of considerable investments in malaria research, only one malaria vaccine has been licensed to-date, known as the RTS,S/AS01 (RTS,S Clinical Trials Partnership, 2015; Neafsey et al., 2015). This subunit vaccine is based on the major *Plasmodium falciparum* sporozoite surface antigen, termed circumsporozoite protein (CSP) (Cohen et al., 2010). CSP is highly conserved amongst *Plasmodium* species, and essential for sporozoite formation, motility and hepatocyte adhesion. It contains a central repeat structure, which likely further contributes to immune-dominance over minor sporozoite surface antigens (Zavala et al., 1983; Zavala et al., 1985). Modest protection offered by this vaccine is strongly associated with humoral immunity and, to a lesser extent, T-cell mediated responses (Stoute et al., 1998; Cohen et al., 2010). Employing murine malaria models it was shown that CSP contains immunogenic targets of protective H2-K^d-restricted $CD8^+$ T cell responses that are vital for protection against sporozoite infections (Rodrigues et al., 1991; Sedegah et al., 1992). But more recent studies have shown that sterile protection can also be achieved in the absence of CSP-specific T cells (Kumar et al., 2006; Grüner et al., 2007; Gibbins et al., 2020). While these findings might partly explain the inadequate protective efficacy of the RTS,S/AS01 vaccine they also highlight the need to investigate non-CSP antigens.

For the identification and evaluation of immunogenic pre-erythrocytic stage $CD8^+$ T cell epitopes two inbred mice strains, H2-K/D^b- and H2-K^d-restricted C57BL/6 (B6) and BALB/c mice, respectively, have been largely used. Immunizing either mouse strains with *Plasmodium berghei* (*Pb*) or *Plasmodium yoelii* (*Py*) γspz is able to induce highly protective responses (Romero et al., 1989; Rodrigues et al., 1991; Sano et al., 2001). Candidate $CD8^+$ T cell epitopes are typically selected based on the amount of IFNγ from activated $CD8^+$ T cells upon stimulation with soluble peptides as a proxy for recognition of immunogenic MHC I-restricted epitopes. Between the two mouse strains, B6 mice appear to represent a more accurate model for immunological studies as the elicited H2-K^b-restricted $CD8^+$ T cell responses during sporozoite infection are more diverse. Reliance on multiple doses for protective immunity suggest a closer resemblance to that of humans, in contrast to the ease of eliciting protective immunity in BALB/c mice due to the immunodominance of the CSP epitope (Hafalla et al., 2013). Furthermore, the inability of B6 mice to recognize the H2-K^d-restricted CSP epitope as a consequence of MHC haplotype restriction allows identification of non-CSP-mediated immunity. A genome-wide screening for candidate pre-erythrocytic stage H2-K/D^b-restricted $CD8^+$ T cell epitopes in B6 mice returned only two epitopes that correlate with protracted $CD8^+$ T cell responses (Hafalla et al., 2013). One H2-D^b-restricted epitope originated from the thrombospondin-related adhesion protein ($TRAP_{130-138}$) and displayed cytotoxic $CD8^+$ T cell responses after a single immunization with γspz. Importantly, partial protection could be achieved by eliciting high levels of TRAP-specific $CD8^+$ T cells *via* a heterologous prime-boost regimen.

Strikingly, the other identified H2-K^b-restricted target of $CD8^+$ T cells ($S20_{318-326}$) found in that screening, which maps to the sporozoite-specific gene 20 (Kaiser et al., 2004), did not induce cytotoxic immune responses. In good agreement, tolerization with $S20_{318-326}$ peptide failed to completely reverse protection, in contrast to $TRAP_{130-138}$ (Hafalla et al., 2013). In this study, we aimed to investigate this unusual $CD8^+$ T cell response by generating *S20* knock-out parasites to confirm the origin of the epitope and to study potential contributions of $S20_{318-326}$ toward protection in whole sporozoite immunizations.

RESULTS

S20 Is Highly Conserved Among *Plasmodium* Species and Primarily Expressed in Sporozoites

Since the sporozoite-specific protein S20 (PBANKA_1429200) was first identified in *Vinckeia* species (Kaiser et al., 2004), we first verified whether it is also present in other *Plasmodium* species and *Toxoplasma gondii*. This analysis revealed S20 orthologs in all *Plasmodium* species and a similar protein in *T. gondii* (TGGT1_229000). Examples of representative apicomplexan S20

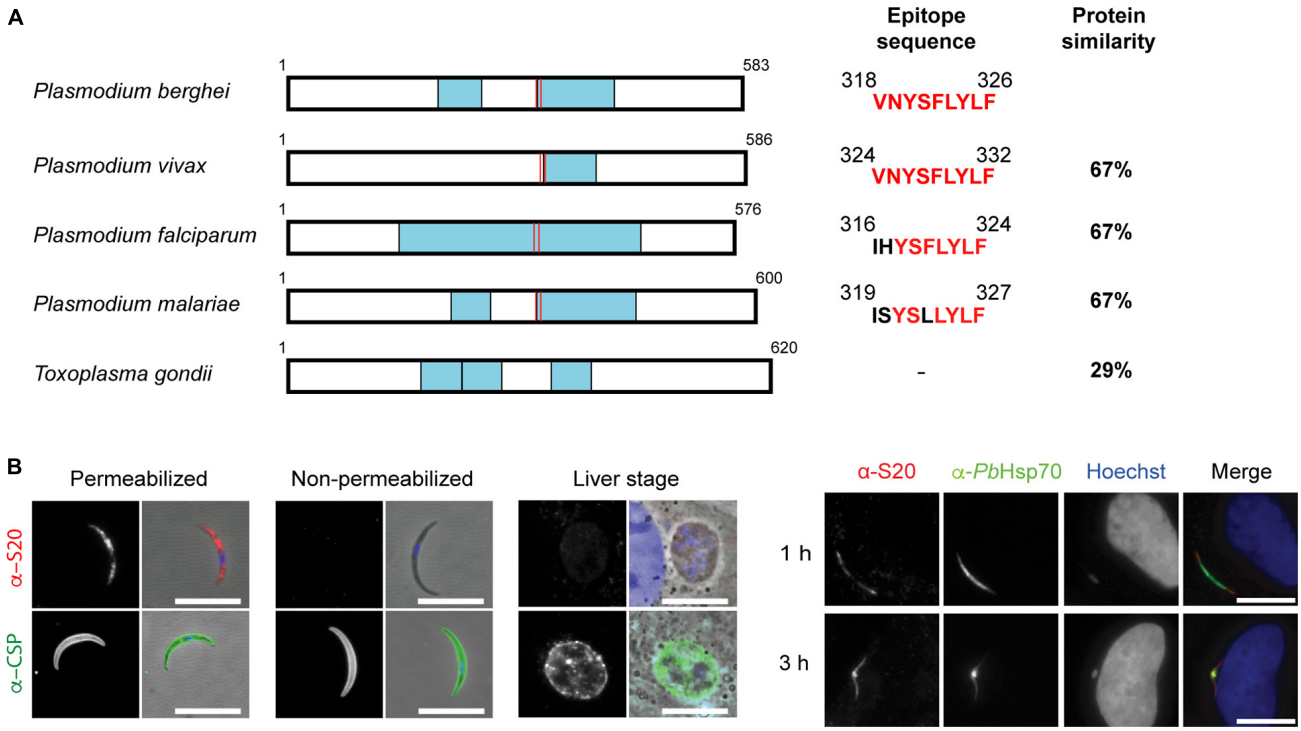

FIGURE 1 | Conservation and expression of *Plasmodium berghei* S20. **(A)** Primary structure of *Plasmodium* and *Toxoplasma* S20 proteins. Predicted Kelch domains are boxed in blue, and the position of the epitope is shown by red lines. *P. berghei* (PBANKA_1429200; XP_034424116.1), *Plasmodium vivax* (PVP01_1432200; XP_001617233.1), *P. falciparum* (PF3D7_1213400; XP_001350539.1), *Plasmodium malariae* (PmUG01_14048200; XP_028864377.1), and *Toxoplasma gondii* (TGGT1_229000; EPR64070). Accession numbers are according to EuPathDB (Aurrecoechea et al., 2017), and alignments were generated using the BLAST algorithm (Altschul et al., 1990). **(B)** Detection of *P. berghei S20* by indirect immunofluorescence. Shown are immune stainings of permeabilized and non-permeabilized sporozoites, early liver stages 24 h after infection, and infected hepatoma cells 1 and 3 h after sporozoite addition. Stainings were done with an anti-*Pb*S20 serum, anti-*Pb*CSP antibody, anti-*Pb*HSP70 antibody and corresponding secondary antibodies. Shown are immune stainings and merge, including DNA stains (Hoechst, blue) and bright field images. Scale bars, 10 μm.

orthologs are displayed in **Figure 1A**. S20 orthologs are also present in other Coccidia, for instance *Sarcocystis neurona* (SRCN_6348), *Besnoitia besnoiti* (BESB_083580), *Eimeria tenella* (ETH_00029095), and *Cyclospora cayetanensis* (cyc_00626), but not Piroplasms. S20 proteins contain kelch motifs, segments of approximately 50 amino acid residues that form a single four-stranded, antiparallel beta-sheet (Bork and Doolittle, 1994). Kelch motifs are widely distributed in eukaryotic and prokaryotic proteins with divergent functions. The high degree of S20 protein sequence conservation among *Plasmodium* is indicative of a possible conserved function. The sequence of H2-K^b-restricted epitope VNYSFLYFL (Hafalla et al., 2013) is also relatively well maintained across *Plasmodium* species.

We next profiled *S20* expression in pre-erythrocytic stages. In good agreement with published data (Kaiser et al., 2004), we detected up-regulation of *PbS20* mRNA in midgut and salivary gland sporozoites (**Supplementary Figure 1**). As expected, the relative transcript abundance of *S20* was lower than the steady state levels of the *CSP* transcripts that encode the major sporozoite surface protein. Transcript levels dropped toward the end of liver stage maturation and remained low during blood infection (**Supplementary Figure 1**), in good agreement with the original description (Kaiser et al., 2004).

In order to gain insights into protein expression and localization, we generated polyclonal anti-*Pb*S20 peptide sera. S20 could be detected in salivary gland sporozoites and in sporozoites that recently invaded hepatoma cells (**Figure 1B**). However, 24 h after invasion, S20 was no longer detectable. The S20 antisera could only recognize S20 in sporozoites that had been permeabilized, which indicates that in contrast to CSP, S20 is restricted to the sporozoite interior. The specificity of the *S20* signal in sporozoites was verified in immunofluorescence assays (IFAs) using *s20*(-) *P. berghei*, where no signal was detected (**Figure 2D**; see below).

Targeted Deletion of *Plasmodium berghei S20*

We were interested in characterizing potential roles of *PbS20* for sporozoite transmission and liver infection and to explore the contribution of $S20_{318-326}$-specific CD8$^+$ T cell responses to immunity elicited by whole sporozoite immunization. However, the latter can only be tested using this strategy if *s20*(-) sporozoites induce blood infections as efficiently as wild-type (WT) sporozoites. To this end, we deleted *PbS20* by double homologous recombination to replace the open reading frame

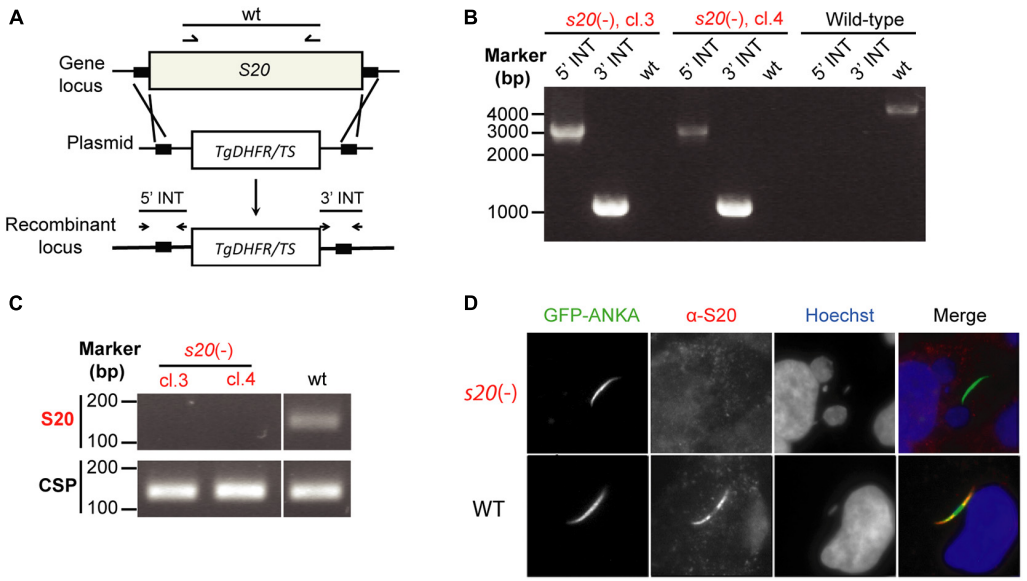

FIGURE 2 | Targeted gene deletion of *P. berghei S20*. **(A)** Schematic diagram of the replacement strategy to generate *s20*(-) parasites. After linearization with *Sac*II and *Kpn*I, the replacement vector containing portions of the 5′ and 3′ flanking regions of *S20* coding sequence and the *Toxoplasma gondii dihydrofolate reductase/thymidylate synthase (Tgdhfr/ts)* selectable marker was transfected into *P. berghei* ANKA wild-type parasites. **(B)** Diagnostic PCR to confirm successful replacement of the *S20* genomic locus with the positive selection marker in *s20*(-) parasites. Shown are the results from clone 3 and 4. 5′- and 3′-integration-specific primer combinations (5′ INT and 3′ INT) amplify the predicted fragment only in the recombinant locus. Wild-type-specific primer pairs (wt) do not produce a PCR fragment in the recombinant locus confirming absence of residual WT parasites. **(C)** Verification of absence of *S20* transcripts in *s20*(-) clones 3 and 4 salivary gland sporozoites by RT-PCR. Note that *s20* mRNA (top) is only detectable in WT sporozoites. *CSP* mRNA (bottom) serves as positive control. **(D)** Indirect immunofluorescent stainings of permeabilized infected hepatoma cells 1 h after *s20*(-) (top) or WT (bottom) sporozoite addition. Stainings were done with anti-GFP antibody, an anti-*Pb*S20 serum, and corresponding secondary antibodies. Shown are immune stainings, DNA stains (Hoechst, blue) and merge images.

with the *Tgdhfr/ts* resistance cassette for positive selection *in vivo* (**Figure 2A**). Successful transfection and cloning by limiting dilution resulted in clonal *s20*(-) parasites. For this study, two clonal parasite populations, termed clones 3 and 4, were obtained after two independent transfection experiments. Genotyping by diagnostic PCR verified the desired gene deletion and absence of WT parasites from the clonal lines (**Figure 2B**). Additional confirmation of the absence of *S20* was obtained by RT-PCR from total RNA isolated from *s20*(-) and WT salivary gland sporozoites (**Figure 2C**). In contrast to *CSP* control transcripts, *S20* mRNA was only present in WT, but not in *s20*(-) sporozoites. As noted above, immunofluorescent staining using the polyclonal anti-*Pb*S20 peptide sera for WT- and *s20*(-)-infected hepatoma cells showed a loss of signal in *s20*(-), but not WT, parasites (**Figure 2D**). Because initial analysis revealed that both clonal parasite populations are phenotypically indistinguishable, one population (clone 4) was selected for the experiments to uncover the roles of *S20* in *Plasmodium* life cycle progression and subsequently, the H2-K^b-restricted $S20_{318-326}$ $CD8^+$ T cell epitope in vaccine-induced protection. Swift selection of asexual *s20*(-) parasites corroborated the notion that *S20* is not required for *Plasmodium* blood infection.

s20(-) Sporozoites Display Full Infectivity to Mice

Conservation of *S20* across all *Plasmodium* species might indicate critical functions during pre-erythrocytic stages. Accordingly, we monitored life cycle progression in the mosquito vector and during sporozoite transmission. Quantification of *s20*(-) midgut oocysts and salivary gland sporozoites from infected *Anopheles* mosquitoes showed no differences in comparison to WT parasites (**Supplementary Table 1**).

Salivary gland sporozoites were isolated and analyzed for their capacity to perform gliding locomotion and infect cultured hepatoma cells and mice (**Figure 3**). Freshly isolated *s20*(-) sporozoites displayed continuous, circular gliding locomotion on BSA-coated glass slides similar to WT parasites (**Figure 3A**). When deposited onto cultured Huh7 hepatoma cells, formation of liver stages was indistinguishable from WT parasites, both quantitatively and morphologically (**Figures 3B,C**). To rule out any defects in sporozoite infectivity *in vivo*, pre-patency, i.e., the time to detection of the first blood stage parasite, and the course of blood infection were determined by daily microscopic examination of blood films from B6 mice following intravenous injection of 10,000 *s20*(-) or WT salivary gland sporozoites, or exposure of the mice to bites of *s20*(-) or WT-infected mosquitoes (**Figure 3D** and **Supplementary Table 2**). All mice infected with either *s20*(-) or WT intravenously or by mosquito bites were blood stage-positive on day 3 after sporozoite inoculation. No differences in the course of blood infection between the two parasite groups were detectable. In good agreement, quantification of the relative liver infection load 42 h after intravenous delivery of 10,000 sporozoites by quantitative RT-PCR (qRT-PCR)

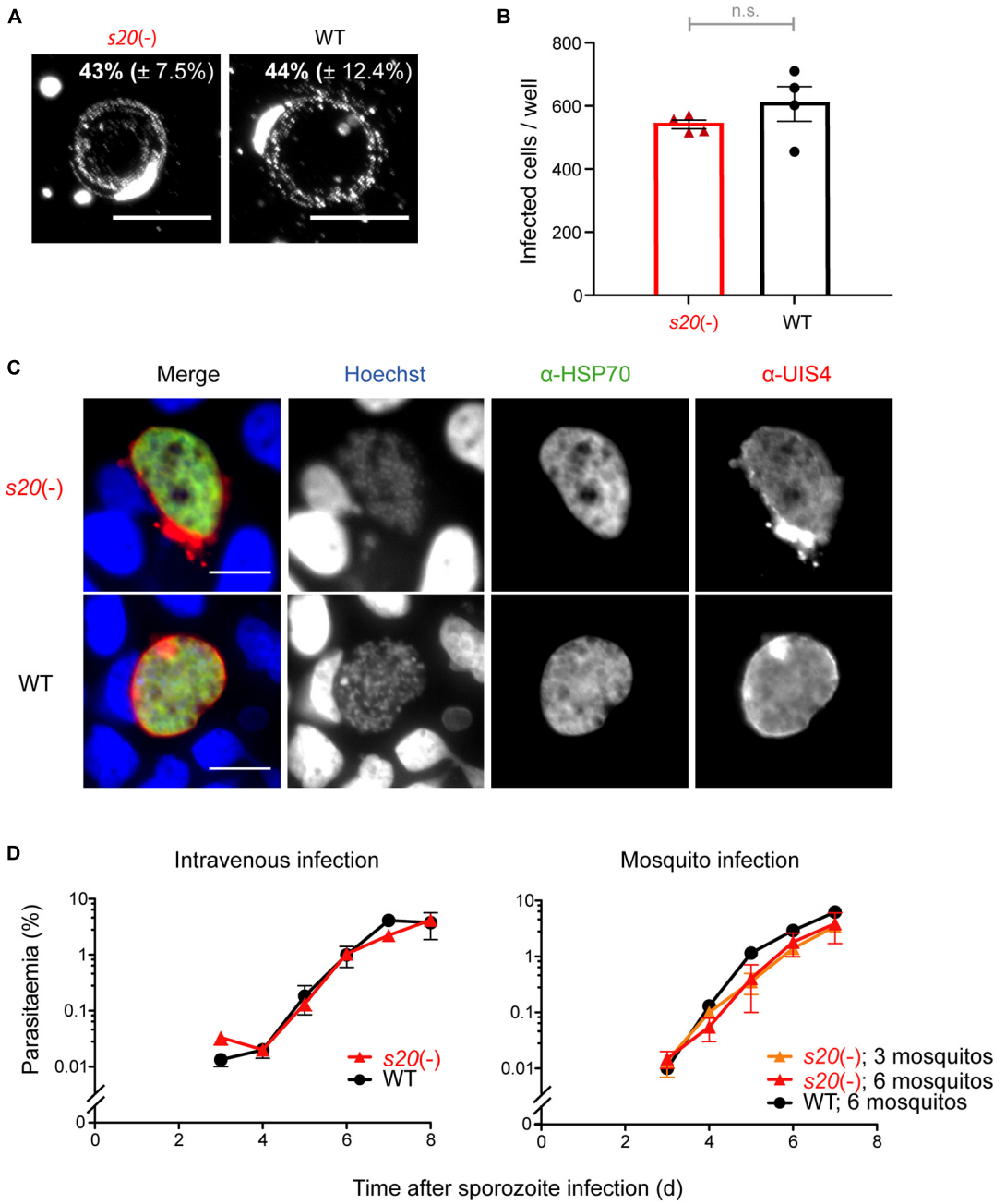

FIGURE 3 | Normal life cycle progression of *s20*(-) parasites. **(A)** Fluorescence micrographs of *s20*(-) and WT sporozoites that were permitted to glide on BSA-coated glass slides. Sporozoites and trails are visualized with an anti-*Pb*CSP and anti-mouse secondary antibodies. Numbers show mean percentage (±SD) of gliding sporozoites. **(B)** Quantification of *s20*(-) and WT-infected hepatoma (Huh7) cells by fluorescence microscopy 48 h after infection. Shown are mean values (±SEM); $n = 1$; n.s., non-significant (unpaired *t*-test). **(C)** Representative fluorescence images of *s20*(-) and WT liver stages. α-HSP70 antibody (green; parasite cytoplasm), α-UIS4 antibody (red; parasitophorous vacuole), and Hoechst (blue; nucleic acid). Scale bars, 10 μm. **(D)** Blood infection after sporozoite-induced infection. B6 mice were infected by intravenous injection of 10,000 *s20*(-) or WT sporozoites ($n = 3$ each) or mosquito bites (WT, six infected mosquitoes, $n = 1$; *s20*(-), 3 or 6 infected mosquitoes, $n = 2$ each). Blood infection was monitored by daily microscopic examination of Giemsa-stained blood films. Shown are mean values (±SEM).

revealed no difference between *s20*(-) and WT parasites (**Supplementary Figure 2**).

Together, *s20*(-) sporozoites displayed no apparent defects in sporozoite, liver stage or blood stage functions, permitting its use in immunization protocols.

Effective Immunizations With Irradiated *s20*(-) Sporozoites

Intravenous immunizations with metabolically active, irradiation-attenuated sporozoites remains the benchmark for pre-clinical and clinical evaluation of experimental malaria

TABLE 1 | Vaccine-induced protection against WT sporozoite challenge infections.

Immunizations[1]	Protected/challenged	Prepatency[2]
3 × 10,000 WT γspz	10/10 (100%)	–
3 × 10,000 *s20*(-) γspz	9/9 (100%)	–
none	0/3 (0%)	day 3

[1] *Immunizations were done by intravenous injection of irradiated (γ) sporozoites.*
[2] *Prepatency is defined as time to the first detection of a single blood stage parasite.*

vaccines. In humans and mice, sterile protection against sporozoite-induced infections can be routinely achieved after multiple doses of γspz (Nussenzweig et al., 1967; Hoffman et al., 2002, 2010). We initiated our study by immunizing groups of mice with three doses of 10,000 γspz. Immunized and control animals were infected by a challenge dose of 10,000 WT sporozoites 29 days after the last immunization (**Table 1**). All immunized animals remained blood stage negative, while the control animals became parasitaemia-positive 3 days after the challenge.

In order to capture potential differences in protective efficacy offered by *s20*(-) and WT γspz, we next employed a sub-optimal immunization schedule consisting of only two doses of 10,000 *s20*(-) or WT γspz, which has been demonstrated to induce incomplete protection (Friesen and Matuschewski, 2011). Immunized mice were challenged by intravenous injection of 10,000 WT sporozoites 35 days after the last immunization (**Figure 4A**). Control mice became blood stage positive on day 3 after challenge inoculation. Challenge infections of *s20*(-) γspz-immunized mice resulted in blood stage parasites in 4 of 10 immunized mice with a mean pre-patent period of 8 days, whereas 3 of 9 WT γspz-immunized mice became positive for blood stage parasitaemia with a mean pre-patent period of 7 days (**Figure 4A**). To independently confirm the results, we performed a second immunization experiment involving single- and two dose-immunization schedule, and quantified parasite loads in the liver 48 h after challenge with 10,000 WT sporozoites by qRT-PCR (**Figure 4B**). In this analysis we also could not detect any differences between the relative parasite loads in livers of *s20*(-) and WT γspz-immunized mice. Together, these findings suggest that the $S20_{318-326}$ reactive $CD8^+$ T cell population does not contribute markedly to vaccine-induced protection.

Lack of $S20_{318-326}$-Specific $CD8^+$ T Cells in *s20*(-) Sporozoite-Immunized Mice

Finally, we wanted to unequivocally confirm that the cells in immunized mice that recognize the S20 peptide VNYSFLYLF were stimulated by this epitope in *Pb*S20. Therefore, we performed fluorescence-activated cell sorting (FACS) analysis and ELISPOT assays to detect restimulated peptide-specific splenic $CD8^+$ T cells from γspz-immunized mice (**Figure 5** and **Supplementary Figure 3**). As expected, only background signals of IFNγ responses after stimulation with $S20_{318-326}$ peptide were detected in naive and *s20*(-)-immunized mice (Hafalla et al., 2013; Müller et al., 2017). In contrast, activated splenic $CD8^+$ T cells from WT-immunized mice could be restimulated with $S20_{318-326}$ peptide. The cell population responding to the $TRAP_{130-138}$ peptide was noticeably higher, as observed in both WT- and *s20*(-)-immunized mice. As controls, we included cells from naive B6 mice (**Supplementary Figure 4**). Together,

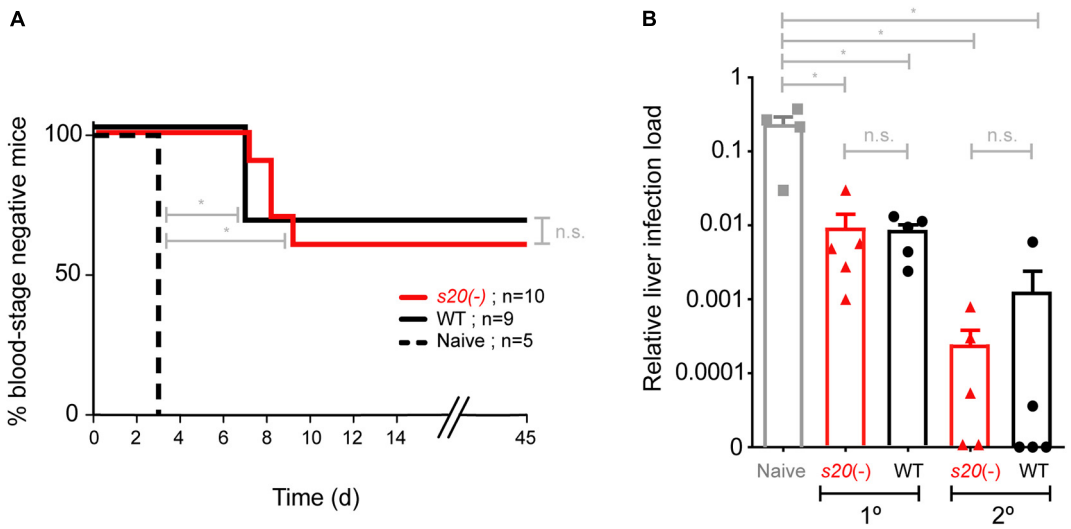

FIGURE 4 | Loss of *S20* does not affect vaccine-induced protection. **(A)** Immunization and challenge protocol. Groups of B6 mice were immunized twice with 10,000 *s20*(-) ($n = 10$) or WT γ-sporozoites ($n = 9$) and challenged 35 days after the last immunization by intravenous injection of 10,000 WT sporozoites. Naïve mice ($n = 5$) served as a control. Shown is a Kaplan-Meier analysis of time to blood infection after challenge infection. From day 3 onward mice were monitored daily for blood stage parasitaemia by microscopic examination of Giemsa-stained blood films. n.s., non-significant; $^*p < 0.05$ (Mann Whitney *U* test). **(B)** Protective efficacy as measured by qRT-PCR. *S20*(-) and WT single or double immunized were challenged with 10,000 infectious sporozoites ($n = 5$ each). Naive mice ($n = 4$) served as controls. The relative liver load was determined 42 h later after liver removal, RNA extraction and qRT-PCR with *Pb*18S rRNA primers normalized to mouse GAPDH. Shown are mean values (±SEM); $n = 1$.

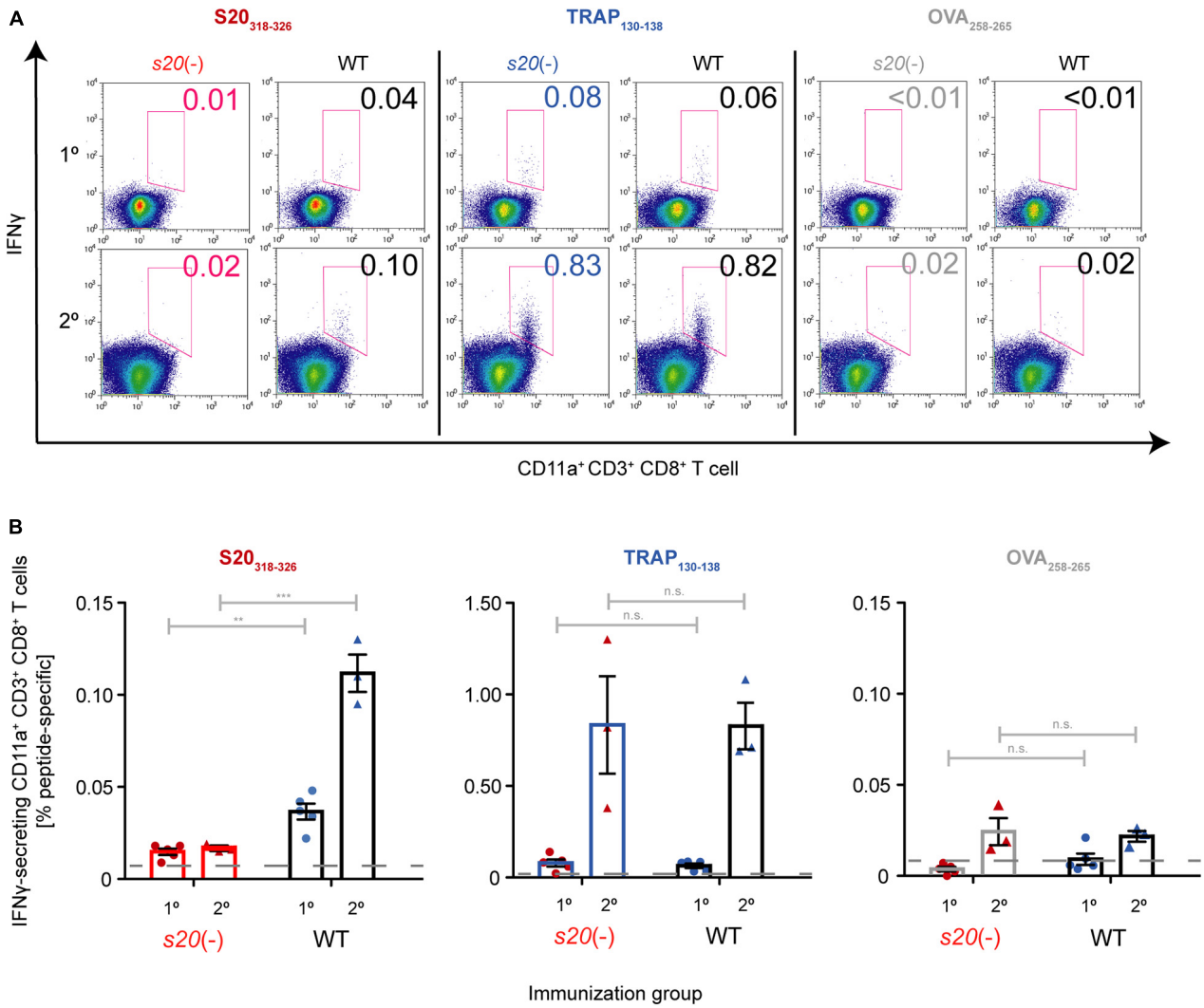

FIGURE 5 | Absence of $S20_{318-326}$-specific splenic $CD8^+$ T cells in *s20*(-)-immunized mice. B6 mice were immunized once (1°; $n = 5$ each) or twice (2°; $n = 3$ each) with *s20*(-) (red) or WT (black) attenuated sporozoites. Peptide-specific splenic $CD8^+$ T cell responses were quantified after restimulation by intracellular staining 11 or 7 days later, respectively. **(A)** Representative FACS plots showing the gating strategy to identify IFNγ-secreting $CD11a^+$ $CD3^+$ $CD8^+$ T cells. The percentage of activated $IFN\gamma^+$ $CD8^+$ T cells among total $CD8^+$ T cells after stimulation with either $S20_{318-326}$ (red), $TRAP_{130-138}$ (blue), or unrelated $OVA_{258-265}$ (gray) peptide is indicated. **(B)** Quantification of activated, $IFN\gamma^+$ $CD11a^+$ $CD8^+$ T cells among total $CD8^+$ T cells after stimulation with either $S20_{318-326}$ (red), $TRAP_{130-138}$ (blue), or unrelated $OVA_{258-265}$ (gray) peptide. Shown are mean percentage (±SEM), $n = 1$. Striped lines represent baseline responses from peptide-restimulated splenic cells of naïve mice. n.s.,non-significant; $^{**}p < 0.01$; $^{***}p < 0.001$ (Unpaired *t*-test).

these results show that the $S20_{318-326}$ specific responses can be attributed to the presence of *Pb*S20 in sporozoites used for immunization.

DISCUSSION

In this study, we deleted a previously identified $CD8^+$ T cell reactive epitope together with its corresponding gene, the sporozoite-specific protein S20 (PBANKA_1429200) (Kaiser et al., 2004; Hafalla et al., 2013; Müller et al., 2017). Validating candidate antigens recognized by $CD8^+$ T cells is an important aspect toward a mechanistic understanding of immune responses. As an example, previous work on identification of reactive $CD8^+$ T cells in a transgenic mouse model, so called *Pb* T-1 cells, erroneously assigned the reactive peptide to PBANKA_0714500 (Lau et al., 2014) to later correct this to the ribosomal protein RPL6 (Valencia-Hernandez et al., 2020). Here, we could assign the $CD8^+$ T cell-reactive, H2-K^b-restricted epitope VNYSFLYFL to *P. berghei* S20. Since we also wanted to explore the cellular function of *PbS20* we employed double homologous recombination to delete the entire gene locus. We could show that *s20*(-) parasites progress normally through the *P. berghei* life cycle and induce typical exponential blood infections when animals are inoculated with *s20*(-) sporozoites. This was surprising considering the degree

of conservation of S20 across the genus *Plasmodium*. The WT-like sporozoite signatures, including gliding motility, liver infectivity, and prepatency permitted us to directly compare vaccine efficacy of *s20*(-) γspz in comparison to WT γspz. Despite the absence of $S20_{318-326}$-reactive, IFNγ-secreting $CD8^+$ T cells we could not detect differences in γspz-induced protective efficacy in double or triple immunization protocols. An attractive hypothesis is that sporozoites express the immunogenic *S20* as a decoy to divert protective immune responses from sporozoites and developing liver stages. In support of this notion, prior studies investigating the *P. berghei* $S20_{318-326}$ epitope uncovered a surprising lack of *in vivo* cytotoxicity of $S20_{318-326}$-specific $CD8^+$ T cells (Hafalla et al., 2013) and an inability of $S20_{318-326}$-specific responses to confer protection in mice (Doll et al., 2016). In marked contrast, $TRAP_{130-138}$-specific $CD8^+$ T cells are cytotoxic, and subunit immunization strategies against *Pb*TRAP elicit protective immunity (Hafalla et al., 2013; Doll et al., 2016). The presence of a similar protein in *T. gondii*, which however lacks the $CD8^+$ T cell epitope under investigation, hints at a potential alternative hypothesis. S20 could be a remnant apicomplexan sporozoite protein, which no longer exerts a central role in *Plasmodium* sporozoites. We consider this possibility less likely due to the high degree of conservation. Experimental genetics studies in coocidian parasites are warranted to determine the role of the kelch-containing proteins in these parasites and infer a potential loss of function in Haemosporidae.

Identifying immunogenic targets of protective immunity against *Plasmodium* infection remains a priority in malaria research. Early work with γspz immunizations has established that protracted, sterilizing pre-erythrocytic protection can be largely attributed to memory effector $CD8^+$ T cells (Schofield et al., 1987; Weiss et al., 1988; Guebre-Xabier et al., 1999; Krzych et al., 2000; Schmidt et al., 2008). However, robust protection cannot be directly inferred from the magnitude of epitope-specific $IFN\gamma^+$ $CD8^+$ T cell populations (Hafalla et al., 2013; Kimura et al., 2013; Müller et al., 2021). For instance, heterologous prime-boost immunizations with TRAP-expressing adenovirus and Modified Vaccinia Ankara (Ad-M) generated very high levels of $TRAP_{130-138}$-reactive effector $CD8^+$ T cells in H2-K/D^b- restricted B6 mice, but provided only partial protection against sporozoite challenge infections (Hafalla et al., 2013). On the other hand, rendering the $OVA_{258-265}$ model epitope poorly immunogenic by placing it in the context of a liver stage antigen still resulted in efficient killing of parasite-infected cells by vaccination (Müller et al., 2021). In the H2-K^d-restricted BALB/c model vaccine efficacy can be largely predicted by the magnitude of $CD8^+$ T cells reactive to the immunodominant CSP-specific epitope (SYVPSAEQI) (Bruña-Romero et al., 2001; González-Aseguinolaza et al., 2003). Hence, in order to design subunit vaccine strategies that are as potent as the protracted sterile protection induced by γspz, many factors including specificity of $CD8^+$ T cell responses and magnitude of responses have to be considered.

To date, most targets of γspz-induced $CD8^+$ T cells are likely either poorly defined or remain unrecognized, and whether γspz-induced protection requires presentation of many or just a few pre-erythrocytic stage epitopes remains unclear. Previous work has focused on identifying and investigating individual $CD8^+$ T cell epitopes using subunit vaccine strategies (Bruña-Romero et al., 2001; Hafalla et al., 2013; Doll et al., 2016), but the reverse approach, to test whether individual epitopes are required for sterile immunity offered by γspz, remains largely unexplored. Previous studies have demonstrated the ability to elicit sterile immunity in H-2K^d-restricted BALB/c mice in the absence of CSP-specific responses (Grüner et al., 2007; Gibbins et al., 2020). The findings suggested that sterile protection does not necessarily depend on CSP-reactive $CD8^+$ T cells, and indicated that inclusion of additional, non-CSP epitopes to subunit vaccine strategies is warranted. Another important stepping stone toward a better understanding of the underlying mechanisms of vaccine-induced protection is distinction of protective from non-protective epitopes by experimental genetics, as exemplified in this study.

Sterile immunity offered by γspz in the absence of *S20* clearly suggests that S20 is not a promising malaria vaccine candidate, fully supporting the findings that prime-boost immunization against $S20_{318-326}$ epitope in mice did not elicit sterilizing immunity despite robust $CD8^+$ T cell responses (Doll et al., 2016). For viral infections, compensatory $CD8^+$ T cell responses were shown to be induced by subdominant epitopes when immunodominant epitope-specific effector $CD8^+$ T cells are absent (Rodriguez et al., 2002; van der Most et al., 2003). Apparently, immunosuppressive effects of IFNγ secreted in large amounts by dominant $CD8^+$ T cell responses are abolished, thus allowing subdominant epitope-specific precursor $CD8^+$ T cells to proliferate. As a result, the subdominance is alleviated and compensatory responses are generated without suppression by IFNγ. Therefore, IFNγ plays a vital role in shaping the epitope immunodominance hierarchy, and subdominant epitopes are key players in inducing these compensatory responses in the absence of immunodominant epitopes. Together, the absence of the subdominant $S20_{318-326}$ epitope in *P. berghei*, as demonstrated by inferior IFNγ responses in comparison to $TRAP_{130-138}$, apparently did not result in compensatory responses generated toward other $CD8^+$ T cell epitopes. Hence, maintenance of sterile protection observed in the absence of S20-specific responses was achieved by the sum of all γspz-induced responses other than $S20_{318-326}$. This hypothesis can be experimentally addressed by a similar strategy as presented herein, by removal of the dominant H2-D^b-restricted $TRAP_{130-138}$ $CD8^+$ T cell epitope.

The anti-*Pb*S20 peptide antiserum detected a cytoplasmic location of S20 in sporozoites and very early liver stages. The effect of antigen localization on protective immunity was also examined with the model antigen ovalbumin (OVA) in transgenic *P. berghei*-expressing exported or non-exported OVA (Montagna et al., 2014). *P. berghei* parasites expressing secreted OVA were found to enhance $CD8^+$ T cell proliferation and MHC I presentation by infected hepatocytes during immunization, resulting in improved liver stage clearance following homologous sporozoite challenge. Importantly, large differences in immunogenicity

due to antigen origin in malaria pre−erythrocytic stages are overcome by robust recognition by vaccine−induced, antigen-specific effector $CD8^+$ T cells, leading to comparable high levels of protection (Müller et al., 2021). Hence, although intracellular antigens might have marginal impacts on the level of $CD8^+$ T cell responses to whole sporozoite immunization, immunogenic $CD8^+$ T cell epitopes derived from intracellular proteins should not be disregarded as potential candidates in subunit vaccine design.

In conclusion, our results revealed a non-vital role of *S20* in *Plasmodium* life cycle progression *in vivo* and surrogate cell culture assays, despite being a highly conserved gene across all *Plasmodium* species. Protective immunity from *s20*(-) γspz immunizations was similar to WT γspz. Our findings exemplify that malarial parasites express conserved, immunogenic proteins that are not required to establish infection in a new mammalian host but might play potential roles in diverting cellular immune responses. Molecular and immunological characterization of candidate *Plasmodium* antigens can assist in prioritizing candidates for urgently needed second-generation malaria vaccines.

MATERIALS AND METHODS

Ethics Statement

All animal work was conducted in accordance with the German "Tierschutzgesetz in der Fassung vom 18. Mai 2006 (BGBl. I S. 1207)," which implements the directive 86/609/EEC from the European Union and the European Convention for the protection of vertebrate animals used for experimental and other scientific purposes. The ethics committee of MPI-IB and the Berlin state authorities (LAGeSo Reg# G0469/09 and G0294/15) approved the protocol.

Parasites and Experimental Animals

Plasmodium berghei ANKA cl507 parasites that constitutively express GFP under the *PbEF1α* promoter were used in our experiments (Franke-Fayard et al., 2004). Six- to Eight-weeks old female NMRI and SWISS or B6 mice used in this study were either purchased from Charles River Laboratories or bred in-house. NMRI mice were used for transfection experiments, blood stage infections and transmission to *Anopheles stephensi* mosquitos. B6 mice were used for sporozoite infections and subsequent immunological studies.

Targeted Gene Deletion and Expression of *S20*

The *P. berghei S20* gene was deleted by a double homologous recombination strategy using a standard replacement knockout plasmid (pB3D; van Dijk et al., 1995). For this aim, fragments from the 5′ and 3′ ends were amplified with primers S20SacII and S20NotI, and with the primer pair S20HindIII and S20KpnI using PCR. Subsequently, the 5′ PCR fragment was double digested overnight at 37°C with the restriction enzymes *Sac*II and *Not*I, while the restriction enzymes *Hind*III and *Kpn*I were used for the 3′ fragment digestion. 10 μg plasmid was linearized with *Sac*II and *Kpn*I for transfection. Transfection experiments were carried out twice, as previously described (Janse et al., 2006), to obtain two independent clones for phenotypical analysis; clone 3 and 4. Successful integration was tested on genomic DNA by conventional PCR using the primers Test1S20fw and JFUTRrv for 5′ integration, and TgPro and Test2S20rv for 3′ integration. Absence of WT parasites in the clonal population was verified using Test1S20fw and Test2S20rv primers. The PCR was carried out as follows: Initial denaturation for 3 min at 94°C, followed by 35 cycles of 30 s denaturation at 94°C, annealing for 45 s at 55°C, and extension at 60°C for 2 min 30 s. A final extension was carried out for 10 min at 60°C. For studying the expression of *S20* during the *P. berghei* life cycle, amplification was performed by qPCR with the primers qS20fw and qS20rv on cDNA of midgut sporozoites, salivary gland sporozoites, early liver stages, late liver stages, mixed blood stages and gametocytes obtained from *P. berghei* ANKA cl507 parasites, which constitutively express GFP under the *PbEF1α* promoter (Janse et al., 2006). Expression levels were normalized to the *GFP* transcript levels determined by primers qGFPfw and qGFPrv.

Salivary Gland Sporozoite Isolation

Wild-type GFP-expressing *P. berghei* ANKA and *P. berghei s20*(-) strains were maintained by continuous cycling between rodent hosts (B6 or NMRI and SWISS mice) and female *A. stephensi* mosquito vectors (Vanderberg, 1975). Mosquitoes were kept at 28°C (non-infected) or 20°C (infected) at 80% humidity. After 10–14 days, midguts were isolated and oocyst development analyzed by fluorescent microscopy. Salivary gland sporozoites were isolated from mosquitos in DMEM medium containing 10% fetal calf serum (FCS).

Polyclonal Anti-S20 Antibody Generation

Polyclonal antibodies against S20 were raised in rabbits immunized with synthetic peptides (MSDISDFSDIDDFSE+C and C+TFTSKKLTENPGKRAY) (Eurogentec, Seraing, Belgium).

Immunofluorescence Staining of Salivary Gland Sporozoites

The gliding motility of salivary gland sporozoites was evaluated by IFA. 5,000 WT or *s20*(-) salivary gland sporozoites suspended in 3% BSA-RPMI were added into each ring of a Medco glass slide pre-coated with 3% BSA-RPMI. The sporozoites were incubated for 45 min at 37°C, during which the parasites glide and shed surface proteins into the extracellular environment. To visualize gliding motility, sporozoites and trails of shed proteins were stained with mouse anti-sporozoite surface antibody, followed by anti-mouse Alexa Fluor 488-coupled antibody (Invitrogen, Carlsbad, CA, United States) and the nuclei stain Hoechst 33342 (Invitrogen, Carlsbad, CA, United States) Slides were mounted with Fluoromount-G (SouthernBiotech) prior to analysis by fluorescence microscopy using Zeiss Axio Imager Z2. To detect S20 by immunofluorescence, sporozoites were

fixed in 3% PFA and permeabilized as indicated with 0.3% Triton X-100 prior to staining with custom-made anti-S20 peptide antiserum or monoclonal anti-CSP (3D11) antibody (Yoshida et al., 1980), and Hoechst 33342 (Invitrogen, Carlsbad, CA, United States).

Hepatoma Cell Infection *in vitro* and Immunofluorescence Staining

Nunc Lab-Tek II 8-well Chamber Slides (Thermo Fisher Scientific, New York, NY, United States) were seeded with 30,000 Huh7 cells per well 24 h before infection. 10,000 WT or *s20*(-) salivary gland sporozoites suspended in 100 μl DMEM-complete were added and allowed to settle for 1 h at RT. *P. berghei* S20 was immunostained to investigate the expression of *S20* during liver stage development. Here, infected hepatoma cells were incubated at 37°C for 1 and 3 h after infection prior to fixation with 4% paraformaldehyde and staining with monoclonal anti-HSP70 antibody (Tsuji et al., 1994), anti-S20 peptide antiserum, and Hoechst 33342 (Invitrogen, Carlsbad, CA, United States). Phenotypic analysis of parasite liver stage development was monitored by IFA in Huh7 cells 48 h post-infection at 37°C. The infected cells were permeabilized with 0.2% Triton-X 100 (Roth, Karlsruhe, Germany) and analyzed 48 h later after fixation with 4% PFA by staining with mouse anti-HSP70 antibody (Tsuji et al., 1994) followed by goat anti-mouse Alexa Fluor 488 antibody (Invitrogen, Carlsbad, CA, United States) and Hoechst 33342 (Invitrogen, Carlsbad, CA, United States). Slides were mounted with Fluoromount-G (SouthernBiotech) and imaged by fluorescence microscopy (Zeiss Axio Imager Z2). At least 20 intracellular parasites per sample were visualized.

s20(-) Parasite Infectivity *in vivo*

To determine the infectivity of sporozoites, B6 mice were infected intravenously with either 10,000 WT or *s20*(-) salivary gland sporozoites suspended in 100 μl PBS per mouse. Simultaneously, another group of B6 mice were infected through direct bites from WT or *s20*(-)-infected *A. stephensi* mosquitos for 20 min. In order to confirm the number of mosquitos that received a blood meal, the mosquitos were paralyzed briefly at −20°C and observed for blood in the abdomen under a compound microscope. The pre-patent period was determined by daily microscopic examination of Giemsa-stained blood smears.

Quantification of Parasite Development *in vivo*

To rule out a defect of *s20*(-) parasites during liver stage development and to determine protective outcome of immunized mice against homologous sporozoite challenge, *P. berghei* 18S rRNA level during liver stage infection was quantified. Naïve B6 mice were inoculated with either 10,000 WT or *s20*(-) sporozoites intravenously for phenotypic characterization, and in the sterile protection experiment, female B6 mice were challenged with 10,000 WT sporozoites 35 days after the last immunization. 42 h after infection, the mice were sacrificed and livers were removed to isolate total RNA using Qiagen RNeasy kit, followed by reverse transcription of the RNA using RETROscript kit. Quantitative Real-Time PCR was performed on cDNA samples using Pb18S ribosomal subunit primer pairs (Gene ID: 160641; sense and antisense primers), mouse GAPDH primer pairs (Gene ID: 281199965; sense primer and antisense primers). Relative liver infection loads were then determined using the ΔC_t method as previously described (Friesen et al., 2010).

Immunization With Attenuated WT and *s20*(-) Sporozoites

Salivary gland sporozoites were attenuated either by a γ-irradiation dose of 12×10^4 cGy, or with azithromycin (AZ) cover (4.8 mg in 200 μl of sodium chloride solution per mouse) (Friesen et al., 2010). For challenge experiments, B6 mice were immunized with two and three doses of WT and *s20*(-) γspz. Immunizations in the two-dose regimen with 10,000 sporozoites were carried out on day 0 and 7. Challenge with 10,000 sporozoites was on day 42, including an addition of 5 age-matched naïve B6 mice. The priming dose of the three-dose regimen consisted of 15,000 sporozoites, while the subsequent two boosts comprised of 10,000 sporozoites. The immunization doses were given at days 0, 35, and 55, followed by a challenge with 10,000 WT sporozoites on day 84, including three naïve animals. All mice were checked for parasitemia by microscopical examination of Giemsa-stained blood smears starting at day 3 after challenge inoculation until day 14. Those animals that remained parasitemia-free were continuously checked for parasitemia up till 45 days after the challenge.

Quantification of $S20_{318-326}$-Specific Splenic $CD8^+$ T Cells in Immunized Mice

Each B6 mouse in immunological studies was immunized intravenously with attenuated sporozoites resuspended in 1× PBS *via* the lateral tail vein. FACS after restimulation and staining was done to determine the absence of $S20_{318-326}$-specific splenic $CD8^+$ T cell responses. B6 mice were immunized with either a single-dose of 15,000 AZ-attenuated sporozoites, or two-dose regimen of γspz followed by AZ-attenuated sporozoites carried out on day 0 and 7, respectively, where each dose consisted of 10,000 sporozoites. B6 mice used in enzyme-linked immune absorbent spot (ELISPOT) experiments were immunized twice with irradiated *s20*(-) or WT irradiated sporozoites at days 0 and 7. Another two groups were immunized in parallel at day 7. Sixteen days after the last immunization, animals were challenged with 10,000 sporozoites, including five naïve mice. 42 h after challenge mouse spleens were used to extract $CD8^+$ T cells and analyzed for their capacity to induce IFNγ responses specific for $S20_{318-326}$ and $TRAP_{130-138}$-specific $CD8^+$ epitopes.

The peptides VNYSFLYLF ($S20_{318-326}$), SALLNVDNL ($TRAP_{130-138}$) (Hafalla et al., 2013), and SIINFEKL ($OVA_{258-265}$) were synthesized by Peptides & Elephants (Potsdam, Germany), and reconstituted in DMSO/water (1:1)

at a concentration of 1 mM. Female B6 mice that received a single-dose or prime-boost sporozoite immunization were dissected 11 and 7 days after last immunization, respectively, along with naïve control animals, to obtain splenic lymphocyte cell suspension using a cell strainer. Red blood cell lysis was then carried out with BD Pharm Lyse^{TM} lysing buffer (Becton, Dickinson and Company, United States) as described in the manufacturer's protocol. In order to quantify sporozoite-induced CD8$^+$ T cells, the lymphocytes were restimulated with peptides for 5–6 h in the presence of Brefeldin A (Invitrogen, Carlsbad, CA, United States), followed by extracellular and intracellular staining procedures specific for CD3, CD11a, CD8a, and IFNγ using the following anti-mouse antibodies; CD3e PE-Cy7 (eBioscience, Inc., San Diego, CA, United States), CD8a PerCP Cy5.5 (eBioscience, Inc., San Diego, CA, United States), CD11a e450 (Invitrogen, United States), and IFNγ-APC (eBioscience, Inc., San Diego, CA, United States). The cells were analyzed using a BD LSR Fortessa flow cytometer (Becton, Dickinson and Company, United States) and data analysis was performed on FLOWJO software (Becton, Dickinson and Company, United States). Target CD8$^+$ T cells were identified from the gated lymphocyte population by the removal of doublets followed by the exclusion of cell debris, artifacts, and other non-target cells (**Supplementary Figure 4B**).

To support the findings from FACS analysis, ELISPOTs were also carried out on splenic CD8$^+$ T cells from immunized female B6 mice (see above) using the same VNYSFLYLF ($S20_{318-326}$) and SALLNVDNL ($TRAP_{130-138}$) (Hafalla et al., 2013) peptides for restimulation. Sterile high protein binding Immobilon-P MultiScreen 96-Well Plate (Millipore, Germany) with 0.45 μm pore size were used as ELISPOT plates. Prior to plating of the cells, plates were pre-wet for 1 min with 35% EtOH, washed with sterile water and incubated overnight with 75 μl of rat anti-mouse IFNγ antibody (AN-18; rat IgG1; eBioscience) at a concentration of 8 μg/ml in sterile PBS at 4°C. After washing with sterile PBS, plates were blocked with DMEM containing 10% FCS and Penicillin/Streptomycin for 2 h at 37°C. Splenic cell suspensions from immunized and control animals were prepared using a cell strainer, and red blood cells were lysed with BD Pharm Lyse lysing buffer as described in the manufacturer's protocol. 10^8 cells were used for isolation of CD8$^+$ cells by positive selection using CD8a (Ly-2) MicroBeads (Miltenyi, Germany) following the manufacturer's instructions. 200,000 CD8$^+$ cells and the same number of antigen-presenting cells were used per well. Naïve spleen cells were incubated with 2 μM peptide for 2 h at 37°C. Afterward, antigen-presenting cells were γ-irradiated for 28 min and washed twice before co-incubation for at least 20 h with CD8$^+$ T cells at 37°C. Plates were washed three times with 1× PBS and three times with 1× PBS containing 0.05% Tween 20 (PBST20), and were subsequently incubated with 100 μl PBST20 containing 0.5% FCS with 1 μg/ml of the biotinylated detection antibody anti-mouse IFNγ mAb R4-6A2 (Mabtech, Germany) overnight at 4°C. On the following day, plates were washed four times in PBST20 and incubated further for 1 h at room temperature with streptavidin-conjugated alkaline phosphatase (BD Pharmingen, Germany) in PBST20 containing 1% FCS. After washing four times with PBST20 and 1× PBS, ELISPOT plates were developed using the Bio-Rad AP color development kit until spots were visible, which were then counted using a binocular.

Statistics

Statistical analysis (see Figure Legends) were performed using Prism software (GraphPad Software Inc., United States).

DATA AVAILABILITY STATEMENT

The original contributions presented in the study are included in the article/**Supplementary Material**, further inquiries can be directed to the corresponding author/s.

ETHICS STATEMENT

The animal study was reviewed and approved by the Ethics Committee of MPI-IB and the Berlin state authorities (LAGeSo Reg# G0469/09 and G0294/15) approved the protocol.

AUTHOR CONTRIBUTIONS

KMa, JF, CH, JH, and KMü designed the experiments. CH and JF performed the experiments and analyzed the data. AI performed and analyzed the sporozoite IFA. DS generated knockout parasite lines. KMa, CH, and JF wrote the manuscript. All authors commented and revised the manuscript.

FUNDING

This work was funded by the Deutsche Forschungsgemeinschaft through the research training group–Ph.D. program 2046 "From Experimental Models to Natural Systems" (project B1) and in part by the Max Planck Society.

ACKNOWLEDGMENTS

We acknowledge support by the German Research Foundation (DFG) and the Open Access Publication Fund of Humboldt-Universität zu Berlin.

SUPPLEMENTARY MATERIAL

The Supplementary Material for this article can be found online at: https://www.frontiersin.org/articles/10.3389/fmicb.2021.703804/full#supplementary-material

REFERENCES

Altschul, S. F., Gish, W., Miller, W., Myers, E. W., and Lipman, D. J. (1990). Basic local alignment search tool. *J. Mol. Biol.* 215, 403–410. doi: 10.1016/S0022-2836(05)80360-2

Aurrecoechea, C., Barreto, A., Basenko, E. Y., Brestelli, J., Brunk, B. P., Cade, S., et al. (2017). EuPathDB: the eukaryotic pathogen genomics database resource. *Nucl. Acids Res.* 45 (D1), D581–D591. doi: 10.1093/nar/gkw1105

Bork, P., and Doolittle, R. F. (1994). *Drosophila* kelch motif is derived from a common enzyme fold. *J. Mol. Biol.* 236, 1277–1282. doi: 10.1016/0022-2836(94)90056-6

Bruña-Romero, O., González-Aseguinolaza, G., Hafalla, J. C. R., Tsuji, M., and Nussenzweig, R. S. (2001). Complete, long-lasting protection against malaria of mice primed and boosted with two distinct viral vectors expressing the same plasmodial antigen. *Proc. Natl. Acad. Sci. U.S.A.* 98, 11491–11496. doi: 10.1073/pnas.191380898

Butler, N. S., Schmidt, N. W., and Harty, J. T. (2010). Differential effector pathways regulate memory CD8 T cell immunity against *Plasmodium berghei* versus P. *yoelii* sporozoites. *J. Immunol.* 184, 2528–2538. doi: 10.4049/jimmunol.0903529

Clyde, D. F., Most, H., McCarthy, V. C., and Vanderberg, J. P. (1973). Immunization of man against sporozoite-induced falciparum malaria. *Am. J. Med. Sci.* 266, 169–177. doi: 10.1097/00000441-197309000-00002

Cohen, J., Nussenzweig, V., Nussenzweig, R., Vekemans, J., and Leach, A. (2010). From the circumspo-rozoite protein to the RTS, S/AS candidate vaccine. *Hum. Vaccin.* 6, 90–96. doi: 10.4161/hv.6.1.9677

Depinay, N., Franetich, J. F., Grüner, A. C., Mauduit, M., Chavatte, J. M., Luty, A. J. F., et al. (2011). Inhibitory effect of TNF-α on malaria pre-erythrocytic stage development: Influence of host hepato-cyte/parasite combinations. *PLoS One* 6:e17464. doi: 10.1371/journal.pone.0017464

Doll, K. L., Pewe, L. L., Kurup, S. P., and Harty, J. T. (2016). Discriminating protective from non-protective *Plasmodium*-specific CD8+ T cell responses. *J. Immunol.* 196, 4253–4262. doi: 10.4049/jimmunol.1600155

Doolan, D. L., and Hoffman, S. L. (2000). The complexity of protective immunity against liver-stage ma-laria. *J. Immunol.* 165, 1453–1462. doi: 10.4049/jimmunol.165.3.1453

Ferreira, A., Schofield, L., Enea, V., Schellekens, H., van der Meide, P., Collins, W., et al. (1986). Inhibition of development of exoerythrocytic forms of malaria parasites by gamma-interferon. *Science* 232, 881–884. doi: 10.1126/science.3085218

Franke-Fayard, B., Trueman, H., Ramesar, J., Mendoza, J., van der Keur, M., van der Linden, R., et al. (2004). A *Plasmodium berghei* reference line that constitutively expresses GFP at a high level throughout the complete life cycle. *Mol. Biochem. Parasitol.* 137, 23–33. doi: 10.1016/j.molbiopara.2004.04.007

Friesen, J., and Matuschewski, K. (2011). Comparative efficacy of pre-erythrocytic whole organism vaccine strategies against the malaria parasite. *Vaccine* 29, 7002–7008. doi: 10.1016/j.vaccine.2011.07.034

Friesen, J., Silvie, O., Putrianti, E. D., Hafalla, J. C. R., Matuschewski, K., and Borrmann, S. (2010). Natural immunization against malaria: causal prophylaxis with antibiotics. *Sci. Transl. Med.* 2:ra49. doi: 10.1126/scitranslmed.3001058

Gibbins, M. P., Müller, K., Glover, M., Liu, J., Putrianti, E. D., Bauza, K., et al. (2020). Importance of the immunodominant CD8+ T cell epitope of *Plasmodium berghei* circumsporozoite protein in parasite- and vaccine-induced protection. *Infect. Immun.* 88, e383–20. doi: 10.1128/IAI.00383-20

González-Aseguinolaza, G., Nakaya, Y., Molano, A., Dy, E., Esteban, M., Rodríguez, D., et al. (2003). Induction of protective immunity against malaria by priming-boosting immunization with recombinant cold-adapted influenza and modified vaccinia Ankara viruses expressing a CD8+-T-cell epitope derived from the *circumsporozoite* protein of Plasmodium yoelii. *J. Virol.* 77, 11859–11866. doi: 10.1128/jvi.77.21.11859-11866.2003

Grüner, A. C., Mauduit, M., Tewari, R., Romero, J. F., Depinay, N., Kayibanda, M., et al. (2007). Sterile protection against malaria is independent of immune responses to the circumsporozoite protein. *PLoS One* 2:e1371. doi: 10.1371/journal.pone.0001371

Guebre-Xabier, M., Schwenk, R., and Krzych, U. (1999). Memory phenotype CD8+ T cells persist in livers of mice protected against malaria by immunization with attenuated *Plasmodium berghei* sporozoites. *Eur. J. Immunol.* 29, 3978–3986. doi: 10.1002/(sici)1521-4141(199912)29:12<3978::aid-immu3978>3.0.co;2-0

Hafalla, J. C., Silvie, O., and Matuschewski, K. (2011). Cell biology and immunology of malaria. *Immunol. Rev.* 240, 297–316. doi: 10.1111/j.1600-065X.2010.00988.x

Hafalla, J. C. R., Bauza, K., Friesen, J., Gonzalez-Aseguinolaza, G., Hill, A. V. S., and Matuschewski, K. (2013). Identification of targets of CD8+ T cell responses to malaria liver stages by genome-wide epitope profiling. *PLoS Pathogens* 9:e1003303. doi: 10.1371/journal.ppat.1003303

Hoffman, S. L., Billingsley, P. F., James, E., Richman, A., Loyevsky, M., Li, T., et al. (2010). Development of a metabolically active, non-replicating sporozoite vaccine to prevent *Plasmodium falciparum* malaria. *Hum. Vaccin.* 6, 97–106. doi: 10.4161/hv.6.1.10396

Hoffman, S. L., Goh, L. M., Luke, T. C., Schneider, I., Le, T. P., Doolan, D. L., et al. (2002). Protection of humans against malaria by immunization with radiation-attenuated *Plasmodium falciparum* sporozoites. *J. Infect. Dis.* 185, 1155–1164.

Janse, C. J., Franke-Fayard, B., Mair, G. R., Ramesar, J., Thiel, C., Engelmann, S., et al. (2006). High efficiency transfection of *Plasmodium berghei* facilitates novel selection procedures. *Mol. Biochem. Parasitol.* 145, 60–70. doi: 10.1016/j.molbiopara.2005.09.007

Kaiser, K., Matuschewski, K., Camargo, N., Ross, J., and Kappe, S. H. (2004). Differential transcriptome profiling identifies *Plasmodium* genes encoding pre-erythrocytic stage-specific proteins. *Mol. Microbiol.* 51, 1221–1232. doi: 10.1046/j.1365-2958.2003.03909.x

Kimura, K., Kimura, D., Matsushima, Y., Miyakoda, M., Honma, K., Yuda, M., et al. (2013). CD8+ T cells specific for a malaria cytoplasmic antigen form clusters around infected hepatocytes and are protective at the liver stage of infection. *Infect. Immun.* 81, 3825–3834. doi: 10.1128/IAI.00570-13

Krzych, U., Schwenk, R., Guebre-Xabier, M., Sun, P., Palmer, D., White, K., et al. (2000). The role of intrahepatic lymphocytes in mediating protective immunity by attenuated *Plasmodium berghei* sporozoites. *Immunol. Rev.* 174, 123–134. doi: 10.1034/j.1600-0528.2002.00013h.x

Kumar, K. A., Sano, G., Boscardin, S., Nussenzweig, R. S., Nussenzweig, M. C., Zavala, F., et al. (2006). The circumsporozoite protein is an immunodominant protective antigen in irradiated sporozoites. *Nature* 444, 937–940. doi: 10.1038/nature05361

Lau, L. S., Fernandez-Ruiz, D., Mollard, V., Sturm, A., Neller, M. A., Cozijnsen, A., et al. (2014). CD8+ T cells from a novel T cell receptor transgenic mouse induce liver-stage immunity that can be boosted by blood-stage infection in rodent malaria. *PLoS Pathogens* 10:e1004135. doi: 10.1371/journal.ppat.1004135

Montagna, G. N., Beigier-Bompadre, M., Becker, M., Kroczek, R. A., Kaufmann, S. H. E., and Matuschewski, K. (2014). Antigen export during liver infection of the malaria parasite augments protective immunity. *mBio* 5:e1321–14. doi: 10.1128/mBio.01321-14

Müller, K., Gibbins, M. P., Matuschewski, K., and Hafalla, J. C. R. (2017). Evidence of cross-stage CD8+ T cell epitopes in malaria pre-erythrocytic and blood stage infections. *Parasite Immunol.* 39:e12434. doi: 10.1111/pim.12434

Müller, K., Gibbins, M. P., Roberts, M., Reyes−Sandoval, A., Hill, A. V. S., Draper, S. J., et al. (2021). Low immunogenicity of malaria pre−erythrocytic stages can be overcome by vaccination. *EMBO Mol. Med.* 13:e13390. doi: 10.15252/emmm.202013390

Neafsey, D. E., Juraska, M., Bedford, T., Benkeser, D., Valim, C., Griggs, A., et al. (2015). Genetic diversity and protective efficacy of the RTS,S/AS01 malaria vaccine. *N. Engl. J. Med.* 373, 2025–2037. doi: 10.1056/nejmoa1505819

Nussenzweig, R. S., Vanderberg, J., Most, H., and Orton, C. (1967). Protective immunity produced by the injection of x-irradiated sporozoites of *Plasmodium berghei*. *Nature* 216, 160–162. doi: 10.1038/216160a0

Richie, T. L., Billingsley, P. F., Sim, B. K. L., James, E. R., Chakravarty, S., Epstein, J. E., et al. (2015). Progress with *Plasmodium falciparum* sporozoite (PfSPZ)-based malaria vaccines. *Vaccine* 33, 7452–7461. doi: 10.1016/j.vaccine.2015.09.096

Rodrigues, M., Nussenzweig, R. S., and Zavala, F. (1993). The relative contribution of antibodies, CD4+ and CD8+ T cells to sporozoite-induced protection against malaria. *Immunology* 80, 1–5.

Rodrigues, M. M., Cordey, A. S., Arreaza, G., Corradin, G., Romero, P., Maryanski, J. L., et al. (1991). CD8+ cytolytic T cell clones derived against the *Plasmodium yoelii* circumsporozoite protein protect against malaria. *Int. Immunol.* 3, 579–585. doi: 10.1093/intimm/3.6.579

Rodriguez, F., Harkins, S., Slifka, M. K., and Whitton, J. L. (2002). Immunodominance in virus-induced CD8+ T-cell responses is dramatically modified by DNA immunization and is regulated by gamma interferon. *J. Virol.* 76, 4251–4259. doi: 10.1128/jvi.76.9.4251-4259.2002

Romero, P., Maryanski, J. L., Corradin, G., Nussenzweig, R. S., Nussenzweig, V., and Zavala, F. (1989). Cloned cytotoxic T cells recognize an epitope in the circumsporozoite protein and protect against malaria. *Nature* 341, 323–326. doi: 10.1038/341323a0

RTS,S Clinical Trials Partnership (2015). Efficacy and safety of RTS,S/AS01 malaria vaccine with or without a booster dose in infants and children in Africa: final results of a phase 3, individually randomized, controlled trial. *Lancet* 386, 31–45. doi: 10.1016/S0140-6736(15)60721-8

Sano, G. I., Hafalla, J. C. R., Morrot, A., Abe, R., Lafaille, J. J., and Zavala, F. (2001). Swift development of protective effector functions in naive CD8+ T cells against malaria liver stages. *J. Exp. Med.* 194, 173–180. doi: 10.1084/jem.194.2.173

Schmidt, N. W., Podyminogin, R. L., Butler, N. S., Baovinac, V. P., Tucker, B. J., Bahjat, K. S., et al. (2008). Memory CD8 T cell responses exceeding a large but definable threshold provide long-term immunity to malaria. *Proc. Natl. Acad. Sci. U.S.A.* 105, 14017–14022. doi: 10.1073/pnas.0805452105

Schofield, L., Villaquiran, J., Ferreira, A., Schellekens, H., Nussenzweig, R., and Nussenzweig, V. (1987). γ interferon,CD8+ T cells and antibodies required for immunity to malaria sporozoites. *Nature* 330, 664–666. doi: 10.1038/330664a0

Sedegah, M., Sim, B. K. L., Mason, C., Nutman, T., Malik, A., Roberts, C., et al. (1992). Naturally acquired CD8+ cytotoxic T lymphocytes against the *Plasmodium falciparum* circumsporozoite protein. *J. Immunol.* 149, 966–971.

Stoute, J. A., Kester, K. E., Krzych, U., Wellde, B. T., Hall, T., White, K., et al. (1998). Long-term efficacy and immune responses following immunization with the RTS,S malaria vaccine. *J. Infect. Dis.* 178, 1139–1144. doi: 10.1086/515657

Tsuji, M., Mattei, D., Nussenzweig, R. S., Eichinger, D., and Zavala, F. (1994). Demonstration of heat-shock protein 70 in the sporozoite stage of malaria parasites. *Parasitol. Res.* 80, 16–21. doi: 10.1007/BF00932618

Valencia-Hernandez, A. M., Ng, W. Y., Ghazanfari, N., Ghilas, S., de Menezes, M. N., Holz, L. E., et al. (2020). A natural peptide antigen within the *Plasmodium* ribosomal protein RPL6 confers liver TRM cell-mediated immunity against malaria in mice. *Cell Host Microbe* 27, 950–962. doi: 10.1016/j.chom.2020.04.010

van der Most, R. G., Murali-Krishna, K., Lanier, J. G., Wherry, E. J., Puglielli, M. T., Blattman, J. N., et al. (2003). Changing immunodominance patterns in antiviral CD8 T-cell responses after loss of epitope presentation or chronic antigenic stimulation. *Virology* 315, 93–102. doi: 10.1016/j.virol.2003.07.001

van Dijk, M. R., Waters, A. P., and Janse, C. J. (1995). Stable transfection of malaria parasite blood stages. *Science* 268, 1358–1362. doi: 10.1126/science.7761856

Vanderberg, J. P. (1975). Development of infectivity by the *Plasmodium berghei* sporozoite. *J. Para-Sitol.* 61, 43–50. doi: 10.2307/3279102

Weiss, W. R., and Jiang, C. G. (2012). Protective CD8+ T lymphocytes in primates immunized with malaria sporozoites. *PLoS One* 7:e31247. doi: 10.1371/journal.pone.0031247

Weiss, W. R., Sedegah, M., Beaudoin, R. L., Miller, L. H., and Good, M. F. (1988). CD8+ T cells (cytotoxic/suppressors) are required for protection in mice immunized with malaria sporozoites. *Proc. Natl. Acad. Sci. U.S.A.* 85, 573–576. doi: 10.1073/pnas.85.2.573

World Health Organisation (2020). *World Malaria Report 2020*. Geneva: World Health Organisation.

Yoshida, N., Nussenzweig, R. S., Potocnjak, P., Nussenzweig, V., and Aikawa, M. (1980). Hybridoma produces protective antibodies directed against the sporozoite stage of malaria parasite. *Science* 207, 71–73. doi: 10.1126/science.6985745

Zavala, F., Cochrane, A. H., Nardin, E. H., Nussenzweig, R. S., and Nussenzweig, V. (1983). Circumsporozoite proteins of malaria parasites contain a single immunodominant region with two or more identical epitopes. *J. Exp. Med.* 157, 1947–1957. doi: 10.1084/jem.157.6.1947

Zavala, F., Masuda, A., Graves, P. M., Nussenzweig, V., and Nussenzweig, R. S. (1985). Ubiquity of the repetitive epitope of the CS protein in different isolates of human malaria parasites. *J. Immunol.* 135, 2790–2793.

Conflict of Interest: The authors declare that the research was conducted in the absence of any commercial or financial relationships that could be construed as a potential conflict of interest.

Publisher's Note: All claims expressed in this article are solely those of the authors and do not necessarily represent those of their affiliated organizations, or those of the publisher, the editors and the reviewers. Any product that may be evaluated in this article, or claim that may be made by its manufacturer, is not guaranteed or endorsed by the publisher.

frontiers in Microbiology

ORIGINAL RESEARCH
published: 31 August 2021
doi: 10.3389/fmicb.2021.703059

The Role of Type II Fatty Acid Synthesis Enzymes FabZ, ODSCI, and ODSCII in the Pathogenesis of *Toxoplasma gondii* Infection

Xiao-Pei Xu[1,2], Hany M. Elsheikha[3], Wen-Ge Liu[1], Zhi-Wei Zhang[1], Li-Xiu Sun[1], Qin-Li Liang[1], Ming-Xin Song[2] and Xing-Quan Zhu[1,4,5]**

[1] State Key Laboratory of Veterinary Etiological Biology, Key Laboratory of Veterinary Parasitology of Gansu Province, Lanzhou Veterinary Research Institute, Chinese Academy of Agricultural Sciences, Lanzhou, China, [2] Heilongjiang Key Laboratory for Zoonosis, College of Veterinary Medicine, Northeast Agricultural University, Harbin, China, [3] Faculty of Medicine and Health Sciences, School of Veterinary Medicine and Science, University of Nottingham, Nottingham, United Kingdom, [4] College of Veterinary Medicine, Shanxi Agricultural University, Taigu, China, [5] Key Laboratory of Veterinary Public Health of Higher Education of Yunnan Province, College of Veterinary Medicine, Yunnan Agricultural University, Kunming, China

OPEN ACCESS

Edited by:
Hong-Juan Peng, Southern Medical University, China

Reviewed by:
Shaojun Long, China Agricultural University, China
Stephen Seah, University of Guelph, Canada

***Correspondence:**
Ming-Xin Song
songmx@neau.edu.cn
Xing-Quan Zhu
xingquanzhu1@hotmail.com

Specialty section:
This article was submitted to Infectious Diseases, a section of the journal Frontiers in Microbiology

Received: *30 April 2021*
Accepted: *30 July 2021*
Published: *31 August 2021*

Citation:
Xu X-P, Elsheikha HM, Liu W-G, Zhang Z-W, Sun L-X, Liang Q-L, Song M-X and Zhu X-Q (2021) The Role of Type II Fatty Acid Synthesis Enzymes FabZ, ODSCI, and ODSCII in the Pathogenesis of Toxoplasma gondii Infection. Front. Microbiol. 12:703059. doi: 10.3389/fmicb.2021.703059

Toxoplasma gondii is an obligate intracellular protozoan parasite, which has a worldwide distribution and can infect a large number of warm-blooded animals and humans. *T. gondii* must colonize and proliferate inside the host cells in order to maintain its own survival by securing essential nutrients for the development of the newly generated tachyzoites. The type II fatty acid biosynthesis pathway (FASII) in the apicoplast is essential for the growth and survival of *T. gondii*. We investigated whether deletion of genes in the FASII pathway influences the *in vitro* growth and *in vivo* virulence of *T. gondii*. We focused on beta-hydroxyacyl-acyl carrier protein dehydratase (FabZ) and oxidoreductase, short chain dehydrogenase/reductase family proteins ODSCI and ODSCII. We constructed *T. gondii* strains deficient in *FabZ, ODSCI*, and *ODSCII* using CRISPR-Cas9 gene editing technology. The results of immunofluorescence assay, plaque assay, proliferation assay and egress assay showed that in RHΔ*FabZ* strain the apicoplast was partly lost and the growth ability of the parasite *in vitro* was significantly inhibited, while for RHΔ*ODSCI* and RHΔ*ODSCII* mutant strains no similar changes were detected. RHΔ*FabZ* exhibited reduced virulence for mice compared with RHΔ*ODSCI* and RHΔ*ODSCII*, as shown by the improved survival rate. Deletion of *FabZ* in the PRU strain significantly decreased the brain cyst burden in mice compared with PRUΔ*ODSCI* and PRUΔ*ODSCII*. Collectively, these findings suggest that FabZ contributes to the growth and virulence of *T. gondii*, while ODSCI and ODSCII do not contribute to these traits.

Keywords: *Toxoplasma gondii*, virulence factors, FASII enzymes, FabZ, ODSCI, ODSCII

INTRODUCTION

Toxoplasma gondii is an obligate intracellular protozoan, which is distributed all over the world. This parasite can cause adverse health impacts on the immunodeficient individuals such as AIDS patients or organ transplant recipients (Xiao et al., 2010; Robert-Gangneux and Dardé, 2012; Chemoh et al., 2015). *T. gondii* can survive in nearly all nucleated cells (Blume et al., 2009; MacRae et al., 2012; Xia et al., 2019) and completes its intracellular reproduction inside a parasitophorous vacuole (PV) after invading the host cell. The synthesis or uptake of fatty acids and other molecules from the host cell is important for the growth and proliferation of intracellular pathogens. Fatty acids are the main components of the PV, the membranes of the apicoplast and other organelles in *T. gondii*, underscoring the significance of fatty acids for the survival of *T. gondii* (Mordue et al., 1999; Ramakrishnan et al., 2012; Botté et al., 2013).

The type II fatty acid biosynthesis pathway (FASII) in apicomplexan protozoa is located in a unique organelle known as apicoplast, which has an independent genome of prokaryotic origin with no counterpart in the human or animal host (Ralph et al., 2004), which makes apicoplast and FASII a source of novel drug targets for *T. gondii* (Wiesner et al., 2008; Aygün and Mutlu, 2020). FASII, via a variety of enzymes, plays an important role in fatty acid metabolism. Phosphoenolpyruvate, after import to the apicoplast, is metabolized into pyruvate and converted into acetyl-CoA (a key precursor for FASII) via the action of pyruvate dehydrogenase complex (PDH) (Fleige et al., 2007). Acetyl-CoA can be also produced in the nucleus and cytosol via the cation of acetyl-CoA synthetase and ATP citrate lyase (Tymoshenko et al., 2015), and in the mitochondrion via the action of branched-chain α-keto acid dehydrogenase-complex (Oppenheim et al., 2014). Although cytosolic acetyl-CoA is required for the synthesis of parasite fatty acids, metabolic adaptation by the parasite compensates for any loss of mitochondrial acetyl-CoA (Kloehn et al., 2020).

The acyl carrier protein (ACP) plays a role in FASII. Deletion of ACP causes growth defect and decreases the virulence of *T. gondii* (Mazumdar et al., 2006). The synthesis of FASII in the apicoplast of *T. gondii* plays a key role in the survival of *T. gondii*, and the β-hydroxyacylacyl carrier protein dehydratase (FabZ; TGME49_321570) is essential for FASII metabolism in *T. gondii* (Wu et al., 2018; Krishnan et al., 2020). The protein coding genes *ODSCI* (TGGT1_269400) and *ODSCII* (TGGT1_313050) (ToxoDB database) belong to oxidoreductase, short-chain dehydrogenase/reductase family (Kowalik et al., 2009). According to KEGG analysis, *ODSCI* and *ODSCII* are involved in the FASII pathway. According to Enzyme Commission classification, they also belong to 3-oxoacyl-[acyl-carrier-protein] reductase, which is involved in type II fatty acid biosynthesis.

The knockout of *FabZ* led to the loss of apicoplast of *T. gondii* tachyzoites, and decreased the level of myristate (C14: 0) and palmitate (C16: 0), the synthetic products of FASII, which resulted in the inhibition of the growth of *T. gondii* (Krishnan et al., 2020). In the present study, we hypothesized that mutation in *T. gondii* genes *FabZ, ODSCI*, and *ODSCII* involved in fatty acid biosynthesis and metabolism may render the mutant parasite strains less virulent and incapable of establishing an infection. We constructed knockout strains using CRISPR-Cas9 technology, and evaluated the effects of deletion of *FabZ*, *ODSCI*, and *ODSCII* on the virulence of the mutant strains in mice and on the *in vitro* growth using plaque assay, intracellular proliferation assay and egress assay.

MATERIALS AND METHODS

Toxoplasma gondii Cultures

T. gondii tachyzoites of the virulent RH (Genotype I) and less virulent PRU (Genotype II) strains were maintained *in vitro* in human foreskin fibroblasts (HFFs, ATCC®, SCRC-1041™) as described previously (Zhang et al., 2021). The HFF cells were grown in Dulbecco's Modified Eagle medium (DMEM) supplemented with 10% fetal bovine serum (FBS), 10 mM HEPES (pH 7.2), 100 Ug/ml streptomycin and 100 U/ml penicillin, and maintained at 37°C with 5% CO_2.

Construction of Knockout Strains

FabZ, *ODSCI*, and *ODSCII* knockout strains were constructed using CRISPR-Cas9 technology as described previously (Wang et al., 2020). Briefly, the single-guide RNA (sgRNA) of each gene was inserted into the template pSAG1-Cas9-SgUPRT plasmid using Q5 mutation kit (NEB) to replace the target RNA. The plasmid was sequenced and the positive plasmid was extracted using Endo-Free Plasmid DNA Mini Kit (Omega, Georgia, United States). The 5′ and 3′ homologous fragments of each gene were amplified from the genomic DNA of *T. gondii* RH strain using the designed 5′ and 3′ homologous arm specific primers. All the primers used in this study are listed in **Supplementary Table 1**. The DHFR resistant fragments were amplified using the pUPRT-DHFR-D plasmid as a template, and the three fragments (5′ and 3′ homologous arm and DHFR fragment) were cloned into the plasmid pUC19 employing the multi-fragment cloning approach using the CloneExpress II one-step cloning kit (Vazyme Biotech, Nanjing, China). The 5HR-DHFR-3HR fragment was amplified using the positive plasmid as a template to produce a homologous template, which was purified by agarose gel electrophoresis. About 40 μg of the CRISPR-Cas9 plasmid and 15 μg of the purified 5HR-DHFR-3HR fragment were co-transfected into freshly egressed *T. gondii* tachyzoites by electroporation. Finally, the clonal strain was obtained using a limiting dilution assay and 96-well plastic culture plates containing 3 μM pyrimethamine. The knockout strains were verified by PCR analysis. PCR 1 and PCR 3 were amplified from 5′ to 3′ of *FabZ*, *ODSCI*, and *ODSCII* by PCR1F/R and PCR3F/R, respectively, to verify whether the DHFR resistant fragment was successfully inserted into the corresponding knockout strain. PCR2F/R amplified product was about 700 bp in length, the knockout primers were designed at the upstream and downstream of *FabZ*, *ODSCI*, and *ODSCII* sgRNA-F to verify the successful knockout of

the three genes (PCR2), and the wild-type (WT) strain was used as the control. The PCR reaction conditions were as follows: initial denaturation at 95°C for 4 min, followed by 35 amplification cycles (denaturation at 95°C for 30 s, annealing at 56°C for 30 s and extension at 72°C for 1 min), and a final extension step at 72°C for 10 min. The amplified products were examined on a 1.5% agarose gel with TAE buffer containing ethidium bromide.

C-Terminal Tagging

The C-Terminal HA epitope tagging was used to establish the subcellular localization of *FabZ*, *ODSCI*, and *ODSCII*. CRISPR-Cas9 plasmids targeting the 3′ region of each gene were constructed as previously described (Cao et al., 2019). Using pLIC-3 × HA-DHFR plasmid as a template, PCR products containing about 1.5 kb (except stop codon) and 3 × HA and DHFR fragments at the 3′ of the target gene were amplified using specific primers and purified using agarose gel electrophoresis. The purified fragment and the constructed C-terminal (3′ region) specific CRISPR-Cas9 plasmid were electro-transfected into freshly egressed tachyzoites. To identify single positive clones and verify whether the HA fragment was successfully inserted into *T. gondii* tachyzoites, we used PCR and specific primers to amplify the *FabZ* gene. We also used immunofluorescence assay (IFA) to localize FabZ and acyl carrier proteins (ACP). Briefly, HFFs were infected with 1×10^6 tachyzoites of RHΔ*FabZ* strain for 24 h. The cells were fixed with 4% paraformaldehyde (PFA) for 1 h, permealized for 30 min using 0.2% Triton X-100/phosphate-buffered saline (PBS), and blocked using 5% BSA for 30 min. Cells were incubated with primary antibodies (1:1,000), including mouse anti-SAG1 antibody to stain the tachyzoite's plasma membrane or anti-ACP antibody to stain the apicoplast, and rabbit anti-HA antibody, overnight at 4°C; followed by incubation with the secondary antibody (Alexa Fluor 594 goat anti-mouse IgG;1:1,000) to stain SAG1 and ACP, or the secondary antibody (Alexa Fluor 488 anti-rabbit IgG; 1:1,000) to stain HA, for 1 h. Image analysis was performed using an TCS SP8 confocal scanning microscope (Leica, Germany).

Immunofluorescence Localization of Apicoplast

HFFs were infected with 1×10^6 tachyzoites of each of the knockout strains (RHΔ*FabZ*, RHΔ*ODSCI*, RHΔ*ODSCII*) and the WT RH strain and cultured at 37°C for 24 h. Subsequently, the cells were fixed with 4% paraformaldehyde (PFA) for 1 h, permealized for 30 min using 0.2% Triton X-100/PBS, and blocked using 5% bovine serum albumin (BSA) for 30 min. Cells were incubated with the primary antibodies (1:1,000), including rabbit anti-IMC1 (inner membrane complex) mouse antibody to stain the tachyzoites and anti-acyl carrier protein (ACP) antibody to stain the apicoplast, overnight at 4°C, followed by incubation with the secondary antibody (Alexa Fluor 488 anti-rabbit IgG; 1:1,000) to stain IMC1 or (Alexa Fluor 594 goat anti-mouse IgG;1:1,000) to stain the ACP 37°C for 1 h. Image analysis was performed using an TCS SP8 confocal scanning microscope (Leica, Germany).

Plaque Assay

Approximately 500 tachyzoites of the three mutant RH strains and the WT strain were inoculated into 12-well culture plates containing HFF cell monolayers. Infected plates were incubated in 37°C and 5% CO_2 for 7 days. After removing the culture medium, the infected cells were fixed with 4% PFA for 1 h and stained with 0.5% crystal violet solution for 30 min. The number and size of plaques were counted and analyzed as described previously (Wang et al., 2020).

Intracellular Proliferation Assay

Tachyzoites (1×10^5) of the three mutant strains and the WT strain were inoculated into cell culture dishes containing HFF cell monolayers. After 1 h, the medium was removed and the culture dishes were washed 3 times to remove any remaining extracellular tachyzoites. Fresh medium was then added to the infected cells and incubated at 37°C and 5% CO_2 for 23 h. The cells were fixed with 4% PFA for 1 h, and then stained with mouse anti-SAG1 and Alexa Fluor 594 goat-anti mouse IgG. Parasitophorous vacuoles (PVs) were randomly examined under a fluorescence microscope, and the number of tachyzoites inside the PVs was determined.

Egress Assay

Tachyzoites (1×10^5) of the three mutant strains and the WT strain were inoculated into cell culture dishes containing HFF cell monolayers. After incubation at 37°C with 5% CO_2 for 1 h, cultures were washed 3 times with PBS to remove any extracellular tachyzoites. Fresh medium was then added and culture was future incubated for 36 h, and infected cells were treated with 3 μM calcium ionophore A23187 diluted in DMEM as described previously (Zhang et al., 2021). Live cell microscopy was used to monitor and image the tachyzoite egress from the host cell.

Quantitative Polymerase Chain Reaction (qPCR) Assay

Quantitative PCR (qPCR) was performed to quantify the expression of uracil phosphoribosyltransferase [(UPRT) (TGGT1_312480)] gene and apicoplast gene (TGGT1_302050) between WT strain and Δ*FabZ* strain. The 18 s rRNA gene was used as an internal reference for normalization. The qPCR assay was performed as described previously (Wu et al., 2009; Yeh and DeRisi, 2011; Reiff et al., 2012; Bansal et al., 2017). Genomic DNA was isolated from freshly egressed tachyzoites using Tiangen DNA extraction kit according to the manufacturer's directions. The apicoplast and UPRT-specific gene sequences were amplified using Max Super-Fidelity DNA Polymerase (Vazyme). The amplification reaction mixture included 10 μl of 2 × SYBR Green *pro Taq HS* Premix (final concentration 1 ×) (Accurate Biology), 0.4 μl of 10 μM of each primer, 40 ng of the extracted *T. gondii* DNA, 0.4 μl of ROX Reference Dye, and sterile water to a final volume of 20 μl. qPCR was performed using an

initial denaturation at 95°C for 30 s; followed by 40 cycles of amplification at 95°C for 10 s, 56°C for 20 s, and 72°C for 30 s.

Tachyzoite-Bradyzoite Transformation

Tachyzoites of the knockout strains (PRUΔ*FabZ*, PRUΔ*ODSCI,* and PRUΔ*ODSCII*) and the WT PRU strain were used to infect the HFF cells cultured in alkaline RPMI-1640 medium (pH 8.2). After 3 days, the cells were fixed with 4% PFA for 1 h, subjected to permeabilization with 0.2% Triton X-100/PBS for 30 min at room temperature. Cells were blocked with PBS plus 5% BSA for 30 min and then incubated with the primary antibody (rabbit anti-IMC1) (1:1,000) overnight at 4°C, washed, and then incubated with goat anti-rabbit IgG Alexa Fluor 594 (1:1,000, Invitrogen, California, United States) 37°C for 1 h. Fluorescein isothiocyanate (FITC)-conjugated Dolichos biflorus lectin (DBL) was used to show the cyst wall (green). Slides were analyzed using a TCS SP8 confocal scanning microscope (Leica, Germany). We also quantified the rate of tachyzoite-bradyzoite transformation by subjecting *T. gondii*-infected HFF cells to immunostaining using DBL (a bradyzoite-specific marker) and IMC1 (stain of total parasites) as described previously (Xia et al., 2018). At least 100 PVs were examined in each parasite strain, and the experiment was repeated at least 3 independent times. The transformation rate of bradyzoites was calculated by dividing the number of DBL positive PVs by the number of IMC1 positive PVs.

Characterization of RHΔ*FabZ*, RHΔ*ODSCI*, RHΔ*ODSCII* in Mice

Female specific-pathogen-free (SPF) Kunming mice (7-weeks-old) were purchased from the Center of Laboratory Animals, Lanzhou Veterinary Research Institute, Chinese Academy of Agricultural Sciences. Mice (8 mice/cage/group) were housed in SPF environment for 1 week in order to acclimatize to the experimental environment. Mice were housed in enriched conditions with 12-h light/dark cycle. The food and water were provided *ad libitum*. Mice were infected intraperitoneally (i.p.) with freshly egressed tachyzoites of the respective mutant strains or WT strains. The number of tachyzoites of RH or PRU strain used in the inoculation was 100 and 5×10^4 per mouse, respectively. The level of disease severity in RH and PRU-infected mouse groups was carefully monitored twice daily. Well-defined humane endpoints were used to identify mice that must be euthanized to avoid unnecessary suffering. The number of cysts in the brain homogenates of the PRU-infected mice that survived until 30 days after infection were recorded as described previously (Wang et al., 2018).

Bioinformatics Analysis

Information on the genomic characteristics of each gene, *FabZ*, *ODSCI*, and *ODSCII*, including the number of signal peptides, exons and transmembrane domains, and the temporal expression during the parasite cell cycle stages and in different *T. gondii* genotypes were obtained from ToxoDB.[1]

[1]http://toxodb.org

Data Analysis

The data were analyzed by GraphPad Prism 7 (GraphPad Software, La Jolla, CA, United States). All the experiments were repeated 3 times and data are presented as means ± standard errors of the means (SEMs). The *F*-test was used for equal variance detection, and the means were compared using Student's *t*-test or the Wilcoxon test.

RESULTS AND DISCUSSION

In this study we investigated whether deletion of *FabZ*, *ODSCI*, and *ODSCII* genes involved in the FASII pathway, using CRISPR-Cas9, influences the *in vitro* growth and *in vivo* virulence of *T. gondii*.

Localization of *FabZ*, *ODSCI*, and *ODSCII*

The *FabZ*, *ODSCI*, and *ODSCII* were tagged with three HA epitopes at the C terminus to characterize their cellular localization. The results of IFA analysis showed that for FabZ, a fluorescence signal can be observed in the apicoplast, indicating that *Tg*-FabZ is expressed in the apicoplast in the WT strain (**Figures 1A,B**). In contrast, no fluorescence signal was detected in the apicoplast in case of *Tg*-ODSCI and *Tg*-ODSCII (data not shown), possibly due to their low expression in the tachyzoite stage.

Construction of Δ*FabZ*, Δ*ODSCI,* and Δ*ODSCII* Strains

To study the biological function of FabZ, ODSCI, and ODSCII in *T. gondii*, we deleted the corresponding encoding genes in RH and PRU strains using CRISPR-Cas9 system. The coding regions of *FabZ*, *ODSCI*, and *ODSCII* were replaced by 5HR-DHFR-3HR fragments using homologous recombination (**Figure 2A**). Then, the constructed Δ*FabZ*, Δ*ODSCI,* and Δ*ODSCII* strains were confirmed by PCR analysis. PCR1 and PCR3 were used to establish whether DHFR was successfully

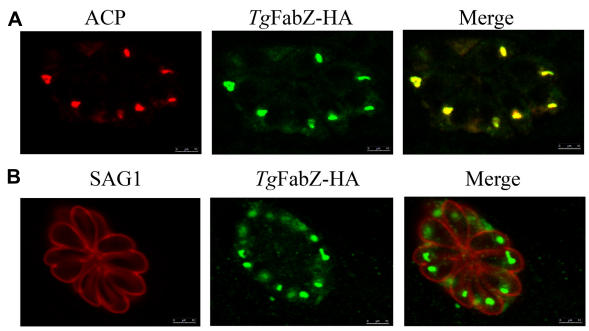

FIGURE 1 | Colocalization of FabZ and apicoplast in *T. gondii* as determined by indirect immunofluorescence analysis. **(A)** Colocalization of acyl carrier protein (ACP) in the apicoplast (red) and *Tg*FabZ-HA (green). **(B)** Colocalization of the plasma membrane protein SAG1 of *T. gondii* tachyzoites (red) and *Tg*FabZ-HA (green). The results indicate that FabZ is located in the apicoplast. Scale bars, 10 μm.

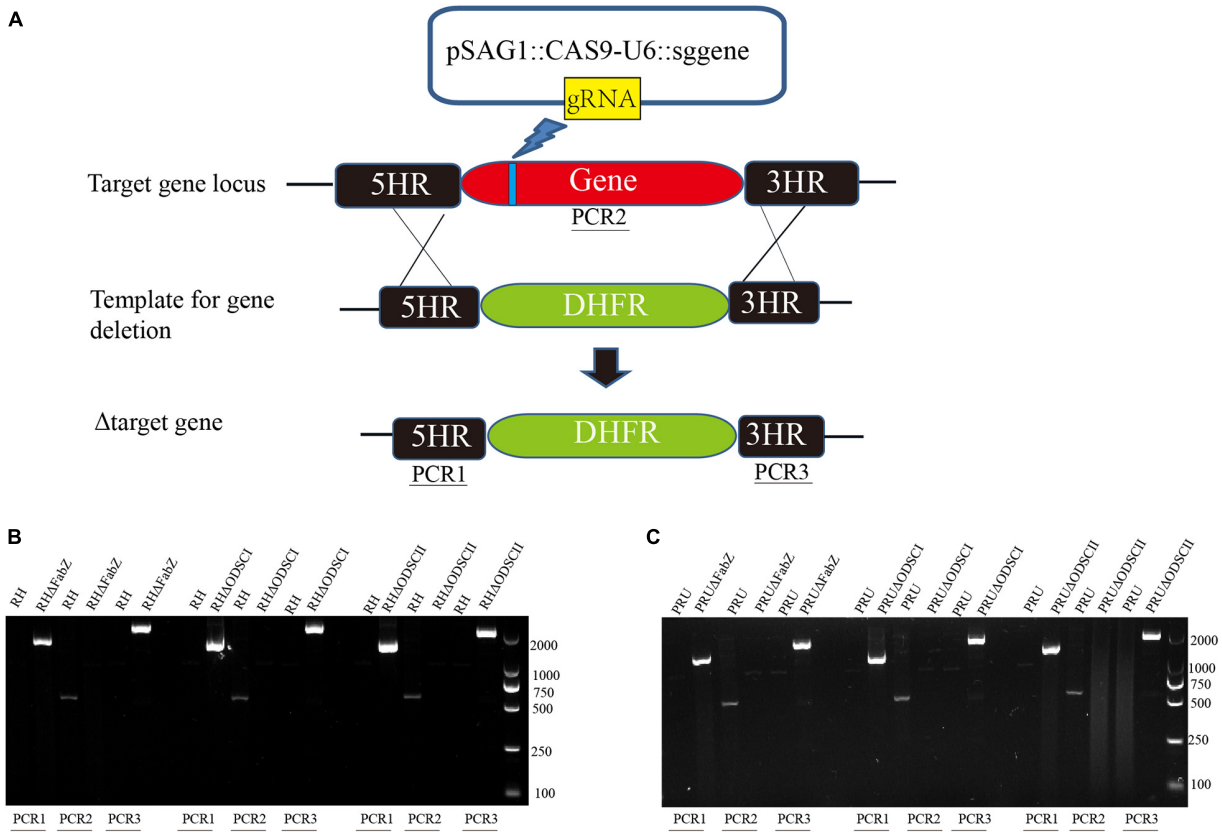

FIGURE 2 | Construction of gene knockout strain using CRISPR-Cas9 system. **(A)** Schematic diagram of the CRISPR-Cas9 strategy used to knockout the target genes *FabZ*, *ODSCI*, and *ODSCII*. **(B,C)** The knockout strains were verified by PCR analysis. The results showed that PCR1 and PCR3 amplified bands in knockout strains, while RH and PRU wild strains had no bands, indicating that DHFR fragments were successfully inserted into knockout strains from 5′ to 3′ ends by homologous recombination. PCR2 showed that bands were amplified in RH and PRU wild-type strains, while knockout strains had no bands, showing that genes were successfully deleted.

inserted into the target gene sequence. The PCR products were detected in the clonal mutant strains, but not in the parental RH or PRU strain. PCR2 was used to verify that the target gene is successfully deleted, where the amplified fragments were detected in the parental strain but not in the knockout strain (**Figures 2B,C**). These results showed that mutant strains, Δ*FabZ*, Δ*ODSCI,* and Δ*ODSCII*, were successfully constructed.

The Effects on the *in vitro* Growth of *T. gondii*

In the present study, we determined whether FabZ, ODSCI, and ODSCII play a role in the growth of *T. gondii* by using the plaque assay, replication assay and egress assay. Significantly smaller and fewer plaques were formed by Δ*FabZ* strain compared to that produced by WT RH strain. There was no difference in the size and number of plaques formed by Δ*ODSCI* or Δ*ODSCII* when compared with WT RH strain (**Figures 3A,B**). These results show that lack of *FabZ* gene causes a considerable reduction in the growth of the RH strain; however, deletion of *ODSCI* and *ODSCII* did not have any impact on the rate of the parasite's growth.

The results of intracellular proliferation assay showed that there were mainly 2 and 4 parasites in the PVs of Δ*FabZ* strain, and the number of PVs with 8 and 16 tachyzoites were significantly less than those detected in the PVs produced by the WT strain (**Figure 3C**), indicating that *FabZ* disruption significantly inhibited the replication of *T. gondii*. In contrast, *ODSCI* and *ODSCII* do not contribute to the parasite growth *in vitro* (**Figure 3C**). A similar finding was detected in *P. yoelii* where deletion of *FabZ*, a key enzyme in the FASII pathway, was found to prevent *P. yoelii* from forming merozoites during the liver infection stage (Vaughan et al., 2009).

We examined whether the deletion of *FabZ*, *ODSCI*, and *ODSCII* had an impact on *T. gondii* egress. The egress of *T. gondii* occurs when there are 64 or more tachyzoites inside the PV, and calcium is a key factor in mediating this process. 3 μM calcium ionophore A23187 was used to stimulate the tachyzoites release from the PV (Black et al., 2000a; Black and Boothroyd, 2000b; Arrizabalaga et al., 2004; Caldas et al., 2009). The results showed that most tachyzoites of Δ*FabZ*, Δ*ODSCI,* or Δ*ODSCII* and WT strain egressed within 2 min, indicating that the knockout of these three genes do not have any impact on the egress of *T. gondii* (**Figure 3D**).

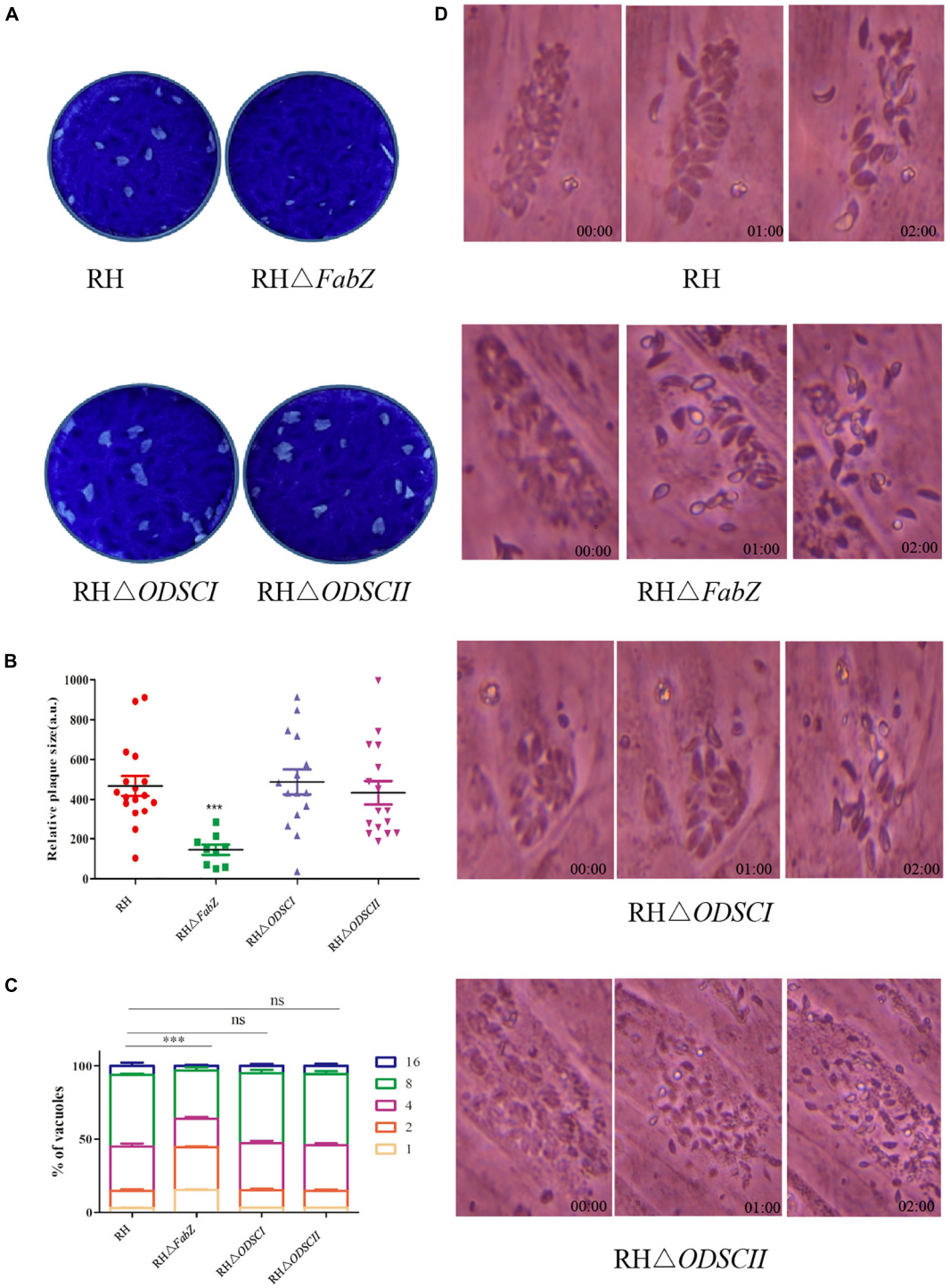

FIGURE 3 | Characterization of the growth kinetics of the knockout strains *in vitro.* **(A)** Representative images of the plaque assay of HFFs infected with RH WT strain and mutant strains (RHΔ*FabZ*, RHΔ*ODSCI,* and RHΔ*ODSCII*) for 7 days. **(B)** Plaque's size presented as arbitrary units (a. u.). The relative size of RHΔ*FabZ* plaque was significantly smaller and the number of plaque was fewer that of RH WT strain, and there was no significant difference between RHΔ*ODSCI* or RHΔ*ODSCII* and RH WT strain. **(C)** The replication of *T. gondii* in HFFs was quantified by counting the number of *T. gondii* tachyzoites (1, 2, 4, 8, 16) per vacuole 24 h after infection with RH WT strain, RHΔ*FabZ*, RHΔ*ODSCI,* or RHΔ*ODSCII* strain. RHΔ*FabZ* replication was significantly inhibited, while RHΔ*ODSCII* and RHΔ*ODSCII* strains had similar intracellular replication kinetics to WT strain. **(D)** HFFs were infected with RH WT strain, RHΔ*FabZ,* RHΔ*ODSCI,* or RHΔ*ODSCII* strain for 36 h, followed by treatment with 3 μM calcium ionophore A23187 to monitor the egress of tachyzoites at 0, 1, and 2 min after treatment. The results showed that the egressed pattern of WT strain was similar to that of all mutant strains. The data are presented as means ± SEMs ($n = 3$ in triplicates). ***$P < 0.001$; ns, non-significant by Student's *t*-test and Gehan-Breslow-Wilcoxon test.

Effect of *FabZ*, *ODSCI*, and *ODSCII* Deletion on Apicoplast of *T. gondii*

The ACP fluorescent signal was hardly observed in the apicoplast of Δ*FabZ* tachyzoites, but was clearly detected in the tachyzoites of Δ*ODSCI* or Δ*ODSCII* and WT strains (**Figure 4A**). We further investigated the role of Δ*FabZ* in the stability of the apicoplast genome by comparing the replication of the apicoplast gene and the nuclear gene in Δ*FabZ* compared with WT by using qPCR. The results showed that compared with WT strain, the apicoplast gene expression of Δ*FabZ* was significantly decreased (**Figure 4B**), indicating that the presence of *FabZ* is essential for the maintenance of apicoplast genome of *T. gondii*.

In this study, the apicoplast gene (TGGT1_302050) and UPRT gene (TGGT1_312480) of *T. gondii* were successfully amplified. We also found that the apicoplast of Δ*FabZ* was lost, and the replications of the apicoplast genome, and the growth and intracellular proliferation were significantly reduced, indicating that FabZ plays a key role in the growth of *T. gondii*. These results show that the interruption of FASII pathway in the apicoplast by deleting *FabZ* may be the cause of the observed growth defects in Δ*FabZ* strain.

Effect of Deletion of *FabZ*, *ODSCI*, and *ODSCII* on Phenotypic Transformation

After incubating tachyzoites with RPMI-1640 (pH 8.2) for 3 days, the parasite cyst wall and tachyzoites were stained with DBL and IMC1, respectively. IFA results showed that Δ*FabZ*, Δ*ODSCI,* and Δ*ODSCII* were similar to WT PRU strain, all of the analyzed strains exhibit parasite DBL positive signal (green) (**Figure 5A**), suggesting that FabZ, ODSCI, and ODSCII do not contribute to the tachyzoite-bradyzoite transformation process. No significant difference was detected in the tachyzoite-bradyzoite transformation rate between any of the examined *T. gondii* WT and mutant PRU strains (**Figure 5B**).

The Virulence of Δ*FabZ*, Δ*ODSCI,* and Δ*ODSCII* in Mice

We examined the impact of deletion of *FabZ*, *ODSCI*, and *ODSCII* on the pathogenicity of *T. gondii*. Approximately 100 tachyzoites of each strain, including RH, RHΔ*FabZ*, RHΔ*ODSCI,* and RHΔ*ODSCII*, were injected into Kunming mice by i.p. inoculation. The mice infected by RHΔ*FabZ* strain reached their humane endpoint up to 15 dpi, while mice infected by RHΔ*ODSCI*, RHΔ*ODSCII,* or WT strain reached their humane endpoint up to 11 dpi (**Figure 6A**). The survival rate of mice inoculated with wild-type PRU was 62.5%, and the survival rates of mice inoculated with knockout strains PRUΔ*FabZ*, PRUΔ*ODSCI,* and PRUΔ*ODSCII* were 50, 50, and 62.5%, respectively, indicating that *FabZ*, *ODSCI*, and *ODSCII* genes do not play any role in the virulence of *T. gondii* PRU strain in mice (**Figure 6B**).

We examined the effects of PRUΔ*FabZ*, PRUΔ*ODSCI,* and PRUΔ*ODSCII* on the cyst formation of *T. gondii*. Approximately 5×10^4 tachyzoites of WT PRU and each of the three mutant strains were injected by the i.p. route into Kunming mice. After 30 days the number of cysts in the brain of the survived mice was counted. As shown in **Figure 6C**, the number of cysts in mice infected by PRUΔ*FabZ* (51.25 ± 3.198) was significantly ($P < 0.01$) lower than that in mice infected by WT (103.7 ± 8.686), while the number of cysts in mice infected with PRUΔ*ODSCI* and PRUΔ*ODSCII* was not significantly different from that of the WT-infected mice.

Previous studies have shown that ACP is a key enzyme in the FASII pathway, and that deletion of the corresponding gene leads to defects in the growth of parasites *in vitro*, and increases the survival time of mice infected with mutant strain compared to mice infected by WT strain (Behnke et al., 2006; Mazumdar et al., 2006). Our results showed that deletion of *FabZ* induced defects in the growth of *T. gondii in vitro*, improved the survival of mice infected by the RH strain, and decreased the number of brain

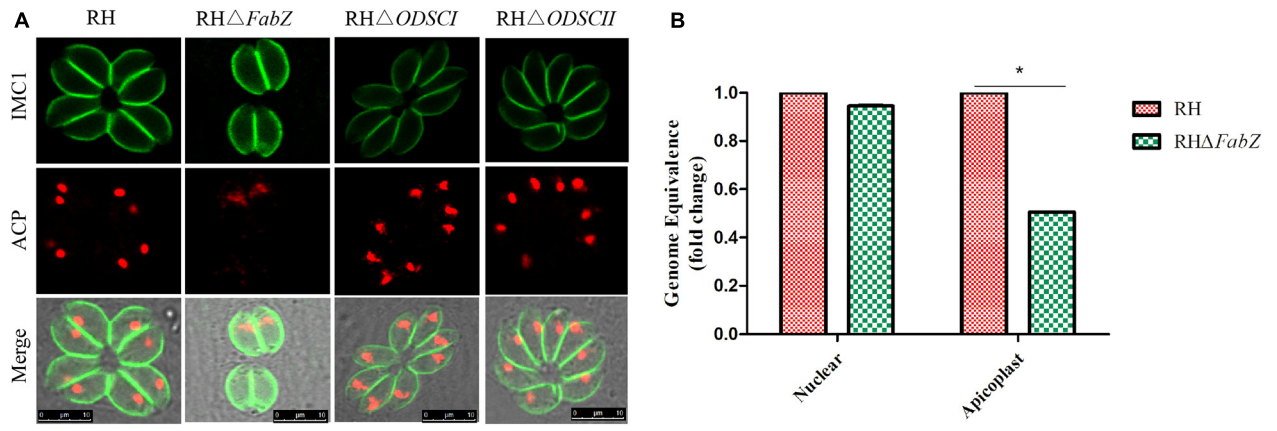

FIGURE 4 | The effect of gene knockout on the apicoplast of *T. gondii* RH strain. **(A)** Immunofluorescence localization of the anti-acyl carrier protein (ACP) in the apicoplast using an apicoplast-specific antibody. The ACP specific fluorescence was hardly detected in the apicoplast of tachyzoites of Δ*FabZ*, but was clearly visible in the tachyzoites of Δ*ODSCI*, Δ*ODSCII,* and WT strains. Scale bars, 10 μm. **(B)** Quantitative PCR was performed to detect apicoplast and nuclear gene in Δ*FabZ* and WT RH strains. The expression of the apicoplast gene in Δ*FabZ* strain was significantly decreased. The data are presented as means ± SEMs ($n = 3$ in triplicates). *$P < 0.05$; ns, non-significant by Student's *t*-test and Gehan-Breslow-Wilcoxon test.

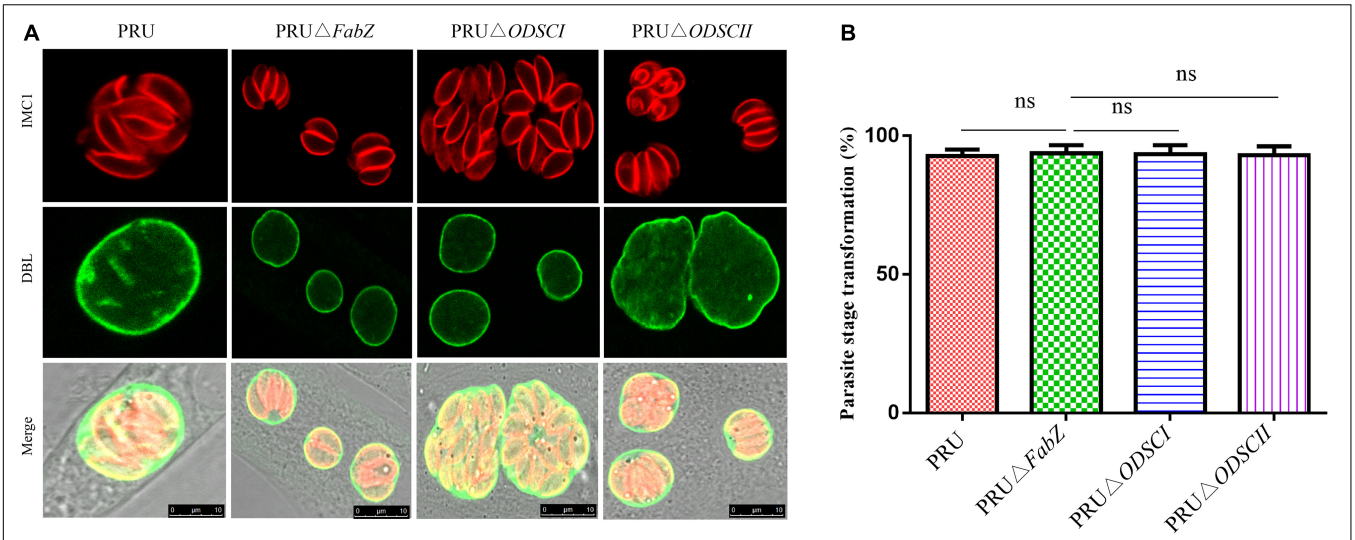

FIGURE 5 | Tachyzoite-bradyzoite transformation of Δ*FabZ*, Δ*ODSCI,* or Δ*ODSCII* using immunofluorescence analysis. HFFs were infected with PRU WT, PRUΔ*FabZ*, PRUΔ*ODSCI,* or PRUΔ*ODSCII* strains and maintained in alkaline medium (pH = 8.2) for 3 days, then the parasites were stained with anti-IMC1 (inner membrane complex) and Alexa Fluor 594 (red). The parasite cyst walls were stained with FITC-conjugated Dolichos biflorus lectin, DBL (green). **(A)** The deletion of *FabZ*, *ODSCI*, or *ODSCII* in PRU strain did not have any remarkable impact on the tachyzoite-bradyzoite transformation ability. Scale bars, 10 μm. **(B)** No significant difference in the parasite stage transformation was detected between any of the tested parasite strains.

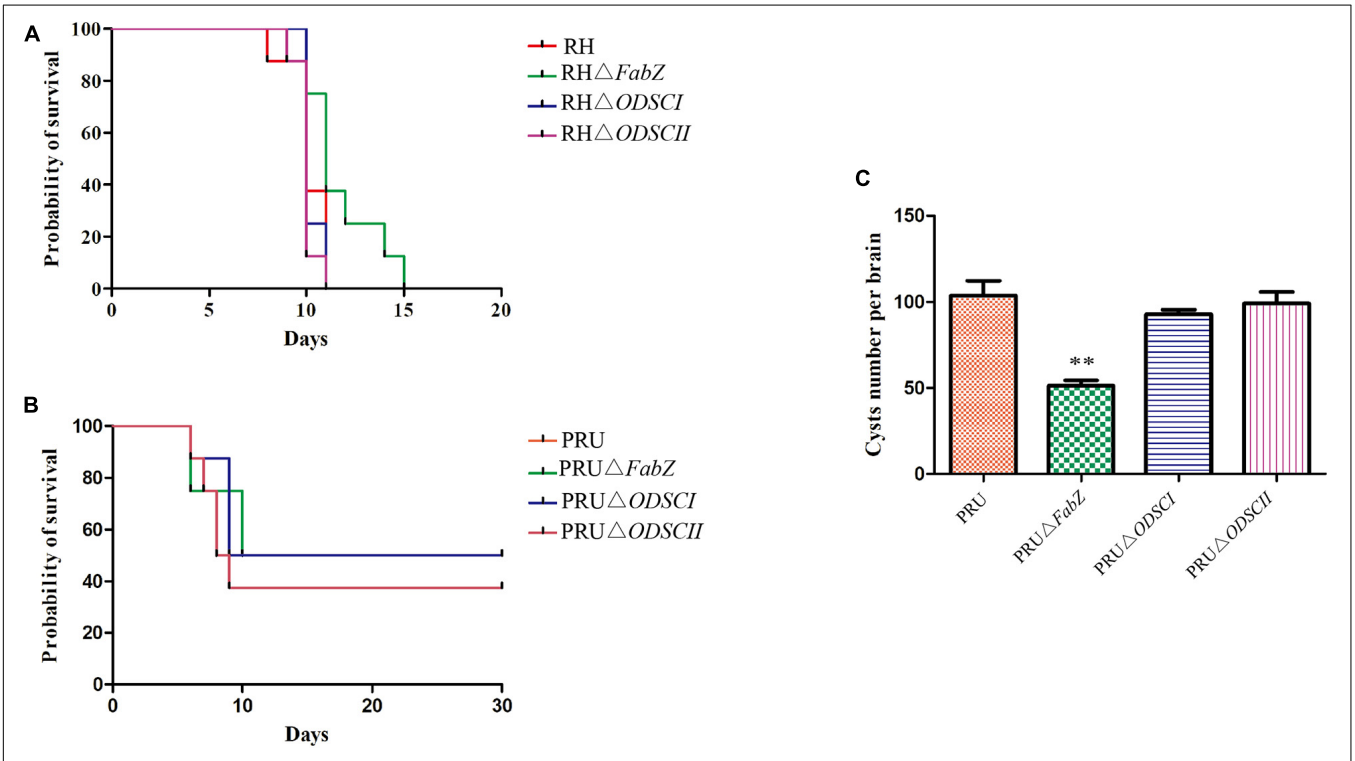

FIGURE 6 | The virulence and cyst forming ability of Δ*FabZ*, Δ*ODSCI,* or Δ*ODSCII in vivo*. **(A)** The survival of Kunming mice inoculated by 100 tachyzoites of the RH (mutant or wild-type) strains. **(B)** The survival of Kunming mice infected by 5×10^4 tachyzoites of the PRU (mutant and wild-type) strains. Mice infected by RH **(A)** or PRU **(B)** strain were checked twice daily by two independent observers for clinical signs and a Kaplan Meier survival curve plotted the infected mice that reached their humane endpoints. **(C)** The number of cysts in the mouse brain homogenates were counted at 30 days after mice were infected by 5×10^4 PRU tachyzoites. The data are shown as means ± SEMs (8 mice/group). $^{**}P < 0.01$; ns, non-significant by Student's *t*-test.

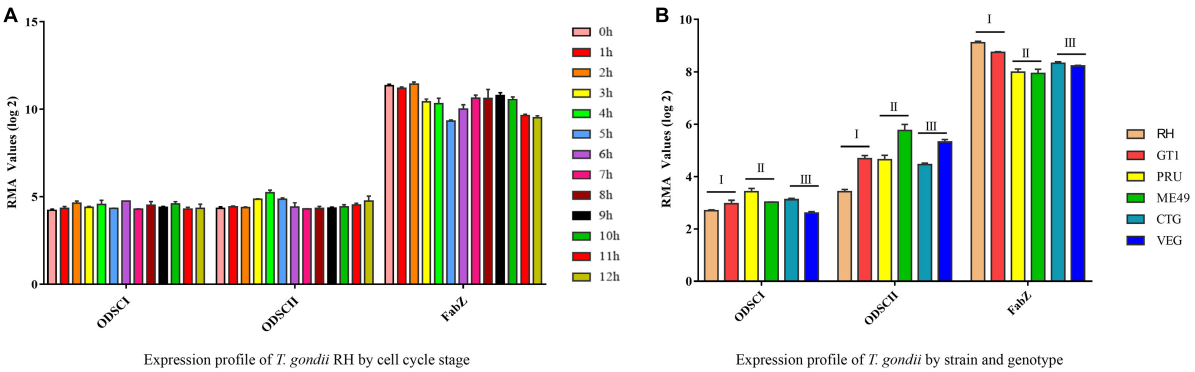

FIGURE 7 | Expression profiles of *FabZ*, *ODSCI*, and *ODSCII* in *T. gondii*. **(A)** The temporal expression profile of *FabZ*, *ODSCI*, and *ODSCII* during the cell cycle of *T. gondii* RH strain. **(B)** The expression profile of *FabZ*, *ODSCI*, and *ODSCII* of *T. gondii* in type I (RH and GT1), type II (PRU and ME49) and type III (CTG and VEG) strains of *T. gondii*.

TABLE 1 | Bioinformatic characteristics of *Toxoplasma gondii* genes.

Name	Gene ID	Product description	Exons	Phenotype value	TMHMM[a]	Predicted signal peptide
FabZ	TGME49_321570	Beta-hydroxyacyl-acyl carrier protein dehydratase	2	0.67	No	Yes
ODSCI	TGGT1_269400	Oxidoreductase, short chain dehydrogenase/reductase family protein	5	0.08	No	No
ODSCII	TGGT1_313050	Oxidoreductase, short chain dehydrogenase/reductase family protein	6	0.37	No	No

[a] *Prediction of transmembrane helices was performed using the TMHMM program version 2.0.*

cysts of the PRU strain, indicating the important role that FabZ plays in the growth and virulence of *T. gondii*.

Expression Profiles of *FabZ*, *ODSCI*, and *ODSCII*

Many genes exhibit temporal expression patterns during the replication of *T. gondii* tachyzoites, which is related to biological processes specific to the parasite development and replication (Behnke et al., 2006). Previous studies have found that some ROP genes, such as *ROP5*, *ROP16*, and *ROP17*, are cell cycle-dependent (Behnke et al., 2006). However, some ROPs do not show periodic expression characteristics, such as *ROP21*, *ROP27*, and *ROP28* (Jones et al., 2017).

The expression profiles of *FabZ*, *ODSCI*, and *ODSCII* genes involved in FASII pathway were analyzed under different conditions according to the data available in ToxoDB. There was no difference in the expression of *FabZ* at different time points in the parasite's respective cell cycle stages, but the expression of *FabZ* was significantly higher than that of *ODSCI* and *ODSCII* at the same time points (**Figure 7A**) (Behnke et al., 2010). Likewise, there was no difference in the expression of each gene between strains of the three main *T. gondii* genotypes (Type I, Type II, and Type III); however, the expression of *FabZ* was higher than that of *ODSCI* and *ODSCII* in the same examined strains (**Figure 7B**).

Studies have shown that the biological characteristics of some genes in *T. gondii* are expressed from a single exon and contain predicted signal peptides, and most proteins enter the secretory pathway mediated by signal peptides in eukaryotic cells (Devillers-Thiery et al., 1975; Lorenzi et al., 2016). The bioinformatics features, including the exon number, signal peptide and transmembrane domain of *FabZ*, *ODSCI*, and *ODSCII* are summarized in **Table 1**. Most of the proteins that perform biological functions in the apicoplast of *T. gondii* are encoded by the nuclear genome and transported to the apicoplast. Studies have shown that the signal peptide of the malaria parasite can transport proteins to the parasite's apicoplast (Meyer et al., 2018). The present and previous studies detected specific signals of FabZ and ACP (Waller et al., 1998, 2000) in the apicoplast. These results suggest that *FabZ* and *ACP*, encoded by the nuclear genome of *T. gondii*, are transported to the apicoplast likely via signal peptides to exert their functions (Waller et al., 1998, 2000).

CONCLUSION

In this study, *FabZ*, *ODSCI*, and *ODSCII* involved in FASII pathway of the apicoplast were deleted using CRISPR-Cas9 system, and the *in vitro* growth and *in vivo* pathogenicity of the mutant strains were studied. Deletion of *FabZ* caused the loss of the apicoplast and reduced the growth of *T. gondii in vitro*, while deletion of *ODSCI* and *ODSCII* had no effect on the parasite's growth. Deletion of *FabZ* reduced the virulence of the RH strain and decreased the brain cyst burden of the PRU strain

in Kunming mice. Bioinformatics analysis showed that *FabZ* is likely to be transported to the apicoplast, via its signal peptides, to participate in the FASII pathway. These findings show that *FabZ* plays an important role in the pathogenesis of *T. gondii* infection.

DATA AVAILABILITY STATEMENT

The original contributions presented in the study are included in the article/**Supplementary Material**, further inquiries can be directed to the corresponding author/s.

ETHICS STATEMENT

The animal study was reviewed and approved by the Animal Ethics Committee of Lanzhou Veterinary Research Institute, Chinese Academy of Agricultural Sciences.

AUTHOR CONTRIBUTIONS

X-QZ, M-XS, and HE conceived and designed this study, and critically revised the manuscript. X-PX performed the experiments, analyzed the data, and drafted the manuscript. W-GL, Z-WZ, L-XS, and Q-LL participated in the implementation of the study. All authors read and approved the final version of the manuscript.

FUNDING

Project support was kindly provided by the Agricultural Science and Technology Innovation Program (ASTIP) of China (Grant No. CAAS-ASTIP-2016-LVRI-03), the Fund for Shanxi "1331 Project" (Grant No. 20211331-13), the Yunnan Expert Workstation (Grant No. 202005AF150041), and the Veterinary Public Health Innovation Team of Yunnan Province.

ACKNOWLEDGMENTS

We are grateful to Prof. Bang Shen (Huazhong Agricultural University) for providing pSAG1::CAS9-U6::sgUPRT and pUPRT-DHFR-D vectors.

SUPPLEMENTARY MATERIAL

The Supplementary Material for this article can be found online at: https://www.frontiersin.org/articles/10.3389/fmicb.2021.703059/full#supplementary-material

REFERENCES

Arrizabalaga, G., Ruiz, F., Moreno, S., and Boothroyd, J. C. (2004). Ionophore-resistant mutant of *Toxoplasma gondii* reveals involvement of a sodium/hydrogen exchanger in calcium regulation. *J. Cell Biol.* 165, 653–662. doi: 10.1083/jcb.200309097

Aygün, C., and Mutlu, Ö. (2020). Computational characterisation of *Toxoplasma gondii* FabG (3-oxoacyl-[acyl-carrier-protein] reductase): a combined virtual screening and all-atom molecular dynamics simulation study. *J. Biomol. Struct. Dyn.* 52, 1–18. doi: 10.1080/07391102.2020.1834456

Bansal, P., Tripathi, A., Thakur, V., Mohmmed, A., and Sharma, P. (2017). Autophagy-related protein ATG18 regulates apicoplast biogenesis in apicomplexan parasites. *mBio* 8, e1468–e1417. doi: 10.1128/mBio.01468-17

Behnke, M. S., Wootton, J. C., Lehmann, M. M., Radke, J. B., Lucas, O., Nawas, J., et al. (2006). Apicoplast fatty acid synthesis is essential for organelle biogenesis and parasite survival in *Toxoplasma gondii*. *Proc. Natl. Acad. Sci. U.S.A.* 103, 13192–13197. doi: 10.1073/pnas.0603391103

Behnke, M. S., Wootton, J. C., Lehmann, M. M., Radke, J. B., Lucas, O., Nawas, J., et al. (2010). Coordinated progression through two subtranscriptomes underlies the tachyzoite cycle of *Toxoplasma gondii*. *PLoS One* 5:e12354. doi: 10.1371/journal.pone.0012354

Black, M. W., Arrizabalaga, G., and Boothroyd, J. C. (2000a). Ionophore-resistant mutants of *Toxoplasma gondii* reveal host cell permeabilization as an early event in egress. *Mol. Cell. Biol.* 20, 9399–9408. doi: 10.1128/mcb.20.24.9399-9408.2000

Black, M. W., and Boothroyd, J. C. (2000b). Lytic cycle of *Toxoplasma gondii*. *Microbiol. Mol. Biol. Rev.* 64, 607–623. doi: 10.1128/mmbr.64.3.607-623.2000

Blume, M., Rodriguez-Contreras, D., Landfear, S., Fleige, T., Soldati-Favre, D., Lucius, R., et al. (2009). Host-derived glucose and its transporter in the obligate intracellular pathogen *Toxoplasma gondii* are dispensable by glutaminolysis. *Proc. Natl. Acad. Sci. U.S.A.* 106, 12998–13003. doi: 10.1073/pnas.0903831106

Botté, C. Y., Yamaryo-Botté, Y., Rupasinghe, T. W., Mullin, K. A., MacRae, J. I., Spurck, T. P., et al. (2013). Atypical lipid composition in the purified relict plastid (apicoplast) of malaria parasites. *Proc. Natl. Acad. Sci. U.S.A.* 110, 7506–7511. doi: 10.1073/pnas.1301251110

Caldas, L. A., de Souza, W., and Attias, M. (2009). Microscopic analysis of calcium ionophore activated egress of *Toxoplasma gondii* from the host cell. *Vet. Parasitol.* 167, 8–18. doi: 10.1016/j.vetpar.2009.09.051

Cao, X. Z., Wang, J. L., Elsheikha, H. M., Li, T. T., Sun, L. X., Liang, Q. L., et al. (2019). Characterization of the role of amylo-alpha-1,6-glucosidase protein in the infectivity of *Toxoplasma gondii*. *Front. Cell. Infect. Microbiol.* 9:418. doi: 10.3389/fcimb.2019.00418

Chemoh, W., Sawangjaroen, N., Siripaitoon, P., Andiappan, H., Hortiwakul, T., Sermwittayawong, N., et al. (2015). *Toxoplasma gondii* - prevalence and risk factors in HIV-infected patients from Songklanagarind Hospital, southern Thailand. *Front. Microbiol.* 6:1304. doi: 10.3389/fmicb.2015.01304

Devillers-Thiery, A., Kindt, T., Scheele, G., and Blobel, G. (1975). Homology in amino-terminal sequence of precursors to pancreatic secretory proteins. *Proc. Natl. Acad. Sci. U.S.A.* 72, 5016–5020. doi: 10.1073/pnas.72.12.5016

Fleige, T., Fischer, K., Ferguson, D. J., Gross, U., and Bohne, W. (2007). Carbohydrate metabolism in the *Toxoplasma gondii* apicoplast: localization of three glycolytic isoenzymes, the single pyruvate dehydrogenase complex, and a plastid phosphate translocator. *Eukaryot. Cell* 6, 984–996. doi: 10.1128/EC.00061-07

Jones, N. G., Wang, Q., and Sibley, L. D. (2017). Secreted protein kinases regulate cyst burden during chronic toxoplasmosis. *Cell. Microbiol.* 19:10. doi: 10.1111/cmi.12651

Kloehn, J., Oppenheim, R. D., Siddiqui, G., De Bock, P.-J., Kumar Dogga, S., Coute, Y., et al. (2020). Multi-omics analysis delineates the distinct functions of sub-cellular acetyl-CoA pools in *Toxoplasma gondii*. *BMC Biol.* 18:67. doi: 10.1186/s12915-020-00791-7

Kowalik, D., Haller, F., Adamski, J., and Moeller, G. (2009). In search for function of two human orphan SDR enzymes: hydroxysteroid dehydrogenase like 2 (HSDL2) and short-chain dehydrogenase/reductase-orphan (SDR-O). *J. Steroid Biochem. Mol. Biol.* 117, 117–124. doi: 10.1016/j.jsbmb.2009.08.001

Krishnan, A., Kloehn, J., Lunghi, M., Chiappino-Pepe, A., Waldman, B. S., Nicolas, D., et al. (2020). Functional and computational genomics reveal unprecedented flexibility in stage-specific *Toxoplasma* metabolism. *Cell Host Microbe* 27, 290–306. doi: 10.1016/j.chom.2020.01.002

Lorenzi, H., Khan, A., Behnke, M. S., Namasivayam, S., Swapna, L. S., Hadjithomas, M., et al. (2016). Local admixture of amplified and diversified secreted pathogenesis determinants shapes mosaic *Toxoplasma gondii* genomes. *Nat. Commun.* 7:10147. doi: 10.1038/ncomms10147

MacRae, J. I., Sheiner, L., Nahid, A., Tonkin, C., Striepen, B., and McConville, M. J. (2012). Mitochondrial metabolism of glucose and glutamine is required for intracellular growth of *Toxoplasma gondii*. *Cell Host Microbe* 12, 682–692. doi: 10.1016/j.chom.2012.09.013

Mazumdar, J., Wilson, E., Masek, K., Hunter, C. A., and Striepen, B. (2006). Apicoplast fatty acid synthesis is essential for organelle biogenesis and parasite survival in *Toxoplasma gondii*. *Proc. Natl. Acad. Sci. U.S.A.* 103, 13192–13197. doi: 10.1073/pnas.0603391103

Meyer, C., Barniol, L., Hiss, J. A., and Przyborski, J. M. (2018). The N-terminal extension of the *P. falciparum* GBP130 signal peptide is irrelevant for signal sequence function. *Int. J. Med. Microbiol.* 308, 3–12. doi: 10.1016/j.ijmm.2017.07.003

Mordue, D. G., Håkansson, S., Niesman, I., and Sibley, L. D. (1999). *Toxoplasma gondii* resides in a vacuole that avoids fusion with host cell endocytic and exocytic vesicular trafficking pathways. *Exp. Parasitol.* 92, 87–99. doi: 10.1006/expr.1999.4412

Oppenheim, R. D., Creek, D. J., Macrae, J. I., Modrzynska, K. K., Pino, P., Limenitakis, J., et al. (2014). BCKDH: the missing link in apicomplexan mitochondrial metabolism is required for full virulence of *Toxoplasma gondii* and *Plasmodium berghei*. *PLoS Pathog*. 10:e1004263. doi: 10.1371/journal.ppat.1004263

Ralph, S. A., van, Dooren, G. G., Waller, R. F., Crawford, M. J., Fraunholz, M. J., Foth, B. J., et al. (2004). Tropical infectious diseases: metabolic maps and functions of the *Plasmodium falciparum* apicoplast. *Nat. Rev. Microbiol.* 2, 203–216. doi: 10.1038/nrmicro843

Ramakrishnan, S., Docampo, M. D., Macrae, J. I., Pujol, F. M., Brooks, C. F., van Dooren, G. G., et al. (2012). Apicoplast and endoplasmic reticulum cooperate in fatty acid biosynthesis in apicomplexan parasite *Toxoplasma gondii*. *J. Biol. Chem.* 287, 4957–4971. doi: 10.1074/jbc.M111.310144

Reiff, S. B., Vaishnava, S., and Striepen, B. (2012). The HU protein is important for apicoplast genome maintenance and inheritance in *Toxoplasma gondii*. *Eukaryot. Cell* 11, 905–915. doi: 10.1128/EC.00029-12

Robert-Gangneux, F., and Dardé, M. L. (2012). Epidemiology of and diagnostic strategies for toxoplasmosis. *Clin .Microbiol. Rev.* 25, 264–296. doi: 10.1128/CMR.05013-11

Tymoshenko, S., Oppenheim, R. D., Agren, R., Nielsen, J., Soldati-Favre, D., Hatzimanikatis, V., et al. (2015). Metabolic needs and capabilities of *Toxoplasma gondii* through combined computational and experimental analysis. *PLoS Comput. Biol.* 11:e1004261. doi: 10.1371/journal.pcbi.1004261

Vaughan, A. M., O'Neill, M. T., Tarun, A. S., Camargo, N., Phuong, T. M., Aly, A. S., et al. (2009). Type II fatty acid synthesis is essential only for malaria parasite late liver stage development. *Cell. Microbiol.* 11, 506–520. doi: 10.1111/j.1462-5822.2008.01270

Waller, R. F., Keeling, P. J., Donald, R. G., Striepen, B., Handman, E., Lang-Unnasch, N., et al. (1998). Nuclear-encoded proteins target to the plastid in *Toxoplasma gondii* and *Plasmodium falciparum*. *Proc. Natl. Acad. Sci. U.S.A.* 95, 12352–12357. doi: 10.1073/pnas.95.21.12352

Waller, R. F., Reed, M. B., Cowman, A. F., and McFadden, G. I. (2000). Protein trafficking to the plastid of *Plasmodium falciparum* is via the secretory pathway. *EMBO J.* 19, 1794–1802. doi: 10.1093/emboj/19.8.1794

Wang, J. L., Bai, M. J., Elsheikha, H. M., Liang, Q. L., Li, T. T., Cao, X. Z., et al. (2020). Novel roles of dense granule protein 12 (GRA12) in *Toxoplasma gondii* infection. *FASEB. J.* 34, 3165–3178. doi: 10.1096/fj.201901416RR

Wang, J. L., Li, T. T., Elsheikha, H. M., Chen, K., Cong, W., Yang, W. B., et al. (2018). Live attenuated PRU:Δ*cdpk2* strain of *Toxoplasma gondii* protects against acute, chronic, and congenital toxoplasmosis. *J. Infect. Dis.* 218, 768–777. doi: 10.1093/infdis/jiy211

Wiesner, J., Reichenberg, A., Heinrich, S., Schlitzer, M., and Jomaa, H. (2008). The plastid-like organelle of apicomplexan parasites as drug target. *Curr. Pharm. Des.* 14, 855–871. doi: 10.2174/138161208784041105

Wu, L., Chen, S. X., Jiang, X. G., and Cao, J. P. (2009). *Toxoplasma gondii*: a simple real-time PCR assay to quantify the proliferation of the apicoplast. *Exp. Parasitol.* 123, 384–387. doi: 10.1016/j.exppara.2009.08.013

Wu, L., Tang, C., Wang, J., Jin, X., Jiang, X., and Chen, S. (2018). Induction of FAS II Metabolic disorders to cause delayed death of *Toxoplasma gondii*. *J. Nanosci. Nanotechnol.* 18, 8155–8159. doi: 10.1166/jnn.2018.16396

Xia, N., Yang, J., Ye, S., Zhang, L., Zhou, Y., Zhao, J., et al. (2018). Functional analysis of *Toxoplasma* lactate dehydrogenases suggests critical roles of lactate fermentation for parasite growth *in vivo*. *Cell. Microbiol.* 20:e12794. doi: 10.1111/cmi.12794

Xia, N., Ye, S., Liang, X., Chen, P., Zhou, Y., Fang, R., et al. (2019). Pyruvate homeostasis as a determinant of parasite growth and metabolic plasticity in *Toxoplasma gondii*. *mBio* 10:e00898. doi: 10.1128/mBio.00898-19

Xiao, Y., Yin, J., Jiang, N., Xiang, M., Hao, L., Lu, H., et al. (2010). Seroepidemiology of human *Toxoplasma gondii* infection in China. *BMC Infect. Dis.* 10:4. doi: 10.1186/1471-2334-10-4

Yeh, E., and DeRisi, J. L. (2011). Chemical rescue of malaria parasites lacking an apicoplast defines organelle function in blood-stage *Plasmodium falciparum*. *PLoS Biol.* 9:e1001138. doi: 10.1371/journal.pbio.100113

Zhang, Z. W., Li, T. T., Wang, J. L., Liang, Q. L., Zhang, H. S., Sun, L. X., et al. (2021). Functional characterization of two thioredoxin proteins of *Toxoplasma gondii* using the CRISPR-Cas9 system. *Front. Vet. Sci.* 7:614759. doi: 10.3389/fvets.2020.614759

Conflict of Interest: The authors declare that the research was conducted in the absence of any commercial or financial relationships that could be construed as a potential conflict of interest.

Publisher's Note: All claims expressed in this article are solely those of the authors and do not necessarily represent those of their affiliated organizations, or those of the publisher, the editors and the reviewers. Any product that may be evaluated in this article, or claim that may be made by its manufacturer, is not guaranteed or endorsed by the publisher.

Frontiers in Microbiology

Explores the habitable world and the potential of microbial life

The largest and most cited microbiology journal which advances our understanding of the role microbes play in addressing global challenges such as healthcare, food security, and climate change.

Discover the latest Research Topics

See more →

Frontiers

Avenue du Tribunal-Fédéral 34
1005 Lausanne, Switzerland
frontiersin.org

Contact us

+41 (0)21 510 17 00
frontiersin.org/about/contact